Proteomic Techniques for the Discovery of Biomarkers associated with Uveal Melanoma and Cutaneous Melanoma Disease Progression

Deirdre O'Flynn

Ph.D 2014

Proteomic Techniques for the Discovery of Biomarkers associated with Uveal Melanoma and Cutaneous Melanoma Disease Progression

A thesis submitted for the degree of Ph.D.

by

Deirdre O'Flynn, B.A. (Mod.) Microbiology

Research work described in this thesis was performed under the supervision of

Dr. Paula Meleady and Prof. Martin Clynes

School of Biotechnology

National Institute for Cellular Biotechnology

Dublin City University

May 2014

I hereby certify that this material, which I now submit for assessment on the programme of study leading to the award of Ph.D. is entirely my own work, that I have exercised reasonable care to ensure that the work is original, and does not to the best of my knowledge breach any law of copyright, and has not been taken from the work of others save and to the extent that such work has been cited and acknowledged within the text of my work.

Signed: _____ ID No.: 55007607

Date:

This thesis is dedicated to my parents, Michael and Olive.

ACKNOWLEDGEMENTS

I would first like to thank Prof. Martin Clynes and Dr. Paula Meleady for giving me the chance to do this Ph.D. They have always been supportive, helpful, and understanding, both in the lab and in life. Thanks so much to both of them for being such great supervisors.

I would like to thank Mick "The Mass Spec Guru" Henry for all of the hours that he spent helping and teaching me. And for all of those Saturdays he spent guiding me through mass spec troubleshooting over the phone while trying to enjoy a round of golf. I also owe so much gratitude to Annett! She taught me so much and never once refused to help, all while being a good friend and wonderful scientist.

Thanks also to Paul Dowling for answering my 1,000,001 questions and for constantly offering good scientific advice. I would also like to thank Clair Gallagher for help and support with all of the apoptosis assays and Joanne Keenan for her assistance in the ROS assays.

Thanks to Michael Moriarty and Vincent Lynch for their help, advice and expertise in any clinical queries I had. I would like to thank Benvon Moran, Susan Kennedy and Pathma Ramasamy for their help in clinical sample collections, characterisations and general advice. Thanks also to all of the clinicians and patients involved in the studies, without which, none of this work would have been possible.

Huge gratitude goes out to Colin Clarke. His (statistically) significant help and positive attitude made writing the thesis so much easier. Thanks also to Stephen Madden for his work on the microarray study and to Annemarie for her help with the immunohistochemistry analysis.

Thanks to Gillian Smith and, previously, Joe Carey for their help in stores and the prep room. I'll miss our little chats Gillian! Thanks also to Carol, Yvonne and Geraldine in the office for all of their help with everything, particularly at the thesis printing stage!

Thank you to all of my second floor comrades; Mark, Shane, Paul, Martin, Alan, Andrew and Gemma. I might not miss the dodgy lunchtime conversations but I will miss singing along to Whitney, the random frights, the sneaky coffees, and the chats!

Thanks so much to Karen and Trish, also known as Krish. They made the last year bearable with their constant support, good chats and mostly, the bants which they provided. Thanks also to Neil who reminded me that a pun can be worse than any bad day in the lab.

Huge thanks go out to my parents who have always helped me through my education and who have got me to where I am today. I appreciate every little thing that they've done for me and their support throughout my Ph.D. has been invaluable. I hope that I've made you both proud! Thanks also to Ed, "The Other Child". He has always helped me without question on any little technical issue, proof reading, and has even fed me the best burritos and cookies I've ever eaten.

Last but not least, thanks to Damian for being the best scientific advisor/proof reader/steak chef/housekeeper/provider of quality TV shows/boyfriend a gal could ask for! Through thick and thin, he has supported me more than he will ever know and never once failed in helping me. Thank you from the bottom of my heart, Dr. Damo.

ABBREVIATIONS

2-D DIGE	-	2-Dimensional Differential Gel Electrophoresis
2-D LC-MS/MS	-	2-Dimensional Liquid Chromatography Tandem Mass Spectrometry
2-D PAGE	-	2-Dimensional Polyacrylamide Gel Electrophoresis
AJCC	-	American Joint Committee on Cancer
Arp2/3	-	Actin-Related Protein 2/3
AUC	-	Area Under the Curve
BACE-2	-	Beta Secretase 2
BAP1	-	BRCA1-associated protein-1
BRAF	-	V-raf Murine Sarcoma Viral Oncogene Homolog B1
BRB	-	Blood Retina Barrier
BSA	-	Bovine Serum Albumin
CAM	-	Cell-Cell Adhesion Molecules
CBS	-	Cerebrospinal Fluid
CDK	-	Cyclin-Dependent Kinase D
CDKN2A	-	Cyclin-Dependent Kinase Inhibitor 2A
CI	-	Confidence Interval
CTLA-4	-	Cytotoxic T-lymphocyte Associated-Antigen 4
CXCL12	-	C-X-C chemokine ligand 12
CXCR4	-	C-X-C motif chemokine receptor 4
DAVID	-	Database for Annotation, Visualization and Integrated Discovery
DCF	-	2',7'-dichlorofluorescein
DCFH-DA	-	2',7'-dichlorofluorescein-diacetate
DMF	-	Dimethylformamide
DMO	-	Diabetic Macular Oedema
DTT	-	dithiothreitol
ECL	-	Enhanced Chemiluminescence
ECM	-	Extracellular Matrix
EDTA	-	Ethylenediaminetetraacetic Acid
EEF1G	-	Elongation Factor 1 Gamma
ELISA	-	Enzyme Linked Immunosorbent Assay
ESI	-	Electrospray Ionisation
FABP3	-	Fatty Acid Binding Protein 3
FCS	-	Foetal Calf Serum

FFPE	-	Formalin-fixed Paraffin Embedded Tissue
FGF2	-	Fibroblast Growth Factor 2
GAPDH	-	Glyceraldehyde-3-Phosphate Dehydrogenase
GEO	-	Gene Expression Omnibus
GNA11	-	Guanine nucleotide-binding protein G(q) subunit alpha-11
GNAQ	-	G(q) Subunit Alpha
GO	-	Gene Ontology
gp100	-	Glycoprotein 100
GPCR	-	G-coupled receptor
HDAC	-	Histone Deacetylase
HDIL-2	-	High-Dose Interleukin-2
HPLC	-	High Performance Liquid Chromatography
IEF	-	Isoelectric Focusing
IFNɣ	-	Interferon 1 Gamma
Ig	-	Immunoglobulin
IGF	-	Insulin-like growth factor
IGF-1R	-	Insulin-like growth factor 1 receptor
IHC	-	Immunohistochemistry
IMAC	-	Immobilised Metal Affinity Chromatography
IMS	-	Industrial Methylated Spirits
IPG	-	Immobiline pH Gradient
IQR	-	Interquartile Range
KPNB1	-	Importin Subunit Beta 1
LC-MS	-	Liquid Chromatography – Mass Spectrometry
LDH	-	Lactate Dehydrogenase
LOH	-	Loss of heterozygosity
m/z	-	Mass to charge ratio
MALDI	-	Matrix-Enhanced Laser Desorption/Ionisation
MAPK/ERK	-	Mitogen-Activated Protein Kinase/Extracellular Signal-Related Kinase
MARS	-	Multiple Affinity Removal System
MDM2	-	Murine Double Minute 2
MEK	-	Mitogen-Activated Protein Kinase Kinase
MIA	-	Melanoma inhibitory activity
MIP1α	-	Macrophage Inhibitory Protein 1 Alpha

MMP	-	Matrix Metalloproteases
MRM	-	Multiple Reaction Monitoring
mRNA	-	Messenger RNA
MS	-	Mass Spectrometry
MS/MS	-	Tandem Mass Spectrometry
mTOR	-	Target of Rapamycin
MW	-	Molecular Weight
NPDR	-	Non-Proliferative Diabetic Retinopathy
NRAS	-	Neuroblastoma RAS viral (v-ras) oncogene homolog
P13K/AKT	-	Phosphoinositide 3-kinase/Protein Kinase B
PBS	-	Phosphate Buffered Saline
PD-1	-	Programmed Death-1
PDR	-	Proliferative Diabetic Retinopathy
PEDF	-	Pigment Epithelium-Derived Factor
pI	-	Isoelectric point
PLCβ	-	β phospholipase C
PMT	-	Photo Multiplier Tube
PTEN	-	Phosphatase and Tensin Homolog
PVR	-	Proliferative Vitreoretinopathy
Rb	-	retinoblastoma tumour suppressor
RISC	-	RNA-induced silencing complex
RNAi	-	RNA Interfernce
RRD	-	Rhegmatogenous retinal detachment
S/N	-	Signal to Noise Ratio
S110B	-	S100 calcium binding protein B
SDS-PAGE	-	Sodium Dodecyl Sulphate-Polyacrylamide Gel Electrophoresis
SELDI	-	Surface Enhanced Laser Desorption/Ionisation
SELENBP1	-	Selenium-Binding Protein
SF	-	Serum Free
SF3B1	-	Splicing Factor 3B, subunit 1
SILAC	-	Stable Isotope Labelling with Amino Acids in Culture
siRNA	-	Small Interfering RNA
SPA	-	Sinapinic Acid
TBS	-	Tris-Buffered Saline

TIC	-	Total Ion Chromatogram
TIMP-1	-	Tissue inhibitor of metalloproteinase 1
TOF	-	Time of Flight
TPI1	-	Triosephosphate isomerase
UHP	-	Ultrapure Water
UM	-	Uveal Melanoma
VEGF	-	Vascular Endothelial Growth factor
XC	-	X Correlation

TABLE OF CONTENTS

ABSTRACT

PROTEOMIC TECHNIQUES FOR THE DISCOVERY OF BIOMARKERS ASSOCIATED WITH UVEAL MELANOMA AND CUTANEOUS MELANOMA DISEASE PROGRESSION

Deirdre O'Flynn

Uveal melanoma is the most common primary intraocular cancer. Cutaneous melanoma accounts for the highest number of deaths of any skin cancer. This research outlines the discovery of proteins potentially associated with disease progression in uveal and cutaneous melanomas.

It was hypothesised that patterns of differential protein expression would be observed between primary uveal melanoma tumour tissues of patients who subsequently developed metastasis versus those who did not and that such proteins could be used as potential biomarkers of disease progression. Using 2-D DIGE and quantitative LC-MS/MS, and functional validation by siRNA knockdown, five proteins were identified; EEF1G, SELENBP1, KPNB1, TPI1, and FABP3, which were found to play a role in invasion and migration in uveal melanoma cell lines.

Vitreous fluid from patients with uveal melanoma was subjected to various sample pre-treatments and analyses in order to determine an optimal method for studying this biofluid. Fractionation by copper-activated IMAC resin and subsequent LC-MS analysis was carried out which resulted in the identification of 62 differentially expressed proteins between patients with monosomy 3 tumours (associated with poor prognosis) and patients with disomy 3 tumours (good prognosis).

It was hypothesised that protein expression differences would be present throughout the process of cutaneous melanoma disease progression. Using quantitative label-free LC-MS/MS, 57 proteins differentially expressed between the control and disease groups were identified. Four of these proteins, and three targets from a previous transcriptomic microarray analysis, were analysed across a panel of control, cutaneous melanoma (benign, early stage, advanced), and uveal melanoma sera using ELISA. This identified two potential markers of melanoma progression; lactotransferrin and BACE-2.

Cutaneous melanoma serum and healthy, control serum were profiled and compared by SELDI TOF MS. This analysis revealed an 8.9 kDa candidate which was overexpressed in the disease samples in comparison to the control samples. In an attempt to identify the potential marker, IMAC purification with 1-D gel electrophoresis and quantitative LC-MS was used. 34 proteins were found to be differentially expressed between control and advanced cutaneous melanoma sera.

CHAPTER ONE

Introduction

1.1 General Introduction

Cancer is defined as the unregulated growth of cells. Cells which grow uncontrollably can eventually form a large cell mass; a neoplasm, more commonly known as a tumour. These tumours grow exponentially as each cell divides to produce two daughter cells, with cells in rapidly-growing tumours replicating every one to four weeks, while the cells of a slow-growing tumour may double every six months. Benign tumours are those which remain in one location and are often removed from the area to which they are confined through the use of surgery; however metastatic tumours are those which contain more aggressive cells. The cells of malignant tumours have a higher invasive potential than those of benign tumours and so, are capable of spreading from the primary location to distant organs.

Although there are more than 100 cancer types, it has been suggested that virtually all show the same hallmarks which are required to breach any physiological barriers and to thus achieve a state of malignancy (Figure 1.1). For example, neoplastic cells must increase and sustain a level of angiogenesis which is conducive to providing the tumour with the oxygen and nutrients it needs for growth, while growth signals must successfully be produced or mimicked, and anti-growth signals supressed, in order to promote proliferation. If a neoplasm achieves such hallmarks, it can eventually reach a point where it will spread and form secondary neoplasms in regions of the body where space and nutrients are more plentiful (Hanahan and Weinberg 2011).

Figure 1.1 The hallmarks of cancer which ultimately contribute to the development of metastases. As adapted from (Hanahan and Weinberg 2011).

Melanomas are malignancies which derive from dendritic melanocytes, i.e. pigment-producing cells, found in the skin, eye, mucosal epithelia, and leptomeniges. However, the skin is the most common site of melanoma development; this type of neoplasm is referred to as a cutaneous melanoma (Hurst, Harbour et al. 2003). Cutaneous melanoma is currently regarded as being a life-threatening malignancy, and a steady increase in incidence has been observed over the past few decades (van den Bosch, Kilic et al. 2010). Cutaneous melanoma accounts for more than 90% of all melanomas. However, melanoma is recognised as being difficult to treat, mainly due to the large number of patients who are resistant to immune therapy as well as chemotherapy (Mehnert and Kluger 2012). Moreover, malignant melanoma often exhibits unpredictable behaviour. For example, many patients with significant vertical growth remain metastasis-free while some with thin lesions subsequently perish as a result of their disease (Torabian and Kashani-Sabet 2005). A better

understanding of the mechanisms of disease initiation and progression involved in cutaneous melanoma is critical for the development of predictive biomarkers which, to-date, have been elusive.

Uveal melanoma only accounts for 5% of all melanomas, albeit, it is the most common intraocular malignancy, accounting for 85% of all cases in the western world. The incidence of uveal melanoma remains reasonably steady at approximately 7 people per million per year, a figure which increases with age (van den Bosch, Kilic et al. 2010). The disease is rarely caused by inherited mutations and develops from melanocytoma (tumour of melanocytes of the ophthalmic disc) (Damato 2004). The uvea consists of the iris, the choroid and the ciliary body, with the disease arising in the choroid of 90% of cases, the ciliary body in 5-10% of patients, and in the iris of 3% of patients, which is associated with the best outcome (Damato 2004, Pardo, Dwek et al. 2007). The 5-year survival rate of uveal melanoma is 72%, however, the median survival rate following metastasis is approximately six months (Triozzi, Eng et al. 2008). This is due to the highly aggressive nature of the metastatic disease which spreads to vital organs such as the kidneys, bone, lungs, and in 95% of metastatic cases, the liver (Damato 2004). As there are no current protein biomarkers available for the detection of uveal melanoma, a prognostic marker would greatly help in the detection and possible treatment of the metastatic disease.

Although uveal and cutaneous melanomas both derive from melanocytes, they are distinct in their mechanisms of tumorigenesis and metastasis, as well as in their therapeutic response and genetic aberrations (van den Bosch, Kilic et al. 2010). The differences between both melanomas are poorly understood, but it is hoped that genetic and proteomic analyses of the nature of melanoma as a disease will aid us in understanding variations between both melanomas.

Proteomic analysis is used for the characterisation of the proteins, and associated protein and peptide modifications which compose signalling networks. Hence, it can be useful, particularly when used in conjunction with genomic markers, in determining deregulated pathways in cancer, thus furthering our understanding of the disease and potentially identifying new drug targets. In addition to this, proteomic analysis can be used for the detection of biomarkers, i.e. features which

are measured and evaluated as indicators of normal or disease state, disease progression or response to therapy. Biomarkers can often be used in the clinic for diagnostic or prognostic tests. Ideally, if a biomarker is intended for use in the clinic, it should illustrate an unbiased diagnosis result, whether or not the patient is symptomatic. The marker should also demonstrate high specificity, high sensitivity, ease of use, regularity, and clarity in results. Proteomic studies for the identification of biomarkers are typically carried out in clinical specimens such as blood (which may be separated into serum and plasma), urine, cerebrospinal fluid (CBS), saliva, and sputum. Techniques such as mass spectrometry (MS), and matrix-assisted laser desorption and ionisation with time-of-flight (MALDI-TOF) have been key methods in the search for differential protein expression patterns in both clinical and cell culture specimens (Lee and Kohn 2010, Boja, Hiltke et al. 2011).

1.2 Uveal Melanoma

Uveal melanoma is the most common primary intraocular malignancy affecting approximately 5 people per million in the Western world each year, however this incidence increases with age (Pardo, Dwek et al. 2007). Uveal melanoma is rarely caused by inherited mutations but can develop from melanocytoma (Damato 2004).

The uvea consists of the iris, the choroid and the ciliary body (Pardo, Dwek et al. 2007). The malignancy arises in the iris of 3% of patients and has the best prognosis in comparison to uveal melanoma of the choroid (90% of patients) or of the ciliary body (5-10% of cases) (Damato 2004). It is unclear why this is but may be due to the fact that iris melanoma is generally smaller than either of the posterior ciliary or choroid tumours at the time of diagnosis. Most iris melanomas consist of spindle cells, according to the Callender classification (Henderson and Margo 2008). Choroidal melanoma tumours have been classified by spindle, epithelioid and mixed cell populations. Spindle cell tumours are associated with a much more promising prognosis than epithelioid cell tumours (Albert 1998).

The 5-year survival rate of uveal melanoma is 72%, however in a 15-year follow up, 53% have been shown to die of metastatic disease. The median survival rate following metastasis is approximately six months (Triozzi, Eng et al. 2008). In 95% of metastatic cases, uveal melanoma spreads to the liver, but it can also spread to

regions such as the kidneys, the bone and the lungs (Damato 2004). Clinical features which are associated with metastatic death include large tumour size, ciliary body involvement and higher patient age. Epithelioid cytology, tumour infiltration by macrophages and/or lymphocytes, and nucleolar size are all histopathologic features which can indicate poor prognosis (Landreville, Agapova et al. 2008).

1.2.1 Pathogenesis of Uveal Melanoma

Uveal melanoma is characterised by a number of disrupted molecular signalling pathways including the retinoblastoma pathway, p53 signalling, Phosphoinositide 3-kinase/Protein Kinase B (P13K/AKT) and mitogen-activated protein kinase/extracellular signal-related kinase pathways (MAPK/ERK) (Coupland, Lake et al. 2013).

The retinoblastoma pathway is mediated by the interaction between the anti-growth protein retinoblastoma tumour suppressor (Rb) and the E2F transcription factor. Rb function is regulated through phosphorylation by the D-type cyclin-dependent kinases. Growth stimulation is induced by D-cyclin/cyclin-dependent kinase 4 (cdk4) activity which induces a cascade of events leading to E2F accumulation and the transition from G_1 to S-phase. Overexpression of cyclin D1 causes a disruption of the Rb pathway in uveal melanoma through the hyperphosphorylation and inactivation of Rb, hence disrupting signalling and causing uncontrolled cell proliferation (Nevins 2001, Onken, Worley et al. 2008). Previous research has shown that overexpression of cyclin D1 may be driven by the $BRAF^{V599E}$/MEK/ERK pathway, as one group illustrated when MEK/ERK inhibition significantly decreased the proliferation rate of uveal melanoma cells in culture (Calipel, Lefevre et al. 2003). Significant cyclin D1 over-expression has been associated in the literature with unfavourable outcome when tumour tissue was examined using immunohistochemistry and has been associated with the presence of extraocular extension of the tumour (Coupland, Anastassiou et al. 2000). High levels of cyclin D1 are found in choroidal melanomas which are the more aggressive tumours and have poorer prognosis in comparison to their iris and ciliary body counterparts (Calipel, Lefevre et al. 2003).

Mutations of the p53 tumour suppressor gene, *TP53*, are present in over half of human neoplasia, making it one of the most frequent molecular events in human cancer (Davies, Spiller et al. 2011). p53 initiates growth arrest, thus antagonising cyclin D1, or apoptosis due to stressful conditions. Murine double minute 2 (MDM2) is necessary for the regulation of p53, however it is a proto-oncogene, independent of p53, which is often overexpressed in human cancers. Previous research has illustrated a potential link between MDM2 over-expression and the development of metastases (Coupland, Anastassiou et al. 2000). In uveal melanoma, high expression of the *MDM2* gene, located on chromosome 12q15, occurs in 97% of cases, resulting in the inhibition of p53 (van den Bosch, Kilic et al. 2010).

PI3K signalling is activated by receptor tyrosine kinases and G-coupled receptors. Once activated, PI3K triggers a series of events which allows for the activation of AKT (essential for several proliferation and survival pathways). This process is regulated by phosphatase and tensin homolog (PTEN), a protein which antagonises PI3K signalling through the conversion of Phosphatidylinositol (3,4,5)-trisphosphate (PIP3) to Phosphatidylinositol 4,5-bisphosphate (PIP2). A total loss of PTEN is associated with a more aggressive uveal melanoma; patients have a median survival of 60 months in comparison to those with normal or close to normal expression. A decrease in PTEN relative to another primary uveal melanoma is correlated with a more aggressive tumour (Patel, Smyth et al. 2011).

During the screening of potential oncogenes which could potentially activate the Mitogen-activated protein kinase (MAPK) pathways, mutations were discovered in Guanine nucleotide-binding protein G(q) subunit alpha (*GNAQ*), a stimulatory heterotrimeric G protein α-subunit, and Guanine nucleotide-binding protein G(q) subunit alpha-11 (*GNA11*), its paralogue (Gaudi and Messina 2011). *GNAQ* mediates signalling between G protein-coupled receptors (GPCRs) and catalyses the hydrolysis of PIP2 through the stimulation of all isoforms of β phospholipase C (PLCβ). Mutations of *GNAQ* and *GNA11* have been detected in 83% of uveal melanomas, both primary and metastatic, and exclusively affect exon 5 (Q209) and exon 4 (R183). This causes constitutive activation of the MAPK pathway in the absence of Neuroblastoma RAS viral (v-ras) oncogene homolog (*NRAS*) and *BRAF* mutations, thus *GNAQ* acts as a dominant oncogene (Lamba, Felicioni et al. 2009, Van Raamsdonk, Griewank et al. 2010, Metz, Scheulen et al. 2013). It is possible

that *GNAQ* and *GNA11* mutations represent an early stage in tumour development and that these mutations may contribute directly to the risk of hereditary melanoma in families with an increased incidence of uveal melanoma. However, previous research has suggested an absence of germ-line mutations in exon 5 of *GNAQ* and *GNA11* in familial melanoma patients (Hawkes, Campbell et al. 2013).

The Insulin-like growth factor (IGF) signalling pathway plays a role in both cell-cell adhesion and tumour invasiveness through the binding of Insulin-like growth factor 1 (IGF-1) to Insulin-like growth factor 1 receptor (IGF-1R) for the activation of the intrinsic receptor tyrosine kinase activity and phosphorylation of insulin receptor substrate. IGF-1R is expressed on primary uveal melanoma tumours; however, IGF-1 is neither secreted nor expressed by melanoma cells. Despite this, it is produced by the liver which is the main site of metastasis for uveal melanoma. A decrease in IGF-1R has been shown to affect uveal melanoma cell line proliferation as well as metastatic potential (All-Ericsson, Girnita et al. 2002). Recent research has illustrated that a decrease in IGF-1 levels in serum can be directly correlated to prognosis. In one such study, IGF-1 serum levels of 10-years disease-free patients were lower than those of their healthy counterparts, and lower again were those of metastatic patients (Frenkel, Zloto et al. 2013). Indications which illustrate the potential role of IGF-1 in follow-up care have been noted, such as an increased IGF-1 6-month post-operative serum level in relation to pre-operative specimens (Topcu-Yilmaz, Kiratli et al. 2010).

BRCA1-associated protein-1 (*BAP1*) is a tumour suppressor which can mediate its effects through transcriptional regulation and chromatin modulation. It is also possible that it acts through the ubiquitin-proteasome system and the DNA damage response pathway. *BAP1* mutations can occur in the germline, thus leading to a familial cancer syndrome in malignancies such as mesothelioma, renal cell carcinoma, and cutaneous melanoma (Murali, Wiesner et al. 2013). An increased susceptibility is associated with a number of cancers such as cutaneous melanoma, epithelioid atypical Spitz tumours and uveal melanoma. Mutations of *BAP1* appear to occur later in tumour progression in comparison to other uveal melanoma-associated molecular defects and are associated with metastasis (Harbour 2013, Murali, Wiesner et al. 2013). Somatic mutations of *BAP1* are found to occur in 84% of metastatic uveal melanoma cases but also in 3-4% of sporadic uveal melanoma

cases where there is a *BAP1* germline mutation (Njauw, Kim et al. 2012, Aoude, Vajdic et al. 2013).

Perhaps the most recently identified recurrent mutation, associated with 18.6% of uveal melanoma cases, is in splicing factor 3B subunit 1 (*SF3B1*), which affects codon 625. *SF3B1* is a splice factor; hence, mutations in this gene result in altered pre-mRNA splicing. However, the target of the altered splicing is unknown and might be cell dependent. In terms of melanoma, *SF3B1* mutations are uveal melanoma-specific as they do not appear to occur in cutaneous melanoma (Schilling, Bielefeld et al. 2013). Mutations in *SF3B1* have previously been identified in myeloid malignancies as well as in breast cancer (Papaemmanuil, Cazzola et al. 2011, Ellis, Ding et al. 2012). Such mutations have been associated with good prognostic features in uveal melanoma, such as a younger patient age, and fewer undifferentiated epithelioid cells. In addition to this, they were found to be inversely linked with features of poor prognosis such as monosomy three and *BAP1* mutations (Harbour, Roberson et al. 2013).

c-KIT, a receptor protein tyrosine kinase involved in numerous processes including the development of uveal melanocytes, has been shown to be expressed in 63-78% of primary uveal melanoma cases as well as being expressed in the majority of metastatic cases (Daniels and Abramson 2009, Mahipal, Tijani et al. 2012).

1.2.2 Chromosomal Status and Classification of Uveal Melanoma

Cytogenetic aberrations occur as part of uveal melanoma disease progression. Typically, regions of chromosome gain are thought to harbour oncogenes while regions of chromosome loss may contain tumour suppressors. Along with features such as tumour size and histology, chromosome status, particularly that of chromosomes 1, 3, 6, and 8, is now recognised in contributing to the risk of metastasis in uveal melanoma.

Loss of chromosome 1p occurs frequently in many other cancers, such as neuroblastoma where it is an indicator of poor prognosis. In uveal melanoma, it has been found to be indicative of metastasising tumours and its loss has also been identified as concurrent with monosomy three; an indicator of poor prognosis (Kilic,

Naus et al. 2005). Loss of 1p has been associated with large ciliary body tumours and also with secondary tumours, i.e. those which have metastasised (Sisley, Parsons et al. 2000, Aalto, Eriksson et al. 2001).

An imbalance of chromosome six has been described as a recurrent aberration associated with uveal melanoma. Typically, a gain of 6p and/or a loss of 6q are observed, albeit not as frequently as other abnormalities. Gain of 6p has been reported in 18% of cases while loss of 6q has been shown to occur in 28% (Kilic, van Gils et al. 2006). Gain of 6p has been associated with a good prognosis, while the loss of 6q implies the presence of tumour suppressors in this region (Damato and Coupland 2009). However, the deletion and amplification of these regions has been shown to occur independently of other abnormalities on chromosomes 1p, 3, and 8 (van Gils, Kilic et al. 2008).

Abnormalities of chromosome eight, namely trisomy eight and isochromosome 8q, have been reported in uveal melanoma (Damato and Coupland 2009). Trisomy eight is often associated with monosomy three, for an overall risk of metastasis. However, when trisomy eight occurs in conjunction with disomy three, it is not linked with the spread of disease (Thomas, Putter et al. 2012). In addition to this, monosomy three and aneusomy eight have been shown to be present in liver metastases (Singh, Tubbs et al. 2009).

In 1996, Prescher et al. unearthed a link between monosomy of chromosome three and metastasis-associated death in uveal melanoma (Prescher, Bornfeld et al. 1996). Through the years, this finding has been proven by multiple studies (Sisley, Rennie et al. 1997, White, Chambers et al. 1998, Scholes, Damato et al. 2003). Monosomy three is thought to occur as an early event, with the loss of 1p, 8p, and gain of 8q occurring later on in disease progression as secondary events (Kilic, van Gils et al. 2006). As mentioned above, the combination of chromosome 8q gain and chromosome three loss further modulates the metastatic progression of monosomy three tumours and has been associated with hepatic metastases (Singh, Tubbs et al. 2009). It is clear that chromosome three loss provides valuable prognostic information, however, not all tumours can be classified as high or low risk based on chromosome three status alone as some tumours have been shown to undergo a partial loss of chromosome three. This has been illustrated to provide inconsistent

prognostic information, although Thomas et al. recently found that patients with "equivocal abnormality" of chromosome three are more likely to develop and die from metastases (Thomas, Putter et al. 2012).

Harbour et al., using cytogenetic analysis and genome-wide profiling, have developed a gene expression profile which distinguishes uveal melanoma tumours into two genomic groups; class 1 and class 2, based on the expression of 15 genes (Harbour 2014). Each class is used as a determinant of outcome due to the correlation between gene expression and prognosis. Class 1 tumours are deemed to have a low risk of metastasis, typically associated with gain of chromosome 6p or disomy three. In contrast, class 2 tumours carry a high risk of metastasis, often characterised by loss of chromosome three or gain of 8q (Onken, Worley et al. 2004, Couturier and Saule 2012).This method has been shown to superior in its prognostic accuracy in comparison to other prognostic biomarkers available, including monosomy three status alone (Onken, Worley et al. 2010, Harbour 2014). The gene expression profile is available as a quantitative polymerase chain reaction (qPCR)-based assay, known commercially as DecisionDX-UM, which is used on a routine basis on very small samples acquired through fine needle aspiration and on archival formalin-fixed samples, as well as on samples acquired in a multi-centre study (Harbour and Chen 2013, Harbour 2014). For the prognostic characterisation of uveal melanomas, DecisionDX-UM illustrated sensitivity and specificity values of 84.6% and 92.9% respectively. Monosomy three detected by array comparative genomic hybridisation illustrated sensitivity and specificity values of only 58.3% and 85.7%, respectively. Monosomy three detected by FISH illustrated even lower sensitivity and specificity values of 50% and 72.7%, respectively (Worley, Onken et al. 2007).

Class 1 tumours can be divided into two groups; 1A and 1B. Class 1A shows a 2% 5-year tumour-survival rate while 1B has a rate of 21%. In contrast to class 2 lesions, class 1 cells are well-differentiated and typically maintain disomy three, generally a more promising indication in terms of prognosis. The metastatic rate is low as is the rate of chromosomal aneuploidy, despite chromosome 6p gain (Gill and Char 2012).

Typically, class 2 uveal melanoma lesions demonstrate high levels of aneuploidy, particularly monosomy three, i.e. loss of heterozygosity (LOH) for chromosome three (Ehlers, Worley et al. 2008, Gill and Char 2012). Approximately 25% of class 2 tumours, class 2B, have a deletion mutation of the chromosome fragment 8p which increases the aggressiveness of the malignancy. Class 2 tumours often exhibit stem-cell like ectodermal differentiation, a high rate of metastasis and a tumour-related mortality rate of 40-60% (Gill and Char 2012). Clinical and histological features such as a large basal tumour diameter, high mitotic rate, epithelioid morphology and ciliary body involvement are also associated with such tumours (Scholes, Damato et al. 2003, Kilic, van Gils et al. 2006, Damato, Duke et al. 2007).

Among the deregulated pathways in uveal melanoma, exome sequencing has identified mutations associated with class 2 tumours; overexpression of *PTP4A3*, which maps to chromosome 8q and a high rate of inactivating mutations in *BAP1*, which maps to chromosome 3p (Couturier and Saule 2012). Harbour et al. implicated loss of *BAP1* in the onset of uveal melanoma metastasis. They also noted that this occurred independently of the presence or absence of *GNAQ* activating mutations at codon 209. It is important to note that mutations in *GNAQ* occur early in uveal melanoma and are not sufficient for malignant transformation however they may create a reliance of the tumour cells on *GNAQ* activity. Mutations of *BAP1* occur at a later stage of disease progression and, as illustrated above, coincide with the development of metastatic disease. The dual targeting of both *BAP1* and *GNAQ* mutations could therefore act as a synergistic therapy for uveal melanoma (Onken, Worley et al. 2008, Harbour, Onken et al. 2010). Somatic mutations in exon five at position 209 in *GNA11* were found to be present in 57% of uveal melanoma metastases, in contrast to *GNAQ*, where the Q209 mutation was identified in 22% of metastases. This mutation affects the production of glutamine, thus blocking intrinsic GTPase activity. Overall, 83% of uveal melanomas have been shown to have a constitutive mutation in either *GNAQ* or *GNA11* (Van Raamsdonk, Griewank et al. 2010). However, it has recently been reported that mutations in either *GNAQ* or *GNA11* are not associated with patient outcome (Koopmans, Vaarwater et al. 2013). A mutation at Arg625 in *SF3B1* in disomy three uveal melanomas has been shown to correlate with a good prognosis. An absence of the mutation appears to be

associated with metastasis, regardless of the chromosome status of the tumour (Martin, Masshofer et al. 2013).

It is unclear if class 1 tumours can evolve into class 2 tumours or if they simply develop along different pathways. Harbour et al. suggested that the presence of a class 1 tumour with a *BAP1* mutation may represent a transition state which suggests that *BAP1* mutations develop prior to the emergence of the class 2 signature. Fully understanding this would impact on primary tumour therapy; if the tumour can change from class 1 to 2 then the treatment of the primary tumour could potentially be entirely curative and early treatment would be critical, if it cannot evolve between stages then it is possible that primary tumour treatment would have no impact on survival (Harbour 2006, Harbour, Onken et al. 2010).

1.2.3 Clinical Treatment Options for Uveal Melanoma

Enucleation, or removal of the eye, has traditionally been the method of choice for uveal melanoma treatment. Nowadays, primary ocular tumours can be treated by a variety of methods tailored to factors such as size, extent and location (Damato 2012).

Unfortunately, there are very few systemic treatments available for metastatic uveal melanoma, all with doubtful efficacy. However, as our molecular knowledge improves, so does the potential for the development of better treatment options (Velho, Kapiteijn et al. 2012).

1.2.3.1 Enucleation

Historically, enucleation has been the definitive treatment for uveal melanoma. Today more than a third of patients still require enucleation; occasionally due to pain, such as in the case of intraocular pressure elevation; and due also to the excessive size of the tumour when there is no hope for useful vision (De Potter 2003, Damato 2012). However, the cosmetic trauma of losing an eye can often be difficult for the patient psychologically. The possibility of sparing vision is also destroyed by enucleation. Therefore a number of alternative treatments have been developed including; plaque or proton beam radiotherapy; stereotactic radiosurgery; trans-

scleral or trans-retinal local resection; and transpupillary thermotherapy (Damato 2012).

1.2.3.2 Radiotherapy and Radiosurgery

Plaque brachytherapy and proton beam radiotherapy are some of the more common forms of radiotherapy used in the treatment of uveal melanoma, particularly in the case of small and medium sized tumours. The possibility of either method preserving the eye and/or retaining vision is dependent on the tumour size and location. The type of radiotherapy used can depend on factors such as; tumour location, tumour size, and adjacent radiation-sensitive ocular structures (Finger 1997, Munzenrider 2001, De Potter 2003).

Ophthalmic plaque brachytherapy involves the use of a thin implant composing of a radioactive element such as iodine, ruthenium, or cobalt which can vary in its dimensions, depending on the tumour size and shape (Giblin, Shields et al. 1989). The purpose of the plaque is to deliver a highly concentrated dose of radiation therapy to a specific region of the eye where the tumour is located. Plaque brachytherapy has been shown to be effective in terms of local control with recurrence following treatment at only 15%, however this rate may be as high as 37% at 15 years in the case of metastatic disease (Freire, De Potter et al. 1997, Munzenrider 2001).

Proton beam radiotherapy is a much more effective method than conventional radiotherapy as it provides a superior distribution of the dose due to the physical nature of protons (Weber, Mirimanoff et al. 2007). If vision is reduced in the affected eye, tumours of all sizes, including some large tumours, can be treated with the proton beam, with a 75-80% probability of preservation of the eye and of some visual function (Munzenrider 2001).

Gamma knife surgery is a form of stereotactic radiosurgery which has been used as an alternative to enucleation for the reduction of the tumour while maintaining the structure of the eyeball and its function. In one study, tumour regression was observed in 90.9% of the sample set (Kang, Lee et al. 2012). The growth control rates and long-term outcome of the method compare well with enucleation and

brachytherapy and so it has been suggested as an alternative treatment for uveal melanoma (Toktas, Bicer et al. 2010). However, retinal detachment, cataract and radiation-induced retinopathy are most commonly reported as side-effects of the procedure (Toktas, Bicer et al. 2010, Kang, Lee et al. 2012).

1.2.3.3 Local Tumour Resection

Trans-scleral resection is generally suitable for certain iris, ciliary body, or anterior choroidal melanoma, especially in those with smaller basal dimensions and greater thickness (De Potter 2003).

1.2.3.4 Transpupillary Thermotherapy

Transpupillary thermotherapy with an infrared diode laser is used as a primary treatment or as a complement to radiotherapy or surgical resection in selected cases of choroidal melanoma. Using thermotherapy as part of a combined therapy appears to be more effective in reducing the intraocular tumour recurrence rate (De Potter 2003).

1.2.3.5 Systemic Treatment

Although the above methods are successful in the eradication of the primary tumour, there is currently no standard systemic therapy available for metastatic uveal melanoma treatment, with typical options, such as immunotherapy, rarely prolonging life. Chemotherapeutic agents, used both in combination and alone, have also been tested, albeit showing poor anti-tumour activity with the response rate ranging from 0 to 15% and a median overall survival time of 6 to 12 months (Pons, Plana et al. 2011).

Currently, the most promising therapies appear to be mitogen-activated protein kinase kinase (MEK) and Histone deacetylase (HDAC) inhibitors. HDAC inhibitors are capable of blocking the Bmi1/Ring1 complex which is responsible for the monoubiquitinylation of histone H2A. This in turn may be able to replace deubiquitinating activity to the cells which is absent following the loss of *BAP1*.

Hence, HDAC inhibitors such as valproic acid, LBH-589, and trichostatin A may be able to reverse the hyperubiquitinylation of histone H2A resulting from *BAP1* loss (Harbour 2012). Cell culture and animal studies have illustrated the therapeutic potential of this approach in uveal melanoma metastasis treatment (Landreville, Agapova et al. 2012). *GNAQ/11* mutations are also currently being investigated as potential therapeutic targets. As the direct inhibition of either gene would not be possible due to the role of the mutations in abrogating intrinsic GTPase activity, the goal of this approach would be to inhibit oncogenic signalling downstream as a result of the mutations. MEK would be a suitable target in this regard as it is a member of the MAPK pathway which is activated by *GNAQ/11* mutations. Recently, selumetinib was shown to induce tumour shrinkage in 50% of metastatic uveal melanoma patients with 15.9 weeks progression-free survival, in comparison to seven weeks in those treated with temozolomide, a chemotherapy drug (AACR 2013). The combined use of selumetinib with a target of rapamycin (mTOR) inhibitor, AZD8055, has also been described. mTOR inhibitors target the PI3K/AKT/mTOR pathway, which has been thought to cooperate with MAPK activation to generate and preserve the malignant phenotype in uveal melanoma. The results from this cell line-based study indicated that the dual-inhibition approach appeared to be effective in certain genotypes; the viability of *BRAF* and *GNAQ* mutant cells was suppressed with the treatment but apoptosis was only induced in *BRAF* mutant cells. In addition to this, tumour regression was only observed in the *BRAF* mutant xenograft model (Ho, Musi et al. 2012). Temozolomide and the MEK inhibitor AZD6244 are currently being tested in a randomized phase II trial; clinical trial identifier NCT01143402. This two-pronged approach uses a chemotherapeutic agent, temozolomide, to kill tumour cells and targeted therapy, AZD6244, to prevent tumour cell growth (Lima, Schoenfield et al. 2011, www.clinicaltrials.gov 2013).

There are some ongoing phase II clinical trials which are testing the use of targeted therapies for the treatment of metastatic uveal melanoma. The anti-angiogenic monoclonal antibody, Bevacizumab, which targets vascular endothelial growth factor (VEGF), has been tested as a treatment for choroidal melanoma as VEGF levels have been noted to be elevated in choroidal melanoma; however it was found that the drug did not halt tumour progression but in fact masked its presence thus delaying appropriate diagnosis (Lima, Schoenfield et al. 2011). Bevacizumab was

found to be useful in the management of complications due to current therapies, such as in the case of retinopathy following plaque brachytherapy treatment through the reduction of macular oedema. Bevacizumab is currently undergoing clinical trials for intravitreal use in the treatment of large uveal melanoma in the hope that it will significantly reduce tumour size in patients scheduled to undergo enucleation. It is also being used as a combination therapy with temozolomide in the treatment of metastatic ocular melanoma. Ranibizumab, another monoclonal antibody treatment derived from the same mouse monoclonal antibody fragment as bevacizumab, is also being tested in clinical trials in combination with proton beam radiotherapy for its safety and tolerability in the treatment of choroidal melanoma (Lima, Schoenfield et al. 2011).

Various drugs known to be effective in the treatment of cutaneous melanoma have been tested on uveal melanoma with little or no success. Ipilimumab, the monoclonal antibody therapy which targets cytotoxic T-lymphocyte associated-antigen 4 (CTLA-4) in order to block its downregulation of the pathways of T-cell activation and hence induce antitumour effects, has been approved for use in the treatment of advanced cutaneous melanoma as it shows a survival benefit in randomised trials. A limited number of initial trials have been conducted in relation to its use as a therapy for uveal melanoma patients where it was reported to be a well-tolerated treatment with no objective responses (Danielli, Ridolfi et al. 2012). In one study, two out of five patients maintained stable disease following ipilimumab administration. One of these patients was found to have maintained disease control at 11 months following treatment and showed a 10% reduction in tumour mass. The other individual developed progressive disease after 15 months. The response patterns of the patients and tumour kinetics resembled those of cutaneous melanoma following ipilimumab therapy. The other three patients developed progressive disease despite treatment. This early clinical trial indicates that ipilimumab may be used in the future as a therapy for uveal melanoma, however, further tests are now required (Khattak, Fisher et al. 2013).

As shown above, many of the therapies being developed target genetic anomalies as there are currently no protein biomarkers for uveal melanoma. The identification of such proteins could provide a therapeutic target for the treatment of the disease.

1.2.4 Proteomic Analysis of Uveal Melanoma

A limited number of proteomic studies have been performed in relation to uveal melanoma to date. A summary of these studies is illustrated in Table 1.1.

Many studies which have been carried out involve differential protein expression analysis of cell lysates using two-dimensional (2-D) based methods in combination with mass spectrometry (MS). Zuidervaart et al. isolated and compared cell lines derived from a primary tumour and from two liver metastases of a patient, identifying twenty-four differentially expressed proteins using two-dimensional differential gel electrophoresis (2-D DIGE) and MS, most of which were previously correlated with metastasis (Zuidervaart, Hensbergen et al. 2006). Using 2-D gel electrophoresis (2-DE) and MS, Pardo et al. identified MUC18 and HMG-1 in uveal melanoma cell lines and using functional assays, correlated their expression levels with invasion. They also found DJ-1 oncoprotein to be both expressed and secreted by uveal melanoma cell lines as well as being detected in uveal malignant melanoma patient serum and therefore could be used as a potential, non-invasive biomarker (Pardo, Garcia et al. 2006). Wang et al. recently used a combination of stable isotope labelling with amino acids in culture (SILAC) and two-dimensional liquid chromatography tandem mass spectrometry (2-D LC-MS/MS) to assess proteomic changes in 92.1 uveal melanoma cell lines following exposure to radiation. The study illustrated a number of proteins which were associated with cell suspension induced by irradiation, such as those associated with cell cycle regulation, DNA replication, cell growth and senescence. From this they identified the downregulation of S100A11, PHB1, PHB2, and TPI1, and upregulation of HSP-27. However the combination of SILAC and 2-D LC-MS/MS was not conducive to smaller, lower abundant proteins as they were often masked by more numerous, high abundant proteins (Wang, Bing et al. 2013). Yan et al. also combined SILAC and MS/MS for the analysis of irradiated uveal melanoma cell lines and identified 29 proteins which correlated with cell survival, cell cycle arrest and growth inhibition (Yan, Shi et al. 2013).

Although cell culture-based studies are a useful method for initial proteomic analysis and may identify markers of disease, these markers may not always occur in the same pattern as they would in their natural biological setting. Therefore, pure cell culture-based studies do not consistently bear an accurate representation of the

disease. Using uveal melanoma cell lines; UM-A, SP6.5, UW-1, 92.1, OCM-1, and one-dimensional (1-D) electrophoresis combined with MS, Pardo et al. identified a number of secreted proteins. From this, they used autoantibodies to verify 15 secreted proteins which induced a humoral response in the serum of cancer patients. Using 2-D DIGE, 61 differentially-expressed proteins were found between control and uveal melanoma sample sets, with 38 of these being identified. However, none of the secreted proteins were found in this analysis (Pardo, Garcia et al. 2006). It may be useful to follow-up clinical specimen research, such as in serum, tissue or vitreous fluid, with cell culture studies, thereby identifying a potential target by one method and validating it by the other.

Therefore, a number of studies have used clinical specimens for the discovery of biomarker in uveal melanoma. Coupland et al. examined primary uveal melanoma tumour tissue from monosomy three and disomy three specimens using 2-D gel electrophoresis and western blot validation for the identification of heat shock protein 27 (HSP-27), vimentin, and pyruvate dehydrogenase beta (PDHB) as being differentially expressed between the sample sets. They correlated the downregulation of HSP-27 expression with monosomy three status and hence, metastatic mortality (Coupland, Vorum et al. 2010). Our group also conducted a proteomic analysis of primary tumour tissue looking at the differential expression of proteins between primary tumours which subsequently metastasised and those which did not. From this study, we identified triosephosphate isomerase (TPI1) and fatty acid binding protein 3 (FABP3) to be upregulated in those which metastasised, and showed that they played a vital role in the invasion and migration of uveal melanoma cells (Linge, Kennedy et al. 2012). The results of this work are outlined in chapter three.

A small number of proteins have been suggested as potential biomarkers for uveal melanoma but to-date none have been followed-up in a clinical setting or as a potential target VEGF has been identified as a potential marker of disease progression and metastasis in uveal melanoma as it was found to be significantly overexpressed in primary tumour tissue, and in serum following the development of secondary neoplasms, in both murine models and patient samples (Notting, Missotten et al. 2006, Barak, Pe'er et al. 2011, Crosby, Yang et al. 2011). Correlations between VEGF, C-X-C motif chemokine receptor 4 (CXCR4) and its

ligand, C-X-C chemokine ligand 12 (CXCL12) have also been noted. The cross-talk between these three proteins insinuates a role in uveal melanoma metastasis (Franco, Botti et al. 2010). As malignant cells are CXCR4-positive and solely bind to CXCL12, this mono-axis has been implicated in guiding cells to specific CXCL12-producing organs, such as the liver. In addition to this, inhibition of the axis has been shown to repress the metastatic process (Bakalian, Marshall et al. 2008). Coupland et al. illustrated that cyclin D1, as determined by immunohistochemical analysis of 95 enucleated eyes, is a marker for aggressive uveal melanoma (Coupland, Anastassiou et al. 2000). Lack of IGF-1 expression has been associated with uveal melanoma metastasis and was examined by Frenkel et al. when serum from healthy, disease-free subjects, and metastatic uveal melanoma patients serum was compared using enzyme-linked immunosorbent assays (ELISA). The study illustrated that IGF-1 levels decrease along the progression to metastasis with the highest expression of IGF-1 being associated with healthy serum and the lowest with metastatic melanoma (Frenkel, Zloto et al. 2013). They postulated that this may be due to the fact that IGF-1R has been reported to be highly overexpressed in liver metastases and as the secondary tumour grows, more IGF-1, which is produced in the liver, binds. Therefore, once IGF-1 binds to its receptor, less circulating ligand is available. It has also been suggested that IGF-1R may have a chemoattractant role in establishing liver metastases. This implies that IGF-1 could be used as a predictive biomarker for liver metastases in uveal melanoma, when continuously measured (Economou, Andersson et al. 2008, Frenkel, Zloto et al. 2013). Other protein expression patterns have been implicated with preferential spread of uveal melanoma to the liver such as the down-regulation of hepatocyte growth factor (HGF) and up-regulation of c-MET, its receptor. This may be a similar scenario to IGF-1/IGF-1R but research suggests that IGF-1R has a more significant prognostic value than that of c-MET (Mallikarjuna, Pushparaj et al. 2007, Bakalian, Marshall et al. 2008, Abdel-Rahman, Boru et al. 2010).

The identification of proteins which indicate the prognosis of a tumour could improve our understanding of the biology of the metastatic disease, and could possibly lead to the discovery of a therapeutic target against which a rational therapy may be designed. Biomarkers, in conjunction with genetic information, may also help in a clinical setting when monitoring patients who are at risk of metastasis.

However, the search for potential targets is hindered by the relatively small sample numbers available for study, due to the rarity of the disease. Larger studies are needed to improve the statistical power of biomarker identification and validation in uveal melanoma. The uveal melanoma tumour tissue acquired is often a very small specimen, which also limits proteomic research.

Author	Study Type	Principal Findings
(Janssen, Kuntze et al. 1996)	Immunohistochemistry analysis of primary tissues	Upregulation of p53 in choroidal melanoma
(Martins, Scull et al. 1997)	Differential proteomics of primary tissues	Upregulation of HMB-45 in uveal melanoma
(Chowers, Folberg et al. 2002)	Differential proteomics of primary tissues	p53 correlated with high proliferation and epithelioid cell type
(Pardo, Garcia et al. 2005)	Global proteome of UM cell line	683 proteins, 96% of which were novel in uveal melanoma
(Pardo, Garcia et al. 2006)	Differential proteomics of UM cell lines	Upregulation of DJ-1, HMG-1 and MUC18 in aggressive UM
(Pardo, Garcia et al. 2007)	Global secretome of 5 UM cell lines	Cathepsin D, gp100 and syntenin-1
(Zuidervaart, Hensbergen et al. 2006)	Differential proteomics of UM cell lines derived from primary and metastatic tumours	Upregulation of HSP-27, αB-crystallin and cofilin in metastatic cell line
(Coupland, Vorum et al. 2010)	Differential proteomics of primary tissues	Downregulation of HSP-27 in monosomy three UM tumours
(Bande, Santiago et al. 2012)	Differential proteomics of serum	Upregulation of serum DJ-1 assoociated with transformation of choroidal nevi
(Linge, Kennedy et al. 2012)	Differential proteomics of primary tissues	Upregulation of FABP3 and TPI1 in aggressive primary UM tumours
(Wang, Bing et al. 2013)	Differential proteomics of irradiated UM cell line	Downregulation of S100A11, PHB1, PHB2,TPI1 and upregulation of HSP-27 in irradiated cells.
(Yan, Shi et al. 2013)	Differential proteomics of irradiated UM cell line	Downregulation of PKFM and upregulation LDHB in irradiated cells.

Table 1.1 Summary of all uveal melanoma proteomic studies carried out to-date.

1.3 Vitreous Fluid

Vitreous humour is a hydrogel-like substance which makes up approximately 80% of the eyeball volume (Grus, Joachim et al. 2007). The vitreous can be a useful tool for analysing pathophysiological events which take place within the orbit of the eye, such as in the case of diabetic retinopathy, and may contain valuable proteomic information (Simo-Servat, Hernandez et al. 2012). In recent years, ocular fluids have been more frequently examined on a proteomic-level. This is mainly due to

advances in protein analysis in areas such as MS, which measures the mass to charge ratio of a molecule, and multiplexing methods. Such advances allow us to better understand major ocular diseases, such as diabetic retinopathy, as they can be associated with pathological concentrations of many proteins within the aqueous and vitreous humour (Pollreisz, Funk et al. 2013).

1.3.1 Vitreous Fluid Sample Preparation

There are many challenges in using vitreous fluid for proteomic analysis, such as contaminating the specimen by rupturing of the blood retina barrier (BRB) or varying protein concentration of samples. The BRB can easily be damaged during sample collection or rupture as a side-effect of the disease and would result in an influx of serum proteins such as serum albumin, therefore contaminating the specimen with other biological fluids (Simo-Servat, Hernandez et al. 2012). Vitreous humour can vary in its protein concentration between control and disease specimens, see Figure 1.2, but also within groups of samples from the same condition (Shitama, Hayashi et al. 2008). In addition to the above, the volume of sample acquired can often also be low, which can hinder experiments requiring a significant protein concentration.

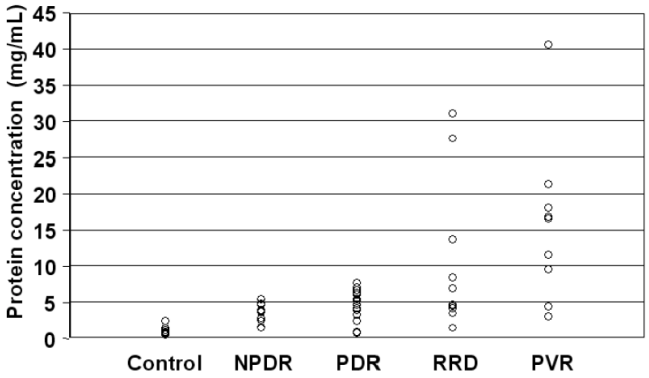

Figure 1.2 Illustration of the variation in protein concentration between control (collected from patients with benign disease or from a healthy post-mortem donor) vitreous and vitreous samples taken from patients with various forms of retinopathy; Non-proliferative diabetic retinopathy (NPDR), Proliferative diabetic retinopathy

(PDR), Rhegmatogenous retinal detachment (RRD), Proliferative vitreoretinopathy (PVR) (Shitama, Hayashi et al. 2008).

Typically, the proteomics workflow of vitreous humour analysis is a multi-step process. It begins with appropriate collection of approximately 1-3 mL of fluid, depending on the underlying condition. Any haemorrhaging must be taken into account during collection as this can affect later analysis. The preservation of the biological nature of the specimen is of paramount importance and hence it must be protected against proteolytic degradation, preferably by snap freezing and storage at -80°C. The high viscosity of vitreous samples can hinder sample manipulation, for example during pipetting, hence it is necessary to centrifuge the samples at high-speed prior to experimental use (Angi, Kalirai et al. 2012).

Vitreous from patients with macular hole or macular epiretinal membrane are often used as controls as vitreous fluid cannot be collected from healthy eyes. Ocular fluid can only be collected during surgery, such as vitrectomy, or enucleation (Grus, Joachim et al. 2007, Wang, Feng et al. 2012).

The gel-like consistency of the fluid is mainly due to the hydrated network of fibular macro-molecules, such as proteoglycans and collagen fibrils, however the majority of vitreous fluid is composed of high abundance proteins such as albumin, immunoglobulin G (IgG) and apolipoproteins. Hence, it is similar to serum in composition (Feener 2012). Therefore, the viscosity and proteomic nature of vitreous make sample pre-treatment a necessary step (Thierauf, Musshoff et al. 2009).

Pre-treatment, such as immunoaffinity subtraction (Section 1.6.1) can be used in order to promote the detection of less abundant proteins in later experiments (Pollreisz, Funk et al. 2013). Immunodepletion may involve removing one or more prominent high molecular weight proteins and is compatible with all downstream applications, but it has been shown to produce the best spectrum of results when used with LC-MS/MS (Smith, Wood et al. 2011). However, it is also possible that by removing many of the high abundance proteins, the protein concentration will be severely decreased and thus inadequate for research. Kim et al. speculated that this could be due to the fact that the majority of the vitreous fluid proteome is composed of high abundance proteins, to which low abundance proteins may be bound. Hence,

some low abundance proteins can be removed along with the depleted proteins (Kim, Kim et al. 2007). ProteoMiner, a protein equalising technology, allows for the simultaneous depletion of high abundance proteins and concentration of low abundance proteins may be a better option (Section 1.6.1).

1.3.2 Proteomic Fractionation and Analysis of Vitreous Fluid

Despite pre-treating vitreous specimens, due to the complexity of the proteome, further fractionation is often required in order to gain a comprehensive view of all proteins in the specimen, particularly low abundant proteins. This may be done using protein fractionation methods which separate all proteins present and hence allow access to the entire proteome. Following this, the entire proteome would be digested into peptides, which are then fractionated and identified by MS. This is known as "shotgun proteomics" and is useful for gaining quantitative information (Angi, Kalirai et al. 2012).

1-D electrophoresis can be used as a basic fractionation method whereby proteins are separated based on their size. 2-D electrophoresis is a useful gel-based method for separating proteins based on both their mass and charge through the combination of sodium dodecyl sulphate-polyacrylamide gel electrophoresis (SDS-PAGE) and isoelectric focusing to generate a "spot map" of proteins of interest. This technique is described in more detail in section 1.6.3. Protein gels are visualised using staining methods such as fluorescent dyes which have high a dynamic range and sensitivity, e.g. SYPRO Ruby, or a global protein stain such as colloidal silver stain or Coomassie Brilliant Blue. Stained protein spots can then be excised from the gel and directly compared to those of another gel in the same region for their protein content following peptide fractionation and identification. Using vitreous fluid, Ouchi et al. identified 6 proteins as being differentially regulated between patients with and without diabetic macular oedema (DMO) using 2-D electrophoresis and optical density analysis of protein spots (Ouchi, West et al. 2005). 2-D DIGE (2-Dimensional Difference Gel Electrophoresis), is one of the most sensitive staining methods available for 2-D electrophoresis, and continues to be the method of choice for differential protein expression analysis in vitreous fluid (Kim, Kim et al. 2007, Wang, Feng et al. 2012, Hernandez, Garcia-Ramirez et al. 2013). Using DIGE,

Hernandez et al. identified four proteins as being exclusively associated with DMO, when 8 control vitreous were compared to 8 DMO vitreous; four with proliferative diabetic retinopathy (PDR) and four without. All targets were subsequently validated using ELISA. They concluded that DIGE proved to be an accurate method for making quantitative comparisons and allowed for the identification of new candidates in DMO pathogenesis (Hernandez, Garcia-Ramirez et al. 2013).

Proteins of interest are ultimately identified using MS. This process is described in more detail in section 1.6.4. In terms of vitreous fluid analysis, Kim et al. utilised both 2-D electrophoresis and LC-MS/MS for the analysis of the same vitreous fluid sample set and identified 49 and 531 proteins, respectively. This illustrates the power of new proteomics technologies and how the quality of results generated from a sample may be dependent in the technology used (Kim, Kim et al. 2007, Angi, Kalirai et al. 2012). Quantitative label-free proteomics is also being more commonly used for vitreous fluid analysis. Hauck et al. used quantitative LC-MS/MS in combination with pathway analysis for the identification of two proteins which led to the discovery of retinal Müeller glial cells involved in autoimmune triggers of uveitis (Hauck, Hofmaier et al. 2012). 1-D SDS-PAGE has also proved useful when utilised in conjunction with reverse-phase LC-MS/MS. Yu et al. used both techniques for the characterisation of the vitreous proteome in rhegmatogenous retinal detatchment (RRD) patients with Proliferative vitreoretinopathy (PVR) and identified 516 proteins. (Yu, Peng et al. 2012).

1.3.3 Clinical Significance of Analysis of the Vitreous Fluid Proteome

Variations in protein composition occur within the vitreous. For example, in the proximity of the cortex, collagen isoforms are significantly more concentrated than in the central vitreous. Such extracellular matrix proteins provide a framework for the binding of molecules and soluble proteins, hence influencing biochemical transport within the eye. This compartmentalisation of proteins also suggests that soluble proteins are heterogeneously distributed within the fluid. This extracellular network allows for the diffusion of proteins between the vitreous and its surrounding tissues, such as the retina and it is in this regard that the vitreous can be seen as a hub of biochemical indicators representative of the surrounding environment since it

is directly impacted by ongoing disease related events (Feener 2012). Therefore, the vitreous is most interesting to analyse when it is close to the site of damage or disease, for example in the case of uveal melanoma or DMO (Grus, Joachim et al. 2007).

Proteins relating to both proliferative and non-proliferative diabetic retinopathy have been studied in the vitreous. Diabetic retinopathy is a progressive disease caused by chronic exposure to hyperglycaemia and is the main cause of vision loss in adults in the developed world. Many proteomic studies have been carried out in the vitreous for the development of a therapeutic target. The disease can be divided into proliferative and non-proliferative retinopathy, depending on the stage of disease. In addition to this, DMO can occur which involves the breakdown of the BRB, hence leading to visual impairment (Ouchi, West et al. 2005, Wang, Feng et al. 2013). Wang et al. used reverse-phase HPLC coupled to ESI-MS/MS for the quantitative analysis of the vitreous proteome in PDR patients. They identified 96 proteins which were differentially expressed between PDR and control vitreous, with many of these proteins being correlated to pathways such as glycolysis/gluconeogenesis and complement and coagulation cascades. Using label-free quantification proteomics methods, they identified a total of 62 proteins which were not yet associated with PDR (Wang, Feng et al. 2013). Other studies attempting to understand the basis of PDR and DMO through the proteomic analysis of the vitreous have also recently been carried out; with MS-based methods being used more frequently (Gao, Chen et al. 2008, Hernandez, Garcia-Ramirez et al. 2010). In spite of this, 2-D electrophoresis methods are still relevant and are commonly used (Garcia-Ramirez, Canals et al. 2007, Wang, Feng et al. 2012).

Uveitis is an inflammatory disease of the uveal tract which is poorly understood and, as there is no therapy available, can lead to loss of vision (Turgut, Gul et al. 2013). Proteomic analysis of the vitreous fluid has been carried out in equine models in order to better understand the disease in both horses and humans. Using label-free LC-MS/MS quantification followed by pathway analysis, they identified a number of human and equine shared auto-antigens, including cellular retinaldehyde-binding protein (CRALBP), involved in autoimmune uveitis and found that the Wnt signal transduction pathway was highly involved in pathogenesis of uveitis (Hauck, Hofmaier et al. 2012). Turgut et al. used ELISA for the analysis of potential uveitis

treatments using vitreous fluid, identifying IL-1, IL-6 and TNF-α as all being upregulated in murine uveitis models despite treatment with gherlin (Turgut, Gul et al. 2013).

1.4 Cutaneous Melanoma

Cutaneous melanoma is a cancer which affects skin melanocytes. Despite accounting for only 4% of all skin cancer cases, it is the form of skin cancer which has the highest death toll in the USA and Europe (Ugurel, Utikal et al. 2009). The rate of incidence of melanoma is rising; in stark contrast to many other cancers. In the USA in 1935, the lifetime risk of developing the cancer was 1 in 1,500. It has now risen to 1 in 68, despite improved patient awareness and better surveillance (Balch, Buzaid et al. 2001, Siegel, Naishadham et al. 2013). However, melanoma has been traditionally known as being difficult to treat, mainly due to the large number of patients who are resistant to immune therapy as well as chemotherapy (Mehnert and Kluger 2012). In addition to this, malignant melanoma often exhibits unpredictable behaviour. For example, many patients with significant vertical growth remain metastasis-free while some patients with thin die as a result of their disease (Torabian and Kashani-Sabet 2005). Therefore, a more thorough understanding of the pathways of cutaneous melanoma is critical for the development of predictive biomarkers.

1.4.1 Cutaneous Melanoma Staging

Primary cutaneous melanomas are characterised by horizontal growth within the epidermis only. However, the malignancies can become more aggressive which leads to rapid growth and invasion of the dermis. Later stages of the disease are associated with rapid invasion and metastasis of tissues other than the dermis. When melanoma is detected and treated prior to the development of lymph node metastasis, the five-year survival rate is 99%, however, the five-year survival rate for distant stage melanoma patients is approximately 15% (Al-Ghoul, Bruck et al. 2008).

Cutaneous melanoma is staged by the TNM system devised by the American Joint Committee on Cancer (AJCC). This determines how widespread the cancer is by taking into account the status of three main criteria; tumour, lymph nodes, and metastasis (TNM) using both clinical staging and pathologic staining.

The tumour category (T) is defined by thickness, ulceration and mitotic rate. Using Breslow measurement, the thickness of a melanoma is determined. The extensiveness of tumour infiltration is defined by a number ranging from 0 to 4 and ulceration and mitotic rate, i.e. the rate of cell proliferation, defined by a letter; a or b. Melanomas which have a higher mitotic rate and are ulcerated tend to have a poorer prognosis. (Balch, Gershenwald et al. 2009, http://www.cancer.org/ 2013).

Lymph node (N) involvement is decided by spread of the malignancy to nearby nodes or lymphatic channels attached and is designated a number from 0 to 3, depending on the degree of melanoma spread in the lymphatic system. As sentinal lymph node biopsies are now considered to be necessary for the staging of microscopic nodal metastases, a letter, a, b, or c, which is based on pathological staining of lymph node tissue can also be assigned. This spread may also be macroscopic or simply composed of satellite tumours which are close to but have not yet reached the lymph nodes (Balch, Gershenwald et al. 2009).

Finally, the M category is defined by spread, or metastasis, of the cancer to distant organs and blood levels of lactate dehydrogenase (LDH) found in such organs. Levels of LDH are now taken into account as a prognostic value for stage IV patients. Indeed, LDH measurements now appear to act as an independent and significant indicator of survival outcome in advanced stage patients. This is further discussed in section 1.4.3. Unfortunately, melanoma can spread to virtually any site in the body which can make detection and diagnosis of metastases both time-consuming and challenging. It most commonly spreads to regions such as the lungs, abdomen, pelvis and the brain (Davies, Liu et al. 2011, Kedinger, Meulle et al. 2013, Trout, Rabinowitz et al. 2013). The spread of melanoma to the brain is often most indicative of poor outcome as 54% of all melanoma deaths are due to the presence of brain metastases (Davies, Liu et al. 2011).

The result from each category is then combined to give an overall TNM stage (Table 1.2).

	Clinical Staging				Pathological Staging		
	T	N	M		T	N	M
0	Tis	N0	M0	0	Tis	N0	M0
IA	T1a	N0	M0	IA	T1a	N0	M0
IB	T1b	N0	M0	IB	T1b	N0	M0
	T2a	N0	M0		T2a	N0	M0
IIA	T2b	N0	M0	IIA	T2b	N0	M0
	T3a	N0	M0		T3a	N0	M0
IIB	T3b	N0	M0	IIB	T3b	N0	M0
	T4a	N0	M0		T4a	N0	M0
IIC	T4b	N0	M0	IIC	T4b	N0	M0
III	Any T	N > N0	M0	IIIA	T1-4a	N1a	M0
					T1-4a	N2a	M0
				IIIB	T1-4b	N1a	M0
					T1-4b	N2a	M0
					T1-4a	N1b	M0
					T1-4a	N2b	M0
					T1-4a	N2c	M0
				IIIC	T1-4b	N1b	M0
					T1-4b	N2b	M0
					T1-4b	N2c	M0
					Any T	N3	M0
IV	Any T	Any N	M1	IV	Any T	Any N	M1

Table 1.2 Anatomic Stage Groupings for Cutaneous Melanoma. As adapted from Balch, Gershenwald et al. 2009.

1.4.2 Pathogenesis of Cutaneous Melanoma

Many genetic studies have been carried out on malignant melanoma. Some of the best characterised mutations and epigenetic changes have involved the receptor tyrosine kinase (RTK) pathway.

V-raf murine sarcoma viral oncogene homolog B1 (*BRAF*) was the first commonly occurring somatic mutation identified in cutaneous melanoma (Davies, Bignell et al. 2002). *BRAF* is a cytoplasmic serine/threonine kinase of the RAS-RAF-MEK-ERK-

MAP kinase pathway, a cascade which is responsible for cellular responses to growth signalling. RAS is responsible for the regulation of *BRAF* however, in approximately 15% of cancers RAS is mutated into an oncogenic form. 66% of melanomas contain a single mutation, valine is substituted for glutamic acid at position 600, associated with *BRAF*. When $BRAF^{V600E}$ is expressed in melanoma cell lines, the MAPK pathway is hyperstimulated which leads to malignant cellular transformation (Davies, Bignell et al. 2002, Jakob, Bassett et al. 2012, Mehnert and Kluger 2012). It has been illustrated that *BRAF* mutations more commonly develop in skin which is intermittently exposed to sun exposure than in unexposed regions such as palms, soles and mucosal membranes. It has also been found that such mutations do not occur in melanomas on chronically sun-damaged skin (Maldonado, Fridlyand et al. 2003). *BRAF* mutations appear to occur early on in the development of melanoma as benign nevi contain a high number of such mutations. Both early stage melanocytic lesions and metastatic lesions also seem to harbour a similar number of *BRAF* mutations (Mehnert and Kluger 2012). It is also notable that patients treated with *BRAF* inhibitors had a better prognosis than those who were not, indicating the significance of *BRAF* activation throughout the disease, despite its mutation being an early event (Davies, Liu et al. 2011).

Neuroblastoma RAS viral (v-ras) oncogene homolog (*NRAS*) is a member of the RAS family which includes *HRAS* and *KRAS*, and is central to the development of the malignant phenotype. *NRAS* codes for a guanine triphosphate (GTP)-binding protein and once mutated can constitutively activate the downstream RAS-RAF-MEK-MAPK pathway via exclusive point mutations found primarily on codon 61, but also on codon 12 and 13. *NRAS* is mutated in 15-20% of melanomas, making it the second most commonly mutated gene in cutaneous melanoma (Aguissa-Toure and Li 2012, Jakob, Bassett et al. 2012, Posch and Ortiz-Urda 2013). Interestingly, most melanomas have either a $BRAF^{V600E}$ or an *NRAS* mutation but not both (Banerji, Affolter et al. 2008, Jakob, Bassett et al. 2012). It has been found that the incidence of either *BRAF* or *NRAS* may be due to differences in histological type and tumour site, based on the extent of sun exposure. *BRAF* mutations typically occur in patients with superficial spreading melanoma, in skin which has not been chronically sun damaged. In contrast, *NRAS* mutations are found in patients with nodular melanoma and have been correlated to continuous ultraviolet (UV) light exposure as

it is suggested that sunlight acts as a mutagenic agent in the development of *NRAS* anomalies (van 't Veer, Burgering et al. 1989, Lee, Choi et al. 2011). *NRAS* mutations are associated with a higher rate of metastasis to the central nervous system (CNS) in comparison to the wild type counterpart and have been identified as a potential, independent indicator of poor prognosis following diagnosis of advanced melanoma (Jakob, Bassett et al. 2012).

PTEN is one of the most commonly inactivated tumour suppressor genes in sporadic cancers and has been detected in a wide spectrum of cancers including, breast, thyroid and prostate. It occurs at a frequency of 30-40% in melanoma cell lines and at 10% in primary melanomas. PTEN protein has both lipid and protein phosphatase activity and is necessary for cell-cycle regulation (Aguissa-Toure and Li 2012). It has also been suggested that it may inhibit tumorgenicity and metastasis through the regulation of matrix metalloproteases (MMP), insulin-like growth factor (IGF) and VEGF expression (Hwang, Yi et al. 2001). Loss of PTEN function results in aberrant cell growth, uncontrolled migration and lack of apoptosis. It appears to explain many phenotypic hallmarks of melanoma, although, *PTEN* mutation is also associated with other genetic changes which clouds our understanding of its role. Loss of function of *PTEN* occurs later on in melanoma progression but may be implicated in early-stage tumorigenesis (Palmieri, Capone et al. 2009, Aguissa-Toure and Li 2012). In addition to this, mutations of *PTEN* are often linked with other melanoma-associated mutated genes, such as Cyclin-Dependent Kinase Inhibitor 2A (*CDKN2A*) and *BRAF*; loss of *CDKN2A* may work in cooperation with *PTEN* in relation to tumorigenesis, and *PTEN* is involved in the inhibition of growth-factor stimulated MAPK signalling which can cause a knock-on effect on the BRAF-MAPK pathway (Palmieri, Capone et al. 2009).

CDKN2A has been found to be mutated in a variety of cancers, including familial melanoma where germline mutations occur. The gene, which is located on chromosome 9p21, encodes for p14 and p16. p14 has an anti-proliferative function through the regulation of the cell cycle at G1/G2 transition stage. p16 is a cyclin-dependent kinase inhibitor necessary in the regulation of G1/S phase through the inhibition of cyclin-dependent kinase D (CDK). Mutated p16 is unable to interact with CDK4, thus preventing the regulation of cell cycle arrest, allowing for the uncontrolled progression through the cell cycle and aiding in the development of

neoplastic transformation. *CDKN2A* is frequently mutated or deleted in tumour cells, which suggests the role of p16 as a tumour suppressor (Mehnert and Kluger 2012, Szponar-Bojda, Pietrzak et al. 2012). Familial melanoma as a result of *CDK4* germline mutations has been observed, which is associated with the subsequent development of additional malignancies such as pancreatic cancer (Goldstein, Struewing et al. 2000). Sporadic melanoma has also occurred as a result of somatic mutations in *p16* and *CDK4* (Gast, Scherer et al. 2010).

Chromosomal aberrations are found throughout melanoma, each of which are often correlated with a particular outcome due to the associated genes present on each chromosome. LOH has been reported at frequency of 47% in chromosome arm 9p and is known to occur prior to the loss of other chromosome arms. LOH of chromosome regions 3p, 6q, 10q, 11q, and 17p have also been described as regularly occurring. Of these LOH of 6q, 11q and 17 p are associated with invasiveness (Healy, Rehman et al. 1995).

Fountain et al. were the first to convincingly associate aberrations of chromosome 10 with melanoma (Fountain, Bale et al. 1990). Both chromosomes 9 and 10 have been found to be most interesting, despite other chromosomes being more regularly altered, due to their singularity in early irregularities and dysplastic lesions. LOH of chromosome 10q in particular has been commonly identified as a feature of melanoma as it is found to occur at a frequency of 30-50%. Due to the presence of a number of tumour suppressor genes on chromosome 10q, such as *PTEN*, its loss is associated with tumour progression (Herbst, Weiss et al. 1994, Aguissa-Toure and Li 2012).

1.4.3 Current Protein Biomarkers for Cutaneous Melanoma

To date, few protein biomarkers have been identified as prognostic indicators of cutaneous melanoma and even less are used in the clinic as tools for diagnosis or prognosis.

LDH has been extensively studied in melanoma patient serum for nearly 60 years. It has been identified as an initial marker of disease recurrence in 12.5% of stage II patients, and has shown sensitivity and specificity values of 72% and 97%. In

relation to liver metastases, it was found to have sensitivity and specificity of 95% and 82% in the stage II group and 86% and 57% in the stage III group (Finck, Giuliano et al. 1983). Serum LDH has also been associated with the presence of extra- and intracranial metastases and the overall survival as a result of such (Partl, Richtig et al. 2013). In addition to this, elevated LDH has been reported to be associated with decreased survival, regardless of the presence or absence of liver metastases (Finck, Giuliano et al. 1983). Due to the strong correlation between increased serum LDH concentration and diminished survival following multivariate analysis, the AJCC has decided to include LDH in its cutaneous melanoma staging system as a factor used to delineate the M categories into three groups (Balch, Buzaid et al. 2001).

S100 calcium binding protein B (S100B) is a calcium-binding protein, which was first described in melanoma cell cultures and is now a well-used marker for pigmented lesions of the skin (Gogas, Eggermont et al. 2009). Despite extensive research, the function of S100B is not yet fully understood. As it is known to interact with the p53 tumour suppressor gene, it is thought that it may have a prominent role in cutaneous melanoma pathogenesis (Vereecken, Cornelis et al. 2012). It is highly abundant in neuronal tissue and can be measured in the cerebrospinal fluid (CSF) or the blood; for example, it is found to be elevated in the blood following brain trauma (Astrand, Unden et al. 2013). S100B is also significantly overexpressed in malignant melanoma serum (Astrand, Unden et al. 2013). The clinical significance of S100B in monitoring and staging was first identified when its levels in serum were directly proportional to disease progression. As well as this, a decline in S100B expression correlated with response to treatment (Guo, Stoffel-Wagner et al. 1995). Other such studies have reaffirmed this observation, describing S100B as an indicator of poor prognosis and in some cases, as an indicator of metastasis (Zissimopoulos, Karpouzis et al. 2006, Mocellin, Zavagno et al. 2008). Serum S100B protein has been shown to be more effective than LDH in predicting prognosis and response to treatment for patients with advanced melanoma and it has been suggested that it should be used as part of the AJCC staging system (Torabian and Kashani-Sabet 2005, Egberts, Pollex et al. 2008). In fact, Switzerland and Germany both recommend measuring serum S100B every 3-6 months in patients with a tumour thickness of less than 1 mm (Gogas, Eggermont et al. 2009). Despite its

effectiveness as an advanced stage marker of prognosis, S100B has been found to be limited in its determination of prognosis in early stages, i.e. stages I and II. Also, S100B is not melanoma specific and can be over-expressed in other disorders such as AIDS, non-melanoma skin cancer, liver and renal injury, central nervous system cancers and various inflammatory conditions (Peric, Zagar et al. 2011, Vereecken, Cornelis et al. 2012).

Melanoma inhibitory activity (MIA) is a low-molecular weight autocrine growth inhibitor which has multiple roles including regulation of cell growth and cell adhesion (Vereecken, Cornelis et al. 2012). It was initially found to be over-expressed in malignant melanoma cells *in vitro* but not in benign skin melanocytes or benign melanocytic nevi. In malignant tumour tissue, MIA messenger RNA (mRNA) was detected at elevated levels in 100% of malignant melanoma samples, and when compared to normal skin, benign human skin melanocytes, benign melanocytic nevi, and malignant melanomas, MIA mRNA levels mirrored the progressive malignancy of the lesions (Bosserhoff, Kaufmann et al. 1997). The comparison of early stage patient sera to advanced stage sera, illustrated that MIA was up-regulated in 13% and 23% of stage I and II patients, respectively, in comparison to 100% of those with stage III and IV disease. Any patients who expressed MIA at a normal level did not develop metastases in the follow-up period of 6-12 months (Bosserhoff, Kaufmann et al. 1997). Other studies have correlated MIA with the development of metastases and suggest that it could be useful as a serum marker for the detection of secondary malignancies (Stahlecker, Gauger et al. 2000). Despite this, MIA has been described as a less reliable tumour marker in comparison to S100B or S100B in combination with LDH (Krahn, Kaskel et al. 2001). It has also been suggested that MIA, when added to combinations of other markers, does not improve the overall efficacy of stage III – IV detection (Garnier, Letellier et al. 2007).

Better prognostic and predictive markers in cutaneous melanoma are sorely needed, but to date have been elusive. The experimental work detailed here was intended to further understand the cutaneous melanoma serum proteome over the course of disease progression. Therefore, this work could lead to the development of a prognostic test which could easily be used in a clinical setting and could also potentially lead to the discovery of a therapeutic target in cutaneous melanoma.

1.4.4 Clinical Treatment Options for Cutaneous Melanoma

Prior to 2011, the treatment options for metastatic melanoma were limited; chemotherapy and high-dose interleukin-2 (HDIL-2) were the only approved options (Burgeiro, Mollinedo et al. 2013). Due to the high rate of resistance to such treatment, the efficacy of chemotherapy was poor. HDIL-2 was also a limited therapy as most patients were ineligible for treatment due to a high, associated toxicity. As well as this, patient response rates are low. Treatment using other conventional methods, such as radiotherapy and immunotherapy, failed due to significant resistance (Burgeiro, Mollinedo et al. 2013, Salama 2013). In recent years, a number of advances have been made in better understanding immune regulation and driver mutations in melanoma which have driven the development of new therapies which, according to stage III clinical trials, demonstrate an overall survival benefit in metastatic melanoma patients (Salama 2013).

Cytotoxic T-lymphocyte-associated protein 4 (CTLA-4) is a modulator of the immune system whose protein expression is induced through the interaction between a T-cell receptor (TCR) and an antigen. CTLA-4 suppresses T-cell activation by recruiting tyrosine and serine or threonine phosphatases and outcompeting CD28; a co-stimulatory receptor which binds the same ligands in order to induce signalling cascades related to proliferation, cytokine secretion, metabolism and apoptosis (Melero, Hervas-Stubbs et al. 2007). Ipilimumab is a humanised, IgG1 monoclonal antibody which blocks CTLA-4 in order to induce an anti-tumour immune response and reduce tolerance to tumour-associated antigens (Burgeiro, Mollinedo et al. 2013). It has successfully been used in the treatment of other cancers such as ovarian carcinoma and metastatic renal cell cancer (Hodi, Mihm et al. 2003, Yang, Hughes et al. 2007). Ipilimumab was the first therapy to improve overall survival in phase III randomised controlled trials in previously treated metastatic melanoma patients both in combination with experimental vaccine glycoprotein 100 (gp100) and without. It was found that ipilimumab decreased the risk of death by 32-34%, leading to FDA approval in 2011 for unresectable or metastatic melanoma (Hodi, O'Day et al. 2010, Salama 2013). These findings have also been confirmed in untreated patients, regardless of the presence of other prognostic factors such as serum LDH level. In addition to this, the inclusion of dacarbazine in ipilimumab treatment decreased the chance of death by 28% in comparison to chemotherapy alone and improved the

median overall survival by 2.1 months (Robert, Thomas et al. 2011). Recently, chemotherapy in combination with ipilimumab has been tested illustrating that no pharmacokinetic or pharmacodynamic interactions occur between the monoclonal antibody and paclitaxel, dacarbazine, or its metabolite, 5-aminoimidazole-4-carboxamide (Weber, Hamid et al. 2013). As ipilimumab is an antibody, it is unable to cross the blood-brain barrier; however this may not be essential for it to exert anti-tumour effects as it activates T-cells which can migrate into the CNS. A phase II trial has shown that 16.67% and 25% of patients with stable brain metastases who were treated with the agent showed a partial response or stable disease, respectively. The median overall survival of all ipilimumab-treated patients in the study was 14 months. Further to this, a separate trial has taken place which illustrated the efficacy of combining ipilimumab and foretmustine, a chemotherapeutic drug which can penetrate the blood-brain barrier (Murrell and Board 2013).

Programmed death-1 (PD-1), a member of the CD28 family, is an inhibitory co-receptor expressed on antigen-activated T-lymphocytes, on antigen-specific T-lymphocytes chronically exposed to antigen, and on B-lymphocytes. One of its ligands is B7-H1/PD-L1, the predominant mediator of PD-1 immunosuppression. Hence, tumours express PD-L1 as part of a mechanism to evade the immune system (Simeone and Ascierto 2012). The suppression of effector T-cell function through PD-1 interaction has been shown to prevent deletion/apoptosis, inhibition of proliferation, and production of cytokines. In conjunction with chronic antigen exposure, this results in T-cell exhaustion, hence, deeming PD-1 to be a potential target for the augmentation of the immune response (Fong and Small 2008). The anti-PD1 monoclonal antibody, nivolumab, is actively being examined for use as an immune activator; both on its own and in combination with Ipilimumab for enhancing its effectiveness (Gogas, Polyzos et al. 2013).

Vemurafenib is an orally-administered, small molecule inhibitor of the $BRAF^{V600E}$ mutation which has been shown to be highly effective in the treatment of cutaneous melanoma through the inhibition of unregulated cell growth. A phase III randomised clinical trial comparing vemurafenib to dacarbazine illustrated that metastatic melanoma patients treated with vemurafenib alone showed a reduction in the risk of death by 63% and a 74% reduction in the risk of disease progression. Response rates were 48% and 5% for vemurafenib and dacarbazine, respectively (Chapman,

Hauschild et al. 2011). A study is currently ongoing to determine the efficacy of vemurafenib in treating melanoma patients who developed brain metastases (NCT01378975), however preliminary studies suggest that a synergistic combination of vemurafenib with radiation therapy appears to be a favourable method of treatment for brain metastases with a median survival time of 13.7 months observed (Narayana, Mathew et al. 2013, www.clinicaltrials.gov 2013). Up to 50% of patients respond to vemurafenib; however this response generally lasts only 6 months due to the emergence of resistance mechanisms (Coit and Olszanski 2013). Despite the significant success of *BRAF* inhibitor treatment, a subset of patients has been found to develop resistance to the therapy following chronic treatment, despite an initial response. This is likely due to *BRAF* reactivation or number of mutations along the MAPK pathway, which is essential for tumour survival, thus inducing a bypass to *BRAF* inhibition. Villanueva et al. illustrated that upon chronic *BRAF* inhibition, melanoma cells can overcome the therapy by flexibly altering their signalling in order to exploit another RAF isoform, such as *CRAF* or *ARAF*, by an unknown mechanism. It has also been found that persistent *BRAF* inhibition in resistant cells is associated with enhanced IGF-1R and PI3K/AKT activity. Therefore, the targeting of both MEK and IGF-1R/PI3K using drug combinations may be a solution to overcome *BRAF* inhibitor resistance (Villanueva, Vultur et al. 2010).

Dabrafenib is a small molecule inhibitor which also targets the V600E mutation of melanoma, although it works on a more general scale to vemurafenib, targeting both wild-type and mutant *CRAF* and *BRAF*. Data has also suggested that it is effective against the non-V600E *BRAF* mutation; V600 (Denton, Minthorn et al. 2013, Medina, Amaria et al. 2013). In a recent stage III clinical trial, dabrafenib-treated patients reached a median progression-free survival of 5.1 months with an overall response rate of 50%, in comparison to dacarbazine-treated patients who reached 2.7 months with an overall response rate of 6% (Huang, Karsy et al. 2013). However, the therapeutic use of dabrafenib has been associated with the development of squamous cell carcinoma (SCC) due to an upregulation of the MAPK pathway as a consequence of increased phosphorylated ERK in wild-type *BRAF* cells. Therefore, the use of dabrafenib in combination with a MEK inhibitor, such as trametinib, has been tested by King at al. They found that the two-pronged approach reduced the

occurrence of skin lesions in rats and enhanced the inhibition of tumour growth in human melanoma xenograft studies in mice. Clinical trials to test the combination therapy in melanoma patients are currently ongoing, however, data from a phase 1/2 trial have illustrated an improvement in progression-free survival and a non-significant reduction in the occurrence of skin lesions (King, Arnone et al. 2013).

A summary of the targeted therapies for cutaneous melanoma mentioned above are shown in Table 1.3.

Treatment	Target	Mechanism
Ipilimumab	CTLA-4	Blocks CTLA-4 in order to induce an anti-tumour response
Nivolumab	PD-1	Suppression of PD-1 expression in order to activate the immune system
Vemurafenib	$BRAF^{V600E}$	Inhibits hyperstimulation of the MAPK pathway in order to halt unregulated cell growth
Dabrafenib	$CRAF/CRAF^{V600E}$, $BRAF/BRAF^{V600E}$	Inhibits hyperstimulation of the MAPK pathway in order to halt unregulated cell growth

Table 1.3 Summary of the most promising targeted therapies used in the systemic treatment of cutaneous melanoma.

1.5 Comparing the Molecular Basis of Uveal and Cutaneous Melanomas

Although cutaneous and uveal melanomas are of a similar embryonic origin, they notably differ in behaviour such as tumorigenesis, metastatic spread and therapeutic response. The differences between both melanomas are poorly understood, albeit, it is hoped that genetic and proteomic analyses of the nature of melanoma as a disease will aid us in understanding variations between both melanomas.

Chromosomal aberrations transpire differently in both melanomas. Most frequently in uveal melanoma, loss of one or two copies of chromosome three occurs or the gain of chromosome 8q, however both anomalies can arise together. Monosomy three also occurs at a rate of 50% in uveal melanoma, but is rarely found in cutaneous melanoma (Hoglund, Gisselsson et al. 2004). Other modifications have been reported in uveal melanoma in relation to chromosome 1p36 where loss can occur in combination with monosomy three. This appears to indicate a poorer

prognosis than either factor occurring alone (Kilic, Naus et al. 2005). Loss of chromosome 1p is reported in 28% of uveal melanoma cases; however gain occurs more frequently at a rate of 33%. Gain of chromosome 6p occurs in both uveal and cutaneous melanoma. It is an indicator of low risk of metastasis in uveal melanoma and rarely occurs with monosomy three (van den Bosch, Kilic et al. 2010). Monosomy ten is the most frequent chromosomal aberration seen in cutaneous melanoma, at a rate of 60% of all cases. It also occurs in uveal melanoma, however at a less significant rate of 27% (van den Bosch, Kilic et al. 2010).

There are a number of genetic mutations which mutually occur in both melanomas. Genetic mutations associated with either cutaneous or uveal melanoma and their relative frequencies are outlined in Table 1.4.

		Cutaneous Melanoma			Uveal Melanoma		
	Gene	Mechanism	Location	Cases (%)	Mechanism	Location	Cases (%)
Proto oncogenes	*NRAS*	Mutation	1p13	15–25	Mutation	1p13	*
	AKT3	Amplification	1q44	40–67	Amplification	1q44	—
	BRAF	Mutation	7q34	36–61	Mutation	7q34	48*[2]
	NBS1	Amplification	8q21	*	Amplification	8q21	50
	MYC	Amplification	8q24	1–40	Amplification	8q24	43
	DDEF1	Amplification	8q24	—	Amplification	8q24	50
	GNAQ	Mutation	9p21	83*[1]	Mutation	9p21	46
	CCND1	Amplification	11q13	6–44	Amplification	11q13	65
	HDM2	Amplification	12q15	—	Amplification	12q15	97
	BCL-2	Amplification	18q21	>90	Amplification	18q21	100
	GNA11	Mutation	19p13	—	Mutation	19p13	32
	KIT	Mutation	4q12	28-39*[3]	Mutation	4q12	63-78
Tumor suppressor genes	*LZTS1*	Deletion, mutation	8p21	—	Deletion	8p21	—
	CDKN2A-sporadic	Deletion, mutation	9p21	*	Deletion, mutation	9p21	*
	CDKN2A-familial	Deletion, mutation	9p21	30–80	Deletion, mutation	9p21	*
	PTEN	Deletion, mutation	10q23	10–40	Deletion, mutation	10q23	15
	SF3B1	Mutation	2q33	—	Mutation	2q33	18.6
	BAP1	Deletion, mutation	3p21	5	Deletion, mutation	3p21	40

Table 1.4 Frequency of Genetic Changes in uveal and cutaneous melanoma. *Rarely observed or sporadic reports in literature. *[1] Observed in 83% of blue naevi. *[2] Observed in 48% of iris melanomas. *[3] Only melanomas arising in chronically sun-damaged skin, or acral and mucosal melanomas

Proteomic similarities have been identified between the melanomas, such as CXCR4 and its ligand, CXCL12. CXCR4 is known to activate processes such as chemotaxis, angiogenesis, and proliferation. In addition to this, its inhibition has been shown to inhibit metastasis. 41.4% and 43.4% of uveal melanoma cases illustrate an overexpression of CXCR4 and CXCL12, respectively, which are shown to correlate with disease progression (Franco, Botti et al. 2010). Similarly, an over-expression of CXCR4 and CXCL12 has been associated with high clinical risk in cutaneous melanoma, while their under-expression is associated with a better prognosis. However, both proteins have been found to be overexpressed in a number of neoplasms which suggests that they may be considered to be general biomarkers for

cancer (Toyozawa, Kaminaka et al. 2012). Melanoma cell adhesion molecule (MCAM) has been correlated with poor outcome in uveal melanoma according to immunohistochemical analysis of primary uveal melanoma paraffin sections (Beutel, Wegner et al. 2009). In addition to this it has been identified as a significant independent variable within advanced stage cutaneous melanoma patients and as a marker of negative treatment outcome in 43% of non-surgically treated individuals with stage IV melanoma (Rapanotti, Ricozzi et al. 2013, Reid, Millward et al. 2013). IGF-1R is closely associated with cutaneous melanoma as an increase in its expression is related to the transition from benign to malignant nevi (Ucar, Kurenova et al. 2012). Topu-Yilmaz et al. found that IGF-1R expression was found to be directly proportional to the degree of pigmentation, necrosis and lymphocyte infiltration in uveal melanoma tissue studies. Vitreal and serum specimens studied using ELISA confirmed that IGF-1 was increased in patients with scleral invasion. This suggests that IGF-1R is related to clincopathological features of uveal melanoma while IGF-1 has a role in disease progression and development (Topcu-Yilmaz, Kiratli et al. 2010). Arrays of mutual proteins which exhibit similar expression patterns have been identified in both cutaneous and uveal melanoma. These include induced nitric oxide synthases (iNOS) which are necessary for tumour growth, and Hepatocyte growth factor (HGF), a protein known to be involved in processes such as angiogenesis and epithelial morphogenesis (Massi, Franchi et al. 2001, Johansson, Mougiakakos et al. 2010, Topcu-Yilmaz, Kiratli et al. 2010, Lee, Kim et al. 2011). This illustrates that both uveal and cutaneous melanoma are linked through common paths of protein expression for establishing tumorigenesis, disease progression, and melanoma development.

It has been reported that patients with uveal melanoma are approximately 4.6 times more likely to develop cutaneous melanoma than “healthy” individuals; however the same cannot be said for cutaneous melanoma patients developing uveal melanoma. This may be due to the fact that those who have developed uveal melanoma have been sufficiently exposed to enough UV radiation to develop cutaneous melanoma also (Shors and Weiss 2004). Of course, this may also be related to genetic factors but there is currently no evidence to support this.

1.6 Clinical Proteomics Methods

The search for biomarkers is currently carried out, for the most part, using MS-based methods in combination with chromatography or gel electrophoresis techniques. Biomarker validation methods include immunohistochemistry (IHC), multiple reaction monitoring (MRM) and ELISA.

Commonly analysed clinical specimens include serum and plasma, which are blood extracts. Serum is prepared when the blood sample is allowed to clot, centrifuged, and the blood clot is removed. Plasma on the other hand is prepared through the centrifugation of blood in order to remove red and white blood cells. Anti-coagulants, such as ethylenediaminetetraacetic acid (EDTA) and heparin, are used during this procedure in order to prevent blood clots from forming (Lam, Rainer et al. 2004).

However, prior to proteomic investigation, many samples, particularly serum and plasma, require a pre-treatment step. This is due to the fact that complex protein mixtures, such as blood, contain an abundance of 20 of the most common proteins which can interfere with the detection of potentially more interesting and less abundant proteins (Fernandez-Costa, Calamia et al. 2012).

1.6.1 Sample Pre-Fractionation

Clinical specimens are clearly a valid source of potential biomarkers, however, as explained, many can contain a large proportion of high abundant proteins, hence fractionation is required to remove these proteins (Kim and Kim 2007).

Using biological fluids such as serum and plasma can be very useful in the biomarker discovery process as they most likely contain proteins and peptides from the site of disease and are minimally invasive during collection. Despite this, 99% of the total protein mass of plasma or serum is composed of 22 proteins; see Figure 1.3, which is the primary disadvantage of using such specimens. Immunodepletion involves the removal of any number of the most abundant proteins through an immunocapture-based technique. An example of an immunodepletion method includes the range of Multiple Affinity Removal System (MARS) columns (Agilent, CA, USA), which can variably remove 6, 7 or 14 abundant proteins, or the

ProteoPrep20 (Sigma-Aldrich, UK), which removes 20 proteins (Smith, Wood et al. 2011). There have been questions over the benefit of depleting increased numbers of proteins in comparison to fewer proteins. Roche et al. immunodepleted one, six, 12 or 20 high abundance proteins and subsequently analysed the treated sera using proteomic approaches such as SELDI-TOF and 2-D electrophoresis. An overall evaluation of results clearly demonstrated the benefit of immunodepletion in the detection of lower abundant and potentially more interesting proteins. However, they noticed that there was a limited advantage in increasing the number of depleted proteins from 12 to 20. By removing 20 proteins, this may also allow for the depletion of associated peptides and proteins, which could negatively impact on the discovery of biomarkers (Roche, Tiers et al. 2009). Other studies have shown that the "depletome" can often contain associated potential disease markers of interest and that more attention should be paid to such proteins and peptides (Koutroukides, Guest et al. 2011).

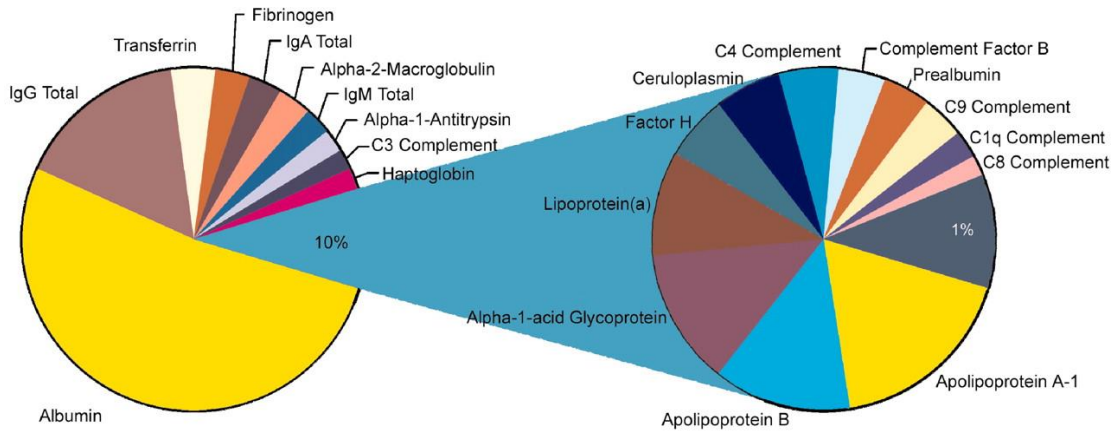

Figure 1.3 The majority of the serum proteome is composed of highly abundant proteins, thus masking lower abundant proteins which may indicate the disease state of a patient (Tirumalai, Chan et al. 2003).

Newer technologies, such as ProteoMiner, can also be employed for sample pre-treatment in order to analyse the "hidden proteome" (Boschetti and Righetti 2008). This involves using a vastly heterogeneous library of hexapeptides bound to poly(hydromethacrylate) beads which allows for the compression of the dynamic

range of protein concentrations. Each hexapeptide binds to an exclusive protein sequence and as there are a finite number of ligands available for each molecule to bind, highly abundant proteins will quickly saturate theirs, with any excess being washed away. Simultaneously, any low abundance proteins are concentrated on their ligands (Figure 1.4). When bound proteins are eluted from the column, the dynamic range of proteins available is decreased, allowing for a greater range of proteins to be analysed in downstream analysis. It is therefore a useful method for quantitative analysis of low abundance proteins in complex clinical samples (Sennels, Salek et al. 2007, Hartwig, Czibere et al. 2009). ProteoMiner equalises the protein in a sample without immunodepletion, which as mentioned above can lead to the loss of small proteins bound to highly abundant ones. ProteoMiner can also be used on many biological samples or a cell or tissue lysate and is compatible with many downstream protein analysis techniques. Sennels et al. used the protein equalising technology for the enrichment of human blood serum proteins, identifying 1559 proteins in the resulting elution, of which 58% had not previously been reported in the literature (Sennels, Salek et al. 2007). ProteoMiner has also been used on a variety of other biological samples including urine, saliva, and colostrum (Castagna, Cecconi et al. 2005, Coscia, Orru et al. 2012, Jagtap, Bandhakavi et al. 2012).

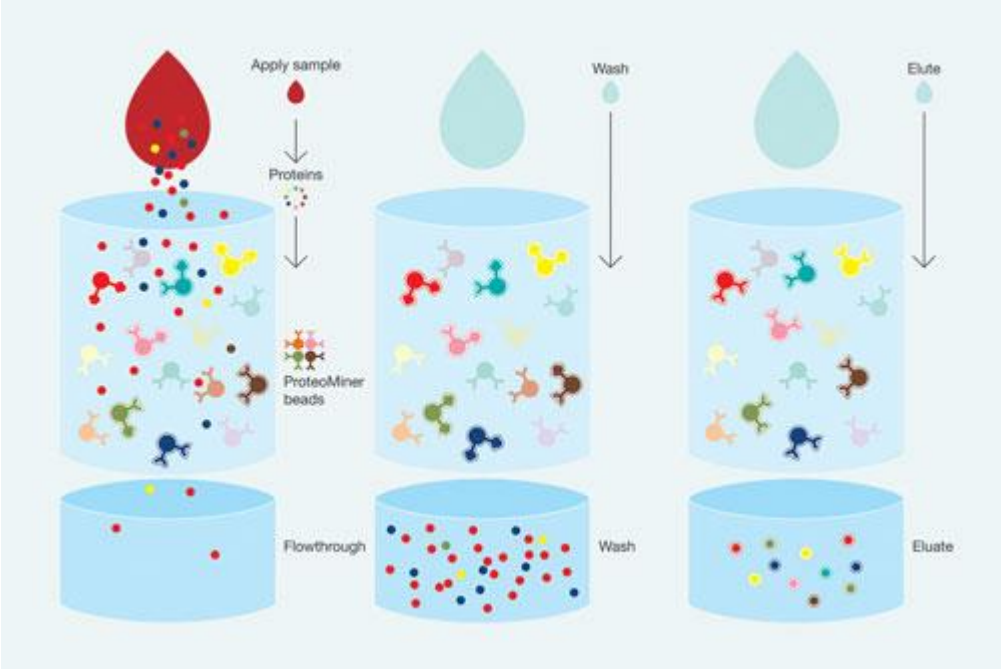

Figure 1.4 ProteoMiner allows for the simultaneous enrichment of low abundance proteins and depletion of high abundance proteins (http://www.genengnews.com/ 2010)

Hydrogel nanoparticles are another method used in the separation of highly abundant and low abundant proteins. These "smart" nanoparticles allow the enrichment and encapsulation of selected classes of proteins from complex mixtures, such as a clinical specimen, while protecting the analytes from degradation following separation (Figure 1.5). The captured proteins can then be extracted from the particles by electrophoresis and quantified (Luchini, Geho et al. 2008). As the fractionation method combines size exclusion, affinity separation, concentration, and stabilisation of proteins from a complex mix, it provides an ideal environment for biomarker discovery in complex biological specimens.

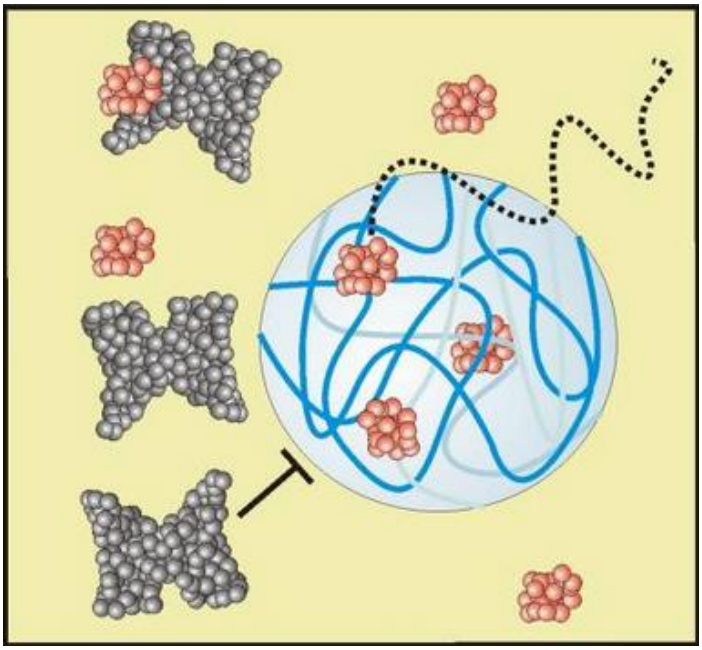

Figure 1.5 Animated representation of the molecular sieving property of hydrogel nanoparticles. Using an affinity bait and defined porosity, low molecular weight proteins (pink) are harvested while high molecular weight proteins are excluded (grey) (Luchini, Geho et al. 2008).

1.6.2 Protein Fractionation

The aim of proteomics is to have a global view of all of the proteins produced in a biological system, usually in order to understand a differential protein expression pattern (Berth, Moser et al. 2007). It is essentially used for the analysis of the final level of gene expression, and is widely utilised in the search for biomarkers of disease. In order to do this, it is first necessary to separate all of the proteins in the sample for analysis, such as by electrophoresis, as there are approximately 100,000 proteins produced in humans and 2-D gels may separate up to 10,000 protein spots on one gel (Wang, Li et al. 2006, Berth, Moser et al. 2007). The subsequent identification of proteins is carried out using MS methods, such as MALDI-TOF and LC-MS/MS.

1.6.3 Two-Dimensional Polyacrylamide Gel Electrophoresis (2-D PAGE)

One of the oldest and most useful methods for protein separation is two-dimensional polyacrylamide gel electrophoresis (2-D PAGE). This initially involves separating a fixed quantity of protein, as determined by protein assay, based on the isoelectric point (pI) of the proteins using immobilised pH gradient (IPG) strips, in the first dimension. The pI of a protein is described as the pH at which its net charge is zero, hence the protein cannot move freely in an electrical field. The strips are attached to the top of a polyacrylamide gel slab and once charge is applied, proteins migrate from the strip into the gel and are separated based on their size, using sodium dodecyl sulphate electrophoresis, in the second dimension. The result of this process is a 2-D gel which, when stained produces a series of spots, with each spot corresponding to a protein. Commonly used protein stains include Coomassie Brilliant Blue and silver nitrate colloidal stain, both of which are global protein stains.

Although 2-D PAGE has been useful for the separation of complex protein mixtures, it was a very limited technique until the advent of micro-analytical techniques, such as quantitative LC-MS (O'Farrell 1975, Rabilloud 2002).

1.6.3.1 Two-Dimensional Differential Gel Electrophoresis (2-D DIGE)

2-D DIGE (Two-Dimensional Differential Gel Electrophoresis) is a highly sensitive method of minimal protein labelling of up to three different conditions using separate fluorescent dyes and their subsequent co-electrophoresis in order to examine the quantitative differential expression of proteins between the conditions (Alban, David et al. 2003).

This technique uses three covalently-bound dyes: Cy2, Cy3 and Cy5, of which the NHS-ester reactive group of one molecule of each binds to the epsilon amino group of lysines in one protein through an amide linkage. The Cy3 dye is used to stain one sample group and Cy5 to stain the other. A pool of all samples can then be created and labelled with Cy2 which acts as an internal standard and is used on all gels. All gels can be normalised against the Cy2 standard which results in accurate reproducibility and protein abundance comparisons between gels. All three of the

dyes are size and charge matched, pH insensitive, photostable, sensitive, and spectrally resolvable (https://www.gelifesciences.com/ , Alban, David et al. 2003) .

The gels are scanned at the appropriate excitation and emission wavelengths and the acquired images are imported onto a computer for analysis by software such as Progenesis SameSpots (Non-Linear Dynamics) or DeCyder (GE Life Sciences). These programmes accurately detect statistically significant protein abundance changes between the gels and effectively minimise gel-to-gel variation (https://www.gelifesciences.com/). The analysis of spot maps is divided into two categories, depending on the work flow; spot detection first, including aligning spots between gels, calculating spot volumes and subsequent expression profile generation, or image modification first, with a separate spot detection step, for removing running differences between gels using whole image information and generating expression profiles based on differences between spot maps. Newer programmes such as Z3, Decyder, Delta2D and Progenesis SameSpots all depend on the latter method (Berth, Moser et al. 2007). An overview of the process is shown in Figure 1.6.

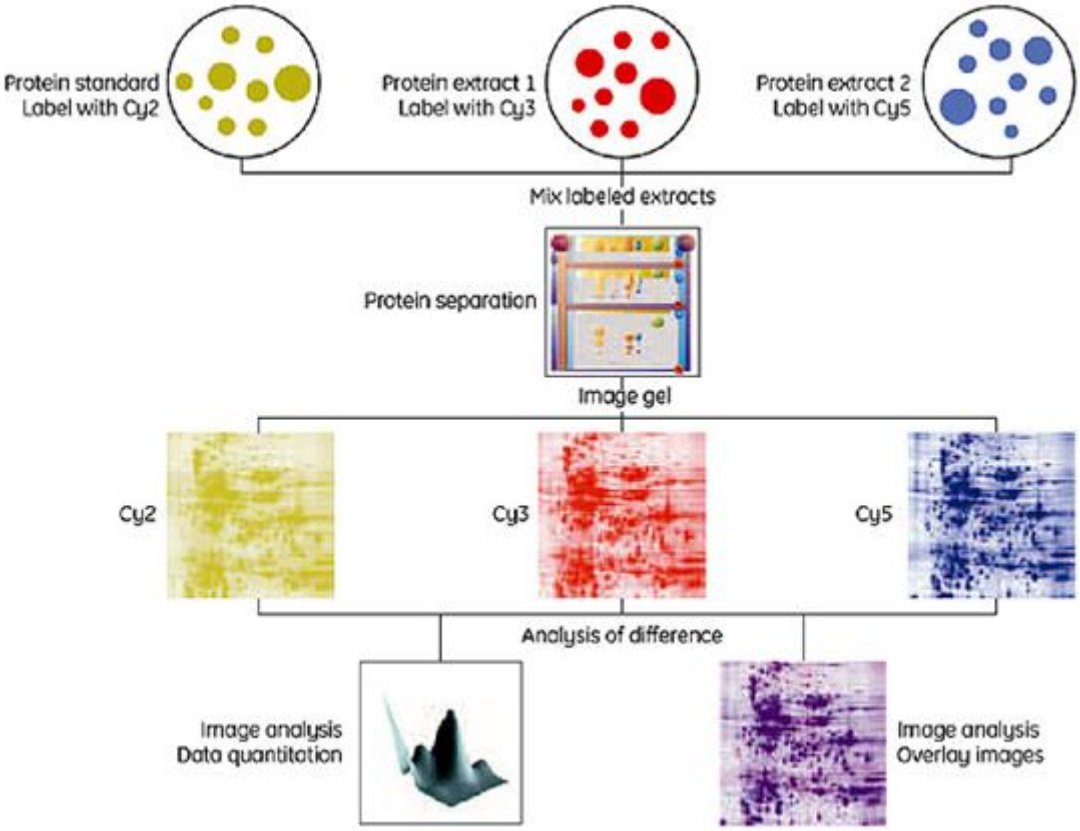

Figure 1.6 A 2-D DIGE workflow from protein labelling with Cy3, Cy5 and Cy2 (internal standard) to image acquisition using a fluorescent imager (https://www.gelifesciences.com/).

As described above, 2D-DIGE has been used for many clinical studies in the past in the hunt for biomarkers and it is still relevant today, primarily due to its high sensitivity. However, there are a number of problems with gel-based methods; single protein spots can often contain more than one protein as molecules of similar charge and size would migrate together, and also, resolution can vary depending on the properties of the protein such as very high molecular weight and hydrophobicity.

1.6.4 Mass Spectrometry

MS is a method of protein fragmentation and identification. Traditionally, this involves digesting the protein at specific sites and fragmenting the peptides in the gas phase.

1.6.4.1 Ionisation

In order to separate neutral molecules through an electromagnetic field, they must first be converted to ions and may be changed to a gas, i.e. desorption. Both processes are carried out using an ionisation source. A number of methods are available for the procedure although, ESI and MALDI are the most efficient ways in which to ionise peptides (Canas, Lopez-Ferrer et al. 2006).

MALDI relies on the saturation and co-crystallisation of matrix with analyte in a low vacuum. When the sample combined with the matrix is bombarded with UV light, the matrix absorbs the energy which causes it to become vaporised along with the sample peptides. This produces a "plume" within which a transfer of protons occurs between the analyte and the matrix, thus producing analyte ions (Canas, Lopez-Ferrer et al. 2006).

The principle of ESI is based on the fact that if a high voltage is applied to a stream of liquid flowing through a narrow capillary, an electrical spray is created. ESI allows for ions to gain multiple charges, such as in the case of peptide ions which are often doubly or triply charged, thereby requiring less activation energy for fragmentation and giving information-rich results for database searches (Canas, Lopez-Ferrer et al. 2006).

1.6.4.2 Mass Analysis

A mass analysis step is used in order to examine ions based on their mass. ESI and MALDI mass spectrometers are combined with various mass analysers, depending on the sample and the research question. Mass analysers can be based on electric and/or magnetic fields for the separation of ions in the gaseous phase and can be used alone or in tandem (Aebersold and Mann 2003).

TOF, the most basic mass analyser, accelerates ions with equal energies in a strong electric field through a high vacuum flight tube. Peptides are measured based on their velocity, as the velocity of each particle is inversely proportional to its mass, i.e. the heavier the peptides, the slower are in reaching the detector. (Canas, Lopez-Ferrer et al. 2006).

In ion trap MS, ions are stored until the trap is full. Using radio frequency voltage, ions are ejected out and are detected by the electron multiplier. The orbitrap is a highly sensitive form of ion trap (Fitzgerald, O'Neal et al. 1997).

1.6.4.3 Protein Identification

The acquired data is then searched against a database in order to generate a set of identifications. For determining the mass of a peptide, peptide mass fingerprinting, which compares mass spectra to a protein database for matching molecular weights, or tandem mass spectrometry (MS/MS), which determines the mass and generates a partial amino acid sequence for further fragmentation, can be used. Software packages which can interpret proteomic data are available, such as MASCOT and Phenyx (Wright, Noirel et al. 2012).

1.6.5 Surface enhanced laser desorption/ionisation (SELDI)

Surface enhanced laser desorption/ionisation (SELDI) is an ionization method in MS that is used for the analysis of protein mixtures. It is a variation of MALDI that uses a target modified to achieve biochemical affinity with the analyte and is useful for the comparison of protein levels between patients and so, can be used for biomarker discovery.

Initially, a chip-based target is charged and activated to bind a specific subset of proteins. The surface may consist of various materials of different affinity characteristics such as hydrophobic or hydrophilic properties, containing metal ions (such as immobilised metal affinity capture: IMAC) or anion and cation exchangers (Kiehntopf, Siegmund et al. 2007), or it can be pre-activated for the coupling of capture molecules such as protein, DNA, or RNA prior to sample loading. Any unbound proteins can be washed away, thus acting as a separation step. The sample is mixed with a matrix, such as sinapinic acid, which is allowed to dry and co-crystallise with the analyte on a chip surface. A laser then strikes the mixture, causing ionisation of any bound proteins present. TOF is used to measure the m/z of each molecule which generates a spectrum where each peak corresponds to a protein.

A wide variety of biofluids can be used on a SELDI chip such as, serum, plasma, vitreous fluid and saliva. Although SELDI-TOF is a rapid method of protein profiling which requires little sample, it does not produce protein identifications; only the m/z ratio and the intensity of the peak (Peng, Stanley et al. 2009, De Bock, de Seny et al. 2010).

1.6.6 Quantitative Label-Free LC-MS/MS

LC-MS/MS is quickly becoming the method of choice for the analysis of complex samples due to its high sensitivity and exceptional dynamic range. This involves the use of nano-high performance liquid chromatography (HPLC) with reverse phase chromatography prior to MS/MS.

Label-free proteomics identifies proteins through both bioinformatics and MS. The label-free approach is based on the separate LC-MS/MS analysis of all samples, followed by retention time control and normalisation between generated MS/MS spectra using a programme such as Progenesis LC-MS (Non-Linear Dynamics). Quantitative LC-MS/MS can be broken into two groups; area under the curve (AUC) or signal intensity measurement based on precursor ion spectra, and spectral counting, which is based on counting the number of peptides assigned to a protein in an MS/MS experiment. (Figure 1.7) (Neilson, Ali et al. , Zhu, Smith et al.).

Measurement by ion intensity infers quantification through precursor ion signals at specific retention times without the use of a stable isotope standard. As ionised peptides elute from a reverse-phase column into the mass spectrometer, their ion intensities can be measured within the chosen detection limits, and differentially expressed peptides can be subsequently compared with those from other samples (Neilson, Ali et al.). This method requires that all data is collected in data-dependent ‘Triple Play’ mode (allowing MS scan, Zoom scan, and MS/MS scan) and these together with chromatographic retention time determine the analytical accuracy of protein identification and quantification by ion intensity (Higgs, Knierman et al. 2005).

Spectral counting relies on the principal that the more of a specific protein present in a sample, the more MS/MS spectra collected for peptides of that protein. Hence, the

relative abundance of that protein can be obtained by comparing the number of MS/MS spectra between sample sets. Although this method has the advantage of simultaneous quantification and identification, it depends on the quality of MS/MS generated (Bantscheff, Schirle et al. 2007, Wang, You et al. 2008).

As the quantitative label-free LC-MS/MS method does not require sample labelling, bias is limited while throughput is significantly increased; a highly reproducible LC profile must be generated to maximise mass resolution, accuracy, and proteome coverage.

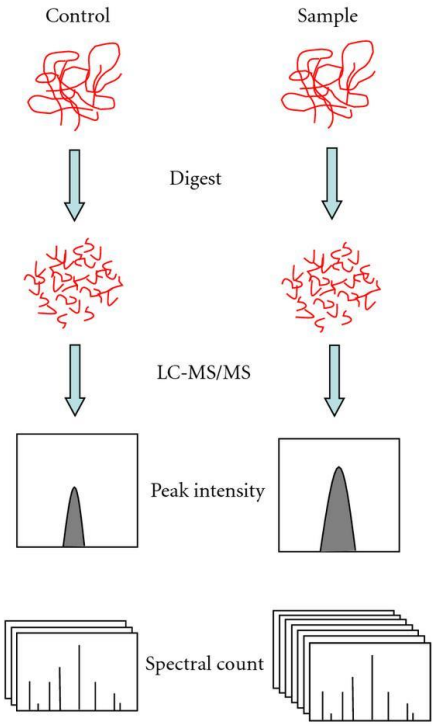

Figure 1.7 Label-free quantitative proteomics. Control and sample are subjected to individual LC-MS/MS analysis. Quantification is based on the comparison of peak intensity of the same peptide or the spectral count of the same protein (Zhu, Smith et al. 2010).

AIMS OF THESIS

The goal of this thesis was to identify differential protein expression patterns between metastatic uveal melanoma in comparison to the non-metastatic disease and also, to determine potential biomarkers in the progression of cutaneous melanoma. It was intended that the analysis of both melanoma types would allow for a better understanding of the molecular mechanisms of the metastatic phenotype. It was also a possibility that this research could the lead to the discovery of biomarkers for the development of targeted therapies for disease treatment and the early detection of disease using proteomics tests. Specifically, the aims of this thesis were the following:

- To identify protein expression differences in primary tumour tissue between two sets of uveal melanoma sample groups; those who subsequently developed metastasis in comparison to those who did not, using 2D-DIGE and quantitative label-free LC-MS, and to elucidate the role of such proteins in metastasis using functional analysis which may improve our understanding of the metastatic phenotype of the disease.

- To compare control serum from disease-free patients to that of late stage cutaneous melanoma patients using fractionation methods in order to identify highly significant protein expression differences and to subsequently examine such differences across an array of control, benign, early stage melanoma, and advanced melanoma sera using ELISA in order to further understand the progression of the disease.

- To optimise a protocol for the use of vitreous fluid from uveal melanoma patients in proteomic experiments by minimising the quantity of highly abundant proteins, while enhancing the presence of low abundance proteins.

- To determine potential, differentially expressed biomarkers for uveal melanoma in the vitreous fluid between patients with monosomy of chromosome three status and those with disomy of chromosome three. It also intended to identify

proteins which were differentially expressed between control vitreous, which was collected from macular degeneration patients, and that of uveal melanoma patients.

- To use surface-enhanced laser desorption-ionisation time-of-flight (SELDI-TOF MS) for the proteomic profiling of advanced cutaneous melanoma serum, the vitreous fluid of uveal melanoma patients and the conditioned media of cutaneous melanoma cultured cells, in comparison to relevant controls for the direct analysis of potential biomarker expression between the sample sets.

CHAPTER TWO

Materials and Methods

2.1 Cell Culture

2.1.1 Preparation of Cell Culture Media

Ultrapure water (UHP) was purified to a standard of 12-18 MΩ/cm resistance by a reverse osmosis system (Millipore MillI-RO 10 Plus, Elgastat UHP). Glassware required for cell culture related applications were soaked in a 2% RBS-25 (Chemical Products R. Borghgraef S.A.) for 1 hour, washed in an industrial dishwasher, using Neodisher detergent and rinsed twice with UHP. All thermostable solutions, water and glassware were sterilised by autoclaving at 121°C for 20 minutes at 15 bar (Thermolabile solutions were filtered through 0.22 μm sterile filters (Millipore, Millex-GV SLGV025BS)). Complete media was prepared by adding serum as required (Table 2.1). An aliquot of complete medium was kept in a T-25cm^2 flask in an incubator over 5-7 days to ensure that the complete medium is free of contamination at the time of use. Complete media was also stored at 4°C for a maximum of one month in the dark.

Cell Lines	Growth Media Components
SK-MEL 5	RPMI-1640 (Sigma-Aldrich, R0883), 10% (v/v) fetal calf serum (PAA, A15-101)
MEL202	RPMI-1640 (Sigma-Aldrich, R0883), 10% (v/v) fetal calf serum (PAA, A15-101)
92.1	RPMI-1640 (Sigma-Aldrich, R0883), 10% (v/v) fetal calf serum (PAA, A15-101)

Table 2.1 Details of cell lines and complete growth media components

2.1.2 Cell Lines and Cell Culture

All cell culture work was carried out in a class II laminar air-flow cabinet (Nuaire). Before and after use the laminar air-flow cabinet was cleaned with 70% industrial methylated spirits (IMS). Any items brought into the cabinet were also swabbed down with IMS. At any time only one cell line was used in the laminar air-flow cabinet and upon completion of work with any given cell line, 15 minutes clearance was given to eliminate any possibilities of cross-contamination between the various cell lines. The cabinet was cleaned weekly with Virkon (Antech International, P0550) and IMS. Details pertaining to the cell lines used for the experiments are

provided in Table 2.2. All cells were incubated at 37°C and where required, in an atmosphere of 5% CO2. Cells were fed with fresh media or subcultured (see section 2.1.1) every 2-3 days or as required in order to maintain active cell growth.

2.1.3 Subculturing of Adherent Cell Lines

The cell lines used during the course of this study, their sources, and detailed information are listed in Table 2.2. Exhausted cell culture medium was removed from the tissue culture flask and discarded into a sterile bottle. The flask was then rinsed out with 2 mL of PBS solution to ensure the removal of any residual media. Depending on the size of the flask, 2-5 mL of trypsin solution (0.25% (v/v) of trypsin (Gibco, 043-05090) and 0.01% (v/v) of EDTA (Sigma, E9884) solution in PBS (Oxoid, BRI4a)) was then added. Cells were incubated at 37°C for approximately 2-5 minutes until all of the cells detached from the inside surface of the flask. This was monitored by microscopic observation. An equal volume of complete media was added to the flask to deactivate the trypsin. The cell suspension was removed from the flask and placed in a sterile universal container (Sterilin, 128a) and centrifuged at 1000 rpm for 5 minutes. The supernatant was then discarded from the universal and the pellet was suspended gently in fresh complete medium. A cell count was performed as described in section 2.1.4 and an aliquot of cells was used to seed a flask at the required density. All cell waste or media exposed to cells was autoclaved before disposal.

Cell Lines	Established by	Source	Cell Line Code	Detailed Information
SK-MEL 5	Old, Lloyd J. Takahashi, T.	ATCC	HTB-70	Malignant Melanoma
MEL202	(Ksander, Rubsamen et al. 1991)	ESTDAB, University of Tubingen, Center for Medical Research, Germany	ESTDAB-128	Primary Uveal Melanoma Tumour
92.1	(De Waard-Siebinga, Blom et al. 1995)	ESTDAB, University of Tubingen, Center for Medical Research, Germany	ESTDAB-127	Primary Uveal Melanoma Tumour

Table 2.2 Details of cell lines used in this investigation.

2.1.4 Assessment of Cell Number and Viability

Prior to cell counts, cells were prepared by subculturing as detailed in section 2.1.3 An aliquot of the cell suspension was then added to trypan blue (Gibco, 525) at a ratio of 1:1 (v/v). The mixture was incubated for 2-3 minutes at room temperature. An aliquot (10 μL) was then applied to the chamber of a glass coverslip-enclosed haemocytometer. For each of the four grids, cells in the 16 squares were counted. Non-viable cells stained blue, while viable cells excluded the trypan blue dye as their membrane remained intact, and remained unstained. The average number of viable and dead cells per 16 squares was multiplied by a factor of $5X10^3$ (volume of the grid) and the relevant dilution factor to determine the average cell number per mL in the original cell suspension. Using the data for viable and non-viable cells, percentage viability was calculated.

The Cedex Automated Cell Counter (Roche), an automated cell counting system based on the Trypan Blue exclusion method, was also used for accurate determination of cell number. Cells were trypsinised and incubated with trypan blue in the same manner as above, prior to assessment of cell number through Cedex analysis. This involved pipetting 10 μL of Trypan Blue/cell suspension mix onto a Cedex Smart Slide (05650801001, Roche) and measuring the cell number using the automated system.

2.1.5 Cryopreservation of Cells

Cells for cryopreservation were harvested in the mid-log phase of growth and counted as described in section 2.1.4. Cell pellets were resuspended in a suitable volume of serum. An equal volume of filter sterilized solution of 10% (v/v) DMSO in serum was added dropwise with mixing into the cell suspension. 1 mL of cell suspension was then aliqoted into the cryovials (Greiner, 122278) and immediately placed in the -20 °C freezer for 1 hour and then placed in a -80 °C freezer for four hours or overnight. The cryovials were then transferred to liquid nitrogen tank for long term storage (-196 °C).

2.1.6 Thawing of Cryopreserved Cells

A volume of 5 mL of fresh complete culture medium was added to a sterile universal and into a T-25 cm^2 flask and incubated at 37 °C for ~1 hour. The cryopreserved cells were removed from the liquid nitrogen and thawed at 37 °C as quickly as possible. The cells were removed from the vials and transferred into the pre-warmed aliquoted media in the universal. The resulting cell suspension was centrifuged at 250 g for 5 minutes. The supernatant was removed and the pellet was resuspended in the pre-warmed culture medium from T-25 cm^2 flask. This cell suspension was then transferred to T-25 cm^2 flask and allowed to attach and grow overnight in incubator. The following day, the culture media was replaced with fresh complete culture medium to remove any non-viable cells and floating cells.

2.1.7 *Mycoplasma* Analysis of Cell Lines

Mycoplasma testing was carried out for all cell lines for possible *Mycoplasma* contamination in house by Mr. Michael Henry at the NICB. All cell lines are found to be *Mycoplasma* free.

2.1.7.1 Indirect Staining Procedure for Mycoplasma Analysis

Normal rat kidney fibroblast (NRK) cells were seeded onto sterile coverslips in sterile Petri dishes (Greiner, 633 185) at a cell density of $2x10^3$ cells/ml and were allowed to attach overnight at 37°C in a 5% CO_2 humidified incubator. 1 mL of cell-free supernatant from each test cell line was inoculated onto an NRK petri dish and incubated as before until the cells reached 20-50% confluency. After this time, the waste medium was removed from the dishes, the coverslips (Chance Propper, 22 x 22 mm) washed twice with sterile PBS, once with a cold PBS/Carnoys (50/50) solution and fixed with 2ml of Carnoys solution (acetic acid:methanol, 1:3) for 10 minutes. The fixative was removed and dried coverslips were washed twice in deionised water and stained with 2ml of Hoechst stain (BDH) (50ng/ml) for 10 minutes. From this point on, work proceeded without direct light to limit quenching of the fluorescent stain. The coverslips were rinsed three times in PBS. They were then mounted in 50% (v/v) glycerol in 0.05 M citric acid and 0.1 M disodium

phosphate and examined using a fluorescent microscope with a UV filter. A Mycoplasma infection would be seen as small fluorescent bodies in and sometimes outside the cells.

2.2 Tumour Tissue Sample Preparation for 2-D DIGE Analysis

Uveal melanoma tissue specimens were homogenised using a sample grinding kit (GE Healthcare, 80-6483-37) by placing the tissue specimen in a 1.5 mL eppindorf tube containing grinding resin. 2-D lysis buffer containing 7 M urea (Sigma Aldrich, 208884), 2 M thiourea, 4% (w/v) (Sigma Aldrich, T8656), CHAPS (Sigma Aldrich, C3023), 40 mM DTT (Sigma Aldrich, D9163) and 0.5% IPG buffer pH 3-11 (GE, 17-6000-86) was added to the tube and the tissue was degraded using a pestle. Insoluble material was removed by centrifugation at 14,000 rpm for 5 min at room temperature and supernatants were stored at -80 °C until required.

2.3 Protein Quantification

Protein concentration was determined using the thiourea-compatible Quick Start Bradford Protein Assay Kit (Bio-Rad, 500-0201), containing 2 mg/mL of bovine serum albumin (BSA) solution as a known standard. Dilutions of BSA stock for 0.125, 0.25, 0.5 and 1.0 mg/mL was prepared and used for generating a protein standard curve. 5μL of protein standard dilution or sample (diluted 1:10) was added to a 96-well plate. 245 μL/well of thiourea-compatible Bradford protein assay reagent (Bio-Rad, 500-0205) was then added to the plate. All samples were assayed in triplicate. After 5 minutes incubation, the absorbance was assessed at 595nm. The concentration of the protein samples was determined from the plot of the absorbance at 595nm versus the concentration of the protein standard.

2.4 2D-DIGE Sample Preparation

2.4.1 Preparation of CyDye DIGE Fluor Minimal Dye Stock Solution

The three CyDye DIGE Fluor Minimal dyes (Cy3, Cy5 and Cy2) (GE Life Sciences, 25-8010-65) were thawed from –20 ^{o}C to room temperature for 5 minutes. To each microfuge tube dimethylformamide (DMF) (Sigma Aldrich, 22,705-6) was added to

a concentration of 1 nmol/µL. Each microfuge tube was vortexed vigorously for 30 seconds to dissolve the dye. The tubes were then centrifuged for 30 seconds at 14,000 rpm in a microcentrifuge. The reconstituted dyes can be stored at –20 ^{o}C for up to two months.

2.4.2 Preparation of 10 µl working dye solution (200 pmol/µL)

On thawing, the dye stock solutions were centrifuged in a microcentrifuge for 30 seconds. To make 10 µL of the three working dye solutions, 8 µL of DMF was added to three fresh eppendorfs labelled Cy2, Cy3 and Cy5. A 0.2 nmol/µL volume of each of the reconstituted dye stock solutions was added to their respective tubes. The dyes can be stored at -20 ^{o}C in tinfoil in the dark for 3 months.

2.4.3 Protein sample labelling

A volume of the protein samples equivalent to 50 µg was placed into eppendorf tubes. An eppendorf tube for the Cy2 pool made up from aliquots from all the protein samples contained enough protein for 50ug for each gel. Each tube was mixed by vortexing, centrifuged and then left on ice for 30 minutes in the dark. To stop the reaction, 1 µL of 10 mM lysine (Sigma Aldrich, L5501) was added, the tubes were vortexed, centrifuged briefly, and left on ice for 10 minutes in the dark. The labelled samples were stored at –80 ^{o}C. To this tube 1 µl of working dye solution was added.

2.4.4 Preparing the labelled samples for the first dimension

The protein samples labelled with Cy2 (pooled internal standard), Cy3 and Cy5 were thawed on ice (in the dark), combined by placing into a single eppendorf tube and mixed. An equal volume of 2X sample buffer (2.5 mL rehydration buffer stock solution (8M urea, 4% CHAPS), pharmalyte broad range pH 4-7 (2%) (GE Life Sciences, 17-6000-86), DTT (2%) (Sigma, D9163)) was added to the labelled protein samples. The mixture was left on ice for at least 10 minutes then applied to Immobiline DryStrips for isoelectric focussing.

2.4.5 First dimension separation - isoelectric focussing methodologies

Isoelectric focussing of all samples was carried out using pH 3-11, 24 cm immobiline pH gradient (IPG) strips (GE Life Sciences, 17-6003-77).

2.4.5.1 Strip rehydration using Immobiline DryStrip reswelling tray

A Immobiline Dry Strip Reswelling tray (GE Life Sciences, 17-1233-01) was levelled using the spirit level. A 350µl volume of rehydration buffer solution containing 7 M urea, 2 M thiourea, 4% CHAPS, 0.5% IPG buffer pH 3-11, 50 mM DTT was slowly pipetted into the centre of each slot, all air bubbles generated were removed. The cover film from the IPG strip was removed and positioned with the gel side down and lowered, ensuring that the entire strip was evenly coated buffer and that no air bubbles were present.

Each strip was overlaid with about 3 mL IPG Cover Fluid (GE Life Sciences, 17-1335-01) starting on both ends of the strip, moving to the centre. The protective lid was then replaced and the strips were left at room temperature to rehydrate overnight (or at least 12 hours).

2.4.5.2 Isoelectric focussing using the IPGphor manifold

Following the rehydration procedure, the Manifold (GE Life Sciences) was placed onto the IPGphor unit by inserting the "T" shape into the hollow provided. A 9 mL volume of Cover Fluid was placed into each of the twelve lanes in the tray in order to cover the surface. Two wicks (GE Life Sciences, 80-6499-14) per strip were rehydrated with 150 µl of UHP water. The rehydrated strips were placed in the correct orientation (+ to anode) and aligned just below the indented mark, to allow for the wicks to overlap the strip. The rehydrated wicks were then placed over both ends of all the strips, ensuring that they were positioned over the gel portion of the strip and avoiding the indent in the lane so as to guarantee a good contact with the electrodes. The sample cups (GE Life Sciences, 80-6498-95) were then positioned approximately 1 cm from the cathodic end of the strip and an insertion tool was used to securely "click" the cups into place. The electrodes were then fitted, in direct contact with the wicks.

The amount of protein loaded per strip was 150 μg for DIGE or 400 μg for spot picking and identification. The protein samples were prepared by centrifuging to remove any insoluble material and the appropriate volume was loaded with a pipette tip placed just beneath the surface of the cover fluid. The cover of the IPGphor unit was closed and the desired programme selected. The temperature was set for 20^{o}C with 50μA/strip. The IEF parameters are as follows: step 1: 300 volts for 3 hours (step-and-hold), step 2: 600 volts for 3 hours (gradient), step 3 1000 volts for 3 hours (gradient), step 4: 8000 volts for 3 hours (gradient). The IEF was left at 8000 volts (step-and –hold) until ready for SDS-PAGE step. On completion of the IEF run, the strips were drained of the cover fluid and stored in glass tubes at –80 ^{o}C or used directly in the second dimension.

2.4.6 Second Dimension – SDS polyacrylamide gel electrophoresis

2.4.6.1 Casting gels in the ETTAN Dalt-12 gel caster

For all 2-D gels, a 12.5% acrylamide gel solution was prepared in a glass beaker (acrylamide/bis 40%, 1.5 M Tris pH 8.8, 10% SDS). Prior to pouring, 10% ammonium persulfate (Sigma Aldrich, A3678) and neat TEMED (Sigma Aldrich, T-9281) were added.

Gels for use in DIGE experiments were poured into a sandwich of low fluorescent plates while those used for preparative gels were poured into hinged plates. Following pouring the acrylamide solution into the appropriate glass plate mould, a displacement solution (0.375M Tris-Cl 1.5M pH 8.8, 30% glycerol, UHP and bromophenol blue) was added to the reservoir, forcing the remaining gel solution into the gel caster. The gels were then overlaid with 1 mL of saturated butanol or sprayed with 0.1 % SDS solution and left to set for at least three hours at room temperature. The set gels were rinsed with distilled water and stored for up to four days in 1X running buffer at 4 ^{o}C, if they were not for immediate use.

If gels were to be used for "spot picking" the plates were silanised to stick the acrylamide mixture to the plates. 2 mL of the following solution; 8 mL ethanol, 200 μL glacial acetic acid, 10 μL bind-silane (GE Life Sciences, 17-1330-01) and 1.8 mL UHP was pipetted over the glass plate and wiped over with a lint free cloth. This was left to air dry for 15 minutes, after which 2 mL ethanol and 2 mL UHP were each

pipetted over the plate and wiped off respectively. The plate was left to air dry for approximately 1 hour 30 minutes.

2.4.6.2 Preparing the ETTAN DALT 12 electrophoresis unit

The electrophoresis chamber was prepared by adding 6.48 litres of UHP and 720 mL of 10X SDS running buffer. The pump was then turned on to cool the system to 10 ^{o}C.

2.4.6.3 Equilibration and loading of focussed Immobiline DryStrips

SDS equilibration buffer (30% glycerol, 6 M urea, 50 nM 1.5M Tris-Cl pH 8.8, 2% SDS, bromophenol blue and UHP) with either dithiothreitol (DTT) (65 mM) (Sigma Aldrich, D9163) or iodoacetamide (240 mM) (Sigma Aldrich, I1149) were prepared. Using a forceps, the rehydrated strips were removed from the IPGphor unit, and the cover fluid was drained off. Equilibration buffer (10 mL containing DTT) was added to each tube and incubated for 15 minutes with gentle agitation using an orbital shaker. The DTT containing equilibration solution was the removed and 5 mL of iodoacetamide containing equilibration buffer added. The strips were incubated for 10 minutes with gentle agitation.

The IPG strips were rinsed in 1X SDS electrophoresis running buffer and placed between the two glass plates of the gel. The strip was pushed down gently using a thin plastic spacer until it came in contact with the surface of the gel, gently removing any air bubbles trapped between the gel surface and the strip. Approximately 1 mL of the 0.5% agarose overlay solution was applied over the IPG strip to seal it in place.

2.4.6.4 Inserting the gels into the Ettan DALT 12 electrophoresis buffer tank

When the running buffer reached the desired temperature (10 ^{o}C) the loaded gel cassettes were inserted into the tank, filling any empty spaces with dummy plates if required. The upper chamber was filled with 2X running buffer. The cover of the unit was replaced and the required running conditions selected. The unit was run for 18–24 hours at 1.5 Watts per gel at 10 °C or until the bromophenol blue dye front

reached the bottom of the gel. When the run was completed, the gel cassettes were removed from the tank one at a time using the DALT cassette removal tool and rinsed with UHP to remove the running buffer.

2.4.6.5 Method for scanning DIGE labelled samples

The Typhoon Variable Mode Imager (GE Healthcare) was turned on and left to warm up for 30 minutes prior to scanning. The scanning control software was opened and the fluorescence mode was selected. The appropriate emission filters and lasers were then selected for the separate dyes (Cy2 520 BP40 Blue (488), Cy3 580 BP30 Green (532) and Cy5 670 BP 30 Red (633)). The first gel was placed in the scanner and pre-scanned at a 1000 pixel resolution in order to obtain the correct photo multiplier tube (PMT) value (to prevent saturation of the signal from high abundant spots). Once the correct PMT value was identified (a value ranging between 40,000 and 60,000) the gel was scanned at 100 pixel resolution, resulting in the generation of three images, one each for Cy2, Cy3 and Cy5. Once the scanning was completed, the gel images were imported into the Progenesis SameSpots version 4.0 (NonLinear Dynamics) software.

2.4.7 Differential Analysis of Gel Images

Scanned fluorescent gel images were analysed using Progenesis SameSpots software. Images were loaded into the software and went through a process of quality assessment to optimise image capture. This highlights any positional errors which were introduced during scanning and allows for their correction using image cropping, flipping, or rotating. This also illustrates any gels or regions of the gel which may have been scanned at the incorrect wavelength and resulted in overexposed areas. Protein spots were detected and normalisation between gels was carried out. The spots on the gels were aligned against all gels in the experiment which allows for 100% matching.

The software calculates the degree of difference in the standardized protein abundance between two spots from different groups and expressed these differences as average ratio. The values by the software are displayed in the range of $-\infty$ to -1 for a decrease in expression and +1 to $+\infty$ for an increase in expression. For example, a two-fold increase and decrease is represented by +2 and -2, respectively. The

'average ratio' has also been termed as 'fold change' in this thesis. The software also calculates the consistency of the differences between samples across all the gels and applies statistics to associate a level of confidence (p-value) for each of the differences. Progenesis SameSpots also details t-test scores between sample sets to determine the expected proportion of false positives if the features p-value is chosen as the significant threshold.

The spots with statistically significant changes in protein expression (±1.2 fold with p-value <0.05) were considered as differentially expressed proteins. These differentially expressed proteins observed using Progenesis SameSpots were designated "proteins of interest" and placed in a pick-list to pick from a preparative gel with the ETTAN Spot Picker (GE Healthcare) for identification using LC-MS/MS.

Preparative gels for spot picking with 300 µg of protein/gel were focussed and run out on SDS-PAGE gels. The gels were then stained with colloidal Coomassie (section 2.4.8). Spots that showed differential protein expression were picked with the ETTAN Spot Picker (section 2.4.10).

2.4.8 Brilliant Blue G Colloidal Coomassie Staining

After electrophoresis, plates attached to the preparative gels were placed in boxes containing fixing solution (7% glacial acetic acid in 40% (v/v) methanol) for at least one hour. During this step, a 1X working solution of Brilliant Blue G colloidal coomassie (Sigma, B2025) was prepared by adding 800 mL UHP to the stock bottle. Following the fixing step, a solution containing 4 parts of 1X working colloidal coomassie solution and 1 part methanol was made, mixed by vortexing for 30 seconds and then placed on top of the gels. The gels were left to stain for 2 hours. To destain, a solution containing 10% acetic acid in 25% methanol was poured over the shaking gels for 60 seconds. The gels were then rinsed with 25% methanol for 30 seconds and then destained with 25% methanol for 24 hours.

2.4.9 Other Staining Methods

2.4.9.1 Silver staining

After 2-DE, plates attached to the preparative gels were placed into a box containing fixing solution (50 mL ethanol, 12.5 mL acetic acid (Lennox) and 62.5 mL UHP).

The gel boxes were placed on an orbital shaker and fixed for at least 1 hour (usually overnight). After fixing, the solution was drained from the gels. The gels were then washed three times with 150 mL of UHP for 5 minutes each time and drained. The gels were next sensitised (60 mL ethanol, 13.6 g sodium acetate, 0.4 g sodium thiosulfate and UHP in 200 mL) for 30 minutes on the orbital shaker.

Following this, the gels were washed three times, for 10 minutes each. Following the washes, 200 mL of silver staining solution (0.5 g silver nitrate, 80 µL formaldehyde and 200 mL UHP) was added and the boxes returned to the orbital shaker. After 20 minutes the silver solution was drained and the gels were washed twice for 5 minutes each with UHP water. After the last wash, 200 mL of developer (5 g sodium carbonate, 40 µL formaldehyde and 200 mL UHP) was added to each of the boxes. The gels were placed on the orbital shaker and allowed to develop. When the desired amount of spots appeared, the developer was drained into the silver-containing 5 L drum (this precipitated out the silver) and 200 mL of stopping solution (2.92 g EDTA and 200 mL UHP) was added. The gels were left on the orbital shaker for at least 10 minutes. The gels could then be stored in UHP water.

2.4.10 Spot picking

The glass surface of the gel plate was dried and two reference markers (GE Healthcare, 18-1143-34) were attached to the underside of the glass plate before scanning at 300 dpi resolution using a flatbed image scanner (GE Life Sciences). The resulting image was imported into the ImageMaster software (GE Healthcare) and the spots were detected, normalised and the reference markers selected. While keeping the shift key depressed, all spots of interest were manually selected. The resulting image was saved and exported into the Ettan Spot Picker software (GE Healthcare). The stained gel was placed in the tray of the Ettan Spot Picker (GE Life Sciences, 18-1145-28) with reference markers aligned appropriately and covered with UHP. The imported pick list was opened, the syringe primed and the system was set up for picking the spots from the pick list. The spots were robotically picked and placed in 50 µL of LC-MS grade water (Fluka, 14263) in polypropylene 96-well plates (Greiner Bio One, 651201) and covered in parafilm, and stored at 4 °C until gel destaining which is outlined in section 2.6.1.

2.5 Excision of Protein Bands from 1-D Gels

The gel was placed on a piece of parafilm which had been swabbed with 70% methanol. The work surface had also been cleaned with 70% methanol. Each lane of the gel was sliced into thin sections, across the width of the lane, using a scalpel and cut into six smaller pieces. The pieces from each band were placed into individual wells of a polypropylene 96-well plate (Greiner Bio One, 651201) with 50 µL of LC-MS grade water in each. The plate can then be stored at 4 °C, covered in parafilm, or the proteins can be destained as described in section 2.6.1.

2.6 Identification of proteins with LC–MS/MS

2.6.1 Destaining Gel Plugs

2.6.1.1 Coomassie-Stained Gel Pieces

Gel pieces were washed three times in a 96-well polypropylene plate using 100mM ammonium bicarbonate/acetonitrile (1:1, vol/vol) for 10 minutes each until the pieces were fully destained.

2.6.1.2 Silver-Stained Gel Pieces

Gel pieces were destained in a 96-well polypropylene plate using 100 mM sodium thiosulfate/30 mM potassium ferricyanide (1:1, vol/vol) and incubated for 30 minutes until the pieces are fully destained.

2.6.2 In-Gel Digestion of Proteins

50 µL of neat acetonitrile was then added to each well at room temperature until the plug becomes dehydrated, i.e. white and shrunken. The acetonitrile was removed and the gel pieces were dried. 50 µl of 10 mM DTT in 100 mM ammonium bicarbonate was added to cover the gel piece and incubated for 30 minutes at 56 °C. The DTT solution was removed and the gel pieces were cooled to room temperature. Once cooled, 50 µL of neat acetonitrile was added to each gel piece until they became dehydrated again. The acetonitrile was removed and 50 µL of 55 mM iodoacetamide in 100 mM ammonium bicarbonate was added. The gel pieces were then incubated for 20 minutes in the dark at room temperature. 50 µL of neat acetonitrile was added to each gel piece at room temperature to dehydrate them. After drying, the individual

gel pieces were rehydrated in 10 µL digestion buffer. The digestion buffer was made fresh and consisted of 12.5 ng sequence-grade trypsin (Promega, V5111) (a 100 µg vial of trypsin was dissolved in 100 µL of 50 mM acetic acid and stored in 10 µl aliquots at -20 °C) per µL of 10% acetonitrile, 40 mM ammonium bicarbonate. Sufficient buffer was added to cover the dried gel pieces and the plate was stored at 37 °C for 30 minutes. After this time, the pieces were checked to ensure that the buffer was absorbed and if more needed to be added. The gel pieces were left for another 90 minutes to saturate them with trypsin and then an additional 10-20 µL of ammonium bicarbonate buffer was added to cover the gel pieces and maintain moisture for the digestion.

Exhaustive digestion was carried out overnight at 37 °C. Peptides were extracted from the gel pieces twice using 50 µL of 1:2 (vol/vol) 5% TFA in acetonitrile (made fresh daily) for 15 minutes each time at 37 °C with gentle agitation. The extracted peptides were transferred to a new 96 well plate and lyophilised using a Maxi Dry Plus vacuum (MSC). The plate were then stored at -20 °C, wrapped in parafilm, or the proteins were resuspended in 20 µL of 0.1% TFA containing 0.1% acetonitrile and analysed using mass spectrometry.

2.6.3 Digestion of Proteins for Quantitative Label-Free LC-MS/MS Analysis

100 µg of protein from the sample of interest (determined by Quick Start Bradford assay) was placed into an eppendorf and the protein was precipitated using a 2-D-clean-up kit (Bio-Rad, 163-2130), overnight in acetone. The protein pellet was resuspended in 6M Urea, 2M Thiourea, 10mM Tris, pH 8. 0.4% ProteaseMAX (Promega, V2071), a surfactant and trypsin enhancer added to improve protein solubility. The sample was sonicated and vortexed to ensure complete suspension.

A Quick Start Bradford assay was performed and 5 µg of protein was transferred into a new eppendorf. 1 µL of reduction buffer was added to the sample (100 mM DTT in 50mM ammonium bicarbonate), vortexed and incubated at 56 ºC for 30 minutes. 1 µL of alkylation buffer was added to the sample (300 mM iodoacetamide in 50 mM ammonium bicarbonate), vortexed and incubated for 20 minutes at room temperature in the dark. 0.5 µL of 1% ProteaseMAX and Lys-C (Promega, V1071), added at a ratio of 1:50 (enzyme:protein), were added and the mixture was incubated for 1 hour at 37 ºC. Samples were diluted with four volumes of 50 mM ammonium bicarbonate

to dilute the urea concentration to below 1 M and sequence grade trypsin (Promega, V5111) was added at a ratio of 1:25 (enzyme:protein) and incubated overnight at 37 ºC, after which the reaction was stopped by adding 50% TFA in LC-MS grade water at a ratio of 1:25.

Samples were then cleaned up using PepClean C18 spin columns (Thermo, 89870), dried under a vacuum and stored at −20 °C until use.

The resulting lyophilised peptides were re-suspended in 0.1% TFA in 2% acetonitrile with agitation and sonication. 1 µg of sample was then analysed by LC-MS/MS.

2.6.4 Mass Spectrometry using LC/MS Analysis

Nano LC–MS/MS analysis was carried out using either an Ultimate 3000 nanoLC system (Dionex) coupled to either a hybrid linear ion trap/Orbitrap mass spectrometer (LTQ Orbitrap XL; Thermo Fisher Scientific) for quantitative analyses or Hybrid linear ion trap mass spectrometer (LTQ XL; Thermo Fisher Scientific) for qualitative analyses.

A 5 µL injection of digested sample were picked up using an Ultimate 3000 nanoLC system (Dionex) autosampler using direct injection pickup onto a 20 µL injection loop. The sample was loaded onto a C18 trap column (C18 PepMap, 300 µm ID × 5 mm, 5 µm particle size, 100 Å pore size; Dionex) and desalted for 10 min using a flow rate of 25 µL/min in loading buffer (0.1% TFA, 2% acetonitrile). The trap column was then switched online with the analytical column (PepMap C18, 75 µm ID × 250 mm, 3 µm particle and 100 Å pore size; (Dionex)) using a column oven at 35 °C and peptides were eluted with the following binary gradients of:

30 minute reverse phase gradient

Mobile phase buffer A (0.1% formic acid in 2% acetonitrile) and Mobile phase buffer B (0.08% formic acid in 80% acetonitrile): 0–100% solvent B in 30 minutes where solvent A consisted of 2% acetonitrile (ACN) and 0.1% formic acid in water and solvent B consisted of 80% ACN and 0.08% formic acid in water. Column flow rate was set to 350 nL/min. This method was used for all qualitative analysis of proteins extracted from gel pieces.

60 minute reverse phase gradient

Mobile phase buffer A (0.1% formic acid in 2% acetonitrile) and Mobile phase buffer B (0.08% formic acid in 80% acetonitrile): 0–50% solvent B in 50 min and 50–100% solvent B in a further 10 min, where solvent A consisted of 2% acetonitrile (ACN) and 0.1% formic acid in water and solvent B consisted of 80% ACN and 0.08% formic acid in water. Column flow rate was set to 350 nL/min. This method was used for the quantitative label-free LC-MS analysis of proteins differentially expressed between monosomy three and disomy three fractionated vitreous fluid, section 4.9.

180 minute reverse phase gradient

Mobile phase buffer A (0.1% formic acid in 2% acetonitrile) and Mobile phase buffer B (0.08% formic acid in 80% acetonitrile): 0–25% solvent B in 120 min and 25–50% solvent B in a further 60 min, where solvent A consisted of 2% acetonitrile (ACN) and 0.1% formic acid in water and solvent B consisted of 80% ACN and 0.08% formic acid in water. Column flow rate was set to 350 nL/min. This method was used for the quantitative label-free LC-MS analysis of proteins differentially expressed between healthy and advanced melanoma fractionated sera, section 5.4.

Data were acquired with Xcalibur software, version 2.0.7 (Thermo Fisher Scientific). The Hybrid linear ion trap/Orbitrap mass spectrometer (LTQ Orbitrap XL; Thermo Fisher Scientific) was operated in data-dependent mode and externally calibrated.

Survey MS scans were acquired in the Orbitrap in the 400–1800 *m*/*z* range with the resolution set to a value of 30,000 at *m*/*z* 400. Up to three of the most intense ions (1+, 2+ and 3+) per scan were CID fragmented in the linear ion trap. A dynamic exclusion was enabled with a repeat count of 1, repeat duration of 30 seconds, exclusion list size of 500 and exclusion duration of 40 seconds. The minimum signal was set to 500. All tandem mass spectra were collected using a normalised collision energy of 35%, an isolation window of 2 *m*/*z*, activation Q was set to 0.250 with an activation time of 30.

The Hybrid linear ion trap mass spectrometer (LTQ XL; Thermo Fisher Scientific) was operated in data-dependent mode. Survey MS scans were acquired in profile

mode at 400–1800 *m*/*z* range. Up to sixteen of the most intense ions (1+, 2+ and 3+) per scan were CID fragmented in the linear ion trap. A dynamic exclusion was enabled with a repeat count of 2, repeat duration of 30 seconds, exclusion list size of 500 and exclusion duration of 40 seconds. The minimum signal was set to 500. All tandem mass spectra were collected using a normalised collision energy of 30%, an isolation window of 2 *m*/*z*, activation Q was set to 0.250 with an activation time of 30.

2.6.5 Identification of Proteins from Mass Spectrometry Data

Mass spectrometry data, generated as *.RAW files from LTQ XL and Orbitrap instruments, was analysed using the search algorithm TurboSequest (Thermo Fisher Scientific) through Bioworks Browser version 3.3.1 (Thermo Fisher Scientific) for qualitative analyses and the MASCOT (v2.3.01, Matrix Science, London, UK) search algorithm for quantitative analyses. In both cases, the human fasta database was downloaded from UniProKB/SwissProt (January 2013) ftp://ftp.uniprot.org/pub/databases/uniprot/current_release/knowledgebase/complete

The MASCOT search parameters that were used allowed two missed cleavages, fixed modification of cysteine (carbamidomethyl-cysteine) and variable modification of methionine (oxidised). Peptide tolerance depended on the instrument used to acquire the mass spectrometry data, in this case the Hybrid linear ion trap/Orbitrap mass spectrometer used a peptide tolerance of 20 ppm. The MS/MS tolerance was set at 0.6 Da. On completion of the database search the peptide results were filtered using MASCOT criteria of 95% confidence interval (C.I.) threshold ($p<0.05$), with a minimum ion score of ≥ 40. Protein identifications were accepted if they had one matched peptide.

The following TurboSequest filters were applied following database searches: for charge state 1, $X_{Corr} > 1.8$; for charge state 2, $X_{Corr} > 2.0$; for charge state 3, $X_{Corr} > 2.5$, a peptide probability of 0.05 and a delta CN of 0.1. Protein identifications were accepted if they had at least two matched identified peptides.

2.6.5.1 Bioworks Browser

Bioworks Browser was used in the analysis of all qualitative identifications. Outputs from the analytical software illustrated the protein accession code, number of matched peptides, and per cent coverage. The protein accession number represents the UniProtKB/Swiss-Prot protein code. Number of peptides matched refers to the number of identified peptides which correspond to the protein. The per cent coverage represents the percentage of the protein's sequence represented by the peptides identified. The Xcorr score (XC) represents the cross correlation value from the search; that is the degree of how well theoretical spectra match to observed spectra. XC values are higher for well-matched, large peptides.

2.6.5.2 Progenesis LCMS

The resulting total ion chromatograms (TIC) of quantitative label-free LC-MS data were subjected to statistical analysis using Progenesis LC-MS software (NonLinear Dynamics). This programme imports all runs in an "ion intensity map" format which maps the ions discovered in the run, by plotting retention time against the mass/charge ratio. All ion maps may be aligned against one reference run which allows for any shift in retention time between runs. The intensity of each ion may then be compared against that of all other runs, thus generating quantitative data on patterns of differential expression between sample sets which may be analysed with statistical analysis tools such as ANOVA, and principal component analysis.

For all experiments, unless stated otherwise, all peptides, and all proteins demonstrated ANOVA scores of ≤ 0.05 for differential analysis between sample sets.

For all quantitative LC-MS/MS data, Progenesis provides the following information; protein accession number, peptide count, number of peptides matched, confidence score, an ANOVA value, the maximum fold change, and the average normalised abundance. The protein accession number represents the code corresponding to the protein in the UniProtKB/Swiss-Prot protein database. "Peptide count" refers to the number of peptides identified and "number of peptides matched" refers to the number of peptides which were matched to the protein. The MASCOT score (or ion score) is calculated from the combined scores of how well each peptide matches to the protein sequence. The significance of the differential expression between the two

groups is represented by an ANOVA score (p-value). The fold change, or average ratio, illustrates the greatest fold different in protein ion abundance between the two groups. The average normalised abundance is calculated from the sum of all peptide abundances from every run for each protein.

2.7 Western blot Analysis

2.7.1 1-D Gel electrophoresis

Proteins for analysis by Western blotting were resolved using 4-12% NuPAGE Bis-Tris Gels (Life Technologies, NP0322PK2) in XCell SureLock™ Mini-Cell (Life technologies, EI0001) running instrument. Western blotting protein samples (2 μg/μL) were prepared by diluting samples with PBS and then an equal volume of 2X loading buffer (Sigma, S3401). The samples were heated at 95 °C for 5 minutes and placed on ice prior to being centrifuged. 10-40 μg of protein and 5μL of molecular weight marker (Thermo, 26634) were loaded onto gels. The samples were electrophoretically separated at 200 V and 45 mA using a 1X MOPS/SDS running buffer (Life Technologies, NP001) until the bromophenol blue dye reached the bottom of the gel.

2.7.2 Western blotting

Once electrophoresis had been completed, the gel was equilibrated in a 1X tris-glycine transfer buffer (Bio-Rad, 161-0734) containing 20% methanol for approximately 10 minutes. Five sheets of Whatman 3 mm filter paper (Whatman, 1001824) were soaked in freshly prepared transfer buffer. These were then placed on the cathode plate of a semi-dry blotting apparatus (Bio-Rad). Air pockets were then removed from between the filter paper. PVDF membrane (GE Healthcare, 10600021), which had been equilibrated in the same transfer buffer, was placed over the filter paper on the cathode plate. Air pockets were once again removed. The gels were then aligned onto the membrane. Five additional sheets of transfer buffer-soaked filter paper were placed on top of the gel, all air pockets removed and excess transfer buffer removed from the cathode plate. All proteins were transferred from the gel to the membrane at a current of 340 mA at 15 V for 23 minutes (FABP3 was

transferred under the same conditions for 20 minutes), until all colour markers had transferred.

Following protein transfer, membranes were stained using Ponceau (Sigma, P7170) to ensure efficient protein transfer. The membranes were then blocked for two hours using 5% Marvel (Cadburys; Marvel skimmed milk) in TBS-T (a mixture of 1X tris-buffered saline (TBS) (Sigma, t5912) containing 0.05% Tween 20 (Sigma, P5927)). The membranes were washed with TBS-T prior to the addition of the primary antibody, prepared in 5% Marvel in TBS-T at recommended dilutions, and then incubated overnight at 4 °C. The membranes were then rinsed 3 times with TBS-T for a total of 30 minutes. Relevant secondary antibody (1/2000 dilution of anti-mouse (Dako Cytomation, P0260) or anti-rabbit (Dako Cytomation, P0448) or anti-goat (Santa Cruz Biotechnology, Sc2098) IgG peroxidase conjugate in 5% Marvel/TBS-T) was added for 2 hours at room temperature. The membranes were again washed three times thoroughly in TBS-T for 30 minutes.

All primary and secondary antibodies used are shown in Tables 2.3 and 2.4.

Antibody	Dilution	Details
TPI1	1:4000	Genetex, GTX104618
FABP3	1 µg/µL	Abcam, ab45966
EEF1G	3 µg	Abnova, H00001937
SELENBP1	1 µg/µL	Abcam, ab90135
KPNB1	1:1000	Pierce, PA-18450
PRDX3	1:1500	Genetex, GTX82299
CNDP2	1:2000	Pierce, PA5-30694
ApoAII	1:250	Invitrogen, 701236
GAPDH	1:2000	Abcam, ab8245

Table 2.3 Primary antibodies and dilutions

Antibody	Dilution	Details
Anti-Rabbit	1:2000	Dako, P0448
Anti-Mouse	1:2000	Dako, P0447
Anti-Goat	1:2000	Dako, P044901-2

Table 2.4 Secondary antibodies and dilutions

2.7.3 Enhanced chemiluminescence detection using autoradiographic films

Immunoblots were developed using an enhanced chemiluminescence (ECL) kit (GE Life Sciences, RPN2106), which facilitated the detection of bound peroxidase-conjugated secondary antibody. Following the final washing, membranes were subjected to ECL. The membrane was placed on a sheet of transparent plastic and 3 mL of a freshly prepared 1:1 (v/v) mixture of ECL reagent A and B was used to cover the membrane. The ECL reagent mixture was completely removed after a period of five minutes and the membrane was covered in a layer of transparent plastic. All excess air bubbles were removed. The membrane was then exposed to autoradiographic film (GE Life Sciences, 95017-681) for various times (from 10 seconds to 15 minutes depending on the intensity of the signal). The exposed autoradiographic film was developed for 3 minutes in developer solution (Kodak, LX24, diluted 1:5 in water). The film was then washed in water for 15 seconds and transferred to a fixative solution (Kodak, FX-40, diluted 1:5 in water) for 5 minutes. The film was washed with water for 5-10 minutes and left to dry at room temperature.

2.8 RNA Interference

RNAi using small interfering RNAs (siRNAs) was carried out to silence the *FABP3*, *TPI1*, *EEF1G*, *SELENBP1*, and *KPNB1* genes. Two independent siRNA molecules were used for each protein (Applied Biosystems). These siRNAs were 21-23 bps in length and were introduced to the cells via reverse transfection with Lipofectamine RNAiMAX Transfection Reagent (Life Technologies, 13778150).

2.8.1 Transfection optimisation

In order to determine the optimal conditions for siRNA transfection, optimisation with kinesin siRNA (Life Technologies, 16704) was carried out for the 92.1 and MEL202 cell lines.

Cell suspensions were prepared at $5X10^4$, 7.5 X 10^4, 1X 10^5, 2.5 X 10^5, and 5 X 10^5 cells per well. Solutions of negative control and kinesin siRNA at a final concentration of 50 nM were prepared in optiMEM (GibcoTM, 31985047)**.** Lipofectamine RNAiMAX solutions at a range of concentrations were added the solutions and was mixed well and incubated for 12 minutes at room temperature. 100 µL of the siRNA/lipofectamine solutions were added in a dropwise fashion to each well of a 6-well plate, of which each well contained 1 mL of a cell suspension. The plates were mixed gently and incubated at 37 °C for either 6 hours or overnight (depending on the cell line). After this time, the transfection mixture was removed from the cells and the plates were fed with fresh serum-containing medium. The plates were assayed for changes in proliferation at 72 hours using the acid phosphatase assay (Section 2.9). Optimal conditions for siRNA transfection were determined as the combination of conditions, which gave the greatest reduction in cell number after kinesin siRNA transfection and also the least cell kill in the presence of transfection reagent. Western blot analysis was used to establish the optimum conditions for a siRNA transfection. The optimised conditions for the cell lines are shown in Table 2.5.

Cell Line	siRNA Concentration (nM)	RNAiMAX Lipofectamine Volume (µL)	Cell Number
92.1	20	5.4	$7.5X10^4$
MEL202	20	5.4	$1X10^5$

Table 2.5 Optimised conditions for the siRNA transfection of 92.1 and MEL202 cell lines.

2.8.2 siRNA Functional Analysis of Targets of Interest

Two pre-designed siRNAs were chosen for the protein/gene targets and transfected into cells. In some cases two siRNAs were sufficient, however multiple siRNA were usually tested.

For each set of siRNA transfections carried out, control, non-transfected cells and a scrambled siRNA transfected negative control were used. Scrambled siRNA are sequences that do not have homology to any genomic sequence. The scrambled non-targeting siRNA used in this study is commercially produced, and guarantees siRNA with a sequence that does not target any gene product. It has also been functionally proven to have no significant effects on cell proliferation, morphology and viability.

For each set of experiments investigating the effect of siRNA, the cells transfected with target-specific siRNAs were compared to cells transfected with scrambled siRNA. This took account of any effects due to the siRNA transfection procedure, reagents, and also any random effects of the scrambled siRNA. Western blots were used to determine if siRNA had an efficient knock-down effect at a protein-level.

All siRNA used in these experiments are shown in Table 2.6.

Targeted Gene	siRNA Details
KPNB1	Ambion; s7919, s7917
EEF1G	Ambion; s4488, s60392
SELENBP1	Ambion; s17151, s17152
FABP3	Ambion; s4973, s4974
TPI1	Ambion; s14339, s224747
PRDX3	Ambion; s21507, s21508
Scrambled (Negative Control)	Ambion; 4390843
Kinesin	Ambion; 14851

Table 2.6 siRNA used in uveal melanoma cell line transfections

2.9 Acid Phosphatase Assay

Following an incubation period of 96 hours, media was removed from the plates. Each well on the plate was washed twice with 2 mL PBS. This was then removed and 2 mL of freshly prepared phosphatase substrate (10 mM p-nitrophenol phosphate

(Sigma 104-0) in 0.1 M sodium acetate (Sigma, S8625), 0.1% triton X-100 (Sigma, X100), pH 5.5) was added to each well. The plates were then incubated in the dark at 37 °C for 2 hours. Colour development was monitored during this time. The enzymatic reaction was stopped by the addition of 1 mL of 1 M NaOH. The plate was read in a dual beam plate reader at 405 nm with a reference wavelength of 620 nm.

2.10 Proliferation assays on siRNA transfected cells

As described, cells were seeded using 5.4 μL RNAiMAx Lipofectamine to transfect 20 nM siRNA in a cell density of either $1X10^5$ or $7.5X10^4$ per well of a 6-well plate. After either 6 hours or overnight, the transfection medium was replaced with fresh media and cells were allowed to grow until they reached 80-90% confluency; a total of 96 hours. Cell viability was assessed using the acid phosphatase assay (section 2.9). All experiments were carried out independently at least three times.

2.11 Invasion assay

2.11.1 Preparation of invasion chambers

Invasion assays were carried out in Boyden chambers (8 μm pore size) (BD Biosciences, 35309) which were coated in 100 μL of matrigel (BD Biosciences, 734-1100) diluted to 1 mg/mL in serum-free RPMI-1640 and incubated over-night at 4 °C. Cell suspensions were prepared in serum-free basal media. 750 μL of complete media was added to the lower chamber of the insert in the 24-well plate. A volume of 500 μL of the cell suspension was then added into the insert. The invasion assays were then incubated for 48 hours at 37 °C and 5% CO2.

2.11.2 Staining of invasive cells

After incubation, the non-invading cells were removed by wiping the inner side of the insert with a PBS-soaked cotton swab (Johnson and Johnson). The outer side of the insert was then stained with 0.25% crystal violet for 10 min. Excess stain was rinsed off the inserts with sterile water and allowed to dry.

2.11.3 Counting of invading cells

To determine the total number of invading or migrating cells, the number of cells/field in 15 fields was counted at 200x magnification. The average number of cells per field was then multiplied by a conversion factor of 140 (growth area of membrane divided by field of viewed area at 200x magnification (calibrated using a microscope graticule)). All assays were subjected to statistical analysis using Student's t-tests (2-tailed, 2-sample unequal variance).

2.12 Migration Assays

Migration assays were carried out using an identical protocol to that of section 2.11 except that uncoated 8 μm inserts were used.

2.13 Apoptosis and FACS

The effect of SELENBP1, EEF1G and KPNB1siRNA-mediated knockdown on apoptosis in the 92.1 uveal melanoma cell line was assessed by Annexin-V/7-AAD-positive staining. Following detachment, cells were stained using PE Annexin V Apoptosis Detection Kit I (BD Pharmingen, 559763) according to manufacturer's instructions and analysed via flow cytometry (BD FACSAria, Ox, UK). Photomultiplier tube (PMT) voltages were set as described (Table 2.7) and a compensation matrix determined using single colour stained controls (Table 2.8). The percentage of early apoptotic (Annexin V positive only) and late apoptotic/dead (Annexin V and 7-AAD positive) cells were compared to those of the scramble control.

PMT detector	Data collection	Voltage
FSC (forward scatter)	Linear	280
SSC (side scatter)	Linear	360
PE	Logarithmetic	310
PerCP-Cy5.5	Logarithmetic	480

Table 2.7 Flow cytometer settings for apoptosis Annexin-V/7AAD assay. Linear scales were used to collect forward and side scatter signals while logarithmetic scales were applied for detection of fluorescent PE and PerCP-Cy5.5 signals.

Fluorochrome	-% Fluorochrome	Spectral overlap
PerCP-Cy5.5	PE	74.89
PE	PerCP-Cy5.5	1.0

Table 2.8 Flow cytometer compensation matrix for apoptosis Annexin-V/7AAD assay.

2.14 Analysis of Reactive Oxygen Species (ROS)

92.1 cells were transfected with two independent SELENBP siRNA as described previously and set up at $1X10^5$ cells/well in a 24-well plate with at least two wells per condition. After overnight incubation, the medium was removed and the cells were washed in PBS. Half of the wells were exposed to 5 μM DCFDA (Sigma, cat 21884) in DMSO (Sigma, cat D2438) and diluted into HBSS (Invitrogen, cat 14025-050), the remaining wells were exposed to HBSS (this allows for background fluorescence to be taken into account). The cells were exposed to DCFDA for 15 minutes and then washed twice with PBS to remove un-incorporated DCFDA. The cells were fed with RPMI-1640 medium containing 1% FCS and incubated for 2 hours at 37 ˚C after which time the cells were washed twice with PBS and read on a fluorescent plate reader with excitation of 485 nm and emission of 528 nm. Sodium selenite was used as a pro-oxidant control and Trolox (Sigma, cat 238813) as an anti-oxidant control. siRNA transfected cells and controls were exposed to 200 μM hydrogen peroxide (Sigma, cat H1009) during the 2 hour incubation in order to observe ROS. The wells incubated with HBSS alone were used subtracted from the wells exposed to DCFDA for each condition.

2.15 Zymography

Serum-free conditioned media was collected from $1.5X10^5$ 92.1 and $2X10^5$ MEL202 cells which were transfected with siRNA against SELENBP, EEF1G, and KNPB1. Samples were mixed 1:1 with 2X Tris-Glycine SDS sample buffer (Serva, 42528.01) and were loaded onto the gel. A 5 μl aliquot of molecular weight marker (Thermo, 26634) was also loaded onto the gel. The gelatin gels (Invitrogen, EC6175BOX) were run at 30 mA per gel in 1X Tris-Glycine SDS running buffer (Life Technologies, LC26755) until the dye front reached the bottom of the gel. After

electrophoresis, gels were soaked in renaturing buffer (Life Technologies, LC2670) at room temperature with gentle shaking for 30 min. The gels were then incubated in developing buffer (Life Technologies, LC2671) for 30 minutes after which time the buffer was decanted and fresh developing buffer was added. The gels were stored at 37 °C overnight. The following day, the gels were stained with Coomassie as described in section 2.4.8. Gelatinase activity was illustrated as distinct, clear bands.

2.16 Immunodepletion

Immunodepletion of serum was performed using Multiple Affinity Removal Column Human-14 (Agilient, 5188-6560) according to the manufacturer's instructions.

2.17 ProteoMiner

2.17.1 Sequential Elution

ProteoMiner sample enrichment was performed using a ProteoMiner sequential elution kit (Bio-Rad, 163-3010). The small capacity kit was used in which 200 µL of serum was added to the column. After following a standard protocol, four elution fractions were acquired per sample (each elution buffer is outlined in Table 2.9) and the protein from each was precipitated overnight using a 2-D clean-up kit (Bio-Rad, 163-2130). The resulting protein pellets were resuspended in 6 M urea, 2 M thiourea, 10 mM tris (pH 8) and stored at -80 °C until further analysis.

	Buffer Constituents	Buffer Properties
Elution Reagent 1	1 M Sodium chloride 20 mM HEPES	Disrupts ionic interactions
Elution Reagent 2	200 mM Glycine	Disrupts hydrogen bond/hydrophobic interactions
Elution Reagent 3	60% Ethylene Glycol in Water	Disrupts mildly hydrophobic interactions
Elution Reagent 4	33.3% 2-Propanol 16.7% Acetonitrile 0.1% Trifluoroacetic Acid	Disrupts hydrophobic interactions

Table 2.9 ProteoMiner sequential elution buffers and their corresponding chemical properties.

2.17.2 Modified ProteoMiner Protocol for Vitreous Fluid Treatment

As the vitreous fluid specimens to be analysed were neither sufficiently concentrated nor plentiful, it was decided to modify the process of ProteoMiner treatment. This involved resuspending the resin in each column in 200 µL of wash buffer, and mixing each well by vortexing. 100 µL of resin was then immediately removed from each unit. This would reduce the volume of settled beads from 20 µL to 10 µL, This would also change the optimal sample volume to 100 µL, which provides the correct sample to beads ratio of 10:1. The adjusted protocol allowed for 300 µg of protein to be loaded onto the beads, which was present in the vitreous samples.

Following this, the ProteoMiner protocol was adjusted to account for the lower bead volume although all of the reagents supplied with the kit (Bio-Rad, 163-3006) were utilised. Briefly, 100 µL of wash buffer was applied to the resin and incubated for five minutes while rotating. The buffer was then removed by centrifugation at 1000 g for 30 seconds following the removal of both caps. The bottom cap was reapplied and 100 µL of sample was added to the resin bed. The top cap was then replaced and the unit was allowed to rotate for a total of two hours incubation time at room temperature. Both caps were removed and unbound sample was discarded by centrifuging the tube at 1000 g for 30 seconds. 100 µL of wash buffer was applied to the resin and the tube caps were replaced prior to rotating the column for five

minutes. The buffer was then removed by centrifugation as before and the wash step was repeated. 100 µL of deionised water was added to the sealed tube and the column was rotated for one minute. The water was then removed by centrifugation as before and the column was resealed. 10 µL of rehydrated elution reagent was added to the column and the top cap was replaced prior to lightly vortexing the tube for five seconds. The elution buffer and resin were allowed to incubate for 15 minutes, during which time the tube was lightly vortexed several times. The elution fraction was collected into a clean eppindorf tube by centrifugation at 1000 g for 30 seconds. The elution step was repeated twice and all elutions were then pooled and stored at -20 °C until use.

2.18 Enzyme-Linked Immunosorbent Assay (ELISA)

The majority of ELISAs performed for validation of cutaneous melanoma biomarker targets were sandwich ELISAs. These 96-well plates come with capture antibody precoated to the surface of the wells. Protein standards that come with the kit were prepared and along with serum samples at a kit specific dilution are added to the wells, with the standards in duplicate and a proportion of the serum samples in duplicate and triplicate. After incubation the plate was washed to remove any unbound antigen. An enzyme-linked detection antibody was added which binds specifically to the antigen. After another incubation period the plate was washed to remove any unbound detection antibody.

A competitive ELISA involves the initial incubation of unlabelled primary antibody with serum. The samples, with the bound antibody/antigen complexes, were then added to an antigen coated well. The plate was washed so that unbound antibody is removed (the antibody/antigen complexes from initial incubation were removed).

For both types of ELISA, a substrate was added that was converted by the enzyme into a colour or fluorescent signal. This colour or fluorescence was measured at a wavelength recommended in the ELISA manual to determine the presence and quantity of the antigen. From the standard curve produced from the standards of known concentrations, the concentration of antigen present in the serum sample was determined and comparisons were be made between the various types of samples.

Standard protocols were followed for each ELISA. An overview of all ELISA used is shown in Table 2.10.

ELISA Target	Manufacturer	Product Code	Standard Curve Range	Sample Dilution	ELISA Type
Apolipoprotein A-II	AssayPro	EA5222-1	4, 1, 0.25, 0.063, 0.016, 0.004, 0 µg/mL	1:1000	Sandwich
Azurocidin	Cusabio	CSB-E09698h	500, 250, 125, 62.5, 31.2, 15.6, 7.8, 0 pg/mL	1:4	Sandwich
Plasma Serine Protease Inhibitor	Cusabio	CSB-EL021061HU	10, 5, 2.5, 1.25, 0.625, 0.312, 0.156, 0 ng/mL	1:1000	Sandwich
BACE-2	Cusabio	CSB-E11867h	10, 5, 2.5, 1.25, 0.625, 0.312, 0.156, 0 ng/mL	1:4.75	Sandwich
Lacotransferrin	AssayPro	EL2011-1	40, 20, 10, 5, 2.5, 1.25, 0.625, 0 ng/mL	1:50	Sandwich
Sertransferrin	AssayPro	ET2105-1	25, 6.25, 1.563, 0.391, 0.098, 0 µg/mL	1:2000	Competitive
TIMP-1	Sigma Aldrich	RAB0466	18000, 6000, 2000, 666.7, 222.2, 74.07, 24.69, 0 pg/mL	1:25	Sandwich
MMP-1	Sigma Aldrich	RAB0361	18000, 6000, 2000, 666.7, 222.2, 74.07, 24.69, 0 pg/mL	1:5	Sandwich

Table 2.10 Overview of conditions and details of ELISA used.

2.19 Luminex Multiplex Bead-Based Assays

A Luminex 12-plex cytokine/chemokine assay was performed according to Millipore Milliplex Map Kit protocol (Millipore). The assay quantified the levels of FGF2, IFNγ, TNFα, TGFα, MIP1α, IL-10, IL-15, IL-1α, IL-2, IL-6, IL-8, and IP10. Initially, the 96-well filter bottom plate was pre-wet by adding 200 µL assay buffer. The microparticles of the panel were pooled together and 25 µL of the diluted microparticle solution and 25 µL of sample and standards and controls were also added to the necessary wells. 25 µL assay buffer was added to all wells. Next the plate was incubated overnight at 4 ºC and next day washed three times with wash buffer. Afterwards, 50 µL of diluted biotin antibody was added to each well and incubated for 1 hour. The plate was then washed as described above and 50 µL of diluted Streptavidin-PE was added to each well and incubated for 30 minutes. All incubations were performed at room temperature on an orbital shaker set at 15 g. Finally, the plate was washed again with 100 µL of Sheath Fluid. The median relative fluorescence units were measured using the Luminex 100 analyzer (Luminex, Austin, TX, USA).

2.20 SELDI-ToF MS

2.20.1 Conditioned Media Preparation and Collection

Cells ($3X10^6$) were seeded in four biological replicates in T-175 cm^2 flasks and allowed to grow until 50-60% confluent. The cell-containing flasks were then washed three times with 10 mL of serum-free (SF) basal media and incubated in 15 mL of SF basal media for 60 minutes. After this time, cells were washed twice with SF basal media and 15 mL of fresh SF basal media was added to the cells and incubated for 72 hours. After such time, conditioned media was collected, centrifuged for 15 minutes at 250 g, and stored at –80 °C. At the time of analysis conditioned media was concentrated using 5,000 dalton (Da) molecular weight cut-off concentrators (Millipore, UFC 900524). A volume of 15 mL was concentrated to 500 µL by centrifuging at 1000 g at 4 °C.

2.20.2 Preparation of IMAC30 Chip Surface

IMAC30 array, 8-spot (Biorad, C730043) was activated by adding 5 µL of 100 mM $CuSO_4$ (Sigma, 2091198) to each chip surface for a total of 30 minutes (2x15 minute applications), and then rinsed with high-performance liquid chromatography grade water (Sigma, 39295). The copper ions were charged by applying 50 µL of 100 mM sodium acetate (Sigma, S8625) for 5 minutes. The chip was placed in a bioprocessor (Biorad) and washed twice with 300 µL of 250 mM sodium chloride containing 0.1% Triton X-100 (Sigma Aldrich, T9284). The protein sample was diluted in 300 µL of 250 mM sodium chloride containing 0.1% Triton X-100 and samples were applied to the spots of the array. The array was placed on a shaker and gently agitated for 90 minutes to allow for interaction with the array surface. After removing the sample, the array was washed x2 with 300 µL of 250 mM sodium chloride for 5 minutes, followed by a brief high-performance liquid chromatography grade water wash. 5 mg of Sinapinic acid (Biorad, C730078) solution was prepared by dissolving in 200 µL of 50% LC-MS grade acetonitrile (Sigma, 34967) containing 0.5% LC-MS grade trifluoroacetic acid (Sigma, 302031). After removing the array from the bioprocessor, a 0.8 µL aliquot of saturated sinapinic acid was added to the spots, allowed to dry and repeated.

2.20.3 Analysis of Protein Chip Array in SELDI TOF Reader

The IMAC-30 arrays were analyzed in a Ciphergen Series PBS-IIC ProteinChip® System, and time-of-flight (TOF) data was generated by averaging a total of 220 laser shots collected at a laser intensity of 200, a detector sensitivity of 8 and molecular mass range from 5–20,000 Da for low molecular weight range and 20,000-100,000 Da for high molecular weight range.

2.20.4 Analysis of Differential Expression of Proteins/Peptides

Molecular weights were calibrated externally using an all-in-1 protein standard (Biorad, N76006). All data was analyzed using Biomarker Wizards Software, version 3.1 (Bio-Rad). After automatic baseline noise correction, all of the spectra were normalized together by the ‘‘total ion content’’ method as described by the manufacturer, i.e. with an m/z between 5,000 and 100,000. The peaks with an m/z value <3000 were excluded, as these peaks were mainly ion noise from the matrix (sinapinic acid). Peak clusters were generated by automatically detecting qualified mass peaks with a signal to noise ratio (S/N) >5 in the first pass, completed with a second-pass peak selection of S/N >3, with a 0.3% mass error for 5000-20,000 Da, and the same for 20,000-100,000 Da. Statistically significant peaks were considered to be those with $p < 0.05$.

2.20.5 IMAC-Cu^{2+} Based Fractionation Using Imidazole

The uncharged IMAC resin (Bio-Rad, 156-0123) was mixed in order to thoroughly resuspend the resin. 200 µL was then transferred into an eppindorf tube containing a spin column with a 0.22 µm filter (Sigma, CLS8161-100EA). The resin was centrifuged at 1000 g for 15 seconds in order to pack the resin and then washed with 500 µL of distilled water. The centrifugation step was repeated. Following this, the resin was equilibrated with 500 µL of 50 mM sodium acetate, 0.3 M sodium chloride, pH4, and the column was centrifuged at 1000 g for 15 seconds. This step was repeated. 500 µL of a 0.2 M copper sulphate solution (of neutral to weakly acidic pH) was applied to the resin and removed by centrifugation. This step was repeated. The column was washed twice with 500 µL of 50 mM sodium acetate, 0.3

M sodium chloride, pH 4 prior to being washed twice with 500 µL of deionised water.

To pre-equilibrate the resin before sample binding, 500 µL of binding buffer was applied (50 mM sodium phosphate, 300 mM sodium chloride, 5 mM imidazole (Sigma Aldrich I0125), pH 8) and removed by centrifugation. This step was repeated. 2 mg of protein in a volume of ≤500 µL was added to the resin and mixed by pipetting up and down five times. It was then incubated for up to 15 minutes and centrifuged at 1000 g for one minute. This step was repeated by reloading the flow-through onto the resin bed. The unbound fraction was then collected. The spin column was placed into a new eppindorf and 500 µL of wash buffer (50 mM sodium phosphate, 300 mM sodium chloride, 20 mM imidazole, pH 8) was applied to the resin and mixed by pipetting up and down five times followed by centrifugation at 1000 g for one minute. This wash step was then repeated after which the fraction was collected. The column was placed into a new collection vessel and an elution buffer (50 mM sodium phosphate, 300 mM sodium chloride, 50 mM imidazole, pH 8) was applied, the fraction was collected as before. Following this, any number of elutions can be collected by increasing the concentration of the imidazole in the elution buffer to a maximum of 500 mM.

The protein present in the fractions was then precipitated by applying five volumes chilled acetone to each elution and storing at -20 °C overnight. The following day, the elution fractions were centrifuged at 14,000 rpm at 4 °C for 10 minutes and the acetone was removed from each sample. The resulting pellets were allowed to air dry for two minutes prior to being resuspended in 6 M Urea, 2 M Thiourea, 10 mM Tris, pH 8 and stored at -20 °C.

2.20.6 On-Chip Elution of IMAC Cu^{2+} -Bound Proteins

The SELDI chip surface was prepared and the appropriate specimen was allowed to bind, followed by a wash step as described in section 2.20.2. However, the matrix was not applied. Instead, an elution buffer (250 mM sodium chloride, 0.1% Triton X-100, 10 mM imidazole) was applied to the chip, and gently agitated for ten minutes in order to remove bound proteins. The elution was removed and the process was repeated using elution buffers containing 50 mM and 100 mM imidazole. The three

fractions were then treated with PepClean C-18 Spin Columns (Thermo, 89870) according to the manufacturer's instructions, and further analysed.

2.21 MALDI ToF Analysis

All experiments were carried out on an AB Sciex 4800 Plus analyser equipped with TOF/TOF ion optics and a diode pumped Nd:YAG laser with 200 Hz repetition rate. The MS/MS capabilities of the instrument are facilitated through a timed ion selector, a deceleration lens, a collision cell, and a second ion source. All the MS/MS spectra resulted from accumulation of at least 1600 laser shots. Air was used as the collision gas such that nominally single collision conditions were achieved. A wide mass window was utilized so that all the precursor ions could pass the gate to enter the collision. Generally, the width of mass window is set to 100 Da for precursor masses between 5000 Da and 9000 Da. MS/MS data were acquired using the instrument default calibration, without applying internal or external calibration. The digitizer, voltage and calibration parameters used are shown in Table 2.11.

Digitiser Settings	
Bin Size	2
Vertical Scale (V Full Scale)	0.5
Input Bandwidth (Mhz)	25
Detector Voltage Multiplier	0.9
Final Detector Voltage	1.971
Laser Intensity	5000
Voltage Settings	**kiloVolts (kV)**
Source 1	8
Source 2	15
Grid 1	7.293
Source 1 Focus	4.2
Source 1 Lens	3.2
Y1 Deflector	0.08
X1 Deflector	0
Y2 Deflector	0.048
X2 Deflector	0
Mirror 1	10.207
Mirror 2	17.77
Collision Cell	7
Deceleration stack	6.3
Lens 1	2.7

Table 2.11 Digitiser, laser intensity, and voltage settings for MALDI-TOF

2.22 Statistical Analysis

Patterns of differential protein abundance between disease and control groups were measured and, using statistical analysis, only the proteins which illustrated a significant difference between the groups were followed up. A two-tailed Student's t-test was utilised to determine if the protein fold changes observed were statistically significant. Protein changes with a p-value of ≤ 0.05 were considered statistically significant. Any keratin identifications which were discovered in protein lists were considered to be of little interest as this may be indicative of contamination and may not accurately reflect the proteome in question. Any outliers present in ELISA readings were determined using Tukey's method which considers values at a distance of 1.5 times the interquartile range (IQR) below Q1 (quartile one) or at 1.5 times the

IQR above Q3 (quartile three) to be possible outliers (Tukey 1977). Identified outliers were subsequently removed from the analysis.

CHAPTER THREE

Proteomic Analysis of Uveal Melanoma Tumour Tissue

3.1 Background

To date, only a very limited number of proteomic studies have been carried out investigating the biology of the metastatic phenotype of uveal melanoma. In addition to this, the majority of these studies have used cell line models, as outlined in section 1.2.4. It was hypothesised that patterns of differential protein expression would be observed between primary uveal melanoma tumour tissues of patients who subsequently developed metastasis versus those who did not. By examining differential protein expression patterns between these tumour tissue types, this may improve our understanding of the biology of uveal melanoma tumours. As few therapeutic targets currently exist for the treatment of metastatic disease, proteins which indicate prognosis may be developed as targeted therapies. In addition to this, protein biomarkers predicting metastatic uveal melanoma could (along with genetic analysis) improve interim monitoring of patients whose tumours are likely to metastasise.

The purpose of this study was to identify differentially expressed proteins in uveal melanoma tissue specimens from patients with a minimum of seven years clinical follow-up comparing those who developed metastases to those who did not. Only primary tumours specimens were used in this analysis as secondary tumour tissue was not available.

Nine subsequently metastasised and 16 non-metastasised primary tissue samples were compared using 2-D DIGE for the analysis of differential protein expression. This work was subsequently published with follow-up IHC analyses (Linge, Kennedy et al. 2012). In parallel, eight tumour tissue specimens from each group were compared using quantitative label-free LC-MS analysis. Identified proteins of interest from both studies were then followed up using functional analysis in cell line models.

3.2 Clinical Specimens Included in the Analysis

A total of 27 uveal melanoma primary tumour tissue specimens obtained by enucleation were included in a 2D-DIGE study carried out in collaboration with the Royal Victoria Eye and Ear Hospital, Dublin (RVEEH). These samples were

acquired from Prof. Susan Kennedy (RVEEH). The study was approved by the Research and Ethics Committee of the Royal Victoria Eye and Ear Hospital, Dublin and the research adhered to tenets of the Declaration of Helsinki. Ten of these specimens subsequently metastasised to regions such as the liver (six cases), lungs (two cases), kidney (one case) and both the liver and skin (one case). According to the Callender classification, of the tumours which metastasised, three were of the epithelioid cell type, four were of the spindle type and three were mixed.

Chromosome three status was available for 14 of the non-metastatic patients which showed disomy in 12 and trisomy in two cases. In eight out of the ten patients who developed metastasis, loss of heterozygosity for chromosome three was observed which is in agreement with previous studies, detailed in section 1.2.2., which correlate loss of heterozygosity of chromosome 3 with poor outcome.

25 of the samples were used in 2-D DIGE analysis while 16 were used in immunohistochemistry (IHC) analysis. This was due to the fact that this was intended to be a discovery-phase, pilot study and hence, eight samples from each group were chosen, see table 3.1 for details on the samples used.

				Clinical characteristics			Histopathological characteristics				
Sample ID	Sex	Age at diagnosis (years)	Follow-up time[†] (years)	Metastatic sites	Ciliary body involvement	Extrascleral extension	Cell type	LTD (mm)	No. of mitotic cells (per 40 HPF)	Chromosome 3 status	Study
1	F	49	**	Kidney	N	N	S	12	4	Monosomy	DIGE, IHC
2	F	51	1	Liver	N	N	E	15	4	Monosomy	DIGE, IHC
3	F	73	1	Liver	Y	N	E	10	1	Monosomy	DIGE, IHC
4	F	58	5	Liver	Y	N	M	15	0	Monosomy	DIGE, IHC
5	F	32	6	Liver	Y	Y	S	8	12	Disomy	IHC
6	F	49	5	Liver, Skin	N	Y	S	9	1	Monosomy	DIGE, IHC
7	M	71	2	Lung	N	N	M	11	16	Monosomy	DIGE, IHC
8	M	64	10	Lung	Y	N	M	10	12	Disomy	DIGE, IHC
9	F	69	11	Liver	N	N	S	12	16	Monosomy	DIGE
10	M	71	7	Liver	Y	Y	E	20	6	Monosomy	DIGE
11	F	52	12	N	N	Y	M	10	2	Disomy	DIGE, IHC
12	F	55	12	N	N	N	E	20	0	Disomy	DIGE, IHC
13	F	76	12	N	N	N	M	8	4	Disomy	DIGE, IHC
14	M	53	12	N	N	N	M	10	8	Trisomy	DIGE, IHC
15	F	42	11	N	N	N	S	17	1	Disomy	DIGE, IHC
16	M	68	9	N	Y	N	S	20	18	Disomy	DIGE, IHC
17	M	68	11	N	N	N	E	12	20	Trisomy	DIGE, IHC
18	F	64	10	N	N	N	E	8	8	Disomy	IHC
19	F	46	11	N	N	N	E	23	4	Disomy	DIGE
20	M	34	17	N	N	N	M	15	4	Disomy	DIGE
21	F	75	11	N	N	N	S	22	4	Disomy	DIGE
22	M	52	10	N	N	N	S	19	0	Disomy	DIGE
23	M	50	11	N	N	N	M	17	4	Disomy	DIGE
24	M	86	9	N	N	N	S	12	0	*	DIGE
25	M	62	9	N	N	N	S	8	4	*	DIGE
26	F	70	9	N	N	N	M	9	4	Disomy	DIGE
27	F	74	7	N	N	N	M	14	1	*	DIGE

Table 3.1 Clinical and histopathological features of the patients included in the 2D DIGE and immunohistochemical studies. Those which were labelled "DIGE, IHC" indicates that the sample was used in both studies. Those marked "DIGE" were only used in the DIGE study while those marked "IHC" were only used in the immunohistochemistry study. F, Female; M, Male; N, no; Y, yes; S, spindle cells; E, epitheloid cells; M, mixed cells; LTD largest tumour diameter; HPF, high power field; DIGE, two dimensional difference gel electrophoresis; IHC, immunohistochemistry.

3.3 Differential Protein Expression Analysis Between Non-Metastasised and Subsequently Metastasised Primary Tumour Tissue using 2-D DIGE

In order to extract protein from the tumour specimens, a sample grinding kit with lysis buffer was used. Protein lysates of uveal melanoma primary tumour tissues were collected from both patient groups.

A pool of two fluorescently labelled samples (from different groups) was mixed with the internal standard, which allows for normalisation between gels and for the comparison of protein abundances, and separated by isoelectric focusing (IEF). Each protein applied to the strip migrates toward its isoelectric point (pI); the point at which its net charge is zero. This represents the first dimension of two-dimensional (2-D) electrophoresis. The IPG strips were then overlaid onto a gel where the proteins were separated based on their size in the second dimension.

Gels were scanned on a Typhoon 9400 Variable Mode Imager to generate images at the appropriate excitation and emission wavelengths. Progenesis Same Spots software statistically analysed these acquired images by comparing non-metastasised primary tumour tissue to that which metastasised in order to identify differentially regulated proteins. Proteins were defined as differentially expressed if the observed average ratio was ±1.2 with a *t*-test score <0.05 between sample groups.

Fourteen protein spots were found to be differentially expressed between the two groups. These proteins were identified using MS. The list of identified differentially expressed proteins is outlined in Table 3.2. Their location on a representative 2D DIGE gel is shown in Figure 3.1.

The following proteins were found to show increased expression in primary uveal melanomas that metastasised compared to non-metastasised uveal melanomas; protein disulphide-isomerase A3 precursor (PDIA3), selenium-binding protein 1 (SELENBP1), alpha-enolase, F-actin capping protein subunit alpha-1 (CAPZA1), endoplasmic reticulum protein ERp29 precursor, triosephosphate isomerase (TPI1), protein DJ-1 (PARK7), and fatty acid-binding protein, heart-type (FABP3). Both CAPZA1 and FABP3 protein spots are shown in Figure 3.2. Protein identification of spot number 2 yielded two protein identifications, vimentin and beta-hexosaminidase subunit alpha. Eukaryotic translation initiation factor 2 subunit 1,

proteasome subunit alpha type 3, 40S ribosomal protein SA, tubulin beta chain and tubulin alpha-1B chain were shown to have decreased expression in uveal melanoma tissues of patients who subsequently developed metastatic disease.

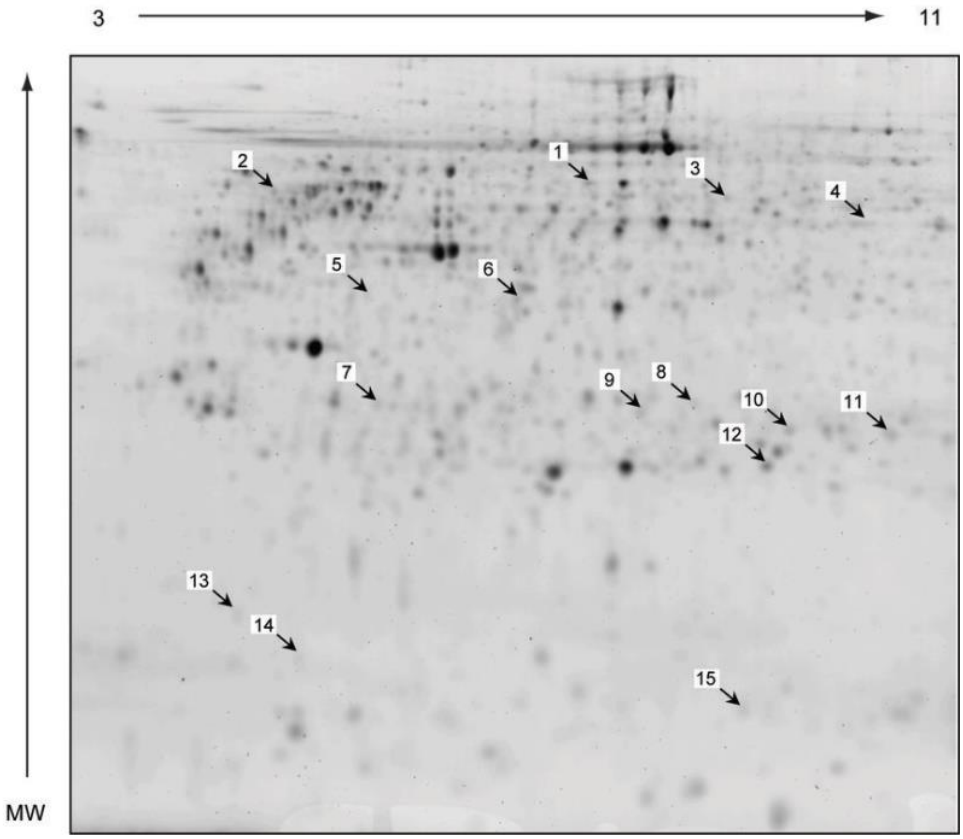

Figure 3.1 Representative 2D DIGE gel image of Cy2-labelled pool of protein lysates from primary uveal melanomas that were subsequently found to have metastasised (n=9) and the primary uveal melanomas that did not metastasise (n=16). Differentially expressed proteins that were successfully identified by LC/MS-MS are represented on the gel. Proteins are labelled numerically for clarity and are outlined in Table 3.2.

Spot no. [a]	Protein accession no.	Gene name	Protein name	MW [Da]	pI	% coverage	Mascot score	Average ratio	*t*-test
1	P30101	PDIA3	Protein disulfide-isomerase A3 precursor	57146	5.98	37	3396	1.5	0.011
2	P08670	VIM	Vimentin	53676	5.06	50	1445	1.8	0.007
	P06865	HEXA	Beta-hexosaminidase subunit alpha	61106	5.04	24	525	1.8	0.007
3	Q13228	SELENBP1	Selenium-binding protein 1	52907	6.13	39	2426	1.3	0.044
4	P06733	ENO1	Alpha-enolase	47481	7.01	53	4944	1.4	0.007
5	P05198	EIF2S1	Eukaryotic translation initiation factor 2 subunit 1	36374	5.02	57	1648	-1.6	0.035
6	P52907	CAPZA1	F-actin capping protein subunit alpha-1	33073	5.45	50	2522	1.3	0.028
7	P25788	PSMA3	Proteasome subunit alpha type 3	28643	5.19	26	1267	-1.2	0.026
8	P08865	RPSA	40S ribosomal protein SA	32947	4.79	30	861	-1.4	0.023
9	P30040	ERP29	Endoplasmic reticulum protein ERp29	29032	6.77	34	2592	1.4	0.04
10	P60174	TPI1	Triosephosphate isomerase	26938	6.45	61	2987	1.6	0.00057
11	P60174	TPI1	Triosephosphate isomerase	26938	6.45	30	317	1.7	0.00009
12	Q99497	PARK7	Protein DJ-1	20050	6.33	34	2037	1.2	0.018
13	P07437	TUBB	Tubulin beta chain	50095	4.78	10	587	-1.7	0.017
14	P68363	TUBA1B	Tubulin alpha-1B chain	50804	4.94	13	553	-1.9	0.006
15	P05413	FABP3	Fatty acid-binding protein, heart	14906	6.29	51	1790	2.2	0.00035

Table 3.2 Proteins which are differentially expressed between subsequently metastasised (n=9), and non-metastasised (n=16) primary tumour tissue according to their relevant protein spots. The differential expression patterns of these proteins was identified by 2-D DIGE and LC-MS/MS was used to identify the proteins. [a] The spot location is shown in Figure 3.1. MW, molecular weight; pI, isoelectric point. All terms are explained in section 2.6.5.2.

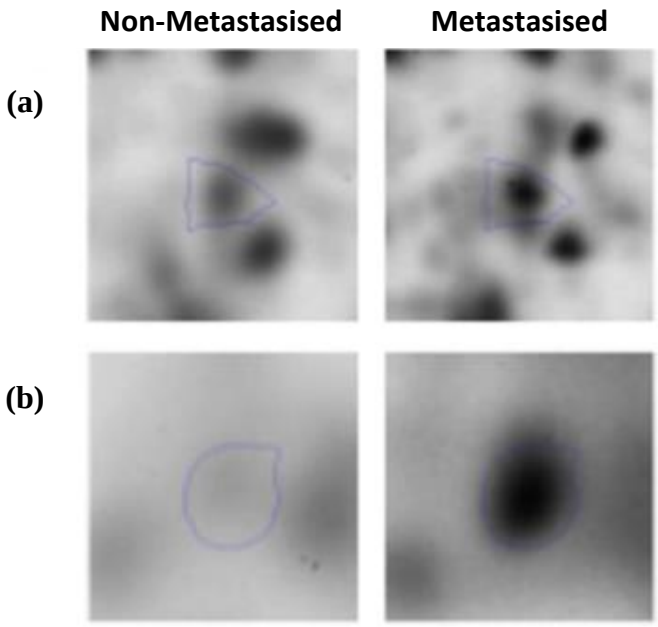

Figure 3.2 Two examples of differentially expressed protein spots as illustrated by Progenesis SameSpots software. Samples of non-metastasised specimens were compared to those which subsequently metastasised. (a) Spot number 6 was identified as F-actin capping protein subunit alpha-1 (CAPZA1), with an average ratio of 1.3 and p=0.028 between experimental groups. (b) Spot number 15 was found to be fatty acid-binding protein, heart type (FABP3), with an average ratio of 2.2 and $p=3.5\text{x}10^{4}$ between experimental groups.

3.4 Enrichment analysis within differentially expressed protein lists using DAVID

In order to determine significant enrichment of biological processes, molecular functions, and cellular compartments involved within the differentially expressed protein lists, Database for Annotation, Visualization and Integrated Discovery (DAVID) and Gene Ontology (GO) analysis was used (http://david.abcc.ncifcrf.gov/). DAVID provides a comprehensive set of functional annotation tools in order to understand the biological meaning behind lists of differentially regulated proteins.

Enrichment was considered to be significant when the Bonferroni p-value adjustment was ≤ 0.05. Differentially expressed proteins were divided into two groups; those which showed an increase in expression in subsequently metastasised primary uveal melanoma tumour tissue and those which showed a decrease in expression, and were analysed individually.

This study identified the cytosol as being significantly involved in the list of upregulated features found in the metastasised tissue, as gene products of PARK7, TPI1, ENO1, FABP3, SELENBP1, and VIM were all found to be localised there (Table 3.3). In addition to this, intramolecular oxioreductase activity was identified as a molecular process involved in the overexpression of the following genes; TPI1, PDIA3, and ERP29 (Table 3.3).

Up in Metastasised				
Cellular Compartment	**Count**	**Associated Genes**	***p*-value**	**Adjusted *p*-value**
Cytosol	6	PARK 7	1.10E-03	4.20E-02
		TPI1		
		ENO1		
		FABP3		
		SELENBP1		
		VIM		
Molecular Function	**Count**	**Associated Genes**	***p*-value**	**Adjusted *p*-value**
Intramolecular oxidoreductase activity	3	TPI1	3.00E-04	1.60E-02
		PDIA3		
		ERP29		

Table 3.3 GO cellular compartment and molecular function enrichment for differentially expressed proteins which were upregulated in subsequently metastasised primary uveal melanoma tumour tissue (n=9). Enrichment was considered significant upon observation of a p-value ≤0.05 and a Bonferroni adjusted p-value ≤0.05. Count corresponds to the overlap between proteins on the list and a particular GO category.

3.5 Follow-Up of Selected 2-D DIGE Targets by Immunohistochemistry

For follow-up of the 2D DIGE study, Dr. Annett Linge (a medical doctor with an interest in pathology in the lab) performed immunohistochemical analysis on eight non-metastasised uveal melanoma tissue specimens and eight uveal melanoma specimens of patients who did subsequently develop metastatic disease (see Table 3.1 for clinical and histopathological features of the patients included in the study; note that two samples differ to the 2D DIGE study due to sample availability). Uveal melanoma tissue sections from the two patient groups were analysed for the expression of FABP3, TPI1, CAPZA1, PDIA3, SELENBP1 and PARK7. For semi-quantitative immunohistochemical analysis, a combined score was obtained by multiplying the scores for the overall positivity and the intensity of stained tumour cells, giving a maximum score of 12.

3.5.1 FABP3

FABP3 showed positive cytoplasmic staining in fifteen of the sixteen of the uveal melanoma cases that were studied. Increased cytoplasmic positivity and membranous reactivity for FABP3 was observed in uveal melanomas that were found to have subsequently metastasised compared to those that did not (mean combined score, 8.5 versus 5) (Figure 3.3 (A)).

3.5.2 TPI1

TPI1 protein showed expression in the cytoplasm and the nucleus in the majority of the cases analysed (Figure 3.3 (B)). Increased positivity for TPI1 was observed in uveal melanomas that were found to have subsequently metastasised compared to 13 those that did not (mean combined score, 8.75 versus 6.25). Two out of eight of the non-metastasised uveal melanomas were found to be completely negative for TPI1 protein expression.

3.5.3 CAPZA1

CAPZA1 showed an overall reduced cytoplasmic expression pattern in the majority of the uveal melanoma tissues that were found to have subsequently metastasised

(mean combined score, 4) compared to those that did not (mean combined score, 10) (Figure 3.4 (A) and (B)). Parallel staining of sections for CAPZA1 and the histiocyte/monocyte/macrophage marker CD68 confirmed CAPZA1 positivity in both tumour cells and tumour-infiltrating macrophages, but not all of those macrophages stained positive for CAPZA1.

3.5.4 PDIA3

PDIA3 (Figure 3.5 (A)) showed decreased expression in uveal melanomas that were found to have subsequently metastasised compared to those that did not (mean combined score, 5.25 versus 7.5).

3.5.5 SELENBP1

SELENBP1 (Figure 3.5 (B)) showed only weak or no cytoplasmic expression in the majority of both non-metastasised and subsequently metastasised uveal melanoma groups (mean combined score, 2.875 versus 2.25).

3.5.6 PARK7

For PARK7 (Figure 3.5 (C)) positive, heterogeneous staining was observed in both non-metastasised and subsequently metastasised uveal melanoma groups (mean combined score, 5 versus 6.6).

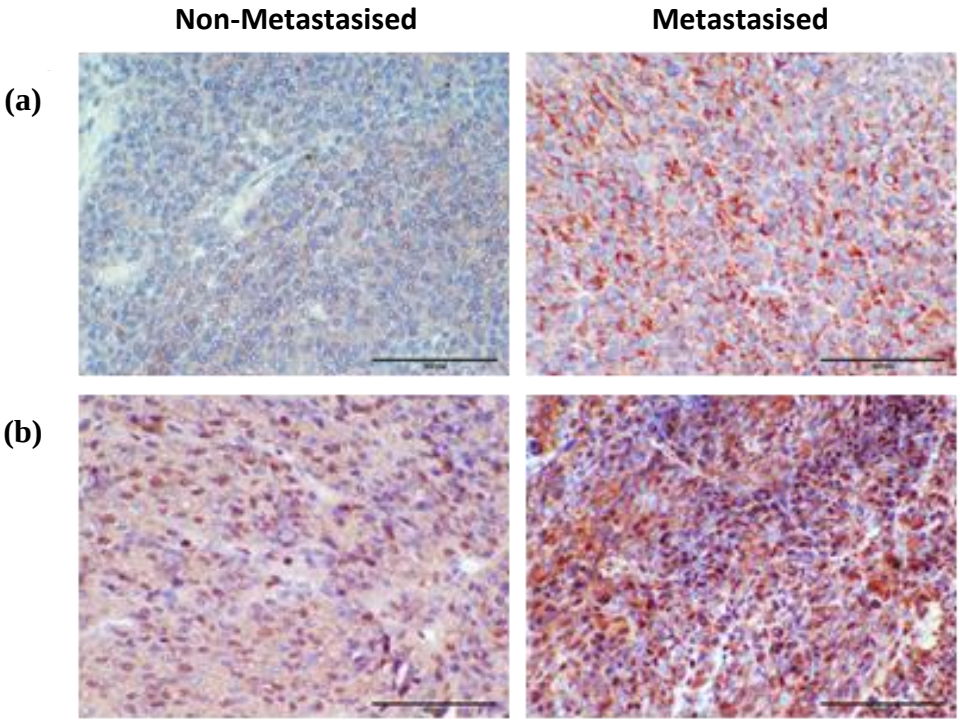

Figure 3.3 Images representing immunohistochemical analysis of (a) FABP3 (p=0.15) and (b) TPI1 (p=0.27) in primary uveal melanomas which subsequently metastasised (right, n=8) in comparison to those which did not (left, n=8). Magnification x400; scale bar = 100 μm.

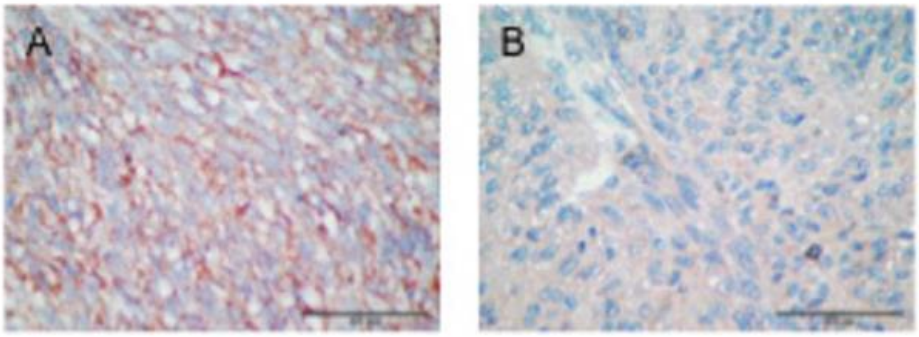

Figure 3.4 Images representing immunohistochemical analysis of (a) CAPZA1 expression in primary uveal melanomas which remained as non-metastasised (n=8) and of (b) CAPZA1 expression in primary uveal melanomas which subsequently metastasised (n=8). Magnification x400; scale bar = 100 μm; *p*=0.08.

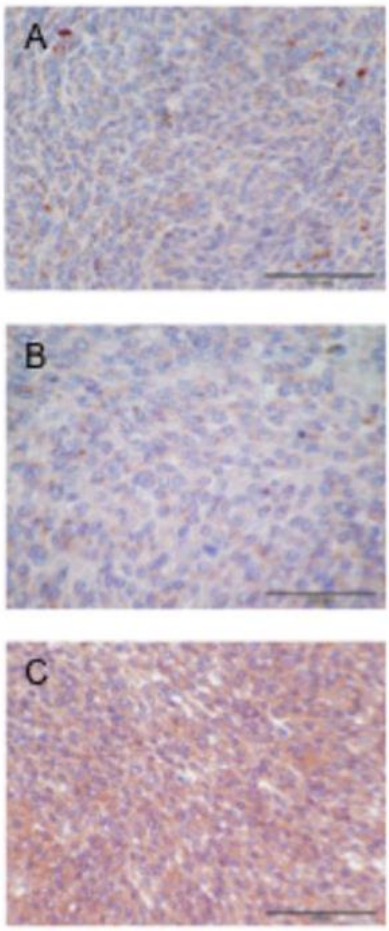

Figure 3.5 Representative images of the immunohistochemical analysis of (a) PDIA3 (p=0.20), (b) SELENBP1 (p=0.69) and (c) PARK7 (p=0.39) in non-metastasised (n=8) primary uveal melanoma tumour tissue. Magnification x400; scale bar = 100 μm.

From the immunohistochemical analysis of CAPZA1, PDIA3, FABP3, TPI1, SELENBP1, and PARK7, it was decided to follow up FABP3, TPI1, and SELENBP1 with functional analysis (Section 3.7).

From the 2-D DIGE study, TPI1 was found to be significantly upregulated in subsequently metastasised uveal melanoma tissue. The immunohistochemical staining for this protein also indicated a trend for upregulation in uveal melanomas which did metastasise. Both results illustrate that the potential biomarker may be involved in the development of the metastatic phenotype in uveal melanoma. TPI1 is a glycolytic enzyme which catalyses the conversion of dihydroxyacetone phosphate to glyceraldehyde 3-phosphate; a high rate of glycolysis is required to support tumour growth (Albery and Knowles 1976, Bui and Thompson 2006). TPI1 has also previously been shown to be expressed in uveal melanoma primary cell cultures (Pardo, Garcia et al. 2005).

FABP3 was found to be upregulated by 2.2-fold in primary uveal melanoma tissue which metastasised. This result correlated with the outcome of the FABP3 immunohistochemistry study. However, the function of FABP3 is poorly understood. It has been shown to exhibit inhibitory activity of mammary epithelial cell proliferation and reduce the tumorgenicity of breast cancer cells in nude mice (Yang, Spitzer et al. 1994). Positive correlations of FABP3 expression with tumour cell invasion, lymph node metastasis and poor patient survival have been identified in gastric carcinomas (Hashimoto, Kusakabe et al. 2004).

SELENBP1 was found to be significantly upregulated in subsequently metastasised primary tumour tissue in comparison to non-metastasised tissue. However, the immunohistochemical analysis was non-conclusive due to the weak/absence of staining in both the metastasised and non-metastasised tumour tissue. SELENBP1 has previously been suggested as a tumour suppressor as its expression is lost in several epithelial cancers (Scortegagna, Martin et al. 2009). Unlike PDIA3 and PARK7, SELENBP1 had not previously been associated with ocular cancer and hence, was novel in this regard (Pardo, Garcia et al. 2005, Bande, Santiago et al.

2012). Therefore, it was decided to follow up SELENBP1 with functional analysis (Section 3.7).

3.6 Differential Protein Expression Analysis Between Non-Metastasised and Subsequently Metastasised Primary Tumour Tissue using Quantitative Label-Free LC-MS Analysis

Dr. Pathma Ramasamy (a medical doctor) and Mr. Michael Henry (a mass spectrometry specialist in the lab) carried out a quantitative LC-MS proteomic analysis of eight non-metastasised tumour tissues and eight which subsequently metastasised, 14 of which were also used in the 2-D DIGE study. The sample details are illustrated in Table 3.4.

From this analysis, 50 proteins with a minimum of three matched peptides were identified as being differentially expressed between both sample sets (Table 3.4). Of these proteins, five had previously been identified in the 2-D DIGE study. Vimentin, alpha-enolase, TPI1, beta-hexosaminidase subunit alpha, and FABP3 were all found to be upregulated in primary uveal melanoma tissue which had metastasised, which correlated with the 2-D DIGE findings, see Table 3.2. In addition to this, heat shock protein beta-1 (HSP-27) was found at a lower abundance in the subsequently metastasised tissue in comparison to non-metastasised primary tissue. This result agrees with a study previously carried out by Jmor et al. which demonstrated that HSP-27 was expressed at a lower level in monosomy three tumours (which are typically associated with metastasis) than in disomy three tumours (often linked with a non-metastatic outcome) (Jmor, Kalirai et al. 2012).

Of the proteins identified by quantitative label-free LC-MS, cytosolic non-specific dipeptidase (CNDP2), thioredoxin-dependent peroxide reductase (PRDX3), importin subunit beta-1 (KPNB1), and elongation factor 1-gamma (EEF1G) were selected for functional analysis. Dr. Ramasamy carried out the follow-up of other targets, using immunohistochemistry, for his M.D. thesis.

The four selected proteins were chosen as, although some of these had previously been linked with other cancer studies, they had not been associated with uveal melanoma. In addition to this, they illustrated some of the lowest ANOVA scores of

the analysis, deeming them as a number of the most significant potential targets from the generated list (Table 3.5).

Sample	Sex	Age (At Diagnosis)	Metastasis	Survival After Diagnosis (Years)	Ciliary Body Involvement	Extraocular Extension	Cell Type	LTD (mm)	Chromosome 3 Status
1	F	40	Liver, Lung	2	Y	N	S	18	N/A
2	F	49	Kidney	N/A	N	N	S	12	Monosomy
3	M	71	Liver	7	Y	Y	E	20	Monosomy
4	F	58	Liver	5	Y	N	M	15	Monosomy
5	M	71	Lung	2	N	N	M	11	Monosomy
6	F	69	Liver	11	N	N	S	12	Monosomy
7	F	51	Liver	1	N	N	E	15	Monosomy
8	M	64	Lung	10	Y	N	M	10	Disomy
9	F	76	_	_	N	N	M	8	Disomy
10	F	46	_	_	N	N	E	23	Disomy
11	F	74	_	_	N	N	M	14	N/A
12	M	68	_	_	N	N	S	20	Disomy
13	F	52	_	_	N	Y	M	10	Disomy
14	F	75	_	_	N	N	S	22	Disomy
15	F	42	_	_	N	N	S	17	Disomy
16	M	50	_	_	N	N	M	17	Disomy

Table 3.4 Patient details of eight subsequently metastasised primary uveal melanoma tumour tissues and eight non-metastasised uveal melanoma primary specimens. N, no; Y, yes; S, spindle cells; E, epitheloid cells; M, mixed cells; LTD, largest tumour diameter; NA, not available.

	Protein Name	Accession No.	Peptide count	No. Peptides Matched	Confidence score	Anova (p)	Max fold change	Average Normalised Abundace	
								Metastasised	Non-Metastasised
Up in Metastasised	**Elongation factor 1-gamma**	**P26641**	**3**	**3**	**142.69**	**3.87E-04**	**2.02**	**2.68E+05**	**1.32E+05**
	Alpha-enolase	P06733	10	10	662.16	7.26E-04	1.68	8.99E+06	5.36E+06
	Nucleoside diphosphate kinase A	P15531	5	5	235.99	9.47E-04	1.89	8.48E+05	4.48E+05
	Thioredoxin-dependent peroxide reductase, mitochondrial	**P30048**	**4**	**4**	**273.05**	**2.18E-03**	**1.58**	**8.99E+05**	**5.70E+05**
	Transitional endoplasmic reticulum ATPase	P55072	4	4	301.59	2.62E-03	1.45	5.19E+05	3.57E+05
	Heat shock cognate 71 kDa protein	P11142	5	5	306.74	2.68E-03	1.54	1.74E+06	1.13E+06
	Importin subunit beta-1	**Q14974**	**4**	**4**	**271.69**	**2.92E-03**	**1.47**	**2.71E+05**	**1.84E+05**
	Rab GDP dissociation inhibitor beta	P50395	5	5	280.72	3.14E-03	1.61	8.76E+05	5.43E+05
	Actin, cytoplasmic 1	P60709	5	5	259.7	5.12E-03	3.54	1.25E+06	3.55E+05
	Heterogeneous nuclear ribonucleoprotein K	P61978	3	3	189.73	6.17E-03	1.56	1.42E+06	9.09E+05
	Beta-crystallin B2	P43320	3	3	168.38	6.19E-03	42.66	5.35E+04	1.25E+03
	Triosephosphate isomerase	P60174	8	8	523.06	6.64E-03	1.79	1.33E+07	7.42E+06
	78 kDa glucose-regulated protein	P11021	6	6	488.32	7.79E-03	1.45	1.21E+06	8.34E+05
	Peptidyl-prolyl cis-trans isomerase A	P62937	3	3	169.95	8.40E-03	1.33	2.09E+06	1.57E+06
	Mast/stem cell growth factor receptor	P10721	6	6	273.77	8.74E-03	4.85	4.54E+04	9.35E+03
	Serum albumin	P02768	4	4	292.09	1.21E-02	2.66	7.46E+06	2.80E+06
	Vimentin	P08670	23	23	1409.7	1.67E-02	1.98	3.77E+07	1.91E+07
	Beta-hexosaminidase subunit alpha	P06865	7	7	484.38	1.80E-02	3.04	2.32E+06	7.61E+05
	Myosin-11	P35749	5	5	262.63	2.03E-02	9.99	5.60E+04	5.61E+03
	Sarcoplasmic/endoplasmic reticulum calcium ATPase 2	P16615	6	6	342.56	2.33E-02	1.76	1.40E+05	7.95E+04
	Serine/threonine-protein phosphatase PP1-beta catalytic subunit	P62140	3	3	128	2.34E-02	2.04	8.42E+04	4.12E+04
	Glucose-6-phosphate isomerase	P06744	5	5	461.9	2.41E-02	1.54	3.50E+06	2.27E+06
	Dihydrolipoyllysine-residue succinyltransferase component of 2-oxoglutarate dehydrogenase complex, mitochondrial	P36957	3	3	128.45	2.55E-02	1.99	1.12E+05	5.62E+04
	Nucleolin	P19338	10	10	726.89	2.75E-02	1.75	2.77E+06	1.59E+06
	Annexin A5	P08758	3	3	172.89	2.84E-02	3.98	1.09E+06	2.73E+05
	Polyadenylate-binding protein 1	P11940	3	3	167.51	2.86E-02	1.37	8.76E+04	6.39E+04
	Elongation factor 2	P13639	5	5	228.5	3.43E-02	1.80	9.36E+05	5.19E+05
	Fatty acid-binding protein, heart	P05413	4	4	289.17	4.19E-02	2.46	8.20E+04	3.34E+04
	Beta-hexosaminidase subunit beta	P07686	6	6	413.84	4.34E-02	2.39	2.58E+06	1.08E+06
Down in Metastasised	**Cytosolic non-specific dipeptidase**	**Q96KP4**	**6**	**6**	**304.06**	**1.32E-03**	**1.75**	**3.67E+05**	**6.41E+05**
	Spectrin alpha chain, brain	Q13813	8	8	352.15	1.87E-03	2.30	4.74E+04	1.09E+05
	15-hydroxyprostaglandin dehydrogenase [NAD+]	P15428	4	4	234	4.46E-03	38.81	4.83E+02	1.88E+04
	Protein kinase C and casein kinase substrate in neurons protein 2	Q9UNF0	3	3	104.12	6.19E-03	3.53	1.26E+04	4.45E+04
	Programmed cell death 6-interacting protein	Q8WUM4	4	4	247.14	7.61E-03	2.27	3.20E+04	7.26E+04
	Alpha-crystallin B chain	P02511	3	3	179.54	1.72E-02	4.27	3.30E+04	1.41E+05
	Cartilage acidic protein 1	Q9NQ79	3	3	116.9	1.88E-02	1.97	5.28E+03	1.04E+04
	Transketolase	P29401	5	5	257.21	1.96E-02	3.43	8.10E+04	2.78E+05
	Synaptic vesicle membrane protein VAT-1 homolog	Q99536	4	4	170.67	2.58E-02	2.09	4.72E+05	9.88E+05
	Sodium/potassium-transporting ATPase subunit alpha-1	P05023	3	3	178.83	2.64E-02	1.81	8.17E+04	1.48E+05
	3-hydroxyisobutyrate dehydrogenase, mitochondrial	P31937	4	4	344.15	2.94E-02	1.46	3.69E+05	5.40E+05

Down in Metastasised	60S ribosomal protein L15	P61313	3	3	129.17	2.99E-02	4.63	3.05E+03	1.41E+04
	Protein Niban	Q9BZQ8	5	5	314.36	3.30E-02	1.66	8.81E+04	1.46E+05
	Microtubule-associated protein 4	P27816	14	14	730.03	3.69E-02	2.33	4.06E+05	9.44E+05
	Lamin-B2	Q03252	3	3	136.84	3.88E-02	2.36	2.83E+04	6.69E+04
	Heat shock 70 kDa protein 1A/1B	P08107	3	3	189.72	4.02E-02	3.16	4.92E+04	1.55E+05
	Glycogen phosphorylase, liver form	P06737	2	2	97.49	4.20E-02	2.96	1.93E+04	5.70E+04
	Alpha-1-antitrypsin	P01009	4	4	204.7	4.34E-02	1.99	6.15E+05	1.22E+06
	Apolipoprotein E	P02649	10	10	594.63	4.49E-02	5.82	4.55E+04	2.65E+05
	Tubulin beta-4 chain	P04350	8	8	706.15	4.83E-02	1.41	3.32E+06	4.66E+06
	Heat shock protein beta-1	P04792	6	6	464.12	4.86E-02	1.56	5.14E+06	8.00E+06

Table 3.5 Quantitative label-free LC-MS analysis of non-metastasised primary uveal melanoma tumour tissues (n=8) and subsequently metastasised primary tissues (n=8). 50 proteins with at least three matched peptides were identified as being differentially expressed between the two samples sets. Of these, elongation factor 1-gamma (EEF1G), thioredoxin-dependent peroxide reductase (PRDX3), importin subunit beta-1 (KPNB1), and cytosolic non-specific dipeptidase (CNDP2) were selected for functional analysis.

3.7 Functional Effects of siRNA-Mediated Downregulation of Targets of Interest in Uveal Melanoma Cell Lines

RNA interference (RNAi) is a naturally-occurring mechanism which can exploited for knockdown studies when understanding the role of potential biomarkers. small interfering RNA (siRNA) are RNA duplexes which becomes separated in the cytoplasm of the cell, with the antisense strand bound to the RNA-induced silencing complex (RISC). This RNA-RISC complex then locates mRNA in the cytoplasm with homologous sequences and induces cleavage of the mRNA, thus preventing translation of the protein.

siRNA transfected cells can be monitored for changes in tumorigenicity or metastatic potential following transfection, which can in turn highlight the role of the targets of interest.

In order to determine the roles of the proteins of interest, siRNA were used to downregulate, or "knockdown", their production. Subsequent functional analysis would then be carried out, using the transfected cells.

TPI1, FABP3, and SELENBP1 were selected from the 2-D DIGE results (Table 3.2), while CNDP2, PRDX3, EEF1G, and KPNB1 were selected from the quantitative label-free LC-MS results (Table 3.5).

In order to determine if it was possible to downregulate the proteins of interest, the levels of each protein in 92.1 and MEL202 uveal melanoma cell lines was first determined. This was carried out using Western blotting with antibodies specific to each protein (Figure 3.6). From this, it was clear that all proteins, except CNDP2 which was not noticeably produced (Figure 3.6 (d)), were expressed at sufficient levels in 92.1 and MEL202 cells. This resulted in CNDP2 being excluded from the analysis.

siRNA specific to TPI1, FABP3, SELENBP1, PRDX3, EEF1G, and KPNB1 were selected for the transfection of 92.1 and MEL202 uveal melanoma cell lines. Two independent siRNA molecules were chosen for each target. In some cases, this required multiple siRNA to be tested prior to selecting the molecule which most efficiently downregulated expression. For example, of three siRNAs tested, siRNA #1 and #3 were selected for SELENBP1 knockdown studies.

For all proteins, except PRDX3, significant knockdown of each protein was achieved. The attempted optimisation of transfection conditions for PRDX3 was carried out in both cell lines. However, the transfection heavily impacted on the proliferation of MEL202 cells at an siRNA concentration of 20 nM, resulting in total cell death. At this concentration, knockdown of the protein did not occur (Figure 3.7 (a)); hence the effect on proliferation observed was not as a result of PRDX3 knockdown. In the 92.1 cell line the transfection did not successfully downregulate PRDX3 at siRNA concentrations of 20 nM, 40 nM or 60 nM. These concentrations were tested using 4.5 μL, 6.5 μL and 7.5 μL of transfection reagent (lipofectamine RNAiMax). The transfection was also tested using 80 nM of siRNA, which appeared to marginally reduce the levels of PRDX3 when 6.5 μL and 7.5 μL of lipofectamine were used (Figure 3.7 (b)). However, at high concentrations, siRNA can cause off-target effects which can generate false results. A lower concentration of siRNA was used by pooling of two PRDX3 siRNA. This method was attempted at two concentrations; 20 nM and 40 nM, however, the extent of knockdown was not strong enough at either concentration (Figure 3.7 (c)). It was decided to exclude PRDX3 from the functional analysis as a result.

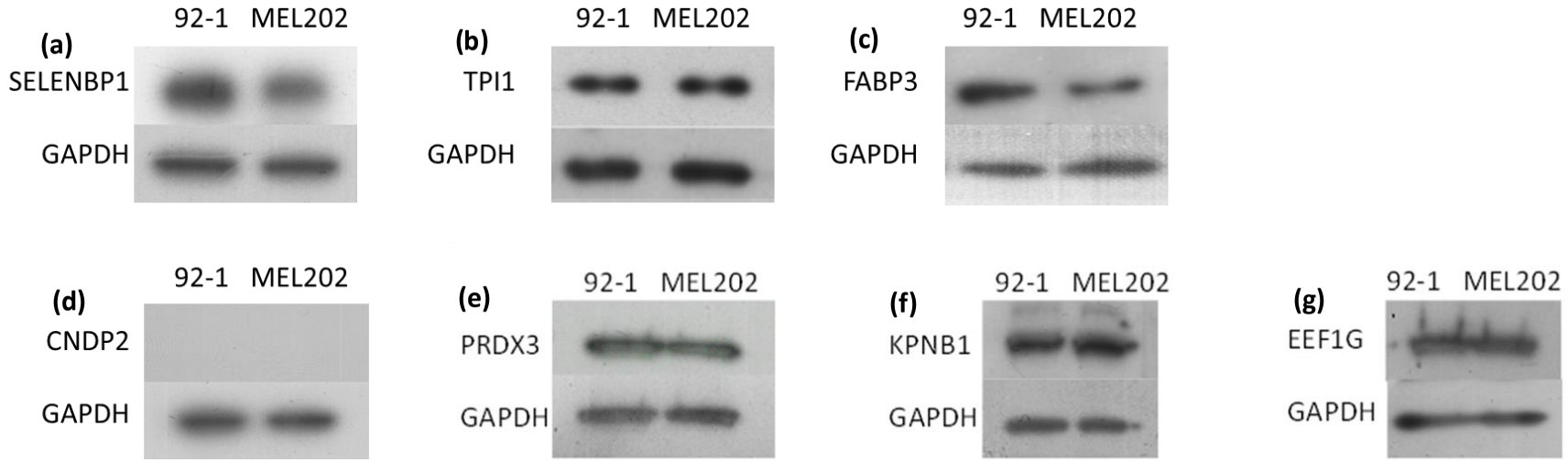

Figure 3.6 Western blotting illustrated that all of the protein targets identified in the 2-D DIGE study; SELENBP1 (a), TPI1 (b), and FABP3 (c), were produced at sufficient levels to carry out downregulation studies using siRNA. Of the proteins of interest identified by the quantitative label-free LC-MS analysis, PRDX3 (e), KPNB1 (f), and EEF1G (g) were all expressed at reasonable levels in 92.1 and MEL202 cells. However, CNDP2 (d) was not expressed in either cell line. Hence, this protein was excluded from subsequent functional analysis.

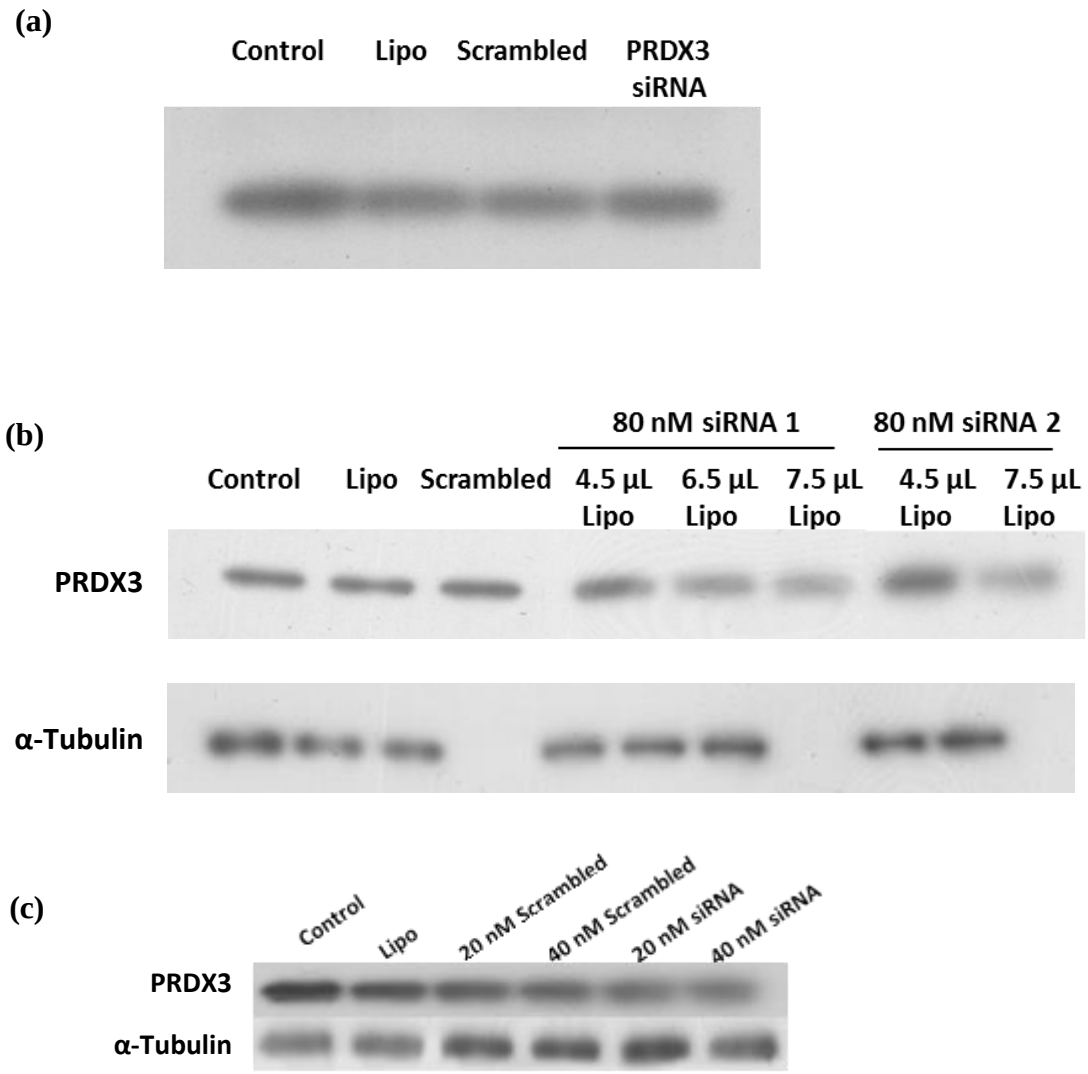

Figure 3.7 The downregulation of PRDX3 in 92.1 and MEL202 cell lines was unsuccessful. (a) In the MEL202 cell line, the transfection of 20 nM PRDX3 siRNA appeared to severely impact proliferation. However, western blotting illustrated that the knockdown of the protein was unsuccessful at this level. This indicates that the observed cell death did not occur as a consequence of the transfection. (b) Knockdown did not occur in the 92.1 cell line at siRNA levels as high as 80 nM, using a range of transfection reagent volumes. (c) Combining two independent siRNA at concentration of 20 nM and 40 nM did not successfully result in the knockdown of PRDX3 in 92.1 cells either. Control refers to healthy, untreated cells. Lipo refers to healthy cells treated with lipofectamine only. Scrambled represents negative control cells which were transfected with a nonsense sequence of siRNA.

3.7.1 TPI1 Downregulation in the 92.1 Uveal Melanoma Cell Line for the Determination of a Potential Role in Proliferation, Invasion and Migration

To study the potential effect of TPI1 on the proliferation, invasion and motility of uveal melanoma cells, down-regulation experiments using siRNA molecules directed against the respective target gene were performed in the 92.1 primary uveal melanoma cell line. Two independent siRNA molecules were used to knockdown TPI1 and the subsequent reduction in protein levels was confirmed by Western blot analysis (Figure 3.8)

3.7.1.1 Proliferation

Proliferation assays were carried out following TPI1 siRNA transfection. No noteworthy effect on proliferation in 92.1 cells was observed when treated cells were compared with scrambled siRNA-treated cells (Figure 3.9 (A)). However, the downregulation of TPI1 notably decreased the rate of proliferation in the MEL202 primary uveal melanoma cell line, with a significant effect observed in the replicate experiments (Figure 3.9 (B)). This could create complications by making it difficult to assess the impact of knockdown on properties such as invasion and migration. Hence, TPI1 knockdown studies were not carried out in this cell line.

3.7.1.2 Invasion

At 72 hours following siRNA transfection, invasion assays were carried out. The total number of 92.1 cells transfected with siRNA #2 invading through the membrane was significantly decreased while a strong effect on invasion was also observed for siRNA #1 transfected cells (Figure 3.10 (A)).

3.7.1.3 Migration

At 72 hours following siRNA transfection, migration assays were carried out. The reduction of TPI1 levels led to a significant decrease in the motility of 92.1 cells (Figure 3.10 (B)).

These results indicate that TPI1 is required for both invasion and migration in 92.1 cells, and hence, may contribute to the metastatic process of uveal melanoma.

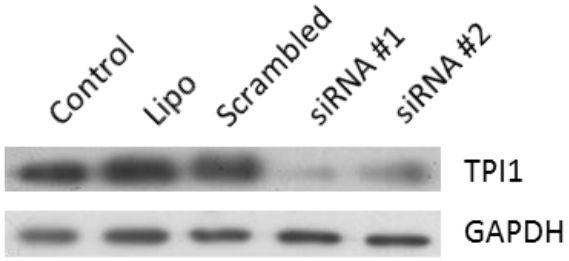

Figure 3.8 Western blot analysis showing the reduction of TPI1 following siRNA knockdown. Control cells (untreated), transfection reagent-treated cells (Lipo), scrambled siRNA treated cells, siRNA #1 and siRNA #2 specific for TPI1-treated cells were lysed 72 hours after transfection and subjected to Western blot analysis. GAPDH served as an internal loading control.

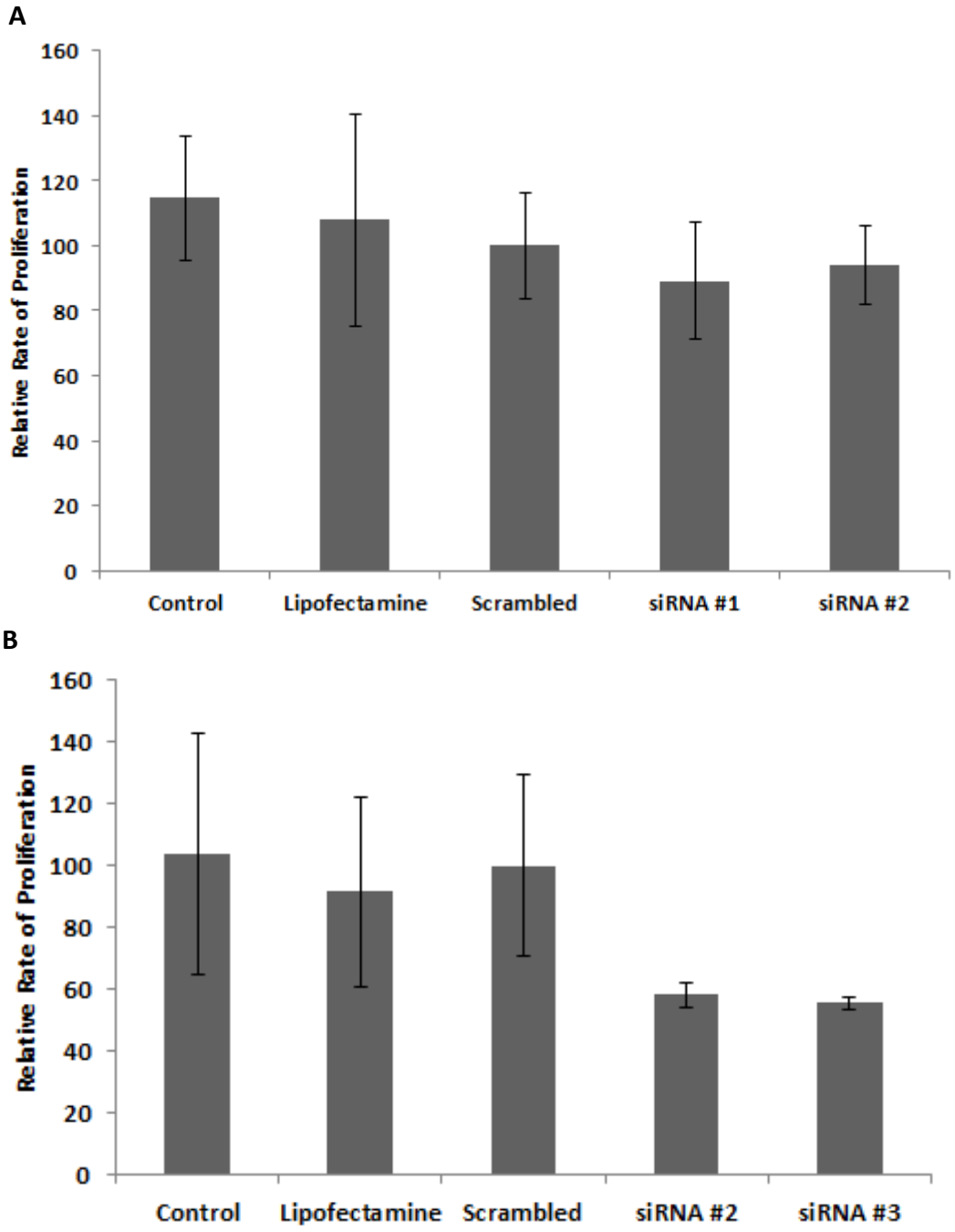

Figure 3.9 Proliferation assay results for (A) 92.1 and (B) MEL202 cells treated with siRNA specific for TPI1. When 92.1 siRNA transfected cells were compared to the scrambled siRNA (negative control), there was no effect on proliferation for either siRNA #1 (p=0.59) or siRNA #2 (p=0.71). However, the knockdown of TPI1 in MEL202 cells strongly affects proliferation in both siRNA #1 (p=0.13) and siRNA #2 (p=0.38) when compared to the negative control (scrambled). The combined result and statistics of three independent experiments is shown. All p-values were determined by comparing each siRNA to the scrambled control. n=3.

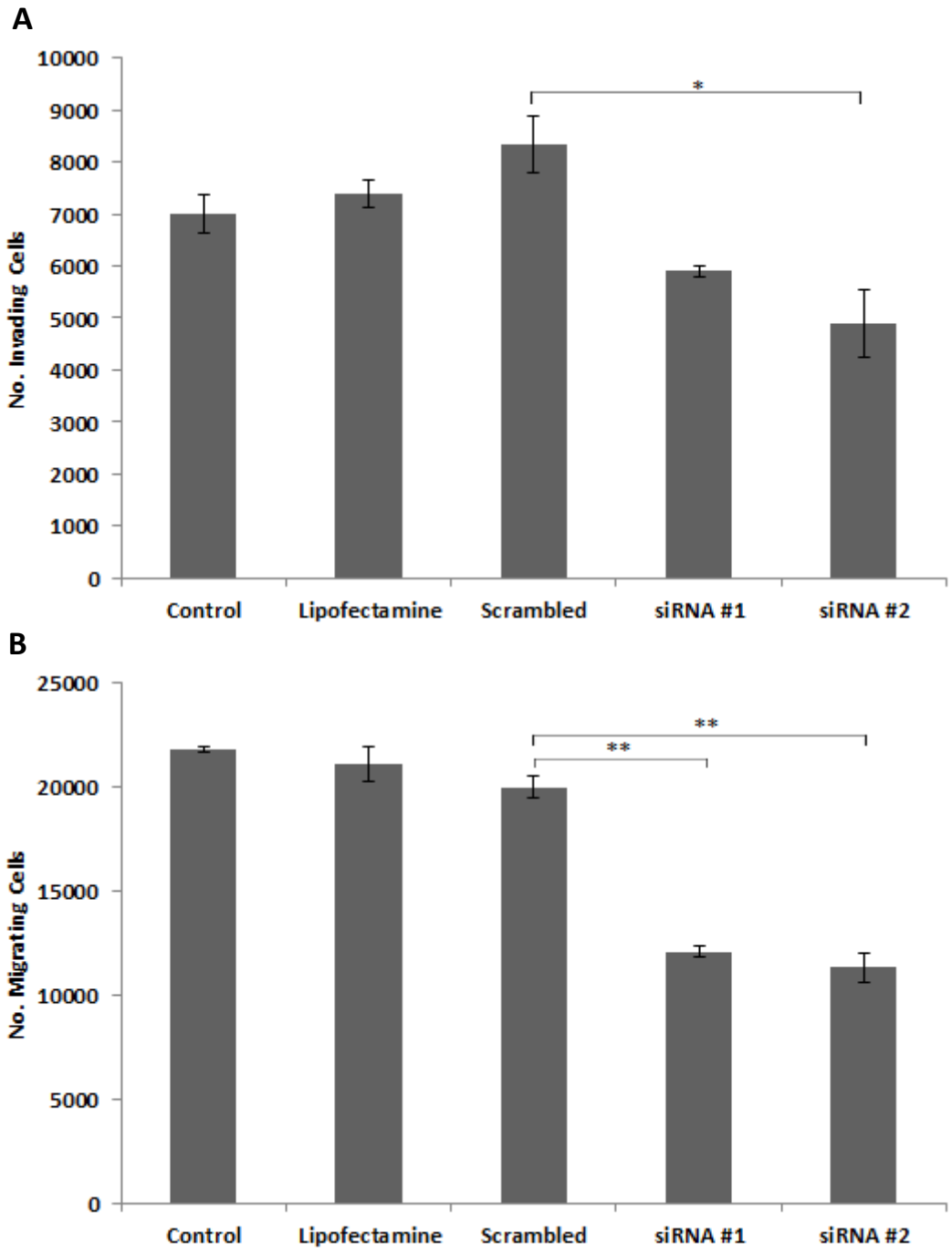

Figure 3.10 siRNA knockdown of TPI1 decreases invasion and motility. (a) Invasion assay of 92.1 cells following siRNA transfection. The total number of 92.1 cells invading through membranes after siRNA transfection is shown. siRNA #1 p=0.08; siRNA #2 p=0.03. (b) Motility assay of 92.1 cells following siRNA transfection. The total number of 92.1 cells migrating through uncoated membrane after siRNA transfection is shown. siRNA #1 p=0.008; siRNA #2 p=0.007. The combined result and statistics of two independent experiments is shown. *p<0.05, **p<0.01 when compared with scrambled siRNA-treated controls. n=2.

3.7.2 FABP3 Downregulation in the 92.1 Uveal Melanoma Cell Line for the Determination of a Potential Role in Proliferation, Invasion and Migration

To study the potential effect of FABP3 on the proliferation, invasion and migration of uveal melanoma cells, down-regulation experiments using siRNA molecules directed against FABP3 were performed in the 92.1 primary uveal melanoma cell line. Two independent siRNA molecules were used to knockdown TPI1 and the subsequent reduction in protein levels was confirmed by Western blot analysis (Figure 3.11).

3.7.2.1 Proliferation

Proliferation assays were carried out following siRNA transfection; no effect on the proliferation of 92.1 cells was observed when treated cells were compared with scrambled siRNA-treated cells (Figure 3.12 (A)). However, the downregulation of FABP3 notably decreased the rate of proliferation in the MEL202 primary uveal melanoma cell line, with a significant effect observed in the individual replicate experiments (Figure 3.12 (B)). This could create complications by making it difficult to assess the impact of knockdown on properties such as invasion and migration. Hence, knockdown studies of FABP3 were not carried out in this cell line.

3.7.2.2 Invasion

At 72 hours following siRNA transfection, invasion assays were carried out. The total number of 92.1 cells invading through the membrane was significantly decreased following transfection (Figure 3.13 (A)). This indicates that FABP3 may be required for invasion.

3.7.2.3 Migration

At 72 hours following siRNA transfection, migration assays were carried out. The knockdown of FABP3 led to a significant decrease in motility of 92.1 cells (Figure 3.13 (B)).

These results indicate that FABP3 may be required for both invasion and migration in 92.1 cells, and hence, may contribute to the metastatic process of uveal melanoma.

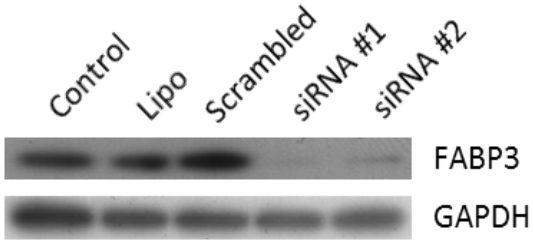

Figure 3.11 Western blot analysis showing the reduction of FABP3 following siRNA knockdown. Control cells (untreated), transfection reagent-treated cells (Lipo), scrambled siRNA treated cells, siRNA #1 and siRNA #2 specific for TPI1-treated cells were lysed 72 hours after transfection and subjected to Western blot analysis. GAPDH served as an internal loading control.

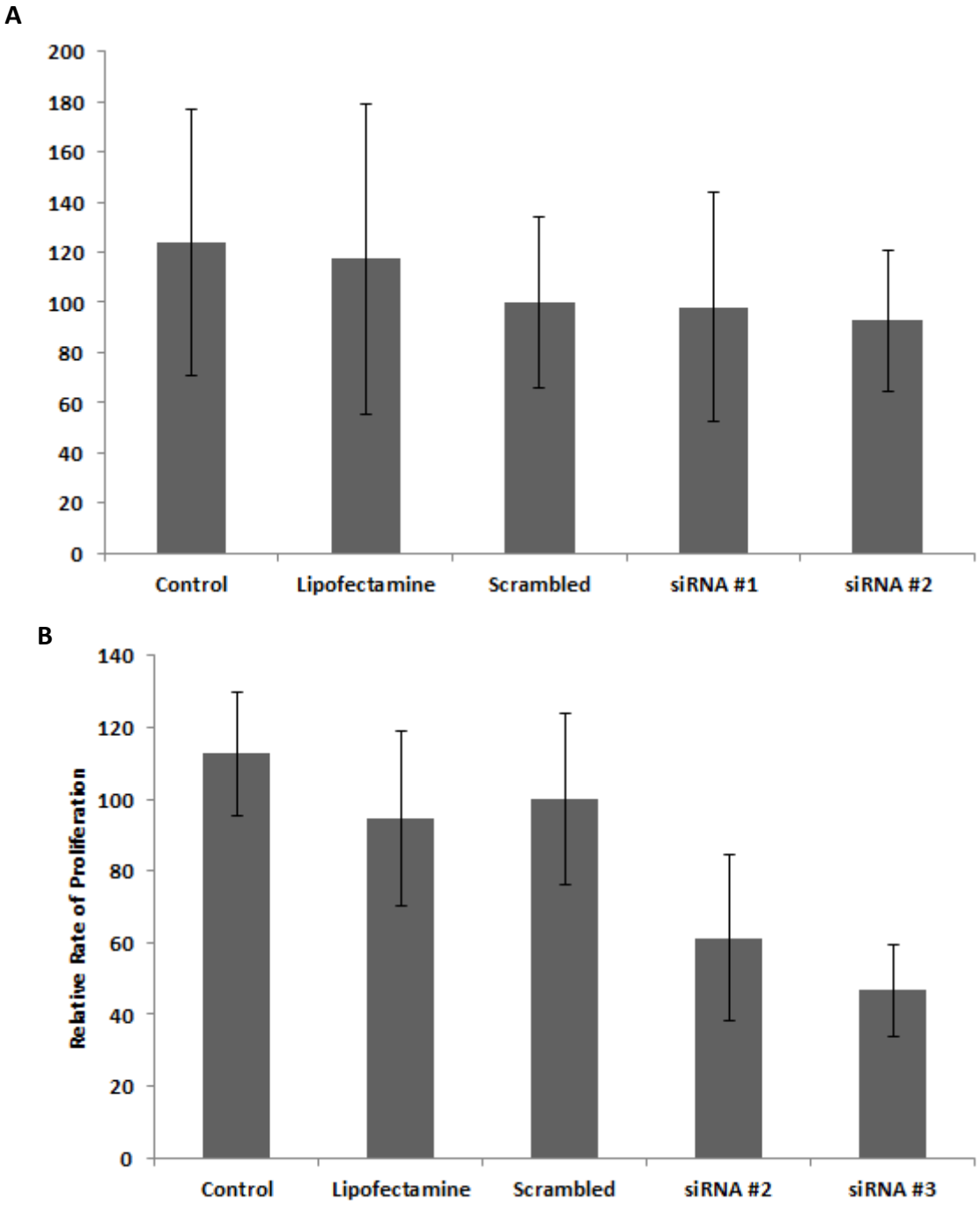

Figure 3.12 Proliferation assay results for (A) 92.1 and (B) MEL202 cells treated with siRNA specific for FABP3. When 92.1 cells were compared to the scrambled siRNA (negative control), the effect of the transfection was minimal on 92.1 cells; siRNA #1 p=0.97 and siRNA #2 p=0.84. The knockdown of FABP3 in MEL202 cells strongly affects proliferation in both siRNA #1 (p=0.13) and siRNA #2 (p=0.38). The combined result and statistics of three independent experiments is shown. All p-values were determined by comparing each siRNA to the scrambled control. n=3.

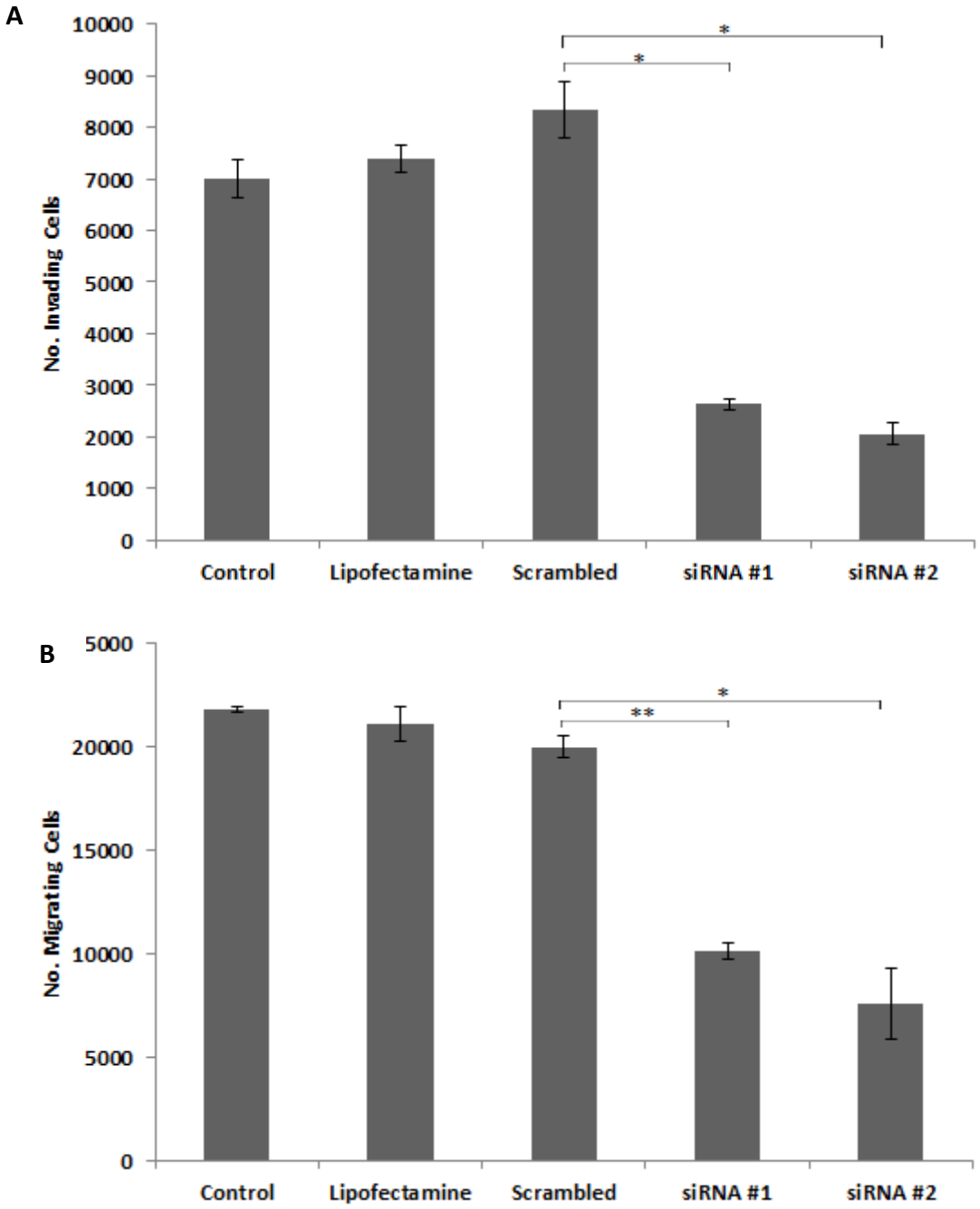

Figure 3.13 siRNA knockdown of FABP3 decreases invasion and motility. (A) Invasion assay of 92.1 cells following siRNA transfection. The total number of 92.1 cells invading through membranes of invasion chambers after siRNA transfection is shown. siRNA #1 p=0.04; siRNA #2 p=0.02. (B) Motility assay of 92.1 cells following siRNA transfection. The total number of 92.1 cells migrating through uncoated membrane after siRNA transfection is shown. siRNA #1 p=0.002; siRNA #2 p=0.04. The combined result and statistics of two independent experiments is shown. *p<0.05, **p<0.01 when compared with scrambled siRNA-treated controls. n=2.

3.7.3 SELENBP1 Downregulation in MEL202 and 92.1 Cell Lines for the Determination of a Potential Role in Proliferation, Invasion, Migration, and Oxidative Metabolism

In order to determine the effect of downregulation of SELENBP1 on the invasion and migration properties of uveal melanoma cells, two siRNA molecules directed against respective target gene, siRNA #1 and #3, were transfected into the 92.1 and MEL202 primary uveal melanoma cell lines. The reduction in protein levels for both cell lines was confirmed by Western blot analysis (Figure 3.14 (A) and (B), i).

3.7.3.1 Proliferation

Proliferation assays were carried out following siRNA transfection which illustrated that there was no significant effect on proliferation in either 92.1 (Figure 3.15 (A)) or MEL202 (Figure 3.12 (B)) cells treated with SELENBP1 siRNA in comparison to scrambled siRNA treated cells Hence, it was decided to carry out the knockdown studies in both cell lines.

3.7.3.2 Invasion

Invasion assays were performed at 72 hours following the transfection of both cell lines. This illustrated that the total number of cells invading through the membrane was significantly decreased following transfection with siRNA molecules specific for SELENBP1 in the 92.1 cell line (Figure 3.13 (A), i). The same was observed in the MEL202 cell line for siRNA #1 but not for siRNA #3.

3.7.3.3 Migration

Migration assays were performed at 72 hours following the transfection for both cell lines. A significant reduction in the migration of 92.1 cells was observed following transfection with siRNA molecules specific for SELENBP1 (Figure 3.13 (A) and (B), ii). However, no significant effect on the migration of MEL202 cells was observed following transfection, although a clear trend in decreased cell number was observed. This may have been due to the nature of MEL202 cells as they aggregate quite easily, creating both dense and sparsely populated areas within the chamber,

hence producing a wide range of cell counts per experiment. This may have therefore affected the overall validity of the experiment.

These results indicate that SELENBP may be required for both invasion and migration in 92.1 and MEL202 cells, and hence, may play a role the process of metastasis in uveal melanoma.

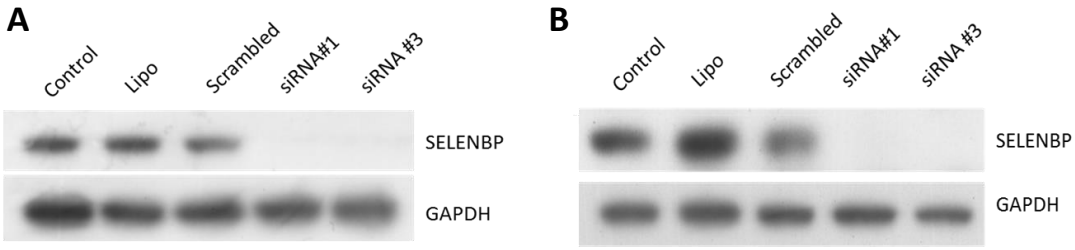

Figure 3.14 Western blot analysis showing the reduction of SELENBP following siRNA knockdown siRNA knockdown of SELENBP in (A) 92.1 and (B) MEL202 uveal melanoma cell lines. Control cells (untreated), transfection reagent-treated cells (Lipo), scrambled siRNA treated cells, siRNA #1 and siRNA #3 specific for SELENBP treated cells were lysed 72 hours after transfection and subjected to Western blot analysis. GAPDH served as an internal loading control.

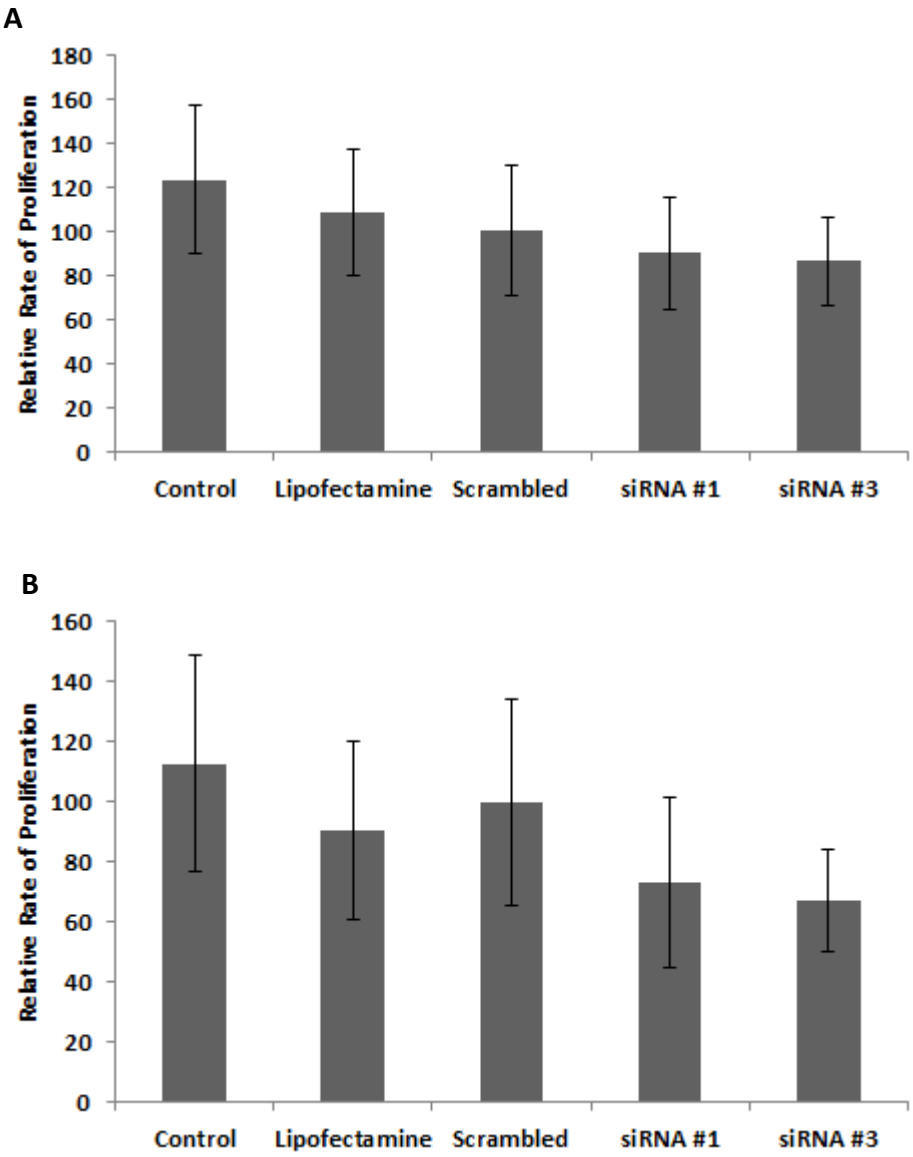

Figure 3.15 Proliferation assay results for (a) 92.1 cells treated with SELENBP1 siRNA #1 (p=0.68) and siRNA #3 (p=0.55), and (b) MEL202 cells treated with SELENBP1 siRNA #1 (p=0.36) and siRNA #3 (p=0.78). No impact on proliferation was noted following siRNA transfection in either the 92-1 or the MEL202 cell line. The combined results and statistics of three independent experiments is shown. All p-values were determined by comparing each siRNA to the scrambled control. n=3.

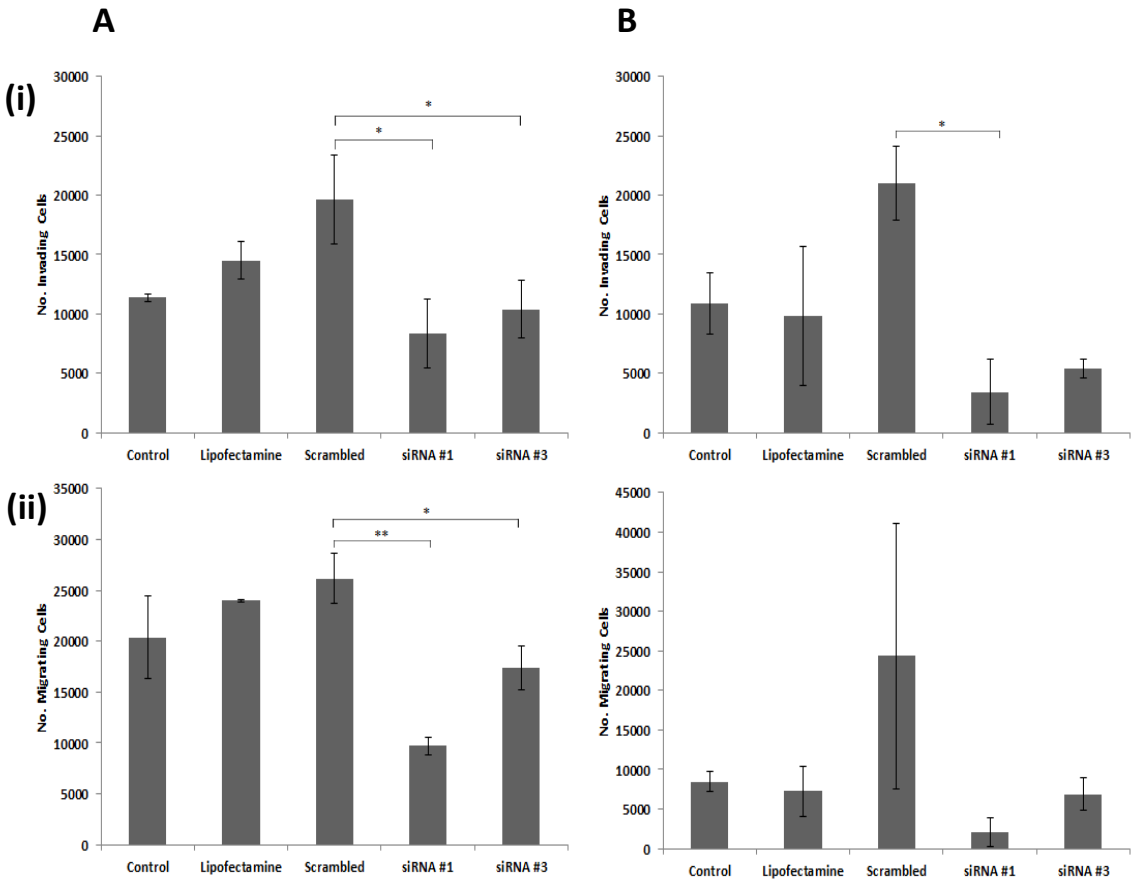

Figure 3.16 siRNA knockdown of SELENBP in the (A) 92.1 and (B) MEL202 uveal melanoma cell line decreases invasion and motility. (i) Invasion assays following siRNA transfection. The total number of cells invading through membranes after siRNA transfection is displayed. 92.1 siRNA #1 p=0.02; siRNA #3 p=0.03. MEL202 siRNA #1 p=0.02; siRNA #3 p=0.03. (ii) Motility assays following siRNA transfection. The total number of cells migrating through uncoated chambers after siRNA transfection is illustrated. 92.1 siRNA #1 p=0.004; siRNA #3 p=0.01. MEL202 siRNA #1 p=0.3; siRNA #3 p=0.4. The combined result and statistics of three independent experiments is shown. *p<0.05, **p<0.01 when compared with scrambled siRNA-treated controls. n=3.

3.7.3.4 Determination of the Effect of SELENBP1 Knockdown on Oxidative Metabolism in 92.1 Uveal Melanoma Cells

Reactive oxygen species (ROS) play an essential role in oxidative metabolism. However when an over-abundance is produced, for example during cell stress such as inflammation, ROS can disrupt the cell through the peroxidation of lipids and destruction of structural proteins, enzymes and nucleic acids. Selenium is an essential trace element which is involved in the function of antioxidant enzymes and proteins that protect the cell against ROS. SELENBP1, a member of the selenoprotein family, is known to bind selenium covalently in order to mediate the intracellular transport of selenium (Zhou, Zhang et al. 2009, Zeng, Yi et al. 2013). Hence, it was decided to examine the ability of 92.1 cells transfected with SELENBP1 siRNA to deactivate ROS, relative to the negative control.

2',7'-dichlorofluorescein-diacetate (DCFH-DA) was used to quantify intracellular produced H_2O_2. DCFH-DA is first transported across the cell membrane where it is deacetylated, becoming trapped within the cell. Through the action of peroxide, it is then converted to 2',7'-dichlorofluorescein (DCF), a highly fluorescent compound, which can be used for measuring the quantity of ROS present. The greater the fluorescence intensity measured, the higher the ROS activity present in the cells.

Overall, no significant difference in ROS activity was observed (Figure 3.14). However, from the Figure 3.14, there appeared to be a mild increase in the activity of ROS in cells transfected with SELENBP1 siRNA in comparison to the lipofectamine-treated controls (Lipo) and negative controls (scrambled). This would suggest that without SELENBP1, selenium cannot sufficiently exert antioxidant effects, hence, the cell cannot control the quantity of ROS produced.

The increase in SELENBP expression does not appear to correlate with the initial establishing of the malignancy, as a significant fold increase was observed in the subsequently metastasised primary uveal melanoma tumour tissue in comparison to the non-metastasised specimens. This increase in abundance may be due to the more aggressive nature of a tumour which has the potential to spread, in comparison to that which does not.

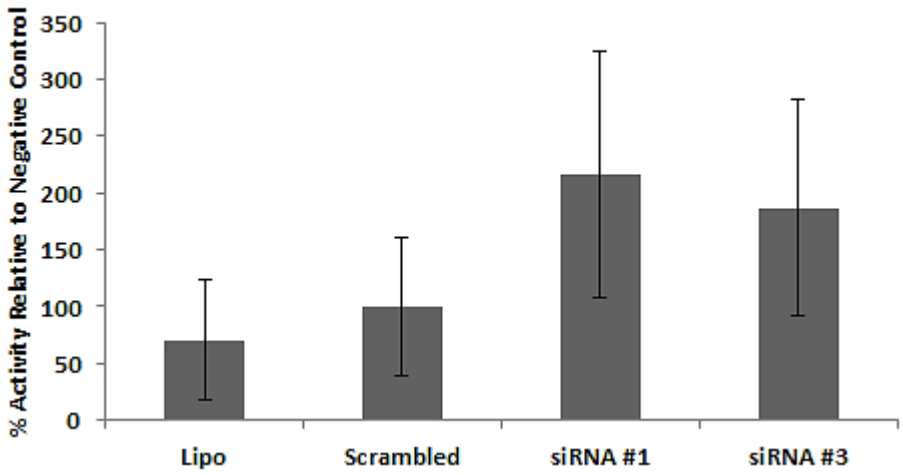

Figure 3.14 Reactive oxygen species (ROS) activity of SELENBP1 siRNA-transfected 92.1 uveal melanoma cells. Analysis was carried out in lipofectamine-treated cells (Lipo), negative controls (scrambled), and cell transfected with two independent siRNA molecules. The ability of SELENBP1 knockdown to increase ROS is shown through increasing fluorescence relative to the negative control. The combined result of three independent experiments is shown. siRNA #1 p=0.14, siRNA #3 p=0.29 when compared to scrambled controls. n=3.

3.7.4 KPNB1 Downregulation in MEL202 and 92.1 Cell Lines for the Determination of a Potential Role in Invasion and Migration

92.1 and MEL202 uveal melanoma cells were transfected with two independent siRNA, siRNA #2 and #3, in order to determine the effect of downregulation of KPNB1 on the invasive and migratory properties of uveal melanoma cells. Using western blotting, the reduction in protein levels of KPNB1 in both cell lines was confirmed (Figure 3.15 (A) and (B)).

3.7.4.1 Proliferation

Proliferation assays illustrated that there was no significant effect on proliferation in either 92.1 or MEL202 cells treated with both KPNB1 siRNA in comparison to scrambled siRNA treated cells (Figure 3.16 (A) and (B)).

3.7.4.2 Invasion

Invasion assays were carried out at 72 hours following transfection. From this, it was found that the total number of cells invading through the membrane was significantly decreased following transfection, in 92.1 cells and in MEL202 cells treated with siRNA #2 (Figure 3.17 (A) and (B), i).

3.7.4.3 Migration

Migration assays were carried out at 72 hours following transfection. From this, it was found that there was a significant reduction in the number of 92.1 cells migrating across the membrane (Figure 3.17 (A), ii). No significant effect on the migration of MEL202 cells was observed following transfection, although a clear trend in decreased cell number was observed. This again may have been due to the nature of MEL202 cells, as outlined in section 3.7.3.3.

These results indicate that KPNB1 may be required for both invasion and migration in 92.1 and MEL202 cells, and hence, may play a role the process of metastasis in uveal melanoma.

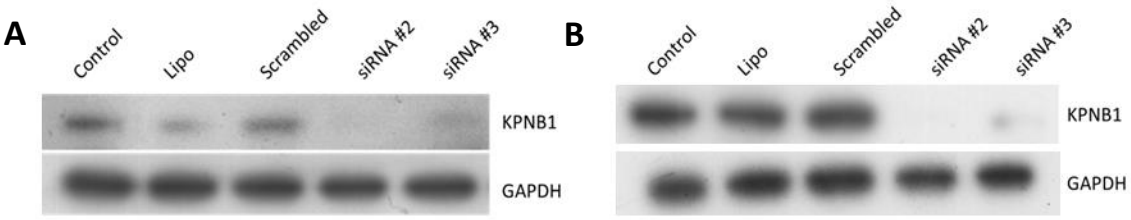

Figure 3.15 Western blot analysis showing the reduction of KPNB1 in (A) 92.1 and (B) MEL202 cell lines following siRNA knockdown. Control cells (untreated), transfection reagent-treated cells (Lipo), scrambled siRNA treated cells, siRNA #1 and siRNA #3 specific for KPNB1 treated cells were lysed 72 hours after transfection and subjected to Western blot analysis. GAPDH served as an internal loading control.

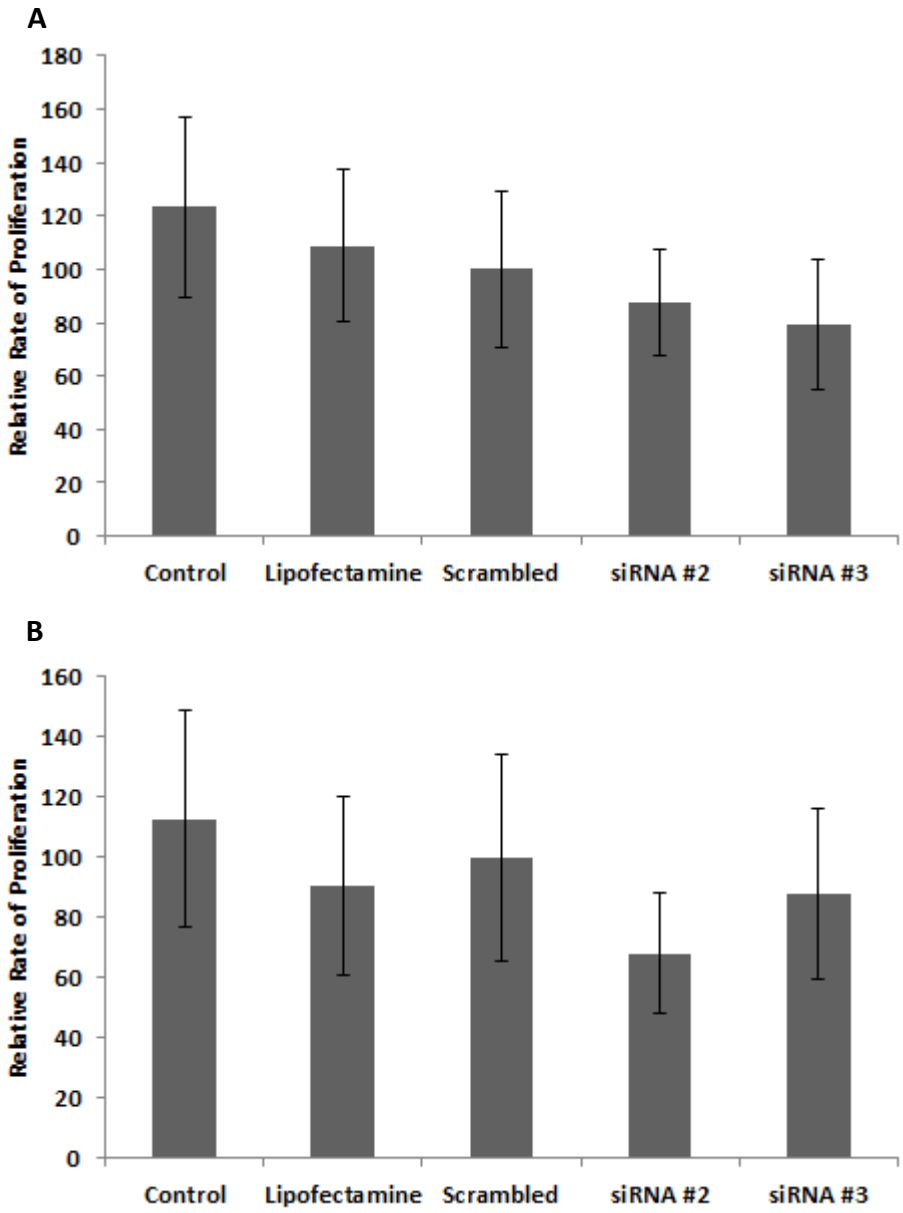

Figure 3.16 Proliferation assay results for (a) 92.1 cells treated with KPNB1 siRNA #2 (p=0.59) and siRNA #3 (p=0.41), and (b) MEL202 cells treated with KPNB1 siRNA #2 (p=0.25) and siRNA #3 (p=0.38). No effect on proliferation was noticed following siRNA transfection in both the 92-1 and MEL202 cell lines. The combined results and statistics of three independent experiments is shown. All p-values were determined by comparing each siRNA to the scrambled control. n=3.

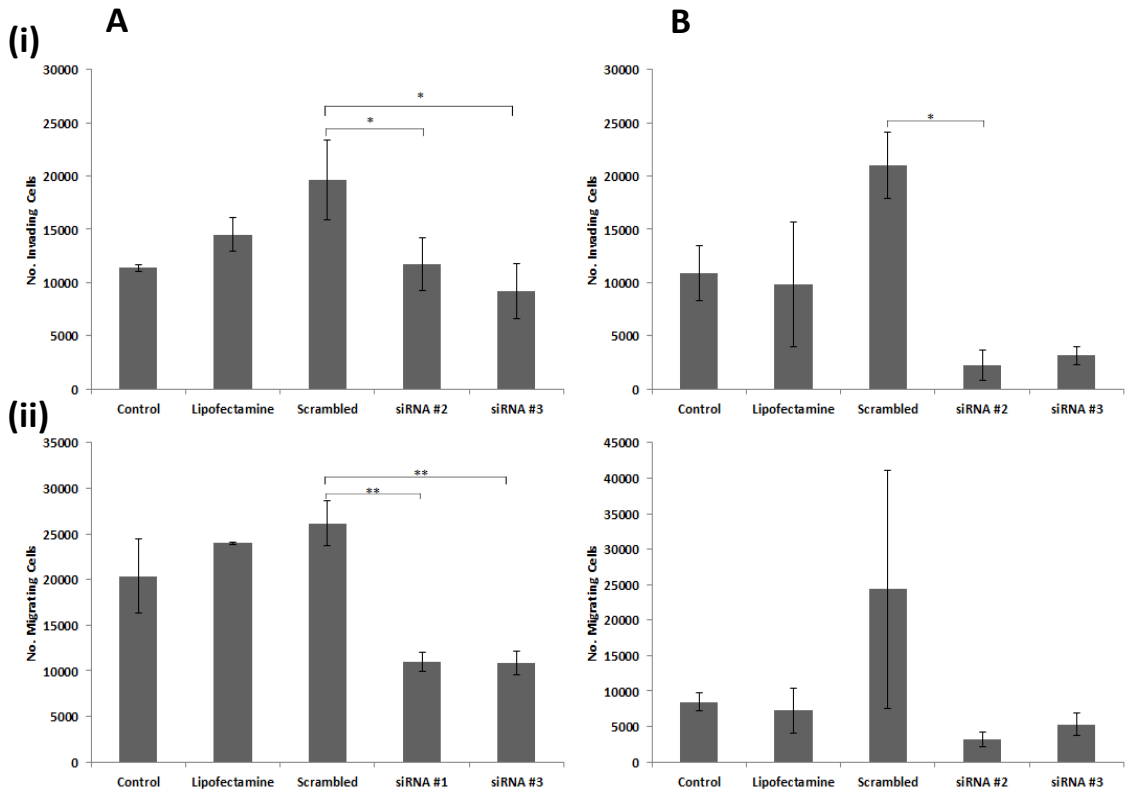

Figure 3.17 siRNA knockdown of KPNB1 in (A) 92.1 and (B) MEL202 cell lines decreases invasion and motility. (i). Invasion assays of 92.1 cells following siRNA transfection. The total number of 92.1 cells invading through membranes of invasion chambers after siRNA transfection is shown. 92.1 siRNA #2 p=0.04; siRNA #3 p=0.02. MEL202 siRNA #2 p=0.04; siRNA #3 p=0.07. (ii) Motility assays of 92.1 cells following siRNA transfection. The total number of 92.1 cells migrating through uncoated membrane after siRNA transfection is shown. 92.1 siRNA #2 p=0.003; siRNA #3 p=0.002. MEL202 siRNA #2 p=0.32; siRNA #3 p=0.35. The combined result and statistics of three independent experiments is shown. *p<0.05, **p<0.01 when compared with scrambled siRNA-treated controls. n=3.

3.7.5 EEF1G Downregulation in MEL202 and 92.1 Cell Lines for the Determination of a Potential Role in Invasion and Migration

Two independent siRNA, siRNA #2 and #4, were transfected into 92.1 and MEL202 uveal melanoma cells in order to downregulate the production of EEF1G. The knockdown cells would then be used to determine the role of the protein in processes of invasion and migration. Western blotting illustrated a reduction in EEF1G levels for both cell lines, thus confirming the transfection (Figure 3.18 (A) and (B), i).

3.7.5.1 Proliferation

Proliferation assays illustrated that there was no effect on proliferation in 92.1 and MEL202 cells treated with EEF1G siRNA in comparison to the negative control (Figure 3.19 (A) and (B)).

3.7.5.2 Invasion

Invasion assays were carried out at 72 hours following the transfection of both cell lines. From this, it was found that the total number of cells invading through the membrane was significantly decreased for both cell lines, as a result of the transfection (Figure 3.20 (A) and (B), i).

3.7.5.3 Migration

Migration assays were carried out 72 hours following the transfection of both cell lines. A significant reduction in the number of 92.1 cells migrating across the membrane was observed (Figure 3.20 (A), ii). No significant effect on the migration of MEL202 cells was observed following transfection, although a clear reduction of cell number was observed. This again may have been due to the nature of MEL202 cells, as outlined in section 3.7.3.3.

These results indicate that EEF1G may be required for invasion and migration in 92.1 and MEL202 cells, and hence, may play a role in metastatic uveal melanoma.

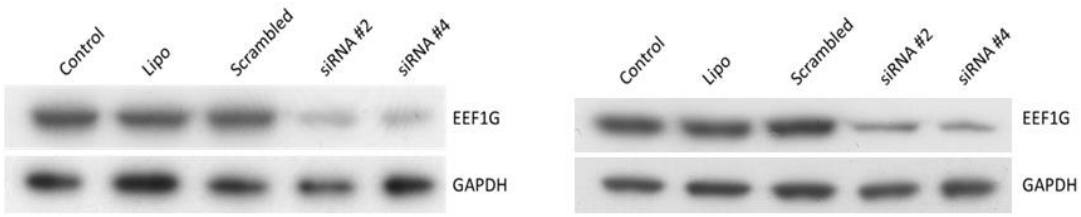

Figure 3.18 Western blot analysis showing the reduction of EEF1G following siRNA knockdown. Control cells (untreated), transfection reagent-treated cells (Lipo), scrambled siRNA treated cells, siRNA #2 and siRNA #4 specific for EEF1G treated cells were lysed 72 hours after transfection and subjected to Western blot analysis. GAPDH served as an internal loading control.

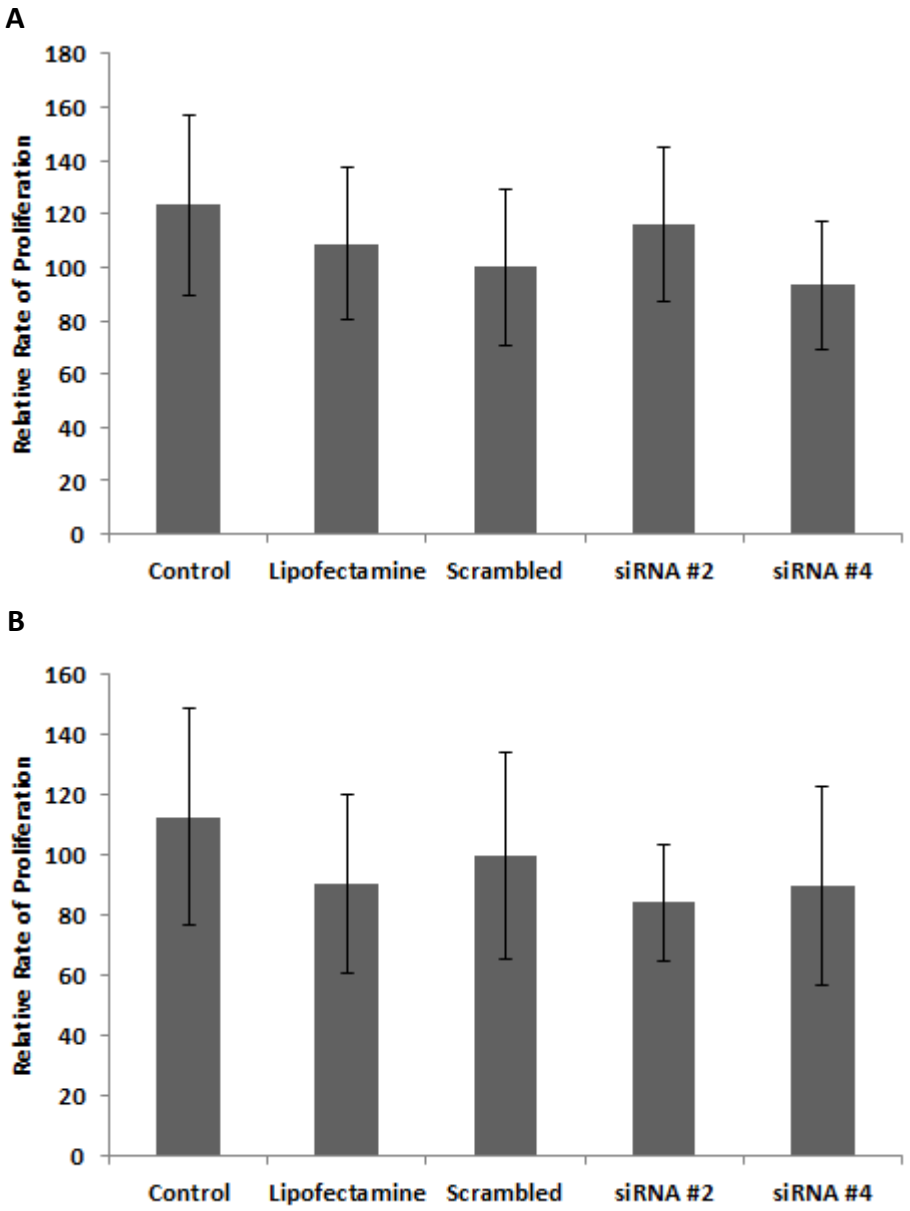

Figure 3.17 Proliferation assay results for (A) 92.1 cells treated with EEF1G siRNA #2 (p=0.53) and siRNA #4 (p=0.77), and (B) MEL202 cells treated with EEF1G siRNA #4 (p=0.54) and siRNA #4 (p=0.82). No effect on proliferation was noticed following transfection in either cell line. The combined results and statistics of three independent experiments is shown. All p-values were determined by comparing each siRNA to the scrambled control. n=3.

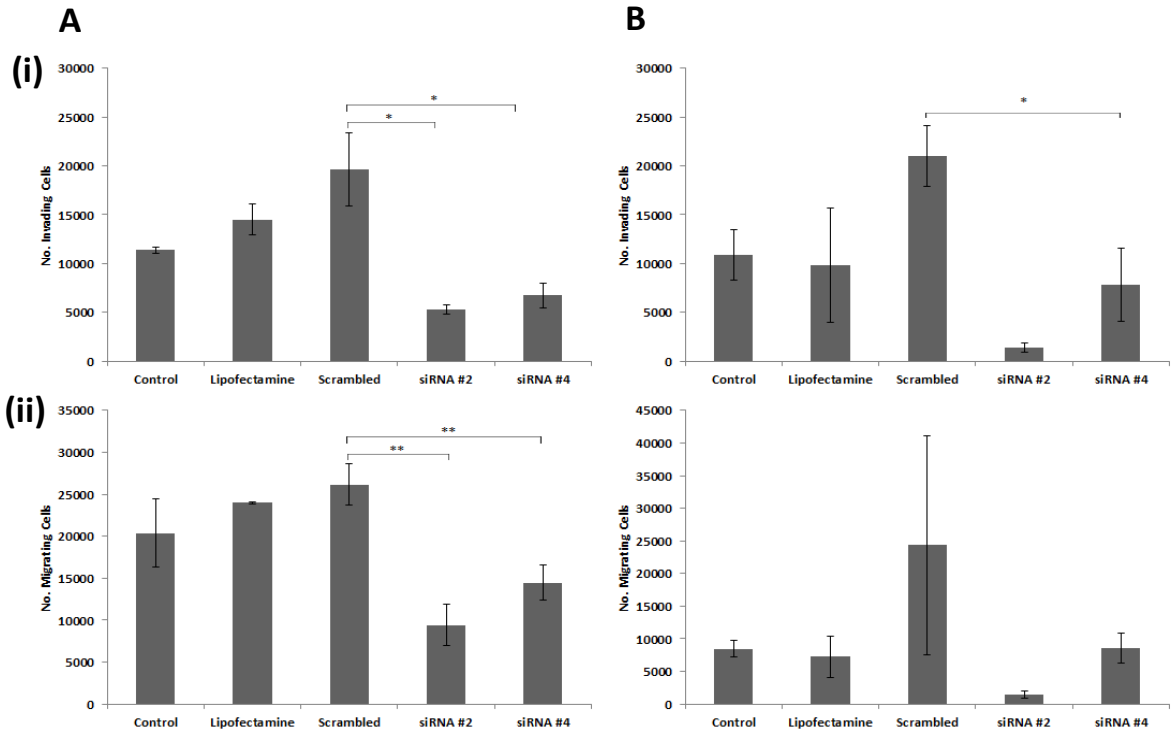

Figure 3.18 siRNA knockdown of EEF1G decreases invasion and motility in (A) 92.1 and (B) MEL202 cell lines. (i). Invasion assays of 92.1 cells following siRNA transfection. The total number of 92.1 cells invading through invasion chamber membranes after siRNA transfection is shown. 92.1 siRNA #2 p=0.02; siRNA #4 p=0.02. MEL202 siRNA #2 p=0.07; siRNA #4 p=0.03. (ii) Motility assays of 92.1 cells following siRNA transfection. The total number of 92.1 cells migrating through uncoated membrane after siRNA transfection is shown. 92.1 siRNA #2 p=0.001; siRNA #4 p=0.004. MEL202 siRNA #2 p=0.3; siRNA #4 p=0.4. The combined results of three independent experiments is shown. *p<0.05, **p<0.01 when compared with scrambled siRNA-treated controls. n=3.

.

3.7.6 Gelatin Zymography Analysis of Cells treated with SELENBP1, KPNB1 and EEF1G siRNA

Zymography can be used to detect and characterise proteases, such as matrix metalloproteases (MMPs), using either casein or gelatin as a substrate, depending on the species of enzyme to be detected. Initially, the proteins are separated under non-reducing and denaturing, i.e. inactivating, conditions. The zymography gel consists of polyacrylamide which is co-polymerised with a substrate. Following electrophoresis, the gel is placed in a solution of Triton X-100 which renatures and reactivates the enzymes, allowing them to digest the substrate. Coomassie Blue is then used to stain the background of undegraded substrate, with MMPs remaining unstained and appearing as clear bands (Snoek-van Beurden and Von den Hoff 2005).

As SELENBP1, EEF1G, and KPNB1 were all found to play a role in invasion, it was hypothesised that MMP-9 and MMP-2 may be involved in this process. MMPs have long been associated with tumour progression and the invasion process, and are often upregulated in tumours and tumour cell lines. In particular, MMP-2 and MMP-9 are often connected with melanoma disease progression (Coussens, Fingleton et al. 2002, Schnaeker, Ossig et al. 2004, Nikkola, Vihinen et al. 2005). MMP-2 and -9 have also previously been implicated in uveal melanoma metastasis (Lai, Conway et al. 2008, Jannie, Stipp et al. 2012).

The 92.1 and MEL202 uveal melanoma cell lines were both transfected with siRNA specific to SELENBP1, KPNB1, and EEF1G. The knockdown cells were then grown for 24 hours before being incubated with serum-free media for a further 48 hours. The media from the cells was then collected, and concentrated prior to zymography. In parallel, conditioned media was collected from large flasks of healthy cells. This analysis indicated that MMP-2 and MMP-9 were unaffected following transfection of either cell line with any of the siRNA (Figure 3.19). This would suggest that neither MMP-2 nor MMP-9 play a role in the invasion pathways affected by the knockdown of any of the three proteins.

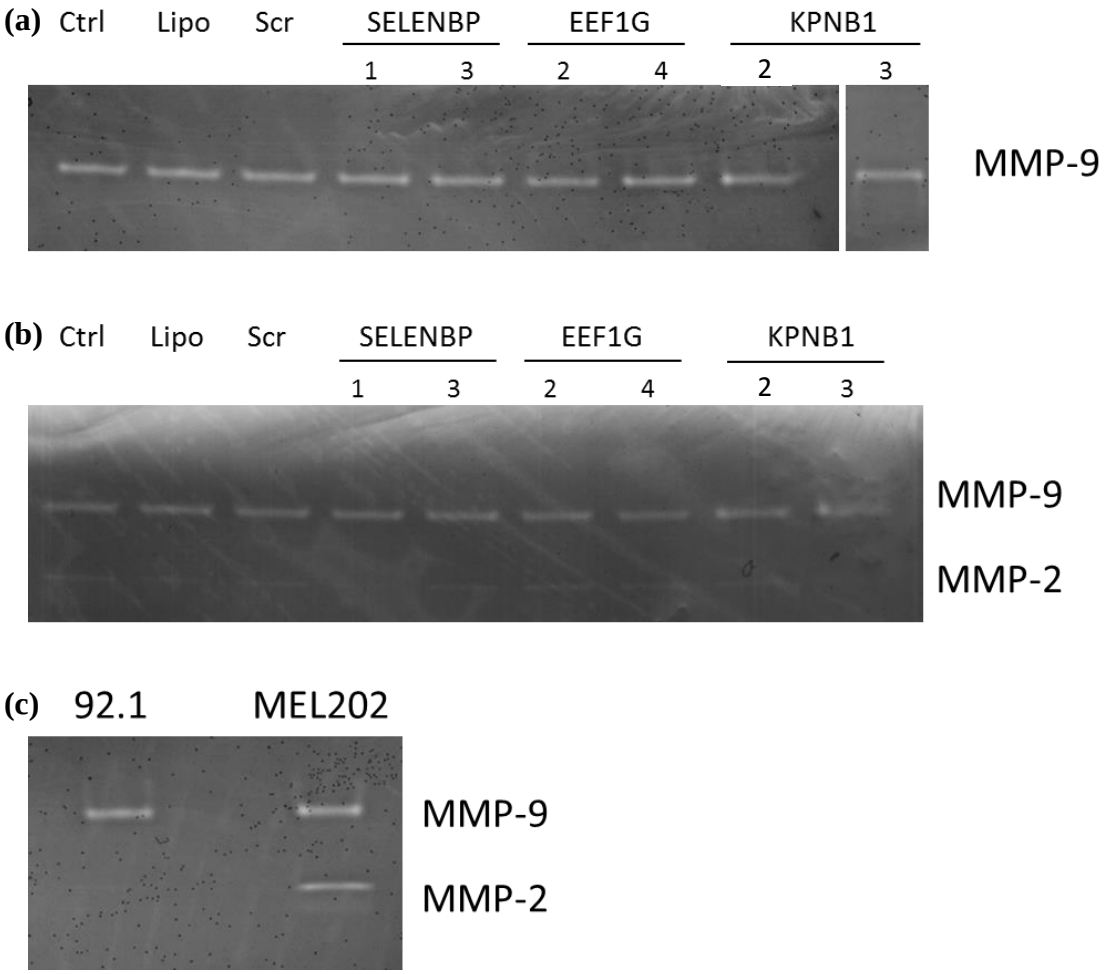

Figure 3.19 Gelatin zymograms illustrating the effect of siRNA-mediated knockdown of SELENBP, EEF1G and KPNB1 on MMP-9 and MMP-2 activity. In both the (a) 92.1 and (b) MEL202 uveal melanoma cell lines, no effect on the abundance of either MMP-2 or -9 was observed following the downregulation of SELENBP1, EEF1G, or KPNB1. (c) When the expression of MMP-2 and MMP-9 was examined in healthy 92.1 and MEL202 cells, MMP-9 was found to be expressed in both cell lines while MMP-2 was only identified in MEL202 cells. n=2.

3.7.7 Analysis of Early, Late, and Total Apoptosis in SELENBP1, EEF1G, and KPNB1 92.1 Knockdowns

Apoptosis is defined as programmed cell death and is essential for tissue homeostasis. Its inhibition is often required for tumorigenesis; for example, the *bcl-2* gene encodes a cell death inhibitory protein which aids the development of cancer and can prevent apoptosis following treatment with an array of toxins or drugs. A high rate of apoptosis may also be observed in various cancers, which can often explain why a tumour, such as a basal cell carcinoma, is slow growing. Both pro- and anti-apoptotic features have been described in uveal melanoma. Tumour necrosis factor-related apoptosis inducing ligand (TRAIL) has been identified as a pro-apoptotic feature while Bcl-2 gene proteins have been shown to inhibit apoptosis in uveal melanoma (Wang, Boonman et al. 2003, Ren, Mayhew et al. 2004, Gill and Char 2012).

In order to determine the potential roles of SELENBP1, EEF1G, and KPNB1 in the apoptotic pathways of uveal melanoma, 92.1 cells were transfected with siRNA specific to each protein and stained with fluorescent markers of apoptosis, followed by measurement of fluorescence using flow cytometry (Figure 3.20).

Apoptosis was examined by labelling the cells with 7-aminactinomycin D (7-AAD) and Phycoerythrin (PE) annexin-V, and measuring the level of fluorescence with flow cytometry. Loss of plasma membrane integrity is one of the earliest features of apoptosis. This involves the translocation of phosphatidylserine (PS) from the inner to the outer leaflet of the membrane. Thus annexin V, which may be conjugated to a fluorochrome such as PE, can bind to the exposed PS and hence, can measure apoptosis at an early stage. PE annexin V is often used in conjunction with a vital dye such as 7-AAD; a fluorescent compound which specifically binds to GC regions of the DNA, to allowing for the identification of early apoptotic cells (e.g. 7-AAD negative, PE annexin V positive). Viable cells with intact membranes exclude 7-AAD, while the membranes of dead and damaged cells are permeable to 7-AAD (Zembruski, Stache et al. 2012).

No statistically significant results were generated from the analysis of early, apoptosis, late apoptosis/death, or total apoptosis across all knockdowns when compared to the negative control (Figure 3.21). This would suggest that none of the

three proteins of interest appear to play a role in apoptosis. Individual graphs for early apoptosis, late apoptosis/death, and total apoptosis are illustrated in Figures 3.22, 3.23, and 3.24, respectively.

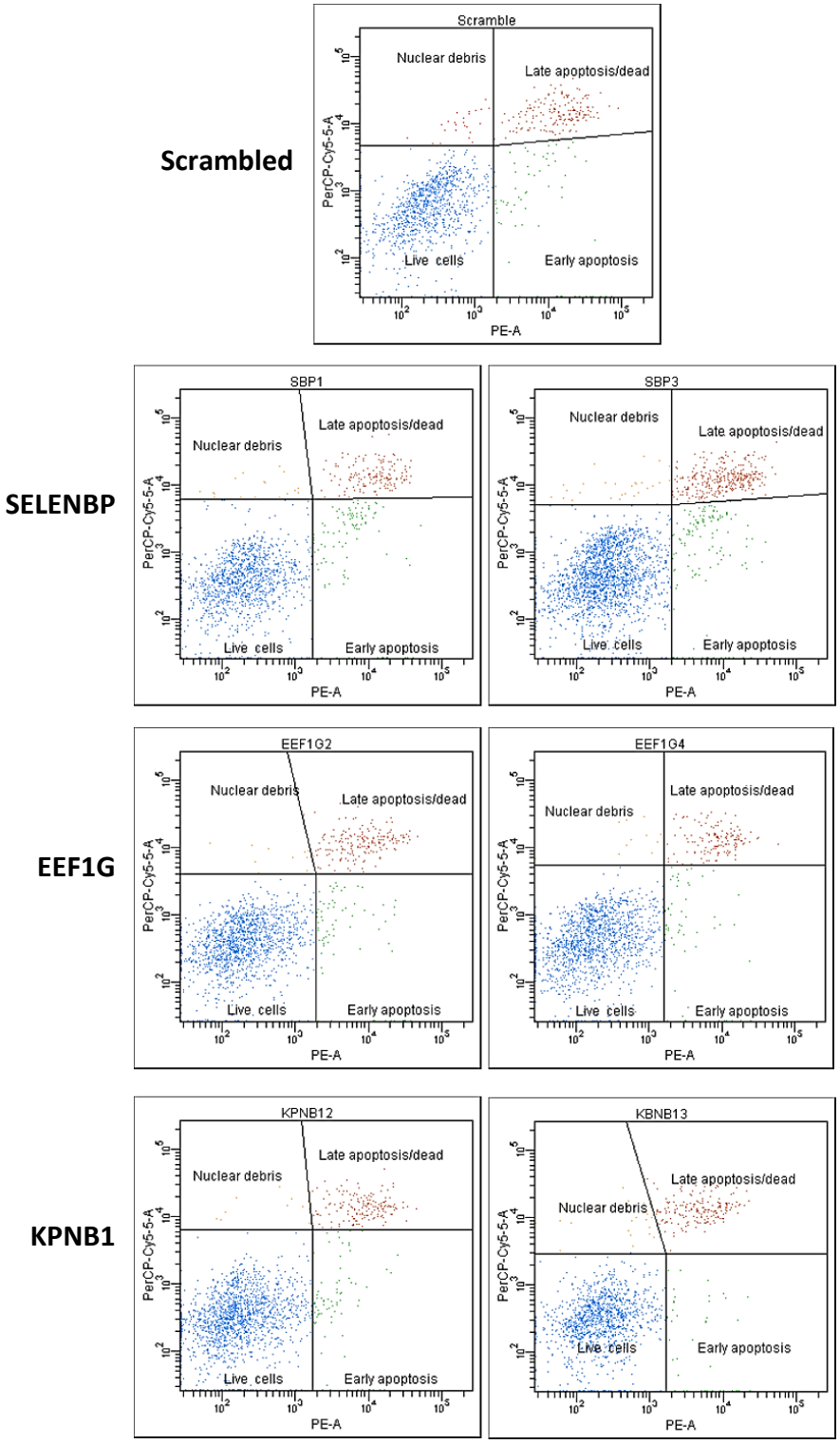

Figure 3.20 Dot plots illustrating the overall trend of healthy cells, and early, and late/death stage apoptosis across all knockdowns with two independent siRNA. No significant differences in the number of apoptosing cells were observed for either of the two independent siRNA used to downregulate the production of each of the three

proteins, when compared to the scrambled (negative) control. One representative result of three independent experiments is shown. n=3.

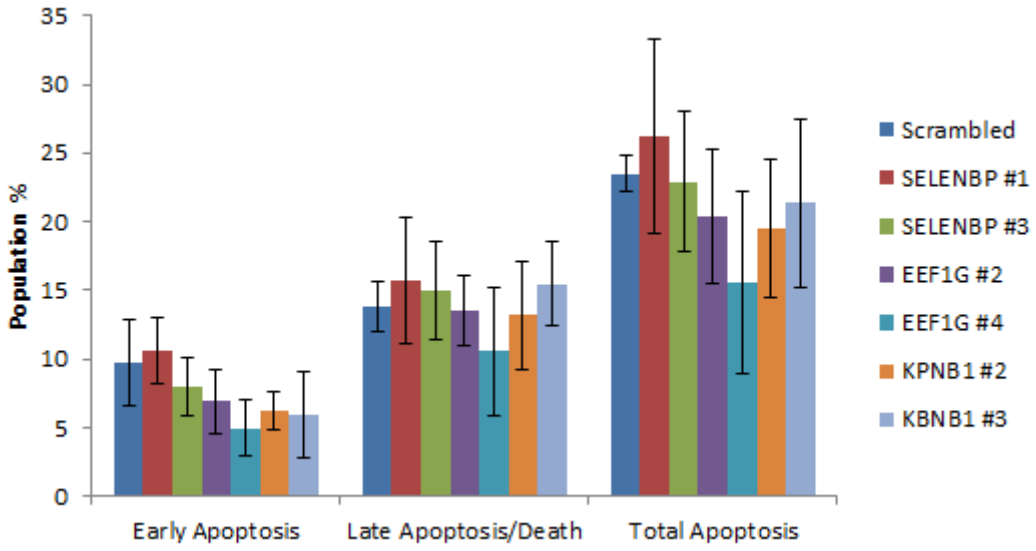

Figure 3.21 Bar charts illustrating the overall trend of early, late/death, and total apoptosis across all knockdowns. No statistically significant differences in the number of cells undergoing apoptosis were observed for either of the two independent siRNA used to downregulate the production of each of the three proteins, in comparison to the scrambled (negative) control. The results shown represent the average of three independent experiments. n=3.

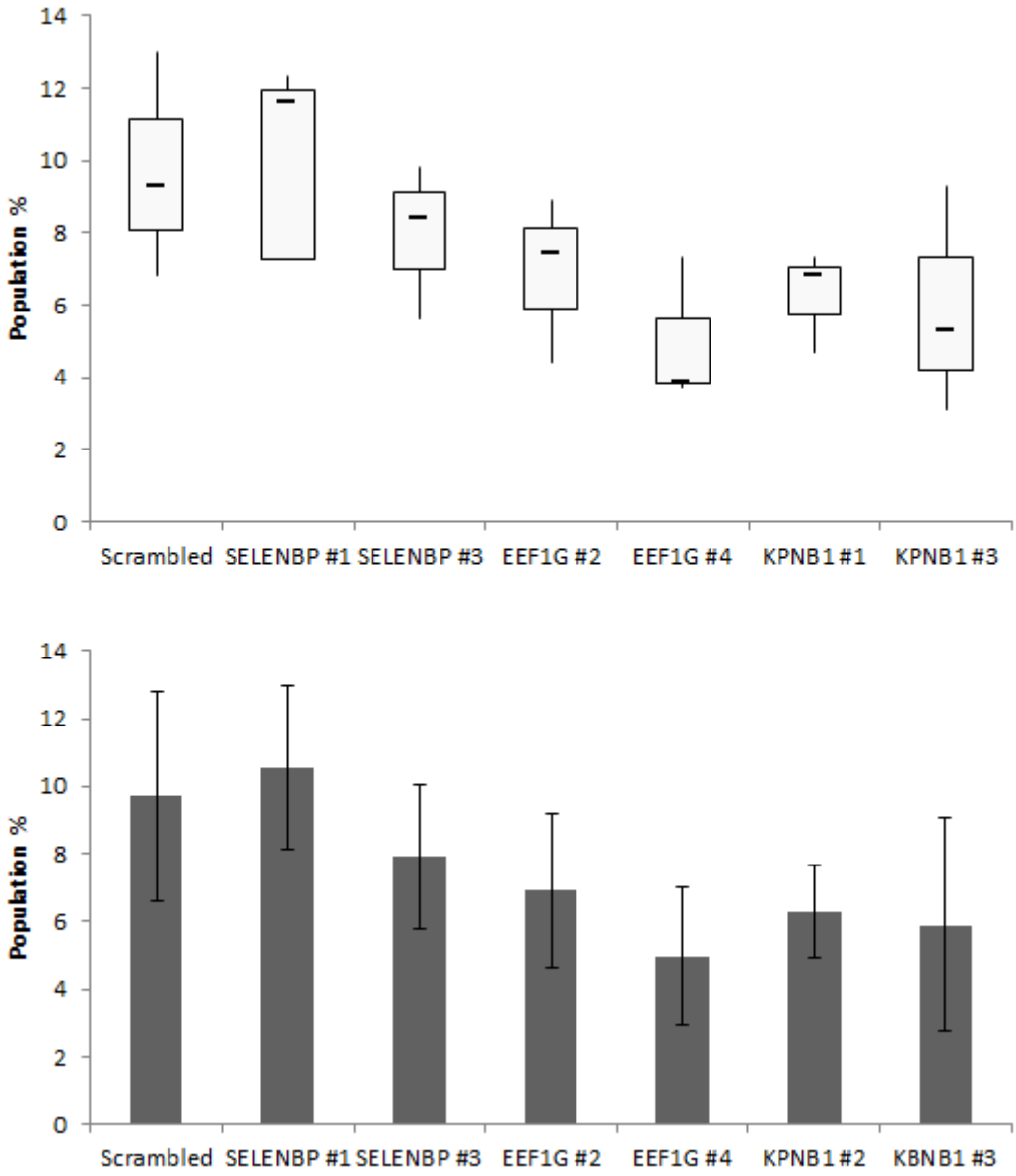

Figure 3.22 Bar chart and box and whisker plot of early apoptosis across all three downregulated proteins of interest, with two independent siRNA each, in 92.1 cells. In comparison to the scrambled (negative) control, no statistically significant change in apoptosis was observed for both siRNA against any of the three proteins. There appeared to be a trend of decreased early apoptosis in EEF1G and KPNB1 transfected cells, however, this was not deemed as significant. n=3.

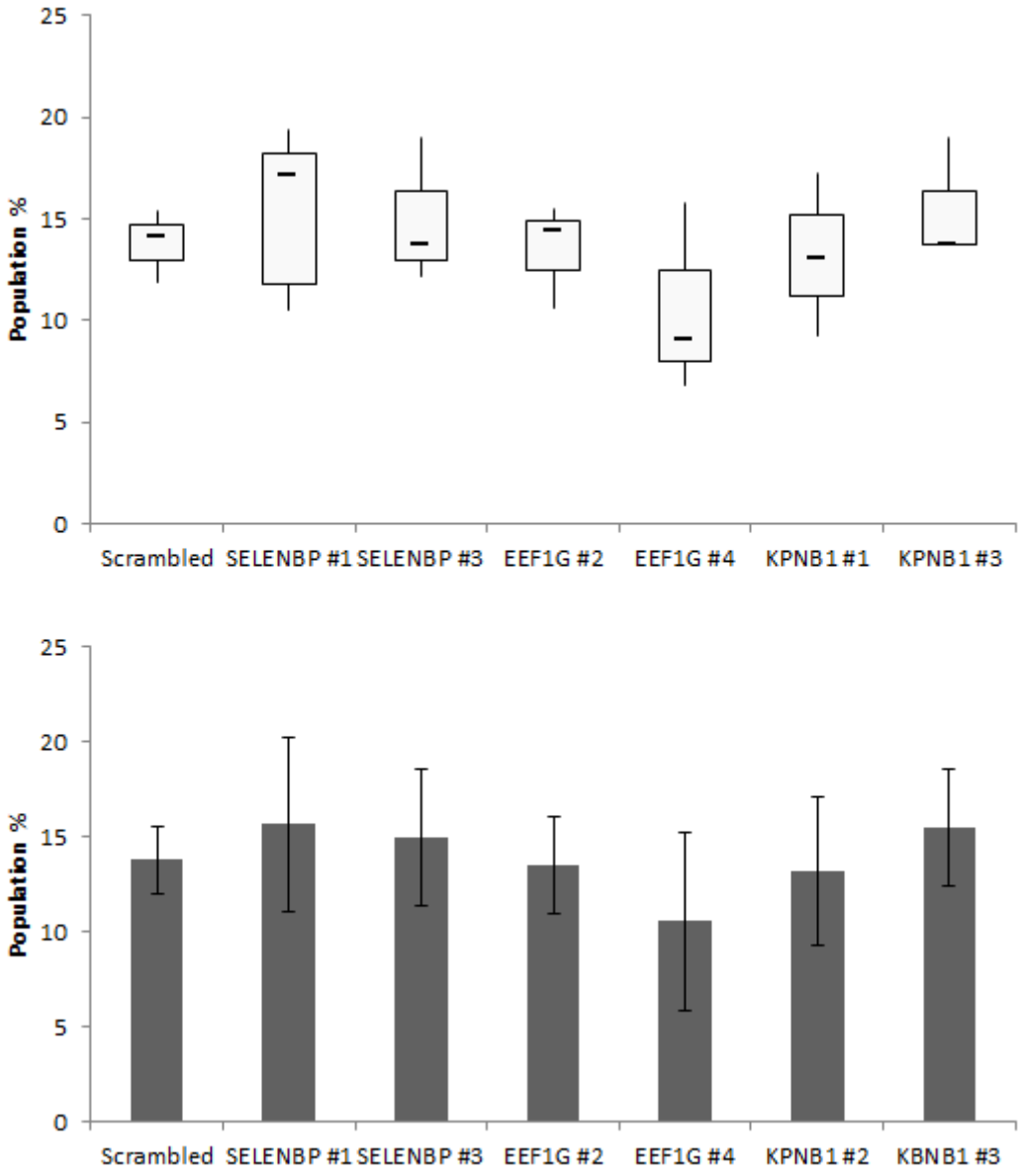

Figure 3.23 Bar chart and box and whisker plot of late apoptosis/deaths across all three downregulated proteins of interest, with two independent siRNA each, in 92.1 cells. In comparison to the scrambled (negative) control, no significant trend in apoptosis was observed for both siRNA against any of the three proteins. n=3.

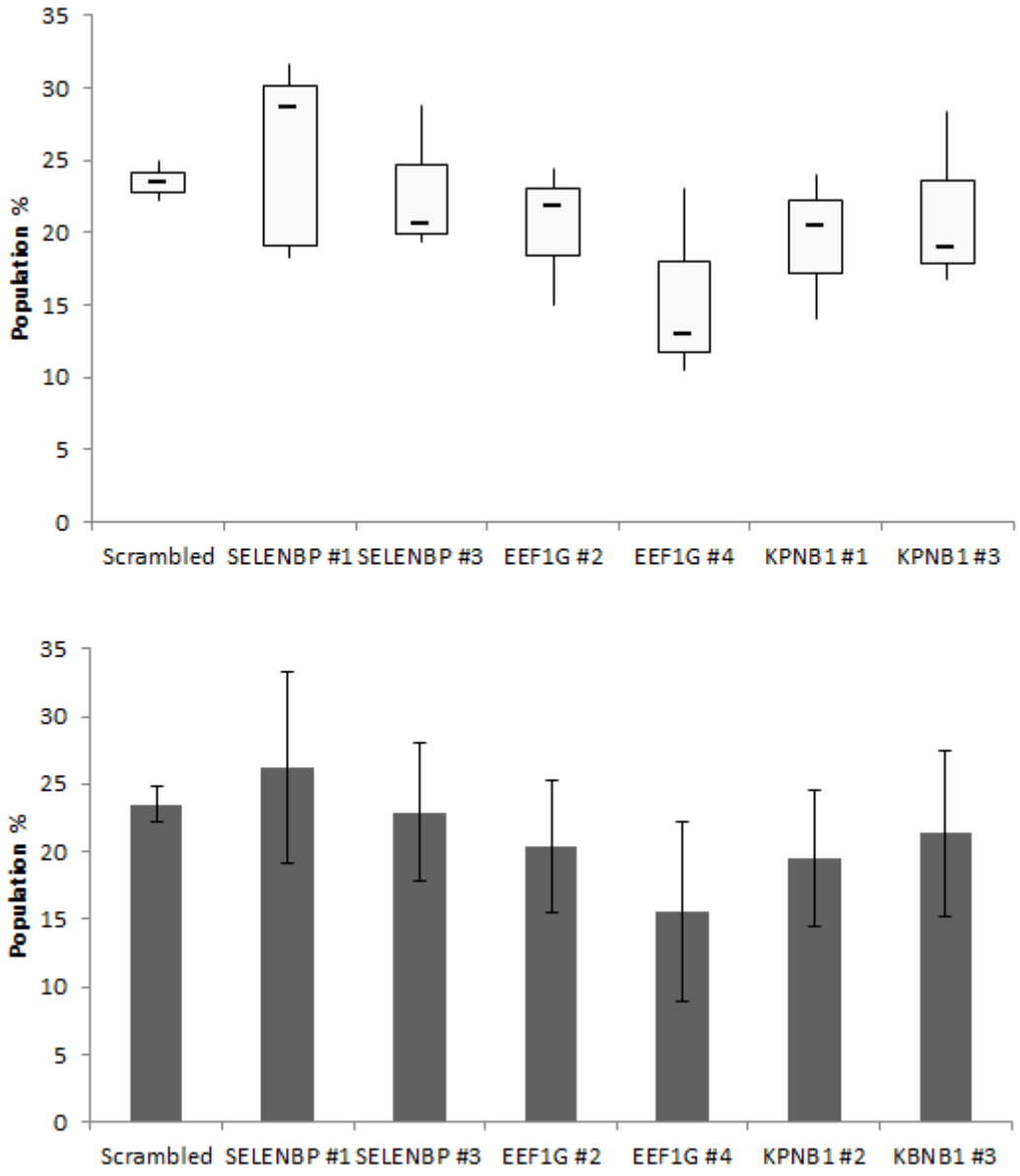

Figure 3.24 Bar chart and box and whisker plot of total apoptosis across all three downregulated proteins of interest, with two independent siRNA each, in 92.1 cells. In comparison to the scrambled (negative) control, no significant trend in apoptosis was observed for both siRNA knockdowns against any of the three proteins. n=3.

CHAPTER FOUR

Vitreous Fluid Sample Optimisation

4.1 Background

Vitreous humour is a gel-like substance contained in the posterior chamber of the eye. As it is often in close proximity to sites of trauma within the eye, it may be a valuable specimen for clinical proteomic analyses.

The fluid may be collected during surgery such as enucleation, hence it can be collected from uveal melanoma patients. However, a minimal number of proteomic studies, which are outlined in chapter one, have been carried out to date in uveal melanoma vitreous specimens. In addition to this, it can be a variable and sometimes difficult specimen to work with, often only providing information on highly abundant proteins (Shitama, Hayashi et al. 2008). Little information was available on the best methods for pre-processing and proteomic analysis of vitreous fluid, as most methods appeared to generate the same data.

In this regard, it was decided that prior to examining the vitreous fluid, methods of sample pre-treatment and analysis would first have to be devised. A summary of all tested pre-treatment and analytical methods used in the work presented is shown at the end of this chapter (Figure 4.21). Following this it would be possible to perform a proteomic analysis of the vitreous extracted from uveal melanoma patients, with the intention of identifying potential biomarkers which may correlate with a poor outcome in uveal melanoma, thus improving our understanding of the metastatic disease and identifying potential therapeutic targets.

4.2 1-D Gel Analysis of Vitreous Fluid

21 vitreous fluid samples were acquired from the Royal Victoria Eye and Ear Hospital, Dublin. Initially, protein assays were performed in order to quantify the protein levels across all of the six control (collected from patients with macular hole degeneration) and 13 disease samples. The protein concentrations varied significantly between the samples with values ranging from 0.27 mg/mL to 34 mg/mL.

In order to get an overall view of the general content of the proteome, two control samples, which had been extracted from macular hole degeneration patients, were selected for preliminary analysis by separation on a 1-D gel (Figure 4.1). Following

staining, it was clear that there were significant levels of high abundant proteins present in the vitreous fluid which had smeared across other regions. This would create difficulties in identifying less abundant proteins as, once digested, high abundance proteins can produce elevated quantities of tryptic peptides thus creating proteolytic background and a bias for the identification of such proteins. Hence, a limited dynamic range is available which can only be improved through extra chromatographic fractionation (Fonslow, Stein et al. 2013).

Despite this, eight regions were excised from the gel and digested using trypsin to generate peptides which were subsequently identified by LC-MS/MS. The table of identifications generated, Table 4.1, illustrates that many of proteins found in the samples were highly abundant and commonly found in clinical specimens such as serum or plasma. As the vitreous fluid proteome is only beginning to be mapped in its entirety, proteins which are known to be of high or medium abundance in the plasma proteome were used as a measure of potentially high or medium abundance proteins in the vitreous. In this way it would be possible to examine how well a pre-treatment method worked. For each qualitative table of this chapter, proteins of high or medium abundance are noted. Serum albumin, transferrin, fibrinogen, alpha-2-macroglobulin, alpha-1-antitrypsin, complement C3, haptoglobin, IgM, IgA, IgG, IgD and their components were all denoted as highly abundant, as 90% of plasma is known to be composed of these proteins. Apolipoprotein A1, apolipoprotein A2, apolipoprotein B, acid-1-glycoprotein, ceruloplasmin, complement C4, complement C1q, prealbumin, and plasminogen, which make up a further 9% of the plasma proteome, were all denoted as being of medium abundance. Only the remaining 1% of the plasma proteome is composed of low abundance proteins which may consist of more potential targets of interest (Anderson and Anderson 2002). It is important to note that although the levels of high abundant proteins were depleted initially, any patterns of differential regulation seen with such proteins later on were not ruled out.

Table 4.1 indicated that vitreous fluid would have to be pre-processed by removing the majority of the high and medium abundant proteins present. This would allow for the identification of any low abundant proteins which may be masked by more highly abundant proteins.

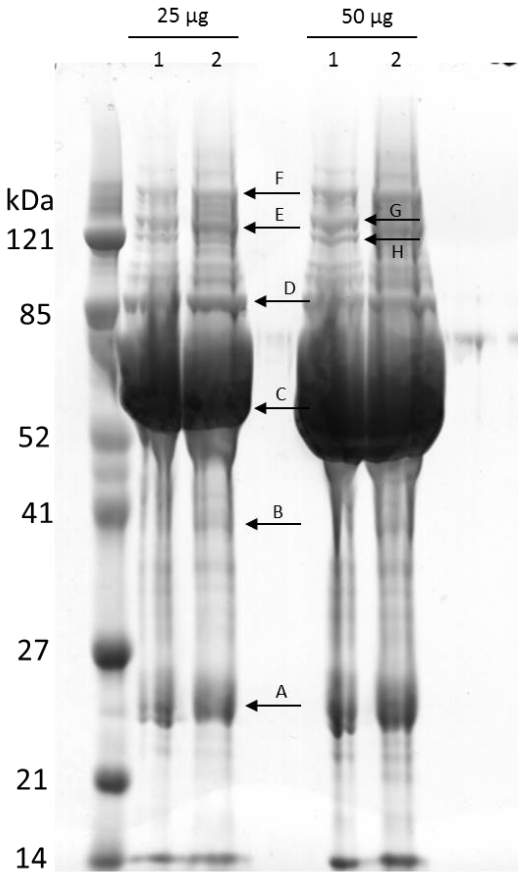

Figure 4.1 1-D separation of control vitreous fluid samples (n=2) was used in order to examine the vitreous fluid proteome. Proteins were separated through a 10% Bis-Tris gel and stained with Coomassie Brilliant Blue. The regions of interest, indicated by an arrow and a corresponding letter, were then excised and the in-gel digestion of proteins to peptides was carried out using trypsin. The samples were analysed in the following order to ensure a minimum carry-over of high abundance proteins; F, H, G, E, D, B, A, C.

Controls 1 & 2	Accession No.	Abundance
Serum albumin	P02768	High
Apolipoprotein A-I	P02647	Medium
Complement C3	P01024	High
Ig kappa chain V-IV region Len	P01625	High
Prostaglandin-H2 D-isomerase	P41222	
Beta-crystallin B1	P53674	
Fibrinogen beta chain	P02675	High
Chitinase-3-like protein 1	P36222	
Haptoglobin	P00738	High
Serotransferrin	P02787	High
Zinc-alpha-2-glycoprotein	P25311	
Fibrinogen gamma chain	P02679	High
Alpha-1-acid glycoprotein 1	P02763	Medium
Clusterin	P10909	
Antithrombin-III	P01008	
Fibrinogen alpha chain	P02671	High
Alpha-1-acid glycoprotein 2	P19652	
Ig gamma-1 chain C region	P01857	High
Haptoglobin-related protein	P00739	
Alpha-1-antichymotrypsin	P01011	
Hemopexin	P02790	
Ig kappa chain C region	P01834	High
Plasma protease C1 inhibitor	P05155	
Afamin	P43652	
Inter-alpha-trypsin inhibitor heavy chain H4	Q14624	
Ceruloplasmin	P00450	Medium
Alpha-1-antitrypsin	P01009	High
Ig alpha-1 chain C region	P01857	High

Table 4.1 Combined protein identifications of control #1 and control #2 from the regions of interest indicated in Figure 4.1. Abundance refers to the quantity of each protein typically found in clinical specimens, such as plasma. Many of the proteins identified were of high or medium abundance (Anderson and Anderson 2002).

As the gel contained a large band which smeared across the gel in the 60-70 kDa region, it was expected that the protein was serum albumin. This band covered the majority of the middle section of the gel and so it contaminated other protein bands. Hence, the vitreous was treated with a multiple affinity removal immunodepletion column which removes 14 of the most abundant proteins found in clinical samples; serum albumin, IgG, antitrypsin, IgA, transferrin, haptoglobin, fibrinogen, alpha2-macroglobulin, alpha1-acid glycoprotein, IgM, apolipoprotein AI, apolipoprotein AII, complement C3 and transthyretin.

A western blot was used to compare the immunodepleted sample to the crude sample (Figure 4.2 (a)). This confirmed the high levels of serum albumin in the crude sample as it was smeared throughout the blot. However, this also illustrated that although the majority of the protein had been removed by immunodepletion, some still remained.

It was decided to immunodeplete the same sample twice and to compare it to the crude sample. This resulted in no detectable serum albumin being identified in the treated sample, while the crude samples remained the same as before (Figure 4.2 (b)).

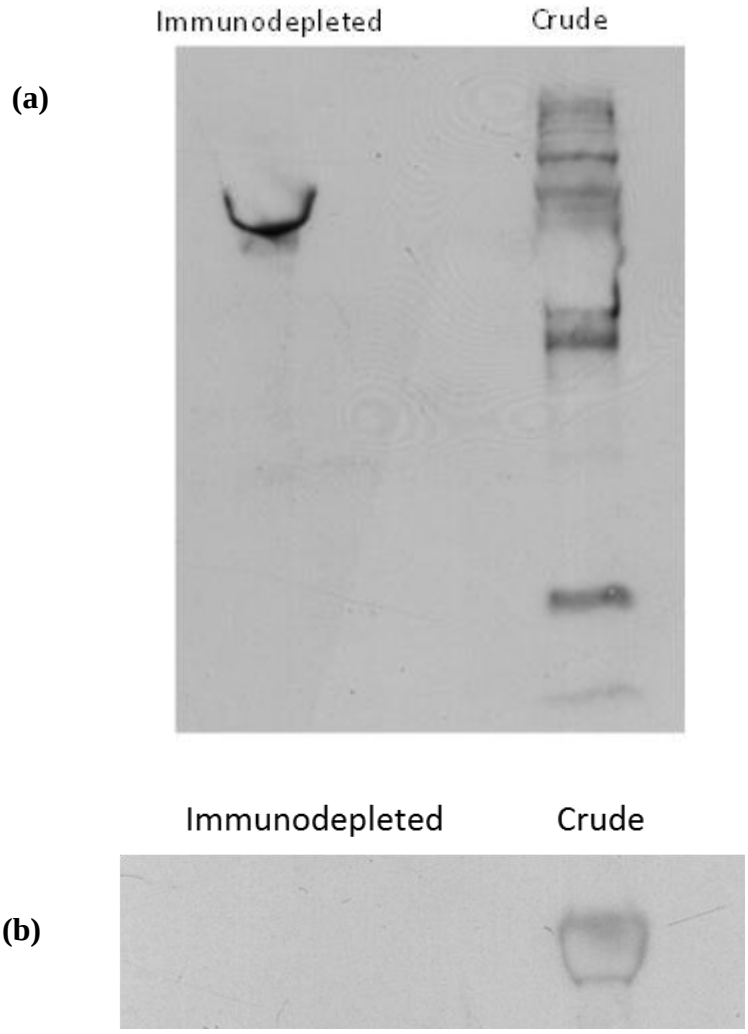

Figure 4.2 Western blot illustrating the effect of immunodepletion on the serum albumin concentration in a control vitreous sample. (a) Following one immunodepletion, the quantity of serum albumin in the vitreous was significantly decreased; however, a second immunodepletion would be required to appropriately deplete the level of serum albumin present. (b) Following a second immunodepletion, the concentration of serum albumin was sufficiently reduced.

The twice-immunodepleted sample was then separated on a 1-D gel which provided a clearer, more balanced view of the proteome with greater number of protein bands being clearly visible (Figure 4.3).

Again, regions of the gel were excised, enzymatically digested and identified by MS. The identifications consisted of a higher number of less abundant and potentially more interesting proteins, while high abundant proteins, such as serum albumin, were less prominent in the list (Table 4.2).

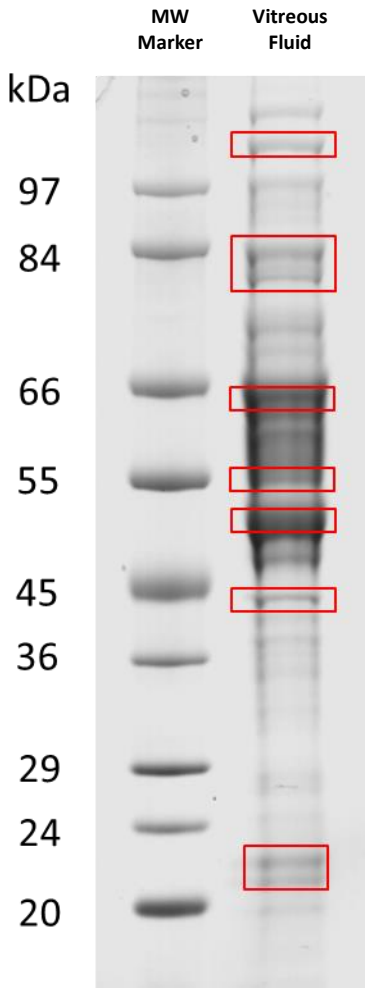

Figure 4.3 1-D gel of twice-immunodepleted vitreous fluid. Various regions of the gel, which are indicated in red, were excised and any proteins present were in-gel digested using trypsin and analysed using mass spectrometry in order to identify them. It was hoped that low abundant proteins would be more easily detected following the removal of highly abundant proteins such as serum albumin.

Accession No.	Coverage (%)	No. Peptides Matched	MW [Da]	Description	Abundance
gi116242676	10.81	18	159917	Neogenin	
gi2851501	15.81	12	101326	Inter-alpha-trypsin inhibitor heavy chain H1	
gi120689	35.44	7	35725	Glyceraldehyde-3-phosphate dehydrogenase	
gi158517847	8.69	12	139005	Complement factor H	
gi119362	14.09	6	92418	Endoplasmin	
gi124894	6.58	9	135278	Retinol-binding protein 3	
gi20178323	23.92	10	46313	Pigment epithelium-derived factor	
gi46577680	14.14	9	54239	Alpha-1B-glycoprotein	
gi51702230	9.08	4	60917	60 kDa heat shock protein, mitochondrial	
gi166899088	3.22	5	145851	Receptor-type tyrosine-protein phosphatase	
gi139641	8.65	6	52929	Vitamin D-binding protein	
gi123647	8.36	3	70761	Heat shock cognate 71 kDa protein	
gi584908	9.03	8	85479	Complement factor B	Medium
gi135496	13.36	3	33323	Tubulin beta chain (Beta-tubulin)	
gi125000	6.03	5	106370	Inter-alpha-trypsin inhibitor heavy chain H2	
gi231506	14.4	3	41729	Actin, cytoplasmic 1	
gi135807	8.2	5	69992	Prothrombin	
gi31077172	4.27	3	45262	Eukaryotic initiation factor 4A-I	
gi116117	33.05	65	122128	Ceruloplasmin	Medium
gi81175238	12.56	21	192650	Complement C4-A	Medium
gi2506872	8.63	17	262442	Fibronectin	
gi112874	24.35	13	47621	Alpha-1-antichymotrypsin	
gi116242595	9.35	13	103261	Inter-alpha-trypsin inhibitor heavy chain H4	
gi1708182	15.37	10	51643	Hemopexin	
gi124096	14.4	8	55119	Plasma protease C1 inhibitor	
gi113936	17.67	9	52569	Antithrombin-III	
gi1168366	8.01	7	69024	Afamin	
gi119370332	5.65	8	187030	Complement C3	High

Table 4.2 Proteins identified from the outlined regions of the gel illustrated in figure 4.3. A significant decrease in the presence of high abundance proteins was observed as well as the identification of a greater number of less common molecules. Proteins which are unique to this list in comparison to Table 4.1 are written in red.

4.3 2-D Proteomic Analysis of Vitreous Fluid

As the twice-immunodepleted vitreous humour appeared to generate the most promising proteomic profile, this sample preparation method was used prior to 2-D DIGE gel analysis. This would allow for the comparison of uveal melanoma vitreous fluid and control vitreous fluid for the identification of differentially expressed proteins.

Separation in the second dimension creates better resolution of the proteome in comparison to a one dimensional separation, which may improve the view of both high and low abundance proteins. A sample which was doubly immunodepleted was compared to its crude counterpart, following 2D separation, in order to test this. The 2-D gels were stained using a colloidal silver stain.

As expected, the high abundance proteins present in the crude sample created a smear across the upper section of the gel, with few well resolved spots visible (Figure 4.4 (a)). In contrast, the immunodepleted gel illustrated clear protein spots with very little background (Figure 4.4 (b)).

A selection of corresponding spots, Figure 4.4 (b), was extracted from an immunodepleted control gel and an immunodepleted uveal melanoma gel for enzymatic digestion and identification of proteins by LC-MS/MS. This produced two purely qualitative lists of proteins. Proteins which were found only in the control vitreous specimen are shown in Table 4.3 while those which were only identified in the uveal melanoma sample are listed in Table 4.4. Although this was not a statistically relevant quantitative comparison between both conditions, it represents a number of proteins which are specific to each sample set and hence, potential biomarkers. It was found that many of the proteins detected in the immunodepleted disease vitreous sample were classed as highly abundant.

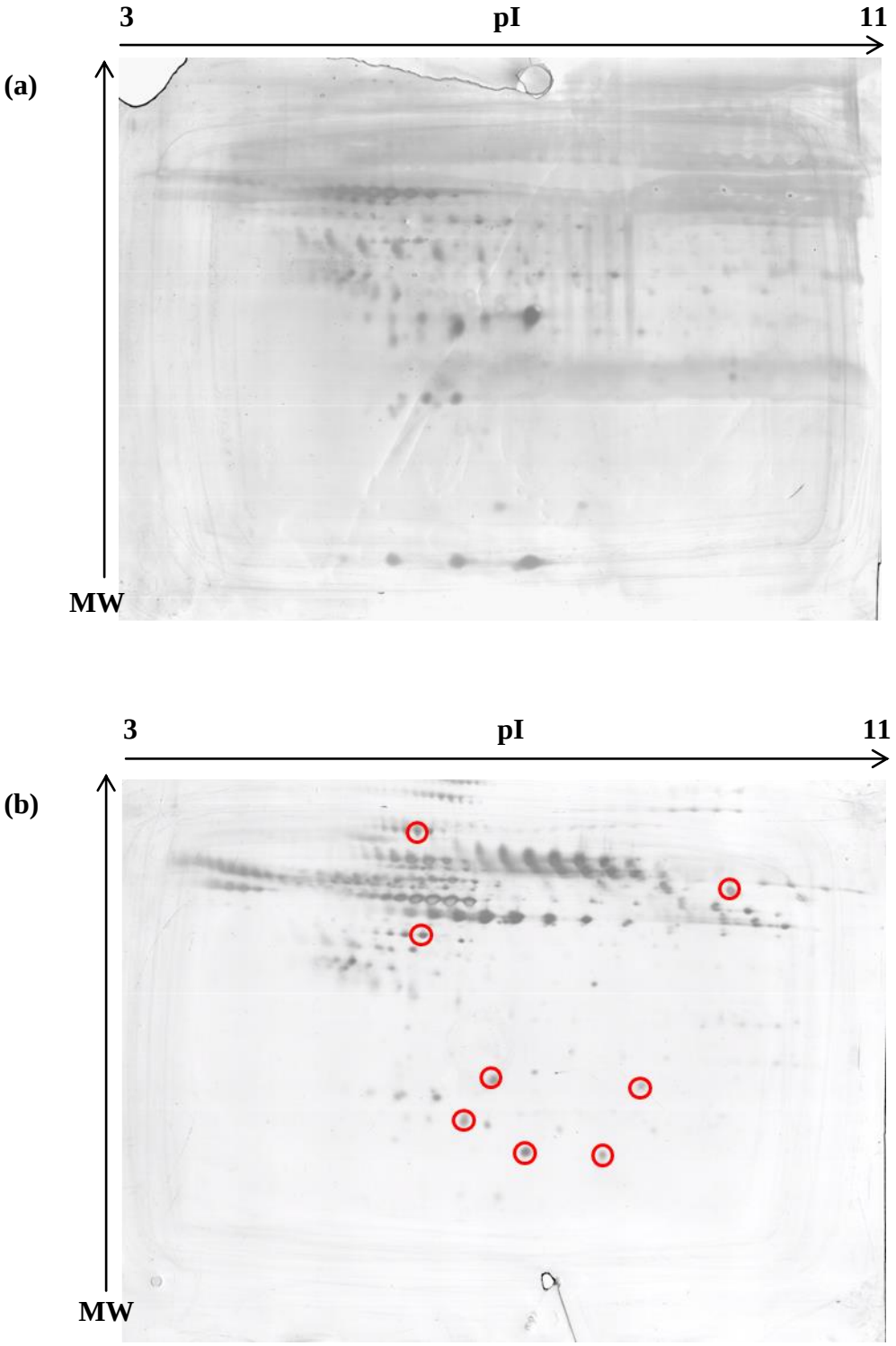

Figure 4.4 Separation of immunodepleted and non-immunodepleted proteins in two dimensions based on pI and size. (a) The non-immunodepleted gel showed areas of high streaking and poor spot resolution (b) The immunodepleted gel was much better resolved with clear spots and little streaking. The region which contained most of the high abundance proteins in the upper region of the gel was also much clearer following immunodepletion. Spots outlined in red were selected for digestion and subsequent identification by LC-MS/MS.

Control Vitreous			
Accession No.	**Description**	**No. Peptides**	**Abundance**
P10745	Retinol-binding protein 3	31	
P06396	Gelsolin	16	
O94985	Calsyntenin-1	12	
P02649	Apolipoprotein E	11	
P10909	Clusterin	11	
P05155	Plasma protease C1 inhibitor	11	
P01034	Cystatin-C	11	
Q13822	Ectonucleotide pyrophosphatase/phosphodiesterase family member 2	9	
P00751	Complement factor B	8	Medium
Q06481	Amyloid-like protein 2	7	
P07339	Cathepsin D	7	
P05067	Amyloid beta A4 protein	7	
P22352	Glutathione peroxidase 3	6	
P02766	Transthyretin	5	
P01019	Angiotensinogen	5	
Q14624	Inter-alpha-trypsin inhibitor heavy chain H4	5	
Q9UBP4	Dickkopf-related protein 3	5	
P43251	Biotinidase	5	
P19022	Cadherin-2	5	
Q9HCB6	Spondin-1	4	
P04217	Alpha-1B-glycoprotein	4	
P04004	Vitronectin	4	
P01042	Kininogen-1	4	
Q9UBM4	Opticin	3	
P01859	Ig gamma-2 chain C region	3	High
P16870	Carboxypeptidase E	3	
P41222	Prostaglandin-H2 D-isomerase	3	
P43652	Afamin	3	
P13611	Versican core protein	3	
P02790	Hemopexin	2	
O43505	N-acetyllactosaminide beta-1,3-N-acetylglucosaminyltransferase	2	
Q14515	SPARC-like protein 1	2	
P25311	Zinc-alpha-2-glycoprotein	2	
P19652	Alpha-1-acid glycoprotein 2	2	
Q9Y5W5	Wnt inhibitory factor 1	2	
P11217	Glycogen phosphorylase, muscle form	2	
Q92765	Secreted frizzled-related protein 3	2	
P07711	Cathepsin L1	2	

Q9Y6R7	IgGFc-binding protein	2	
Q99574	Neuroserpin	2	
Q6MZW2	Follistatin-related protein 4	2	
Q8N475	Follistatin-related protein 5	2	
Q92520	Protein FAM3C	2	
P61769	Beta-2-microglobulin	2	
P01606	Ig kappa chain V-I region OU	2	High
O75326	Semaphorin-7A	2	
Q13510	Acid ceramidase	2	

Table 4.3 Proteins identified in control vitreous fluid which were not found in the uveal melanoma sample. This illustrates the effectiveness of immunodepletion as a vitreous fluid pre-treatment technique for identifying less abundant proteins.

Uveal Melanoma Vitreous			
Accession No.	**Description**	**No. Peptides**	**Abundance**
P01871	Ig mu chain C region	6	High
P02679	Fibrinogen gamma chain	5	High
P0C0L5	Complement C4-B	5	Medium
P00738	Haptoglobin	5	High
P69905	Hemoglobin subunit alpha	5	
P04220	Ig mu heavy chain disease protein	4	High
P02675	Fibrinogen beta chain	4	High
P01860	Ig gamma-3 chain C region	4	High
P68871	Hemoglobin subunit beta	4	
P02750	Leucine-rich alpha-2-glycoprotein	3	
P62736	Actin, aortic smooth muscle	3	
P60709	Actin, cytoplasmic 1	3	
P68032	Actin, alpha cardiac muscle 1	3	
P63261	Actin, cytoplasmic 2	3	
P63267	Actin, gamma-enteric smooth muscle	3	
P68133	Actin, alpha skeletal muscle	3	
P20742	Pregnancy zone protein	3	
P01623	Ig kappa chain V-III region WOL	3	High
P01877	Ig alpha-2 chain C region	2	High
P06733	Alpha-enolase	2	
P01622	Ig kappa chain V-III region Ti	2	High
P04206	Ig kappa chain V-III region GOL	2	High
P01598	Ig kappa chain V-I region EU	2	High
P01842	Ig lambda chain C regions	2	High
P01593	Ig kappa chain V-I region AG	2	High
P01594	Ig kappa chain V-I region AU	2	High
P01599	Ig kappa chain V-I region Gal	2	High
P01600	Ig kappa chain V-I region Hau	2	High
P01607	Ig kappa chain V-I region Rei	2	High
P01608	Ig kappa chain V-I region Roy	2	High
P01609	Ig kappa chain V-I region Scw	2	High
P01610	Ig kappa chain V-I region WEA	2	High
P80362	Ig kappa chain V-I region WAT	2	High
P18135	Ig kappa chain V-III region HAH	2	High
P18136	Ig kappa chain V-III region HIC	2	High
P02042	Hemoglobin subunit delta	2	
P02652	Apolipoprotein A-II	2	
P05109	Protein S100-A8	2	
P01700	Ig lambda chain V-I region HA	2	High

Table 4.4 Proteins identified by mass spectrometry methods which were found

exclusively in uveal melanoma vitreous fluid in comparison to the control ocular fluid. Many of these proteins were highly abundant, despite immunodepletion.

4.4 2-D DIGE Analysis of Uveal Melanoma vs. Control Vitreous Fluid

It was intended to utilise immunodepletion as a vitreous humour pre-treatment prior to 2-D DIGE analysis. Immunodepletion significantly depletes the quantity of protein in the ocular fluid because for the most part it is composed of high abundance proteins. This results in a more dilute sample. In addition to this, a very low volume of vitreous fluid is generally available for analysis. As the protein concentration of many of the vitreous fluid samples acquired was quite low and little sample was available, immunodepletion was not possible for the entire control and uveal melanoma sample sets.

Due to the above issues, 2-D DIGE was carried out using 25 μg of crude uveal melanoma and control vitreous fluids. The 2-D DIGE method is outlined in more detail in section 3.3.

The images generated from the 2-D DIGE analysis (Figure 4.5) illustrated that high abundance proteins which would have been removed by immunodepletion had streaked across the gel. The protein spots of the gels were also poorly resolved; hence, the Progenesis software could not identify protein spot differences between the gels of the two sample sets.

(a)

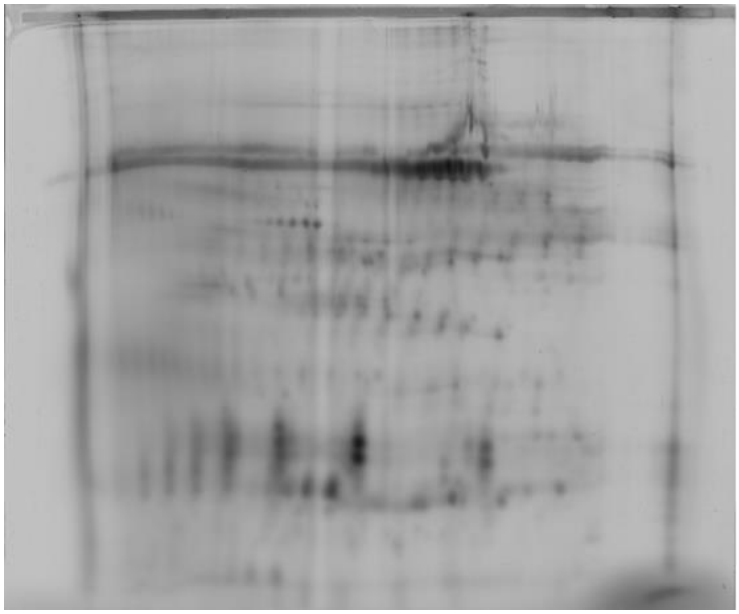

(b)

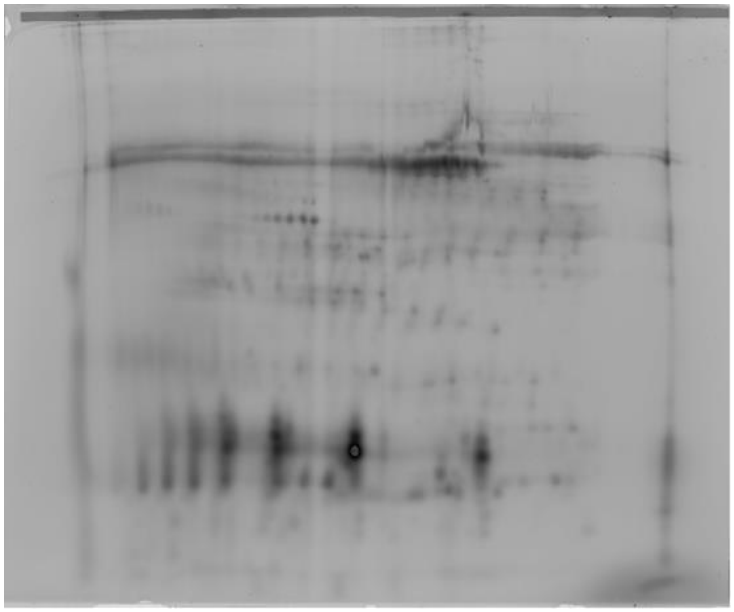

Figure 4.5 2-D DIGE images of 25 μg of non-immunodepleted vitreous fluid protein. As the concentration of protein and sample volume was too low in some of the vitreous fluid samples available, it was not possible to use immunodepletion as a pre-treatment. Streaking and poor protein spot resolution is evident in both images. (a) uveal melanoma vitreous fluid (b) vitreous fluid of a macular hole degeneration patient (control).

4.5 Quantitative Label-Free LC-MS Analysis of Control and Uveal Melanoma Vitreous Fluid

Quantitative label-free proteomics involves the digestion of a fixed quantity of protein and the subsequent analysis of 1 μg of the sample by reverse-phase LC-MS/MS. Acquired total ion chromatograms (TIC) are statistically analysed using Progenesis LC-MS software to generate quantitative information on differential protein expression patterns between the control and disease vitreous fluid. Progenesis LC-MS aligns all of the total ion chromatograms (TIC) generated by selecting a reference TIC to which all other runs are compared, thus correcting any minor drifts in retention times. MS/MS spectra are then exported to a protein identification programme.

It was planned that label-free proteomics would be used to analyse the crude vitreous fluid of uveal melanoma patients in comparison to untreated controls for the detection of differentially expressed proteins. However when the samples were examined using the technique, it was found that the control and the melanoma groups were too different to compare (Figure 4.6). The controls showed similarities in their peak profiles and contained a wide variety of features. However, the disease samples generated very poor total ion chromatograms; the peaks were poor and were totally dissimilar to the control samples with virtually no common peaks detected between the sample sets. This suggests that there were few detectable proteins which were mutual to both groups and hence no patterns of differential protein expression could be found.

The lack of identified proteins in the uveal melanoma vitreous fluid may have been due to the high abundant proteins present; i.e. when the samples were all initially normalised to 10 μg of protein, this could have mainly consisted of background high abundance proteins in the disease sample set. This confirmed that a pre-processing method for the vitreous would be necessary prior to analysis.

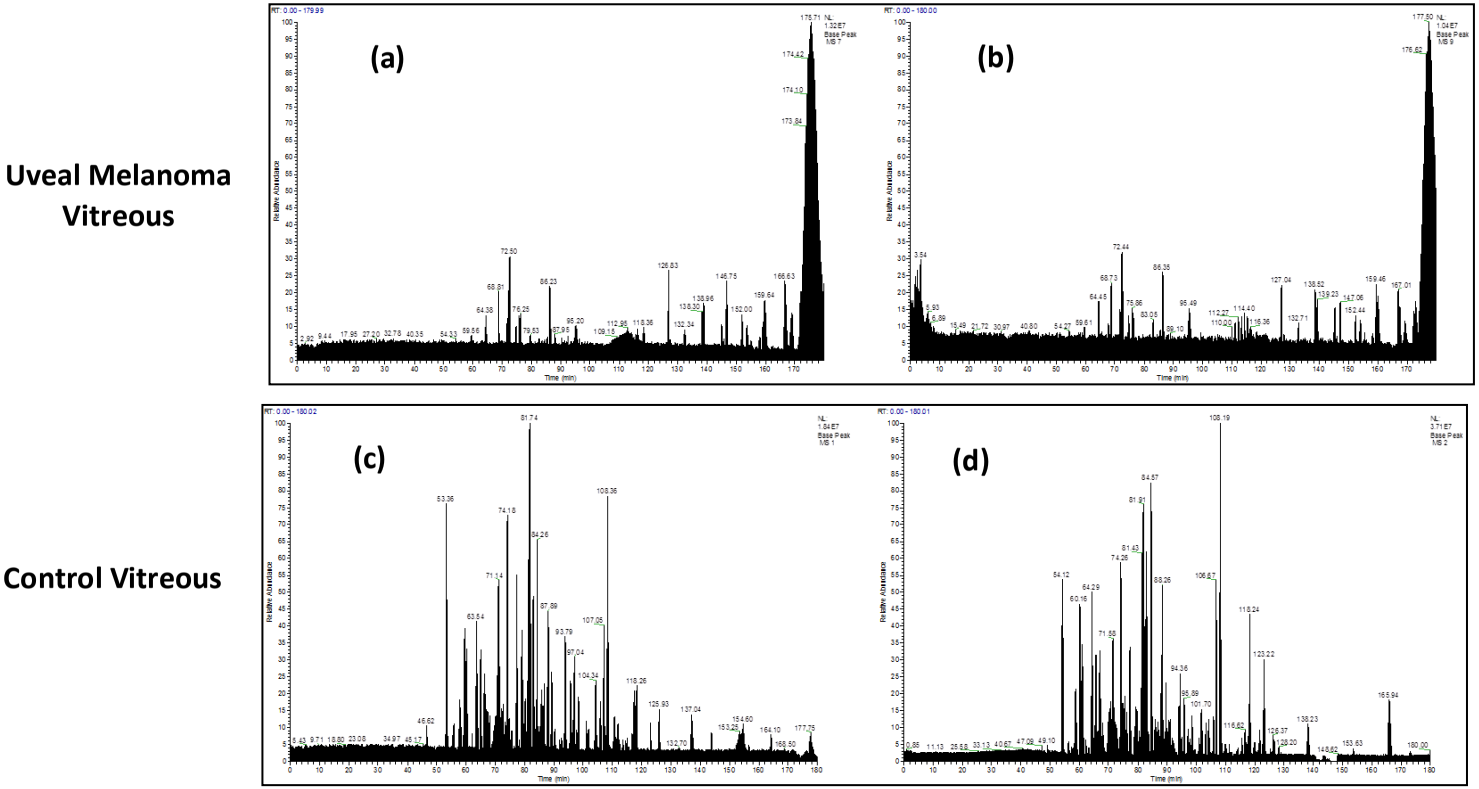

Figure 4.6 Examples of total ion chromatograms (TIC) generated from a quantitative label-free LC-MS analysis comparing uveal melanoma vitreous fluid and control specimens. The uveal melanoma samples, (a) and (b), produced unsatisfactory TIC; the peak profiles were poor and few common peaks were detected between the control and disease samples. The control spectra, (c) and (d), demonstrated a broad variety of peaks and similar peak profiles between samples. The lack of comparable peaks between the sample sets may have been due to a greater proportion of high abundant proteins present in the disease samples in comparison to the controls; i.e. when the protein concentration was normalised to 10 µg, this could have mainly consisted of background high abundance proteins.

4.6 ProteoMiner Pre-Treatment of Vitreous Fluid

ProteoMiner is a bead-based technology used for the compression of the dynamic range of proteins present in complex biological samples through the equalisation of all protein abundances. This provides a representative view of the original proteome while enhancing the presence of proteins which may have been undetected otherwise. The technique is explained further in section 5.2.

A ProteoMiner kit (Bio-Rad) was used in order to normalise the abundance of proteins within each vitreous sample, for both sample sets. It was hoped that this would enhance the concentration of the low abundance proteins which could potentially be of interest. However, the method requires a minimum protein concentration and sample volume higher than available in many of the vitreous samples available. Hence the analysis could not be performed as recommended by the manufacturer.

Instead, an appropriate volume of beads was removed from each unit which ensured that the quantity of remaining beads was sufficient for a lower sample concentration and volume. One control and one uveal melanoma vitreous fluid sample was treated using the modified units and the resulting elution from each was separated via 1-D electrophoresis, along with the untreated samples (Figure 4.7). The resulting gel was stained with colloidal silver. A depletion of background proteins is visible between the crude and the treated sample, although an unknown interference diminished the resolution of the gels. Each lane was cut into sections and digested using trypsin. Through LC-MS, the proteins present in each sample were identified (Table 4.5).

This analysis showed that ten previously unseen proteins were identified in the disease vitreous fluid as a result of the ProteoMiner treatment. However, only 49 identifications were found in the ProteoMiner-treated uveal melanoma specimen in comparison to 57 in its crude counterpart. In the control fluid, 36 proteins were identified in the raw sample while only ten were identified in the ProteoMiner-treated sample. This indicates that the modified technique was unsatisfactory and another method should be utilised.

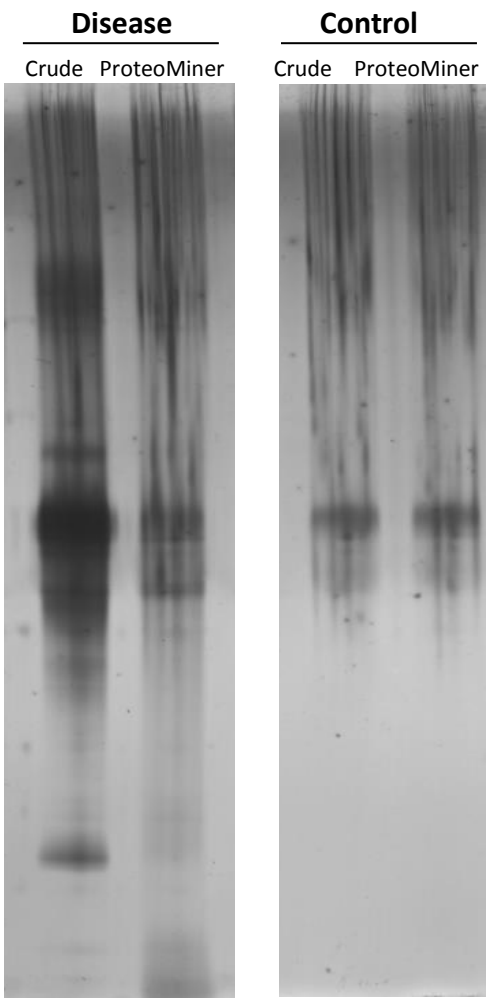

Figure 4.7 15 μg of ProteoMiner-treated and crude vitreous fluid from a control and a uveal melanoma sample was separated by 1-D electrophoresis and stained with a silver nitrate stain. Although an unknown contaminant interfered with the resolution of the gel, it is clear that some of the high abundance proteins, including serum albumin, were depleted from the samples. The gel lanes were excised and digested with trypsin prior to mass spectrometry analysis for the identification of the proteins present.

Uveal Melanoma Vitreous Fluid				Control Vitreous Fluid			
Crude Disease	**Abundance**	**Proteominer-Treated Disease**	**Abundance**	**Crude Control**	**Abundance**	**Proteominer-Treated Control**	**Abundance**
Myosin-9		Ig lambda-2 chain C regions	High	Transthyretin		Ig gamma-1 chain C region	High
Ig gamma-1 chain C region	High	Ig lambda-3 chain C regions	High	Ig kappa chain C region	High	Serum albumin	High
Hemoglobin subunit beta		Ig lambda-6 chain C region	High	Complement C4-A	Medium	Transthyretin	
Hemoglobin subunit delta		Ig lambda-7 chain C region	High	Complement C4-B	Medium	Complement C3	High
Actin, cytoplasmic 1		Ig kappa chain V-I region DEE	High	Ig kappa chain V-III region SIE	High	Pigment epithelium-derived factor	
Actin, cytoplasmic 2		Ig alpha-2 chain C region	High	Ig kappa chain V-III region WOL	High	Inter-alpha-trypsin inhibitor heavy chain H4	
Transthyretin		Immunoglobulin lambda-like polypeptide 5		Ig kappa chain V-III region Ti	High	Ceruloplasmin	Medium
Vitamin D-binding protein		Ig lambda-1 chain C regions	High	Ig kappa chain V-III region GOL	High	Complement C4-A	Medium
Ig kappa chain C region	High	Cathepsin D		Ceruloplasmin	Medium	Complement C4-B	Medium
Alpha-1-antitrypsin	High	Alpha-crystallin A chain		Antithrombin-III		Ig kappa chain C region	High
POTE ankyrin domain family member E		Kininogen-1		Vitamin D-binding protein			
Serotransferrin	High	Plasminogen	Medium	Apolipoprotein A-I	Medium		
Pigment epithelium-derived factor		Alpha-crystallin B chain		Ig gamma-1 chain C region	High		
Serum albumin	High	Transthyretin		Alpha-1B-glycoprotein			
Hemoglobin subunit alpha		Ig kappa chain C region	High	Serum albumin	High		
Ig kappa chain V-III region SIE	High	Ig gamma-1 chain C region	High	Ig kappa chain V-IV region Len	High		
Ig kappa chain V-III region WOL	High	Complement C4-A	Medium	Alpha-1-antitrypsin	High		
Ig kappa chain V-III region Ti	High	Complement C4-B	Medium	Plasminogen	Medium		
Ig kappa chain V-III region GOL	High	Pigment epithelium-derived factor		Apolipoprotein A-IV			
Prostaglandin-H2 D-isomerase		Serum albumin	High	Ig gamma-2 chain C region	High		
Actin, alpha cardiac muscle 1		Alpha-1-antichymotrypsin		Prostaglandin-H2 D-isomerase			
Beta-actin-like protein 2		Vitamin D-binding protein		Alpha-1-antichymotrypsin			
Actin, aortic smooth muscle		Hemoglobin subunit alpha		Alpha-1-acid glycoprotein 1			
Actin, gamma-enteric smooth muscle		Hemoglobin subunit beta		Immunoglobulin lambda-like polypeptide 5			

Alpha-2-HS-glycoprotein		Hemoglobin subunit delta		Ig lambda-1 chain C regions	High
Hemopexin		Ig alpha-1 chain C region	High	Alpha-2-macroglobulin	High
Alpha-1-antichymotrypsin		Alpha-2-HS-glycoprotein		Pregnancy zone protein	
Ig alpha-1 chain C region	High	Ig kappa chain V-III region SIE	High	Ig lambda-2 chain C regions	High
Ig gamma-4 chain C region	High	Ig kappa chain V-III region WOL	High	Ig lambda-3 chain C regions	High
Ig kappa chain V-III region HAH	High	Ig kappa chain V-III region Ti	High	Ig lambda-6 chain C region	High
Ig kappa chain V-III region HIC	High	Ig kappa chain V-III region GOL	High	Ig lambda-7 chain C region	High
Complement C3	High	Ig kappa chain V-III region HAH	High	Ig alpha-1 chain C region	High
Apolipoprotein E		Ig kappa chain V-III region HIC	High	Ig alpha-2 chain C region	High
Ig gamma-3 chain C region	High				

Table 4.5 List of proteins identified in control and disease samples both before and after ProteoMiner treatment. As ProteoMiner is a protein-equalising technology, it should improve the spectrum of proteins identifiable by mass spectrometry methods. In this instance, the vitreous fluid protein concentration and volume was insufficient for ProteoMiner pre-treatment. Therefore, a proportion of the beads were removed from the column in order to correct the protein to bead ratio and to utilise the technology. As shown in the table above, this was insufficient for enhancing the protein content. 57 proteins were identified in the raw disease vitreous, while following ProteoMiner treatment only 49 proteins were identified, although 13 of these were identified as a result of the treatment (shown in red). Fewer proteins were also identified in the ProteoMiner-treated control sample in comparison to the untreated counterpart.

4.7 Profiling of Vitreous Fluid using SELDI-TOF

SELDI-TOF is a variation of MALDI, where an analyte is bound to a surface through a specific, modified target. A number of affinity technologies can be used for this purpose, including cation exchange (CM10) and immobilised metal affinity chromatography (IMAC). The method is further explained in section 6.1.

In this case, copper-activated IMAC chips were used to bind uveal melanoma vitreous fluid, cutaneous melanoma serum and conditioned media collected from cutaneous melanoma cell lines and to compare the protein profiles from each.

In each sample set, an unknown 8.9 kDa potential marker was identified in the disease sample or the media conditioned by a cancer cell line. This work is outlined in more detail in Chapter 6. However, the peak of interest was identified in both crude and immunodepleted uveal melanoma vitreous fluid and remained absent from the control specimen (Figure 4.8). As SELDI cannot identify the protein peaks which it detects, it was necessary to devise a method in order to isolate and identify this protein.

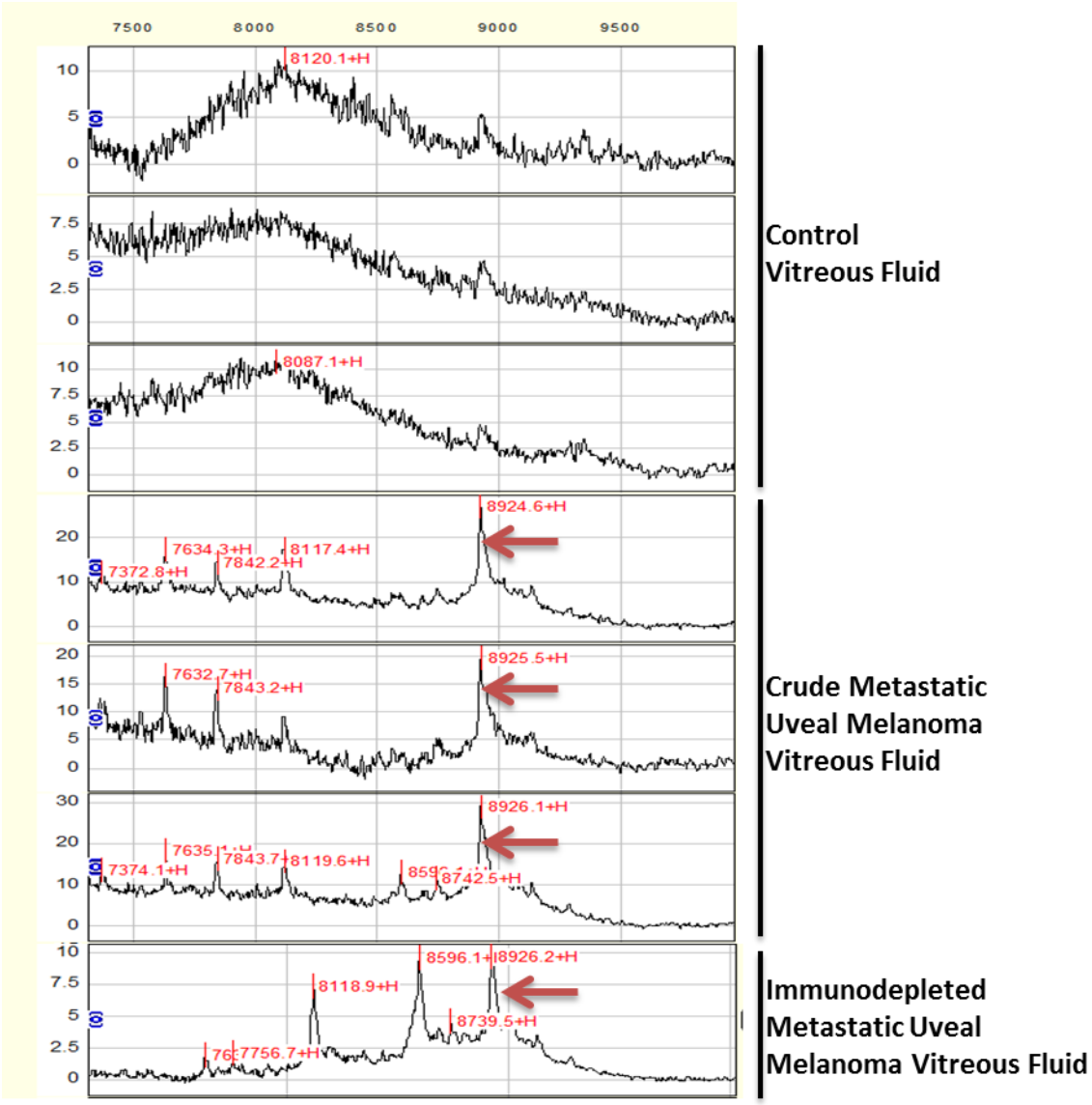

Figure 4.8 SELDI analysis of both crude and immunodepleted vitreous fluid illustrated an 8.9 kDa peptide or protein, as indicated by a red arrow, which consistently appeared in the uveal melanoma specimens but was absent from the control samples. This potential marker also repeatedly appeared in SELDI spectra of advanced cutaneous melanoma sera but remained absent from the corresponding control samples.

A copper-activated IMAC resin contained in spin columns was employed for binding proteins of interest. In this way the resin would mimic the original technology used for SELDI analysis and should bind the protein of interest. This would allow for the elution and possible identification of the protein.

One control and one uveal melanoma vitreous fluid sample were incubated with the copper-activated resin for sample binding. An ascending gradient of the following imidazole concentrations; 25 mM, 50 mM, 100 mM, 200 mM, and 500 mM, was then applied to the column and subsequent elution fractions were collected. The fractions were separated in the first dimension using a 4-20% low molecular weight gel and stained with a colloidal silver stain (Figure 4.9). The lower portion of each lane, beneath the red line in Figure 4.9, was excised and in-gel digested with trypsin for the generation of peptides which were then analysed by LC-MS/MS, with the aim of identifying the 8.9 kDa protein of interest.

The qualitative results of this analysis illustrated that although the technique failed to identify an 8.9 kDa potential biomarker in the vitreous humour, it succeeded in identifying a host of proteins which were not found in the previous attempts to analyse the ocular fluid proteome. Included in these identifications was a family of proteins known as crystallins which are associated with the structure of the eye and associated ocular diseases. Although some of the proteins identified in the low molecular weight region of the gel were shown to have high molecular weights, they may be cleavage products of the larger molecule and hence could migrate to the region in question.

Although this gel-based method does not illustrate significant expression differences between both experimental conditions, the identifications shown in Table 4.6 illustrated substantial differences in peptide numbers between the control and the disease sample.

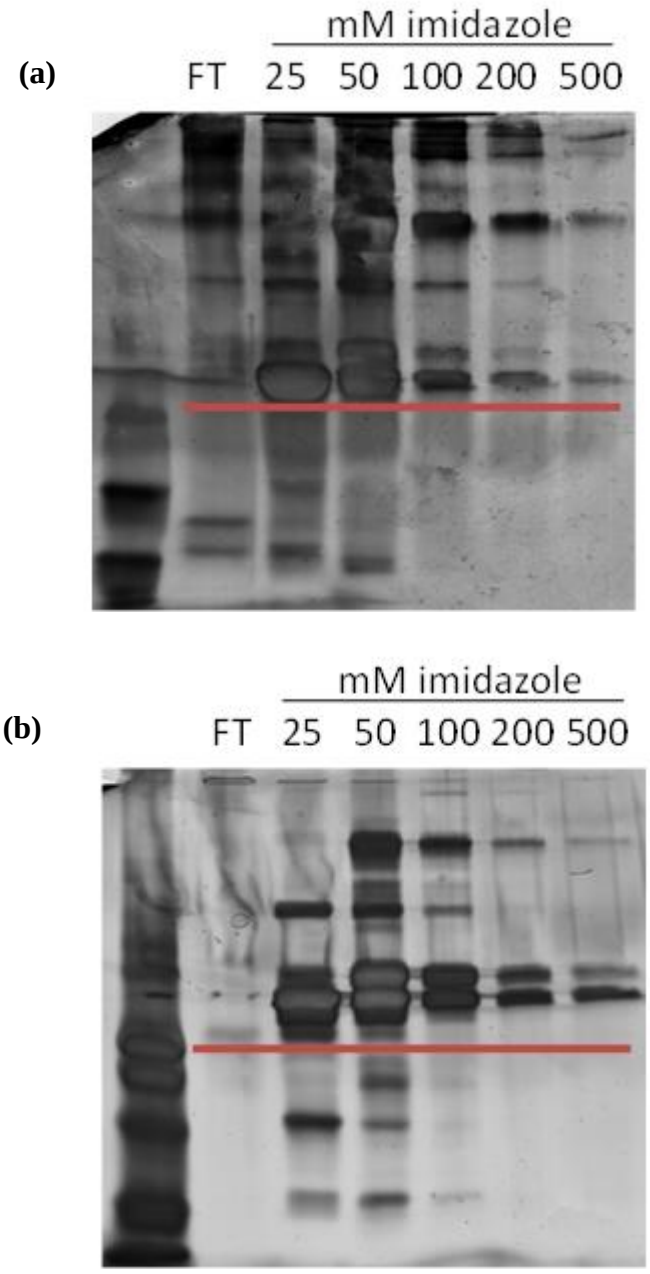

Figure 4.9 1-D gels illustrating protein fractions which were collected from a column containing IMAC resin by applying increasing concentrations of imidazole; 25 mM, 50 mM, 100 mM, 200 mM and 500 mM. The fractions were separated on a low molecular weight gel in the first dimension and stained with a colloidal silver stain. The region below the red line containing proteins weighing 30 kDa or less was then excised from both the disease (a) and control (b) gels. Each fraction in the low molecular weight region of both gels was digested into peptides and analysed by mass spectrometry. FT = flowthrough, i.e. unbound proteins.

Protein Name	Abundance	Accession Number	Molecular Weight (Da)	Number of Peptides Matched: Uveal Melanoma Vitreous	Percent Coverage	Control Vitreous	Percent Coverage
Beta-crystallin B1		P53674	28023	15	67.06%	0	-
Beta-crystallin B2		P43320	23380	12	70.73%	0	-
Alpha-crystallin B chain		P02511	20159	13	57.14%	0	-
Apolipoprotein A-I	Medium	P02647	30788	13	48.31%	4	19.85%
Hemoglobin subunit beta		P68871	15998	12	89.80%	0	-
Serotransferrin	High	P02787	77064	12	21.06%	2	3.44%
Alpha-crystallin A chain		P02489	19909	9	55.49%	3	19.08%
Beta-crystallin A3		P05813	25150	7	42.79%	0	-
Apolipoprotein A-II	Medium	P02652	11175	7	64.00%	0	-
Beta-crystallin S		P22914	21007	6	40.45%	0	-
Gamma-crystallin D		P07320	20738	5	39.66%	0	-
Hemoglobin subunit alpha		P69905	15257	4	48.59%	0	-
Ig kappa chain C region	High	P01834	11609	4	66.98%	0	-
Beta-crystallin A4		P53673	22374	3	23.47%	0	-
Clusterin		P10909	52494	3	9.80%	0	-
Retinol-binding protein 3		P10745	135362	3	5.69%	0	-
Ig gamma-1 chain C region	High	P01857	36106	3	12.42%	0	-

Immunoglobulin lambda-like polypeptide 5		B9A064	23063	3	23.36%	0	-
Complement C3	High	P01024	187147	3	2.53%	1	1.26%
Inter-alpha-trypsin inhibitor heavy chain H4		Q14624	103357	2	3.23%	0	-
Ubiquitin-60S ribosomal protein L40		P62987	14728	2	19.53%	0	-
Ig lambda-2 chain C regions	High	P0CG05	11293	2	27.36%	0	-
Cathepsin D		P07339	44552	2	7.04%	0	-
Tetranectin		P05452	22537	2	17.33%	0	-
Apolipoprotein D		P05090	21275	2	10.58%	0	-

Table 4.6 Selection of proteins identified from the gels shown in Figure 4.8 using mass spectrometry. Although this is a qualitative analysis, a present and absent approach can be used to indicate differentially expressed proteins between sample sets. All but four proteins were absent from the control group, while every protein was identified in the uveal melanoma specimen. Many of the proteins listed had not been identified in any of the previous attempts to optimise the vitreous fluid proteome. Some of the proteins identified were of a high molecular weight which may have been as a result of the presence of cleavage products of larger molecules. Only proteins which were identified by two peptides or more are shown.

4.8 Qualititative Analysis of Vitreous Fluid Fractionated from IMAC Resin

The flowthrough, 20 mM fraction, 50 mM fraction and the raw starting material of one uveal melanoma vitreous fluid sample were separated by 1-D electrophoresis in order to visually represent how well the technique worked (Figure 4.10). This gel illustrates the elevated levels of high abundance proteins, such as serum albumin, which dominate the starting material and flowthrough lanes to the point where they were found to leach into the gel. Although such proteins were still visible in the 20 mM and 50 mM fractions, they were severely depleted.

It was also noticeable that the presence of less abundant proteins had been enriched by the technique and in some cases bands were visible in the imidazole fractions which were previously undetectable.

The fractions and starting material which correspond to the gel were qualitatively analysed by LC-MS/MS (Table 4.7). Overall, 27, 46, 58, and 59 proteins were identified in the starting material, the flowthrough, the 20 mM fraction, and the 50 mM fraction, respectively.

Of the flowthrough identifications, seven proteins were not found in either the 20 mM or the 50 mM fraction. 25 and 29 proteins were found to be unique to the 20 mM and 50 mM elutions, respectively, when compared to the flowthrough protein list.

Of the starting material identifications, four were found to be unique as they were not identified in any of the other fractions. When compared to the starting material list, 31, 39, and 40 proteins were found to be enriched in the flowthrough, 20 mM and 50 mM fractions, respectively, following IMAC fractionation.

A number of crystallins were only detected in the 20 mM and 50 mM fractions and not in the flowthrough or starting material. As crystallins are known to bind IMAC, this would suggest that the fractionation worked.

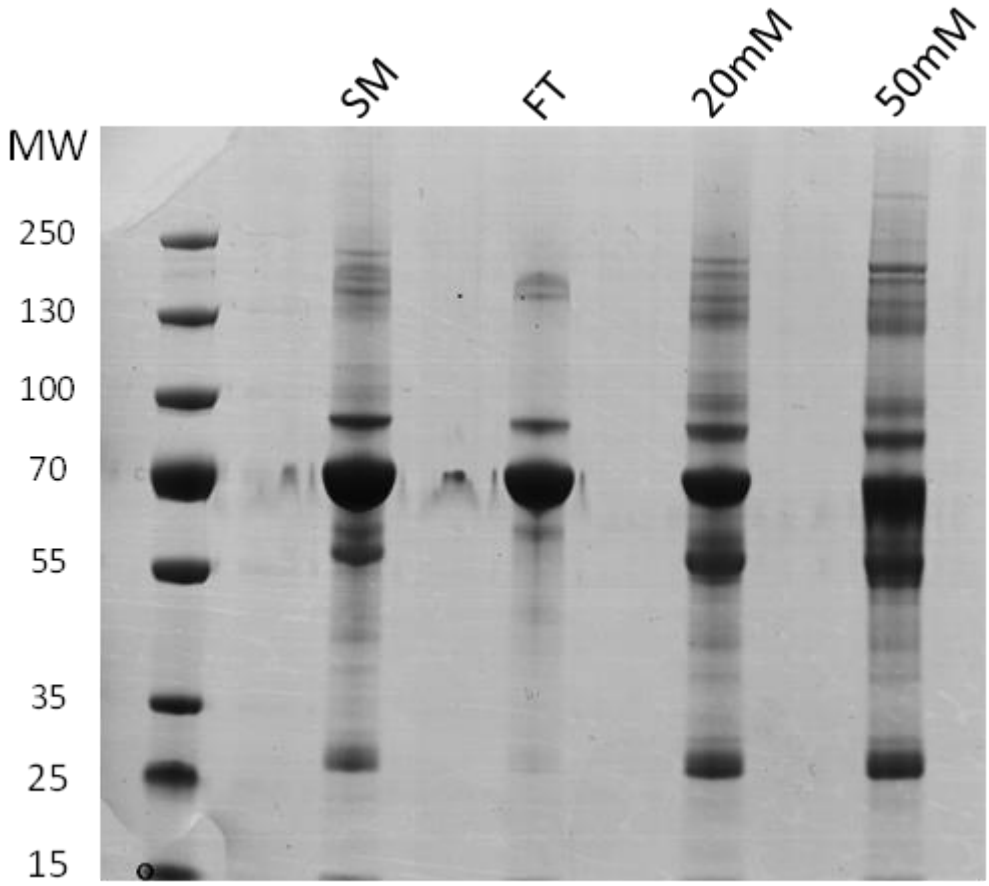

Figure 4.10 Uveal melanoma vitreous fluid fractionated from copper-activated IMAC resin. Although the starting material (SM) contained highly abundant proteins which dominated the lane, the IMAC fractionation method improved the resolution of less prominent bands while reducing the intensity of the more abundant proteins present. SM - Starting Material; FT - Flowthrough; 20 mM – 20 mM imidazole elution fraction; 50 mM - 50mM imidazole elution fraction

Starting Material				Flowthrough Fraction				20 mM Fraction				50 mM Fraction			
Protein Name	Abundance	Accession No.	No. Peptides Matched	Protein Name	Abundance	Accession No.	No. Peptides Matched	Protein Name	Abundance	Accession No.	No. Peptides Matched	Protein Name	Abundance	Accession No.	No. Peptides Matched
Apolipoprotein B-100		P04114	4	Alpha-1-acid glycoprotein 2		P19652	2	Hemopexin		P02790	10	Hemopexin		P02790	9
C4b-binding protein alpha chain		P04003	2	Hornerin		Q86YZ3	3	Fibrinogen beta chain	High	P02675	8	Coagulation factor XII		P00748	5
Ig kappa chain V-I region Mev	High	P01612	2	Cystatin-C		P01034	3	Complement C4-A	Medium	P0C0L4	15	Fibrinogen beta chain	High	P02675	10
Ig kappa chain V-I region Wes	High	P01611	2	Alpha-2-antiplasmin		P08697	3	Beta-crystallin B1		P53674	2	Gelsolin		P06396	10
Ig kappa chain C region	High	P01834	5	Afamin		P43652	3	Inter-alpha-trypsin inhibitor heavy chain H4		Q14624	5	Fibrinogen gamma chain	High	P02679	12
Alpha-2-HS-glycoprotein		P02765	5	Retinol-binding protein 4		P02753	2	Fibrinogen gamma chain	High	P02679	5	Beta-crystallin B2		P43320	3
Haptoglobin	High	P00738	3	Alpha-1B-glycoprotein		P04217	2	Ig gamma-4 chain C region	High	P01861	3	Hemoglobin subunit beta		P68871	7
Prothrombin		P00734	2	Transthyretin		P02766	3	Beta-crystallin A3		P05813	2	Complement component C8 alpha chain		P07357	2
Fibronectin		P02751	2	Ig alpha-1 chain C region	High	P01876	8	Hemoglobin subunit beta		P68871	8	Ig gamma-4 chain C region	High	P01861	3
Ceruloplasmin	Medium	P00450	5	Alpha-1-antichymotrypsin		P01011	5	Gelsolin		P06396	9	Ig gamma-3 chain C region	High	P01860	4
Alpha-2-macroglobulin	High	P01023	10	Inter-alpha-trypsin inhibitor heavy chain H2		P19823	6	Beta-crystallin B2		P43320	3	Ig kappa chain V-III region SIE	High	P01620	3
Complement C3	High	P01024	6	Ig gamma-2 chain C region	High	P01859	3	Ig kappa chain V-III region SIE	High	P01620	2	Fibrinogen alpha chain	High	P02671	8
Plasminogen	Medium	P00747	5	Apolipoprotein A-IV		P06727	11	Complement factor I		P05156	3	Clusterin		P10909	6
Alpha-1-antitrypsin	High	P01009	3	Apolipoprotein E		P02649	9	Ig gamma-3 chain C region	High	P01860	2	Prostaglandin-H2 D-isomerase		P41222	2
Serum albumin	High	P02768	14	Alpha-1-acid glycoprotein 1	Medium	P02763	4	Fibrinogen alpha chain	High	P02671	3	Beta-crystallin A3		P05813	2
Immunoglobulin lambda-like polypeptide 5		B9A064	2	Vitamin D-binding protein		P02774	8	Ig kappa chain V-IV region (Fragment)	High	P06312	2	Histidine-rich glycoprotein		P04196	9
Serotransferrin	High	P02787	4	Pigment epithelium-derived factor		P36955	8	Complement component C8 gamma chain		P07360	2	Complement factor I		P05156	4
Inter-alpha-trypsin inhibitor heavy chain H1		P19827	2	Plasma protease C1 inhibitor		P05155	5	Clusterin		P10909	6	Vitronectin		P04004	4
Complement factor H		P08603	6	Apolipoprotein A-I	Medium	P02647	6	Ig alpha-1 chain C region	High	P01876	9	Inter-alpha-trypsin inhibitor heavy chain H4		Q14624	3
Beta-2-glycoprotein 1		P02749	3	Ig lambda-2 chain C regions	High	P0CG05	2	Alpha-1B-glycoprotein		P04217	6	Alpha-crystallin A chain		P02489	2
Haptoglobin-related protein		P00739	2	Antithrombin-III		P01008	7	Transthyretin		P02766	5	Ig kappa chain V-IV region (Fragment)	High	P06312	2
Hemoglobin subunit alpha		P69905	2	Complement C4-A	Medium	P0C0L4	3	Ig gamma-2 chain C region	High	P01859	5	Transthyretin		P02766	6
Ig gamma-1 chain C region	High	P01857	2	Complement factor B		P00751	7	Apolipoprotein E		P02649	12	Ig gamma-2 chain C region	High	P01859	8
Ig mu chain C region	High	P01871	3	Galectin-3-binding protein		Q08380	2	Apolipoprotein A-I	Medium	P02647	10	Ig alpha-1 chain C region	High	P01876	10
Kininogen-1		P01042	2	Angiotensinogen		P01019	4	Alpha-1-antichymotrypsin		P01011	6	Vitamin D-binding protein		P02774	6
				Apolipoprotein A-II	Medium	P02652	2	Ig lambda-2 chain C regions	High	P0CG05	2	Alpha-1B-glycoprotein		P04217	5
				Clusterin		P10909	2	Inter-alpha-trypsin inhibitor heavy chain H2		P19823	4	Ig lambda-2 chain C regions	High	P0CG05	2
				Prothrombin		P00734	2	Pigment epithelium-derived factor		P36955	3	Complement factor B		P00751	11
				Serum albumin	High	P02768	42	Complement factor B		P00751	9	Alpha-1-acid glycoprotein 1	Medium	P02763	5
				Alpha-1-antitrypsin	High	P01009	17	Plasma protease C1 inhibitor		P05155	3	Pigment epithelium-derived factor		P36955	3
				Kininogen-1		P01042	4	Antithrombin-III		P01008	2	Apolipoprotein A-I	Medium	P02647	8
				Ig kappa chain C region	High	P01834	3	Galectin-3-binding protein		Q08380	2	Apolipoprotein E		P02649	8
				Complement C3	High	P01024	20	Alpha-1-acid glycoprotein 1	Medium	P02763	3	Alpha-1-antichymotrypsin		P01011	6
				Serotransferrin	High	P02787	16	Angiotensinogen		P01019	2	Complement C4-A	Medium	P0C0L4	6

Immunoglobulin lambda-like polypeptide 5		B9A064	4	Apolipoprotein A-IV		P06727	2	Inter-alpha-trypsin inhibitor heavy chain H2		P19823	4
Ig mu chain C region	High	P01871	2	Ceruloplasmin	Medium	P00450	16	Antithrombin-III		P01008	5
Ceruloplasmin	Medium	P00450	3	Alpha-2-HS-glycoprotein		P02765	7	Plasma protease C1 inhibitor		P05155	4
Haptoglobin	High	P00738	5	Alpha-2-macroglobulin	High	P01023	22	Galectin-3-binding protein		Q08380	3
Ig gamma-1 chain C region	High	P01857	5	Hemoglobin subunit alpha		P69905	4	Apolipoprotein A-IV		P06727	4
Beta-2-glycoprotein 1		P02749	3	Fibronectin		P02751	4	Apolipoprotein A-II	Medium	P02652	2
Alpha-2-HS-glycoprotein		P02765	2	Haptoglobin-related protein		P00739	3	Alpha-2-macroglobulin	High	P01023	47
Plasminogen	Medium	P00747	2	Inter-alpha-trypsin inhibitor heavy chain H1		P19827	3	Plasminogen	Medium	P00747	9
				Complement factor H		P08603	3	Alpha-2-HS-glycoprotein		P02765	7
				Serum albumin	High	P02768	32	Complement factor H		P08603	21
				Complement C3	High	P01024	22	Fibronectin		P02751	17
				Ig kappa chain C region	High	P01834	4	Kininogen-1		P01042	8
				Kininogen-1		P01042	4	Hemoglobin subunit alpha		P69905	4
				Plasminogen	Medium	P00747	3	Haptoglobin-related protein		P00739	7
				Alpha-1-antitrypsin	High	P01009	16	Serum albumin	High	P02768	39
				Ig gamma-1 chain C region	High	P01857	10	Complement C3	High	P01024	15
				Serotransferrin	High	P02787	24	Ceruloplasmin	Medium	P00450	14
				Immunoglobulin lambda-like polypeptide 5		B9A064	4	Haptoglobin	High	P00738	7
				Ig mu chain C region	High	P01871	3	Ig kappa chain C region	High	P01834	5
				Haptoglobin	High	P00738	5	Ig gamma-1 chain C region	High	P01857	11
								Beta-2-glycoprotein 1		P02749	3
								Alpha-1-antitrypsin	High	P01009	17
								Serotransferrin	High	P02787	32
								Ig mu chain C region	High	P01871	6
								Immunoglobulin lambda-like polypeptide 5		B9A064	3

Table 4.7 Qualitative analysis of protein fractions shown in Figure 4.10. Overall, 27, 46, 58, and 59 proteins were identified in the starting material, the flowthrough, the 20 mM fraction, and the 50 mM fraction, respectively. Of the starting material identifications, four were found to be unique as they were not identified in any of the other fractions. These proteins are shown in red in the starting material column. When compared to the starting material list, 31, 39, and 40 proteins were found to be unique to the flowthrough, 20 mM and 50 mM fractions, respectively. These identifications are also listed in red in their respective columns. This would suggest that the technique enriched for these proteins. Of the list of flowthrough identifications, seven proteins were not found in either the 20 mM or the 50 mM fraction. 25 and 29 proteins were found to be unique to the 20 mM and 50 mM elutions, respectively, when compared to the flowthrough protein list.

4.9 Quantitative LC-MS Analysis of Differentially Regulated, IMAC-Bound Vitreous Fluid Proteins

In order to examine the efficiency of the IMAC-based fractionation technique with a larger sample set, 13 uveal melanoma vitreous humour specimens were selected for IMAC purification (Table 4.8). This would determine the reproducibility of the technique as a fractionation method and as an enhancer of the low abundance protein population. Six of the samples were collected from patients with monosomy of chromosome three; an indicator of poor prognosis in uveal melanoma, while the other seven were disomy of chromosome three. . It was postulated that proteins would be differentially expressed between specimens collected from patients with monosomy three (associated with poor prognosis) and disomy three (good prognosis) and that this analysis would highlight any potential differential protein expression patterns.

Each specimen was bound to copper-activated IMAC resin as before and eluted in 20 mM, 50 mM, 100 mM, 300 mM and 500 mM fractions. The unbound fraction was also collected. All samples were then quantified, however of the fractions, only enough protein to proceed with the analysis was present in the 20 mM and the 50 mM elutions. The flowthrough and two fractions were in-solution digested with both lys-C and trypsin to produce peptides of which 1 μg was analysed by LC-MS/MS over the course of a one hour gradient. Technical replicates were performed for each sample. The resulting information was analysed with Progenesis LC-MS software. Identifications with ANOVA scores of <0.05 for peptides and proteins were accepted. Protein principal component analyses (PCA), which represents protein abundance variation between features, are shown for the flowthrough, 20 mM, and 50 mM fractions in Figure 4.11. This illustrated good separation of protein abundances between the monosomy three and disomy three sample sets for each of the three fractions.

Sample Identifier	Sex	Age (years)	Chromosome 3 Status	Metastasised
1	F	72	Disomy	No
2	M	77	Disomy	No
3	M	64	Disomy	Lungs
4	M	49	Disomy	No
5	F	85	Disomy	No
6	M	38	Disomy	No
7	F	58	Disomy	No
8	M	42	Monosomy	No
9	F	78	Monosomy	No
10	F	49	Monosomy	Liver, Skin
11	F	73	Monosomy	Liver
12	F	49	Monosomy	Kidneys
13	-	-	Monosomy	-

Table 4.8 Patient details for 13 vitreous humour specimens selected for IMAC fractionation. Seven disomy of chromosome three samples were compared with six monosomy of chromosome three specimens. All fluids were taken from patients with uveal melanoma.

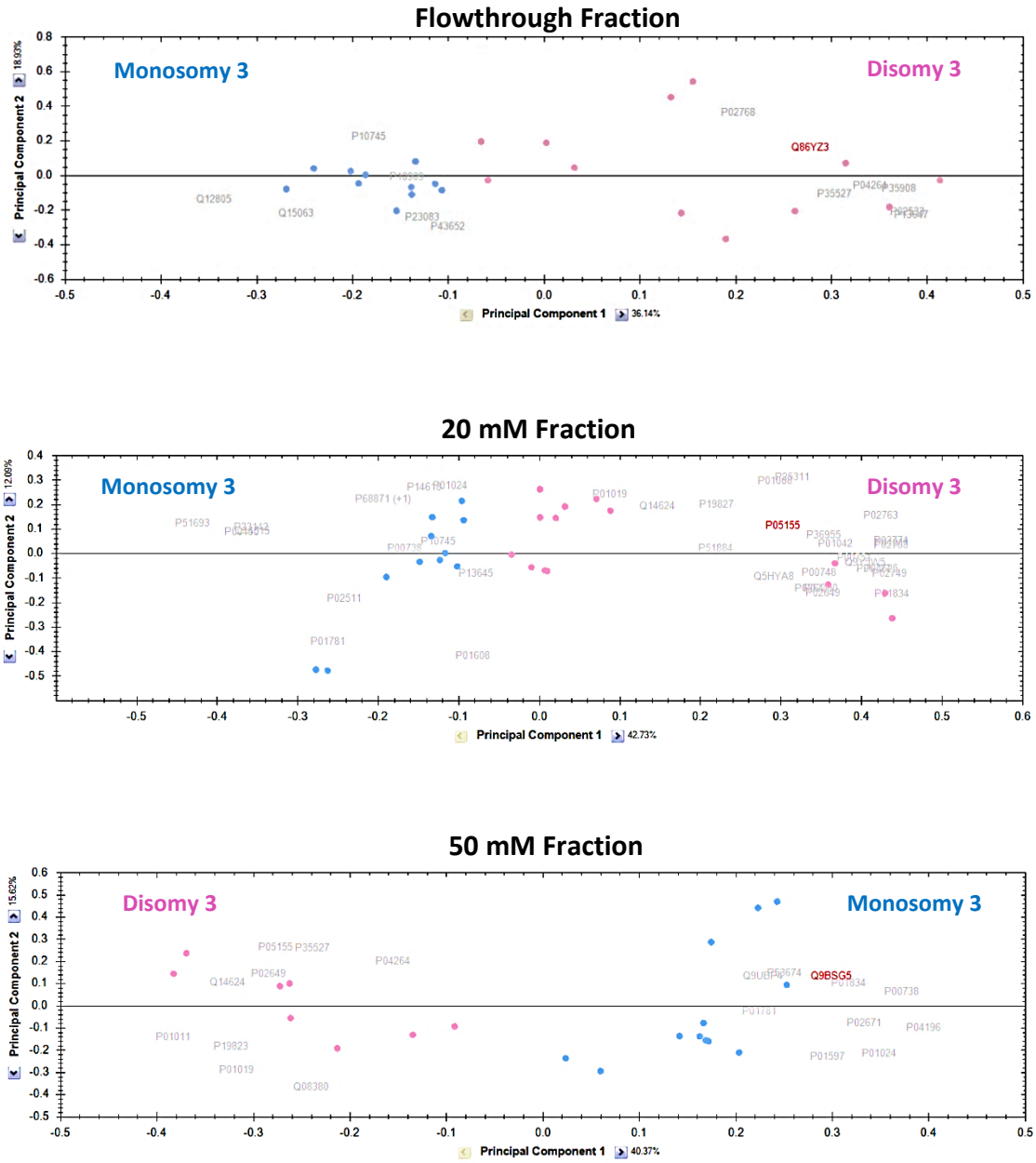

Figure 4.11 Principal component analysis (PCA) for proteins in the flowthrough, 20 mM and 50 mM fractions. Feature abundance levels across runs are plotted to determine the abundance variation between samples. This is useful in identifying run outliers. Each blue point corresponds to a monosomy of chromosome three sample (n=6) while each pink point corresponds to a disomy of chromosome three sample (n=7).

Eight proteins were found to be differentially expressed between monosomy three and disomy three specimens in the flowthrough (Table 4.9). One such identification, Ig heavy chain V-I region V35 (Figure 4.11), had not previously been reported in the literature as being expressed in the vitreous.

	Description	Accession No.	No. Peptides Matched	Score	Anova (p)	Fold	Average Normalised Abundances	
							Disomy 3	Monosomy 3
Down in Monosomy 3	Hornerin	Q86YZ3	1	56.41	1.97E-03	52.72	7.00E+04	1328.13
	Serum albumin	P02768	1	44.17	0.03	11.28	1.31E+06	1.16E+05
Up in Monosomy 3	Clusterin	P10909	2	115.17	0.03	1.67	3.06E+05	5.10E+05
	Retinol-binding protein 3	P10745	2	76.52	0.06	1.68	9.33E+04	1.57E+05
	Ig heavy chain V-I region V35	P23083	1	57.38	0.04	11.28	2.63E+04	2.97E+05
	EGF-containing fibulin-like extracellular matrix protein 1	Q12805	1	46.28	2.11E-03	1.39	4482.65	6213.22
	Afamin	P43652	1	34.43	0.04	2.46	730.46	1794.95
	Periostin	Q15063	1	34.39	0.03	1.39	1.36E+05	1.88E+05

Table 4.9 Proteins which did not bind to the IMAC resin, i.e. the flowthrough, were analysed by quantitative label-free LC-MS. Eight differentially expressed proteins between the vitreous fluid of uveal melanoma patients with monosomy of chromosome 3 (n=6) and those with disomy of chromosome 3 (n=7) were identified by Progenesis LC-MS software.

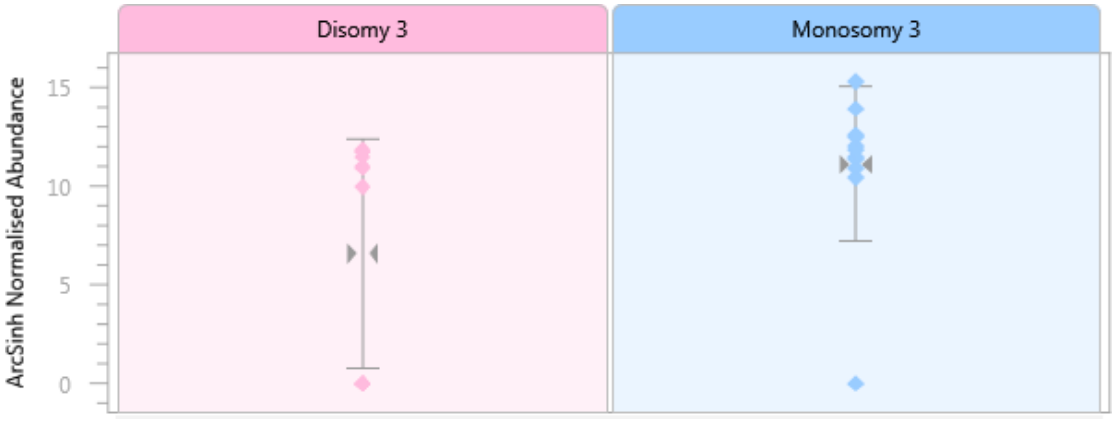

Figure 4.11 Normalised abundance profile for Ig heavy chain V-I region V35 in the flowthrough fraction of IMAC fractionated vitreous fluid. An 11.28 max fold increase was observed in the monosomy three vitreous specimens (n=6, analysed in duplicate) in comparison to those which were disomy three (n=7, analysed in duplicate), p=0.04 between experimental groups. Each spot in the profile corresponds to Ig heavy chain V-I region V35 abundance per sample.

37 proteins were detected as potential targets of interest in the 20 mM fraction, including ocular-related proteins such as retinol-binding protein 3 and alpha crystallin B chain (Table 4.10).

Retinol-binding protein 3 was identified as being upregulated in monosomy of chromosome three specimens in both the flow through and the 20 mM fraction (Figure 4.12). As it functions as a transporter of retinoids between the photoreceptors and the retinal pigment epithelium, it is necessary for normal rod and cone cell function (den Hollander, McGee et al. 2009).

Meckelin, which mediates primary ciliary function, was identified as being decreased in the monosomy three sample set by 2.03-fold, as illustrated in Figure 4.13 (Dawe, Smith et al. 2007). Meckelin, Ig heavy chain V-III region GAL, and Ig kappa chain V-I region Roy, all of which were found to be differentially regulated between the disomy of chromosome three and monosomy of chromosome three sample sets, were not previously identified in vitreous humour, according to the literature, including a recent study carried out by Aretz et al. Using different protein pre-fractionation strategies, such as liquid phase isoelectric focusing, 1-D gel electrophoresis and a combination of both, followed by UPLC-MS/MS analysis of generated peptides, Aretz et al. identified 1111 unique proteins from three separate vitreous specimens (Aretz, Krohne et al. 2013). This is the most comprehensive qualitative study of a control vitreous fluid proteome carried out to date. As some of the proteins identified in this study were not found by Aretz et al., this may suggest that these proteins may be differentially regulated exclusively in uveal melanoma, and may be novel in terms of vitreous fluid proteomics.

Other proteins which were found to be differentially expressed in this study have previously been identified in the vitreous, including pigment epithelium-derived factor (PEDF). PEDF was found to be decreased in the monosomy three sample set by 1.44-fold (Figure 4.14). This secreted protein has been long associated with anti-angiogenic and anti-tumorigenic properties as well as being essential for the health and survival of the retina (Subramanian, Locatelli-Hoops et al. 2013).

	Description	Accession No.	No. Peptides Matched	Score	Anova (p)	Fold	Average Normalised Abundances	
							Disomy 3	Monosomy 3
Down in Monosomy 3	Inter-alpha-trypsin inhibitor heavy chain H1	P19827	3	281.78	0.01	1.43	5.04E+05	3.52E+05
	Alpha-1-antichymotrypsin	P01011	4	252.03	1.39E-03	2.51	3.55E+06	1.41E+06
	Antithrombin-III	P01008	5	239.62	0.01	1.36	1.66E+06	1.22E+06
	Apolipoprotein A-IV	P06727	4	237.63	0.02	2.05	1.67E+06	8.14E+05
	Plasma protease C1 inhibitor	P05155	4	228.22	2.59E-06	1.84	1.59E+06	8.65E+05
	Kininogen-1	P01042	4	221.39	0.01	1.53	2.24E+06	1.46E+06
	Coagulation factor XII	P00748	3	206.01	0.02	2.53	1.49E+06	5.86E+05
	Apolipoprotein E	P02649	3	193.89	1.83E-03	3.83	5.39E+05	1.40E+05
	Angiotensinogen	P01019	2	182.6	6.18E-03	1.69	1.03E+06	6.10E+05
	Complement factor B	P00751	3	141.82	7.67E-04	1.73	1.10E+06	6.37E+05
	Inter-alpha-trypsin inhibitor heavy chain H4	Q14624	3	129.28	0.01	1.52	3.84E+05	2.53E+05
	Vitamin D-binding protein	P02774	3	107.03	9.18E-03	3.02	9.07E+05	3.00E+05
	Serum albumin	P02768	2	88.16	0.01	6.34	1.60E+06	2.53E+05
	Ig kappa chain V-IV region Len	P01625	1	87.89	0.02	5.37	6.75E+05	1.26E+05
	Apolipoprotein A-I	P02647	2	84.62	0.01	1055.83	6.10E+05	577.99
	Alpha-1-acid glycoprotein 1	P02763	1	60.56	0.01	2.86	8.09E+05	2.83E+05
	Pyruvate kinase isozymes M1/M2	P14618	1	58.8	0.05	2	4.32E+04	2.16E+04
	Wnt inhibitory factor 1	Q9Y5W5	1	53.35	0.02	90.84	4.41E+04	485.99
	Beta-2-glycoprotein 1	P02749	1	48.67	2.42E-04	2.98	3.67E+04	1.23E+04
	Lumican	P51884	1	47.35	0.02	1.49	7.40E+04	4.97E+04
	Pigment epithelium-derived factor	P36955	1	46.51	0.04	1.44	6.06E+05	4.22E+05
	Hemopexin	P02790	1	44.9	1.29E-03	226.3	1.40E+05	619.13
	Ig kappa chain C region	P01834	1	40.42	0.05	Infinity	2.42E+04	0
	Zinc-alpha-2-glycoprotein	P25311	1	34.92	0.02	1.36	8.70E+05	6.39E+05
	Meckelin	Q5HYA8	1	34.23	9.59E-03	2.03	8.74E+04	4.31E+04

Up in Monosomy 3	Retinol-binding protein 3	P10745	6	317.11	0.03	2.82	5.23E+05	1.47E+06
	Haptoglobin	P00738	5	270.41	7.47E-05	8.78	2.59E+05	2.27E+06
	Complement C3	P01024	5	231.15	0.04	1.5	7.58E+05	1.13E+06
	Ceruloplasmin	P00450	2	111.3	0.02	1.44	7.07E+05	1.02E+06
	Hemoglobin subunit beta	P68871	2	110.22	0.04	1.63	1.50E+05	2.44E+05
	Keratin, type I cytoskeletal 10	P13645	1	96.13	0.04	4.02	1.50E+05	6.03E+05
	Fibulin-1	P23142	1	66.91	0.05	2.3	8.77E+04	2.02E+05
	Ig heavy chain V-III region GAL	P01781	1	59.47	4.74E-03	2.38	1.86E+05	4.43E+05
	Amyloid-like protein 1	P51693	1	41.39	0.04	1.85	1.29E+04	2.37E+04
	Ig kappa chain V-I region Roy	P01608	1	39.65	0.03	2.18	3.62E+04	7.88E+04
	SPARC-like protein 1	Q14515	1	33.42	8.37E-04	1.43	1.53E+04	2.19E+04
	Alpha-crystallin B chain	P02511	1	30.13	0.04	85.01	162.93	1.38E+04

Table 4.10 Proteins eluted from IMAC resin with 20 mM imidazole were analysed by quantitative label-free LC-MS. 37 statistically-significant differentially expressed proteins between the vitreous fluid of uveal melanoma patients with monosomy of chromosome 3 (n=6) and those with disomy of chromosome 3 (n=7) were identified by Progenesis LC-MS software.

Figure 4.12 Retinol-binding protein 3 was identified as being upregulated by 2.82-fold in the monosomy three specimens of the 20 mM fraction (p=0.03 between experimental groups). However, two technical replicates from one of the samples (circled) appear to have biased the observed fold change. Despite this, the result was still considered significant across all samples (a) Normalised abundance view of retinol-binding protein 3 expression in disomy three (n=7, analysed in duplicate) and monosomy three (n=6, analysed in duplicate) vitreous samples. Each point corresponds to a sample and illustrates the quantity of the protein of interest per specimen. (b) Normalised abundance of identified retinol-binding protein 3 peptides per sample. Each line represents a peptide while each point indicates the abundance of the peptide per sample.

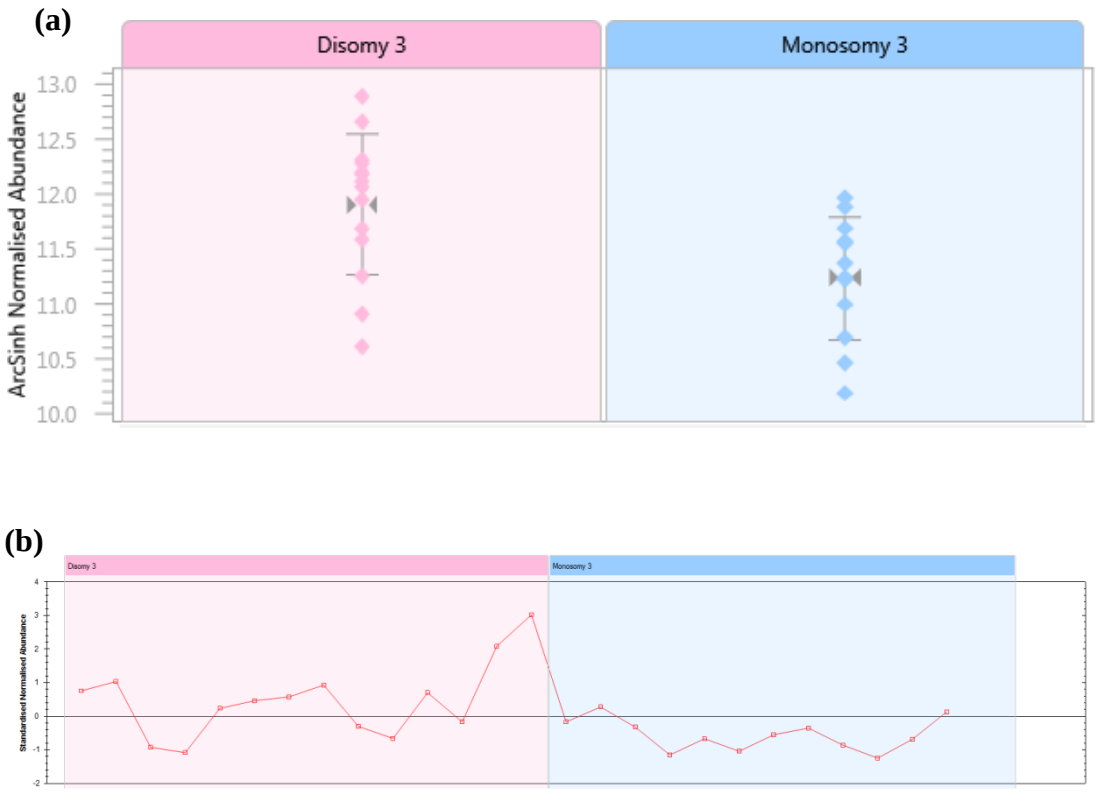

Figure 4.13 Meckelin was identified as being downregulated by 2.03-fold in the monosomy three specimens (n=6, analysed in duplicate) of the 20 mM fraction in comparison to that of the disomy three (n=7, analysed in duplicate), p=9.59x10^{-3} between sample sets. Only one peptide was matched to this sample which indicates that meckelin may be a weak candidate. (a) Normalised abundance view of meckelin expression in disomy three and monosomy three vitreous samples. Each point on the figure corresponds to a sample and indicates the quantity of the protein of interest per specimen. (b) Normalised abundance of identified meckelin peptides per sample. The line represents a peptide while each point indicates the abundance of peptide per sample.

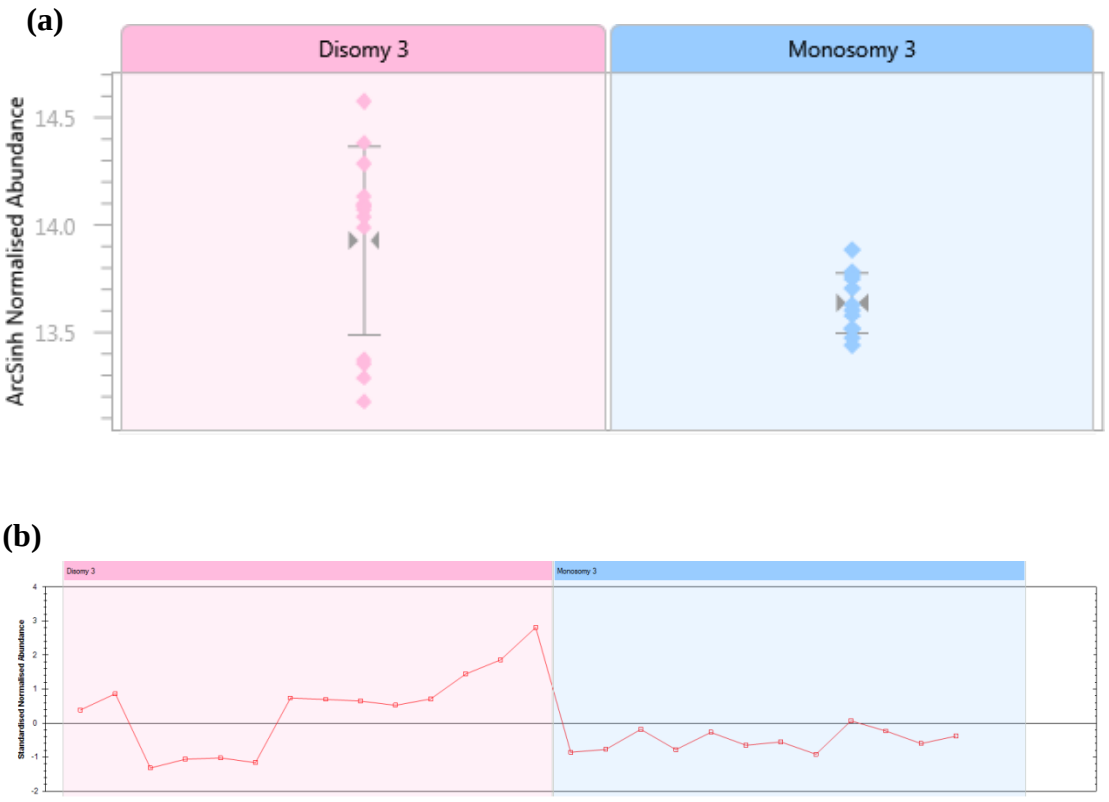

Figure 4.14 Pigment epithelium-derived factor (PEDF) was identified as being downregulated by 1.44-fold in the monosomy three specimens (n=6, analysed in duplicate) of the 20 mM fraction in comparison to the disomy three samples (n=7, analysed in duplicate), *p*=0.04 between sample sets. Only one peptide was matched to this sample which indicates that PEDF may be a weak candidate. (a) Normalised abundance view of PEDF expression in disomy three and monosomy three vitreous samples. Each point on the figure corresponds to a sample and indicates the quantity of the protein of interest per specimen. (b) Normalised abundance of identified PEDF peptides per sample. The line represents a peptide while each point indicates the abundance of peptide per sample.

For the 50 mM fraction, 17 proteins were found to be differentially expressed between both groups (Table 4.11).

Retbindin, a secreted protein, was identified in the 50 mM fraction as showing an decreased abundance in the monosomy of chromosome three sample set (Figure 4.15). This is a relatively novel, secreted protein which is thought to function in flavonoid or carotenoid binding (Wistow, Bernstein et al. 2002). Again, retbindin was not previously identified in vitreous fluid by Aretz et al. or in the literature.

	Description	Accession No.	No. Peptides Matched	Score	Anova (p)	Fold	Average Normalised Abundances	
							Disomy 3	Monosomy 3
Down in Monosomy 3	Apolipoprotein E	P02649	1	90.78	3.17E-03	2	2.90E+06	1.45E+06
	Alpha-1-antichymotrypsin	P01011	2	67.85	1.06E-03	3.11	2.24E+06	7.19E+05
	Angiotensinogen	P01019	1	66.78	0.01	15.86	1.20E+06	7.55E+04
	Galectin-3-binding protein	Q08380	1	61.34	0.05	3.84	1.75E+06	4.56E+05
	Histidine-rich glycoprotein	P04196	1	58.91	2.24E-04	1.01	1.60E+04	1.59E+04
	Inter-alpha-trypsin inhibitor heavy chain H2	P19823	1	41.21	9.23E-03	2.67	1.71E+06	6.38E+05
	Inter-alpha-trypsin inhibitor heavy chain H4	Q14624	1	38.72	1.26E-03	3.53	7.91E+05	2.24E+05
	Plasma protease C1 inhibitor	P05155	1	38.47	0.01	3.84	3.40E+06	8.85E+05
Up in Monosomy 3	Haptoglobin	P00738	4	209.73	2.27E-04	21.39	2.46E+05	5.26E+06
	Retbindin	Q9BSG5	2	177.82	1.62E-04	9.74	2.41E+04	2.35E+05
	Complement C3	P01024	2	89.36	2.80E-04	9.7	2.37E+04	2.30E+05
	Fibrinogen alpha chain	P02671	1	70.38	1.25E-03	5.41	1.71E+04	9.24E+04
	Ig kappa chain C region	P01834	1	54.41	0.01	2.75	9.33E+04	2.56E+05
	Dickkopf-related protein 3	Q9UBP4	1	38.83	7.31E-03	3.33	4.58E+04	1.53E+05
	Beta-crystallin B1	P53674	1	36.61	0.04	Infinity	0	6.15E+04
	Ig kappa chain V-I region DEE	P01597	1	36.57	0.02	3.77	1.16E+05	4.39E+05
	Ig heavy chain V-III region GAL	P01781	1	30.92	0.05	1.87	1.28E+05	2.38E+05

Table 4.11 Proteins eluted from IMAC resin with 50 mM imidazole were analysed by quantitative label-free LC-MS. 17 statistically-significant differentially expressed proteins between the vitreous fluid of uveal melanoma patients with monosomy of chromosome 3 and those with disomy of chromosome 3 were identified.

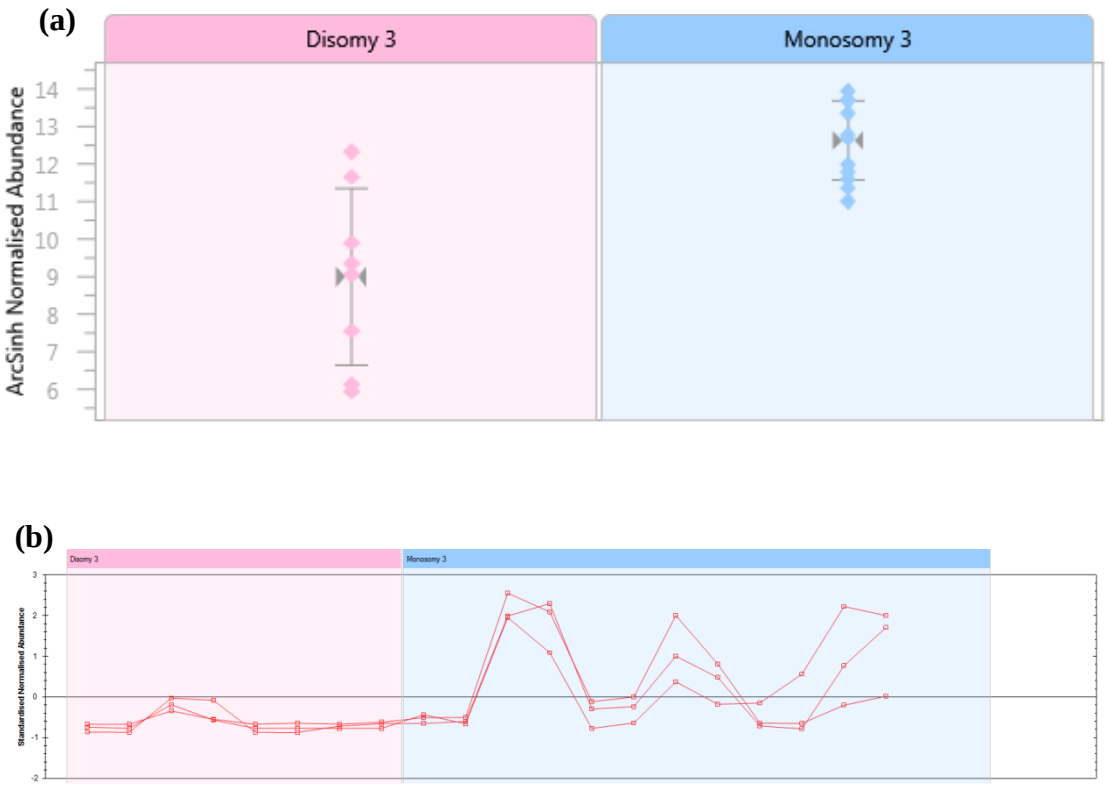

Figure 4.15 Retbindin was identified as being upregulated by a maximum fold value of 9.74 in monosomy three specimens (n=6, with two of the samples analysed in duplicate) in comparison to disomy three specimens (n=7, with six of the samples analysed in duplicate), in the 50 mM fraction, $p=1.62x10^{-4}$ between sample sets. (a) Normalised abundance view of retbindin expression in disomy three and monosomy three vitreous samples. Each point on the figure corresponds to a sample and indicates the quantity of the protein of interest per specimen. (b) Normalised abundance of identified retbindin peptides per sample. The lines represent peptides while each point indicates the abundance of peptide per sample.

For the flowthrough, the 20 mM, and the 50 mM fractions, the TIC profiles were similar between the samples in each group with good alignments of features between samples. This would indicate that the method was reproducible between fractions and hence, successful.

4.10 Enrichment Analysis Within Differentially Expressed Protein Lists Using DAVID

In order to determine significant enrichment of biological processes, molecular functions, and cellular compartments involved within the differentially expressed protein lists, DAVID and (GO analysis was used. Enrichment was considered to be significant when the Bonferroni p-value adjustment was ≤ 0.05. The differentially regulated protein lists for the flowthrough, 20 mM and 50 mM fractions were merged, and proteins either up or downregulated in monosomy three specimens were analysed as two separate lists.

For the list of proteins which were downregulated in monosomy of chromosome three specimens, many of the identifications related to biological processes such as response to trauma, e.g. inflammatory response, regulation of blood coagulation (Table 4.12). This may be due to the breakdown of the blood-retinal barrier which can occur during uveal melanoma. Cellular compartments which were related to the downregulation of proteins in the monosomy of chromosome three sample set were associated with extracellular regions and lipoprotein complexes (Table 4.13). The molecular processes identified by the analysis involved enzyme inhibiting and cholesterol-binding activities (Table 4.14). Overall, DAVID found that the collective decrease in expression of five the proteins identified; kininogen-1, plasma protease C1 inhibitor, antithrombin-III, complement factor B and coagulation factor XII, would impact on B cell receptor signalling pathway in the complement and coagulation cascade (Figure 4.16).

Biological Process	Count	*p*-value	Adjusted *p*-value
Regulation of response to external stimulus	9	4.00E-10	3.00E-07
Positive regulation of cholesterol esterification	4	2.20E-07	1.60E-04
Regulation of inflammatory response	6	2.90E-07	2.20E-04
Regulation of cholesterol esterification	4	3.50E-07	2.60E-04
Regulation of blood coagulation	5	6.10E-07	4.50E-04
Regulation of coagulation	5	1.00E-06	7.80E-04
Acute inflammatory response	6	1.00E-06	7.90E-04
Positive regulation of steroid metabolic process	4	2.30E-06	1.70E-03
Response to wounding	9	4.40E-06	3.30E-03
Negative regulation of blood coagulation	4	1.10E-05	8.10E-03
Defence response	9	1.30E-05	9.80E-03
Negative regulation of coagulation	4	1.60E-05	1.20E-02
Inflammatory response	7	2.80E-05	2.10E-02
Blood coagulation	5	4.00E-05	3.00E-02
Coagulation	5	4.00E-05	3.00E-02
Regulation of steroid metabolic process	4	4.30E-05	3.20E-02
Negative regulation of defence response	4	4.30E-05	3.20E-02
Homeostasis	5	5.00E-05	3.70E-02
Regulation of lipid metabolic process	5	5.80E-05	4.20E-02

Table 4.12 GO biological process enrichment for differentially expressed proteins which were downregulated in monosomy of chromosome three vitreous fluid. Enrichment was considered significant upon observation of a p-value ≤0.05 and a Bonferroni adjusted p-value ≤0.05. Count corresponds to the overlap between proteins on the list and a particular GO category.

Cellular Compartment	Count	*p*-value	Adjusted *p*-value
Extracellular region	25	8.20E-17	6.80E-15
Extracellular space	15	1.50E-11	9.00E-10
Extracellular region part	16	9.10E-11	5.50E-09
Triglyceride-rich lipoprotein particle	4	9.40E-06	5.70E-04
Very-low-density lipoprotein particle	4	9.40E-06	5.70E-04
High-density lipoprotein particle	4	1.90E-05	1.10E-03
Plasma lipoprotein particle	4	5.30E-05	3.20E-03
Protein-lipid complex	4	5.30E-05	3.20E-03
Chylomicron	3	2.80E-04	1.70E-02

Table 4.13 GO cellular compartment enrichment for differentially expressed proteins which were downregulated in monosomy of chromosome three vitreous fluid. Enrichment was considered significant upon observation of a p-value ≤0.05 and a Bonferroni adjusted p-value ≤0.05. Count corresponds to the overlap between proteins on the list and a particular GO category.

Molecular Function	Count	*p*-value	Adjusted *p*-value
Endopeptidase inhibitor activity	10	3.70E-12	4.30E-10
Serine-type endopeptidase inhibitor activity	9	4.60E-12	5.30E-10
Peptidase inhibitor activity	10	6.00E-12	7.00E-10
Enzyme inhibitor activity	10	9.70E-10	1.10E-07
Phosphatidylcholine-sterol O-acyltransferase Activator activity	3	3.50E-05	4.10E-03
Heparin binding	5	4.20E-05	4.80E-03
Glycosaminoglycan binding	5	1.40E-04	1.60E-02
Lipid binding	7	1.70E-04	1.90E-02
Polysaccharide binding	5	2.00E-04	2.30E-02
Pattern binding	5	2.00E-04	2.30E-02
Cholesterol transporter activity	3	2.30E-04	2.70E-02
Sterol transporter activity	3	3.20E-04	3.60E-02

Table 4.14 GO molecular function enrichment for differentially expressed proteins which were downregulated in monosomy of chromosome three vitreous fluid. Enrichment was considered significant upon observation of a p-value ≤0.05 and a Bonferroni adjusted p-value ≤0.05. Count corresponds to the overlap between proteins on the list and a particular GO category.

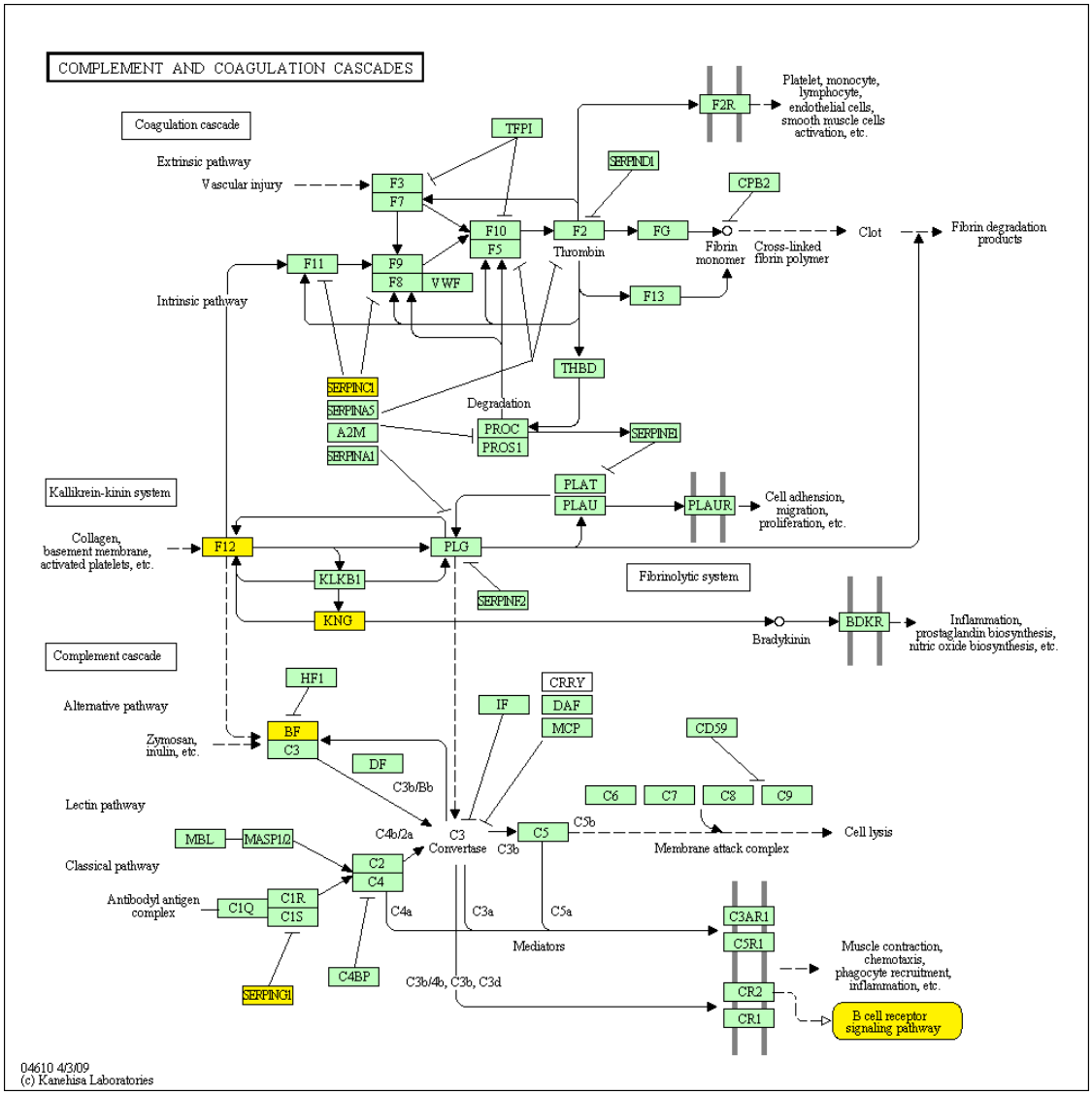

Figure 4.16 DAVID analysis of proteins which were downregulated in monosomy of chromosome three uveal melanoma vitreous fluid specimens found that five identifications; kininogen-1, plasma protease C1 inhibitor, antithrombin-III, complement factor B and coagulation factor XII, were involved in complement and coagulation cascades. The genes which are involved are highlighted in yellow. This illustrated that the downregulation of these proteins would ultimately affect B cell receptor signalling.

Proteins which were upregulated in monosomy of chromosome three ocular fluid were shown to relate to extracellular compartments (Table 4.15). No statistically significant biological or molecular processes were identified for the protein list. Two genes which express proteins from the list; fibrinogen alpha chain and complement C3, were found to play a role in the complement and coagulation cascades (Figure 4.17).

Cellular Compartment	Count	*p*-value	Adjusted *p*-value
Extracellular region part	13	3.70E-10	2.30E-08
Extracellular region	16	4.30E-10	2.70E-08
Extracellular space	8	2.30E-05	1.50E-03
Proteinaceous extracellular matrix	6	6.20E-05	3.90E-03
Extracellular matrix	6	8.90E-05	5.60E-03

Table 4.15 GO cellular compartment enrichment for differentially expressed proteins which were upregulated in monosomy of chromosome three vitreous fluid. Enrichment was considered significant upon observation of a p-value ≤0.05 and a Bonferroni adjusted p-value ≤0.05. Count corresponds to the overlap between proteins on the list and a particular GO category.

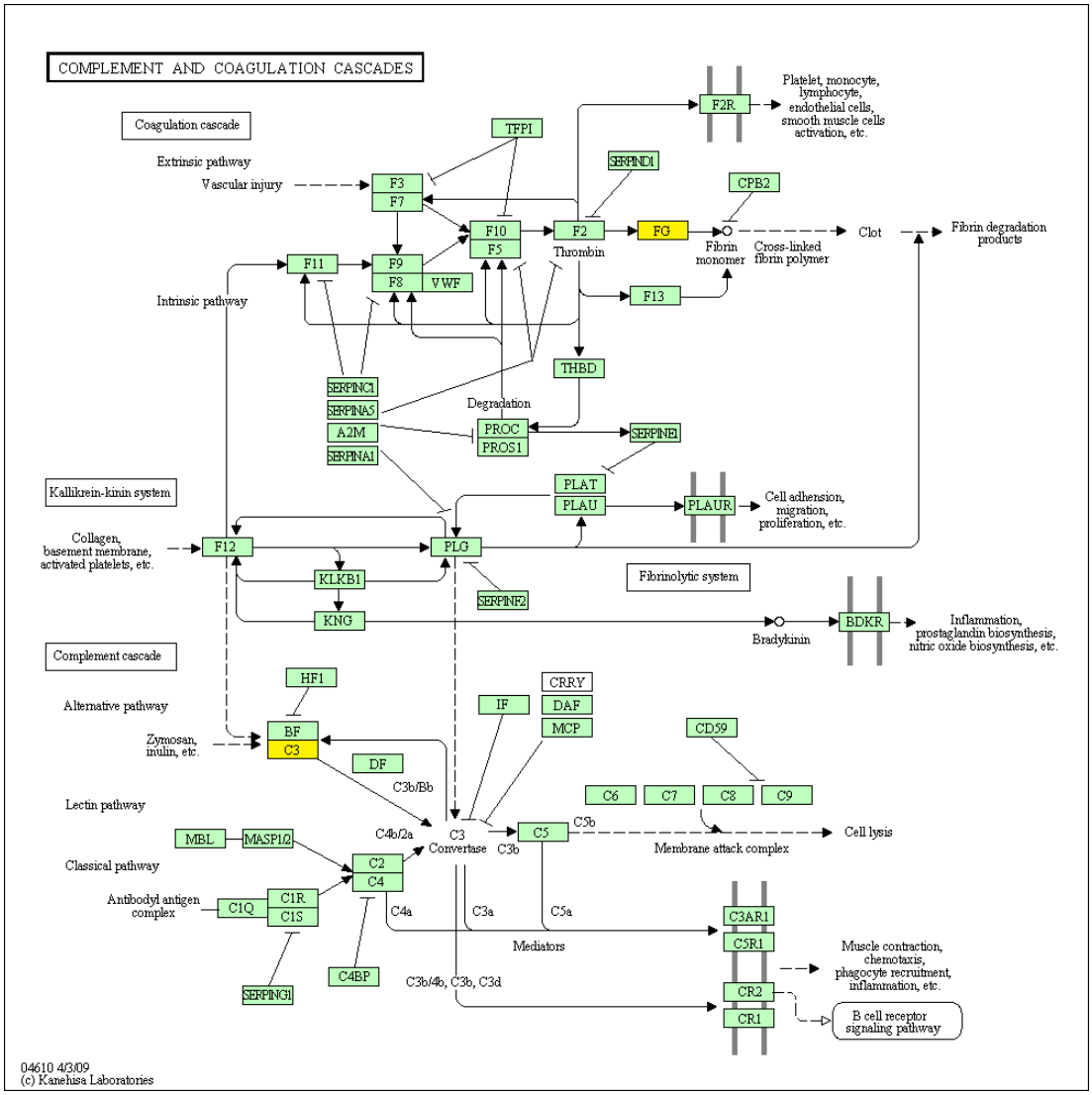

Figure 4.17 DAVID analysis of proteins which were upregulated in monosomy of chromosome three uveal melanoma vitreous fluid specimens found that two identifications; fibrinogen alpha chain and complement C3, were involved in complement and coagulation cascades.

4.11 Analysis of Vitreous Fluid by Luminex Multiplex Assay

The Luminex bioassay system uses xMAP technology which creates a multiplex approach to bioassaying. Through the combination of advanced fluidics, optics, and digital signal processing with a microsphere technology, it is possible to analyse up to 500 analytes per well. The microspheres used are tiny colour-coded polystyrene beads dyed with distinct proportions of red and near-infrared fluorophores. Each bead set can be coated with a reagent specific to a particular bioassay, allowing the capture and detection of specific analytes from a sample. Within the Luminex system, a light source excites the internal dyes which identify each microsphere particle and any reporter dye captured during the assay. Up to one hundred different detection reactions can be carried out simultaneously on the various bead populations in very small volumes.

Results acquired from multiplex analysis can be further examined using MedCalc, a statistical software programme designed for biomedical science. This illustrates the sensitivity and specificity of a potential marker through ROC curve analysis.

A Luminex 12-plex cytokine/chemokine assay was chosen for the analysis of vitreous humour from both uveal melanoma and control patients. The assay quantified the levels of FGF2, IFNɣ, TNFα, TGFα, MIP1α, IL-10, IL-15, IL-1α, IL-2, IL-6, IL-8, and IP10 in eight uveal melanoma and six control vitreous samples. Within the disease sample set were seven patients who developed metastases and one who did not. The six control vitreous were obtained from macular hole degeneration patients. All samples used in the analysis are outlined in Table 4.16. This identified three potential chemokines of interest; basic fibroblast growth factor (FGF2), macrophage inhibitory protein 1 alpha (MIP1α) and interferon gamma (IFNɣ).

In some cases t-test results were poor and ROC test results appeared implausibly high, which may have been due to the small sample set used and to variances between samples.

	Sample Identifier	Sex	Age (years)	Chromosome 3 Status	Metastasised
Control	1		66	-	-
	2		54	-	-
	3		60	-	-
	4		73	-	-
	5		64	-	-
	6		79	-	-
Uveal Melanoma	7	F	73	Monosomy	Liver
	8	F	69	Monosomy	Liver
	9	F	49	Monosomy	Kidneys
	10	F	51	Monosomy	Liver
	11	F	49	Monosomy	Liver, Skin
	12	M	64	Disomy	Lungs
	13	M	71	Monosomy	Liver
	14	M	34	Disomy	No

Table 4.16 Clinical data for control (from macular hole degeneration patients) and uveal melanoma vitreous fluid samples used in the Luminex 12-plex cytokine/chemokine assay.

4.11.1 FGF2

As illustrated in Figure 4.18 (a), FGF2 was not shown to be significantly differentially expressed between the control and the uveal melanoma sample groups, although a trend appeared to indicate a higher abundance of the protein in the disease vitreous.

The result was followed up using MedCalc (Figure 4.18 (b)) which presented a specificity of 100% and a sensitivity of 75%. This would indicate that FGF2 may be of interest as a potential biomarker; however analysis with a larger sample set would first be required.

(a)

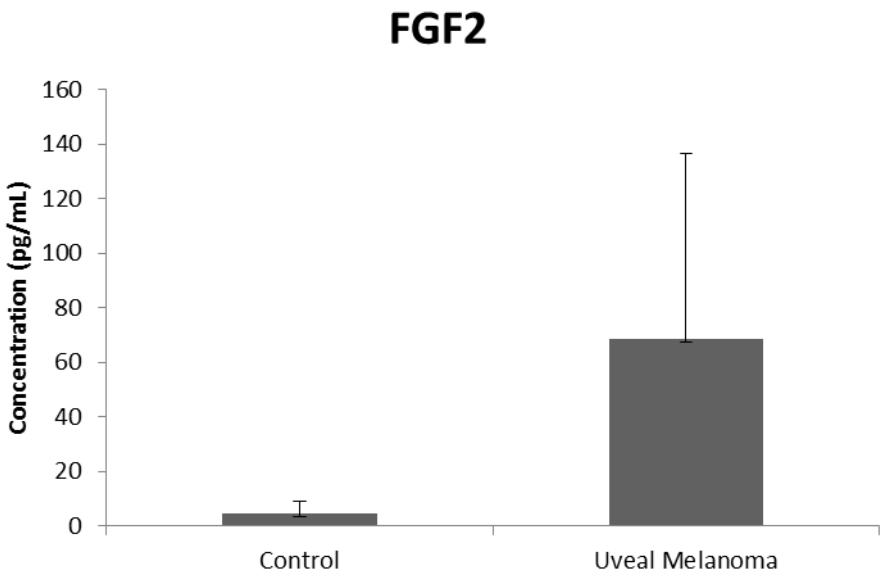

(b)

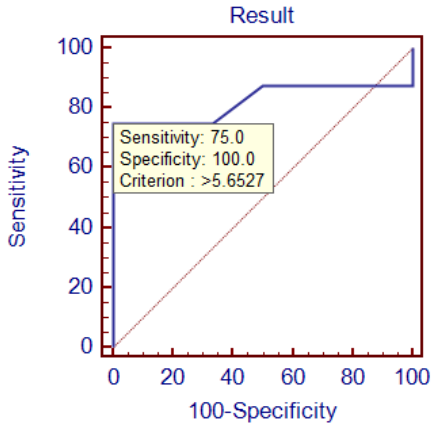

Figure 4.18 Basic fibroblast growth factor (FGF2) was identified in vitreous fluid by a Luminex multiplex bioassay. (a) No statistically significant difference in expression of FGF2 was seen between the control (n=6) and uveal melanoma vitreous samples (n=7). (b) ROC curve analysis indicated the strength of FGF2 as a potentially specific marker. *p*-value=0.09, area under the ROC curve (AUC)=0.823.

4.11.2 MIP-1α

A significant increase in MIP-1α expression was seen in the vitreous of uveal melanoma patients when compared to the controls, with an ANOVA score of <0.01 (Figure 4.19 (a)).

ROC curve analysis confirmed this finding with high sensitivity and specificity values generated for the comparison of control and uveal melanoma vitreous.

(a)

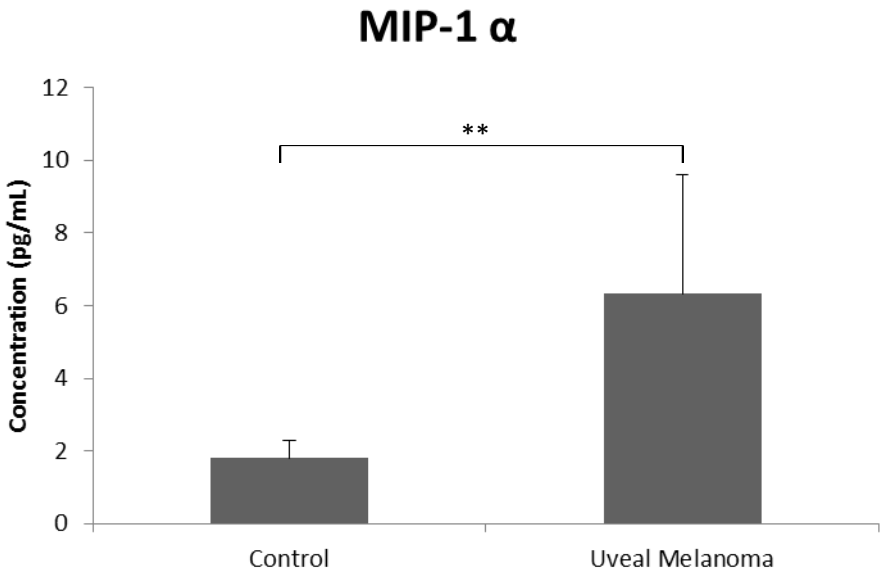

(b)

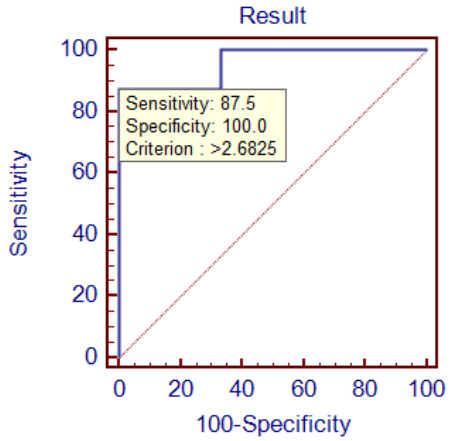

Figure 4.19 (a) Macrophage Inflammatory Protein 1 Alpha (MIP-1α) was found at statistically significantly higher levels in uveal melanoma vitreous (n=7) when compared to control vitreous (n=6) by Luminex multiplex assay. (b) Using ROC curve analysis, MIP-1α was found to be a potential biomarker. *p*-value=6.01×10^{-3}, area under the ROC curve=0.958. ** p <0.01

4.11.3 IFNɣ

IFNɣ was found to be more abundant in uveal melanoma vitreous in comparison to the control vitreous. This was found to be a statistically significant increase in expression, with an ANOVA score of <0.01 (Figure 4.20 (a)).

ROC curve analysis correlated with this finding, illustrating both 100% sensitivity and 100% specificity (Figure 4.20 (b)).

(a)

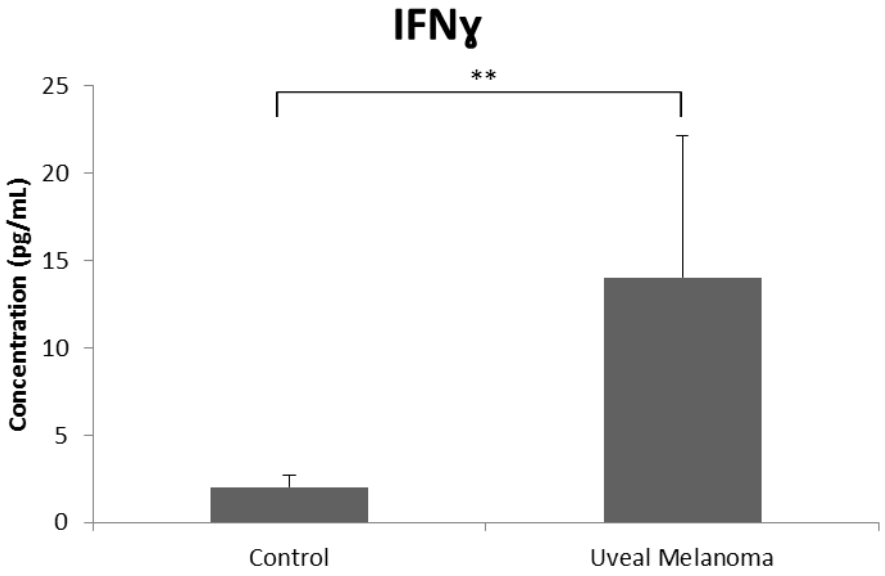

(b)

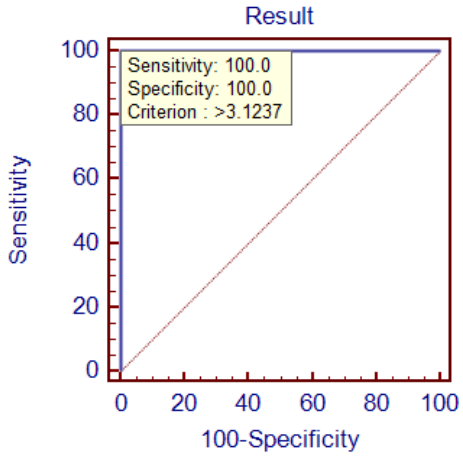

Figure 4.20 (a) Interferon Gamma (IFNγ) was found to be significantly overexpressed in the uveal melanoma vitreous (n=7) in comparison to the control (n=6). (b) ROC curve analysis illustrated high sensitivity and specificity. *p*-value=3.87×10^{-3}, area under the ROC curve (AUC)=1.0. ** p <0.01

Method	Stage	Outcome
Immunodepletion	Pre-Treatment	Following two sequential immunodepletions, highly abundant proteins were successfully removed. However, an insufficient level of protein for further analysis remained.
ProteoMiner	Pre-Treatment	Did not improve the detectable protein content and in some cases, it reduced the number of identifiable proteins.
Cu^{2+} IMAC	Pre-Treatment	Successfully removed a sufficient quantity of highly abundant proteins while enhancing the presence of a subset of low abundance proteins.
2-D DIGE	Analysis	Crude vitreous fluid was too rich in high abundance proteins which caused smearing throughout each gel and resulted in a failed analysis.
Quantitative LC-MS	Analysis	Due to substantial protein content differences between sample sets, it was not possible to compare crude control vitreous fluid and uveal melanoma vitreous fluid. Following Cu^{2+} IMAC treatment, 62 differentially expressed proteins were successfully identified between monosomy 3 and disomy 3 vitreous fluid specimens.
Luminex Multiplex	Analysis	Successfully identified three differentially regulated proteins between untreated control and uveal melanoma vitreous fluids.

Figure 4.21 Summary table illustrating all methods which were tested in the pre-treatment and analysis of vitreous fluid.

CHAPTER FIVE

Proteomic Analysis of Cutaneous Melanoma Disease Progression

5.1 Background

In order to fully comprehend the nature of disease and its progression, a better understanding at the proteomic level is often necessary. It was hypothesised that protein expression differences would be present throughout the process of melanoma disease progression. Such protein differences may in turn lead to the discovery of biomarkers which can then be used in diagnostic tests or as therapeutic targets. It was decided to undertake a complete analysis of the cutaneous melanoma proteome by comparing fractionated advanced cutaneous melanoma serum to fractionated control serum (collected from potentially diabetic patients) using quantitative label-free LC-MS proteomics. Quantitative LC-MS is a highly sensitive, reproducible and accurate method of determining differential protein expression patterns between disease and test groups. Any differentially regulated proteins identified would then be followed up in benign and early stage melanoma serum, as well as in uveal melanoma serum.

It was intended that this approach could improve our understanding of the cutaneous melanoma proteome throughout disease progression and to investigate possible correlations between both uveal and cutaneous melanomas. It could also identify potential biomarkers for metastatic uveal melanoma, in comparison to non-metastatic uveal melanoma.

5.2 Quantitative Label-Free LC-MS Analysis of ProteoMiner Fractionated Serum

ProteoMiner is a bead-based technology used for the compression of the dynamic range of proteins present in complex biological samples. Through the use of a large, bead-based library of combinatorial peptide ligands, ProteoMiner attempts to equalise levels of all proteins throughout the sample. This provides a representative view of the original proteome while enhancing the presence of proteins which may have been undetected otherwise.

A group of eight control sera versus eight stage IV cutaneous melanoma sera were chosen for the experiment (Table 5.1). The control and disease samples were all matched by sex.

A ProteoMiner sequential elution kit was used to treat all of the above samples. This kit combines ProteoMiner bead technology with multiple elution reagents of various chemical properties, as outlined in section 2.17.1, hence providing a protein fractionation based on the characteristics of the individual molecules. This gave four elution fractions per sample, thus resulting in a good overview of the proteome.

Control Sera				Melanoma Sera			
Sample Identifier	Age	Sex		Sample Identifier	Age	Sex	AJCC Stage
DS38	55	F		031	72	F	IV
DS1018	35	F		023	28	F	IV
DS52	38	M		010	36	M	IV
DS114	56	F		017	73	F	IV
DS118	70	M		036	67	M	IV
DS36	38	M		019	45	M	IV
DS37	52	F		039	40	F	III
DS32	36	M		029	27	M	III

Table 5.1 Details of eight advanced cutaneous melanoma sera vs. eight control sera treated using a ProteoMiner Sequential Elution method and subsequently analysed by quantitative label-free LC-MS proteomics for the discovery of differentially expressed proteins between both conditions.

5.3 1-D Analysis of ProteoMiner-Fractionated Serum Samples

All elution fractions were treated with a 2-D clean up kit which involves selective precipitation in order to remove ionic contaminants, that can interfere with downstream analysis, from protein samples. In addition to this, it enables concentration of proteins allowing for higher sample load. The elution fractions were then quantified and an equal concentration of protein from each sample of four elution fractions was separated on a 1-D gel. The gels were subsequently stained with Coomassie Brilliant Blue Colloidal stain in order to give a visual representation of each elution (Figure 5.1). From this, it was clear that elution fractions three and four were very similar in their protein profiles.

Following the visual comparison of all 4 elution fraction 1-D profiles, each lane was excised from gels (a) and (d) shown in Figure 5.1 and in-gel digested using trypsin. LC-MS analysis provided a list of identifications for each elution; 128, 143, 126 and 135 proteins were identified for fractions one, two, three and four, respectively, of the melanoma sera and 138, 127, 113 and 125 were identified in the corresponding fractions of the control sera, respectively.

It was clear, however, that the proteins discovered in elution fraction three were less exclusive and, for the most part, were easily detected in fractions one, two and four. Following a comparison of the melanoma serum identifications acquired, only two proteins were found to be unique to fraction three when compared to fractions one, two and four (Appendix A). Similarly, for the control serum results, only three identifications were noted as exclusive to elution fraction three (Appendix A). Hence, it was decided to exclude fraction three from quantitative label-free LC-MS analysis.

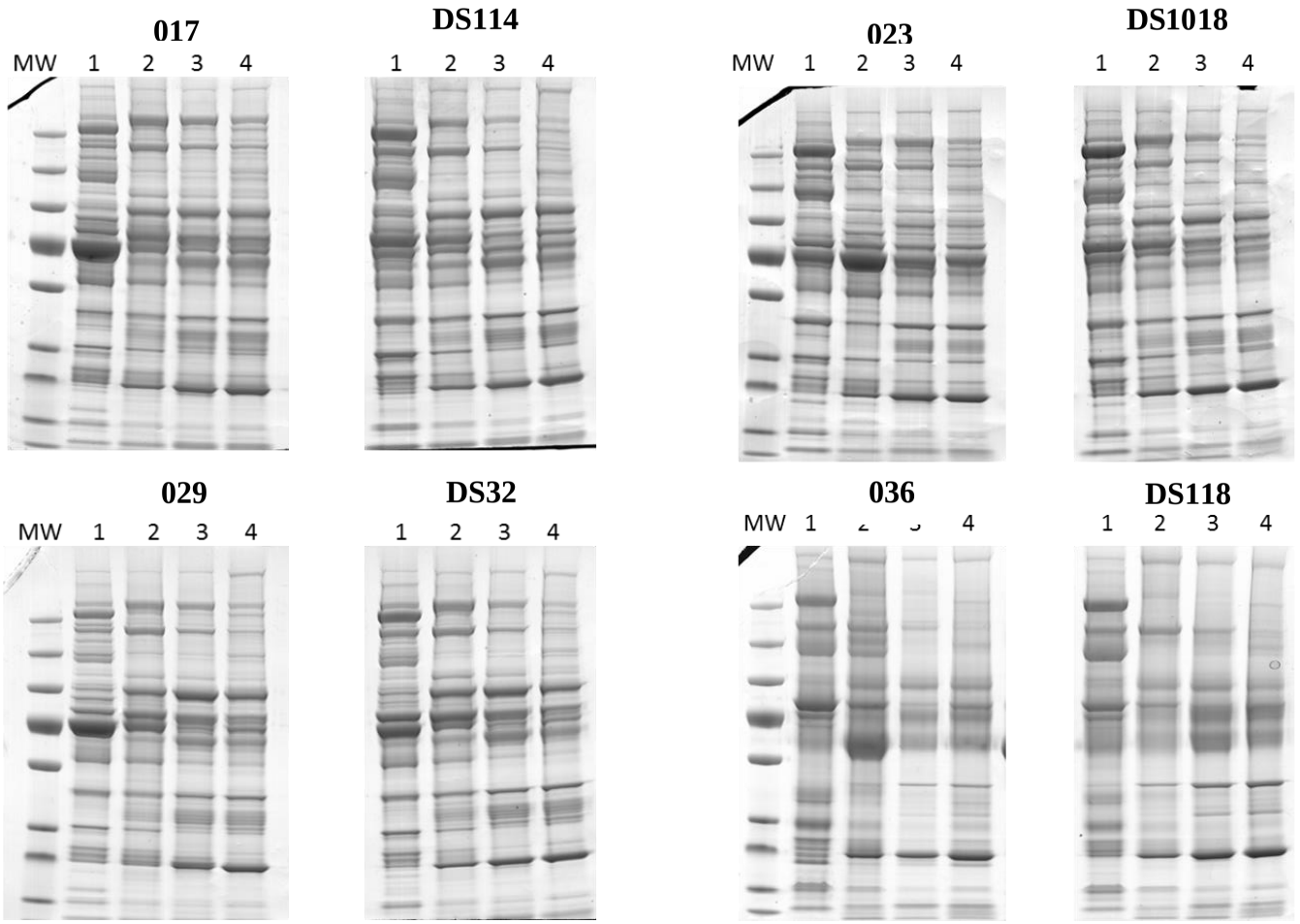

Figure 5.1 1-D gels illustrating the protein profile differences between elution fractions 1-4 of melanoma and control serum samples which were matched by sex. Across the four elution fractions for each melanoma serum sample; 017, 023, 029 and 036, and for each control serum; DS114, DS1018, DS32 and DS118, fraction 3 appeared to be very similar visually in its 1-D protein profile to that of fraction 4.

5.4 Quantitative Label-Free Proteomics Analysis of Fractionated Cutaneous Melanoma Serum

Elution fractions one, two and four of all eight control and eight melanoma sera were processed using C18 reverse-phase resin in order to remove interfering contaminants which could cause a strong signal suppression. C18 technology should reduce these effects, thus improving signal-to-noise ratios and sequence coverage.

Each fraction was analysed by reverse-phase LC-MS/MS and the acquired data were statistically analysed using Progenesis LC-MS software to generate quantitative information on differential protein expression patterns between cutaneous melanoma and control sera. MS/MS spectra with ANOVA values of ≤0.1, and with charge states from +1 to +3 were exported to MASCOT, and subsequent identifications were selected based on a protein ANOVA score of ≤0.05 between experimental groups. From this it was found that 29, 39, and 54 proteins in fractions one, two and four, respectively, were differentially regulated between the control and advanced melanoma groups. Protein identifications for each fraction are outlined in Tables 5.3, 5.4 and 5.5.

However, the protein list generated for elution fraction four illustrated a pattern of downregulation in the cutaneous melanoma proteome in comparison to the control proteome for all but three proteins. This pattern of differential regulation seemed unlikely as some of the proteins identified in elution four showed an opposite trend of expression in comparison to previous elution fractions. For example, Vitamin D-binding protein was upregulated in the cutaneous melanoma proteome by 2.08- and 2.44-fold in elution fractions one and two, respectively, although in elution fraction four it was identified at a level of 2.51-fold higher in the control proteome in comparison to that of the melanoma samples. This unusual trend may have been due to the fourth elution reagent simply stripping all remaining proteins from the ProteoMiner column as it is a stringent organic buffer. It was decided that this may provide a disproportionate view of the proteome and could skew the overall results; hence, elution fraction four was excluded from the analysis.

	Elution 1							
	Description	Accession No.	Peptides	Score	Anova (p)	Fold	Average Normalised Abundances	
							Control	Melanoma
Down in Melanoma	Thrombospondin-1	P07996	3	147.24	2.12E-03	2.37	9.65E+04	4.07E+04
	Complement C4-A	P0C0L4	2	125.28	0.02	1.51	6.66E+04	4.42E+04
	Apolipoprotein A-IV	P06727	1	65.07	0.04	1.93	9.81E+04	5.09E+04
	Keratin, type I cytoskeletal 10	P13645	1	60.79	0.04	Infinity	2019.13	0
	Protein AMBP	P02760	1	58.23	0.04	1.38	6.47E+04	4.68E+04
	Beta-2-glycoprotein 1	P02749	1	55.1	0.04	1.38	6533.24	4721.19
	Antithrombin-III	P01008	1	46.72	4.22E-03	29.42	1745.37	59.32
	Apolipoprotein B-100	P04114	1	44.29	3.17E-03	2.02	8271.17	4101.83
	Hyaluronan-binding protein 2	Q14520	1	43.6	3.02E-03	2.16	1.71E+04	7932.31
	Inter-alpha-trypsin inhibitor heavy chain H4	Q14624	1	41.86	4.06E-03	2.32	1.28E+04	5521.84
	Extracellular matrix protein 1	Q16610	1	34.42	0.01	2.26	4961.23	2193.66
	Complement component C8 beta chain	P07358	1	34.31	0.05	1.55	3497.52	2256.87
	Coagulation factor V	P12259	1	33.42	0.03	1.61	1.41E+04	8795.03
	Sulfhydryl oxidase 1	O00391	1	33.36	0.05	Infinity	532.66	0
Up in Melanoma	Myeloperoxidase	P05164	3	168.27	0.02	5.97	5634.34	3.36E+04
	Plasma protease C1 inhibitor	P05155	2	105.83	3.68E-03	1.52	8.59E+04	1.30E+05
	Lactotransferrin	P02788	2	98.92	2.53E-03	5.07	3633.94	1.84E+04
	Lipopolysaccharide-binding protein	P18428	1	91.61	0.05	2.4	2.36E+04	5.66E+04
	Platelet glycoprotein Ib alpha chain	P07359	1	66.25	1.21E-03	2.66	9917.85	2.64E+04
	Coagulation factor XII	P00748	1	64.98	0.03	1.94	6046.51	1.17E+04
	Complement component C6	P13671	1	53.3	0.02	1.42	1.54E+04	2.20E+04
	Vitamin D-binding protein	P02774	1	44.88	0.03	2.08	2.56E+04	5.33E+04
	Complement C3	P01024	1	42.76	8.81E-03	1.68	7767.28	1.30E+04
	Azurocidin	P20160	1	40.69	0.04	4.57	1291.32	5902.2
	Complement C5	P01031	1	40.35	0.05	2.06	1.84E+04	3.80E+04
	Serum albumin	P02768	1	36.12	0.02	2.39	8223.43	1.97E+04
	Inter-alpha-trypsin inhibitor heavy chain H1	P19827	1	34.16	0.02	8.98	339.16	3045.13
	Protein MB21D2	Q8IYB1	1	32.76	0.03	3.1	4729.07	1.46E+04
	Apolipoprotein L1	O14791	1	32.63	0.03	2.39	2690.63	6434.43

Table 5.3 Elution fraction one contained 29 statistically-significant proteins which were identified as being differentially regulated between control (n=8) and advanced cutaneous melanoma (n=8) sample groups. All differentially expressed proteins have a p-value of ≤0.05 between experimental groups.

	Elution 2							
	Description	Accession No.	Peptides	Score	Anova (p)	Fold	Average Normalised Abundances	
							Control	Melanoma
Down in Melanoma	Plasma serine protease inhibitor	P05154	3	143.31	5.11E-03	2.6	1.83E+05	7.04E+04
	Vitamin K-dependent protein S	P07225	2	105.66	0.01	1.68	2.82E+05	1.68E+05
	Plasminogen	P00747	2	92.16	6.80E-03	1.89	4.10E+05	2.17E+05
	Inter-alpha-trypsin inhibitor heavy chain H4	Q14624	2	84.66	1.70E-04	2.57	2.37E+05	9.22E+04
	Complement factor H-related protein 5	Q9BXR6	1	66.87	8.29E-03	2.59	1.83E+05	7.04E+04
	Keratin, type I cytoskeletal 9	P35527	1	55.49	0.04	2.64	8.99E+04	3.40E+04
	Peroxiredoxin-2	P32119	1	53.91	0.04	3.39	1.55E+04	4568.24
	Insulin-like growth factor-binding protein 3	P17936	1	48.29	2.34E-03	1.79	2.05E+04	1.14E+04
	Phosphatidylinositol-glycan-specific phospholipase D	P80108	1	46.96	0.03	1.93	6503.17	3370.57
	Angiogenin	P03950	1	44.81	0.03	2.06	1.48E+04	7160.48
	Selenoprotein P	P49908	1	43.94	0.04	2.44	5.92E+04	2.43E+04
	Serum amyloid A-4 protein	P35542	1	41.18	1.94E-03	2.31	4685.47	2024.45
	Hyaluronan-binding protein 2	Q14520	1	40.3	0.03	1.87	3.34E+04	1.79E+04
	Ficolin-2	Q15485	1	37.94	0.02	1.78	4.96E+04	2.79E+04
	Apolipoprotein A-I	P02647	1	37.5	0.04	1.74	6747.02	3875.44
	Fibronectin	P02751	1	36.25	0.03	2.16	1.00E+05	4.62E+04
	Cadherin-1	P12830	1	34.92	7.21E-03	1.67	1.80E+04	1.08E+04
	Histidine-rich glycoprotein	P04196	1	32.84	1.53E-03	2.67	1.84E+05	6.90E+04
	Mannan-binding lectin serine protease 2	O00187	1	31.65	0.05	2.15	3703.9	1722.42
	Clusterin	P10909	1	30.33	0.03	1.88	3.26E+05	1.73E+05
Up in Melanoma	Alpha-1-antitrypsin	P01009	6	291.34	6.62E-03	2.53	5.52E+05	1.40E+06
	Serum albumin	P02768	3	211.65	0.01	5.48	1.07E+05	5.88E+05
	Serotransferrin	P02787	3	154.88	9.22E-03	6.01	2.65E+05	1.59E+06
	Lactotransferrin	P02788	3	119.14	4.40E-03	3.3	3.70E+04	1.22E+05
	Vitamin D-binding protein	P02774	3	114.97	2.26E-03	2.44	8.77E+04	2.14E+05
	Alpha-1-antichymotrypsin	P01011	2	111	2.29E-03	4.65	5.85E+04	2.72E+05
	Complement C5	P01031	3	109.48	6.32E-03	2.01	5.79E+04	1.16E+05
	Plasma protease C1 inhibitor	P05155	2	93.84	0.01	1.75	2.02E+05	3.53E+05
	Alpha-2-macroglobulin	P01023	2	91.14	0.02	4.1	1.86E+05	7.64E+05
	Alpha-1B-glycoprotein	P04217	2	88.89	0.02	2.52	3.66E+04	9.22E+04

Up in Melanoma	Haptoglobin	P00738	2	81.41	0.04	2.65	2.33E+05	6.18E+05
	Ig gamma-3 chain C region	P01860	2	78.95	0.02	2.91	4.81E+04	1.40E+05
	Ig lambda chain V-I region HA	P01700	1	46.49	0.05	2.16	9.72E+04	2.10E+05
	C4b-binding protein alpha chain	P04003	1	37.65	0.04	1.77	1.35E+05	7.63E+04
	Alpha-1-acid glycoprotein 1	P02763	1	35.56	0.03	5	1.43E+04	7.13E+04
	Complement C3	P01024	1	34.19	0.04	3.86	8716.87	3.37E+04
	Eukaryotic translation initiation factor 4E type 3	Q8N5X7	1	31.73	3.07E-03	3.55	1.24E+05	4.39E+05
	Uncharacterized protein FLJ44066	Q6ZU11	1	30.48	9.75E-03	4.28	1.67E+05	7.14E+05
	Azurocidin	P20160	1	30.4	0.03	14.19	652.76	9261.02

Table 5.4 Elution fraction two contained 39 proteins which were identified as being differentially regulated between control (n=8) and advanced cutaneous melanoma (n=8) sample groups. All differentially expressed proteins have a p-value of ≤0.05 between experimental groups.

Elution 4

	Description	Accession No.	Peptides	Score	Anova (p)	Fold	Average Normalised Abundances	
							Control	Melanoma
Down in Melanoma	Complement component C9	P02748	4	263.09	8.11E-04	2.11	9.26E+05	4.38E+05
	Complement C1r subcomponent	P00736	6	260.88	1.82E-03	3.22	4.66E+05	1.45E+05
	Fibronectin	P02751	6	258.5	5.75E-04	1.97	2.25E+05	1.14E+05
	Complement C3	P01024	4	227.6	8.74E-04	1.63	8.72E+06	5.35E+06
	Vitamin K-dependent protein S	P07225	4	224.47	8.65E-04	1.56	4.22E+05	2.71E+05
	Coagulation factor V	P12259	3	207.08	1.11E-04	2.11	2.09E+05	9.90E+04
	Serum albumin	P02768	4	205.08	5.52E-03	2.33	6.97E+05	2.99E+05
	Complement factor H	P08603	3	195.45	2.93E-03	2.43	6.39E+05	2.63E+05
	Complement C4-A	P0C0L4	4	181.56	0.04	1.84	3.36E+06	1.83E+06
	Myeloperoxidase	P05164	3	176	9.74E-03	7.43	3.08E+04	4137.5
	C4b-binding protein alpha chain	P04003	4	168.26	9.96E-04	2.09	7.13E+05	3.40E+05
	Plasma protease C1 inhibitor	P05155	4	167.68	4.11E-03	2.24	7.61E+05	3.39E+05
	Lactotransferrin	P02788	2	162.79	9.91E-04	11.59	3.26E+04	2814.83
	Complement component C6	P13671	3	155.54	1.01E-03	2.42	2.16E+05	8.91E+04
	Fibrinogen alpha chain	P02671	2	148.25	7.09E-03	3.28	5.93E+04	1.81E+04
	von Willebrand factor	P04275	2	144.8	8.54E-03	2.57	8.18E+04	3.19E+04
	Complement factor H-related protein 1	Q03591	2	137.91	5.66E-03	2.29	1.05E+05	4.59E+04
	Complement component C8 beta chain	P07358	3	133.61	2.64E-03	2.23	1.05E+05	4.68E+04
	Complement component C8 alpha chain	P07357	2	110.23	6.16E-03	1.56	1.39E+05	8.89E+04
	Vitamin D-binding protein	P02774	2	100.48	3.26E-03	2.51	8.95E+04	3.57E+04
	Prothrombin	P00734	2	100.27	0.01	2.39	1.17E+05	4.90E+04
	Galectin-3-binding protein	Q08380	2	97.45	9.07E-03	1.97	1.04E+05	5.30E+04
	Complement C1s subcomponent	P09871	2	87.8	6.89E-04	1.88	2.67E+05	1.42E+05
	Alpha-1-antitrypsin	P01009	2	86.91	0.01	2.29	1.61E+05	7.07E+04
	Alpha-1-antichymotrypsin	P01011	2	83.66	9.87E-03	2.33	1.50E+04	6440.54
	Apolipoprotein M	O95445	2	80.75	2.91E-03	1.71	1.58E+05	9.24E+04
	Plasma kallikrein	P03952	1	78.27	6.15E-03	2.46	3.84E+04	1.56E+04
	Apolipoprotein A-I	P02647	2	76.39	1.26E-03	3.04	2.60E+05	8.54E+04
	Alpha-1B-glycoprotein	P04217	1	74.63	0.02	1.62	1.91E+04	1.18E+04
	Ig heavy chain V-II region NEWM	P01825	1	72.77	0.02	2.81	8.85E+04	3.15E+04
	Ig gamma-1 chain C region	P01857	1	70.01	0.02	2.19	4.80E+04	2.19E+04
	Complement component C7	P10643	2	68.97	1.09E-03	2.79	1.78E+05	6.37E+04
	Alpha-1-acid glycoprotein 1	P02763	1	60.24	0.03	1.12	1.69E+04	1.51E+04
	Kininogen-1	P01042	1	59.81	2.43E-03	2.05	1.69E+05	8.26E+04
	Protein Z-dependent protease inhibitor	Q9UK55	1	47.98	0.02	1.91	4.01E+04	2.10E+04
	Complement factor B	P00751	1	46.39	0.03	2.01	2.21E+04	1.10E+04
	Heparin cofactor 2	P05546	1	45.1	0.03	1.42	1.34E+05	9.43E+04
	Ig kappa chain V-IV region Len	P01625	1	42.94	0.05	2.15	2.21E+04	1.03E+04
	Complement C1q subcomponent subunit C	P02747	1	42.48	0.03	3.79	7731.55	2041.47
	Complement C5	P01031	1	41.95	0.04	1.86	4.59E+04	2.47E+04
	Titin	Q8WZ42	1	41.51	0.04	4.06	3.43E+04	8434.11

Down in Melanoma	Apolipoprotein L1	O14791	1	40.09	2.93E-03	1.73	2.86E+05	1.65E+05
	Afamin	P43652	1	38.59	0.03	3.17	3848.87	1214.56
	Keratin, type II cytoskeletal 2 epidermal	P35908	1	37.98	0.03	3.01	4.04E+04	1.34E+04
	Serum amyloid A-4 protein	P35542	1	37.82	6.08E-04	5.07	2.30E+04	4526.58
	Antithrombin-III	P01008	1	34.55	0.03	1.74	2.74E+06	1.58E+06
	Inter-alpha-trypsin inhibitor heavy chain H3	Q06033	1	33.48	5.71E-03	2.24	1.33E+05	5.95E+04
	Beta-2-glycoprotein 1	P02749	1	33.46	0.02	3.34	2.32E+04	6941.42
	Phospholipid transfer protein	P55058	1	32.17	2.85E-03	2.08	3.22E+04	1.55E+04
	Phenylalanine--tRNA ligase beta subunit	Q9NSD9	1	31.51	0.02	1.71	1.11E+06	6.53E+05
	Krueppel-like factor 17	Q5JT82	1	30.13	1.51E-03	2.42	8.82E+05	3.65E+05
Up in Melanoma	Vitamin K-dependent protein C	P04070	1	71.48	0.05	1.82	3.05E+04	5.55E+04
	Plasma serine protease inhibitor	P05154	1	48.82	0.02	2.84	1720.3	4885.14
	Ig lambda-2 chain C regions	P0CG05	1	47.97	8.24E-03	523.34	14.44	7554.93

Table 5.5 Elution fraction four contained 54proteins which were identified as being differentially regulated between control (n=8) and advanced cutaneous melanoma (n=8) sample groups. However, the majority of the proteins found were downregulated in the cutaneous melanoma group. All differentially expressed proteins have a p-value of ≤0.05 between experimental groups.

5.5 Analysis of Differential Regulation of Proteins in Recombined Fractions One and Two

Initially, 16 biological samples were fractionated in order to increase protein coverage and to have the best overall view of the proteome. However, in order to investigate how the proteins behave across the whole experiment, fractions of the same sample may be recombined. Progenesis LC-MS software normalises between elution fractions of the same sample and combines protein measurements to provide statistical analyses of the experiment as a whole.

Elution fractions one and two of the same sample were recombined and analysed together to identify differential regulation patterns between eight control sera and eight advanced cutaneous melanoma sera. This resulted in the identification of 57 differentially expressed proteins, of which nine proteins were found in both elution fractions one and two (Table 5.6).

5.6 Comparison of 1-D and Quantitative Label-Free LC-MS Protein Profiles for the Selection of Targets for Validation

The qualitative protein profiles were generated from digesting each band of the gels shown in Figure 5.1 (a) and (d) with trypsin and analysing the peptides over the course of an hour gradient.

Shown in Table 5.7 are qualitative statistically identified proteins which were found in both control samples, DS 118 and DS 114, and both disease samples, 036 and 017. Each identification shown in Table 5.7 was found only in one group, i.e. control or disease. The full list of identifications for elution one and two of 017, 036, DS114, and DS118 can be found in Appendix B.

The proteins listed in Table 5.7 were then compared with the label-free protein list created from recombined fractions one and two (Table 5.6). From this, 10 potential targets of interest were identified (Table 5.8).

Elution 1 & 2								
Accession No.	Peptides	Score	Anova (p)	Fold	Description	Elution	Average Normalised Abundances	
							Control	Melanoma
P02788	2	98.92	2.53E-03	5.07	Lactotransferrin	1	3633.94	**1.84E+04**
P02788	3	119.14	4.40E-03	3.3	Lactotransferrin	2	3.70E+04	**1.22E+05**
P20160	1	40.69	0.04	4.57	Azurocidin	1	1291.32	**5902.2**
P20160	1	30.4	0.03	14.19	Azurocidin	2	652.76	**9261.02**
P02768	1	36.12	0.02	2.39	Serum albumin	1	8223.43	**1.97E+04**
P02768	3	211.65	0.01	5.48	Serum albumin	2	1.07E+05	**5.88E+05**
Q14624	1	41.86	4.06E-03	2.32	Inter-alpha-trypsin inhibitor heavy chain H4	1	**1.28E+04**	5521.84
Q14624	2	84.66	1.70E-04	2.57	Inter-alpha-trypsin inhibitor heavy chain H4	2	**2.37E+05**	9.22E+04
Q14520	1	43.6	3.02E-03	2.16	Hyaluronan-binding protein 2	1	**1.71E+04**	7932.31
Q14520	1	40.3	0.03	1.87	Hyaluronan-binding protein 2	2	**3.34E+04**	1.79E+04
P02774	1	44.88	0.03	2.08	Vitamin D-binding protein	1	2.56E+04	**5.33E+04**
P02774	3	114.97	2.26E-03	2.44	Vitamin D-binding protein	2	8.77E+04	**2.14E+05**
P01031	1	40.35	0.05	2.06	Complement C5	1	1.84E+04	**3.80E+04**
P01031	3	109.48	6.32E-03	2.01	Complement C5	2	5.79E+04	**1.16E+05**
P01024	1	42.76	8.81E-03	1.68	Complement C3	1	7767.28	**1.30E+04**
P01024	1	34.19	0.04	3.86	Complement C3	2	8716.87	**3.37E+04**
P05155	2	105.83	3.68E-03	1.52	Plasma protease C1 inhibitor	1	8.59E+04	**1.30E+05**
P05155	2	93.84	0.01	1.75	Plasma protease C1 inhibitor	2	2.02E+05	**3.53E+05**

Table 5.6 Nine differentially expressed proteins were identified in both elutions one and two following recombination analysis of fractions one and two for each sample. *p*-value=≤0.05.

Elution 1										
036 - 66 proteins	**Score (XC)**	**Coverage**	**MW (Da)**	**Accession**	**No. Peptide**	**017 - 62 Proteins**	**Score (XC)**	**Coverage**	**MW (Da)**	**Accession**	**No. Peptide**
Lactotransferrin	140.31	26.90	78132.0	P02788	14	Lactotransferrin	30.23	4.60	78132.0	P02788	3
Haptoglobin-related protein	40.21	13.20	39004.7	P00739	4	Haptoglobin-related protein	66.26	15.20	39004.7	P00739	7
Haptoglobin	28.19	5.70	45176.6	P00738	3	Haptoglobin	70.30	22.20	45176.6	P00738	7
Complement C5	120.29	12.20	188185.3	P01031	12	Complement C5	40.26	5.10	188185.3	P01031	4
Lipopolysaccharide-binding protein	80.30	21.20	53350.0	P18428	8	Lipopolysaccharide-binding protein	20.30	7.70	53350.0	P18428	2
DS118 - 77 proteins	**Score (XC)**	**Coverage**	**MW (Da)**	**Accession**	**No. Peptide**	**DS114 - 61 Proteins**	**Score (XC)**	**Coverage**	**MW (Da)**	**Accession**	**No. Peptide**
Apolipoprotein B-100	250.31	7.90	515283.6	P04114	25	Apolipoprotein B-100	210.33	6.50	515283.6	P04114	21
Apolipoprotein A-IV	80.24	19.70	45371.5	P06727	8	Apolipoprotein A-IV	70.19	19.20	45371.5	P06727	7
Keratin, type I cytoskeletal 10	50.24	11.50	58791.6	P13645	5	Keratin, type I cytoskeletal 10	70.29	17.60	58791.6	P13645	7
Procollagen C-endopeptidase enhancer 1	40.22	14.00	47942.0	Q15113	4	Procollagen C-endopeptidase enhancer 1	20.27	6.70	47942.0	Q15113	2
Apolipoprotein A-II	20.20	43.00	11167.9	P02652	2	Apolipoprotein A-II	20.20	29.00	11167.9	P02652	2
Gelsolin	110.30	20.80	85644.3	P06396	11	Gelsolin	120.33	22.60	85644.3	P06396	12
Vitronectin	80.24	18.20	54271.2	P04004	8	Vitronectin	60.26	16.10	54271.2	P04004	6
Lysozyme C	50.27	45.30	16526.3	P61626	5	Lysozyme C	30.25	28.40	16526.3	P61626	3

Elution 2										
036 - 73 proteins	**Score (XC)**	**Coverage**	**MW (Da)**	**Accession**	**No. Peptide**	**017 - 70 Proteins**	**Score (XC)**	**Coverage**	**MW (Da)**	**Accession**	**No. Peptide**
Complement C5	30.24	3.60	188185.3	P01031	3	Complement C5	30.17	2.10	188185.3	P01031	3
Serotransferrin	290.31	48.70	77013.7	P02787	29	Serotransferrin	280.32	41.70	77013.7	P02787	28
Alpha-1-acid glycoprotein 1	40.27	23.40	23496.8	P02763	4	Alpha-1-acid glycoprotein 1	40.24	22.90	23496.8	P02763	4
Alpha-1-antichymotrypsin	48.29	12.50	47620.6	P01011	5	Alpha-1-antichymotrypsin	58.25	17.50	47620.6	P01011	6
Haptoglobin	78.25	26.60	45176.6	P00738	8	Haptoglobin	60.24	16.70	45176.6	P00738	6
CD5 antigen-like	20.18	7.20	38063.0	O43866	2	CD5 antigen-like	20.21	9.80	38063.0	O43866	2
Complement component C7	20.17	2.60	93457.3	P10643	2	Complement component C7	20.21	3.70	93457.3	P10643	2
Alpha-1-antitrypsin	100.29	32.80	46707.1	P01009	10	Alpha-1-antitrypsin	170.30	56.70	46707.1	P01009	17
Alpha-2-macroglobulin	240.27	23.20	163187.4	P01023	24	Alpha-2-macroglobulin	220.29	23.30	163187.4	P01023	22
Ig gamma-2 chain C region	50.27	25.80	35877.8	P01859	5	Ig gamma-2 chain C region	50.26	26.40	35877.8	P01859	5
Serum albumin	500.38	76.20	69321.6	P02768	50	Serum albumin	470.37	70.30	69321.6	P02768	47
DS118 - 77 proteins	**Score (XC)**	**Coverage**	**MW (Da)**	**Accession**	**No. Peptide**	**DS114 - 50 Proteins**	**Score (XC)**	**Coverage**	**MW (Da)**	**Accession**	**No. Peptide**
Ficolin-3	50.22	14.70	32882.0	O75636	5	Ficolin-3	40.24	14.00	32882.0	O75636	4
Adiponectin	40.25	29.90	26397.0	Q15848	4	Adiponectin	40.25	31.60	26397.0	Q15848	4
Apolipoprotein E	120.25	42.90	36131.8	P02649	12	Apolipoprotein E	90.26	30.90	36131.8	P02649	9

Table 5.7 Qualitative results of proteins identified in 1-D gels illustrated in Figure 5.1 (a) and (b). Only proteins which were found in both controls, DS118 and DS114, and both disease sera, 036 and 017, are shown. These identifications were then compared with the results from the quantitative label-free LC-MS analysis for the selection of targets for further validation.

Accession No.	Peptides	Score	Anova (p)	Fold	Fractions	Description	Average Normalised Abundances	
							Control	Melanoma
P01031	16	741.94	3.40E-04	1.65	1,2	Complement C5	2.83E+05	4.67E+05
P01011	2	121.15	8.81E-04	3.61	1	Alpha-1-antichymotrypsin	1.29E+04	4.65E+04
P02788	**8**	**392.17**	**1.17E-03**	**4.17**	**1,2**	**Lactotransferrin**	**2.80E+04**	**1.17E+05**
P02763	1	56.33	1.45E-03	3.88	1	Alpha-1-acid glycoprotein 1	5089.57	1.97E+04
P04114	1	44.29	3.17E-03	2.02	2	Apolipoprotein B-100	9422.41	4672.76
P01009	2	95.03	3.76E-03	2.53	1	Alpha-1-antitrypsin	2.22E+04	5.62E+04
P02787	**3**	**134.35**	**6.73E-03**	**3.47**	**1**	**Serotransferrin**	**3.56E+04**	**1.24E+05**
P02768	5	223.53	0.01	3.73	1	Serum albumin	7.74E+04	2.89E+05
P01023	5	369.82	0.03	2.89	1,2	Alpha-2-macroglobulin	1.20E+05	3.47E+05
P06727	1	65.07	0.04	1.93	2	Apolipoprotein A-IV	1.12E+05	5.80E+04

Table 5.8 The protein list created by the quantitative analysis of recombined elution fractions one and two was overlapped with the qualitative results generated from the 1-D analysis. This identified a list of potential targets which could then be followed up by further validation using ELISA

5.7 Selection of Potential Targets for Further Validation

Following the fractionation and subsequent analysis of the differential regulation data acquired, it was decided to follow-up some of the notable targets using ELISA, as this is the method of clinical biomarker detection primarily used in hospitals.

From the quantitative LC-MS label-free analysis combining elution fractions one and two, azurocidin and lactotransferrin (Table 5.6) were selected for follow-up analysis as was serotransferrin, which was identified in both the quantitative label-free LC-MS data and the qualitative 1-D data (Table 5.8). As mentioned, all three targets were found to be upregulated in the advanced cutaneous melanoma serum in comparison to the control during the Progenesis analysis. Plasma serine protease inhibitor (Table 5.4) was also chosen as it was found to be significantly under-expressed in the disease sera in comparison to the controls. Analysis of all proteins of interest demonstrated *p*-values of <0.05 as well as strong Mascot scores and good peptide overlap between samples.

In addition to the above, three targets were chosen from a microarray study carried out by Dr. Paul Dowling and Dr. Steven Madden using Gene Expression Omnibus (GEO). Beta-secretase 2 (BACE-2), Matrix metalloprotease (MMP-1), and Tissue inhibitor of metalloproteinase 1 (TIMP-1) were identified by the analysis of two publically available array data sets for control tissue, and primary and metastasised cutaneous melanoma tumour tissue (Riker, Enkemann et al. 2008, Raskin, Fullen et al. 2013). All three proteins were significantly upregulated in the metastasised and primary tissues in comparison to the control. This data is shown in Table 5.9.

In addition to using benign, early-stage and advanced-stage cutaneous melanoma serum for the analysis of the seven proteins of interest, serum collected from uveal melanoma patients was also included to examine the expression patterns of the proteins of interest between patients with monosomy of chromosome three, which is a known chromosomal aberration correlated with a poor prognosis, and those patients with no evidence of monosomy three, i.e. disomy three. By including serum of ocular melanoma patients, this would also allow for the direct comparison of specific protein expression between uveal and cutaneous melanomas. An overview of the samples used in the ELISA validation of the seven targets is shown in Table 5.10. Cutaneous melanoma sera were collected and clinically characterised by Dr. Benvon Moran of St. James's Hospital.

	Metastasised vs. Control Tissue				Primary vs. Control Tissue			
	Gene Name	**Fold Change**	**Average Expression**	***p*-value**	**Gene Name**	**Fold Change**	**Average Expression**	***p*-value**
Array 1	BACE2	5.990609994	2156.972114	9.59E-05	BACE2	7.431086321	2156.972114	3.94E-08
	TIMP1	4.178272153	6337.021918	2.86E-05	MMP1	34.86258329	760.2056155	1.46E-06
					TIMP1	2.632767658	6337.021918	0.000207766
	Gene Name	**Fold Change**	**Average Expression**	***p*-value**	**Gene Name**	**Fold Change**	**Average Expression**	***p*-value**
Array 2	BACE2	9.736859403	864.550713	0.000992996	BACE2	9.898329678	864.550713	0.005691107
	TIMP1	7.494517947	3642.159455	7.34E-05	MMP1	128.5913889	526.8937612	0.005959777
					TIMP1	6.096281159	3642.159455	0.003123521

Table 5.9 Three proteins; Beta-secretase 2 (BACE-2), Matrix metalloprotease (MMP-1), and Tissue inhibitor of metalloproteinase 1 (TIMP-1) were identified by the analysis of two publically available array data sets for control tissue, and primary and metastasised cutaneous melanoma tumour tissue. All three proteins were significantly upregulated in the metastasised and primary tissues in comparison to controls. This work was carried out by Dr. Stephen Madden and Dr. Paul Dowling.

		Cutaneous Melanoma			Uveal Melanoma	
Sample Set	**Control**	**Benign**	**Early Stage***	**Advanced Stage#**	**Monosomy 3**	**No evidence of Monsomy 3**
Age Range	30 - 62	19 - 81	34 - 89	28 - 84	61 - 85	54 - 79
Total No. Samples	13	18	14	12	7	6
No. Male	6	6	11	8	3	4
No. Female	7	12	2	4	3	-

Table 5.10 Control, cutaneous melanoma and uveal melanoma sera were all used in the further analysis, by ELISA, of the seven proteins of interest; azurocidin, lactotransferrin, serotransferrin, MMP-1, TIMP-1 and BACE-2. A more comprehensive list of samples used is shown in Appendix C.

* The early stage consisted of the following sub-stages; twelve stage I and two stage II.

The advanced stage group consisted of the following sub-stages; four stage III and eight stage IV.

5.8 ELISA Analysis of Potential Biomarkers of Interest

ELISA results are presented in both bar chart and box-and-whisker formats. In addition to the standard bar graphs, box-and-whisker plots were included as they show a more accurate distribution of results. From the box-and-whisker plots the minimum, maximum, and median can be determined as well as the 25^{th} and 75^{th} percentile, giving a more accurate representation of where the overall results lie. Comparisons between experimental groups with T-test ≤ 0.05 are marked by a single asterisk (*) and ≤ 0.01 are marked by two asterisks (**).

5.8.1 Lactotransferrin

Lactotransferrin, a major iron-binding and multifunctional protein, was found to be 4.17-fold upregulated in advanced-stage cutaneous melanoma serum, see Figure 5.2 (a). As illustrated by Figure 5.2 (b), lactotransferrin was identified in both elution fractions one and two in the quantitative LC-MS analysis and showed high reproducibility between samples containing the same eight peptides against lactotransferrin.

According to the ELISA data acquired (Figure 5.3) lactotransferrin was significantly less abundant in benign or early-stage cutaneous melanoma serum when compared to control serum. There was no significant difference between the levels in control and advance-stage cutaneous melanoma serum, however an increase in lactotransferrin was observed in advanced-stage samples when compared to those which were benign.

The uveal melanoma sample set, which contained both monosomy of chromosome three sera and disomy of chromosome three sera, showed a significantly decreased level of lactotransferrin when compared with that of the control sample set, as illustrated in Figure 5.3. When the uveal melanoma serum specimens which were positive for monosomy of chromosome three were compared to those which did not have this anomaly, no significant difference was observed between the two (Figure 5.4).

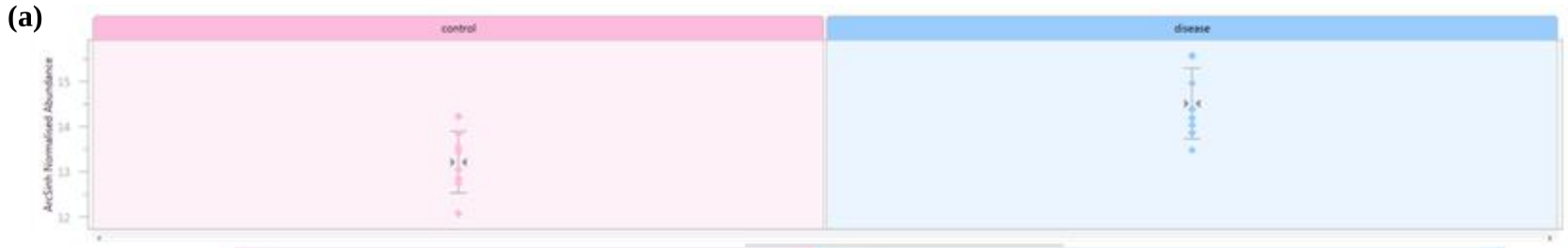

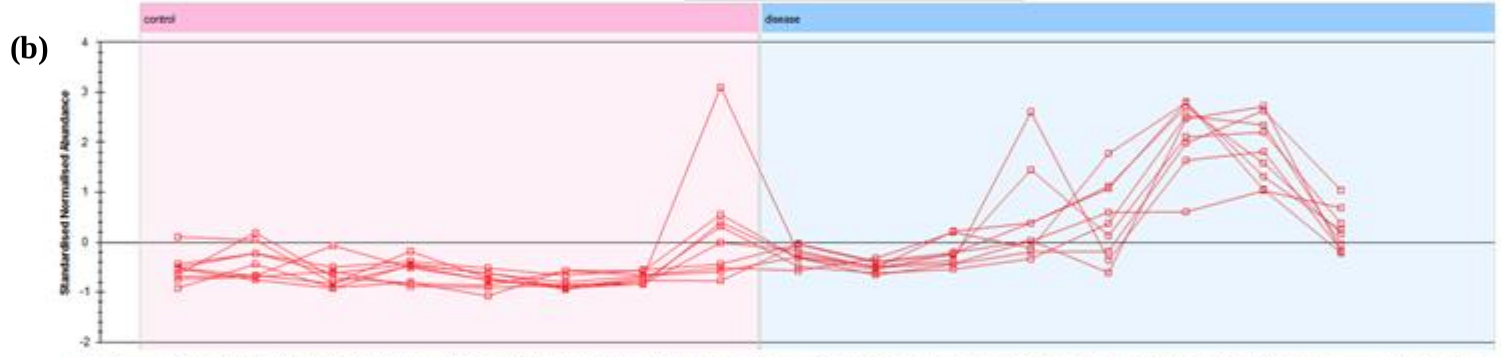

Σ	#	Score	Anova (p)	Max Fold Change	Highest Mean	Lowest Mean	Abundance	m/z	Charge	Retention Time	Fractions	Mass error (ppm)	Peptide Sequence	Modifications
•	3158	32.45	0.00714	5.03	disease	control	3.485E+05	496.243	2	116.129	1 2	0.88	GQFPNLCR	
•	3184	76.42	0.0419	5.9	disease	control	3.627E+05	510.7592	2	151.306	1 2	0.30	DGAGDVAFIR	
•	3597	31.54	0.0735	2.43	disease	control	1.193E+05	462.7111	2	99.834	1 2	0.59	CFQWQR	
•	7352	43.46	0.0293	3.06	disease	control	1.178E+05	695.8703	2	216.688	1 2	0.59	GGSFQLNELQGLK	
•	7462	33.72	0.000146	5.27	disease	control	1.035E+05	429.2311	2	52.889	1 2	-0.13	GPPVSCIK	
•	9792	64.97	0.0319	1.63	disease	control	5.453E+04	468.2746	2	33.269	1 2	-0.23	VPSHAVVAR	
•	7984	36.11	0.00558	3.16	disease	control	1.83E+05	790.3802	2	125.145	1 2	-0.16	NLLFNDNTECLAR	
•	51441	33.31	0.000182	5.68	disease	control	1.583E+04	550.6043	3	52.412	1 2	-1.01	SCHLAMAPNHAVVSR	
•	120588	49.72	0.0286	4.93	disease	control	3767	468.2745	2	29.456	1 2	-0.46	VPSHAVVAR	

Figure 5.2 Quantitative label-free LC-MS data for lactotransferrin. Overall, lactotransferrin was identified in the recombined elution fraction analysis as being over-expressed by 4.17-fold in advanced cutaneous melanoma serum (n=8) in comparison to control serum (n=8), recombined *p*-value=1.17×10^{-3} (a) Standard expression individual protein profile for all 16 samples (b) The peptide measurement view with an accompanying table illustrates unique peptides for lactotransferrin in each sample.

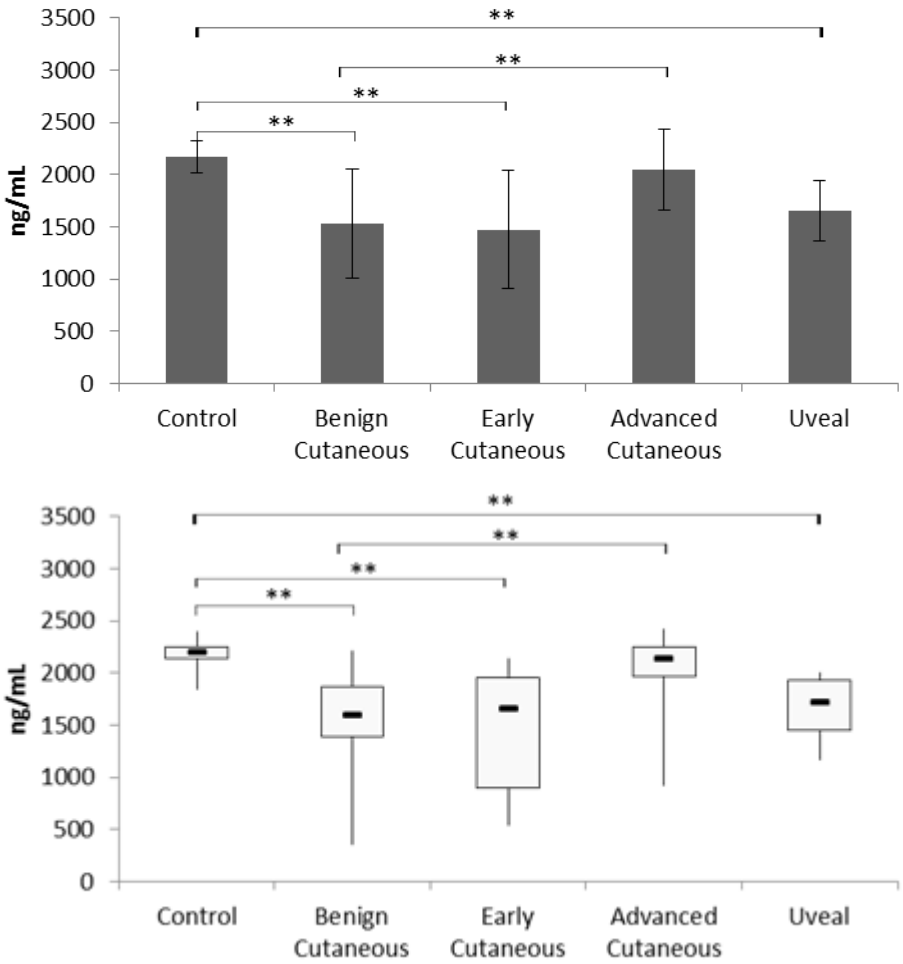

Figure 5.3 Lactotransferrin ELISA data represented by both bar chart and Box and Whisker Plot. Serum samples from a variety of melanoma conditions were used; benign cutaneous melanoma (n=18), early-stage cutaneous disease (n=14), advanced-stage cutaneous disease (n=12), and uveal melanoma (n=13), as well as control serum (n=13). t-test scores: control vs. benign cutaneous = 6.48×10^{-5}; control vs. early cutaneous = 3.93×10^{-4}; control vs. uveal = 3.46×10^{-6}; benign cutaneous vs. advanced cutaneous = 1.78×10^{-4}; * t-test score between experimental groups of ≤0.05, ** t-test score between experimental groups of ≤0.01.

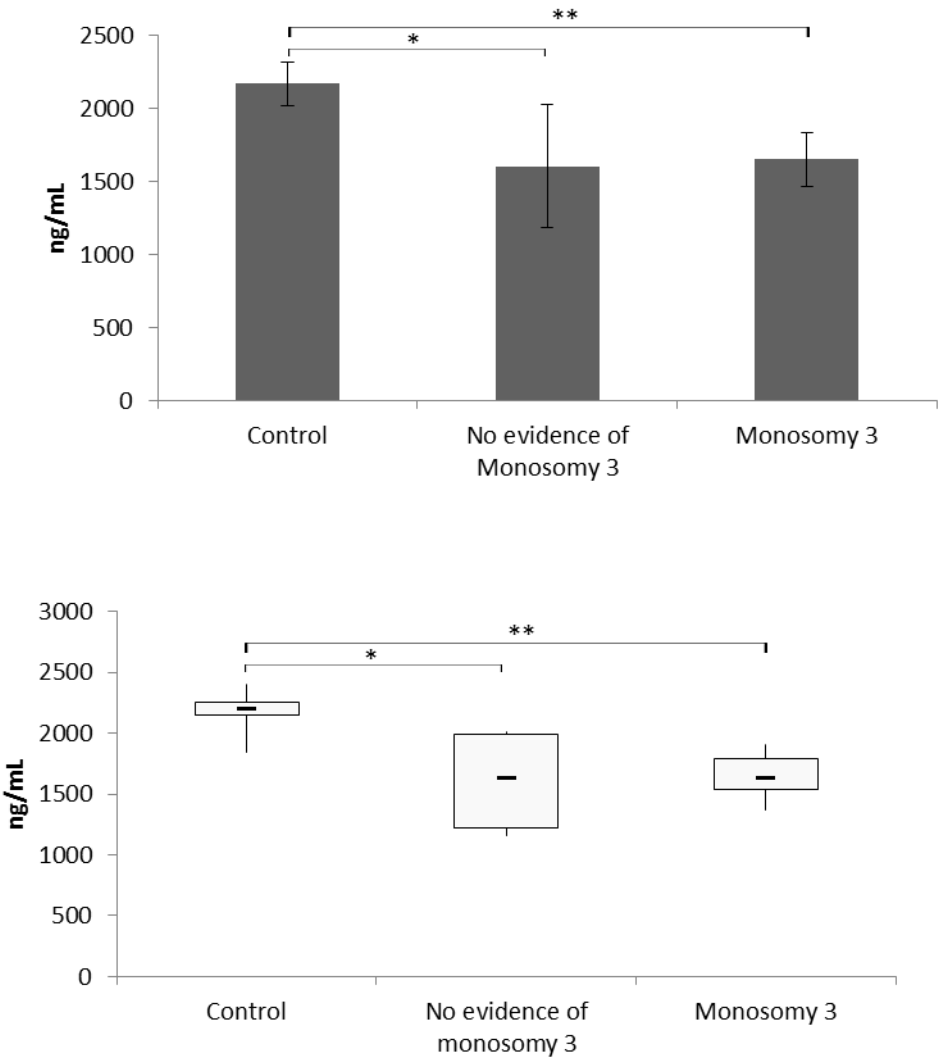

Figure 5.4 Lactotransferrin ELISA data represented by both bar chart and Box and Whisker Plot. Serum samples from two uveal melanoma conditions were used; monosomy of chromosome three (n=7) and no evidence of monosomy of chromosome three (n=6). t-test scores: control vs. no evidence of monosomy three = $1.83x10^{-2}$; control vs. monosomy three = $5.53x10^{-5}$. * t-test score between experimental groups of ≤0.05, ** t-test score between experimental groups of ≤0.01.

5.8.2 Serotransferrin

Serotransferrin was initially found to be over-expressed by 3.47-fold in advanced-stage melanoma sera when compared to healthy sera using quantitative label-free proteomics analysis, Figure 5.5 (a). Three peptides with a *p*-value of ≤0.05 which matched the serotransferrin sequence were identified in elution fraction two only, as shown in Figure 5.5 (b).

However, the ELISA results directly contradicted this quantitative LC-MS data with a statistically significant trend of decreased serotransferrin levels observed in either early or advanced-stage cutaneous disease when compared to the control serum (Figure 5.6). Overall, a trend of decreased serotransferrin abundance was observed across all melanoma samples; benign, early-stage, advanced-stage, in relation to control serum.

A statistically significant decrease in serotransferrin abundance was observed in uveal melanoma serum when compared to control serum, (Figure 5.6), as is the case in monosomy three serum compared to control serum. No statistically significant difference in abundance was observed between monosomy three and disomy three uveal melanoma specimens, when they were compared with one another (Figure 5.7).

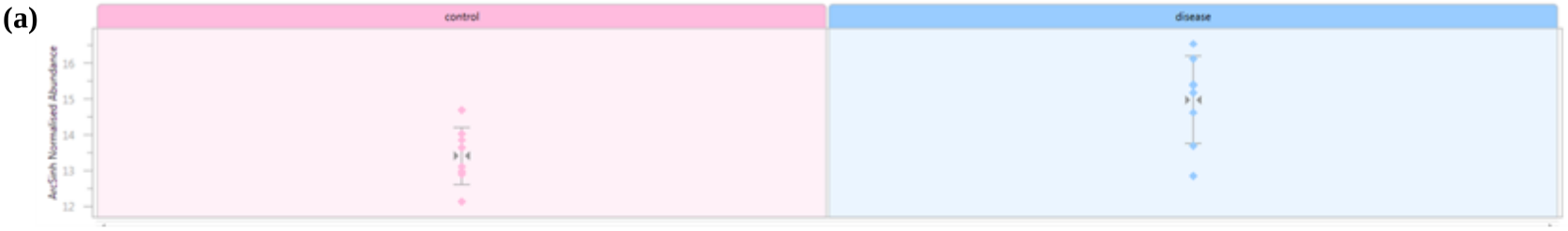

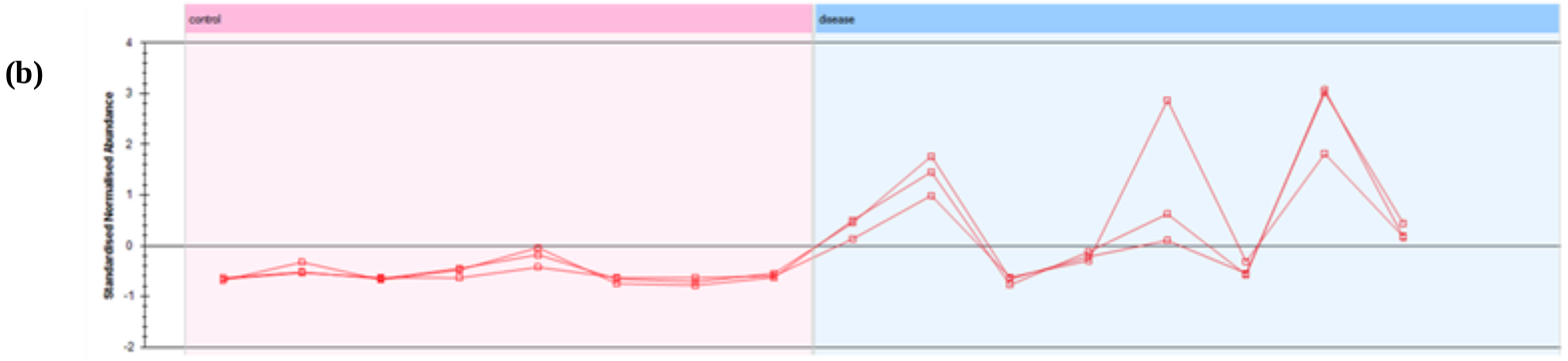

Σ	#	Score	Anova (p)	Max Fold Change	Highest Mean	Lowest Mean	Abundance	m/z	Charge	Retention Time	Fractions	Mass error (ppm)	Peptide Sequence	Modifications
•	1112	71.65	0.00882	6.21	disease	control	2.341E+06	625.3064	2	111.062	1 2	-0.26	SASDLTWDNLK	
•	3787	39.02	0.0226	4.26	disease	control	2.563E+05	414.2063	2	56.971	1 2	0.87	NPDPWAK	
•	16453	44.21	0.00872	18.9	disease	control	4.127E+04	606.2772	2	63.788	1 2	-0.13	DSGFQMNQLR	[6] Oxidation (M)

Figure 5.5 Quantitative label-free LC-MS data for serotransferrin. Overall, serotransferrin was identified in the recombined elution fraction analysis as being over-expressed by 3.47-fold in advanced cutaneous melanoma serum (n=8) in comparison to control serum (n=8), *p*-value=9.22×10^{-3} (a) Standard expression individual protein profile for all 16 samples (b) The peptide measurement view with an accompanying table illustrates unique peptides for serotransferrin in each sample.

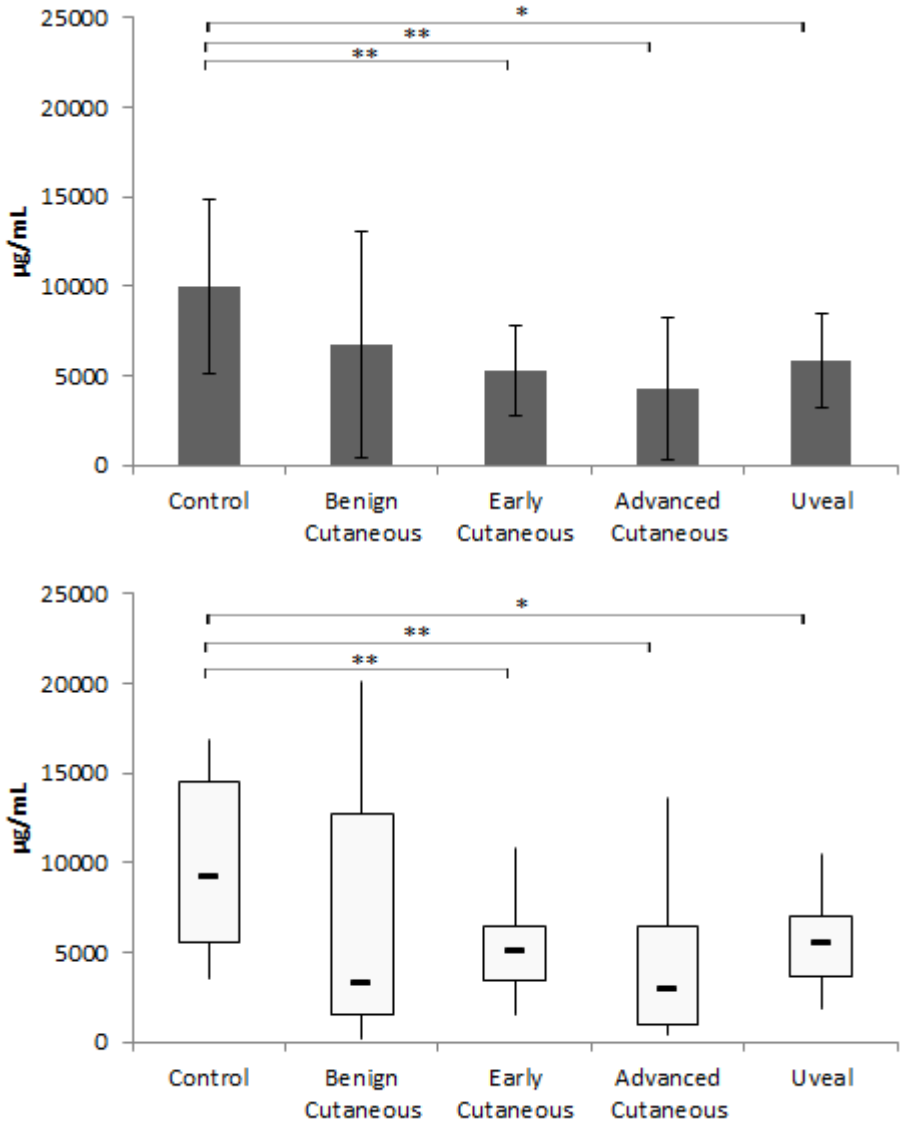

Figure 5.6 Serotransferrin ELISA data represented by both bar chart and Box and Whisker Plot. Serum samples from a variety of melanoma conditions were used; benign cutaneous melanoma (n=18), early-stage cutaneous disease (n=14), advanced-stage cutaneous disease (n=12), and uveal melanoma (n=13), as well as control serum (n=13). t-test scores: control vs. early cutaneous = 6.48×10^{-3}; control vs. advanced cutaneous = 4.16×10^{-3}; control vs. uveal = 1.59×10^{-2} * t-test score between experimental groups of ≤0.05; ** t-test score between experimental groups of ≤0.01.

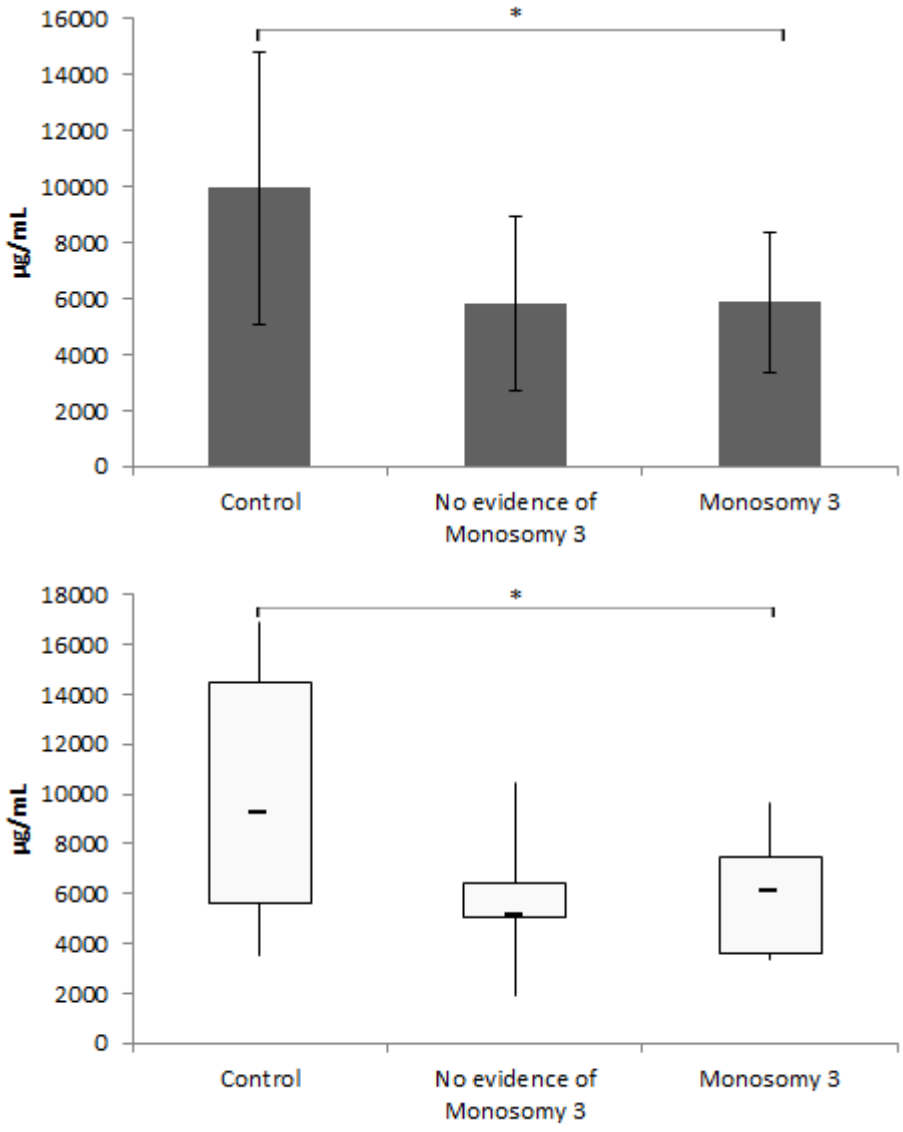

Figure 5.7 Serotransferrin ELISA data represented by both bar chart and Box and Whisker Plot. Serum samples from two uveal melanoma conditions were used; monosomy of chromosome three (n=7) and no evidence of monosomy of chromosome three (n=6). * t-test score between experimental groups of ≤0.05.

5.8.3 Azurocidin

As illustrated in Figure 5.8 (a), azurocidin was over-expressed in late-stage cutaneous melanoma serum specimens according to quantitative label-free LC-MS analysis. One peptide for the protein was found in elution fraction one and in elution fraction two, over-expressed at a maximum observed fold change of 14.2, Figure 5.8 (b).

Although a slight increase in azurocidin abundance was observed in advanced cutaneous melanoma sera in comparison to healthy sera, no statistically significant relationship was identified.

(a)

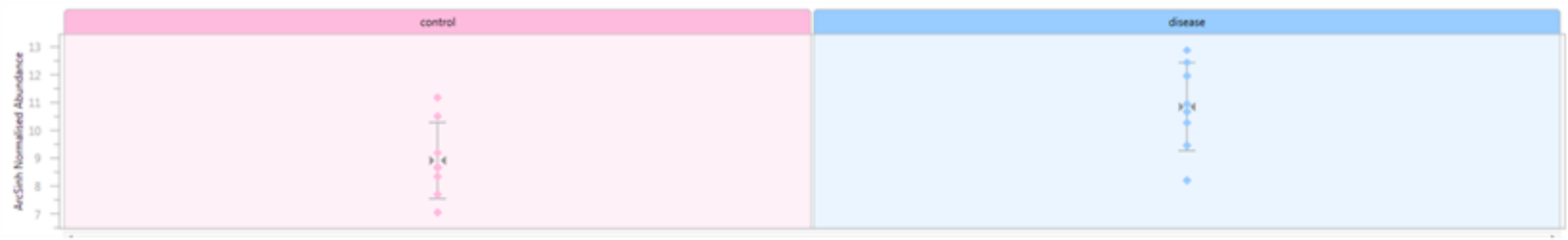

(b)

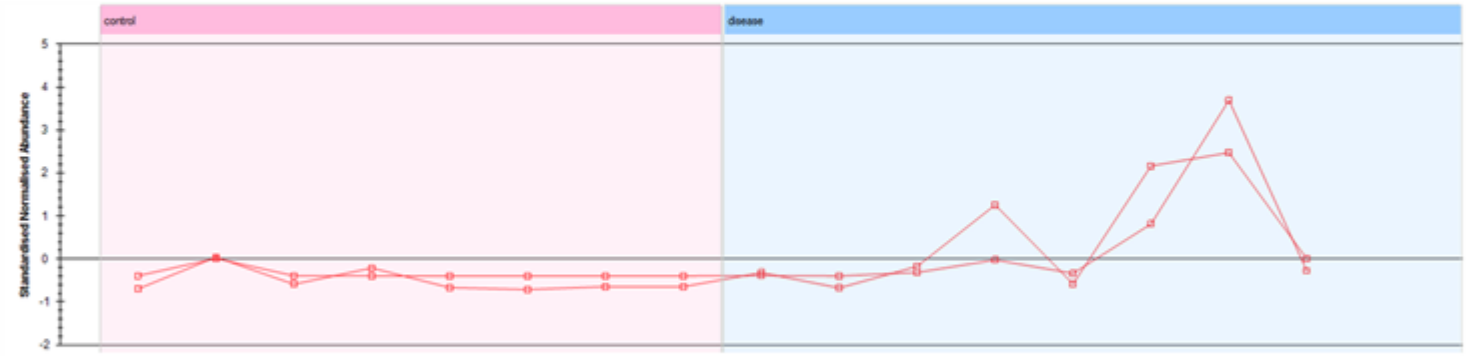

Σ	#	Score	Anova (p)	Max Fold Change	Highest Mean	Lowest Mean	Abundance	m/z	Charge	Retention Time	Fractions	Mass error (ppm)	Peptide Sequence	Modifications
•	8369	40.28	0.02	5.9	disease	control	4.395E+04	420.2057	2	123.453	1 2	-0.67	GPDFFTR	
•	27783	30.4	0.0368	14.2	disease	control	1.536E+04	420.2054	2	87.693	1 2	-1.32	GPDFFTR	

Figure 5.8 Quantitative label-free LC-MS data for azurocidin. Overall, azurocidin was identified in the recombined elution fraction analysis as being over-expressed in advanced cutaneous melanoma serum (n=8) in comparison to control serum (n=8), recombined *p*-value=3.9×10^{-3}. (a) Standard expression individual protein profile for all 16 samples (b) The peptide measurement view with an accompanying table illustrates unique peptides for azurocidin in each sample.

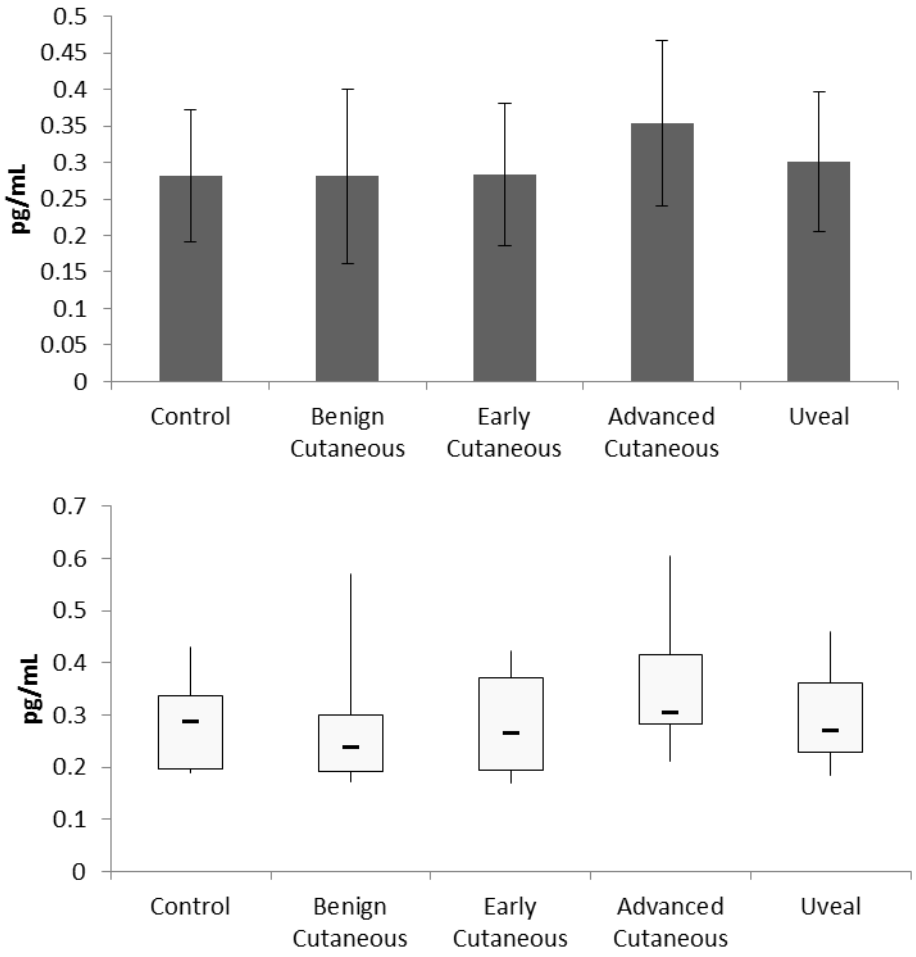

Figure 5.9 Azurocidin ELISA data represented by both bar chart and Box and Whisker Plot. Serum samples from a variety of melanoma conditions were used; benign cutaneous melanoma (n=18), early-stage cutaneous disease (n=14), advanced-stage cutaneous disease (n=12), and uveal melanoma (n=13), as well as control serum (n=13).

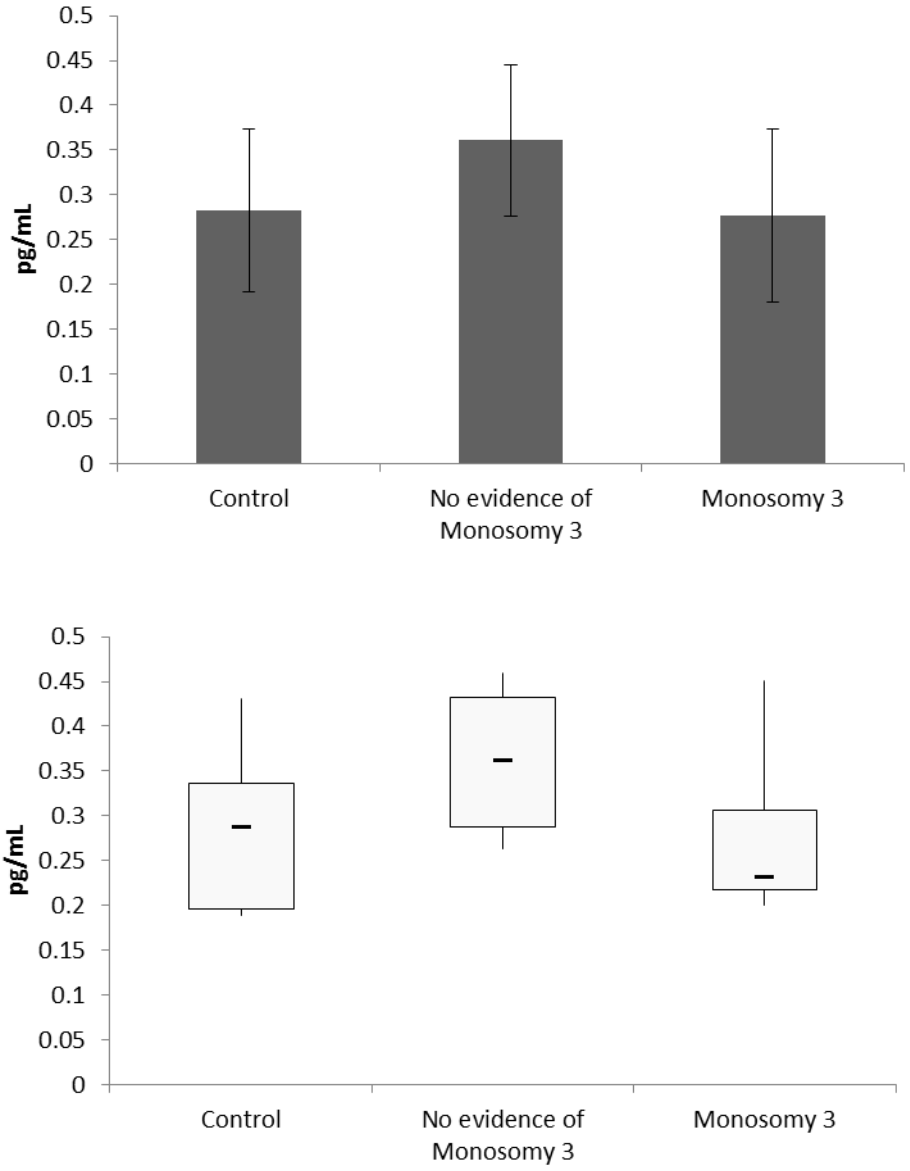

Figure 5.10 Azurocidin ELISA data represented by both bar chart and Box and Whisker Plot. Serum samples from two uveal melanoma conditions were used; monosomy of chromosome three (n=7) and no evidence of monosomy of chromosome three (n=6).

5.8.4 Plasma Serine Protease Inhibitor

Figure 5.11 (a) illustrates the downregulation of plasma serine protease inhibitor in advanced sera in comparison to normal melanoma sera, as detected by quantitative label-free LC-MS analysis. As shown in Figure 5.11 (b), three peptides were detected in elution fraction two, where an average fold change of 2.6 was observed.

In contrast to the above results, a significant increase in the expression of plasma serine protease inhibitor in early stage cutaneous melanoma serum in comparison to that of either control or benign melanoma serum was noted (Figure 5.12). No significant or clear abundance difference of the protein was observed when control and advanced cutaneous melanoma serum were compared. Hence, the results of the ELISA do not validate those of the quantitative label-free LC-MS experiment.

There was a statistically significant increase in the level of plasma serine protease inhibitor in uveal melanoma serum when compared to that of healthy patients (Figure 5.12). This increase in abundance was observed equally in both patients with monosomy of chromosome three and those with disomy of chromosome three, in relation to the level of plasma serine protease inhibitor produced in control serum, as shown in Figure 5.13.

(a)

(b)

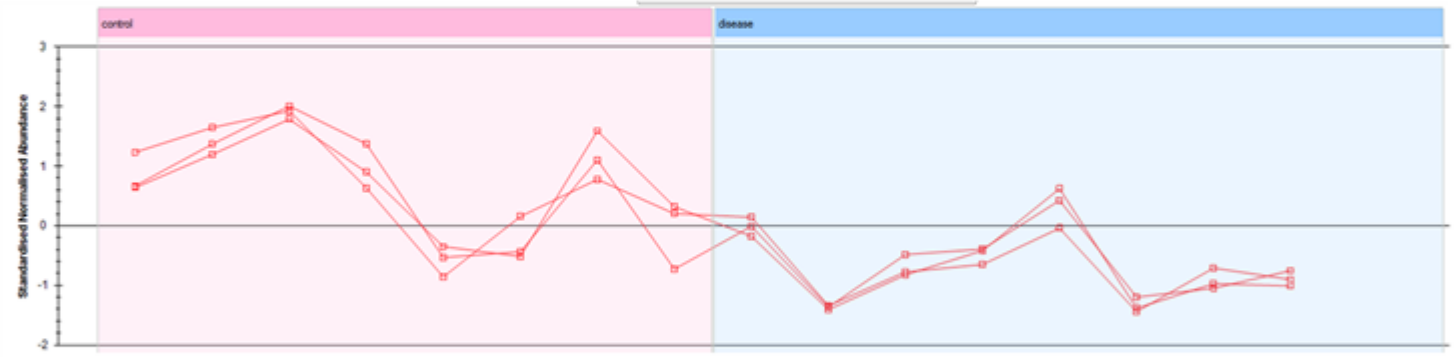

Σ	#	Score	Anova (p)	Max Fold Change	Highest Mean	Lowest Mean	Abundance	m/z	Charge	Retention Time	Fractions	Mass error (ppm)	Peptide Sequence	Modifications
•	6030	37.3	0.00854	2.78	control	disease	1.591E+05	728.9133	2	146.074	1 2	0.15	MQILEGLGLNLQK	
•	10223	50.48	0.00397	2.47	control	disease	9.863E+04	581.2906	2	54.488	1 2	-0.63	AVVEVDESGTR	
•	13791	55.53	0.0187	2.32	control	disease	4.541E+04	631.8055	2	53.333	1 2	-0.63	MQQVENGLSEK	

Figure 5.11 Quantitative label-free LC-MS data for plasma serine protease inhibitor. Overall, plasma serine protease inhibitor was identified in the recombined elution fraction analysis as being underexpressed in advanced cutaneous melanoma serum (n=8) as it was found to be elevated in control serum (n=8) by 2.4-fold, *p*-value=5.11×10^{-3}. (a) Standard expression individual protein profile for all 16 samples (b) The peptide measurement view with an accompanying table illustrates unique peptides for plasma serine protease inhibitor in each sample.

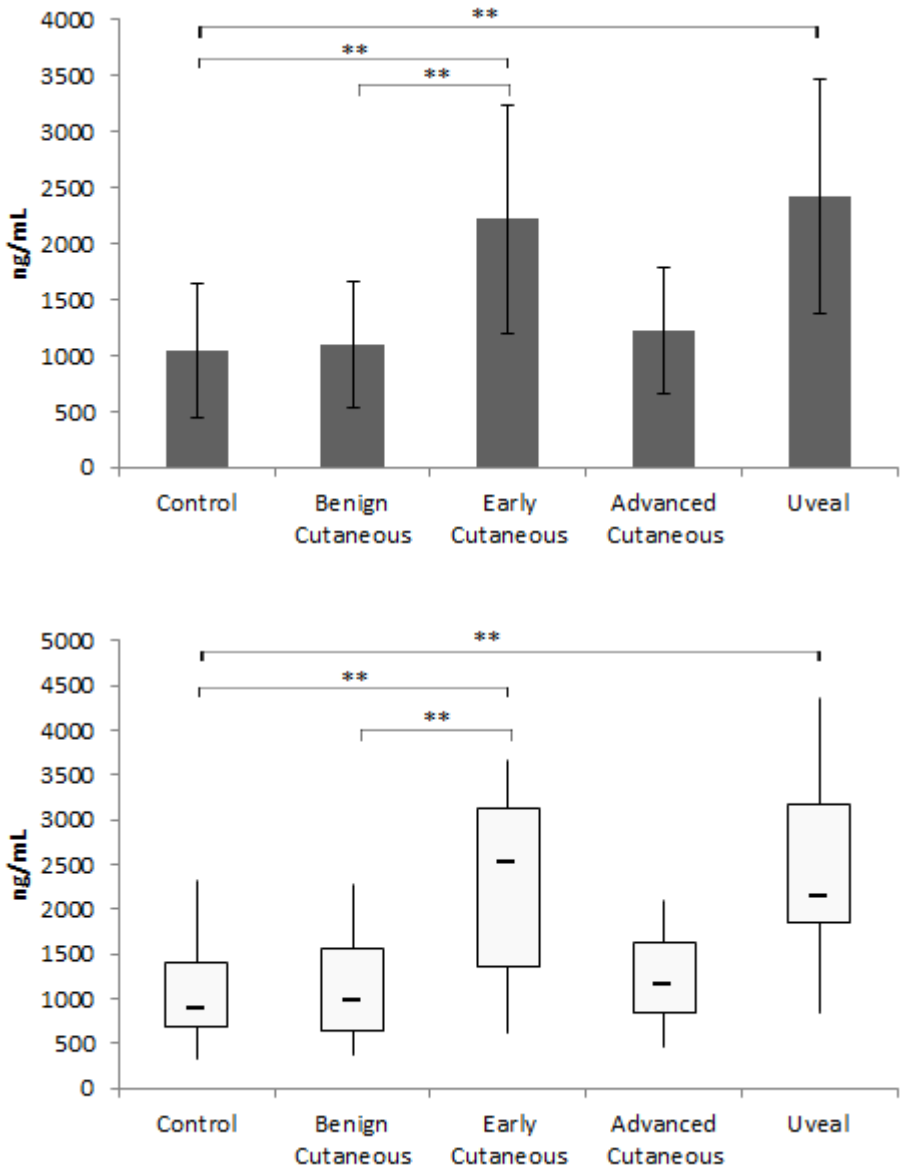

Figure 5.12 Plasma serine protease inhibitor ELISA data represented by both bar chart and Box and Whisker Plot. Serum samples from a variety of melanoma conditions were used; benign cutaneous melanoma (n=18), early-stage cutaneous disease (n=14), advanced-stage cutaneous disease (n=12), and uveal melanoma (n=13), as well as control serum (n=13). t-test scores: control vs. early cutaneous = $1.55x10^{-3}$; control vs. uveal = $6.32x10^{-4}$; benign vs. early cutaneous = $1.56x10^{-3}$. ** t-test score between experimental groups of ≤0.01

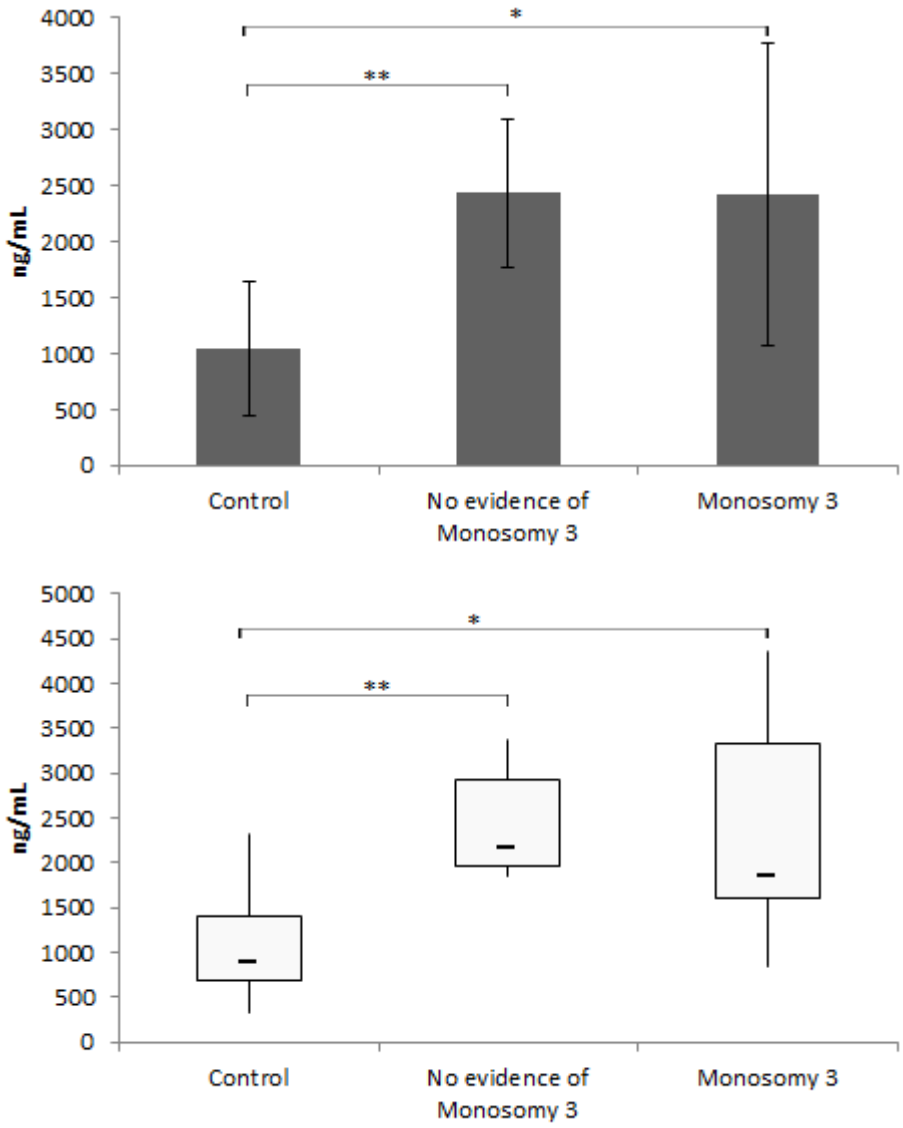

Figure 5.13 Plasma serine protease inhibitor ELISA data represented by both bar chart and Box and Whisker Plot. Serum samples from two uveal melanoma conditions were used; monosomy of chromosome three (n=7) and no evidence of monosomy of chromosome three (n=6). t-test scores: control vs. no evidence of monosomy three = 1.79×10^{-3}; control vs. monosomy three = 0.037. * t-test score between experimental groups of ≤0.05. ** t-test score between experimental groups of ≤0.01

5.8.5 BACE-2

As illustrated in Figure 5.14, BACE-2 was shown to be elevated in both early and late stage cutaneous melanoma in comparison to serum of patients with benign disease. In addition to this, BACE-2 was also shown to be highly abundant in late-stage disease when compared to healthy sera.

No statistically significant difference in BACE-2 production was observed between the uveal melanoma serum group and the control sera, see Figure 5.14; neither was any difference noted between patients with or without monosomy of chromosome three (Figure 5.15).

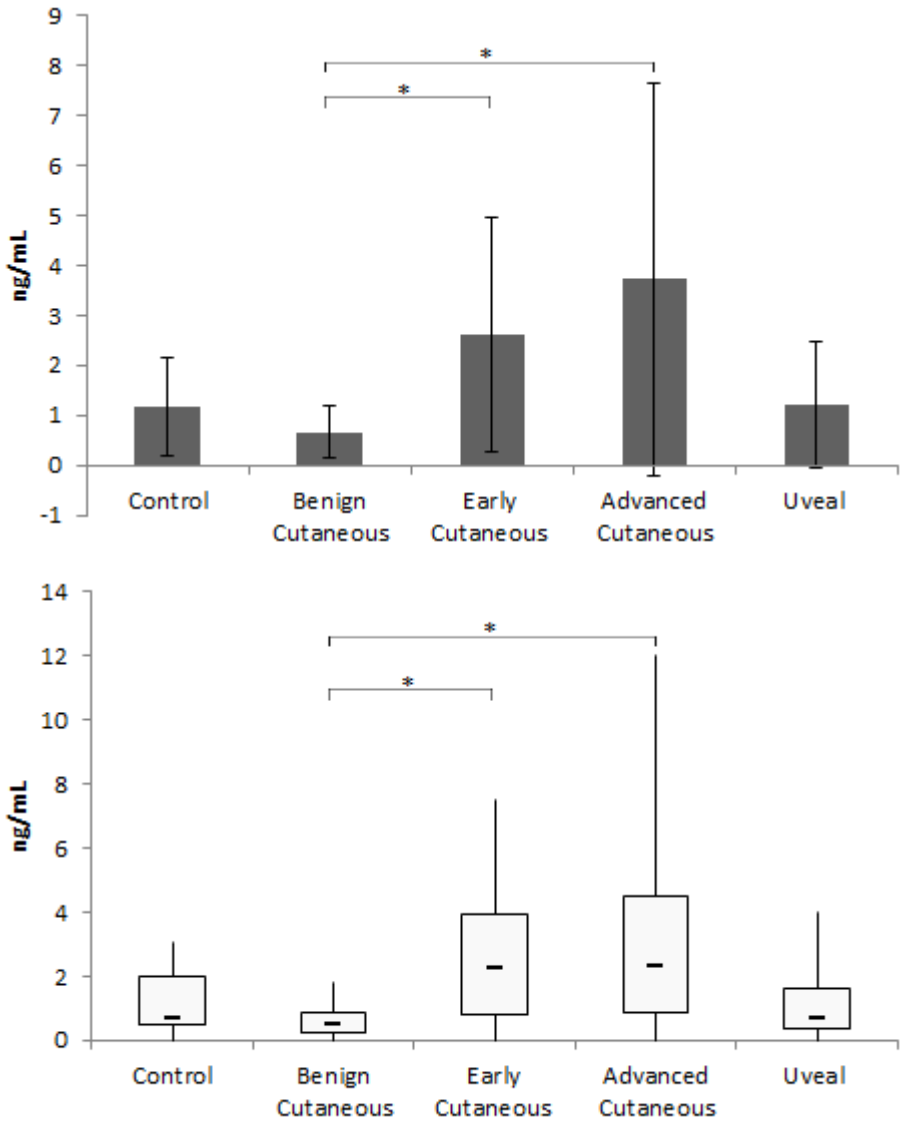

Figure 5.14 BACE-2 ELISA data represented by both bar chart and Box and Whisker Plot. Serum samples from a variety of melanoma conditions were used; benign cutaneous melanoma (n=18), early-stage cutaneous disease (n=14), advanced-stage cutaneous disease (n=12), and uveal melanoma (n=13), as well as control serum (n=13). t-test scores: benign cutaneous vs. early cutaneous = $1.52x10^{-2}$; benign cutaneous vs. advanced cutaneous = $2.78x10^{-2}$. * t-test score between experimental groups of ≤0.05.

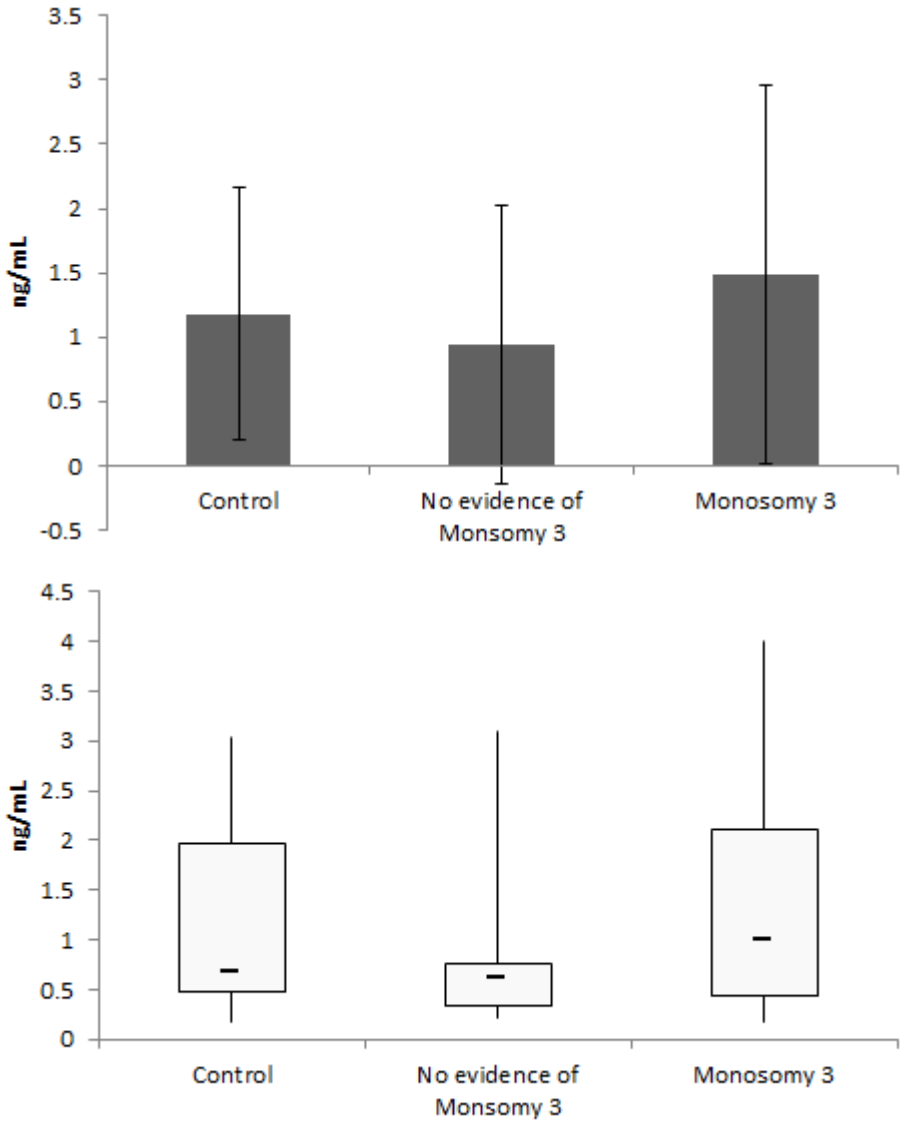

Figure 5.15 BACE-2 ELISA data represented by both bar chart and Box and Whisker Plot. Serum samples from two uveal melanoma conditions were used; monosomy of chromosome three (n=7) and no evidence of monosomy of chromosome three (n=6).

5.8.6 TIMP-1

As shown in Figure 5.16, no significant difference in the abundance of TIMP-1 was observed between control or benign disease serum and early or late stage disease. In addition to this, no differential production of the protein was noted when serum of uveal melanoma patients was compared to healthy serum (Figure 5.16). When the uveal melanoma samples were divided into those with either monosomy of chromosome three or disomy of chromosome three and compared, no differential abundance of TIMP-1 was detected (Figure 5.17).

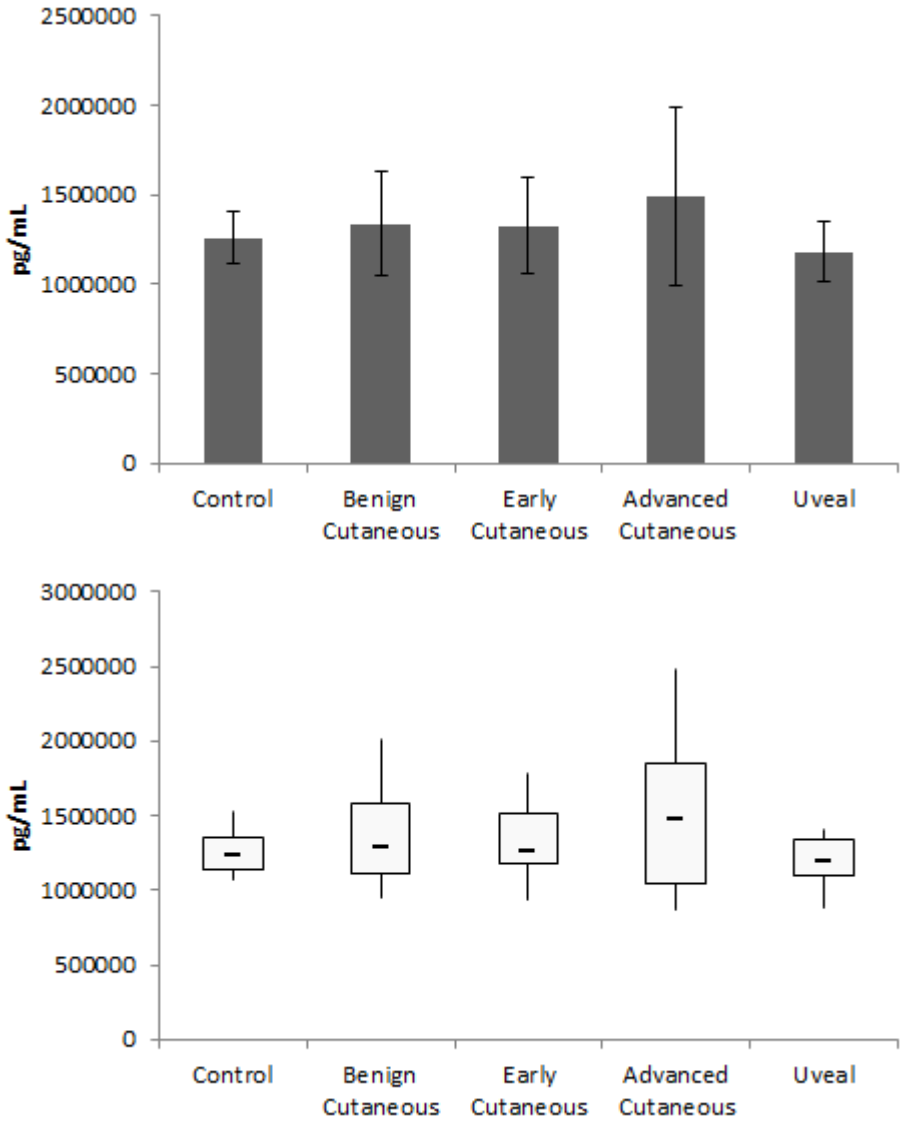

Figure 5.16 TIMP-1 ELISA data represented by both bar chart and Box and Whisker Plot. Serum samples from a variety of melanoma conditions were used; benign cutaneous melanoma (n=18), early-stage cutaneous disease (n=14), advanced-stage cutaneous disease (n=12), and uveal melanoma (n=13), as well as control serum (n=13).

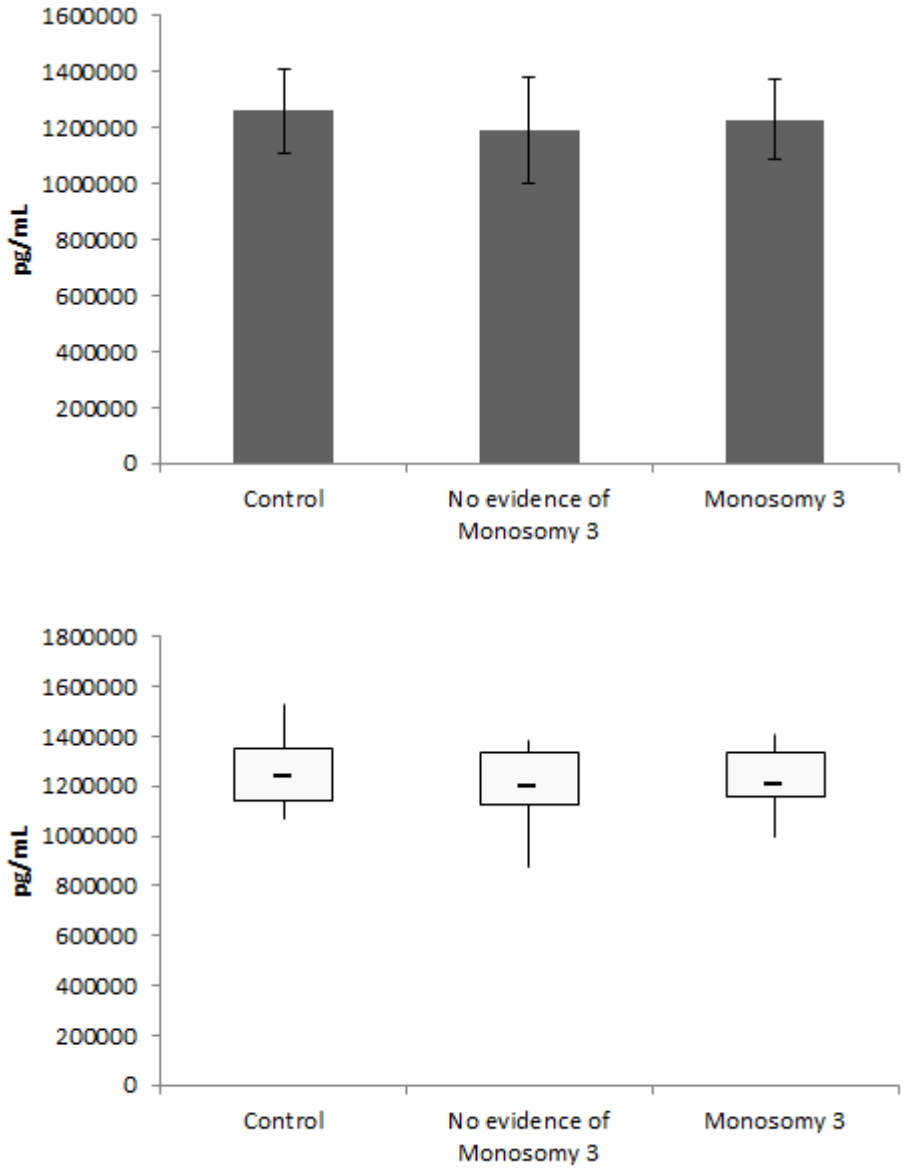

Figure 5.17 TIMP-1 ELISA data represented by both bar chart and Box and Whisker Plot. Serum samples from two uveal melanoma conditions were used; monosomy of chromosome three (n=7) and no evidence of monosomy of chromosome three (n=6).

5.8.7 MMP-1

As shown in Figure 5.18, a statistically significant decrease in the level of MMP-1 was observed in the sera of advanced cutaneous melanoma patients, when compared to control specimens. This result directly contradicts the findings of the microarray study.

Uveal melanoma serum was not found to contain significantly less MMP-1 than that of healthy serum (Figure 5.18), in addition to this there was no significant difference in its abundance between uveal melanoma serum of patients with either monosomy of chromosome three or disomy of chromosome three (Figure 5.19).

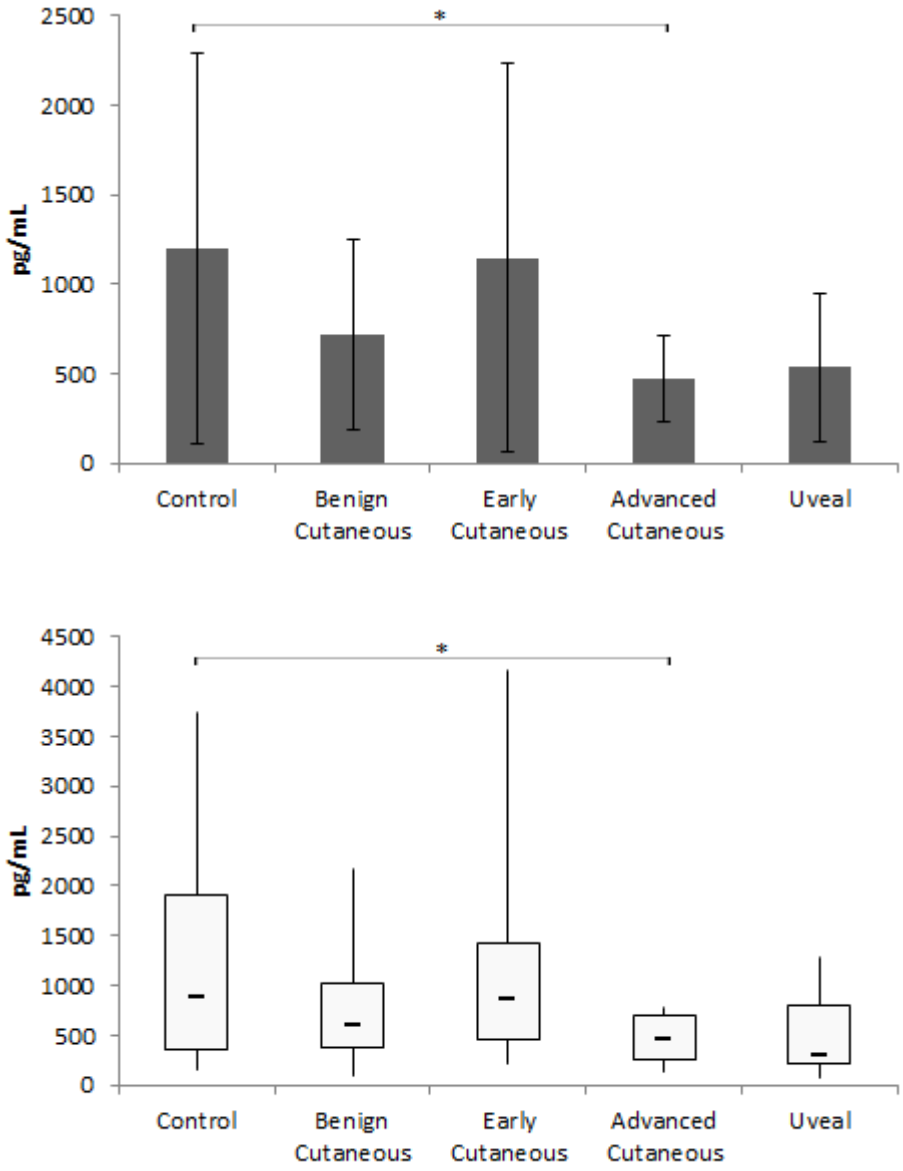

Figure 5.18 MMP-1 ELISA data represented by both bar chart and Box and Whisker Plot. Serum samples from a variety of melanoma conditions were used; benign cutaneous melanoma (n=18), early-stage cutaneous disease (n=14), advanced-stage cutaneous disease (n=12), and uveal melanoma (n=13), as well as control serum (n=13). t-test score: control vs. advanced cutaneous melanoma serum = 0.044. * t-test score between experimental groups of ≤0.05.

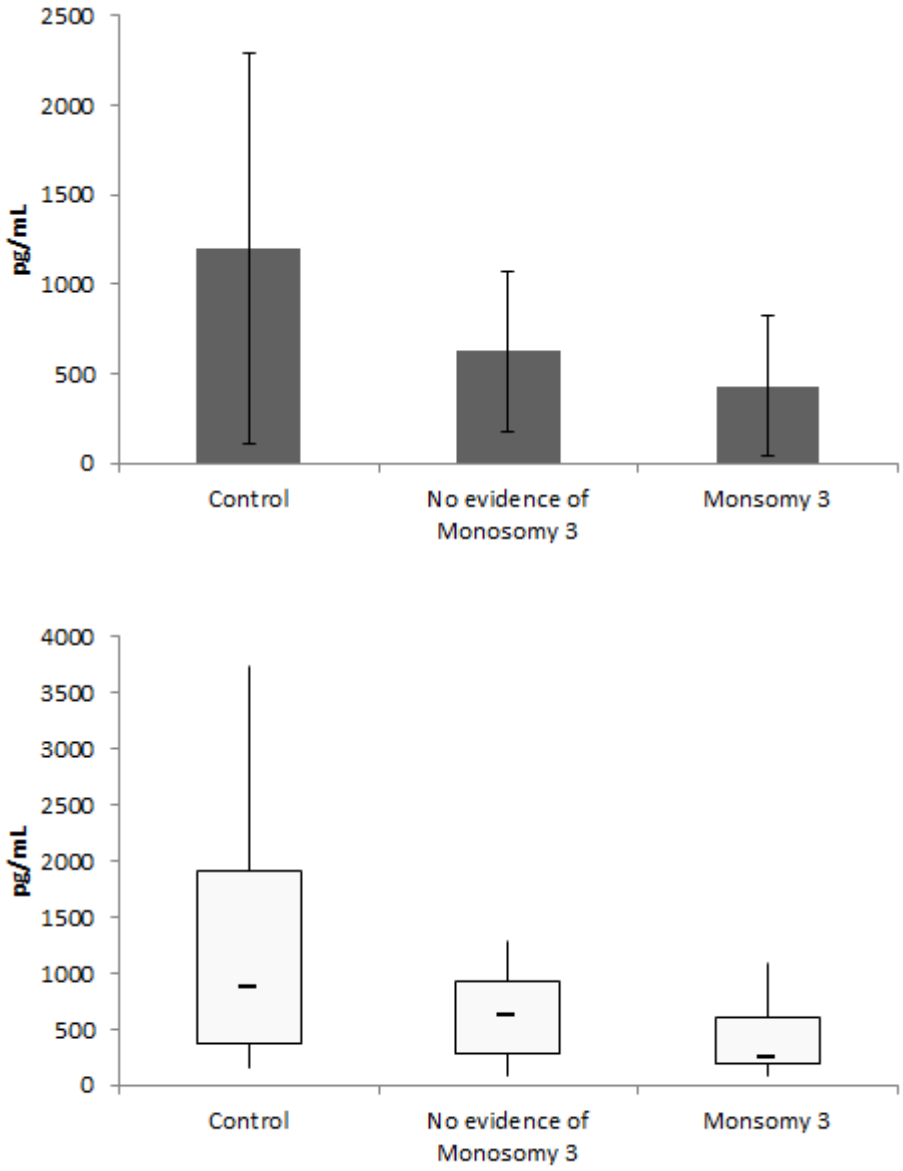

Figure 5.19 MMP-1 ELISA data represented by both bar chart and Box and Whisker Plot. Serum samples from two uveal melanoma conditions were used; monosomy of chromosome three (n=7) and no evidence of monosomy of chromosome three (n=6).

CHAPTER SIX

Discovery of an 8.9 kDa Species by SELDI-ToF MS as a Potential Marker for Disease Progression in Melanoma

6.1 Background

SELDI-TOF is used in biomarker discovery as it quickly and effectively analyses protein mixtures, such as urine, serum, and tissue lysates, in order to illustrate proteomic differences; such as those between control and disease specimens.

Previously, Dr. Priyanka Maurya had used SELDI-TOF MS for the discovery of a 7.6 kDa protein in the conditioned media of a paclitaxel-resistant superinvasive melanoma cell line variant (MDA-MB-435S-F/Taxol10p4pSI) (Dr. Pryanka Maurya, Ph.D. Thesis, 2009). MALDI-TOF/TOF MS subsequently identified the protein as a fragment of bovine transferrin (Dowling, Maurya et al. 2007). Following the profiling of conditioned media collected from a range of melanocytes and melanoma cell lines, it was discovered that the 7.6 kDa fragment was solely expressed in melanoma cell lines. In addition to this, a number of other proteins which were only identified in the melanoma cell lines were discovered, including an 8.5 kDa ubiquitin-like marker, where they were found to be highly upregulated in comparison to normal melanocytes (Dr. Pryanka Maurya, Ph.D. Thesis, 2009).

It was hypothesised that specific protein expression differences between a variety of sample sets could be highlighted using the SELDI TOF method. The aim of the study described here was to analyse the expression of the markers of interest in melanoma serum. Vitreous fluid collected from uveal melanoma patients would also be analysed in order to determine the presence of biomarkers of interest.

6.2 SELDI-TOF MS Analysis

SELDI-TOF MS is MALDI-based method which uses a target modified, e.g. nickel-activated IMAC, to achieve biochemical affinity with the analyte in order to bind a specific subset of proteins. The sample is mixed with a matrix which co-crystallises with the analyte on a chip surface. A laser then strikes the mixture, causing ionisation of any bound proteins present. TOF is used to measure the m/z of each molecule which generates a spectrum where each peak corresponds to a protein.

However, the technique does not provide any protein identifications, only the m/z ratio and the intensity of the peak. In order to identify the peaks, spin columns containing a resin which can mimic the SELDI surface can be employed.

6.3 Determination of the 7.6 kDa and 8.5 kDa Markers in Conditioned Media

Cell lines secrete and shed proteins into the surrounding media. This media, without serum which can mask the secreted or shed proteins, is known as conditioned media. Serum-free RPMI-1640 media was conditioned by SK-MEL-5 cutaneous melanoma cells for 72 hours and the resulting media was analysed by SELDI-TOF using copper-activated IMAC as the target, which identified peaks corresponding to both the 7.6 kDa and 8.5 kDa markers (Figure 6.1 (a)). The conditioned media was also diluted in serum-free media at concentrations of 1:2, 1:10, 1:20 and 1:50 which illustrated that 1:10 and 1:20 were the most dilute levels at which the 7.6 kDa and 8.5 kDa markers could be observed, respectively (Figure 6.1 (b), (c) and (d)).

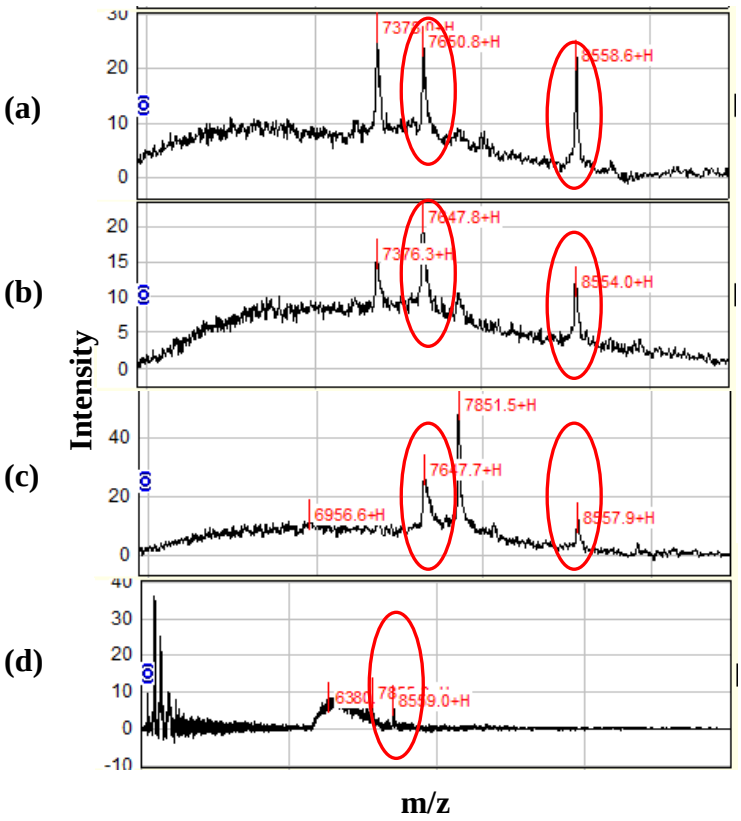

Figure 6.1 Both targets of interest, the 7.6 kDa fragment and 8.5 kDa ubiquitin-like marker, as outlined in red, were found in (a) neat conditioned media of SK-MEL-5 cutaneous melanoma cells, and at dilutions of (b) 1:2 and (c) 1:10 in serum-free media. (d) The 8.5 kDa marker was also found at a dilution of 1:20. One representative result of three is shown.

6.4 Detection of 7.6 kDa and 8.5 kDa Potential Markers in Serum-Diluted Conditioned Media

In order to identify whether or not the markers of interest could be identified in a clinical sample, the SK-MEL-5 conditioned media was diluted in colorectal cancer serum and then analysed by SELDI using copper-activated IMAC 30 chips. This would prevent wasting valuable clinical specimens.

The serum did not contain either biomarker. The markers were not clearly detectable at the 1:5 or the 1:10 dilution (Figure 6.2 (b) and (c)). This may have been due to the fact that the protein-rich serum easily masked the biomarkers in the resulting spectra and so it was difficult to identify the lowest level at which they were still detectable. However an unknown 8.9 kDa protein, or protein cleavage product, was found in all dilutions as well as in the neat conditioned media (Figure 6.2).

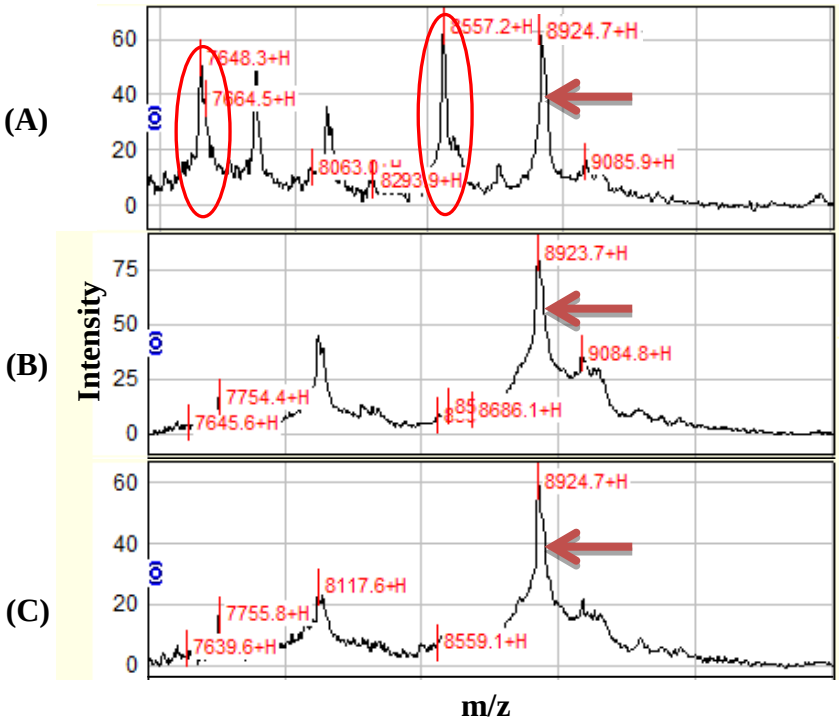

Figure 6.2 SELDI-ToF spectra of (a) undiluted conditioned media, and (b) 1:5 and (c) 1:10 dilutions of SK-MEL-5 conditioned media in serum. The 7.6 kDa transferrin fragment and the 8.5 kDa fragment were potentially found in (b) and (c), albeit at minute levels. In all cases an 8.9 kDa protein, or protein cleavage product, was found. One representative result of three is shown in both cases.

6.5 Detection of an Approximate 8925 m/z Species in Cutaneous Melanoma Serum

Immunodepleted stage IV melanoma sera were examined using SELDI-ToF MS and were compared to immunodepleted control sera (collected from potentially diabetic patients).

The initial biomarkers of interest; a 7.6 kDa transferrin fragment and an 8.5 kDa ubiquitin-like marker, were not found. Despite this, an unknown 8.9 kDa protein was discovered which occurred in 10 of 12 disease samples, for at least one out of three replicates each (Figure 6.3).

The 8.9 kDa protein was identified in three of 12 controls. When further examined, it was found that the levels of the marker were low in the controls in comparison to the levels in the samples (Figure 6.3).

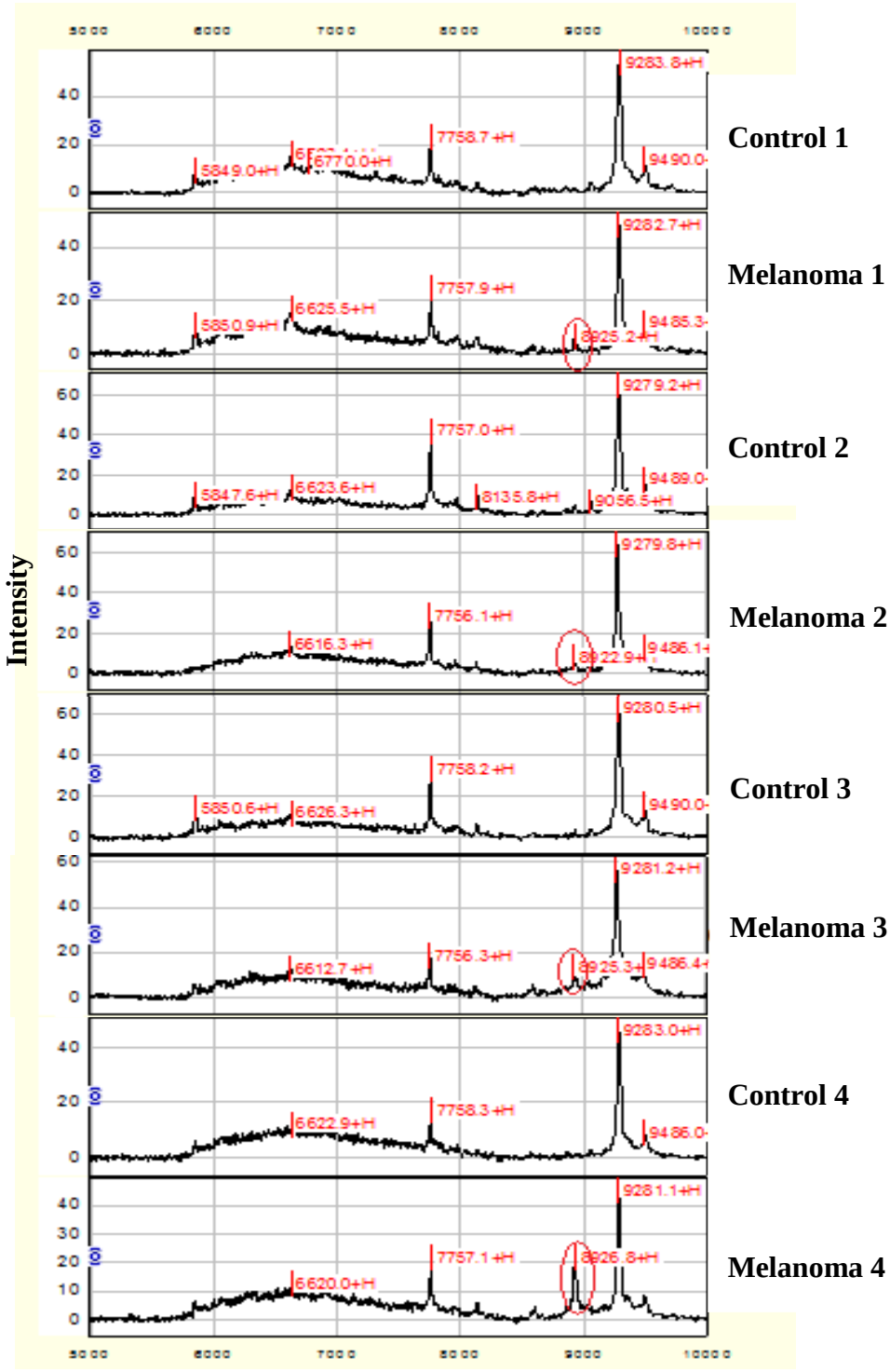
Intensity
m/z
Control 1
Melanoma 1
Control 2
Melanoma 2
Control 3
Melanoma 3
Control 4
Melanoma 4

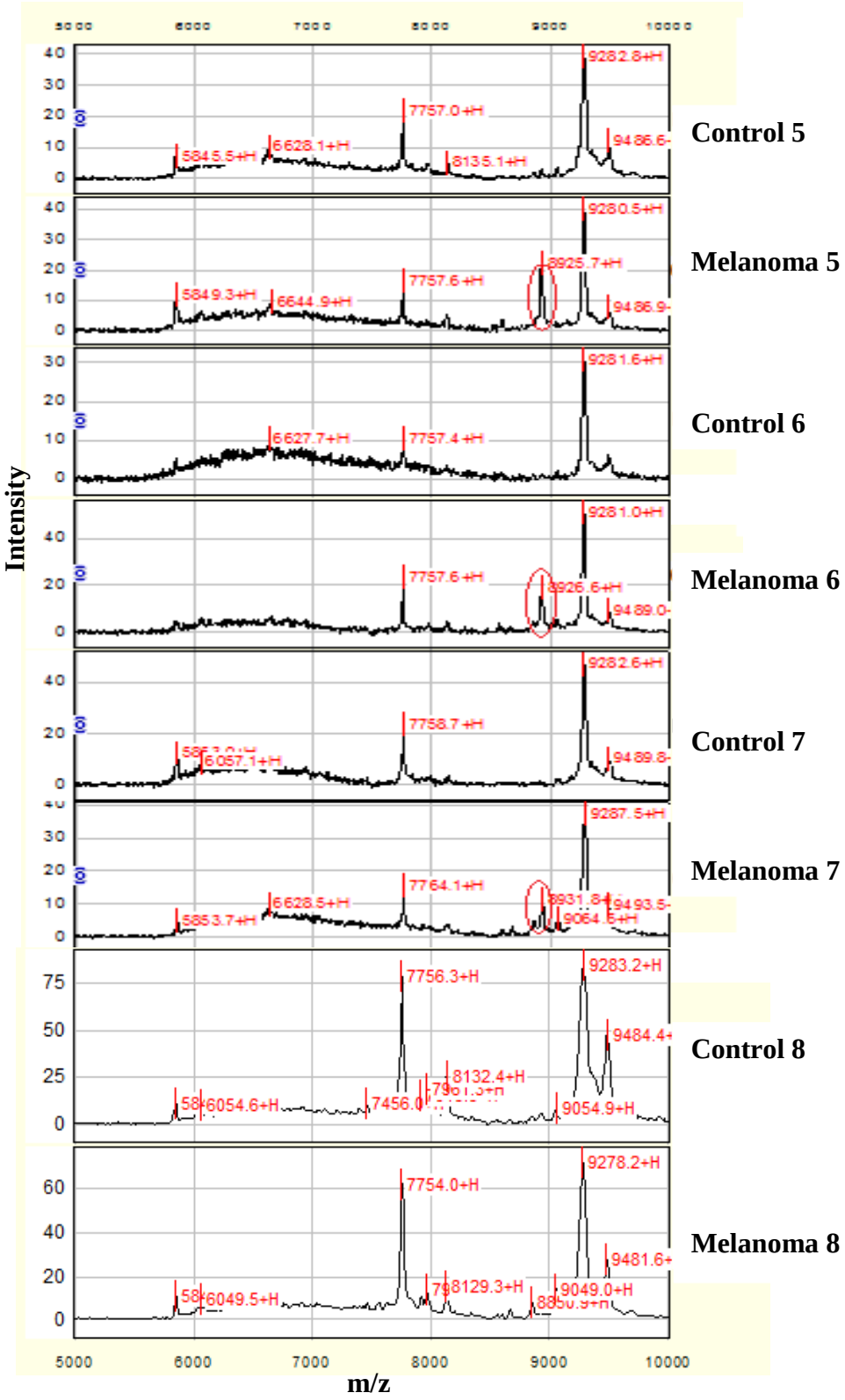
Intensity
m/z
Control 5
Melanoma 5
Control 6
Melanoma 6
Control 7
Melanoma 7
Control 8
Melanoma 8
9282.8+H
7757.0+H
6628.1+H
5845.5+H
8135.1+H
9280.5+H
8925.7+H
7757.6+H
6644.9+H
5849.3+H
9281.6+H
6627.7+H
7757.4+H
9281.0+H
7757.6+H
8926.6+H
9282.6+H
7758.7+H
6057.1+H
9287.5+H
7764.1+H
6628.5+H
5853.7+H
9283.2+H
7756.3+H
8132.4+H
6054.6+H
9054.9+H
9278.2+H
7754.0+H
6049.5+H
8129.3+H
9049.0+H

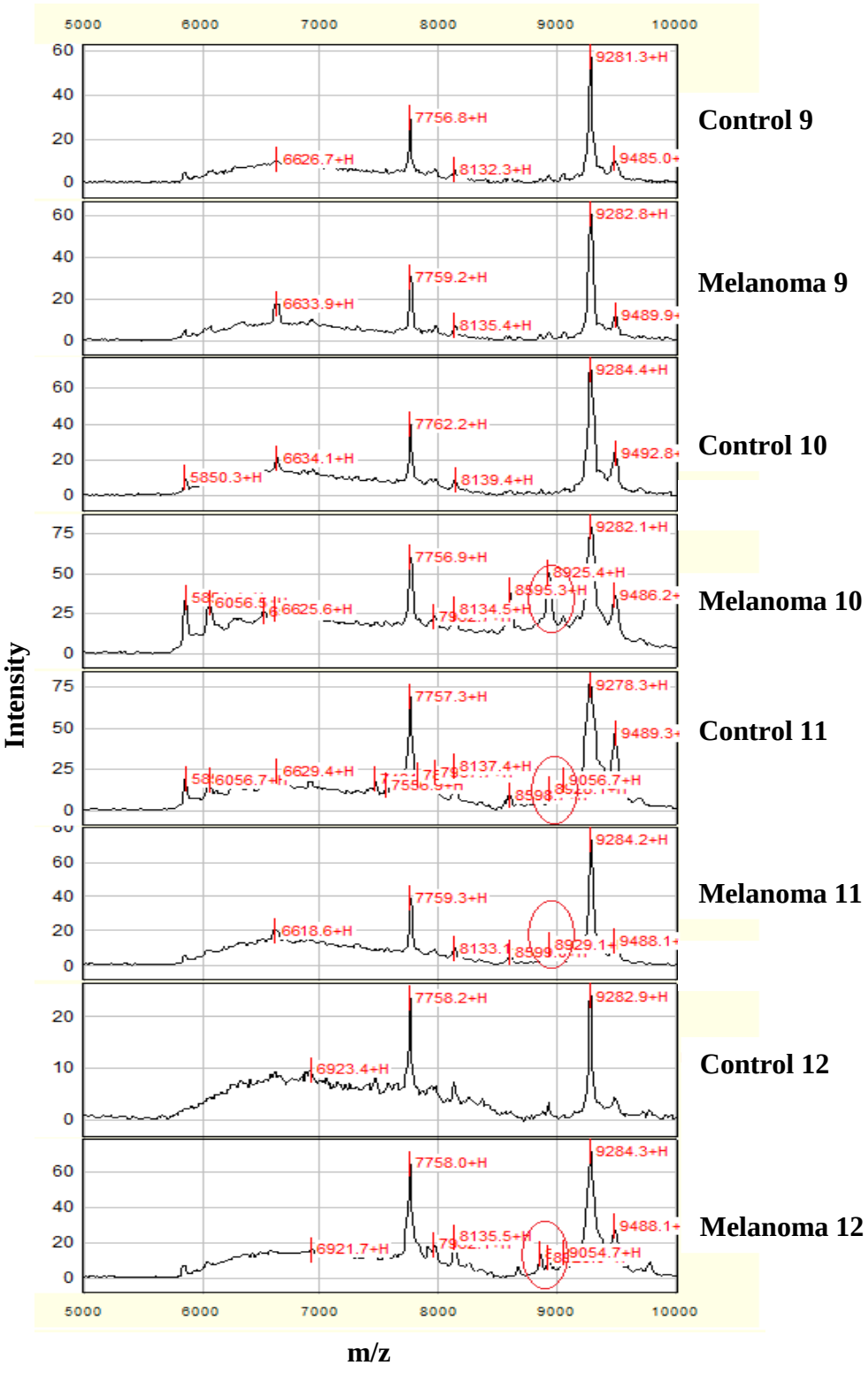

Figure 6.3 SELDI spectra illustrating a protein, or cleavage product of a protein, with an approximate m/z value of 8925, circled in red which was identified in immunodepleted advanced-stage cutaneous melanoma serum (n=12) in comparison to healthy immunodepleted serum controls (n=12). The potential marker was found to occur in each disease sample at least once out of the three times the experiment

was performed. The 8.9 kDa protein was identified in 10 of 12 samples examined and at low levels in only three of 12 controls. One representative result is shown in each case.

6.6 Detection of an Approximate 8925 m/z Species in the Vitreous Fluid of a Patient with Metastatic Uveal Melanoma

SELDI analysis was also performed on one metastatic uveal melanoma ocular fluid sample in order to determine whether or not the 7.6 kDa and 8.5 kDa markers of interest found in the cutaneous melanoma conditioned media, were also present in the vitreous fluid of uveal melanoma and hence, act as potential biomarkers for the disease.

The 7.6 kDa transferrin fragment appeared to be present in both crude and immunodepleted samples. It was more abundant in the crude specimen than the immunodepleted fluid where it was detected at near-baseline levels. The 8.5 kDa ubiquitin-like protein was clearly detectable in the immunodepleted specimen, with only a small peak identified in one crude vitreous specimen (Figure 6.4).

The 8.9 kDa unknown peak of interest was clearly visible in both crude and immunodepleted samples (Figure 6.4).

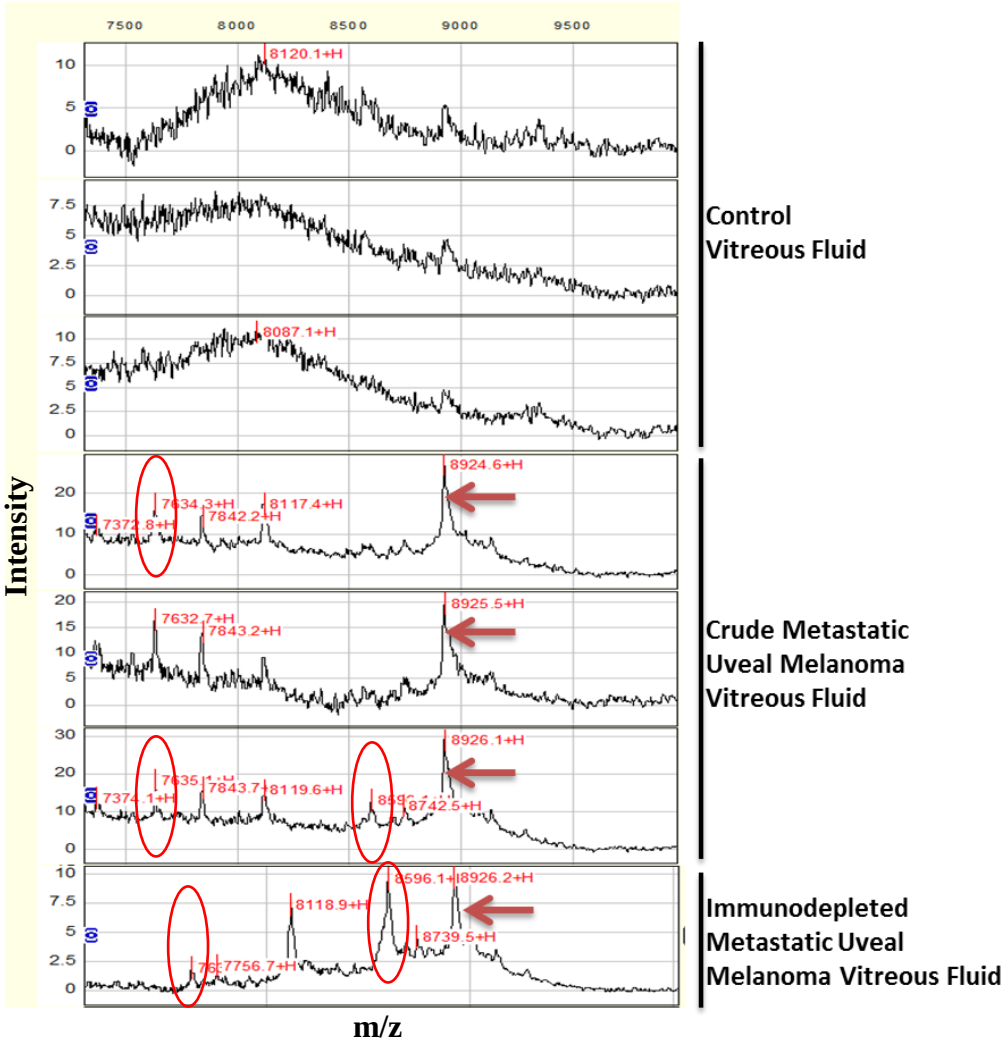

Figure 6.4 SELDI spectra illustrating the presence of an 8.9 kDa species in the vitreous fluid of a uveal melanoma patient (n=1) which was not identified in a corresponding vitreous fluid control (n=1). Red arrows indicate the 8.9 kDa peak of interest while the 7.6 kDa and 8.5 kDa peaks are indicated by a red circle.

6.7 Attempted Purification of the 8.9 kDa Protein Using IMAC Resin

Copper-activated IMAC SELDI chips were used in the discovery of the 8.9 kDa peak of interest. As SELDI cannot be used for the identification of proteins, it was decided to use copper-activated IMAC resin to isolate the subset of proteins which have an affinity for copper. This would allow for the separation of the protein of interest and subsequent attempts to identify it.

IMAC spin columns contain an uncharged resin which is based on the same principle of affinity chromatography as the IMAC SELDI chips. The resin must be activated and charged with a metal ion such as cobalt or nickel, to which proteins with an affinity for these ions bind, often through a histidine residue or a phosphorylation site. In order to elute bound proteins from the column, a pH change or a competitive molecule, such as imidazole, may be employed. In this case, a gradient of increasing imidazole concentration was used. Imidazole would compete with histidine residues of the protein for binding sites on the resin, therefore as the concentration of imidazole increased; more bound protein would be eluted from the column.

Cutaneous melanoma serum samples 4, 5, and 6 shown in Figure 6.3, which contained a high level of the 8.9 m/z potential marker according to their corresponding SELDI spectrum, were selected for IMAC purification and a gradient of 10 mM to 500 mM imidazole was used to elute bound proteins. Normal phase (NP20) SELDI chips, which bind all protein, were used to validate the IMAC resin technique and visualise the protein profile presence of the collected fractions. It was hoped that this would pin-point the concentration of imidazole that most successfully eluted the 8.9 kDa m/z species. However this analysis yielded no peaks whatsoever.

The elution fractions were assayed for protein content, which indicated that no protein was present in the fractions. The fractions were also separated on a 4-20% gradient gel, which should resolve low molecular weight proteins such as the 8.9 kDa target, and stained with a colloidal silver protein stain. This visualised an apparent array of bands in each lane. One band, circled in red, appeared to be located at the approximate molecular weight of 8.9 kDa (Figure 6.5). However, following the in-gel digestion of any proteins in that region and subsequent analysis by LC-

MS/MS, very poor results and few protein identifications were yielded from the analysis.

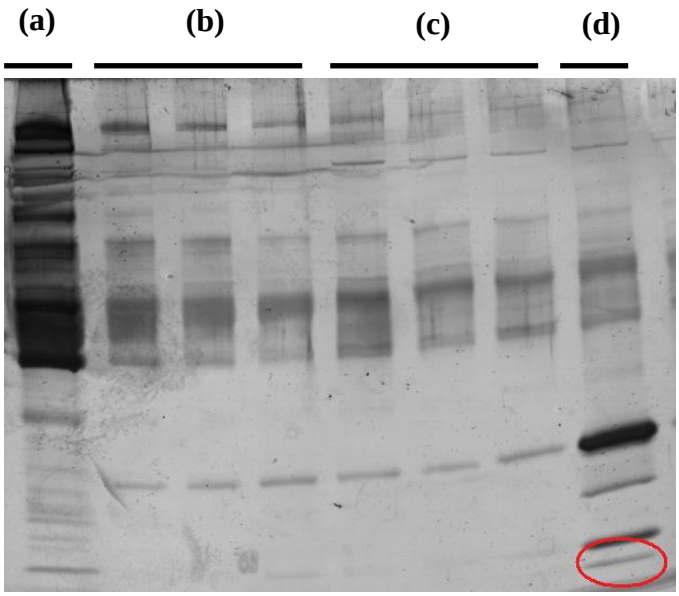

Figure 6.5 Silver-stained gel illustrating advanced-stage cutaneous melanoma serum which was eluted from a copper-activated IMAC spin column using an imidazole gradient. Collected fractions were then separated on a 4-20% Tris-Glycine gel which was subsequently silver stained. The potential band of interest is circled in red. (a) Immunodepleted melanoma serum, (b) 10 mM imidazole fraction, (c) 200 mM imidazole fraction; (d) 500 mM imidazole fraction.

It was hypothesised that staining the gel with colloidal silver may have caused this as it is known to affect the identification of proteins in mass spectrometry, despite using a mass spectrometry-compatible protocol. Hence, the experiment was repeated using a reverse, zinc-based stain which stains the non-proteinaceous regions of the gel, thus leaving any protein bands clear. In this way the stain does not bind to the regions of interest and may improve the number of identifications acquired. This did not seem to improve the quality of identifications acquired which confirmed that the mass spectrometry-compatible silver staining method was not responsible for the poor list of identifications.

LTQ mass spectrometry was used for the identification of proteins in the above analysis. However, Orbitrap-based mass spectrometry has a higher mass accuracy. It was decided to repeat the experiment using the more accurate, Orbitrap-based method of analysis. Additional reduction and alkylation steps were also included in the new method.

The binding of protein to and subsequent imidazole-based elution from copper-activated IMAC resin was repeated. The following samples which had previously confirmed the presence or absence of the 8.9 m/z species were chosen for the experiment; cutaneous melanoma serum, control serum, control vitreous fluid, uveal melanoma vitreous fluid, and media conditioned by SK-MEL-5 cutaneous melanoma cell lines. Imidazole concentrations of 25 mM, 50 mM, 100 mM, 200 mM, and 500 mM were used to fractionate protein from the resin. Collected fractions were separated in the first dimension on a 4-20% gel and silver stained (Figure 6.6). Regions below the red line in Figure 6.6, i.e. the low molecular region of the gel, were excised into bands and in-gel digested with trypsin to generate peptides which were separated over the course of an hour gradient and analysed using an Orbitrap mass spectrometer. The results of the qualitative analysis are shown in Table 6.1. Identifications generated from a single peptide were accepted due to the low molecular weight of the protein or cleavage product of interest. As the low molecular weight region of the gel was excised, many of the proteins identified were larger than expected. This suggested that the protein in question may be a cleavage product of a larger molecule.

In addition to separating the fractions by 1-D electrophoresis, an in-solution digest was also carried out on the elution fractions. However, the results from this mainly consisted of high abundance proteins and did not overlap with those acquired in Table 6.1.

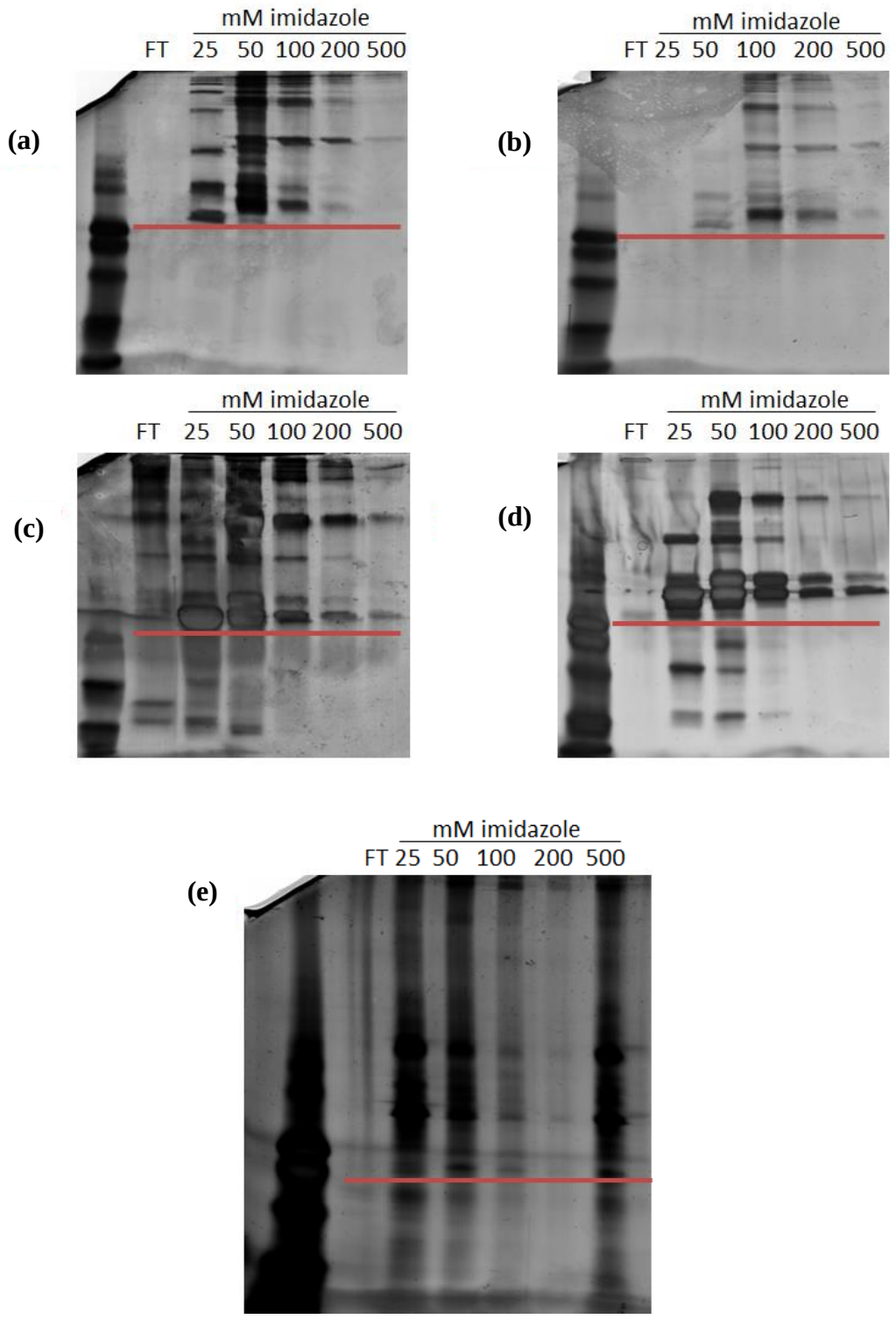

Figure 6.6 Silver-stained 4-20% 1-D gel of (a) melanoma serum, (b) control serum, (c) uveal melanoma vitreous, (d) control vitreous, and (e) SK-MEL-5 conditioned media which were eluted from IMAC spin columns using an imidazole gradient. The low molecular weight region of the gel, the region below the red line, was cut and each lane was sliced and in-gel digested.

Protein Name	Accession number	Molecular Weight (Da)	Number of Peptides (% Coverage)				
			Conditioned Media	Uveal Melanoma Vitreous Fluid	Cutaneous Melanoma Serum	Control Vitreous Fluid	Control Serum
Cystatin-A	P01040	11006	1 (12.24%)	1 (12.24%)	0	0	0
Actin, cytoplasmic 1	P60709	41736	2 (6.13%)	1 (2.67%)	0	0	0
Histone H4	P62805	11367	3 (28.16%)	1 (9.71%)	0	0	0
Glyceraldehyde-3-phosphate dehydrogenase	P04406	36053	2 (6.27%)	3 (12.84%)	0	0	1 (8.36%)
Apolipoprotein E	P02649	36154	0	9 (34.70%)	3 (13.56%)	3 (12.93%)	0
Retinol-binding protein 4	P02753	23010	0	4 (24.88%)	4 (20.90%)	0	2 (13.43%)
Prothrombin	P00734	7003	0	0	4 (11.09%)	0	1 (3.22%)
Serum amyloid P-component	P02743	25387	0	0	4 (21.08%)	0	1 (4.48%)
Hemopexin	P0279	51676	0	0	3 (7.14%)	0	0

Table 6.1 The quantitative analysis of imidazole-eluted fractions from an IMAC spin column produced a list of 9 significant proteins which were identified as potential 8.9 kDa candidates. No one identification was found which appeared in the conditioned media, uveal melanoma vitreous, and advanced cutaneous melanoma serum and which was absent from the controls. Protein identifications generated from one peptide were accepted as it is possible that the protein or cleavage product in question may consist of one 8.9 kDa peptide.

In order to determine an effective method of isolating the 8.9 m/z species, 3-20 kDa cut-off spin devices were used for concentrating the low molecular weight portion of SK-MEL-5 conditioned media of cutaneous melanoma cells following IMAC resin binding and imidazole elution.

The proteins bound to the column were eluted in one fraction (500 mM imidazole) and either run on a 1-D gel and silver stained or acetone precipitated and in-solution digested. This, however, did not produce any proteins which overlapped with Table 6.1. The experiment may have been compromised as the high imidazole concentration may have damaged the columns.

6.8 MALDI-TOF Analysis of Proteins Eluted Directly from IMAC Chips

As SELDI is a form of matrix-enhanced laser desorption ionisation (MALDI), MALDI was used in an attempt to detect the 8.9 kDa protein of interest in a peak profile and subsequently fragment it into peptides whose sequence may be determined, thus identifying the protein.

It was decided to attempt to remove the protein of interest directly from the SELDI chip from which it was known to bind as this may have concentrated the marker more successfully than the resin. The control and disease sera used in the analysis were also immunodepleted in order to reduce any high abundance proteins present. This would minimise the effect of large peaks diminishing the significance of smaller ones.

Cutaneous melanoma and healthy sera were incubated on copper-activated SELDI chips, as before, and one fraction of 500 mM imidazole was used to elute all bound proteins from the surface. The fractions were co-crystallised with a sinapinic acid (SPA) matrix and analysed by MALDI. However, too much interference was present thus masking any peaks. This was due to the low protein concentration and high imidazole levels present in the samples. Hence, it was necessary to increase the concentration of protein being loaded onto the SELDI chip while keeping the quantity of imidazole used to a minimum.

The experiment was repeated using 10 mM, 50 mM and 100 mM imidazole concentrations to sequentially elute bound melanoma and control proteins from copper-activated IMAC SELDI chips (Figure 6.7).

An internal calibrant was used for the accurate determination of size and as an indicator of abundance (Figure 6.8). When the samples were mixed with this internal calibrant, peaks were still visible which would suggest that a notable level of protein was detectable in all samples (Figure 6.9). Despite this, a species in the region of an m/z 8925 was not identified.

Using colorectal serum, the MALDI technique was optimised. The most effective matrix was selected; SPA was found to ionise more efficiently than α-Cyano-4-hydroxycinnamic acid (CHCA), and the most effective method of mixing matrix and sample for best co-crystallisation was also chosen. The chosen method involved layering the sample between matrix. This optimisation also allowed for a high volume of test serum to be used each time, thus avoiding wasting valuable melanoma serum. However, it was found that although a reasonably clear spectrum of protein could be generated (Figure 6.10), successful fragmentation of proteins to peptides was not achieved.

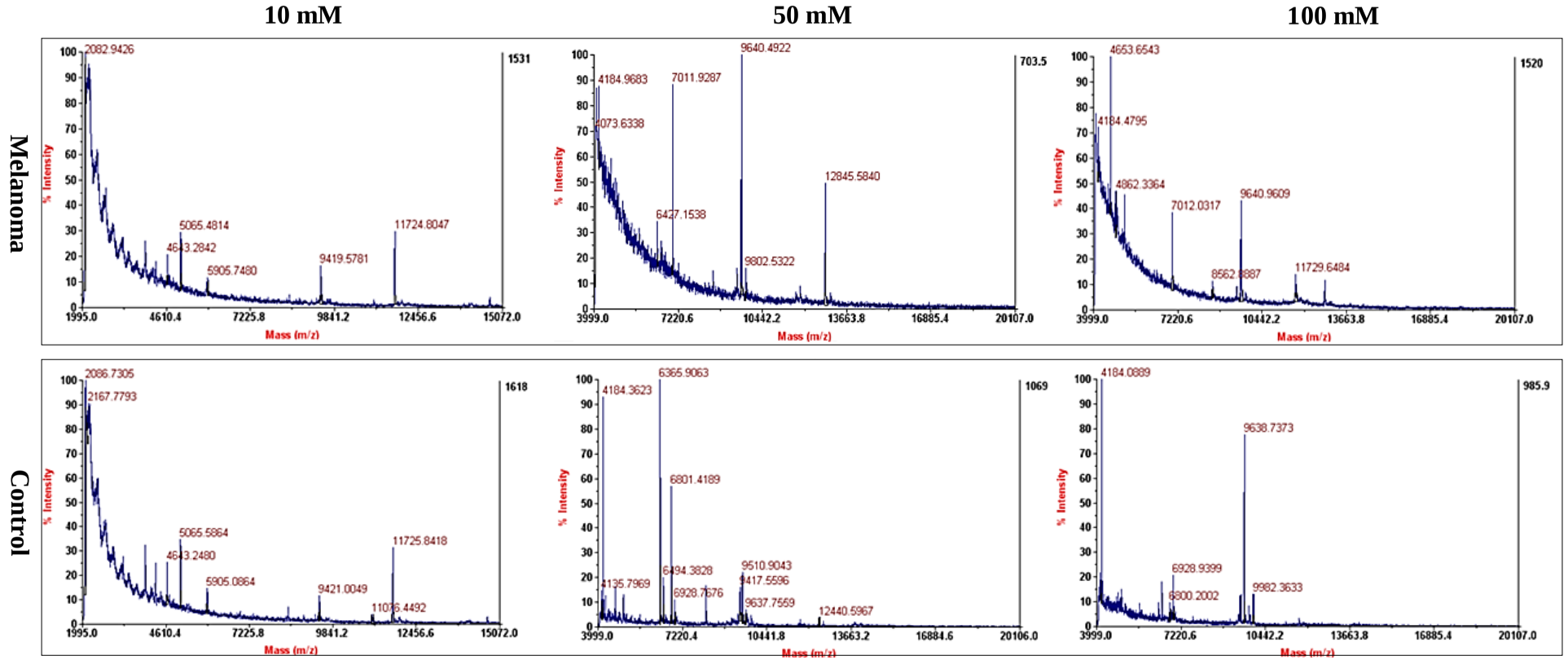

Figure 6.7 MALDI-TOF spectra of control and advanced cutaneous melanoma sera which had been eluted from IMAC resin with 10 mM, 50 mM and 100 mM imidazole. Each elution fraction was analysed by MALDI for the detection of a peak at 8.9 kDa. Due to the imidazole present in each sample, particularly those with high concentrations, as well as the low protein quantities available, a high abundance of interference and small protein peaks were noted.

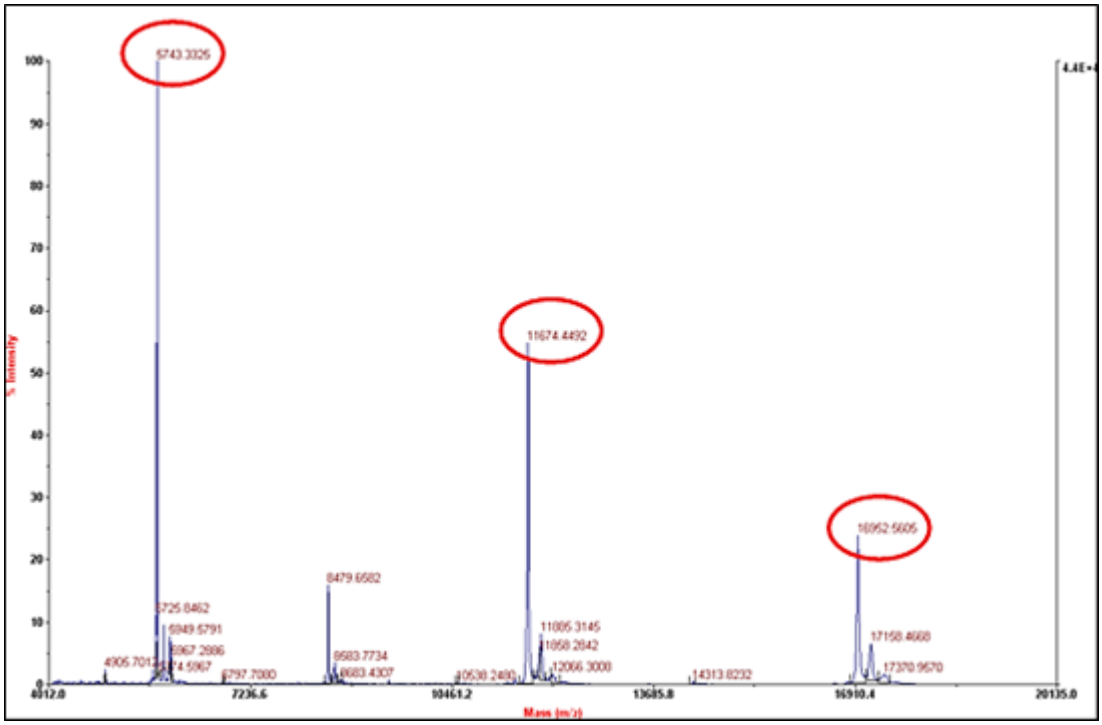

Figure 6.8 MALDI-TOF spectra of a set of internal calibrants used for determination of protein mass and as an indicator of abundance. The following proteins circled in red were included due to their low molecular weights; insulin (5734 m/z), thioredoxin (11674 m/z), apomyoglobin (16952 m/z).

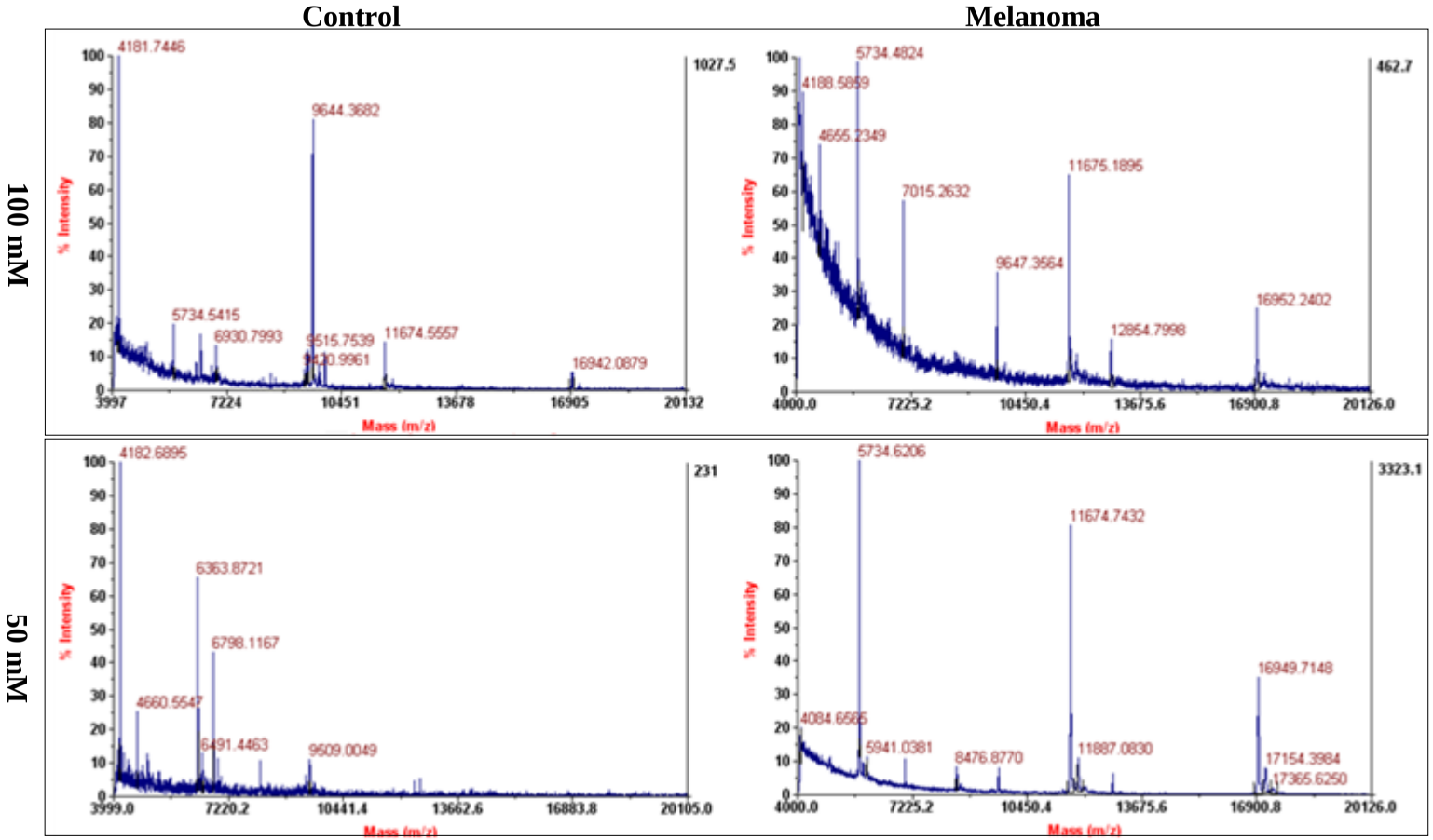

Figure 6.9 MALDI-TOF spectra of control and advanced cutaneous melanoma sera which were combined with internal calibrant. This identified peaks from the sample which indicates that protein was detectable at relatively low levels.

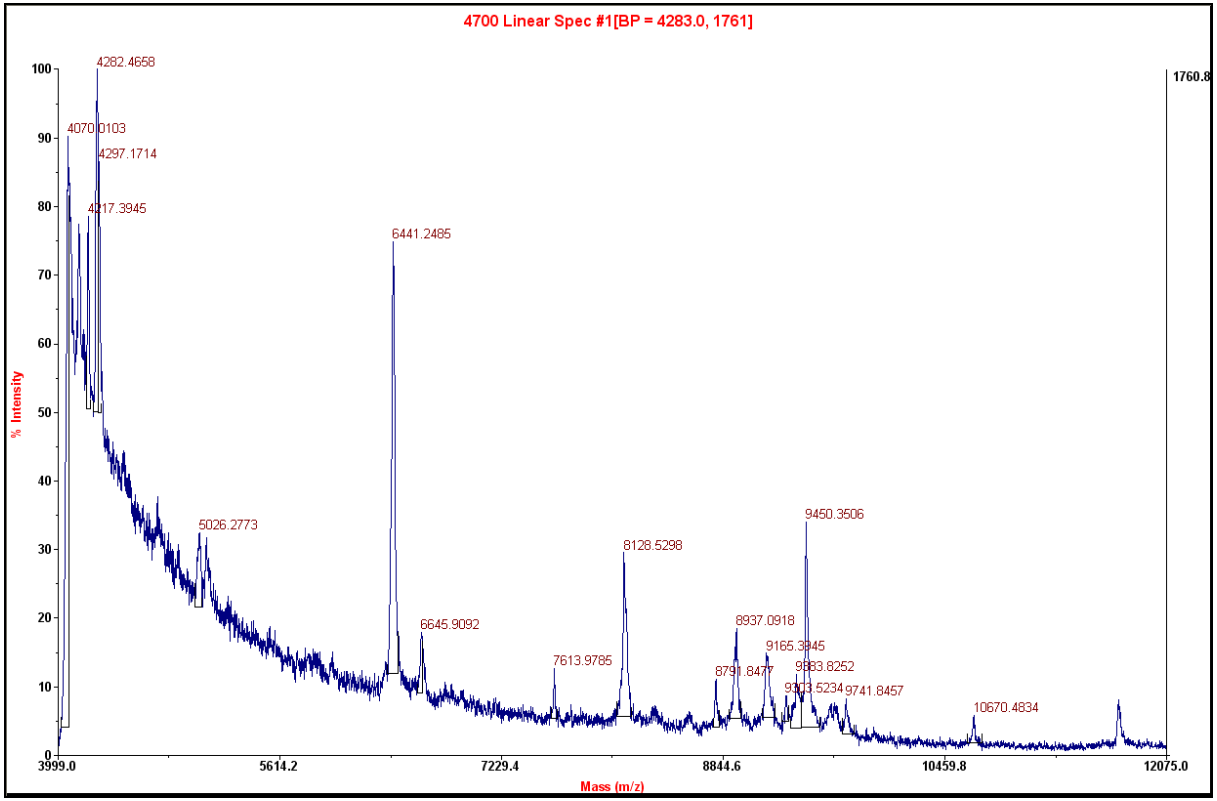

Figure 6.10 MALDI-TOF spectrum of colorectal serum following elution from IMAC resin by imidazole for the optimisation of MALDI conditions. A high volume of serum was allowed to bind to the chip prior to elution. This, along with a reduced imidazole concentration of 100 mM, provided a good spectrum of peaks. Despite this, the fragmentation of proteins to peptides was unsuccessful.

6.9 Quantitative Analysis of Proteins Eluted Directly From IMAC Chips

As the IMAC analysis which originally identified the 8.9 kDa protein of interest was carried out using SELDI chips, it was decided to repeat this procedure by binding and subsequently eluting proteins from the chip. Quantitative LC-MS would then be used for the identification of differentially expressed proteins between control and disease sera which would hopefully identify potential 8.9 kDa candidates.

Two cutaneous melanoma sera and two control sera were incubated on copper-activated IMAC chips. Any bound proteins were subsequently eluted from the chips using 250 mM imidazole. The fractions were then in-solution digested with trypsin and Lys-C to generate peptides which were analysed by quantitative label-free LC-MS/MS.

Apolipoprotein AII was identified as being significantly upregulated in the cutaneous melanoma serum samples in comparison to the controls by 2.46-fold (Figure 6.11). Although the protein is known to have a molecular weight of 17.38 kDa, it has been reported in the literature as having numerous isoforms, one of which occurs at 8.9 kDa and has been identified by SELDI-TOF at approximately 8.9 km/z (Malik, Ward et al. 2005). This suggested that apolipoprotein AII may have been the 8.9 kDa marker of interest which had previously been observed in the SELDI data.

(a)

(b)

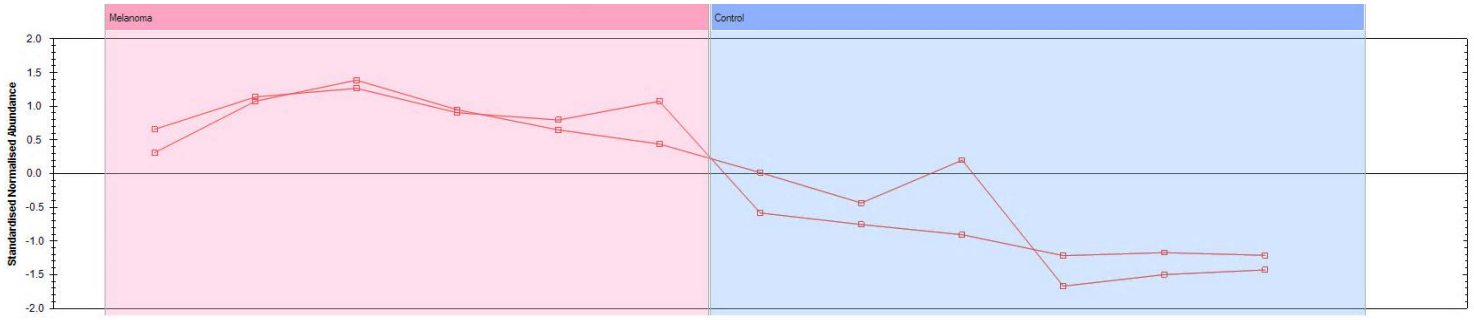

Σ	#	Score	Anova (p)	Max Fold Change	Highest Mean	Lowest Mean	Abundance	m/z	Charge	Retention Time	Mass error (ppm)	Peptide Sequence	Modifications
•	138	75.84	0.00606	2.04	Melanoma	Control	1.066E+04	1175.5452	2	54.384	-3.28	EPCVESLVSQYFQTVTDYGK	
•	572	56.13	0.000125	6.66	Melanoma	Control	3492	1257.146	2	59.767	-2.98	KAGTELVNFLSYFVELGTQPATQ	

Figure 6.11 Quantitative label-free LC-MS determined a significant quantitative difference (p-value=1.97x10^{-3}) in apolipoprotein AII expression between control (n=2) and advanced cutaneous melanoma (n=2) serum samples, each with three technical replicates. Apolipoprotein AII has been reported as an 8.9 kDa isoform in the literature which suggests that it might be the identity of the unknown SELDI peak of interest (a) Standard expression profile for apolipoprotein AII. (b) The peptide measurement view illustrates two peptides for apolipoprotein AII, illustrated by lines, and their abundance across all samples, each illustrated by a point. The accompanying table shows a maximum increase in apolipoprotein AII expression of 6.66-fold, observed in the disease sample set.

This result was further examined using ELISA and western blotting. The ELISA results are shown in Figure 6.12; however, this did not demonstrate an increase in apolipoprotein AII abundance in advanced cutaneous melanoma serum in comparison to the control serum. In addition to this, benign and early stage sera from cutaneous melanoma patients were included which did not illustrate significant differential expression of the protein when compared to the control experimental group. Also, no significant differences in abundance of apolipoprotein AII were noted between control serum and serum of uveal melanoma patients.

A western blot of control and advanced cutaneous melanoma serum was also carried out; however, this was unsuccessful in producing information on the abundance of apolipoprotein AII. This may have been due to the difficult nature of carrying out western blots using serum.

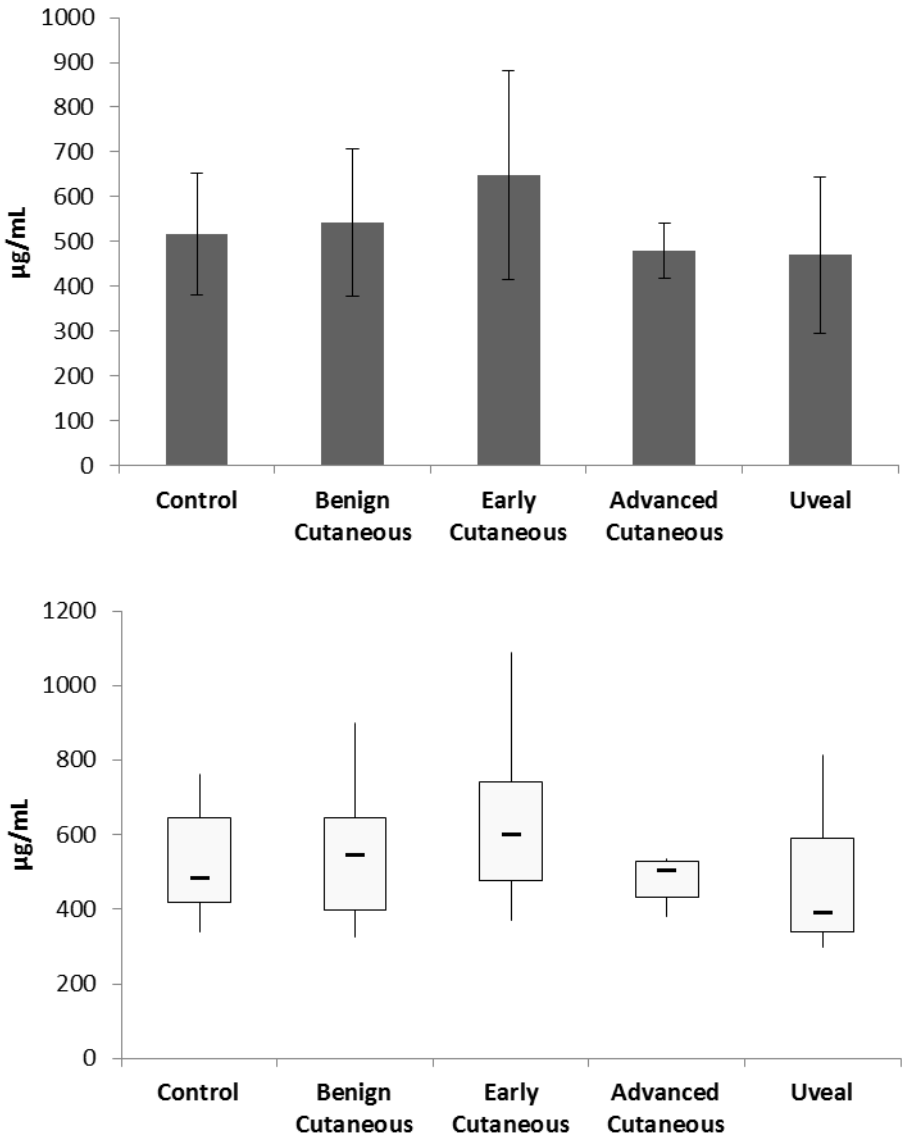

Figure 6.12 Apolipoprotein AII ELISA represented by both bar chart and Box and Whisker Plot. Serum samples from a variety of melanoma conditions were used; benign cutaneous melanoma (n=14), early-stage cutaneous melanoma disease (n=11), advanced-stage cutaneous disease (n=11), and uveal melanoma (n=11), as well as control serum (n=15). No significant difference in expression of apolipoprotein AII was observed between the control and the experimental groups.

It was decided to repeat the quantitative LC-MS experiment using IMAC resin contained in spin columns to fractionate a larger sample set.

One fraction of 250 mM imidazole was used to elute bound proteins and subsequently digest them using Lys-C and trypsin. Generated peptides were separated over the course of a three-hour gradient. The resulting data was analysed with Progenesis LC-MS to check for the presence and expression of apolipoprotein AII in a larger pool of samples.

Although apolipoprotein AII was identified in the analysis, it was found to be overexpressed in the control specimens in comparison to the disease sera (Table 6.2). This directly contradicts the previous result and dismisses the possibility of apolipoprotein AII as the identity of 8.9 kDa SELDI peak.

	Protein Name	Accession No.	Molecular Weight (Da)	No. Peptides Matched	Score	Anova (p)	Fold	Average Normalised Abundances	
								Control	Cutaneous Melanoma
Down in Cutaneous Melanoma	Apolipoprotein B-100	P04114	515605	25	1369.54	1.11E-03	1.65	6.67E+06	4.05E+06
	Serum paraoxonase/arylesterase 1	P27169	39731	1	62.88	0.02	1.57	1.59E+06	1.01E+06
	Serum albumin	P02768	69367	2	108.52	0.01	1.7	1.11E+06	6.57E+05
	Lumican	P51884	38429	1	71.6	0.02	1.44	7.70E+05	5.33E+05
	Gelsolin	P06396	85698	2	69.8	1.28E-03	1.65	5.39E+05	3.27E+05
	Undifferentiated embryonic cell transcription factor 1	Q5T230	36439	1	36.16	0.03	1.59	3.47E+05	2.19E+05
	Ig heavy chain V-III region WEA	P01763	12256	1	61.22	0.01	1.7	2.29E+05	1.35E+05
	Selenoprotein P	P49908	43174	3	140.08	8.52E-04	2.09	1.73E+05	8.29E+04
	Complement C4-A	P0C0L4	192785	1	51.32	0.03	1.88	1.56E+05	8.32E+04
	C4b-binding protein alpha chain	P04003	67033	1	62.03	0.02	1.77	1.36E+05	7.69E+04
	ATP-binding cassette sub-family F member 1	Q8NE71	95926	1	39.22	0.04	2.37	1.19E+05	5.02E+04
	Alpha-2-HS-glycoprotein	P02765	39325	2	77.02	4.88E-03	2.15	9.08E+04	4.22E+04
	Ig kappa chain V-II region Cum	P01614	12676	1	36.33	0.02	1.74	5.20E+04	2.99E+04
	Apolipoprotein A-II	P02652	11175	1	44.77	0.02	1.61	4.03E+04	2.50E+04
	Polymeric immunoglobulin receptor	P01833	83284	1	32.22	0.02	3.33	1.96E+04	5894.59
	Inter-alpha-trypsin inhibitor heavy chain H2	P19823	106463	1	42.99	0.02	1.69	1.84E+04	1.09E+04
	Conserved oligomeric Golgi complex subunit 7	P83436	86344	1	33.78	0.01	2.15	1.20E+04	5593.08
	Histidine-rich glycoprotein	P04196	59578	1	51.98	0.02	1.48	1.17E+04	7861.71
Up in Cutaneous Melanoma	Alpha-1-antichymotrypsin	P01011	47651	2	100.7	8.69E-04	2.55	6.60E+05	1.68E+06
	Complement component C9	P02748	63173	2	92.97	2.17E-03	2.48	1.42E+05	3.52E+05
	Pregnancy zone protein	P20742	163863	1	69.78	6.58E-03	2.92	7.89E+04	2.31E+05
	Inter-alpha-trypsin inhibitor heavy chain H3	Q06033	99849	1	42.36	9.40E-03	2.09	6.22E+04	1.30E+05
	Corticosteroid-binding globulin	P08185	45141	1	38.69	0.04	1.52	3.74E+04	5.67E+04
	Ig gamma-2 chain C region	P01859	35901	1	44.63	0.03	2.28	2.84E+04	6.49E+04
	Neutrophil defensin 1	P59665	10201	2	94.66	2.45E-04	11.7	2.04E+04	2.39E+05

Up in Cutaneous Melanoma	Leucine-rich alpha-2-glycoprotein	P02750	38178	2	97.05	5.90E-03	8.82	1.93E+04	1.70E+05
	Hyaluronan-binding protein 2	Q14520	62672	1	32.14	0.03	1.59	1.08E+04	1.72E+04
	Insulin-like growth factor-binding protein 4	P22692	27934	1	47.93	7.35E-03	2.8	9349.14	2.62E+04
	Scavenger receptor cysteine-rich type 1 protein M130	Q86VB7	125,451	1	60.94	1.95E-03	2.55	6153.44	1.57E+04
	Fibrinogen gamma chain	P02679	51512	1	39.06	0.03	5.88	5287.81	3.11E+04
	Alpha-1-antitrypsin	P01009	46737	2	80.22	3.24E-04	8.6	4608.47	3.96E+04
	von Willebrand factor	P04275	309265	2	93.69	1.16E-03	19.01	3177.58	6.04E+04
	Ig heavy chain V-I region V35	P23083	13009	1	43.22	0.05	21.96	1925.97	4.23E+04
	Complement C1r subcomponent	P00736	80119	1	53.29	0.01	358.1	194.18	6.95E+04

Table 6.2 The quantitative label-free LC-MS analysis of larger control (n=13) and cutaneous melanoma sample sets (n=13) was used to determine the possibility of apolipoprotein AII as the 8.9 km/z species observed during SELDI analysis. This did not confirm the upregulation of the protein in the disease specimens; however it did generate 33 other differentially expressed proteins, all of which illustrated a *p*-value of ≤0.05 between experimental groups. These differentially regulated proteins may be further followed up as potential biomarkers for cutaneous melanoma disease progression.

This analysis provided a list of 34 statistically significant proteins which were found to be differentially expressed between control and cutaneous melanoma serum samples. Of these, 16 proteins were found to be upregulated in the disease sample set while 18 showed a decreased abundance compared to controls. The chromatography of the samples was clear, with good overlap of total ion chromatograms (TIC) between samples. Protein principal component analysis (PCA) is shown in Figure 6.13. This illustrated good separation of protein abundances between the control and disease sample sets.

Many of the proteins which were differentially expressed demonstrate potential as possible serum biomarkers for advanced cutaneous melanoma. For example, alpha 1 antichymotrypsin was found to upregulated in cutaneous melanoma serum by 2.55-fold (Figure 6.14). This has previously been associated with poor prognosis in malignant melanoma as well as in other cancers, such as prostate cancer, where it is complexed to prostate-specific antigen (PSA) (Martinez, Espana et al. 2002, Wang, Jiang et al. 2010). Immune- and inflammation-related proteins such as neutrophil defensin-1, scavenger receptor cysteine-rich type 1 protein M130 and complement component C9 (Figure 6.15) were also found to be significantly upregulated in cutaneous melanoma serum.

A summary of all of the methods used in the attempted identification of the 8.9 kDa protein of interest are outlined in Figure 6.16.

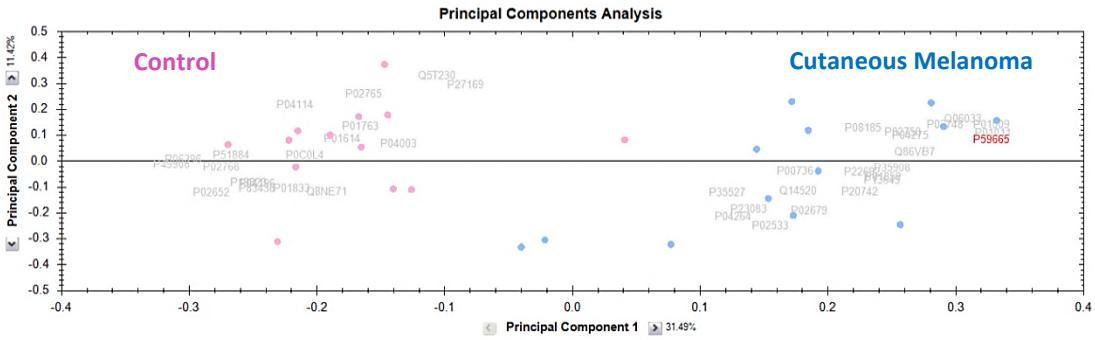

Figure 6.13 Principal component analysis (PCA), generated by Progenesis LCMS, illustrating the separation of protein abundances between the control (n=13) and advanced cutaneous melanoma (n=13) sample sets.

Figure 6.14 Alpha 1 antichymotrypsin was found to upregulated in cutaneous melanoma serum (n=13) in comparison to control serum (n=13) by 2.55-fold, *p*-value=8.69×10^{-4} (a) Normalised abundance view of alpha 1 antichymotrypsin expression in melanoma serum. Each point corresponds to a sample and illustrates the quantity of the protein of interest per specimen. (b) Normalised abundance of two identified alpha 1 antichymotrypsin peptides identified. Each line represents a peptide while each point indicates the abundance of the peptide per sample.

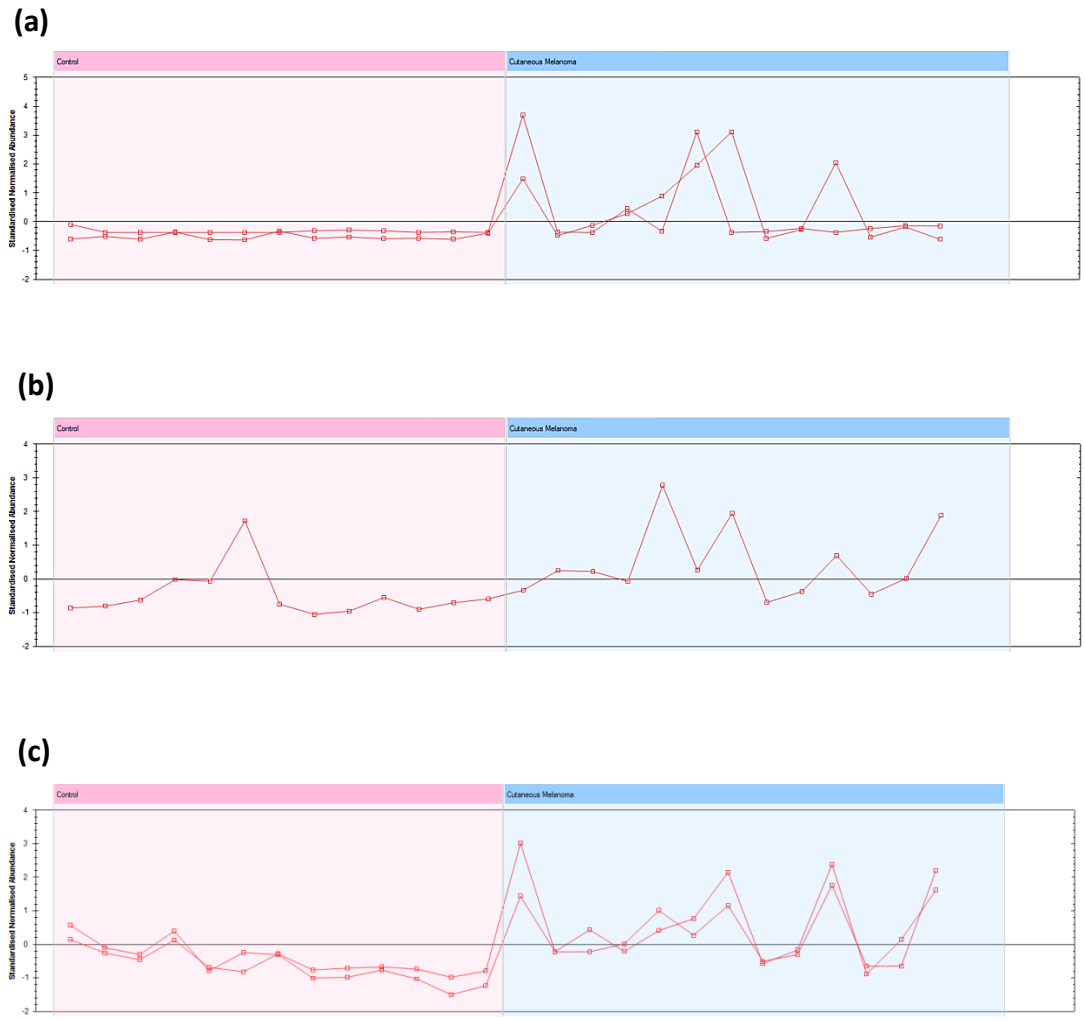

Figure 6.15 (a) Neutrophil defensin-1 (p-value=2.45x10^{-4}), (b) scavenger receptor cysteine-rich type 1 protein M130 (p-value=1.95x10^{-3}), and (c) complement component C9 (p-value=2.17x10^{-3}) were all found to be upregulated in cutaneous melanoma serum (n=13) in comparison to control serum (n=13) by maximum fold values of 11.7, 2.55, and 2.48, respectively. Each line represents a peptide while each point indicates the abundance of the peptide per sample.

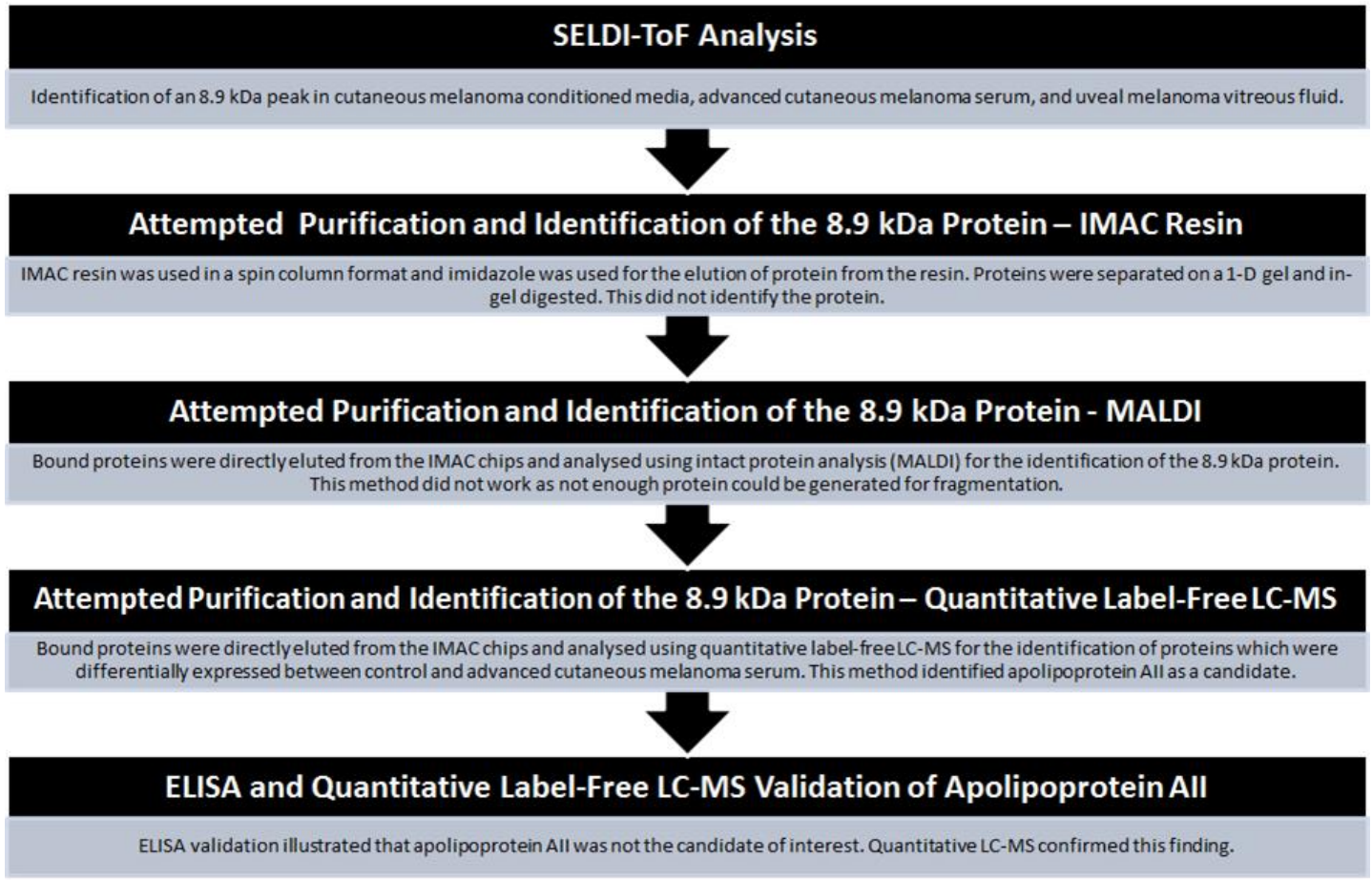

Figure 6.16 Timeline showing the steps taken in the attempted identification of the 8.9 kDa protein.

6.10 Enrichment Analysis of Differentially Regulated Protein Lists Using DAVID

It was decided to use DAVID to determine significant enrichment of biological processes, molecular functions, and cellular compartments associated with the list of proteins identified as being differentially expressed between the control and disease sample sets. Enrichment was considered to be significant when the Bonferroni p-value adjustment was ≤ 0.05. Lists of proteins upregulated in either the control or the melanoma specimens were analysed individually.

For the list of proteins which were downregulated in the cutaneous melanoma sample set in comparison to the control, the identifications related to extracellular regions of the cell (Table 6.3 (a)), with molecular functions based on the inhibition of enzymatic activity (Table 6.3 (b)).

Of the list of proteins upregulated in cutaneous melanoma specimens, enriched biological processes involved a response to trauma, such as inflammation and blood coagulation (Table 6.4 (a)). This may be due to the advanced stage of the tumour where it induces damage as a result of its aggressive, invasive behaviour. Cellular compartments associated with the protein list were all extracellular (Table 6.4 (b)). Molecular functions which were enriched primarily involved anti-enzyme activities. This inhibition may be an anti-tumour response as the inhibition of endopeptidases has been associated with suppressed growth of tumour cells (Suzuki, Sakaguchi et al. 2013). In addition to the above, it was found that the complement pathway was affected in by the upregulation of multiple proteins in the disease proteome; complement C1r subcomponent, complement component 9, fibrinogen gamma chain, von Willebrand factor, and alpha-1-antitrypsin (Figure 6.17).

The 16 proteins upregulated in the disease samples may now be followed up as potential identifications for the 8.9 kDa protein of interest as it is possible that it may be a fragment or an isoform of one of these 16. All 34 differentially expressed proteins can also be further examined as possible biomarkers for advanced cutaneous melanoma.

(a)

Cellular Compartment	Count	*p*-value	Adjusted *p*-value
Extracellular region	14	2.70E-09	2.20E-07
Extracellular region part	9	3.90E-06	3.20E-04
Extracellular space	8	5.40E-06	4.40E-04

(b)

Molecular Function	Count	*p*-value	Adjusted *p*-value
Enzyme inhibitor activity	5	1.10E-04	1.10E-02
Endopeptidase inhibitor activity	4	3.60E-04	3.40E-02
Peptidase inhibitor activity	4	4.20E-04	4.00E-02

Table 6.3 GO cellular compartment (a) and molecular function enrichment (b) for differentially expressed proteins which were downregulated in the cutaneous melanoma sample set in comparison to the control. Enrichment was considered significant upon observation of a p-value ≤0.05 and a Bonferroni adjusted p-value ≤0.05. Count corresponds to the overlap between proteins on the list and a particular GO category.

(a) Biological Process	Count	*p*-value	Adjusted *p*-value
Response to wounding	8	6.70E-07	9.90E-05
Acute inflammatory response	5	3.30E-06	4.90E-04
Inflammatory response	6	1.90E-05	2.80E-03
Defence response	7	3.00E-05	4.50E-03
Blood coagulation	4	1.80E-04	2.60E-02
Coagulation	4	1.80E-04	2.60E-02
Hemostasis	4	2.10E-04	3.10E-02
(b)			
Cellular Compartment	**Count**	***p*-value**	**Adjusted *p*-value**
Extracellular region	16	8.50E-13	3.10E-11
Extracellular region part	8	5.00E-05	1.80E-03
Extracellular space	7	7.60E-05	2.70E-03
(c)			
Molecular Function	**Count**	***p*-value**	**Adjusted *p*-value**
Serine-type endopeptidase inhibitor activity	5	1.10E-06	4.50E-05
Endopeptidase inhibitor activity	5	6.90E-06	2.80E-04
Peptidase inhibitor activity	5	8.50E-06	3.40E-04
Enzyme inhibitor activity	5	7.90E-05	3.20E-03

Table 6.4 GO biological process (a), cellular compartment (b), and molecular function (c) enrichment for differentially expressed proteins which were upregulated in advanced cutaneous melanoma sera compared with control sera. Enrichment was considered significant upon observation of a p-value ≤0.05 and a Bonferroni adjusted p-value ≤0.05. Count corresponds to the overlap between proteins on the list and a particular GO category.

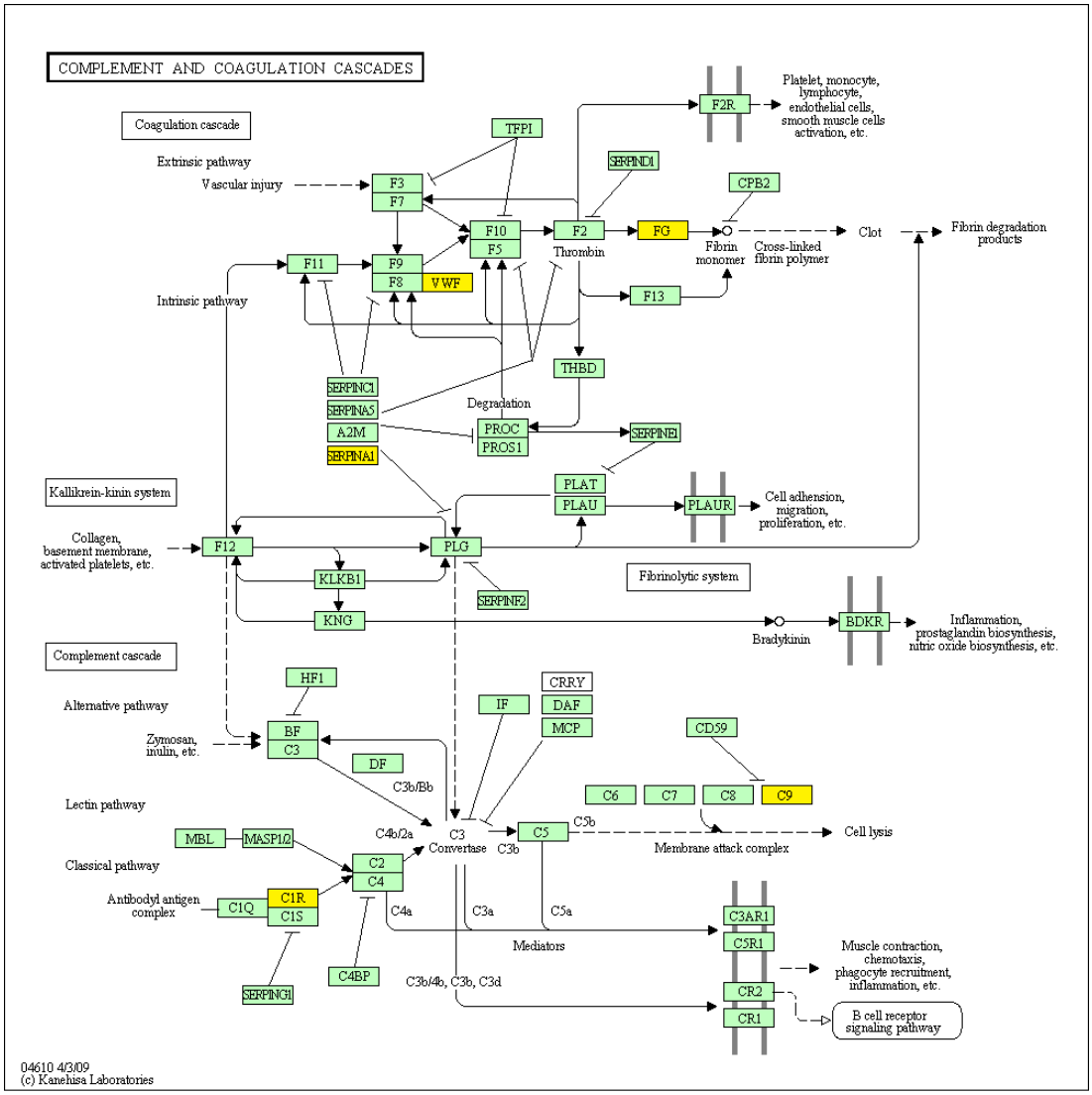

Figure 6.17 DAVID analysis of proteins which were upregulated in advanced cutaneous melanoma sera found that five identifications; complement C1r subcomponent, complement component 9, fibrinogen gamma chain, von Willebrand factor, and alpha-1-antitrypsin, were involved in complement and coagulation cascades. The genes which are involved are highlighted in yellow.

CHAPTER SEVEN

Discussion

7.1 Introduction

Although uveal melanoma is a rare malignancy of the uveal tract; the iris, the choroid, and the ciliary body, it is the most common intraocular malignancy in adults. The overall incidence of uveal melanoma is 5-7 cases per million per year with this number increasing to 20 per million per year after the age of 70. The majority of uveal melanomas develop in the choroid while the remainder (8%) arise in the iris and ciliary body. (Damato 2012, Ramasamy, Murphy et al. 2013).

Substantial advances have been made in the diagnosis and local therapy of uveal melanoma over the past number of decades. The primary clinical diagnosis of uveal melanoma regularly initially involves reduced visual awareness, retinal detachment, and scotoma. Slit lamp biomicroscopy is also used to identify a tumour, while ultrasound investigation can be utilised to determine acoustic hollowness. With treatment, uveal melanoma has a five-year survival rate of 77-84%. Enucleation was the traditional method of treatment, however radioactive plaque brachytherapy, proton beam therapy, and local resection can also be used for the treatment of the primary tumour while maintaining the eyeball (Abildgaard and Vorum 2013).

However, uveal remains classified as a high risk disease in the case of metastasis which occurs in up to 50% of patients. In the majority of cases, uveal melanoma spreads preferentially to the liver; a generally fatal metastasis within 15 months. Currently, metastasis is rarely detected at primary diagnosis, despite thorough investigations, and often develops in the subsequent months and years. Although the risk of metastasis may be predicted by chromosomal testing (monosomy of chromosome three and gain of chromosome eight are both indicative of poor prognosis), cell type (epithelioid tumours are more aggressive than those of spindle cell type), and molecular screening (BAP1 mutations occur late in the disease and signify a high likelihood of metastasis occurring) there is currently no effective treatment for metastatic uveal melanoma (Harbour 2012, Yonekawa and Kim 2012, Ramasamy, Murphy et al. 2013).

Protein biomarkers indicative of prognosis could further our understanding of the biology of uveal melanoma, and could lead to the development of rational therapies which target differentially regulated proteins specific to the disease. Such biomarkers, together with complementary genetic information, may also potentially

aid in determining a prognosis in a clinical setting when monitoring patients who are at risk of metastasis.

Cutaneous melanoma is a malignancy of skin melanocytes. Despite accounting for only 4% of all skin cancer cases, it is the form of skin cancer which has the highest death toll in the USA and Europe (Ugurel, Utikal et al. 2009). It is widely accepted that cutaneous melanoma risk is determined through genetic factors and exposure to sunlight; 80% of melanomas develop in areas which receive intermittent sun exposure or have a history of sunburn (Garbe and Leiter 2009).

Primary cutaneous melanomas are characterised by horizontal growth within the epidermis only. When melanoma is detected and treated prior to the development of lymph node metastasis, the five-year survival rate is 99%. If the malignancy develops and becomes more aggressive, it can lead to rapid growth and invasion of the dermis. Later stages of the disease are associated with rapid invasion and metastasis of tissues other than the dermis; the five-year survival rate for distant stage melanoma patients is approximately 15% (Al-Ghoul, Bruck et al. 2008).

Surgical removal of the tumour is the standard of care for primary cutaneous melanoma, often coupled with high-dose interferon therapy. Systemic metastatic melanoma was traditionally difficult to treat, with poor outcome, as therapies beyond surgery were very toxic. In addition to this, melanoma has been traditionally been recognised as difficult to treat, mainly due to the large number of patients who are resistance to immune therapy as well as chemotherapy (Mehnert and Kluger 2012). New therapeutic strategies such as anti-PDI1 antibodies (such as ipilimumab), BRAF inhibitors (such as vemurafenib or dabrafenib), c-Kit inhibitors, and MEK inhibitors have illustrated significant anti-tumour effects, improving patient survival times and response rates.

To date, few protein biomarkers have been identified as prognostic indicators of cutaneous melanoma and even less are used in the clinic as tools for diagnosis or prognosis. However, lactate dehydrogenase (LDH), melanoma inhibitory activity protein (MIA) and S-100 beta protein (S100B) are currently recognised as seriological markers for the disease.

Better prognostic and predictive markers in cutaneous melanoma are needed, but to date have been elusive. The experimental work detailed here was intended to further understand the cutaneous melanoma serum proteome over the course of disease progression. Therefore, this work could lead to the development of a prognostic test which could easily be used in a clinical setting and could also potentially lead to the discovery of a therapeutic target in cutaneous melanoma.

Both cutaneous and uveal melanoma originate in melanocytes, albeit, their clinical behaviours and molecular mechanisms differ significantly. The differences between both melanomas are poorly understood, albeit, it was hoped that the proteomic analyses of the nature of melanoma as a disease would aid in understanding variations between both melanomas and further our understanding of metastasis.

One aim of this thesis was to identify proteins which were differentially expressed between primary uveal melanoma tumour tissue which metastasised and that which did not. This work could improve our understanding of the biology of uveal melanoma tumours which subsequently metastasise through the identification of potential biomarkers. Such proteins could eventually be developed as targets for rationally designed therapies in the treatment of uveal melanoma, and could, along with genetic information, predict the outcome of the disease. It was also intended to study the vitreous fluid collected from uveal melanoma patients in order to identify unique proteins of interest for the same purposes. In the process of this, an ocular fluid sample preparation method could be developed. The study could also improve our overall understanding of the vitreous proteome. Finally, it was hoped to better understand the proteomic changes which occur throughout the course of cutaneous melanoma disease progression. It was anticipated that this may illustrate potential proteins biomarkers for disease progression in serum, a sample which is minimally invasive to collect and so, could easily be extracted for an assay in a clinical environment.

Throughout this work, there were a number of shortcomings. For example, due to the rarity of uveal melanoma, few primary tumour tissue and vitreous specimens were available. Although cutaneous melanoma is not as rare, few samples were also available. Hence, this work was part of a discovery phase, pilot study. In addition to this, no metastasised uveal melanoma tumour tissue was available for analysis.

There were also a number of strengths of the studies carried out. The availability of rare clinical specimens with at least seven years of follow up was a clear advantage of this work. Also, the involvement of experienced pathologists was useful in determining clinical questions of interest.

7.2 2-D DIGE and Quantitative Label-Free LC-MS Analysis of Uveal Melanoma Tumour Tissue

Biological fluids are considered to be a good source of biomarkers as they are easily accessible and minimally invasive, are relatively cheap to obtain, and can be potentially used for the development of large-scale, prognostic/diagnostic tests (Good, Thongboonkerd et al. 2007).

However, in order to detect tissue specific biomarkers, i.e. proteins directly produced by the tumour, in biological fluid, the target must first be secreted by the tissue. It must also be recognised as disease tissue-specific, which may be difficult as there are a variety of secreted proteins circulating at any one time (Shiwa, Nishimura et al. 2003).

Hence, it may be more efficient to first identify a tumour-specific protein biomarker directly from the tissue and subsequently detect it in fluids such as serum.

7.2.1 Identification of Differentially Expressed Proteins between Non-Metastasised and Subsequently Metastasised Primary Tumour Tissue Using 2-D DIGE

It was decided to compare 16 non-metastasised uveal melanoma primary tumour tissues and nine primary tissues which subsequently metastasised in order to better our understanding of uveal melanoma metastasis through the identification of differentially expressed disease-specific biomarkers. In order to identify differentially regulated proteins, a 2-D DIGE analysis of primary uveal melanoma tumour tissue was carried out.

From this analysis, 14 statistically significant differentially expressed proteins were identified, which agreed with the hypothesis that stated that patterns of differential

protein expression would be observed between both disease states. Protein disulphide-isomerase A3 precursor (PDIA3), selenium-binding protein 1 (SELENBP1), alpha-enolase, F-actin capping protein subunit alpha-1 (CAPZA1), endoplasmic reticulum protein ERp29 precursor, triosephosphate isomerase (TPI1), protein DJ-1 (PARK7), and fatty acid-binding protein, heart-type (FABP3) were all found to be upregulated in subsequently metastasised primary tissue in comparison to non-metastasised tissue. Vimentin and beta-hexosaminidase subunit alpha were identified from the same protein spot which was identified as being more abundant in the metastatic proteome. Eukaryotic translation initiation factor 2 subunit 1, proteasome subunit alpha type 3, 40S ribosomal protein SA, tubulin beta chain and tubulin alpha-1B chain were shown to have decreased expression in uveal melanoma tissues of patients who subsequently developed metastatic disease.

Of these proteins, four had previously been mentioned in the literature in relation to uveal melanoma at that time; vimentin, beta-hexosaminidase subunit alpha, alpha-enolase, and 40S ribosomal protein SA.

Alpha-enolase was previously identified as being downregulated in uveal melanoma cell lines derived from secondary tumours in comparison to a primary tumour cell line which was derived from the same patient (Zuidervaart, Hensbergen et al. 2006). Alpha enolase is a metalloenzyme which is required for catalysing the conversion of 2-phospho-D-glycerate to phosphoenolpyruvate in glycolysis; a critical process in neoplastic cells (Capello, Ferri-Borgogno et al. 2011). Hence, it would be expected that an upregulation of glycolysis would be required for metastatic cells in comparison to the primary tumour cells they were derived from. Zuidervaart et al. explained that their observed result may be explained by the apparent higher growth rate of the primary tumour cell line in comparison to its metastatic counterpart. The result of our study is in agreement with previous tumour tissue studies which link an increase in alpha enolase production with metastasis through the Warburg effect; an increase in aerobic glycolysis (Altenberg and Greulich 2004, Yoshida, Okamoto et al. 2013).

The expression of vimentin intermediate filaments acts a mesenchymal marker, and is typical of melanomas. Vimentin was identified by Hendrix et al. as contributing to the metastatic phenotype of uveal melanoma. They illustrated that uveal melanoma

cell lines which co-expressed keratin and vimentin intermediate filaments were six-fold more invasive than those which expressed vimentin only and eight- to 13- fold more invasive than normal uveal melanocytes. These findings were confirmed with immunohistochemistry of tumour tissue specimens from which the uveal melanoma cell lines were derived (Hendrix, Seftor et al. 1998). Vimentin was also identified by Coupland et al. as being upregulated in uveal melanoma monosomy three tumour tissues in comparison to those which were disomy three (Coupland, Vorum et al. 2010). In our study, vimentin was found to be upregulated in subsequently metastasised primary tissue in comparison to non-metastasised tumour specimens which corresponds with the above findings, thus linking vimentin expression to metastatic potential.

Beta-hexosaminidase subunit beta is known to be required for cellular interaction with adhesion proteins, and hence play an important role in cellular motility. It was previously identified as being upregulated in uveal melanoma cell lines derived from secondary tumours in comparison to a primary tumour cell line which was derived from the same patient (Zuidervaart, Hensbergen et al. 2006). Although it was the alpha subunit which was discovered to be upregulated in the metastatic sample set in our study, beta-hexosaminidase subunit alpha has been linked with the development of metastases in cancers such as glioblastoma (He, Liu et al. 2011). This all concurs with our findings associating beta hexosamidase with metastasis.

40S ribosomal protein SA functions as a laminin receptor; thus playing a role in cell adhesion, as well as being required for the full maturation of ribosomal subunits. As cancer cells can attach to laminin, this may aid the process of metastasis. Previously, gastric cancer cells were found to express 40S ribosomal protein SA on their surface which correlated with tumour aggressiveness (de Manzoni, Guglielmi et al. 1998). It has also been shown to be overexpressed in bile duct carcinoma, colorectal carcinoma, cervical cancer, and breast carcinoma (Kumazoe, Sugihara et al. 2013). The protein was identified as being associated with uveal melanoma primary cell cultures by Pardo et al (Pardo, Garcia et al. 2006). In our study, it was found to downregulated in metastatic specimens in comparison to the non-metastatic group

7.2.1.1 Immunohistochemical Validation of Six Proteins of Interest Identified by 2-D DIGE

Following the identification of 16 differentially-regulated proteins between the metastasised and non-metastasised tissue sample sets, it was decided to follow up six proteins of interest by immunohistochemical staining of FFPE tissue; TPI1, FABP3, PDIA3, CAPZA1, PARK-7, and SELENBP1.

For PDIA3, CAPZA1, and PARK-7, the trends in expression identified by the 2-D DIGE study were not observed in the immunohistochemical analysis. There are several possible reasons for this lack of correlation. Whole tumour homogenates were used for the 2-D DIGE study in order to study total than rather localised protein expression. Also, immunohistochemistry is examining formalin-fixed, paraffin-embedded tissue, whereas the proteins for 2-D DIGE were extracted from snap-frozen tissue, stored at -80 °C prior to use.

In cases where the data from the two methods did not agree, it is not possible to determine, which result better reflects the protein expression in the tumour. However, the two very different approaches yielded concurrent results for FABP3 and TPI1, which support the differential expression of both proteins. In the case of SELENBP, little or no staining was observed in either sample set; metastasised or non-metastasised.

Protein disulfide isomerase (PDIA3) is a thiol oxidoreductase protein of the endoplasmic reticulum which is required for protein folding (Koivunen, Helaakoski et al. 1996, Garbi, Tanaka et al. 2006). In our study, it showed statistically significant differential expression in the 2-D DIGE study, with an abundance increase of 1.5-fold in the metastasised sample set in comparison to the non-metastasised group. PDIA3 has been known to play a role in oesophageal carcinoma (Qi, He et al. 2008). Its expression has been identified in the M14 melanoma cell line, and in other cancer cell lines, HeLa and Raji, where it was found to be bound to regulatory regions of the DNA, prompting the possibility of PDIA3 acting as a transcriptional regulator in non-endoplasmic reticulum regions (Aureli, Gaucci et al. 2013). On this basis, it appeared to be a promising and novel potential target for uveal melanoma. Albeit, our immunohistochemistry results directly contradicted our 2-D DIGE results, with a decreased expression observed in melanomas which

subsequently metastasised in comparison to those which did not, hence it was excluded from further analysis.

F-actin capping protein subunit alpha-1 (CAPZA1) is a cytoskeletal protein. In our differential protein expression analysis, it was found to be upregulated by 1.3-fold in subsequently metastasised uveal tissue samples. Reports on CAPZA1 in cancer are rare; it has been reported to be increased ten-fold in HPV 18-positive oral squamous cell carcinoma patients in comparison to other HPV 18-positive cancers. CAPZA1 was identified in the proteomic analysis of human gastric cancer clinical specimens, with its underexpression being associated with poor prognosis (Lee, Jeong et al. 2013). It has also been identified to be differentially expressed in renal cell carcinoma compared to normal renal cells suggesting its possible involvement in tumorigenesis (Kellner, Lichtenfels et al. 2002). In the immunohistochemical analysis of uveal melanoma tumour tissue, CAPZA1 showed an overall reduced cytoplasmic expression pattern in the majority of primary specimens that were found to have metastasised compared to those that did not. Parallel staining of sections for CAPZA1 and the histiocyte/monocyte/macrophage marker CD68 confirmed CAPZA1 positivity in both tumour cells and tumour-infiltrating macrophages, but not all of those macrophages stained positive for CAPZA1.

PARK-7, also known as DJ-1, is an oncogene which was originally cloned as a putative oncogene which could transform NIH-3T3 cells, with the cooperation of H-ras. It has since been implicated in a number of processes, such as oxidative stress, and is thought to play a role in tumorigenesis; acting as a negative regulator of the tumour suppressor PTEN. Pardo et al. identified PARK-7 as being overexpressed in uveal melanoma cell lines in comparison to normal melanocytes. They also identified the protein as being secreted as it was detected in the serum of uveal melanoma patients. We identified PARK-7 as being upregulated in subsequently metastasised primary tumours by 1.2-fold in comparison to those which remained as non-metastasised. However, an upregulation of PARK7 during metastasis was not observed in the immunohistochemical analysis.

SELENB1, TPI1, and FABP3 were selected for further analysis using *in vitro* functional studies. By using small interfering RNA (siRNA), the consequences of effectively knocking down or reducing expression of a protein of interest can be

examined in an assay of choice, hence illustrating the role of the aberrantly-expressed protein. To understand the biology of a cancer, it is often necessary to study the deviant regulation of its cellular processes; this can be carried out using cell line models. Healthy cells, lipofectamine-treated cells, negative control cells, and cells transfected with two independent siRNA were included for each experiment, and the effects of the knockdown are measured by comparing the downregulated cells to the negative control.

7.2.2 TPI1

Triosephosphate isomerase (TPI1) was identified twice with an 1.6- and 1.7-fold upregulation in uveal melanoma samples of patients who subsequently developed metastatic disease, immunohistochemical analysis also showed a trend for upregulation of TPI1 in uveal melanomas which did metastasise. The double identification of TPI1 as an upregulated protein is very likely due its isoforms (Snapka, Sawyer et al. 1974, Kester and Gracy 1975).

The glycolytic enzyme TPI1 catalyses the conversion of dihydroxyacetone phosphate to glyceraldehyde 3-phosphate (Albery and Knowles 1976), and a high rate of glycolysis is required to support tumour growth (Bui and Thompson 2006). TPI1 has previously been shown to be expressed in uveal melanoma primary cell cultures (Pardo, Garcia et al. 2005).

As the 2-D DIGE and immunohistochemistry results both illustrated that TPI1 was upregulated in subsequently metastasised primary tumour tissue, our proteomics study provided evidence that TPI1 may have been involved in the development of the metastatic phenotype in uveal melanoma. Hence, it was decided to follow up TPI1 with functional analysis to further understand its role.

Abnormal proliferation is required for tumorigenesis, as cancer involves the accumulation of clonal cells. The reduction in tumour cell number, or tumour burden, is often the goal of current cancer therapies. Hence, a better understanding of the key proteins behind abnormal cell proliferation in a cancer could aid the development of more effective targets for therapies (Andreeff 2000). Following the siRNA-mediated downregulation of TPI1 in the 92.1 uveal melanoma cell line, an

acid phosphatase assay was carried out which demonstrated that no extensive effect on proliferation was observed *in vitro* when the two independent siRNA transfections per target were compared against the negative control. However, when the MEL202 uveal melanoma cell line was transfected, a prominent significant decrease in proliferation was noted between the negative control and the transfected cells. The negative effect observed may have been due to the cell line rather than the knockdown of TPI1 as no comparable effect was seen in the 92.1 uveal melanoma cell line. Hence, any subsequent functional assays involving TPI1 were carried out only in the 92.1 cell line.

Invasion and migration of cancer cells allow them to enter the blood or lymphatic system to grow at distant locations to the primary tumour in a process called metastasis. By 'knocking-down' expression, a role in migration and/or invasion of cancer cells can be elucidated. For the TPI1 siRNA-transfected 92.1 cells, a largely significant reduction of both invasion and migration was observed *in vitro* when compared with the negative control.

As TPI1 was identified as being upregulated in subsequently metastasised uveal melanoma tumour tissue in comparison to that which did not metastasise, a result that was confirmed by immunohistochemistry, as well as apparently being involved in the invasiveness and motility of the uveal melanoma cells, it appears to be implicated in the aggressive nature of the metastasised disease. It may be possible to target TPI1 for the inhibition of glycolysis and inhibit the Warburg effect as a therapeutic strategy for uveal melanoma metastasis. The approach of using glycolytic inhibitors as anticancer drugs has been examined as a potential therapeutic strategy and has been experimentally applied to other cancers, such as colon cancer, leukaemia and lymphoma cell lines (Xu, Pelicano et al. 2005, Pelicano, Martin et al. 2006).

7.2.3 FABP3

2-D DIGE analysis revealed a 2.2-fold up-regulation of fatty acid-binding protein three (FABP3) in uveal melanomas which subsequently metastasised. This trend was confirmed by immunohistochemical studies.

FABP3 is a member of a multi-gene family including nine FABPs and the cellular retinoid binding proteins. Fatty acid-binding proteins show a broad tissue distribution, and tissues can contain more than one FABP (Storch and Corsico 2008, Storch and McDermott 2009). Though FABPs are known to be involved in intracellular transport of long-chain fatty acids, their in vivo functions are poorly understood (Ockner and Manning 1974). FABP3 was shown to inhibit cell proliferation in mammary epithelial cells and the ectopic expression of FABP3 in breast cancer cells led to reduced tumorigenicity in nude mice (Yang, Spitzer et al. 1994). In contrast, positive correlations of FABP3 expression with tumour cell invasion, lymph node metastasis and poor patient survival have been found in gastric carcinomas (Hashimoto, Kusakabe et al. 2004).

As the 2-D DIGE and immunohistochemistry results correlated with an upregulation of FABP3 in relation to metastasis, and the target appeared to be novel in uveal melanoma, FABP3 was chosen for follow-up functional studies in order to further understand its potential role in metastasis.

Following the siRNA-mediated downregulation of FABP3 in the 92.1 uveal melanoma cell line, proliferation assays were carried out which demonstrated that no extensive effect was observed *in vitro* when the two independent siRNA transfections were compared against the negative control. However, when FABP3 siRNA were used to transfect the MEL202 uveal melanoma cell line, a strongly significant decrease in proliferation was noted between the negative control and the transfected cells. The negative effect observed may, again, have been due to the MEL202 cells rather than the knockdown of FABP3 as no comparable effect was seen in the 92.1 uveal melanoma cell line. Hence, any subsequent functional assays involving FABP3 were carried out only in the 92.1 cell line.

When the expression of FABP3 was reduced, a largely significant decrease in both invasion and migration was observed when compared to the negative control. This indicates that FABP3 appears to be involved in the processes of invasion and migration in uveal melanoma cells.

Overall, it appears as though FABP3 may play a role in the spread of uveal melanoma as it was upregulated in subsequently metastasised tissue and its

downregulation affected invasion and migration *in vitro*, key processes in the aggressiveness of metastatic malignancies.

7.2.4 SELENBP1

Selenium-binding protein (SELENBP1), a member of the selenoprotein family, is known to bind selenium covalently in order to mediate the intracellular transport of selenium (Zhou, Zhang et al. 2009, Zeng, Yi et al. 2013).

It has previously been suggested as a tumour suppressor as its expression is lost in several epithelial cancers (Scortegagna, Martin et al. 2009, Zeng, Yi et al. 2013). In addition to this, it has been identified as a potential marker for hepatocellular carcinoma by Di Statsio el al. They identified a decrease in SELENBP1 abundance in hepatocellular carcinoma liver tissue specimens. The gradual decrease in selenium levels correlated with an increased malignant grade, with the levels of selenium and of SELENBP1 directly correlating (M, Volpe et al. 2011).

SELENBP1 had not previously been associated with ocular cancer and hence, was considered novel in this regard. In addition to this, SELENBP1 was not typically identified as being upregulated in cancer. Although the immunohistochemistry results did not correspond with the 2-D DIGE results, it was decided to further examine the role of SELENBP1 in uveal melanoma cell lines using functional analysis.

After the downregulation of SELENBP1 in the 92.1 and MEL202 uveal melanoma cell lines, an acid phosphatase assay was carried out. This demonstrated that no extensive effect on proliferation was observed *in vitro* when the two independent siRNA transfections per target were compared against the negative control.

Following the siRNA-mediated knockdown of SELENBP1, a significant reduction of both invasion and migration was observed, in compared to the negative control. This indicates that the protein appears to be involved in the invasiveness and motility of the 92.1 cell line, and possibly also in the MEL202 cell line.

Specific invasion-related proteins, such as matrix metalloproteases (MMPs), may also be identified using zymography, an electrophoresis method by which proteases

present in a sample are detected through the digestion of a substrate-containing gel. 92.1 and MEL202 uveal melanoma cell lines were transfected with siRNA specific to SELENBP1. Conditioned media was then collected from the cells as this contained the secreted MMPs. MMP-2 and -9 are typically implicated in melanoma disease progression and have been associated with uveal melanoma metastasis (Coussens, Fingleton et al. 2002, Lai, Conway et al. 2008). Hence, gelatin-based zymography was used as this is the substrate of choice for MMP-2 and -9. In spite of this, no difference was observed between the transfected cells and the negative controls, for either cell line.

The inhibition of apoptosis is a key feature of many malignant cells as some oncogenic mutations allow for proliferating cancer cells to grow without hindrance by preventing apoptosis. Apoptosis is a tightly regulated mechanism which ensures homeostasis of all tissues and without it leading to tumour initiation, progression or metastasis. Also, mutations which suppress tumour development can affect treatment sensitivity, rendering it less effective (Andreeff 2000, Lowe and Lin 2000). 7-AAV and PE-Annexin V were used to stain DNA and exposed phosphatidyserine, respectively. Fluorescence was subsequently measured using flow cytometry which quantified the degree of apoptosis. Apoptosis was measured in cells which were transfected with siRNA specific for SELENBP1; however, no significant effect on cell death was determined.

Oxygen derived species are recognised as cytotoxic and have been implicated as carcinogens in the process of cancer. Such species may exert their effects through reactive oxygen species (ROS), which are generated during metabolism. Oxidative damage can occur in cellular DNA as a result, which can play a role in the development of various malignancies (Waris and Ahsan 2006). Selenium is an essential trace element which is involved in the function of antioxidant enzymes and proteins that protect the cell against ROS. SELENBP1 is known to bind selenium covalently in order to mediate the intracellular transport of selenium (Zhou, Zhang et al. 2009, Zeng, Yi et al. 2013). Hence, it was decided to downregulate SELENBP1 production in order to determine its potential role in terms of protection from ROS. 2',7'-dichlorofluorescein-diacetate (DCFH-DA) was used to quantify intracellular produced H_2O_2; based on the activity of peroxide, DCFH-DA is converted to a fluorescent compound, 2',7'-dichlorofluorescein (DCF), which indicates the quantity

of ROS present. Overall a visual trend of increased ROS activity was observed in the transfected cells when compared to their negative controls. However, this was not a statistically significant result. Although, the trend does illustrate what is expected, based on the literature. Zeng et al. demonstrated that the knockdown of SELENBP1 induces human bronchial epithelial cell transformation and that it is an early event in in lung squamous cell cancer (Zeng, Yi et al. 2013). This indicates a potential increase in ROS activity as a result of the downregulation of SELENBP1 which may therefore play a role in protecting uveal melanoma cells from oxidative damage.

Typically, SELENBP1 is reported as being downregulated in cancers such as in the case of colorectal cancer, ovarian cancer, lung cancer, and pleural mesothelioma (Pass, Liu et al. 2004, Huang, Park et al. 2006, Kim, Kang et al. 2006, Zeng, Yi et al. 2013). Hence, its upregulation in uveal melanoma is potentially unique and may be a novel marker for metastasis as it was found to be significantly upregulated in subsequently metastasised primary tissue. It clearly plays a role in invasion and migration *in vitro*, but is not involved in proliferation and does not exert anti-apoptotic effects. It is, however, possibly required for protection from oxidative damage.

7.3 Identification of Differentially Expressed Proteins between Non-Metastasised and Subsequently Metastasised Tissue Using Quantitative Label-Free LC-MS

2-D DIGE is a sensitive and high-throughput method for the identification of biomarkers from various sources. It is the most-widely used gel-based method for the detection of differentially regulated proteins. Mass spectrometry-based proteomic analysis has improved greatly since the last decade. The advent of label-free quantitative LC-MS has allowed for the simultaneous and accurate identification of thousands of differentially regulated proteins, even from very minute quantities, thus potentially giving a more comprehensive view of the proteome in question. This advancement has helped enormously in the identification and delivery of candidate biomarkers for cancer diagnosis, prognosis and monitoring of treatment regimen (Paul, Kumar et al. 2013).

It was therefore decided to carry out a quantitative LC-MS proteomic analysis of eight non-metastasised tumour tissues and eight which subsequently metastasised. In total, 14 of these tissues had previously been used in the 2-D DIGE differential expression experiment.

This approach also agreed with the hypothesis as 50 proteins with a minimum of three matched peptides were identified as being differentially expressed between both sample sets. Of these proteins, five were previously identified in the 2-D DIGE study. Vimentin, alpha-enolase, TPI1, beta-hexosaminidase subunit alpha, and FABP3 were all found to be upregulated in primary uveal melanoma tissue that had subsequently metastasised, which correlated with the 2-D DIGE findings.

Heat shock protein beta-1 (HSP-27) was found at a lower level in primary tissue which subsequently metastasised in comparison to primary tissue which remained as non-metastasised. This result agrees with a study previously carried out by Coupland et al. which demonstrated that HSP-27 was expressed at a lower level in monosomy three tumour tissues than in disomy three tumour specimens. Monosomy three is indicative of poor prognosis while disomy three is often suggestive of a better outcome (Coupland, Vorum et al. 2010). This finding was subsequently followed-up by Jmor et al. who illustrated that in combination with basal tumour diameter, melanoma cytomorphology and mitotic rate, the level of HSP-27 enhanced the estimation of survival probability (Jmor, Kalirai et al. 2012).

Vimentin, which was previously identified as being upregulated in the metastasised sample set in comparison to the non-metastasised group in the 2-D DIGE study, was again identified as being overexpressed in uveal melanoma monosomy three tumour tissues in comparison to those which were disomy three.

Of the 50 proteins identified by label-free quantitative LC-MS, CNDP2, PRDX3, KPNB1, and EEF1G were selected for further studies through functional analysis. These were chosen as, although some of these had previously been linked with other cancer studies, they had not been associated with uveal melanoma. In addition to this, they illustrated some of the lowest ANOVA scores of the analysis, deeming them as a number of the most significant potential targets from the generated list. However, functional analysis could not be completed for two of these proteins; CNDP2 and PRDX3.

Cytosolic non-specific dipeptidase (CNDP2) is expressed in all human tissues. The loss of chromosome 18q, which encodes for the protein, results in carnosinemia, a rare autosomal recessive metabolic disorder. In addition to this, it may play a role tumour suppressor, as demonstrated in hepatocellular carcinoma cells (Zhang, Chan et al. 2006). Deletion of the CNDP2 gene has been identified in 27.2% cancer specimens from an aCGH study containing more than 3,000 cancer specimens, including many malignancies of the gastrointestinal tract (Lee, Giovannetti et al. 2012). In our study, CNDP2 was found to be 1.75-fold more abundant in the non-metastasised tissue in comparison to that which subsequently metastasised. This correlates with the above previous work which suggests that the downregulation of CNDP2 may be indicative of a poorer prognosis. However, as CNDP2 was not expressed in either of the chosen uveal melanoma cell lines; 92.1 and MEL202, it was excluded from the functional analysis.

Peroxiredoxins are a family of peroxidases which catalyse the reduction of peroxides in the presence of thioredoxin (Wonsey, Zeller et al. 2002). They are present in all animals existing in multiple isoforms, with at least six isoforms in humans (Seo, Kang et al. 2000). They exhibit different expression patterns, with some providing defence against oxidative damage, and participating in signalling by controlling H_2O_2 concentration, while others have been shown to play a role in apoptosis, and proliferation (Rhee, Kang et al. 2001, Wonsey, Zeller et al. 2002). Thioredoxin-dependent peroxide reductase (PRDX3) has been found to be overexpressed in a number of endocrine tumours such as prostate cancer where it plays an essential role in regulating oxidation-induced apoptosis in anti-androgen resistant cells (Whitaker, Patel et al. 2013). The *PRDX3* gene has also been identified as a target gene of the c-Myc transcription factor. c-Myc functions to accelerate metabolic pathways such as glycolysis. As mitochondria are crucial for the execution of energy production and cell death, mitochondrial proteins such as PRDX3 may be involved in the regulation of proliferation and apoptosis. Hence, PRDX3, and other c-Myc target genes encoding mitochondrial proteins, could play an important role in tumorigenesis (Wonsey, Zeller et al. 2002). PRDX3 was found to be upregulated in subsequently metastasised tumour tissue by 1.58-fold when compared to the non-metastasised specimens. This correlates with the above previous work which suggests that the upregulation of PRDX3 may be indicative of a poorer prognosis. However, despite

many attempts, the optimisation of PRDX3 siRNA-mediated downregulation failed and hence, it was also excluded from the functional analysis.

7.3.1 KPNB1

Importin subunit beta-1 (KPNB1) is a major nuclear receptor protein which is required for the import of proteins, such as transcription factors, into the nuclear envelope and is plays a major role in maintaining normal cell homeostasis.

In cancer cells, KPNB1 is often upregulated in order to maintain a high level of nuclear transport, thus it may be a potential biomarker (van der Watt, Stowell et al. 2013). This pattern has been observed in cervical tumours, non-small cell lung cancer, and head and neck squamous cell carcinoma (van der Watt, Ngarande et al. 2011, Martens-de Kemp, Nagel et al. 2013).

KPNB1 was found to be upregulated by 1.47-fold in subsequently metastasised uveal melanoma tumour tissue in comparison to non-metastasised, which agrees with previous studies that may indicate a role of KPNB1 in tumour progression and ultimately metastasis.

Following the siRNA-mediated downregulation of KPNB1 in the 92.1 and MEL202 uveal melanoma cell lines, an acid phosphatase assay was carried out *in vitro* which demonstrated that no extensive effect on proliferation was observed for the two independent KPNB1 siRNA transfections in comparison to the negative control.

A highly significant reduction of both invasion and migration was observed when the expression of KPNB1 was reduced, in comparison to the negative control, in 92.1 cells. Hence, KPNB1 may play a role in the invasiveness and motility of uveal melanoma cells *in vitro*.

92.1 and MEL202 uveal melanoma cell lines were transfected with siRNA specific to KPNB1. Conditioned media was then collected from the cells as this contained the secreted MMPs. However, using gelatin zymography, no difference in MMP expression was observed between the transfected cells and the negative controls, for either cell line.

Apoptosis was measured in cells which were transfected with siRNA specific for KPNB1; however, no significant effect on cell death was determined.

KPNB1 appears to be necessary for the metastatic phenotype of uveal melanoma as it was found to be upregulated in subsequently metastasised tissue, and its downregulation decreases invasion and migration; however it does this independently of MMP-2 and -9. It also does not play anti-apoptotic role in uveal melanoma, which correlates with its lack of effect on proliferation. It is potentially a useful anticancer therapeutic target as it appears to be somewhat responsible for the increased rate of nuclear transport in cancer. However, the availability of drugs targeting such molecules is currently limited. One such drug which is available is Leptomycin, a small molecule inhibitor of CRM1, a major receptor for the export of nuclear proteins and a member of the karopherin family. Leptomycin has been shown to exhibit anticancer activity both *in vivo* and *in vitro*. Hence, it is very possible that KPNB1 may be affected in a similar manner, as it is also a member of the karyopherin family, and so, may be an effective target (Fornerod, Ohno et al. 1997, van der Watt, Stowell et al. 2013) .

7.3.2 EEF1G

Elongation factor 1-gamma (EEF1G) is a GTP-binding protein involved in translation and protein biosynthesis by mediating the transport of aminoacyl-tRNA to 80S ribosome (Proud 1994, Negrutskii and El'skaya 1998).

EEF1G has been associated with pancreatic cancer tumour tissues, where it was identified in seven out of nine specimens, relative to apparently normal adjacent tissue. It was also found to be overexpressed in 25 out of 29 colorectal carcinomas (Chi, Jones et al. 1992). The overexpression of EEF1G appears to be highly associated with cancers of the gastrointestinal tract and has also been identified in hepatic, ileocecel, duodenal, and colon carcinoma cell lines (Mimori, Mori et al. 1995). It has also been associated with the co-upregulation of TNF receptor-associated protein 1 (TRAP-1), a member of the heat shock protein (HSP) 90 protein family involved in protection from oxidative stress and apoptosis, in colon carcinoma cells (Matassa, Amoroso et al. 2013).

EEF1G was identified as being upregulated by 2.02-fold in uveal melanoma tumours which had subsequently produced metastases in comparison to non-metastasised tissues. It was chosen as it was potentially novel target for uveal melanoma as it appears to play a role in tumour progression.

Following the siRNA-mediated downregulation of EEF1G in the 92.1 and MEL202 uveal melanoma cell lines, a proliferation assay was carried out which demonstrated that the knock-down of the protein had no extensive effect on proliferation *in vitro* in either of the two independent KPNB1 siRNA transfections in comparison to the negative control.

A highly significant reduction of both invasion and migration was observed when the expression of EEF1G was diminished, in comparison to the negative control, in 92.1 cells. An effect was also observed in the MEL202 cell line. This indicates that EEF1G may play a role in the invasiveness and motility of the uveal melanoma cells *in vitro*.

92.1 and MEL202 uveal melanoma cell lines were transfected with siRNA specific to EEF1G. Conditioned media was then collected from the cells as this contained the secreted MMPs. However, using gelatin zymography, no difference was observed between the EEF1G transfected cells and the negative controls, for either cell line.

Apoptosis was measured in cells which were transfected with siRNA specific for EEF1G; however, no significant effect on cell death was determined. EEF1G appears to be necessary for the process of invasion and migration in uveal melanoma *in vitro*, albeit independently of MMP-2 and -9, and hence is required in metastasis. It does not play an anti-apoptotic role in uveal melanoma, which correlates with its lack of effect on proliferation.

Previous studies have identified potent and selective inhibitors of other members of the elongation factor family, which could inhibit growth of the malignancy through downregulation of nutrient transporters and activation of autophagy. Arora et al. screened a series of imidazolium compounds for the inhibition of EEF2 (eukaryotic elongation factor 2) activity in several forms of malignancy. From this, they identified NH125 as a lead compound which decreased the viability of 10 cancer cell lines (Arora, Yang et al. 2003). Hait et al. described the combination of a growth

factor antagonist with an inhibitor of EEF-2 kinase in breast cancer in order to induce cell death (Hait, Wu et al. 2006). This illustrates the potential significance of EEF1G as a potential target for uveal melanoma treatment.

7.4 Conclusion

This proteomics study on primary uveal melanoma tissue samples led to the successful identification of proteins including FABP3, SELENBP1, EEF1G, KPNB1, and TPI1 that are possibly involved in the metastatic phenotype of uveal melanoma *in vitro*. These results correlated with the hypothesis that proteins are differentially expressed between disease states and that such proteins may be potential biomarkers. These proteins showed a strong differential expression and high statistical significance from either the 2-D DIGE or quantitative label-free LC-MS analysis when compared to the non-metastasised group. Their siRNA-based knockdown significantly reduced invasion and migration of uveal melanoma cell lines, suggesting that they are functionally involved in the metastatic phenotype of uveal melanoma *in vitro*, and that they may be suitable candidates for targeted therapies in the treatment of aggressive uveal melanoma. This work has fulfilled the aim of identifying patterns of differential protein expression between subsequently metastasised and non-metastasised primary uveal melanoma tissue, which may further our understanding of the metastatic phenotype of uveal melanoma.

7.5 Sample Preparation and Proteomic Analysis of Uveal Melanoma Vitreous Fluid

The vitreous fluid is a hydrogel-like substance, located in the posterior segment of the eye. Physical and pathological conditions of nearby tissues, such as the retina, may be reflected in the vitreous humour (Angi, Kalirai et al. 2012).

Proteomics of the vitreous fluid is a growing area as the specimen contains a variety of proteins. Soluble proteins are thought to filter from the plasma through fenestrated capillaries of the ciliary body stroma via the iris root. Proteins may also be secreted from posterior chamber tissues which may impact on the protein content of the fluid. Indeed, the vitreous should contain a complex mix of proteins as it

reacts to its environment when attempting to maintain homeostasis. In this regard, alterations in its proteome may be indicative of disease, or illustrate proteins which are actively involved in the pathogenic process (Chowdhury, Madden et al. 2010). Although we are still not close to fully understanding the biochemistry of the vitreous humour, a recent study was carried out which extensively detailed the entire vitreous proteome, listing a total of 1111 proteins (Aretz, Krohne et al. 2013). Therefore, progress is quickly being made in the field of vitreous fluid proteomics.

In addition to this, a number of studies have been carried out which indicate its role in disease and in biomarker discovery, as well as in clinical diagnoses and prognoses. Autoimmune or autoinflammatory uveitis patients' vitreous has been used for the analysis of cytokine production. For example, an elevated level of TNF-alpha has been identified in the vitreous of animal uveitis models (Damato, Angi et al. 2012). The specimen has also successfully been used in the differentiation of infectious, inflammatory, and malignant cases of uveitis (Lobo and Lightman 2003). A significant amount of research has been carried out in the vitreous of diabetic patients for the proteomic analysis of retinopathy. Fluid from patients undergoing vitreoretinal surgery is currently used to indirectly explore the synthesis of mediators of diabetic retinopathy produced by the retina as well as the infiltration of leukocytes (Yoshimura, Sonoda et al. 2009, Simo-Servat, Hernandez et al. 2012). A number of potential biomarkers have also been determined through this research. Orosomucoid was identified as being upregulated in the vitreous of proliferative vitreoretinopathy patients in comparison to that of proliferative diabetic retinopathy patients (Wu, Sauter et al. 2004).

Due to the close proximity of the vitreous to many regions of the eye, high concentrations of proteins may be secreted into the fluid from various sites of disease, such as a tumour, thus illustrating pathophysiological events taking place. Hence, the vitreous humour qualifies as a suitable fluid for the clinical proteomic analysis of uveal melanoma, as it may contain significant numbers of secreted biomarkers.

Little has been carried out in terms of uveal melanoma vitreous fluid proteomics. The majority of studies to date have consisted of multiplex bead arrays, such as those which are discussed in section 7.5.4.

Therefore, it was decided to examine the vitreous collected from uveal melanoma patients as it could be a specimen of interest in detecting potential prognostic markers.

7.5.1 Vitreous Fluid Sample Preparation

The analysis of vitreous fluid can be a challenging process due to the small sample volume and low protein concentration present. Improvements in mass spectrometry have improved the overall process with high sensitivity instruments now available which can provide both qualitative and quantitative information (Pollreisz, Funk et al. 2013). Despite this, the challenge still remains in efficiently mining the proteome to reach the concentration of low abundance proteins, which are often of most interest in terms of biomarker discovery. Hence it is necessary to fractionate the vitreous prior to experimentation in order to extract proteins of interest from the complex mixture (Angi, Kalirai et al. 2012).

Following the separation of a control vitreous fluid sample, collected from a patient with macular hole degeneration, it was evident that the vitreous was rich in serum albumin and other proteins considered to be highly abundant such as; IgG, haptoglobin, complement C3. Following a double immunodepletion, the proteome appeared to be sufficiently "cleaned-up" as large regions of smeared protein were no longer present and less prominent bands were more visible. However, this impacted on the protein concentration, as high abundance proteins make up 80% of the vitreous fluid proteome. This resulted in insufficient quantities of protein being available for pre-fractionation methods, such as ProteoMiner treatment, and separation experiments, such as 2-D DIGE.

A quantitative LC-MS label-free approach was adopted in order to identify potential differentially expressed proteins between the control and uveal melanoma sample sets. Highly sensitive mass spectrometry methods are capable of identifying quantitative differences between low abundance proteins, using the minimal quantity of sample to do so. Such approaches have been effectively used in the study of aqueous humour and tear fluid previously which would suggest that the same process could be successful in vitreous humour (de Souza, Godoy et al. 2006, Chowdhury, Madden et al. 2010). Nevertheless, the results of this analysis did not

produce differentially expressed proteins as spectra generated from the control group were entirely different to those from the disease group and could not be compared. This may have been as a result of the quantity of high abundance proteins which were present in uveal melanoma specimens in comparison to the controls. As all samples were normalised to 10 μg prior to analysis, the majority of this possibly consisted of a few abundant proteins in the uveal samples, hence creating an entirely different spectrum of peaks to the control sample set (which may have contained a variety of proteins).

7.5.2 IMAC Fractionation of Uveal Melanoma Vitreous Fluid

Little has been carried out in vitreous fluid using SELDI technology; hence, it was decided to compare a control and a uveal melanoma specimen as a pilot SELDI TOF MS study.

This identified the presence of three protein peaks which were originally identified in cutaneous melanoma serum and the conditioned media of a cutaneous melanoma cell line. However, SELDI TOF MS does not provide identifications for peaks detected, only spectral profiles. As further explained in sections 7.7.3 and 7.7.4, it was decided to attempt to identify the protein peak at 8.9 kDa.

Using an IMAC column, described in section 7.7.4.1, proteins with an affinity for copper were bound and subsequently eluted with an imidazole gradient from the resin in fractions. These elution fractions were separated in the first dimension using gel electrophoresis and stained. Following this, protein bands from the gel were digested and generated peptides were analysed using LC-MS/MS for their identification.

This qualitative method succeeded in identifying a host of proteins which had not been found in our previous attempts to mine the uveal melanoma vitreous proteome. This fulfilled the aim of developing an effective method of vitreous fluid sample preparation. It was therefore decided to repeat the experiment and to analyse the imidazole fractions quantitatively. In this quantitative LC-MS analysis, six monosomy three uveal melanoma vitreous samples were compared to seven disomy three uveal melanoma vitreous specimens.

Previously, Coupland et al. had compared four primary uveal melanoma tumour tissue specimens from monosomy three patients to those of three disomy three patients, with the intention of identifying differentially regulated proteins between both groups. Monosomy three in uveal melanoma is regarded as an indicator of poor outcome; therefore, a biomarker providing prognostic relevance early on in the disease would be of great benefit. From this 2-D DIGE analysis, they discovered nine differentially expressed proteins, three of which were confirmed by western blotting; HSP-27, vimentin, pyruvate dehydrogenase beta. Immunohistochemistry further validated that low HSP-27 abundance correlated with monosomy three chromosomal status, and that HSP-27 appeared to be a promising prognostic marker (Coupland, Vorum et al. 2010).

Therefore, other biomarkers indicating outcome in uveal melanoma could be detected in vitreous fluid by comparing monosomy three specimens to those of disomy three patients, as this has not been reported previously, using the IMAC quantitative method. It was hoped that this would improve our understanding of the metastatic disease, and potentially indicate any differentially regulated proteins which could act as therapeutic targets.

7.5.3 Proteins of Interest Identified as a Result of IMAC Fractionation

From the quantitative and qualitative analyses of the IMAC vitreous fluid samples a number of proteins of interest were discovered.

From the 1-D gel-based qualitative study, a family of proteins known as crystallins were identified, which illustrated that the technique had uncovered a range of previously undiscovered proteins and hence, was a successful pre-treatment technique.

From the quantitative LC-MS-based study, proteins such as retinol-binding protein three, meckelin, PEDF, retbindin, and alpha crystallin B were discovered to be differentially regulated between the monosomy three and disomy three sample sets. These may potentially be useful as novel prognostic markers, as some of these; retinol-binding protein 3, meckelin, and retbindin, have not previously been identified in relation to uveal melanoma. In addition to this, meckelin, and retbindin

have not been identified in the vitreous fluid. This work agreed with the hypothesis that proteins would be differentially expressed between monosomy 3 and disomy 3 samples. It also satisfied the aim of identifying such proteins which could act as potential biomarkers or therapeutic targets.

Enrichment analysis of the differentially expressed proteins identified in the qualitative study indicated that, overall, the complement and coagulation cascades would be upregulated as a result of the overexpression of proteins in the disomy three samples. This suggests that due to significant trauma caused by the malignancy, the immune system was triggered in an effort to regulate and repair the damage caused. This action may have activated an inflammatory response, as this response was detected following the enrichment of biological processes. This action could activate a cascade of cytokines in response which would potentially be detectable in vitreous fluid, and thus be identifiable using a Luminex multiplex method, such as that in section 7.5.4.

7.5.3.1 Proteins of Interest Discovered in the Qualitative Analysis

7.5.3.1.1 Crystallins

Crystallins are water-soluble proteins of the lens which contribute to its transparency and refractive properties, with age-related post-translational modifications of the crystallins being associated with cataracts. These proteins were originally thought to merely be stable structural components, however, they have been shown to have further roles, such as molecular chaperones, and have been identified outside of the lens. Lens proteins are highly stable and do not age but do eventually undergo post-translational modifications such as deamidation, and protein crosslinking, and can be oxidised by free radicals generated by UV light (Andley 2007).

Beta-crystallin B1, beta-crystallin A4 and beta-crystallin A3, which were identified in our qualitative study, have been shown to be predominantly involved in cataract formation as they are both targets for crosslinking by tissue transglutaminasae (tTG). This crosslinking activity of tTG has also been implicated in many cell processes such as; motility, wound healing, extracellular matrix remodelling, differentiation, and apoptosis. Beta-crystallin B2, also discovered in the qualitative analysis, has been implicated as a potent glutamate substrate for tTG, but also as a target for

deamidation by tTG, which destabilises the protein. These processes of deamidation and crosslinking are thought to play a role, not only in cataractogenesis, but in aging and disintegration of the structural components of the eye (Andley 2007). Mutations of beta crystallin S have been associated with autosomal dominant congenital cataract formation (Sun, Ma et al. 2005).

A mutation in gamma-crystallin D, P23T, is associated with a number of well-known cataract phenotypes through the reduced solubility and subsequent condensation of the mutated protein without demonstrating any change in the protein structure (Pande, Annunziata et al. 2005).

The alpha crystallins, chains A and B, were both discovered in uveal melanoma vitreous fluid following the qualitative analysis. Alpha-crystallin B is a small heat shock protein and has similar properties to those of a molecular chaperone. Increased levels of alpha-crystallin B have been associated with a variety of neurological diseases such as Alzheimer's disease, Parkinson's disease, and Creutzfeldt Jacob disease. However, it does not seem to be required for normal development of the refractive lens. Alpha-crystallin A has been shown to have a protective effect on other crystallins, and in particular gamma crystallin, however the mechanism by how this occurs is elusive (Horwitz 2003). Alpha-crystallin B appears to play an anti-tumorigenic role in nasopharyngeal carcinoma, as well as suppressing the progression of the cancer through its potent effect on invasion and adhesion (Huang, Cheng et al. 2012). The protein has also been linked with poor outcome and nodal status in a number of malignancies such as breast cancer, glioblastoma, renal cell carcinoma and head and neck squamous cell carcinoma (Aoyama, Steiger et al. 1993, Takashi, Katsuno et al. 1998, Moyano, Evans et al. 2006, van de Schootbrugge, Bussink et al. 2013).

Alpha-crystallin B has also been shown to be highly expressed in melanocytes and expressed at a lesser level in melanoma cells, where it is repressed as a result of upregulated BRAF-MEK signalling. It also contributes to the turnover of cyclin D1 in both melanocytes and melanoma cells following DNA damage. Finally, although not discovered in this study, absent in melanoma 1 (AIM1) is an unusual member of the family of crystallins whose expression is known to suppress malignancy in melanoma (Aravind, Wistow et al. 2008).

As crystallins have been shown to bind to IMAC, this illustrates that the method was successful in binding proteins with an affinity for IMAC (Chiou, Huang et al. 2010, Huang, Wang et al. 2011).

Due to using the IMAC fractionation method, it was possible to better observe the vitreous fluid proteome and to isolate a number of members of the crystallin family. These results may indicate the possible role of the crystallins in the vitreous fluid of uveal melanoma patients. In addition to this, this may improve our understanding of the vitreous fluid during malignancy of the uvea, and indeed, better our knowledge of the cancer itself.

7.5.3.2 Differentially Regulated Proteins of Interest Discovered in the Quantitative Analysis

Using quantitative LC-MS following IMAC fractionation, the protein content of monosomy of chromosome three and disomy of chromosome three uveal melanoma vitreous fluid sample sets were compared. This unearthed a total of 62 differentially expressed proteins which were identified from the flowthrough, 20 mM, and 50 mM fractions. From enrichment analysis of pathways involved, it was clear that the greatest effect was observed in downregulation of proteins in the monosomy 3 specimens where complement and coagulation cascades were affected.

A number of proteins which may be followed up are described in the following sub-sections.

7.5.3.2.1 Retinol-Binding Protein 3

Retinol-binding protein 3 is a glycoprotein which functions as a transporter of retinoids between the photoreceptors and the retinal pigment epithelium, and is necessary for normal rod and cone cell function and development (Liou, Fei et al. 1998, den Hollander, McGee et al. 2009). It has been associated with inducing uveoretinitis, and retinitis pigmentosa, a degenerative ocular disease (Eisenfeld, Bunt-Milam et al. 1987, Bianciotto, Shields et al. 2010). In addition to this, its expression has been linked with the development of retinoblastoma and pineocytoma

(Korf, Korf et al. 1992). However, it also may play a protective role as an anti-oxidant (den Hollander, McGee et al. 2009).

In our study, the protein was identified as being upregulated in monosomy of chromosome three specimens in both the flow through and the 20 mM fraction. This may indicate its role in tumour development and disease progression, as it was identified at a lower level in the disomy three sample set, which is less aggressive. It has previously been implicated in malignant cutaneous melanoma in a case where autoantibodies against the metastatic melanoma cross-reacted with retinol-binding protein three, i.e. a retinal autoantigen; this rare condition is referred to as melanoma-associated retinopathy (MAR). MAR is also known to occur in metastatic uveal melanoma, which raises the question if this would explain the observed increase in retinol-binding protein three expression in monosomy three samples, which are typically associated with metastasis, in comparison to the disomy three sample set (Bianciotto, Shields et al. 2010).

However, it is also possible that retinol-binding protein three was upregulated in monosomy three vitreous samples as a result of extensive trauma to the eye due to the aggressive nature of the malignancy. An increase in the transport of retinoids to the retinal pigment epithelium for repair of the extensive damage caused by the tumour may have been necessary.

Retinol-binding protein 3 has previously been discovered in the vitreous fluid (Aretz, Krohne et al. 2013), however, it has not yet been described in relation to uveal melanoma. Hence, it may a potential biomarker of interest for poor prognosis.

7.5.3.2.2 Meckelin

Meckelin is a transmembrane ciliary protein which mediates primary ciliary function. Little is known about the protein but it has been illustrated to be involved in intraflagellar transport and it appears to be critical for cilia function in organs such as the kidneys, liver, and retina (Tiwari, Hudson et al. 2013). Retinal rods and cones use cilia for the connection of the inner and outer segments of photoreceptors, and a disruption of this process may lead to retinal deterioration (Fliegauf, Benzing et al. 2007). Mutations in the MKS3 gene, which encodes for meckelin, can result in eye

abnormalities, such as retinal degeneration (Dawe, Smith et al. 2007, Collin, Won et al. 2012).

In our study, meckelin was identified as being decreased in the monosomy three sample set by 2.03-fold. The protein has not previously been identified in relation to the vitreous or uveal melanoma; hence, it may be an entirely novel protein in this regard. Cellular component enrichment analysis illustrated that lipoprotein particles were involved in the proteins identified at a higher abundance in the disomy three specimens. This may implicate meckelin as it is a transmembrane protein which would therefore be embedded in the lipid bilayer.

7.5.3.2.3 PEDF

Pigment epithelium-derived factor (PEDF) has been long associated as being essential for the health and survival of the retina (Subramanian, Locatelli-Hoops et al. 2013). Its multiple functions include neurogenesis, neuroprotection, anti-angiogenesis, and stem cell renewal, albeit, one of the more prominent features of the protein is its anti-cancer role. The protein appears to exhibit anti-angiogenic and antimetastatic activities, as well as inhibit tumour growth and prolong survival in animal models (Becerra and Notario 2013). PEDF-mediated antitumour activity is due to its action on the tumour microenvironment and on the tumour cells (Fernandez-Barral, Orgaz et al. 2012). A decrease in or loss of PEDF expression has been associated with an increased incidence of metastasis and with poor prognosis in cutaneous melanoma, prostate carcinoma, pancreatic carcinoma, neuroblastoma, and glioma (Yang and Grossniklaus 2010).

PEDF was detected in the monosomy three sample set by a 1.44-fold lower abundance in comparison to the disomy three sample set, which correlates with previous findings of a lower expression of PEDF being associated with more aggressive phenotypes of malignancy.

PEDF is highly expressed in melanocytes and less aggressive melanoma cells, but it is minimally expressed, if at all, in highly aggressive melanoma cells. It was first described as the most potent angiostatic factor of the eye, where it is produced by retinal pigment epithelial cells. PEDF elicits a highly potent inhibitory action on

melanoma cells, inducing apoptosis under stress conditions and annulling migration and invasion (Fernandez-Barral, Orgaz et al. 2012). The protein has been associated with uveal melanoma, where its overexpression has been shown to inhibit growth and hepatic micrometastasis in a mouse model. It has been previously been identified in the vitreous, however, it has not been identified in the uveal melanoma vitreous proteome (Aretz, Krohne et al. 2013).

Therefore, our discovery of the differential expression of PEDF between monosomy three and disomy three vitreous fluid specimens may provide more information on the method of disease progression in uveal melanoma and may be a potential biomarker for prognosis.

7.5.3.2.4 Retbindin

Retbindin is a relatively novel, secreted protein which was originally identified in ocular tissue and is thought to be preferentially expressed in the retina. It is thought to function in flavonoid or carotenoid binding as it shares homology with riboflavin binding proteins (Wistow, Bernstein et al. 2002). Flavonoids have been shown in the past to inhibit multiple drug resistance efflux pump systems in mouse lymphoma and colon cancer cells (Gyemant, Tanaka et al. 2006). They have also illustrated anti-angiogenesis, anti-metastasis, and pro-apoptosis effects on cancer cells. Li et al demonstrated the suppression of migration and invasion of breast cancer cell lines as a result of treatment with a flavonoid derivative (Li, Li et al. 2012). Carotenoids have also indicated anti-tumour effects (Tanaka, Shnimizu et al. 2012).

The protein was identified in the 50 mM fraction as showing a decreased abundance in the monosomy of chromosome three sample set, in comparison to the disomy three sample set. Due to the potential carotenoid/flavonoid binding function of retbindin, an observed lower abundance in monosomy three vitreous samples in comparison to disomy three specimens would concur with previous anti-cancer findings associated with flavonoids and carotenoids.

Retbindin was not previously identified in vitreous fluid nor does it appear to have been located in uveal melanoma or any other malignancy, which deems the protein

to potentially be entirely novel in cancer biomarker discovery. Hence it was decided that retbindin should be followed up in later studies.

7.5.3.2.5 Alpha Crystallin B

As illustrated above, a host of crystallins, including alpha crystallin B, were identified in the qualitative analysis of uveal melanoma vitreous fluid. Alpha crystallin B was also identified in the quantitative analysis as being highly upregulated in the monosomy three specimens.

Alpha crystallin B functions as a stress-induced molecular chaperone which promotes cell survival. The ectopic expression of the protein may also protect an array of cell types against apoptotic signals including TNFα, and TRAIL, as well as conferring protection against oxidative stress. Previous studies have illustrated that by reducing the expression of the protein using RNA interference, cells may be sensitised to apoptosis, and by overexpressing it, the rates of invasion and migration are increased *in vitro* (Moyano, Evans et al. 2006). Alpha crystallin B has formerly been associated with poor outcome in a number of malignancies including; breast cancer, head and neck cancer, and laryngeal squamous cell carcinoma (Chin, Boyle et al. 2005, Moyano, Evans et al. 2006, Mao, Zhang et al. 2012)

Zuidervaart et al. had previously discovered alpha-crystallin B as being overexpressed in two metastatic uveal melanoma cell lines, in comparison to the primary tumour from which they were derived (Zuidervaart, Hensbergen et al. 2006). As it was overexpressed in the uveal melanoma vitreous fluid from patients with monosomy three and has been found to be upregulated in metastatic uveal melanoma cell lines, it appears that it may play a prognostic role. However, it has not yet been detected in uveal melanoma vitreous fluid and hence, may be a potential marker of interest which should be followed-up.

7.5.4 Luminex Multiplex-Based Analysis of Control vs. Uveal Melanoma Vitreous Fluid

Luminex xMAP technology is a highly sensitive bead-based array which allows for the multiplex analysis of proteins or nucleic acids. The microspheres have a capture

antibody covalently immobilized on a small surface area, thus requiring a low quantity of sample (Baker, Murphy et al. 2012).

Vitreous fluid collected from uveal melanoma cases has been successfully studied using the Luminex system. Nagarkatti-Gude et al. studied the presence of inflammatory cytokines in uveal melanoma vitreous fluid in order to determine the relationship between the vitreal concentration of cytokines, and prognostic variables, such as tumour dimensions. Compared with control vitreous, a higher concentration of a variety of inflammatory mediators was identified in the disease fluid, which appeared to directly correlate with the size of the tumour and with the presence of immune cell infiltrate (Nagarkatti-Gude, Bronkhorst et al. 2012). Other such studies have also been carried out in vitreous in order to examine the link between inflammation and tumorigenesis in the uveal melanoma (Dunavoelgyi, Funk et al. 2012).

Prior to the publication of the above studies, it was decided to compare uveal melanoma vitreous samples, from both metastasised and non-metastasised cases, to control specimens using a Luminex 12-plex cytokine/chemokine assay as part of a pilot study. The assay quantified the levels of FGF2, IFNɣ, TNFα, TGFα, MIP1α, IL-10, IL-15, IL-1α, IL-2, IL-6, IL-8, and IP10. From this work, three cytokines of interest were identified; basic fibroblast growth factor (FGF2), macrophage inhibitory protein 1 alpha (MIP1α) and interferon gamma (IFNɣ). These were all validated for their sensitivity and specificity as potential biomarkers, however, a small sample set was used, and did not provide as comprehensive an analysis as other studies (Dunavoelgyi, Funk et al. 2012, Nagarkatti-Gude, Bronkhorst et al. 2012).

7.5.4.1 FGF2

FGF2 is a member of fibroblast growth factor family which has more than 20 structurally-related members. These proteins control a range of functions including; proliferation, motility, survival, and differentiation. FGF2 is known to play an important role in cancer development due to its role in angiogenesis (Polnaszek, Kwabi-Addo et al. 2003).

FGF2 has been described as being overexpressed in a variety of cancers including breast, prostate, melanoma, lung, and bladder (Polnaszek, Kwabi-Addo et al. 2003). In uveal melanoma, it was discovered that FGF2 is highly expressed in primary tumours. When the production of the protein was decreased in uveal melanoma cell lines, this severely impacted on cell proliferation and survival (Lefevre, Babchia et al. 2009). In addition to this, an FGF2-binding peptide has been shown to inhibit proliferation and angiogenesis in uveal melanoma (Yu, Gao et al. 2012).

FGF2 was not shown to be significantly differentially expressed between the control and the uveal melanoma sample groups. The result was followed up using MedCalc which presented a specificity of 100% and a sensitivity of 75%.

7.5.4.2 MIP1α

MIP1α is a member of the C-C subfamily of chemokines which functions as an activator of monocytes and plays a role in host defence (Konishi, Okabe et al. 1996).

It has previously been associated with lung cancer when it was found that lung cancer cells expressed MIP1α, suggesting that these cells can participate in inflammatory cell recruitment through the production of MIP1α (Konishi, Okabe et al. 1996). MIP1α overexpression has also been identified as being upregulated in breast cancer (Wolf, Clark-Lewis et al. 2003, Martinez-Outschoorn, Whitaker-Menezes et al. 2011)

MIP1α has previously been associated with uveal melanoma vitreous humour where it positively correlated with tumour prominence (Nagarkatti-Gude, Bronkhorst et al. 2012). Our study agreed with this finding, illustrating a significant increase in MIP-1α expression in the vitreous of uveal melanoma patients when compared to the controls, with an ANOVA score of <0.01. ROC curve analysis confirmed this finding with high sensitivity and specificity values.

7.5.4.3 IFNɣ

IFNɣ is a cytokine known for protecting against malignancies as it inhibits proliferation, sensitises tumour cells to apoptosis, modulates cell differentiation and stimulates anti-tumour immune activity (Garcia-Tunon, Ricote et al. 2007, Wang, Xu et al. 2013).

IFNɣ has been shown to inhibit the growth of multiple cell lines such as breast cancer cell lines and has been demonstrated to trigger the regression of skin metastases (Garcia-Tunon, Ricote et al. 2007). Reduced levels of IFNɣ in lung cancer have been associated with a shorter survival in lung cancer (Wang, Xu et al. 2013).

IFNɣ has previously identified in uveal melanoma vitreous humour where it directly correlated with tumour size (Nagarkatti-Gude, Bronkhorst et al. 2012). The same results were observed in our study where the cytokine was found to be significantly more abundant in uveal melanoma vitreous in comparison to the control vitreous. ROC curve analysis correlated with this finding, illustrating both 100% sensitivity and 100% specificity. This result differs to what is typically found in the literature, i.e. a decrease in IFNɣ as the disease progresses.

7.5.5 Conclusion

Although vitreous fluid is a reasonably difficult specimen to work with, the IMAC resin fractionation method appears to generate an interesting subset of proteins which may be analysed by gel-based qualitative methods or by LC-MS-based quantitative methods. The label-free quantitative analysis generated a total of 62 differentially-expressed proteins, of which alpha crystallin B, retbindin, retinol-binding protein three, and meckelin can now be followed up.

The Luminex multiplex assay identified three cytokines of interest; FGF2, IFNɣ, and MIP1α. However, it should be noted that these results may be skewed by the small sample sizes used, and a larger study would have to be carried out to follow up these results.

Overall, this work may further our understanding of the process of uveal melanoma metastasis which could lead to the development of potential therapeutic targets.

7.6 ProteoMiner Fractionation and Quantitative Label-Free LC-MS Analysis of Advanced Cutaneous Melanoma Serum

As proteins are continuously varying in their expression, in accordance with the stage of disease or the treatment regimen, their levels can provide key information on a disease at the molecular level. Biomarkers may be secreted into the bloodstream either directly by the tumour, or indirectly through the destruction of cells. The blood is a potentially rich source of biomarkers, while being an easily accessible specimen. (Bougnoux and Solassol 2013).

Many proteomic studies have been carried out where potential biomarkers have been detected in cutaneous melanoma serum specimens, across all stages. However, only LDH is used as a prognostic biomarker in stage IV melanoma, where the survival rate is less than 5%. Hence, new methods for the detection of metastasis at an earlier stage are required (Bougnoux and Solassol 2013).

The majority of cutaneous melanoma profiling experiments have been carried out using SELDI-TOF MS or MALDI-TOF MS, both of which have been effective methods. Caron et al. used SELDI-TOF MS as part of a serum proteome fingerprinting approach to determine if a protein profile could discriminate between healthy individuals and melanoma patients. From this, they identified a peak signature with 98.1% diagnostic accuracy (Caron, Mange et al. 2009). To compare the proteomic profile of serum from those with early stage melanoma to those who had relapsed, Wilson et al. used SELDI-TOF MS. This identified three peaks which appeared to correlate with recurrence following the curative resection of the primary melanoma tumour (Wilson, Tran et al. 2004). MALDI TOF was used in the discovery of serum amyloid A as a differentially regulated protein between early and advanced melanoma, and as a potential marker of prognosis (Findeisen, Zapatka et al. 2009). Newer methods are now coming on-stream, such as hydrogel core shell nanoparticles which are being used for the detection of biomarkers in clinical specimens. This method was used by Mian et al. to detect and compare biomarkers indicative of early or late stage melanoma in serum. This identified a pro-apoptotic protein named Bak the expression of which appeared to correlate with disease progression (Longo, Gambara et al. 2011).

It was decided to use LC-MS, a method which has not been widely used in cutaneous melanoma proteomics, to compare control serum and advanced cutaneous melanoma serum for the identification of potential biomarkers of interest. Any proteins identified would then be followed up over the course of disease progression; benign, early, and advanced stages.

7.6.1 ProteoMiner Fractionation of Control and Advanced Cutaneous Melanoma Serum

Although serum and plasma are highly interesting and potentially information-rich specimens in terms of novel biomarker analysis, 99% of the overall protein content is represented by a few high abundance proteins. Through signal suppression, these proteins can mask the presence of less abundant and potentially more interesting proteins during mass spectrometry analysis (Hartwig, Czibere et al. 2009).

Therefore, it is often necessary to pre-treat serum prior to proteomic analysis. ProteoMiner is a method which enhances the sample proteome through equalisation, using a combinatorial library of hexapeptide ligands bound to beads. High abundance proteins will saturate their beads quickly, with any excess simply being washed away while lower abundance proteins will continue to bind to their appropriate ligands. The total quantity of bound proteins may then be eluted from the column. This results in a depletion of high abundance proteins, while concentrating those of lower abundance (Liang, Tan et al. 2012).

Previous studies have been performed demonstrating the ability of ProteoMiner as a pre-fractionation technique for the analysis of low abundant proteins in the serum proteome. Hartwig at el. demonstrated the effectiveness of the ProteoMiner treatment of serum when combined with 2-D DIGE (Hartwig, Czibere et al. 2009). In addition to this, Fröbel et al. illustrated a significant increase in the resolution of the serum proteome in SELDI-TOF MS profiling following ProteoMiner pre-processing (Frobel, Hartwig et al. 2010). The quantitative LC-MS analysis of the cerebrospinal fluid proteome has been carried out utilising the ProteoMiner system as a pre-treatment method, resulting in the detection of over 1000 proteins from a pooled sample set (Mouton-Barbosa, Roux-Dalvai et al. 2010). The analysis of ProteoMiner-treated serum by quantitative LC-MS has not previously been carried

out according to the literature, however it was decided to utilise this method in order to detect differentially regulated proteins between control and advanced melanoma sera.

Eight control and eight advanced melanoma disease sera were all treated with ProteoMiner in order to improve the likelihood of identifying novel proteins of interest. However, given that there are thousands of proteins present in serum, the fractionation of serum following pre-treatment can simplify the proteome for the most efficient identification of potential biomarkers. Therefore, a ProteoMiner sequential elution kit was used, which allows for bound proteins to be eluted in four separate fractions, with each containing proteins of different properties.

7.6.2 Differential Expression Analysis of Control and Advanced Cutaneous Melanoma Serum Using LC-MS and Progenesis LC-MS

The four fractions per sample were analysed using 1-D gel electrophoresis initially, in order to get a visual overview of how the fractionation worked. Following the in-gel digestion of all protein bands in each lane and subsequent LC-MS/MS analysis, it was determined that elution fraction three did not produce as extensive a list of unique proteins in comparison to the other three fractions, for all samples. Hence, it was excluded from the analysis.

Following quantitative label-free LC-MS analysis of fractions one, two, and four, a pattern of consistent protein upregulation in the control sample set was observed for fraction four. This appeared unlikely as some of the expression trends directly contradicted previously observed results from fractions one and two. It was possible that the fourth elution buffer was simply stripping any remaining proteins from the column. Therefore, fraction four was also excluded.

29 and 39 differentially regulated proteins were identified in elution fraction one and two, respectively, for all samples. Following this, fractions one and two were recombined in order to identify the trends of protein expression across the whole experiment. This identified nine differentially regulated potential targets which were expressed in both fractions, of which two targets were selected for follow-up analysis; lactotransferrin and azurocidin. These were selected as both markers were

somewhat novel in terms of cutaneous melanoma. Lactotransferrin has previously been associated with anti-tumoural activity but has not been identified as a potential serum biomarker for cutaneous melanoma, despite being linked with choroidal melanoma, while azurocidin has not been associated with melanoma at all (Dikovskaya, Trunov et al. 2013). Identifications from the 1-D electrophoresis analysis were also taken into account, overlapping them with data acquired from the recombined analysis, thus identifying 10 mutual proteins, from which serotransferrin was chosen for further analysis. Although serotransferrin has previously been linked with melanoma, it has not been studied in relation to the progression of disease and so, it was decided to follow-up the protein in this regard (Richardson and Baker 1990). Plasma serine protease inhibitor was also selected for follow-up validation as it was found to be significantly upregulated in disease sera in comparison to control sera. As it was not previously associated with cutaneous melanoma, it was decided to follow up plasma serine protease inhibitor also.

Beta-secretase 2 (BACE-2), Matrix metalloprotease (MMP-1), and Tissue inhibitor of metalloproteinase 1 (TIMP-1) were previously identified by the analysis of two publically available array data sets for control tissue, and primary and metastasised cutaneous melanoma tumour tissue (Riker, Enkemann et al. 2008, Raskin, Fullen et al. 2013). All three were significantly upregulated in the metastasised and primary tissues in comparison to the control. BACE-2 had not previously been identified as a potential marker for cutaneous melanoma, and so, it was decided to further examine the protein. Both TIMP-1 and MMP-1 had, however, been identified in malignant melanoma as promoters of tumorigenicity, hence, it was decided to further examine their expression over the course of disease (Hoashi, Kadono et al. 2001, Iida and McCarthy 2007, Toricelli, Melo et al. 2013)

All seven proteins; serotransferrin, lactotransferrin, azurocidin, plasma serine protease inhibitor, BACE-2, MMP-1, TIMP-1, were selected for further validation throughout the course of cutaneous melanoma disease progression.

7.6.3 Validation of Targets as Potential Biomarkers for Cutaneous Melanoma Disease Progression

ELISA-based validation was selected for the follow-up of all seven proteins of interest. It was decided to examine the abundance of each across the course of disease, using serum which was collected from patients with benign, early stage, or advanced stage disease. In addition to this uveal melanoma serum collected from patients was also included. As chromosome status information was available, it was possible to examine the protein levels in both disomy of chromosome three and monosomy of chromosome three. Control sera were also included.

7.6.3.1 Serotransferrin

Serotransferrin is a glycopeptide which is produced by hepatocytes and is involved in cellular iron transport. It has been implicated in breast cancer where it was found to be upregulated in BRCA1 mutation carriers, a marker of poor prognosis (Custodio, Lopez-Farre et al. 2012). In a 2-D electrophoresis-based differential expression study, serotransferrin was identified as being overexpressed in endometrial adenocarcinoma (Byrjalsen, Mose Larsen et al. 1999). In addition to this serotransferrin has been linked with pancreatic carcinoma as it was found to be upregulated in serum in comparison serum collected from to other pancreatic disease patients, gastric carcinoma patients and healthy individuals (Sun, Zhu et al. 2007).

Using quantitative label-free LC-MS analysis, serotransferrin was initially found to be over-expressed by 3.47-fold in advanced-stage melanoma sera when compared to control sera. Hence, this result agreed with studies which link an increase in serotransferrin levels and disease progression.

However, the ELISA results directly contradicted this illustrating a significant decrease in serotransferrin levels in either early or advanced-stage cutaneous disease when compared to the control serum. A statistically significant decrease in serotransferrin levels was observed when uveal melanoma serum was compared with control serum. This was also the case when monosomy three uveal melanoma sera were compared with control sera.

7.6.3.2 Azurocidin

Azurocidin is a mediator of inflammation and functions in host defence, and is a member of the serprocidin family of serine protease homologs (Brandt, Lundell et al. 2011).

It was previously considered to be inactive as a protease homologue, however, azurocidin was identified in the urine of multiple myeloma patients as specifically cleaving insulin-like growth factor-binding protein 1 (IGFBP-1) (Wang, Shafqat et al. 2006). Insulin-like growth factor (IGF-1) is known to foster cellular proliferation and inhibit apoptosis (Terry, Tworoger et al. 2009). IGF-1 and IGFBP-1 are both present in the circulation where they are acted upon by proteases, where IGF is cleaved and is available for biological actions (Khandwala, McCutcheon et al. 2000). Azurocidin was found to cleave IGFBP-1, causing a lower affinity but a higher binding capacity for IGF-1, thus increasing rate of association and dissociation between the molecules. This in turn increased the turnover and IGF availability. It also induced a decreased inhibition of IGF-2-stimulated proliferation and glucose uptake (Wang, Shafqat et al. 2006).

Azurocidin was over-expressed in late-stage cutaneous melanoma serum specimens by a maximum observed fold change of 14.2 according to quantitative label-free LC-MS analysis. IGF-1 has also been shown to be a stimulator of cell growth in metastatic melanoma cell lines, therefore, it may be possible that an upregulation of azurocidin contributes to this phenotype (Khandwala, McCutcheon et al. 2000).

Overall, there appeared to be a non-significant increase in azurocidin levels as the disease progressed from benign to late-stage. This may indicate that a larger sample set would provide a more comprehensive result. No difference in expression was noted between control sera and uveal melanoma sera.

7.6.3.3 Lactotransferrin

Lactotransferrin is a major iron-binding glycoprotein produced by mucosal epithelial cells. It is involved in a variety of activities such as iron homeostasis, and has bacteriostatic and immunomodulatory effects. In addition to this, it elicits anti-tumour behaviour, mediated by mechanisms such anti-growth effects, immune

activation, and enhancement of apoptosis. Indeed, lactotransferrin has been shown on numerous occasions to protect against chemically-induced carcinogenesis in organs such as the liver, tongue, oesophagus, colon and bladder, and to reduce tumour growth and metastasis both *in vitro* and *in vivo* (Ward, Paz et al. 2005, Roseanu, Florian et al. 2010, Deng, Ye et al. 2013).

Typically, lactotransferrin is reported to be downregulated in cancer as the loss of its protective effects increases the likelihood of tumorigenesis and subsequent disease progression (Shaheduzzaman, Vishwanath et al. 2007, Zhou, Zeng et al. 2008, Deng, Ye et al. 2013). However, the protein was found to be 4.17-fold upregulated in advanced-stage cutaneous melanoma serum, in both elution fractions one and two, according to the quantitative LC-MS analysis where it showed high reproducibility between samples.

According to the ELISA data, lactotransferrin was significantly less abundant in benign or early-stage cutaneous melanoma serum when compared to control serum. There was no significant difference between the levels in control and advance-stage cutaneous melanoma serum, however an increase in lactotransferrin was observed in advanced-stage samples when compared to those which were benign. The uveal melanoma sample set, which contained both monosomy of chromosome 3 sera and disomy of chromosome 3 sera, showed a significantly decreased level of lactotransferrin when compared with that of the control sample set. When the uveal melanoma serum specimens which were positive for monosomy of chromosome 3 were compared to those which did not have this anomaly, no significant difference was observed between the two.

The downregulation of lactotransferrin in benign and early-stage melanoma may suggest that knock-down of the protein is required for establishing tumorigenesis. The decrease of lactotransferrin abundance in uveal melanoma serum agrees with this hypothesis.

7.6.3.4 Plasma Serine Protease Inhibitor

Plasma serine protease inhibitor regulates numerous serine proteases, such as thrombin and activated protein C, in the process of coagulation. It has been shown

inactivate cathepsin L, a lysosomal cysteine protease that has been implicated in the destruction of components of the extracellular matrix and can induce diseases such as cancer and atherosclerosis when upregulated. Plasma serine protease inhibitor has been illustrated as regulating breast tumour cell migration through the inhibition of cathepsin L (Fortenberry, Brandal et al. 2010). The protein has been shown to have the same role in renal cell carcinoma where it inhibits urinary plasminogen inhibitor (uPA), a protease which mediates metastasis and invasion (Wakita, Hayashi et al. 2004). Other protein kinases have previously been associated with uveal melanoma, where they exerted anti-tumour behaviour (Wu, Li et al. 2012, Wu, Zhu et al. 2012)

Plasma serine protease inhibitor was identified as being 2.6-fold downregulated in advanced cutaneous melanoma sera in comparison to control sera, as detected by quantitative label-free LC-MS analysis, which agrees with the previous findings from other groups. This may indicate that if the protein is downregulated, there is a higher possibility of tumorigenesis and metastasis.

In contrast to the above results, a significant increase of plasma serine protease inhibitor abundance was observed in early stage cutaneous melanoma serum in comparison to that of either control or benign melanoma serum. No difference in protein levels was observed when control and advanced cutaneous melanoma serum were compared. Hence, the results of the ELISA do not validate those of the quantitative label-free LC-MS experiment.

There was a statistically significant increase in the level of plasma serine protease inhibitor in uveal melanoma serum when compared to that of healthy patients. This increase in abundance was observed equally in both patients with monosomy of chromosome three and those with disomy of chromosome three, in relation to the level of plasma serine protease inhibitor produced in control serum.

7.6.3.5 MMP-1

Matrix metalloproteases (MMPs) are a family of zinc-dependent endopeptidases which hydrolyse extracellular matrix components. These enzymes are required for processes such as wound healing and angiogenesis. They have also been associated with cancer invasiveness and the development of metastases in numerous

malignancies such as colorectal cancer, breast cancer, and pancreatic cancer (Liu, Kato et al. 2012). MMP-1 has been suggested to play a role in malignant melanoma by enhancing processes of proliferation, invasion and anchorage-independent growth (Iida and McCarthy 2007).

MMP-1 was shown to be significantly overexpressed in primary and metastasised tissue in comparison to control tissue according to the results of the microarray, which would correlate with studies observed in the literature.

However, the ELISA illustrated a statistically significant decrease in the levels of MMP-1 in advanced cutaneous melanoma serum when compared with control serum. For the uveal melanoma serum, the ELISA did not indicate a pattern of differential expression of MMP-1 between healthy and uveal melanoma serum.

7.6.3.6 TIMP-1

Tissue inhibitor of metalloprotease-1 (TIMP-1) is an inhibitor of MMPs. Although it might therefore be assumed that the upregulation of TIMP-1 would hence inhibit tumour progression, this is not necessarily true. Several studies have shown that high levels of TIMP-1 are observed in the most aggressive tumours. This may be due to MMP-independent functions, such as inhibition of apoptosis through stimulation of the Akt pathway, that TIMP-1 possibly provides which may enhance the progression of cancer (Grunnet, Mau-Sorensen et al. 2013). TIMP-1 has been demonstrated as a potential prognostic and predictive factor in many cancers such as gastric cancer, breast cancer, and oesophageal cancer (Neri, Megha et al. 2012, Grunnet, Mau-Sorensen et al. 2013, Kozlowski, Laudanski et al. 2013). Using cell culture-based studies, it has also been reported as being involved in stimulating the growth of both primary and metastatic melanoma cell lines (Hoashi, Kadono et al. 2001, Toricelli, Melo et al. 2013).

A significant overexpression of TIMP-1 in primary and metastasised tissue in comparison to control tissue was observed in the microarray results. A higher fold change was noted when comparing the metastasised and control tissue than when comparing the primary and control tissue. This would agree with previous studies

which demonstrated that the level of TIMP-1 correlates with the degree of cancer aggressiveness.

According to the ELISA results, no significant difference in the abundance of TIMP-1 was observed between control or benign disease serum and early or late stage disease. In addition to this, no differential production of the protein was noted when serum of uveal melanoma patients was compared with healthy serum.

7.6.3.7 BACE-2

Beta secretase-2 (BACE-2) is a member of a family of membrane-bound aspartyl proteases (Fluhrer, Capell et al. 2002). Xin et al. previously associated BACE-2 with growth and metastasis in a highly tumorigenic and metastatic breast cancer cell line, MDA-MB-435, and correlated it with breast and colon tumour tissues, as well as liver metastases removed from the colon cancer patient (Xin, Stephans et al. 2000). However, the role of the protein appears to be linked to cell proliferation as it was discovered to be involved in controlling pancreatic beta-cell growth, and hence, it has been viewed as a potential target for diabetes (Southan 2013).

BACE-2 was shown to be significantly upregulated in primary and metastasised cutaneous melanoma tissue in comparison to control tissue according to the results of the microarray.

According to the ELISA results, the protein of interest was shown to be elevated in both early and late stage cutaneous melanoma in comparison to serum of patients with benign disease.

No statistically significant difference in BACE-2 production was observed between the uveal melanoma serum group and the control sera; neither was any difference noted between patients with or without monosomy of chromosome three.

This suggests that BACE-2 is potentially involved in cutaneous melanoma disease progression as it appears to be overexpressed in early and advanced disease sera when compared to controls. In addition to this, the protein was not significantly differentially expressed in the uveal melanoma sample set when compared to the

control which may indicate a disparity between the molecular mechanisms of uveal and cutaneous melanoma.

7.6.4 Conclusion

Overall, it was found that the ProteoMiner sequential elution technique was a less successful fractionation method than anticipated. For some of the identifications, there was an overlap between elution fractions which is not indicative of a good technique.

This may be due to multiple binding mechanisms which a protein can have; some could strongly bind to a ligand, however, others could bind weakly, but multiple weak interactions create a somewhat stronger bond. When bead-bound proteins are sequentially eluted using an increasing gradient of stringency, proteins may be found in more than one fraction. It is possible that this is as a result of both weak and strong binding interactions occurring between one protein type and multiple ligands on various beads (Boschetti and Righetti 2008).

This may explain why inconsistencies were so often observed between the results of the quantitative LC-MS analysis and the results of the ELISA carried out. Considering this, it appears that the technology may not be entirely ready for the deconvolution of an entire proteome and may require further optimisation of affinity interactions.

However, our method of ProteoMiner Sequential elution coupled with quantitative label-free LC-MS was effective as it illustrated differential protein expression patterns which agreed with previous findings in cutaneous melanoma proteomics studies in the literature. For example, a decrease in peroxiredoxin-2 has previously been associated with metastasis in cutaneous melanoma (Lee, Kang et al. 2013). Our study associated with this finding as we identified peroxiredoxin-2 to be expressed at a higher level in control sera in comparison to that of advanced cutaneous melanoma patients. We also identified insulin-like growth factor binding protein 3 (IGFBP-3) to be more abundant in control serum in comparison to that of advanced cutaneous melanoma patients. The reduction in IGFBP3 levels has been associated in with cutaneous melanoma progression, which matches our results (Panasiti, Naspi et al. 2011). This work has fulfilled the aim of identifying differentially expressed proteins

between control and advanced stage cutaneous melanoma serum which were subsequently validated using ELISA. Although, the results did not agree with the hypothesis that protein expression changes would be observed across all stages of disease progression, as in some cases a significant difference was only seen between control or benign and advanced stage disease. As stated above, this may have been affected by the disappointing and somewhat failed method of fractionation.

Some of the targets followed-up in our analysis appear to be promising, such as BACE-2 and lactotransferrin, and may now be further examined as potential markers of melanoma disease progression in larger cohorts of patient samples.

7.7 SELDI-TOF MS Analysis for the Identification of Potential Markers of Uveal and Cutaneous Melanoma

SELDI-TOF can be useful for the discovery of biomarkers as it is high throughput and can demonstrate clear patterns of a proteome, hence illustrating variances between disease and control proteomes across large sample sets. The technique has previously been used for the identification of low molecular weight proteins, i.e. below 40 kDa, as potential biomarkers in clinical specimens (Srinivasan, Daniels et al. 2006). In other proteomic methods, such as 2-D DIGE, this can be difficult and many low molecular weight biomarkers could be missed. A variety of clinical specimens may be used and in the past, analysed body fluids have included; serum, plasma, amniotic fluid, urine, saliva, cerebrospinal liquid, bronchoalveolar wash out, tears, and nipple aspirate fluid. In addition to this, very little sample preparation, and low sample volumes are required (Liu 2011).

Previously, Dr. Priyanka Maurya used SELDI-TOF MS for the discovery of a 7.6 kDa protein in the conditioned media of a paclitaxel-resistant superinvasive cell line variant (MDA-MB-435S-F/Taxol10p4pSI). This was subsequently identified as a fragment of bovine transferrin (Dowling, Maurya et al. 2007). Following the profiling of conditioned media collected from a range of melanocytes and melanoma cell lines, it was discovered that the 7.6 kDa fragment was solely expressed in melanoma cell lines. In addition to this, a number of other proteins which were only identified in the melanoma cell lines were discovered, including an 8.5 kDa ubiquitin-like marker (Dr. Pryanka Maurya, Ph.D. Thesis, 2009).

It was therefore decided to use IMAC SELDI-TOF MS to attempt to locate the 7.6 kDa transferrin fragment and the 8.5 kDa ubiquitin-like marker in cutaneous melanoma serum and uveal melanoma vitreous fluid. This would indicate the possibility of either protein as a potential marker for melanoma. In addition to this, it was decided to profile the serum of advanced cutaneous melanoma patients in comparison to the serum of healthy individuals. A pilot IMAC SELDI-TOF MS analysis of vitreous fluid collected from uveal melanoma patients compared to a control vitreous specimen was also carried out.

7.7.1 SELDI-TOF MS Analysis of Clinical Specimens for the Identification of Potential Biomarkers

The main disadvantage of SELDI is that the identity of a peak of interest is not determined by the technique; it is only possible to acquire the m/z value, and the intensity of the peak. This creates challenges in discovering the identity of a potential biomarker, and hence, in developing commercial assays for use in a clinical environment.

Despite this, SELDI-TOF MS has been used in a variety of clinical studies for the discovery of biomarkers which distinguish between test and control samples. For example, Li et al. utilised nickel-activated IMAC-based SELDI TOF MS technology for the discovery of three biomarkers in 169 sera specimens collected from breast cancer patients. These biomarkers were identified as spectrum peaks at 4.3, 8.1, and 8.92 kDa, respectively. The combined analysis of the three proteins illustrated a sensitivity of 93% for cancer patients and a specificity of 91% for controls (Li, Zhang et al. 2002). Another study identified a number of potential markers, including PC1, PC2, and PC3, which distinguished between prostate cancer and benign prostate disease. They also found that the identified biomarkers illustrated a higher specificity than prostate-specific antigen (PSA) (Li, White et al. 2004).

It should be noted that using a panel of biomarkers could greatly increase the specificity and sensitivity of cancer diagnosis. This is possible using SELDI technology as a panel of peaks may be detected at a time. This was previously carried out in hepatocellular carcinoma (HCC) serum samples, where an 11-protein signature was identified as being overexpressed (Zinkin, Grall et al. 2008).

7.7.2 SELDI-TOF MS Analysis of Cutaneous Melanoma Serum

SELDI-TOF MS analyses of cutaneous melanoma specimens have been carried out, many with the intention of identifying prognostic outcomes. Mian et al. used serum samples collected from 101 early-stage patients which were compared to 104 advanced melanoma sera for the profiling of cutaneous melanoma progression using SELDI technology. They identified signature proteomic profiles which were indicative for different stages of the disease (Mian, Ugurel et al. 2005). Another study used SELDI-TOF MS for the identification of melanoma-associated protein biomarkers of disease recurrence. Multiple protein peaks were identified in the region of 3.3-30 kDa which appeared to discriminate between those who developed recurrence in comparison to those who did not, with high sensitivity and specificity (Wilson, Tran et al. 2004).

In our study, both the 7.6 kDa and the 8.5 kDa proteins of interest were identified as prominent peaks in the conditioned media collected from the SK-MEL5 cutaneous melanoma cell line, which is of low invasive potential. However, when examined for their presence in serum, they were not identified. This would suggest that both proteins are not secreted at a detectable level, or may not be expressed by the tumour, and that they may only be produced in melanoma cell lines. As the serum was immunodepleted, little to no interference from highly abundant proteins was present.

Despite this, another protein, an unknown 8.9 kDa protein, was identified in the conditioned media of SK-MEL 5 cells, even when diluted to levels as low as 1:10. When 12 advanced cutaneous melanoma sera were examined, 10 samples were shown to express the protein of interest, where the potential marker was identified at least once in three replicates. It was also detected in three of 12 controls; however, it was present at a low level in these when compared to melanoma serum samples and hence was still deemed to be of interest.

7.7.3 Pilot SELDI-TOF MS Analysis of Uveal Melanoma Vitreous Fluid

Very little has been reported in the literature as regards the SELDI-TOF MS-based analysis of ocular fluids and nothing has been reported in relation to the vitreous humour of uveal melanoma patients. Using aqueous humour, Ayuso et al.

successfully identified transthyretin as a potential biomarker for juvenile idiopathic arthritis (JIA)-associated uveitis and silent chronic anterior uveitis (AU), inflammatory conditions of the eye (Kalinina Ayuso, de Boer et al. 2013). This illustrates the potential effectiveness of SELDI-TOF MS in determining potential biomarkers in samples which are of low volume or are of a precious nature.

Hence, it was decided to examine vitreous fluid collected from metastatic uveal melanoma patients and control vitreous fluid collected from idopathic macular hole degeneration patients in order to determine the presence of differentially expressed proteins of interest.

From this analysis, the 7.6 kDa transferrin fragment was identified in crude vitreous fluid. However, the 8.5 kDa ubiquitin-like marker was only found in the immunodepleted specimens. This suggests that the potential marker may be easily overshadowed by interference created by high abundance proteins. In the control specimen, this interference was very prominent and hence, no protein peaks were detected. This may have been caused as a result of the notable levels of high abundance proteins, such as serum albumin and immunoglobulin, present in the vitreous which account for over 80% of the whole vitreous fluid proteome (Angi, Kalirai et al. 2012). The 8.9 kDa unknown marker of interest was detected in both the crude and immunodepleted vitreous fluid at high levels.

This suggested that the unknown 8.9 kDa peak could be of great interest as it was identified in SK-MEL 5 conditioned media, advanced cutaneous melanoma serum and metastatic uveal melanoma vitreous fluid, while being absent from either control group. It was therefore decided to attempt to isolate and identify the potential marker.

7.7.4 Attempted Identification of the 8.9 kDa Protein of Interest

As mentioned, the main disadvantage of SELDI-TOF MS is its lack of ability to identify the peaks generated. To overcome this problem, other groups had used spin columns containing a resin which mimicked the surface of the SELDI chip. By allowing the protein to bind to the activated resin using the same chemistry as with a chip, the same protein species may be isolated. Proteins of interest can then be eluted

from the beads using either a competitor ligand, such as imidazole, reduction of the pH, or stripping of the immobilised metal.

7.7.4.1 IMAC-Resin and Imidazole Elution

Following the initial discovery of a peak of interest in rat plasma, Bouchal et al. successfully identified it as retinol-binding 4. As they used IMAC SELDI chips in the initial discovery of the peak, they used IMAC resin to subsequently mimic the chips conditions. Following this it was possible to elute the protein using imidazole, and separate the resulting fraction in the first dimension using an SDS gel. Resulting protein bands were stained and digested into peptides, prior to being identified by MALDI TOF (Bouchal, Jarkovsky et al. 2011).

It was decided to follow this process using conditioned media, vitreous fluid (both control and uveal melanoma), and serum (both control and cutaneous melanoma). Each sample was eluted in fractions, separated in the first dimension and stained. However, the 8.9 kDa protein in question was not identified as no appropriate low molecular weight protein was found in each disease sample which was not present in the controls. It is possible, however, that the 8.9 kDa protein of interest was in fact a fragment of a larger protein. Some of the identifications from this analysis were clearly larger than the expected low molecular weight proteins which indicate that they may have been fragments of larger proteins. This may also have been true for the 8.9 kDa peak of interest.

7.7.4.2 MALDI-TOF

MALDI-TOF can also be used to generate a spectrum of proteins, but, it can also fragment specific peaks and analyse the resulting fragments in TOF/TOF mode in order to identify them (Cazares, Diaz et al. 2008). However, using MALDI-TOF to fragment the proteins present in each elution for the discovery of their identifications, was unsuccessful in this case.

7.7.4.3 On-Chip Elution

It has previously been illustrated that it is possible to identify peaks of interest from a SELDI experiment using an on-chip elution method. Nilsen et al. tested this by binding and subsequently eluting four known proteins directly from a SELDI chip using a change in pH. Subsequently digested peptides were then analysed with LC-MS/MS for the detection of bound proteins (Maeland Nilsen, Uleberg et al. 2011).

It was decided to use an on-chip elution method, using imidazole, for the attempted identification of the 8.9 kDa potential marker. The peptides generated from this analysis were examined using quantitative label-free LC-MS. This identified one main protein of interest; apolipoprotein AII (ApoAII). This protein was found to be significantly upregulated in cutaneous melanoma sera in comparison to control sera. Although ApoAII is reported to have a molecular weight of 11.175 kDa, an 8.9 kDa isoform has been identified. Using LC-MS/MS and immunoassays, Malik et al. identified ApoAII as being upregulated in prostate cancer serum, a finding which correlated with immunohistochemistry results. They also found that the marker appeared to be more specific than PSA, as ApoAII was overexpressed in prostate disease when PSA was not (Malik, Ward et al. 2005).

ApoAII has also been linked with pancreatic adenocarcinoma, where it was shown to be downregulated. However, its exact function in cancer is unclear. In healthy cells, it is required for the transport of lipids, hence, it may be that lipid metabolism is required for malignancies to thrive, such as prostate tumours, and apoAII is necessary for directing the lipid to the cancer. There is significant evidence that cancer cells can specifically alter different aspects of lipid metabolism which may have a knock-on effect on many cellular processes, including cell growth, proliferation, differentiation and motility (Xue, Scarlett et al. 2010, Santos and Schulze 2012).

An ELISA was carried out which indicated that apoAII was not upregulated in advanced cutaneous melanoma sera in comparison to the control, and that it was unchanged across the clinical stages of the disease as well as in uveal melanoma serum. This may be due to the assay detecting other isoforms, as well as the 8.9 kDa potential marker, hence illustrating the abundance of all apoAII isoforms.

A quantitative label-free LC-MS experiment was repeated as before but with a larger cohort of samples. This also indicated that apoAII was not increased in the advanced disease sera. This, in combination with the ELISA results, would suggest that the apoAII isoform may not be the identity of the 8.9 kDa of interest.

All of the above techniques have been shown to be successful in terms of identifying unknown SELDI peaks of interest, however they were not successful in this case, and thus, the identity of the 8.9 kDa potential biomarker remains elusive.

However, the final differential expression analysis of the larger cohort of samples provided a list of 16 proteins which were upregulated in the disease sample set which can now be followed up. It is possible that the 8.9 kDa potential marker may be a fragment of one of these.

7.7.5 34 Differentially Expressed Proteins were Identified Between Control and Advanced Cutaneous Melanoma Sera Using IMAC Purification

From the quantitative label-free LC-MS analysis, 34 statistically significant proteins were found to be differentially regulated between advanced cutaneous melanoma and control sera. These proteins may include potential serum biomarkers for cutaneous melanoma and can now be followed up throughout the progression of melanoma, using serum collected from various stages of the disease.

DAVID analysis indicated that, from the list of proteins upregulated in the cutaneous melanoma sample set, biological processes relating to inflammation and blood coagulation were involved which suggests that such events occurred in response to trauma. This could indicate the damage induced by the aggressive nature of the tumour. Molecular functions which were enriched primarily involved anti-enzyme activities. This inhibition may be an anti-tumour response as the inhibition of endopeptidases has been associated with suppressed growth of tumour cells (Suzuki, Sakaguchi et al. 2013).

Many of the 34 proteins discovered have previously been reported in the literature in relation to cancer. For example, lumican, an anti-tumour proteoglycan, was found by Pietraszek et al. to be involved in the downregulation of melanoma growth and migration (Pietraszek, Brezillon et al. 2013). This result correlates with our study

where we identified it to be downregulated in cutaneous melanoma sera, in comparison to control sera. In addition to this, von Willebrand factor, which we identified as being differentially regulated between control and advanced melanoma sera, has been linked with melanoma-associated thrombin activity (Kerk, Strozyk et al. 2010). From our enrichment analysis, von Willebrand factor was also found to be associated with the upregulation of the complement pathway in advanced cutaneous melanoma. Insulin-like growth factor-binding protein 4 (IGFBP-4), which we identified as being upregulated in the advanced disease serum, has also been associated with the progression from primary to metastatic melanoma (Yu, Warycha et al. 2008).

However, not all have been discussed in terms of melanoma. Below is a selection of some of the identified proteins which may be followed up in cutaneous melanoma serum as part of a future study.

7.7.5.1 Alpha 1-Antitrypsin

Alpha 1-antitrypsin is a circulating protease inhibitor which is known to perform an anti-apoptotic role (Topic, Ljujic et al. 2011). In addition to this, it has been shown to have anti-oxidant and anti-inflammatory activity (Jamnongkan, Techasen et al. 2013).

In our study, it was found to be upregulated in advanced cutaneous melanoma serum by 8.6-fold, in comparison to control serum. Using DAVID analysis, it was noted that anti-enzyme activities such as peptide inhibition, which alpha 1-antitrypsin was involved in, were recognised as statistically significant enriched molecular functions in the list of proteins upregulated in the melanoma group. In addition to this, its overexpression in the advanced disease was found to be associated with the upregulation of the complement pathway.

Alpha 1-antitrypsin has previously been associated with colorectal cancer where it was found to be upregulated in the serum of cancer patients in comparison to controls. In addition to this, it was found to discriminate between early and advanced stages of disease. It has also been linked with gastric cancer where high levels of expression of alpha 1-antitrypsin were found to be produced in the gastric juice

(Bujanda, Sarasqueta et al. 2013). It has been associated with an array of other malignancies such as lung cancer, cholangiocarcinogenesis, and breast cancer (Topic, Ljujic et al. 2011, Lopez-Arias, Aguilar-Lemarroy et al. 2012, Jamnongkan, Techasen et al. 2013).

However, alpha 1-antitrypsin has not previously been identified as a potential serological marker for cutaneous melanoma. Hence, it may of interest to follow its expression over the course of disease.

7.7.5.2 Selenoprotein P

Selenoprotein P is the main transporter of selenium as it can carry up to ten selenocysteine residues, the form of selenium which is incorporated into growing proteins. It has been shown to display anti-oxidant properties, protecting cells such as astrocytes, and endothelial cells from oxidative damage (Gonzalez-Moreno, Boque et al. 2011).

In our study, selenoprotein P was found to be of lower abundance in disease serum in comparison to the control specimens by 2.09-fold, which may indicate that its downregulation is required for tumour progression.

In the literature, selenoprotein has been associated with a number of malignancies including prostate cancer, lung cancer, and colon cancer, in all of which its expression was reduced (Gonzalez-Moreno, Boque et al. 2011).

However, it is not well characterised in cutaneous melanoma and so, it may be an interesting protein to follow up.

7.7.5.3 Alpha 1-Antichymotrypsin

Alpha 1-antichymotrypsin is a serine protease inhibitor which was found to upregulated in our study in cutaneous melanoma sera by 2.55-fold. DAVID analysis indicated that anti-enzymatic molecular functions were found to be enriched in the disease sera, which alpha 1-antichymotrypsin was involved in.

This has previously been associated with poor prognosis in malignant melanoma as well as in other cancers, such as prostate cancer, where it is complexed to prostate-specific antigen (PSA) (Martinez, Espana et al. 2002, Wang, Jiang et al. 2010). In addition this, it has been identified in pancreatic cancer as a possible biomarker for advanced stage pancreatic carcinoma (Roberts, Campa et al. 2012). It was also found to be upregulated in breast cancer and lung adenocarcinoma; in both cases it was thought to play a role in tumorigenesis (Higashiyama, Doi et al. 1995).

As alpha 1-antichymotrypsin has not been linked with cutaneous melanoma serum previously, it may be an interesting protein to further examine.

7.7.6 Conclusion

SELDI-TOF MS is a suitable method for determining the individual protein profiles of sample sets, and for quickly discovering potential variances and potential peaks of interest between them in a high throughput fashion. However, as the identity of a protein may not be determined directly through SELDI-TOF MS, it can be problematic when subsequently identifying potential biomarkers.

Using SELDI TOF MS, the 7.6 kDa transferrin fragment and 8.5 kDa ubiquitin-like marker have been identified in vitreous fluid, however, they were not detected in advanced cutaneous melanoma serum.

Despite not identifying the 8.9 kDa protein/fragment of interest, a number of new potential candidates have been discovered. In addition to this, these proteins may also provide further information on the progression of cutaneous melanoma disease.

Overall, this work fulfilled the aim of using SELDI TOF MS to compare the proteomic profiles of cutaneous melanoma serum, uveal melanoma vitreous fluid, and cutaneous melanoma conditioned media to relevant controls. It also agreed with the hypothesis described as this method highlighted the presence of a potential biomarker present in the disease samples and mostly absent from the control sample sets.

7.8 Comparing the Proteomic Basis of Uveal and Cutaneous Melanoma

The work presented in this thesis illustrates patterns of differential protein expression between stages of disease progression in both uveal and cutaneous melanomas. Both melanomas are of a similar embryonic origin and, as described in section 1.5, some similarities do occur between the two diseases. However, the work illustrated here demonstrates that both melanomas are significantly different in terms of their mechanisms of disease progression.

Although different specimens were examined in both studies; tissue and vitreous fluid in the uveal melanoma work and serum in the cutaneous melanoma work, no common proteins of interest were identified between the two studies. However, this may be due to the differing sample types used and/or the different experimental approaches used.

Uveal melanoma serum was incorporated into the ELISA validation of cutaneous melanoma targets of interest, see section 5.8. This did not identify any patterns of expression which were mutually observed between both melanomas. Again, the lack of correlation observed may be due to the methods by which both melanomas disseminate; uveal melanoma spreads primarily through blood as the eye lacks any lymphatic drainage, while cutaneous melanoma may spread by either system.

From this work, it can be said that both melanomas are entirely different on a proteomic level. However, the lack of correlation between both diseases may be enhanced by the difference in experimental design and the nature of the samples used in both studies.

CHAPTER EIGHT

Conclusions and Future Work

CONCLUSIONS

1. SELENBP1, FABP3, TPI1, EEF1G and KPNB1 all have potential as biomarkers for uveal melanoma metastasis in primary tumour tissue, however more follow-up work is now required.

- All five proteins were identified as being upregulated in subsequently metastasised primary tumour tissue in comparison to that which did not metastasise.
- Each protein was found to be involved in the processes of invasion (independent of MMP-2 and MMP-9) and migration in uveal melanoma cells.
- SELENBP1 may also induce anti-oxidant effects in uveal melanoma cells.
- However, none of the proteins were found to be implicated in either proliferation or apoptosis in uveal melanoma cell lines.
- This work may have improved our understanding of uveal melanoma metastasis, identifying five proteins which may be indicative of poor outcome and may be developed as therapeutic targets in the treatment of metastatic uveal melanoma.

2. Vitreous fluid is a complex sample in terms of its proteomic nature.

- It requires significant pre-processing prior to experimental analysis in order to allow for the identification of a wide variety of both high and, in particular, low abundance proteins. For this purpose, a combination of IMAC chromatography and imidazole fractionation can be used for the successful identification of both low abundant proteins and specific protein subsets in vitreous fluid.

3. Retbindin, retinol-binding protein 3, meckelin, alpha crystallin B, and PEDF were all found to be differentially regulated between the vitreous fluid of monosomy three uveal melanoma patients and that of disomy three uveal melanoma patients. Of these, retbindin, retinol-binding protein three, and meckelin have not previously been identified in uveal melanoma vitreous fluid. All five proteins may be suitable prognostic biomarkers for poor outcome in uveal melanoma, and may act as

therapeutic targets in the treatment of the disease, however, further studies are now required to test this.

4. FGF2, MIP1α and IFNɣ may be useful as potential indicators of uveal melanoma in vitreous fluid, in comparison to control specimens and will now be followed up in a larger sample set.

5. Serotransferrin, lactotransferrin, azurocidin, plasma serine protease inhibitor, MMP-1, TIMP-1 and BACE-2 may be potential biomarkers for cutaneous melanoma and will now be further examined in a larger study.

- Using quantitative LC-MS, serotransferrin, lactotransferrin, and azurocidin were all identified as being upregulated in advanced cutaneous melanoma sera in comparison to control sera from healthy patients, while plasma serine protease inhibitor was found to be overexpressed in the control sample set.
- MMP-1, TIMP-1, and BACE-2 mRNA levels were identified by Dr. Stephen Madden and Dr. Paul Dowling as being significantly upregulated in metastasised cutaneous melanoma tissue and primary melanoma tumour tissue in comparison to the healthy, control tissue.
- Using ELISA, lactotransferrin was found to be significantly overexpressed in advanced cutaneous melanoma sera when compared to the benign disease sample set.
- Using ELISA, BACE-2 was also identified as being significantly overexpressed in advanced cutaneous melanoma sera, when compared to either healthy, control or benign disease sera.

6. SELDI-TOF is a suitable method for quickly and easily determining the individual protein profiles of sample sets, and for quickly discovering differentially expressed potential peaks of interest between them in a high throughput fashion; however, it may be difficult to subsequently determine the identity of these proteins.

- A 7.6 kDa transferrin fragment and an 8.5 kDa ubiquitin-like marker were identified in uveal melanoma vitreous fluid and media conditioned by cutaneous melanoma cells, while being undetectable in control vitreous fluid

collected from a benign disease (macular hole degeneration). However, neither was detected in advanced cutaneous melanoma serum.

- An unknown 8.9 kDa protein was discovered in uveal melanoma vitreous fluid, media conditioned by cutaneous melanoma cells, and in advanced cutaneous melanoma serum, while it was absent from control vitreous fluid, collected from a benign disease, and control serum.
- Following an attempted IMAC purification and subsequent MALDI TOF or quantitative label-free LC-MS analysis of the fractions, the identification of the protein could not be determined.
- Further evaluation discovered a number of proteins which were differentially expressed between control and advanced disease sera which may be candidates for the identity of the 8.9 kDa peak of interest. This protein list may also provide a number of potential biomarkers for advanced cutaneous melanoma.

FUTURE WORK

1. Prior to further analysis, larger sample sets would be used in order to validate the results acquired from the work presented in this thesis. From these discovery phase data, power analysis would be used in order to calculate appropriate sample sizes.

2. As CNDP2 was found to be downregulated in primary tumour tissue which subsequently metastasised in comparison to that which did not, the protein could be overexpressed in 92.1 and MEL202 uveal melanoma cells using a cDNA-based method.

- CNDP2 may play a role as a tumour suppressor, as described in section 7.3, hence, it would be of interest to carry out invasion and migration assays with the transfected cells in order to determine the potential role of CNDP2 in uveal melanoma disease progression and the impact of its upregulation in the metastatic potential of the cells.
- It would also be of relevance to examine the role of CNDP2 in proliferation, using the cDNA transfected uveal melanoma cells.
- In addition to this, anoikis (anchorage-dependent cell death) and apoptosis (programmed cell death) assays could be performed for the analysis of the role of CNDP2 in cell death as part of uveal melanoma disease progression.

3. It may be of interest to further examine the role of TPI1, FABP3, SELENBP1, KPNB1, and EEF1G in uveal melanoma disease progression.

- A uveal melanoma cell line derived from a secondary tumour, such as OMM2.5, could be transfected with siRNA against the respective targets in order to decrease their expression. The transfected cells could then be assessed for changes in their proliferative, invasive and migratory potentials, as this would further indicate the role of the potential targets in metastasis.
- In addition to this, anoikis assays may further determine a function of the five proteins in resistance to anchorage dependent cell death which is a commonly gained feature of cancer cells.

- Proteins of interest may assessed in cell culture as potential therapeutic targets through the application of targeted agents, such as glycolytic inhibitors and nuclear transport inhibitors in the case of TPI1, and KPNB1, respectively. The effects of these agents on cellular processes, such as proliferation, and their levels of toxicity may then be determined.

4. For the vitreous fluid sample preparation, it may be interesting to use alternative methods of protein fractionation.

- This may involve using another resin, such as cation exchange, as this may isolate another subtype of proteins. Hence, this may illustrate a new aspect of the uveal melanoma vitreous proteome and, using differential expression analysis between disease states, may allow for the identification of other proteins which are indicative of diagnosis or prognosis in uveal melanoma.
- It may also be of interest to incorporate an immunodepletion step prior to IMAC-fractionation of the vitreous fluid. This would reduce the level of the most abundant proteins present in the vitreous, thus allowing for the most efficient mining of the low abundance proteome.

5. Potential targets of interest identified as being differentially regulated throughout the progression of cutaneous melanoma, and between monosomy three and disomy three uveal melanoma vitreous fluids, could be further followed up.

- Using ELISA validation, a larger cohort of samples could be used for the further validation of targets identified in the preliminary ELISA analysis, such as BACE-2 and lactotransferrin, as potential biomarkers of disease progression.
- It may also be of interest to follow up panels of potential targets in larger sample sets using logistic regression and ROC curve analysis, as this may lead to the development of predictive models for various disease states, e.g. early stage cutaneous melanoma or monosomy three uveal melanoma, by providing stronger specificity and sensitivity values than the proteins on their own.
- Cutaneous melanoma markers of interest could be examined in cutaneous melanoma cell lines, such as SK-MEL 5 and SK-MEL 28, to discover their

potential functional roles as secreted proteins. Using siRNA transfection, knockdown studies could be carried out in order to understand the potential roles of notable proteins, such as BACE-2 and lactotransferrin, in processes such as proliferation, invasion, and migration.

6. The three targets identified in the preliminary Luminex multiplex assays; IFNγ, MIP1α, and FGF2, could be validated in a larger sample set of vitreous fluid samples consisting of control, uveal melanoma monosomy three, and uveal melanoma disomy three specimens. This could indicate their potential roles in uveal melanoma metastasis, and as prognostic biomarkers for uveal melanoma.

7. Proteins discovered as being differentially expressed between the control and advanced cutaneous melanoma serum samples could be followed up in relation to the elusive 8.9 kDa peak of interest. It is possible that the potential marker of interest is a fragment of one of these proteins.

- Potential targets of interest which were identified in the quantitative LC-MS study as being differentially expressed between control and advanced cutaneous melanoma serum could also be followed up as potential biomarkers for advanced cutaneous melanoma. Using siRNA transfection and functional studies, such as invasion and migration assays, the roles of proteins such as alpha 1-antichymotrypsin and alpha 1-antitrypsin could be further examined in cutaneous melanoma and its progression. This could be carried out using both cell lines of high and low invasive potential, e.g. SK-MEL 5 and SK-MEL 28.
- It may also be of interest to further examine the role of selenoprotein P in oxidative metabolism as it has previously been associated with anti-oxidant properties and was identified in my work as being less abundant in advanced cutaneous melanoma serum in comparison to control serum. This would require over-expression studies in cutaneous melanoma cell lines using cDNA specific to the target, and performing a ROS assay, for the analysis of its role as an anti-oxidant.

REFERENCES

AACR (2013). "Selumetinib shows promise in metastatic uveal melanoma." Cancer Discov **3**(7): OF8.

Aalto, Y., L. Eriksson, S. Seregard, O. Larsson and S. Knuutila (2001). "Concomitant loss of chromosome 3 and whole arm losses and gains of chromosome 1, 6, or 8 in metastasizing primary uveal melanoma." Invest Ophthalmol Vis Sci **42**(2): 313-317.

Abdel-Rahman, M. H., G. Boru, J. Massengill, M. M. Salem and F. H. Davidorf (2010). "MET oncogene inhibition as a potential target of therapy for uveal melanomas." Invest Ophthalmol Vis Sci **51**(7): 3333-3339.

Abildgaard, S. K. and H. Vorum (2013). "Proteomics of Uveal Melanoma: A Minireview." J Oncol **2013**: 820953.

Aguissa-Toure, A. H. and G. Li (2012). "Genetic alterations of PTEN in human melanoma." Cell Mol Life Sci **69**(9): 1475-1491.

Al-Ghoul, M., T. B. Bruck, J. L. Lauer-Fields, V. S. Asirvatham, C. Zapata, R. G. Kerr and G. B. Fields (2008). "Comparative proteomic analysis of matched primary and metastatic melanoma cell lines." J Proteome Res **7**(9): 4107-4118.

Alban, A., S. O. David, L. Bjorkesten, C. Andersson, E. Sloge, S. Lewis and I. Currie (2003). "A novel experimental design for comparative two-dimensional gel analysis: two-dimensional difference gel electrophoresis incorporating a pooled internal standard." Proteomics **3**(1): 36-44.

Albert, D. M. D.-W., M.; Robinson, N.L.; Grossniklaus, H.E.; Green, R. (1998). "Histopathologic characteristics of uveal melanomas in eyes enucleated from the Collaborative Ocular Melanoma Study. COMS report no. 6." Am J Ophthalmol **125**(6): 745-766.

Albery, W. J. and J. R. Knowles (1976). "Free-energy profile of the reaction catalyzed by triosephosphate isomerase." Biochemistry **15**(25): 5627-5631.

All-Ericsson, C., L. Girnita, S. Seregard, A. Bartolazzi, M. J. Jager and O. Larsson (2002). "Insulin-like growth factor-1 receptor in uveal melanoma: a predictor for metastatic disease and a potential therapeutic target." Invest Ophthalmol Vis Sci **43**(1): 1-8.

Altenberg, B. and K. O. Greulich (2004). "Genes of glycolysis are ubiquitously overexpressed in 24 cancer classes." Genomics **84**(6): 1014-1020.

Anderson, N. L. and N. G. Anderson (2002). "The human plasma proteome: history, character, and diagnostic prospects." Mol Cell Proteomics **1**(11): 845-867.

Andley, U. P. (2007). "Crystallins in the eye: Function and pathology." Prog Retin Eye Res **26**(1): 78-98.

Andreeff, M. G., D.W.; Pardee, A.B. (2000). Cell Proliferation, Differentiation, and Apoptosis. Holland-Frei Cancer Medicine. 5th edition. R. C. Bast.

Angi, M., H. Kalirai, S. E. Coupland, B. E. Damato, F. Semeraro and M. R. Romano (2012). "Proteomic analyses of the vitreous humour." Mediators Inflamm **2012**: 148039.

Aoude, L. G., C. M. Vajdic, A. Kricker, B. Armstrong and N. K. Hayward (2013). "Prevalence of germline BAP1 mutation in a population-based sample of uveal melanoma cases." Pigment Cell Melanoma Res **26**(2): 278-279.

Aoyama, A., R. H. Steiger, E. Frohli, R. Schafer, A. von Deimling, O. D. Wiestler and R. Klemenz (1993). "Expression of alpha B-crystallin in human brain tumors." Int J Cancer **55**(5): 760-764.

Aravind, P., G. Wistow, Y. Sharma and R. Sankaranarayanan (2008). "Exploring the limits of sequence and structure in a variant betagamma-crystallin domain of the protein absent in melanoma-1 (AIM1)." J Mol Biol **381**(3): 509-518.

Aretz, S., T. U. Krohne, K. Kammerer, U. Warnken, A. Hotz-Wagenblatt, M. Bergmann, B. V. Stanzel, T. Kempf, F. G. Holz, M. Schnolzer and J. Kopitz (2013). "In-depth mass spectrometric mapping of the human vitreous proteome." Proteome Sci **11**(1): 22.

Arora, S., J. M. Yang, T. G. Kinzy, R. Utsumi, T. Okamoto, T. Kitayama, P. A. Ortiz and W. N. Hait (2003). "Identification and characterization of an inhibitor of eukaryotic elongation factor 2 kinase against human cancer cell lines." Cancer Res **63**(20): 6894-6899.

Astrand, R., J. Unden and B. Romner (2013). "Clinical use of the calcium-binding S100B protein." Methods Mol Biol **963**: 373-384.

Aureli, C., E. Gaucci, V. Arcangeli, C. Grillo, M. Eufemi and S. Chichiarelli (2013). "ERp57/PDIA3 binds specific DNA fragments in a melanoma cell line." Gene **524**(2): 390-395.

Bakalian, S., J. C. Marshall, P. Logan, D. Faingold, S. Maloney, S. Di Cesare, C. Martins, B. F. Fernandes and M. N. Burnier, Jr. (2008). "Molecular pathways mediating liver metastasis in patients with uveal melanoma." Clin Cancer Res **14**(4): 951-956.

Baker, H. N., R. Murphy, E. Lopez and C. Garcia (2012). "Conversion of a capture ELISA to a Luminex xMAP assay using a multiplex antibody screening method." J Vis Exp(65).

Balch, C. M., A. C. Buzaid, S. J. Soong, M. B. Atkins, N. Cascinelli, D. G. Coit, I. D. Fleming, J. E. Gershenwald, A. Houghton, Jr., J. M. Kirkwood, K. M. McMasters, M. F. Mihm, D. L. Morton, D. S. Reintgen, M. I. Ross, A. Sober, J. A. Thompson and J. F. Thompson (2001). "Final version of the American Joint Committee on Cancer staging system for cutaneous melanoma." J Clin Oncol **19**(16): 3635-3648.

Balch, C. M., J. E. Gershenwald, S. J. Soong, J. F. Thompson, M. B. Atkins, D. R. Byrd, A. C. Buzaid, A. J. Cochran, D. G. Coit, S. Ding, A. M. Eggermont, K. T. Flaherty, P. A. Gimotty, J. M. Kirkwood, K. M. McMasters, M. C. Mihm, Jr., D. L. Morton, M. I. Ross, A. J. Sober and V. K. Sondak (2009). "Final version of 2009 AJCC melanoma staging and classification." J Clin Oncol **27**(36): 6199-6206.

Bande, M. F., M. Santiago, M. J. Blanco, P. Mera, C. Capeans, M. X. Rodriguez-Alvarez, M. Pardo and A. Pineiro (2012). "Serum DJ-1/PARK 7 is a potential biomarker of choroidal nevi transformation." Invest Ophthalmol Vis Sci **53**(1): 62-67.

Banerji, U., A. Affolter, I. Judson, R. Marais and P. Workman (2008). "BRAF and NRAS mutations in melanoma: potential relationships to clinical response to HSP90 inhibitors." Mol Cancer Ther **7**(4): 737-739.

Bantscheff, M., M. Schirle, G. Sweetman, J. Rick and B. Kuster (2007). "Quantitative mass spectrometry in proteomics: a critical review." Anal Bioanal Chem **389**(4): 1017-1031.

Barak, V., J. Pe'er, I. Kalickman and S. Frenkel (2011). "VEGF as a biomarker for metastatic uveal melanoma in humans." Curr Eye Res **36**(4): 386-390.

Becerra, S. P. and V. Notario (2013). "The effects of PEDF on cancer biology: mechanisms of action and therapeutic potential." Nat Rev Cancer **13**(4): 258-271.

Berth, M., F. M. Moser, M. Kolbe and J. Bernhardt (2007). "The state of the art in the analysis of two-dimensional gel electrophoresis images." Appl Microbiol Biotechnol **76**(6): 1223-1243.

Beutel, J., J. Wegner, R. Wegner, F. Ziemssen, K. Nassar, J. M. Rohrbach, R. D. Hilgers, M. Luke and S. Grisanti (2009). "Possible implications of MCAM expression in metastasis and non-metastatic of primary uveal melanoma patients." Curr Eye Res **34**(11): 1004-1009.

Bianciotto, C., C. L. Shields, C. E. Thirkill, M. A. Materin and J. A. Shields (2010). "Paraneoplastic retinopathy with multiple detachments of the neurosensory retina and autoantibodies against interphotoreceptor retinoid binding protein (IRBP) in cutaneous melanoma." Br J Ophthalmol **94**(12): 1684-1685, 1696.

Boja, E., T. Hiltke, R. Rivers, C. Kinsinger, A. Rahbar, M. Mesri and H. Rodriguez (2011). "Evolution of clinical proteomics and its role in medicine." J Proteome Res **10**(1): 66-84.

Boschetti, E. and P. G. Righetti (2008). "The ProteoMiner in the proteomic arena: a non-depleting tool for discovering low-abundance species." J Proteomics **71**(3): 255-264.

Bosserhoff, A. K., M. Kaufmann, B. Kaluza, I. Bartke, H. Zirngibl, R. Hein, W. Stolz and R. Buettner (1997). "Melanoma-inhibiting activity, a novel serum marker for progression of malignant melanoma." Cancer Res **57**(15): 3149-3153.

Bouchal, P., J. Jarkovsky, K. Hrazdilova, M. Dvorakova, I. Struharova, L. Hernychova, J. Damborsky, P. Sova and B. Vojtesek (2011). "The new platinum-based anticancer agent LA-12 induces retinol binding protein 4 in vivo." Proteome Sci **9**(1): 68.

Bougnoux, A. C. and J. Solassol (2013). "The contribution of proteomics to the identification of biomarkers for cutaneous malignant melanoma." Clin Biochem **46**(6): 518-523.

Brandt, K., K. Lundell and K. Brismar (2011). "Neutrophil-derived azurocidin cleaves insulin-like growth factor-binding protein-1, -2 and -4." Growth Horm IGF Res **21**(3): 167-173.

Bui, T. and C. B. Thompson (2006). "Cancer's sweet tooth." Cancer Cell **9**(6): 419-420.

Bujanda, L., C. Sarasqueta, A. Cosme, E. Hijona, J. M. Enriquez-Navascues, C. Placer, E. Villarreal, M. Herreros-Villanueva, M. D. Giraldez, M. Gironella, F.

Balaguer and A. Castells (2013). "Evaluation of alpha 1-antitrypsin and the levels of mRNA expression of matrix metalloproteinase 7, urokinase type plasminogen activator receptor and COX-2 for the diagnosis of colorectal cancer." PLoS One **8**(1): e51810.

Burgeiro, A., F. Mollinedo and P. J. Oliveira (2013). "Ipilimumab and vemurafenib: two different routes for targeting melanoma." Curr Cancer Drug Targets **13**(8): 879-894.

Burgeiro, A., F. Mollinedo and P. J. Oliveira (2013). "Ipilimumab and Vemurafenib: Two Different Routes for Targeting Melanoma." Curr Cancer Drug Targets.

Byrjalsen, I., P. Mose Larsen, S. J. Fey, L. Nilas, M. R. Larsen and C. Christiansen (1999). "Two-dimensional gel analysis of human endometrial proteins: characterization of proteins with increased expression in hyperplasia and adenocarcinoma." Mol Hum Reprod **5**(8): 748-756.

Calipel, A., G. Lefevre, C. Pouponnot, F. Mouriaux, A. Eychene and F. Mascarelli (2003). "Mutation of B-Raf in human choroidal melanoma cells mediates cell proliferation and transformation through the MEK/ERK pathway." J Biol Chem **278**(43): 42409-42418.

Canas, B., D. Lopez-Ferrer, A. Ramos-Fernandez, E. Camafeita and E. Calvo (2006). "Mass spectrometry technologies for proteomics." Brief Funct Genomic Proteomic **4**(4): 295-320.

Capello, M., S. Ferri-Borgogno, P. Cappello and F. Novelli (2011). "alpha-Enolase: a promising therapeutic and diagnostic tumor target." FEBS J **278**(7): 1064-1074.

Caron, J., A. Mange, B. Guillot and J. Solassol (2009). "Highly sensitive detection of melanoma based on serum proteomic profiling." J Cancer Res Clin Oncol **135**(9): 1257-1264.

Castagna, A., D. Cecconi, L. Sennels, J. Rappsilber, L. Guerrier, F. Fortis, E. Boschetti, L. Lomas and P. G. Righetti (2005). "Exploring the hidden human urinary proteome via ligand library beads." J Proteome Res **4**(6): 1917-1930.

Cazares, L. H., J. I. Diaz, R. R. Drake and O. J. Semmes (2008). "MALDI/SELDI protein profiling of serum for the identification of cancer biomarkers." Methods Mol Biol **428**: 125-140.

Chapman, P. B., A. Hauschild, C. Robert, J. B. Haanen, P. Ascierto, J. Larkin, R. Dummer, C. Garbe, A. Testori, M. Maio, D. Hogg, P. Lorigan, C. Lebbe, T. Jouary, D. Schadendorf, A. Ribas, S. J. O'Day, J. A. Sosman, J. M. Kirkwood, A. M.

Eggermont, B. Dreno, K. Nolop, J. Li, B. Nelson, J. Hou, R. J. Lee, K. T. Flaherty, G. A. McArthur and B.-S. Group (2011). "Improved survival with vemurafenib in melanoma with BRAF V600E mutation." N Engl J Med **364**(26): 2507-2516.

Chi, K., D. V. Jones and M. L. Frazier (1992). "Expression of an elongation factor 1 gamma-related sequence in adenocarcinomas of the colon." Gastroenterology **103**(1): 98-102.

Chin, D., G. M. Boyle, R. M. Williams, K. Ferguson, N. Pandeya, J. Pedley, C. M. Campbell, D. R. Theile, P. G. Parsons and W. B. Coman (2005). "Alpha B-crystallin, a new independent marker for poor prognosis in head and neck cancer." Laryngoscope **115**(7): 1239-1242.

Chiou, S. H., C. H. Huang, I. L. Lee, Y. T. Wang, N. Y. Liu, Y. G. Tsay and Y. J. Chen (2010). "Identification of in vivo phosphorylation sites of lens proteins from porcine eye lenses by a gel-free phosphoproteomics approach." Mol Vis **16**: 294-302.

Chowdhury, U. R., B. J. Madden, M. C. Charlesworth and M. P. Fautsch (2010). "Proteome analysis of human aqueous humor." Invest Ophthalmol Vis Sci **51**(10): 4921-4931.

Coit, D. G. and A. J. Olszanski (2013). "Progress in the management of melanoma in 2013." J Natl Compr Canc Netw **11**(5 Suppl): 645-648.

Collin, G. B., J. Won, W. L. Hicks, S. A. Cook, P. M. Nishina and J. K. Naggert (2012). "Meckelin is necessary for photoreceptor intraciliary transport and outer segment morphogenesis." Invest Ophthalmol Vis Sci **53**(2): 967-974.

Coscia, A., S. Orru, P. Di Nicola, F. Giuliani, A. Varalda, C. Peila, C. Fabris, A. Conti and E. Bertino (2012). "Detection of cow's milk proteins and minor components in human milk using proteomics techniques." J Matern Fetal Neonatal Med **25 Suppl 4**: 54-56.

Coupland, S. E., G. Anastassiou, A. Stang, H. Schilling, I. Anagnostopoulos, N. Bornfeld and H. Stein (2000). "The prognostic value of cyclin D1, p53, and MDM2 protein expression in uveal melanoma." J Pathol **191**(2): 120-126.

Coupland, S. E., S. L. Lake, M. Zeschnigk and B. E. Damato (2013). "Molecular pathology of uveal melanoma." Eye (Lond) **27**(2): 230-242.

Coupland, S. E., H. Vorum, N. Mandal, H. Kalirai, B. Honore, S. F. Urbak, S. L. Lake, J. Dopierala and B. Damato (2010). "Proteomics of uveal melanomas suggests

HSP-27 as a possible surrogate marker of chromosome 3 loss." Invest Ophthalmol Vis Sci **51**(1): 12-20.

Coussens, L. M., B. Fingleton and L. M. Matrisian (2002). "Matrix metalloproteinase inhibitors and cancer: trials and tribulations." Science **295**(5564): 2387-2392.

Couturier, J. and S. Saule (2012). "Genetic determinants of uveal melanoma." Dev Ophthalmol **49**: 150-165.

Crosby, M. B., H. Yang, W. Gao, L. Zhang and H. E. Grossniklaus (2011). "Serum vascular endothelial growth factor (VEGF) levels correlate with number and location of micrometastases in a murine model of uveal melanoma." Br J Ophthalmol **95**(1): 112-117.

Custodio, A., A. J. Lopez-Farre, J. J. Zamorano-Leon, P. J. Mateos-Caceres, C. Macaya, T. Caldes, M. de la Hoya, E. Olivera, J. Puente, E. Diaz-Rubio and P. Perez-Segura (2012). "Changes in the expression of plasma proteins associated with thrombosis in BRCA1 mutation carriers." J Cancer Res Clin Oncol **138**(5): 867-875.

Damato, B. (2004). "Developments in the management of uveal melanoma." Clin Experiment Ophthalmol **32**(6): 639-647.

Damato, B. (2012). "Progress in the management of patients with uveal melanoma. The 2012 Ashton Lecture." Eye (Lond) **26**(9): 1157-1172.

Damato, B. and S. E. Coupland (2009). "Translating uveal melanoma cytogenetics into clinical care." Arch Ophthalmol **127**(4): 423-429.

Damato, B., C. Duke, S. E. Coupland, P. Hiscott, P. A. Smith, I. Campbell, A. Douglas and P. Howard (2007). "Cytogenetics of uveal melanoma: a 7-year clinical experience." Ophthalmology **114**(10): 1925-1931.

Damato, B. E. (2012). "Treatment selection for uveal melanoma." Dev Ophthalmol **49**: 16-26.

Damato, E. M., M. Angi, M. R. Romano, F. Semeraro and C. Costagliola (2012). "Vitreous analysis in the management of uveitis." Mediators Inflamm **2012**: 863418.

Danielli, R., R. Ridolfi, V. Chiarion-Sileni, P. Queirolo, A. Testori, R. Plummer, M. Boitano, L. Calabro, C. D. Rossi, A. M. Giacomo, P. F. Ferrucci, L. Ridolfi, M. Altomonte, C. Miracco, A. Balestrazzi and M. Maio (2012). "Ipilimumab in pretreated patients with metastatic uveal melanoma: safety and clinical efficacy." Cancer Immunol Immunother **61**(1): 41-48.

Daniels, A. B. and D. H. Abramson (2009). "c-KIT in uveal melanoma: big fish or red herring?" Arch Ophthalmol **127**(5): 695-697.

Davies, H., G. R. Bignell, C. Cox, P. Stephens, S. Edkins, S. Clegg, J. Teague, H. Woffendin, M. J. Garnett, W. Bottomley, N. Davis, E. Dicks, R. Ewing, Y. Floyd, K. Gray, S. Hall, R. Hawes, J. Hughes, V. Kosmidou, A. Menzies, C. Mould, A. Parker, C. Stevens, S. Watt, S. Hooper, R. Wilson, H. Jayatilake, B. A. Gusterson, C. Cooper, J. Shipley, D. Hargrave, K. Pritchard-Jones, N. Maitland, G. Chenevix-Trench, G. J. Riggins, D. D. Bigner, G. Palmieri, A. Cossu, A. Flanagan, A. Nicholson, J. W. Ho, S. Y. Leung, S. T. Yuen, B. L. Weber, H. F. Seigler, T. L. Darrow, H. Paterson, R. Marais, C. J. Marshall, R. Wooster, M. R. Stratton and P. A. Futreal (2002). "Mutations of the BRAF gene in human cancer." Nature **417**(6892): 949-954.

Davies, L., D. Spiller, M. R. White, I. Grierson and L. Paraoan (2011). "PERP expression stabilizes active p53 via modulation of p53-MDM2 interaction in uveal melanoma cells." Cell Death Dis **2**: e136.

Davies, M. A., P. Liu, S. McIntyre, K. B. Kim, N. Papadopoulos, W. J. Hwu, P. Hwu and A. Bedikian (2011). "Prognostic factors for survival in melanoma patients with brain metastases." Cancer **117**(8): 1687-1696.

Dawe, H. R., U. M. Smith, A. R. Cullinane, D. Gerrelli, P. Cox, J. L. Badano, S. Blair-Reid, N. Sriram, N. Katsanis, T. Attie-Bitach, S. C. Afford, A. J. Copp, D. A. Kelly, K. Gull and C. A. Johnson (2007). "The Meckel-Gruber Syndrome proteins MKS1 and meckelin interact and are required for primary cilium formation." Hum Mol Genet **16**(2): 173-186.

De Bock, M., D. de Seny, M. A. Meuwis, J. P. Chapelle, E. Louis, M. Malaise, M. P. Merville and M. Fillet (2010). "Challenges for biomarker discovery in body fluids using SELDI-TOF-MS." J Biomed Biotechnol **2010**: 906082.

de Manzoni, G., A. Guglielmi, G. Verlato, A. Tomezzoli, G. Pelosi, I. Schiavon and C. Cordiano (1998). "Prognostic significance of 67-kDa laminin receptor expression in advanced gastric cancer." Oncology **55**(5): 456-460.

De Potter, P. (2003). "[Treatment of intraocular melanoma: new concepts]." Bull Mem Acad R Med Belg **158**(1-2): 103-111; discussion 111-102.

de Souza, G. A., L. M. Godoy and M. Mann (2006). "Identification of 491 proteins in the tear fluid proteome reveals a large number of proteases and protease inhibitors." Genome Biol **7**(8): R72.

De Waard-Siebinga, I., D. J. Blom, M. Griffioen, P. I. Schrier, E. Hoogendoorn, G. Beverstock, E. H. Danen and M. J. Jager (1995). "Establishment and characterization of an uveal-melanoma cell line." Int J Cancer **62**(2): 155-161.

den Hollander, A. I., T. L. McGee, C. Ziviello, S. Banfi, T. P. Dryja, F. Gonzalez-Fernandez, D. Ghosh and E. L. Berson (2009). "A homozygous missense mutation in the IRBP gene (RBP3) associated with autosomal recessive retinitis pigmentosa." Invest Ophthalmol Vis Sci **50**(4): 1864-1872.

Deng, M., Q. Ye, Z. Qin, Y. Zheng, W. He, H. Tang, Y. Zhou, W. Xiong, M. Zhou, X. Li, Q. Yan, J. Ma and G. Li (2013). "miR-214 promotes tumorigenesis by targeting lactotransferrin in nasopharyngeal carcinoma." Tumour Biol **34**(3): 1793-1800.

Denton, C. L., E. Minthorn, S. W. Carson, G. C. Young, L. E. Richards-Peterson, J. Botbyl, C. Han, R. A. Morrison, S. C. Blackman and D. Ouellet (2013). "Concomitant oral and intravenous pharmacokinetics of dabrafenib, a BRAF inhibitor, in patients with BRAF V600 mutation-positive solid tumors." J Clin Pharmacol.

Dikovskaya, M. A., A. N. Trunov, V. V. Chernykh and T. A. Korolenko (2013). "Cystatin C and lactoferrin concentrations in biological fluids as possible prognostic factors in eye tumor development." Int J Circumpolar Health **72**.

Dowling, P., P. Maurya, P. Meleady, S. A. Glynn, A. J. Dowd, M. Henry and M. Clynes (2007). "Purification and identification of a 7.6-kDa protein in media conditioned by superinvasive cancer cells." Anticancer Res **27**(3A): 1309-1317.

Dunavoelgyi, R., M. Funk, S. Sacu, M. Georgopoulos, G. Zlabinger, M. Zehetmayer and U. Schmidt-Erfurth (2012). "Intraocular activation of angiogenic and inflammatory pathways in uveal melanoma." Retina **32**(7): 1373-1384.

Economou, M. A., S. Andersson, D. Vasilcanu, C. All-Ericsson, E. Menu, A. Girnita, L. Girnita, M. Axelson, S. Seregard and O. Larsson (2008). "Oral picropodophyllin (PPP) is well tolerated in vivo and inhibits IGF-1R expression and growth of uveal melanoma." Invest Ophthalmol Vis Sci **49**(6): 2337-2342.

Egberts, F., A. Pollex, J. H. Egberts, K. C. Kaehler, M. Weichenthal and A. Hauschild (2008). "Long-term survival analysis in metastatic melanoma: serum S100B is an independent prognostic marker and superior to LDH." Onkologie **31**(7): 380-384.

Ehlers, J. P., L. Worley, M. D. Onken and J. W. Harbour (2008). "Integrative genomic analysis of aneuploidy in uveal melanoma." Clin Cancer Res **14**(1): 115-122.

Eisenfeld, A. J., A. H. Bunt-Milam and J. C. Saari (1987). "Uveoretinitis in rabbits following immunization with interphotoreceptor retinoid-binding protein." Exp Eye Res **44**(3): 425-438.

Ellis, M. J., L. Ding, D. Shen, J. Luo, V. J. Suman, J. W. Wallis, B. A. Van Tine, J. Hoog, R. J. Goiffon, T. C. Goldstein, S. Ng, L. Lin, R. Crowder, J. Snider, K. Ballman, J. Weber, K. Chen, D. C. Koboldt, C. Kandoth, W. S. Schierding, J. F. McMichael, C. A. Miller, C. Lu, C. C. Harris, M. D. McLellan, M. C. Wendl, K. DeSchryver, D. C. Allred, L. Esserman, G. Unzeitig, J. Margenthaler, G. V. Babiera, P. K. Marcom, J. M. Guenther, M. Leitch, K. Hunt, J. Olson, Y. Tao, C. A. Maher, L. L. Fulton, R. S. Fulton, M. Harrison, B. Oberkfell, F. Du, R. Demeter, T. L. Vickery, A. Elhammali, H. Piwnica-Worms, S. McDonald, M. Watson, D. J. Dooling, D. Ota, L. W. Chang, R. Bose, T. J. Ley, D. Piwnica-Worms, J. M. Stuart, R. K. Wilson and E. R. Mardis (2012). "Whole-genome analysis informs breast cancer response to aromatase inhibition." Nature **486**(7403): 353-360.

Feener, E. (2012). Proteomics in the Vitreous of Diabetic Retinopathy Patients. Visual Dysfunction in Diabetes. J. Tombran-Tink, C. J. Barnstable and T. W. Gardner, Springer New York**:** 173-188.

Fernandez-Barral, A., J. L. Orgaz, V. Gomez, L. del Peso, M. J. Calzada and B. Jimenez (2012). "Hypoxia negatively regulates antimetastatic PEDF in melanoma cells by a hypoxia inducible factor-independent, autophagy dependent mechanism." PLoS One **7**(3): e32989.

Fernandez-Costa, C., V. Calamia, P. Fernandez-Puente, J. L. Capelo-Martinez, C. Ruiz-Romero and F. J. Blanco (2012). "Sequential depletion of human serum for the search of osteoarthritis biomarkers." Proteome Sci **10**(1): 55.

Finck, S. J., A. E. Giuliano and D. L. Morton (1983). "LDH and melanoma." Cancer **51**(5): 840-843.

Findeisen, P., M. Zapatka, T. Peccerella, H. Matzk, M. Neumaier, D. Schadendorf and S. Ugurel (2009). "Serum amyloid A as a prognostic marker in melanoma identified by proteomic profiling." J Clin Oncol **27**(13): 2199-2208.

Finger, P. T. (1997). "Radiation therapy for choroidal melanoma." Surv Ophthalmol **42**(3): 215-232.

Fitzgerald, R. L., C. L. O'Neal, B. J. Hart, A. Poklis and D. A. Herold (1997). "Comparison of an ion-trap and a quadrupole mass spectrometer using diazepam as a model compound." J Anal Toxicol **21**(6): 445-450.

Fliegauf, M., T. Benzing and H. Omran (2007). "When cilia go bad: cilia defects and ciliopathies." Nat Rev Mol Cell Biol **8**(11): 880-893.

Fluhrer, R., A. Capell, G. Westmeyer, M. Willem, B. Hartung, M. M. Condron, D. B. Teplow, C. Haass and J. Walter (2002). "A non-amyloidogenic function of BACE-2 in the secretory pathway." J Neurochem **81**(5): 1011-1020.

Fong, L. and E. J. Small (2008). "Anti-cytotoxic T-lymphocyte antigen-4 antibody: the first in an emerging class of immunomodulatory antibodies for cancer treatment." J Clin Oncol **26**(32): 5275-5283.

Fonslow, B. R., B. D. Stein, K. J. Webb, T. Xu, J. Choi, S. K. Park and J. R. Yates, 3rd (2013). "Digestion and depletion of abundant proteins improves proteomic coverage." Nat Methods **10**(1): 54-56.

Fornerod, M., M. Ohno, M. Yoshida and I. W. Mattaj (1997). "CRM1 is an export receptor for leucine-rich nuclear export signals." Cell **90**(6): 1051-1060.

Fortenberry, Y. M., S. Brandal, R. C. Bialas and F. C. Church (2010). "Protein C inhibitor regulates both cathepsin L activity and cell-mediated tumor cell migration." Biochim Biophys Acta **1800**(6): 580-590.

Fountain, J. W., S. J. Bale, D. E. Housman and N. C. Dracopoli (1990). "Genetics of melanoma." Cancer Surv **9**(4): 645-671.

Franco, R., G. Botti, M. Mascolo, G. Loquercio, G. Liguori, G. Ilardi, S. Losito, A. La Mura, R. Calemma, C. Ierano, J. Bryce, C. D'Alterio and S. Scala (2010). ""CXCR4-CXCL12 and VEGF correlate to uveal melanoma progression"." Front Biosci (Elite Ed) **2**: 13-21.

Freire, J. E., P. De Potter, L. W. Brady and W. A. Longton (1997). "Brachytherapy in primary ocular tumors." Semin Surg Oncol **13**(3): 167-176.

Frenkel, S., O. Zloto, J. Pe'er and V. Barak (2013). "Insulin-like growth factor-1 as a predictive biomarker for metastatic uveal melanoma in humans." Invest Ophthalmol Vis Sci **54**(1): 490-493.

Frobel, J., S. Hartwig, W. Passlack, J. Eckel, R. Haas, A. Czibere and S. Lehr (2010). "ProteoMiner and SELDI-TOF-MS: a robust and highly reproducible combination for biomarker discovery from whole blood serum." Arch Physiol Biochem **116**(4-5): 174-180.

Gao, B. B., X. Chen, N. Timothy, L. P. Aiello and E. P. Feener (2008). "Characterization of the vitreous proteome in diabetes without diabetic retinopathy and diabetes with proliferative diabetic retinopathy." J Proteome Res **7**(6): 2516-2525.

Garbe, C. and U. Leiter (2009). "Melanoma epidemiology and trends." Clin Dermatol **27**(1): 3-9.

Garbi, N., S. Tanaka, F. Momburg and G. J. Hammerling (2006). "Impaired assembly of the major histocompatibility complex class I peptide-loading complex in mice deficient in the oxidoreductase ERp57." Nat Immunol **7**(1): 93-102.

Garcia-Ramirez, M., F. Canals, C. Hernandez, N. Colome, C. Ferrer, E. Carrasco, J. Garcia-Arumi and R. Simo (2007). "Proteomic analysis of human vitreous fluid by fluorescence-based difference gel electrophoresis (DIGE): a new strategy for identifying potential candidates in the pathogenesis of proliferative diabetic retinopathy." Diabetologia **50**(6): 1294-1303.

Garcia-Tunon, I., M. Ricote, A. A. Ruiz, B. Fraile, R. Paniagua and M. Royuela (2007). "Influence of IFN-gamma and its receptors in human breast cancer." BMC Cancer **7**: 158.

Garnier, J. P., S. Letellier, B. Cassinat, C. Lebbe, D. Kerob, M. Baccard, P. Morel, N. Basset-Seguin, L. Dubertret, B. Bousquet, K. Stoitchkov and T. Le Bricon (2007). "Clinical value of combined determination of plasma L-DOPA/tyrosine ratio, S100B, MIA and LDH in melanoma." Eur J Cancer **43**(4): 816-821.

Gast, A., D. Scherer, B. Chen, S. Bloethner, S. Melchert, A. Sucker, K. Hemminki, D. Schadendorf and R. Kumar (2010). "Somatic alterations in the melanoma genome: a high-resolution array-based comparative genomic hybridization study." Genes Chromosomes Cancer **49**(8): 733-745.

Gaudi, S. and J. L. Messina (2011). "Molecular bases of cutaneous and uveal melanomas." Patholog Res Int **2011**: 159421.

Giblin, M. E., J. A. Shields, J. J. Augsburger and L. W. Brady (1989). "Episcleral plaque radiotherapy for uveal melanoma." Aust N Z J Ophthalmol **17**(2): 153-156.

Gill, H. S. and D. H. Char (2012). "Uveal melanoma prognostication: from lesion size and cell type to molecular class." Can J Ophthalmol **47**(3): 246-253.

Gogas, H., A. M. Eggermont, A. Hauschild, P. Hersey, P. Mohr, D. Schadendorf, A. Spatz and R. Dummer (2009). "Biomarkers in melanoma." Ann Oncol **20 Suppl 6**: vi8-13.

Gogas, H., A. Polyzos and J. Kirkwood (2013). "Immunotherapy for advanced melanoma: fulfilling the promise." Cancer Treat Rev **39**(8): 879-885.

Goldstein, A. M., J. P. Struewing, A. Chidambaram, M. C. Fraser and M. A. Tucker (2000). "Genotype-phenotype relationships in U.S. melanoma-prone families with CDKN2A and CDK4 mutations." J Natl Cancer Inst **92**(12): 1006-1010.

Gonzalez-Moreno, O., N. Boque, M. Redrado, F. Milagro, J. Campion, T. Endermann, K. Takahashi, Y. Saito, R. Catena, L. Schomburg and A. Calvo (2011). "Selenoprotein-P is down-regulated in prostate cancer, which results in lack of protection against oxidative damage." Prostate **71**(8): 824-834.

Good, D. M., V. Thongboonkerd, J. Novak, J. L. Bascands, J. P. Schanstra, J. J. Coon, A. Dominiczak and H. Mischak (2007). "Body fluid proteomics for biomarker discovery: lessons from the past hold the key to success in the future." J Proteome Res **6**(12): 4549-4555.

Grunnet, M., M. Mau-Sorensen and N. Brunner (2013). "Tissue inhibitor of metalloproteinase 1 (TIMP-1) as a biomarker in gastric cancer: a review." Scand J Gastroenterol **48**(8): 899-905.

Grus, F. H., S. C. Joachim and N. Pfeiffer (2007). "Proteomics in ocular fluids." Proteomics Clin Appl **1**(8): 876-888.

Guo, H. B., B. Stoffel-Wagner, T. Bierwirth, J. Mezger and D. Klingmuller (1995). "Clinical significance of serum S100 in metastatic malignant melanoma." Eur J Cancer **31A**(11): 1898-1902.

Gyemant, N., M. Tanaka, P. Molnar, J. Deli, L. Mandoky and J. Molnar (2006). "Reversal of multidrug resistance of cancer cells in vitro: modification of drug resistance by selected carotenoids." Anticancer Res **26**(1A): 367-374.

Hait, W. N., H. Wu, S. Jin and J. M. Yang (2006). "Elongation factor-2 kinase: its role in protein synthesis and autophagy." Autophagy **2**(4): 294-296.

Hanahan, D. and R. A. Weinberg (2011). "Hallmarks of cancer: the next generation." Cell **144**(5): 646-674.

Harbour, J. W. (2006). "Eye cancer: unique insights into oncogenesis: the Cogan Lecture." Invest Ophthalmol Vis Sci **47**(5): 1736-1745.

Harbour, J. W. (2012). "The genetics of uveal melanoma: an emerging framework for targeted therapy." Pigment Cell Melanoma Res **25**(2): 171-181.

Harbour, J. W. (2013). "Genomic, prognostic, and cell-signaling advances in uveal melanoma." Am Soc Clin Oncol Educ Book **2013**: 388-391.

Harbour, J. W. (2014). "A prognostic test to predict the risk of metastasis in uveal melanoma based on a 15-gene expression profile." Methods Mol Biol **1102**: 427-440.

Harbour, J. W. and R. Chen (2013). "The DecisionDx-UM Gene Expression Profile Test Provides Risk Stratification and Individualized Patient Care in Uveal Melanoma." PLoS Curr **5**.

Harbour, J. W., M. D. Onken, E. D. Roberson, S. Duan, L. Cao, L. A. Worley, M. L. Council, K. A. Matatall, C. Helms and A. M. Bowcock (2010). "Frequent mutation of BAP1 in metastasizing uveal melanomas." Science **330**(6009): 1410-1413.

Harbour, J. W., E. D. Roberson, H. Anbunathan, M. D. Onken, L. A. Worley and A. M. Bowcock (2013). "Recurrent mutations at codon 625 of the splicing factor SF3B1 in uveal melanoma." Nat Genet **45**(2): 133-135.

Hartwig, S., A. Czibere, J. Kotzka, W. Passlack, R. Haas, J. Eckel and S. Lehr (2009). "Combinatorial hexapeptide ligand libraries (ProteoMiner): an innovative fractionation tool for differential quantitative clinical proteomics." Arch Physiol Biochem **115**(3): 155-160.

Hashimoto, T., T. Kusakabe, T. Sugino, T. Fukuda, K. Watanabe, Y. Sato, A. Nashimoto, K. Honma, H. Kimura, H. Fujii and T. Suzuki (2004). "Expression of heart-type fatty acid-binding protein in human gastric carcinoma and its association with tumor aggressiveness, metastasis and poor prognosis." Pathobiology **71**(5): 267-273.

Hauck, S. M., F. Hofmaier, J. Dietter, M. E. Swadzba, M. Blindert, B. Amann, J. Behler, E. Kremmer, M. Ueffing and C. A. Deeg (2012). "Label-free LC-MSMS analysis of vitreous from autoimmune uveitis reveals a significant decrease in secreted Wnt signalling inhibitors DKK3 and SFRP2." J Proteomics **75**(14): 4545-4554.

Hawkes, J. E., J. Campbell, D. Garvin, L. Cannon-Albright, P. Cassidy and S. A. Leachman (2013). "Lack of GNAQ and GNA11 Germ-Line Mutations in Familial Melanoma Pedigrees with Uveal Melanoma or Blue Nevi." Front Oncol **3**: 160.

He, J., Y. Liu, T. S. Zhu, X. Xie, M. A. Costello, C. E. Talsma, C. G. Flack, J. G. Crowley, F. Dimeco, A. L. Vescovi, X. Fan and D. M. Lubman (2011). "Glycoproteomic analysis of glioblastoma stem cell differentiation." J Proteome Res **10**(1): 330-338.

Healy, E., I. Rehman, B. Angus and J. L. Rees (1995). "Loss of heterozygosity in sporadic primary cutaneous melanoma." Genes Chromosomes Cancer **12**(2): 152-156.

Henderson, E. and C. E. Margo (2008). "Iris melanoma." Arch Pathol Lab Med **132**(2): 268-272.

Hendrix, M. J., E. A. Seftor, R. E. Seftor, L. M. Gardner, H. C. Boldt, M. Meyer, J. Pe'er and R. Folberg (1998). "Biologic determinants of uveal melanoma metastatic phenotype: role of intermediate filaments as predictive markers." Lab Invest **78**(2): 153-163.

Herbst, R. A., J. Weiss, A. Ehnis, W. K. Cavenee and K. C. Arden (1994). "Loss of heterozygosity for 10q22-10qter in malignant melanoma progression." Cancer Res **54**(12): 3111-3114.

Hernandez, C., M. Garcia-Ramirez, N. Colome, L. Corraliza, L. Garcia-Pascual, J. Casado, F. Canals and R. Simo (2013). "Identification of new pathogenic candidates for diabetic macular edema using fluorescence-based difference gel electrophoresis analysis." Diabetes Metab Res Rev.

Hernandez, C., M. Garcia-Ramirez, N. Colome, M. Villarroel, L. Corraliza, L. Garcia-Pacual, J. Casado, F. Canals and R. Simo (2010). "New pathogenic candidates for diabetic macular edema detected by proteomic analysis." Diabetes Care **33**(7): e92.

Higashiyama, M., O. Doi, H. Yokouchi, K. Kodama, S. Nakamori and R. Tateishi (1995). "Alpha-1-antichymotrypsin expression in lung adenocarcinoma and its possible association with tumor progression." Cancer **76**(8): 1368-1376.

Higgs, R. E., M. D. Knierman, V. Gelfanova, J. P. Butler and J. E. Hale (2005). "Comprehensive label-free method for the relative quantification of proteins from biological samples." J Proteome Res **4**(4): 1442-1450.

Ho, A. L., E. Musi, G. Ambrosini, J. S. Nair, S. Deraje Vasudeva, E. de Stanchina and G. K. Schwartz (2012). "Impact of combined mTOR and MEK inhibition in uveal melanoma is driven by tumor genotype." PLoS One **7**(7): e40439.

Hoashi, T., T. Kadono, K. Kikuchi, T. Etoh and K. Tamaki (2001). "Differential growth regulation in human melanoma cell lines by TIMP-1 and TIMP-2." Biochem Biophys Res Commun **288**(2): 371-379.

Hodi, F. S., M. C. Mihm, R. J. Soiffer, F. G. Haluska, M. Butler, M. V. Seiden, T. Davis, R. Henry-Spires, S. MacRae, A. Willman, R. Padera, M. T. Jaklitsch, S.

Shankar, T. C. Chen, A. Korman, J. P. Allison and G. Dranoff (2003). "Biologic activity of cytotoxic T lymphocyte-associated antigen 4 antibody blockade in previously vaccinated metastatic melanoma and ovarian carcinoma patients." Proc Natl Acad Sci U S A **100**(8): 4712-4717.

Hodi, F. S., S. J. O'Day, D. F. McDermott, R. W. Weber, J. A. Sosman, J. B. Haanen, R. Gonzalez, C. Robert, D. Schadendorf, J. C. Hassel, W. Akerley, A. J. van den Eertwegh, J. Lutzky, P. Lorigan, J. M. Vaubel, G. P. Linette, D. Hogg, C. H. Ottensmeier, C. Lebbe, C. Peschel, I. Quirt, J. I. Clark, J. D. Wolchok, J. S. Weber, J. Tian, M. J. Yellin, G. M. Nichol, A. Hoos and W. J. Urba (2010). "Improved survival with ipilimumab in patients with metastatic melanoma." N Engl J Med **363**(8): 711-723.

Hoglund, M., D. Gisselsson, G. B. Hansen, V. A. White, T. Sall, F. Mitelman and D. Horsman (2004). "Dissecting karyotypic patterns in malignant melanomas: temporal clustering of losses and gains in melanoma karyotypic evolution." Int J Cancer **108**(1): 57-65.

Horwitz, J. (2003). "Alpha-crystallin." Exp Eye Res **76**(2): 145-153.

http://www.cancer.org/. (2013).

http://www.genengnews.com/. (2010).

https://www.gelifesciences.com/.

Huang, C. H., Y. T. Wang, C. F. Tsai, Y. J. Chen, J. S. Lee and S. H. Chiou (2011). "Phosphoproteomics characterization of novel phosphorylated sites of lens proteins from normal and cataractous human eye lenses." Mol Vis **17**: 186-198.

Huang, K. C., D. C. Park, S. K. Ng, J. Y. Lee, X. Ni, W. C. Ng, C. A. Bandera, W. R. Welch, R. S. Berkowitz, S. C. Mok and S. W. Ng (2006). "Selenium binding protein 1 in ovarian cancer." Int J Cancer **118**(10): 2433-2440.

Huang, T., M. Karsy, J. Zhuge, M. Zhong and D. Liu (2013). "B-Raf and the inhibitors: from bench to bedside." J Hematol Oncol **6**: 30.

Huang, Z., Y. Cheng, P. M. Chiu, F. M. Cheung, J. M. Nicholls, D. L. Kwong, A. W. Lee, E. R. Zabarovsky, E. J. Stanbridge, H. L. Lung and M. L. Lung (2012). "Tumor suppressor Alpha B-crystallin (CRYAB) associates with the cadherin/catenin adherens junction and impairs NPC progression-associated properties." Oncogene **31**(32): 3709-3720.

Hurst, E. A., J. W. Harbour and L. A. Cornelius (2003). "Ocular melanoma: a review and the relationship to cutaneous melanoma." Arch Dermatol **139**(8): 1067-1073.

Hwang, P. H., H. K. Yi, D. S. Kim, S. Y. Nam, J. S. Kim and D. Y. Lee (2001). "Suppression of tumorigenicity and metastasis in B16F10 cells by PTEN/MMAC1/TEP1 gene." Cancer Lett **172**(1): 83-91.

Iida, J. and J. B. McCarthy (2007). "Expression of collagenase-1 (MMP-1) promotes melanoma growth through the generation of active transforming growth factor-beta." Melanoma Res **17**(4): 205-213.

Jagtap, P., S. Bandhakavi, L. Higgins, T. McGowan, R. Sa, M. D. Stone, J. Chilton, E. A. Arriaga, S. L. Seymour and T. J. Griffin (2012). "Workflow for analysis of high mass accuracy salivary data set using MaxQuant and ProteinPilot search algorithm." Proteomics **12**(11): 1726-1730.

Jakob, J. A., R. L. Bassett, Jr., C. S. Ng, J. L. Curry, R. W. Joseph, G. C. Alvarado, M. L. Rohlfs, J. Richard, J. E. Gershenwald, K. B. Kim, A. J. Lazar, P. Hwu and M. A. Davies (2012). "NRAS mutation status is an independent prognostic factor in metastatic melanoma." Cancer **118**(16): 4014-4023.

Jamnongkan, W., A. Techasen, R. Thanan, K. Duenngai, P. Sithithaworn, E. Mairiang, W. Loilome, N. Namwat, C. Pairojkul and P. Yongvanit (2013). "Oxidized alpha-1 antitrypsin as a predictive risk marker of opisthorchiasis-associated cholangiocarcinoma." Tumour Biol **34**(2): 695-704.

Jannie, K. M., C. S. Stipp and J. A. Weiner (2012). "ALCAM regulates motility, invasiveness, and adherens junction formation in uveal melanoma cells." PLoS One **7**(6): e39330.

Jmor, F., H. Kalirai, A. Taktak, B. Damato and S. E. Coupland (2012). "HSP-27 protein expression in uveal melanoma: correlation with predicted survival." Acta Ophthalmol **90**(6): 534-539.

Johansson, C. C., D. Mougiakakos, E. Trocme, C. All-Ericsson, M. A. Economou, O. Larsson, S. Seregard and R. Kiessling (2010). "Expression and prognostic significance of iNOS in uveal melanoma." Int J Cancer **126**(11): 2682-2689.

Kalinina Ayuso, V., J. H. de Boer, H. L. Byers, G. R. Coulton, J. Dekkers, L. de Visser, A. M. van Loon, P. A. Schellekens, A. Rothova and J. D. de Groot-Mijnes (2013). "Intraocular biomarker identification in uveitis associated with juvenile idiopathic arthritis." Invest Ophthalmol Vis Sci **54**(5): 3709-3720.

Kang, D. W., S. C. Lee, Y. G. Park and J. H. Chang (2012). "Long-term results of Gamma Knife surgery for uveal melanomas." J Neurosurg **117 Suppl**: 108-114.

Kedinger, V., A. Meulle, O. Zounib, M. E. Bonnet, J. B. Gossart, E. Benoit, M. Messmer, P. Shankaranarayanan, J. P. Behr, P. Erbacher and A. L. Bolcato-Bellemin (2013). "Sticky siRNAs targeting survivin and cyclin B1 exert an antitumoral effect on melanoma subcutaneous xenografts and lung metastases." BMC Cancer **13**(1): 338.

Kellner, R., R. Lichtenfels, D. Atkins, J. Bukur, A. Ackermann, J. Beck, W. Brenner, S. Melchior and B. Seliger (2002). "Targeting of tumor associated antigens in renal cell carcinoma using proteome-based analysis and their clinical significance." Proteomics **2**(12): 1743-1751.

Kerk, N., E. A. Strozyk, B. Poppelmann and S. W. Schneider (2010). "The mechanism of melanoma-associated thrombin activity and von Willebrand factor release from endothelial cells." J Invest Dermatol **130**(9): 2259-2268.

Kester, M. V. and R. W. Gracy (1975). "Alteration of human lymphocyte triosephosphate isomerase isozymes during blastogenesis." Biochem Biophys Res Commun **65**(4): 1270-1277.

Khandwala, H. M., I. E. McCutcheon, A. Flyvbjerg and K. E. Friend (2000). "The effects of insulin-like growth factors on tumorigenesis and neoplastic growth." Endocr Rev **21**(3): 215-244.

Khattak, M. A., R. Fisher, P. Hughes, M. Gore and J. Larkin (2013). "Ipilimumab activity in advanced uveal melanoma." Melanoma Res **23**(1): 79-81.

Kiehntopf, M., R. Siegmund and T. Deufel (2007). "Use of SELDI-TOF mass spectrometry for identification of new biomarkers: potential and limitations." Clin Chem Lab Med **45**(11): 1435-1449.

Kilic, E., N. C. Naus, W. van Gils, C. C. Klaver, M. E. van Til, M. M. Verbiest, T. Stijnen, C. M. Mooy, D. Paridaens, H. B. Beverloo, G. P. Luyten and A. de Klein (2005). "Concurrent loss of chromosome arm 1p and chromosome 3 predicts a decreased disease-free survival in uveal melanoma patients." Invest Ophthalmol Vis Sci **46**(7): 2253-2257.

Kilic, E., W. van Gils, E. Lodder, H. B. Beverloo, M. E. van Til, C. M. Mooy, D. Paridaens, A. de Klein and G. P. Luyten (2006). "Clinical and cytogenetic analyses in uveal melanoma." Invest Ophthalmol Vis Sci **47**(9): 3703-3707.

Kim, H., H. J. Kang, K. T. You, S. H. Kim, K. Y. Lee, T. I. Kim, C. Kim, S. Y. Song, H. J. Kim, C. Lee and H. Kim (2006). "Suppression of human selenium-

binding protein 1 is a late event in colorectal carcinogenesis and is associated with poor survival." Proteomics **6**(11): 3466-3476.

Kim, M. R. and C. W. Kim (2007). "Human blood plasma preparation for two-dimensional gel electrophoresis." J Chromatogr B Analyt Technol Biomed Life Sci **849**(1-2): 203-210.

Kim, T., S. J. Kim, K. Kim, U. B. Kang, C. Lee, K. S. Park, H. G. Yu and Y. Kim (2007). "Profiling of vitreous proteomes from proliferative diabetic retinopathy and nondiabetic patients." Proteomics **7**(22): 4203-4215.

King, A. J., M. R. Arnone, M. R. Bleam, K. G. Moss, J. Yang, K. E. Fedorowicz, K. N. Smitheman, J. A. Erhardt, A. Hughes-Earle, L. S. Kane-Carson, R. H. Sinnamon, H. Qi, T. R. Rheault, D. E. Uehling and S. G. Laquerre (2013). "Dabrafenib; Preclinical Characterization, Increased Efficacy when Combined with Trametinib, while BRAF/MEK Tool Combination Reduced Skin Lesions." PLoS One **8**(7): e67583.

Koivunen, P., T. Helaakoski, P. Annunen, J. Veijola, S. Raisanen, T. Pihlajaniemi and K. I. Kivirikko (1996). "ERp60 does not substitute for protein disulphide isomerase as the beta-subunit of prolyl 4-hydroxylase." Biochem J **316 (Pt 2)**: 599-605.

Konishi, T., H. Okabe, H. Katoh, Y. Fujiyama and A. Mori (1996). "Macrophage inflammatory protein-1 alpha expression in non-neoplastic and neoplastic lung tissue." Virchows Arch **428**(2): 107-111.

Koopmans, A. E., J. Vaarwater, D. Paridaens, N. C. Naus, E. Kilic, A. de Klein and g. Rotterdam Ocular Melanoma Study (2013). "Patient survival in uveal melanoma is not affected by oncogenic mutations in GNAQ and GNA11." Br J Cancer **109**(2): 493-496.

Korf, H. W., B. Korf, W. Schachenmayr, G. J. Chader and B. Wiggert (1992). "Immunocytochemical demonstration of interphotoreceptor retinoid-binding protein in cerebellar medulloblastoma." Acta Neuropathol **83**(5): 482-487.

Koutroukides, T. A., P. C. Guest, F. M. Leweke, D. M. Bailey, H. Rahmoune, S. Bahn and D. Martins-de-Souza (2011). "Characterization of the human serum depletome by label-free shotgun proteomics." J Sep Sci **34**(13): 1621-1626.

Kozlowski, M., W. Laudanski, B. Mroczko, M. Szmitkowski, R. Milewski and G. Lapuc (2013). "Serum tissue inhibitor of metalloproteinase 1 (TIMP-1) and vascular

endothelial growth factor A (VEGF-A) are associated with prognosis in esophageal cancer patients." Adv Med Sci: 1-8.

Krahn, G., P. Kaskel, S. Sander, P. J. Waizenhofer, S. Wortmann, U. Leiter and R. U. Peter (2001). "S100 beta is a more reliable tumor marker in peripheral blood for patients with newly occurred melanoma metastases compared with MIA, albumin and lactate-dehydrogenase." Anticancer Res **21**(2B): 1311-1316.

Ksander, B. R., P. E. Rubsamen, K. R. Olsen, S. W. Cousins and J. W. Streilein (1991). "Studies of tumor-infiltrating lymphocytes from a human choroidal melanoma." Invest Ophthalmol Vis Sci **32**(13): 3198-3208.

Kumazoe, M., K. Sugihara, S. Tsukamoto, Y. Huang, Y. Tsurudome, T. Suzuki, Y. Suemasu, N. Ueda, S. Yamashita, Y. Kim, K. Yamada and H. Tachibana (2013). "67-kDa laminin receptor increases cGMP to induce cancer-selective apoptosis." J Clin Invest **123**(2): 787-799.

Lai, K., R. M. Conway, R. Crouch, M. J. Jager and M. C. Madigan (2008). "Expression and distribution of MMPs and TIMPs in human uveal melanoma." Exp Eye Res **86**(6): 936-941.

Lam, N. Y., T. H. Rainer, R. W. Chiu and Y. M. Lo (2004). "EDTA is a better anticoagulant than heparin or citrate for delayed blood processing for plasma DNA analysis." Clin Chem **50**(1): 256-257.

Lamba, S., L. Felicioni, F. Buttitta, F. E. Bleeker, S. Malatesta, V. Corbo, A. Scarpa, M. Rodolfo, M. Knowles, M. Frattini, A. Marchetti and A. Bardelli (2009). "Mutational profile of GNAQQ209 in human tumors." PLoS One **4**(8): e6833.

Landreville, S., O. A. Agapova and J. W. Harbour (2008). "Emerging insights into the molecular pathogenesis of uveal melanoma." Future Oncol **4**(5): 629-636.

Landreville, S., O. A. Agapova, K. A. Matatall, Z. T. Kneass, M. D. Onken, R. S. Lee, A. M. Bowcock and J. W. Harbour (2012). "Histone deacetylase inhibitors induce growth arrest and differentiation in uveal melanoma." Clin Cancer Res **18**(2): 408-416.

Lee, D. J., D. H. Kang, M. Choi, Y. J. Choi, J. Y. Lee, J. H. Park, Y. J. Park, K. W. Lee and S. W. Kang (2013). "Peroxiredoxin-2 represses melanoma metastasis by increasing E-Cadherin/beta-Catenin complexes in adherens junctions." Cancer Res **73**(15): 4744-4757.

Lee, J. H., J. W. Choi and Y. S. Kim (2011). "Frequencies of BRAF and NRAS mutations are different in histological types and sites of origin of cutaneous melanoma: a meta-analysis." Br J Dermatol **164**(4): 776-784.

Lee, J. H., E. Giovannetti, J. H. Hwang, I. Petrini, Q. Wang, J. Voortman, Y. Wang, S. M. Steinberg, N. Funel, P. S. Meltzer, Y. Wang and G. Giaccone (2012). "Loss of 18q22.3 involving the carboxypeptidase of glutamate-like gene is associated with poor prognosis in resected pancreatic cancer." Clin Cancer Res **18**(2): 524-533.

Lee, J. M. and E. C. Kohn (2010). "Proteomics as a guiding tool for more effective personalized therapy." Ann Oncol **21 Suppl 7**: vii205-210.

Lee, Y. J., S. H. Jeong, S. C. Hong, B. I. Cho, W. S. Ha, S. T. Park, S. K. Choi, E. J. Jung, Y. T. Ju, C. Y. Jeong, J. W. Kim, C. W. Lee, J. Yoo and G. H. Ko (2013). "Prognostic value of CAPZA1 overexpression in gastric cancer." Int J Oncol **42**(5): 1569-1577.

Lee, Y. J., D. H. Kim, S. H. Lee, D. W. Kim, H. S. Nam and M. K. Cho (2011). "Expression of the c-Met Proteins in Malignant Skin Cancers." Ann Dermatol **23**(1): 33-38.

Lefevre, G., N. Babchia, A. Calipel, F. Mouriaux, A. M. Faussat, S. Mrzyk and F. Mascarelli (2009). "Activation of the FGF2/FGFR1 autocrine loop for cell proliferation and survival in uveal melanoma cells." Invest Ophthalmol Vis Sci **50**(3): 1047-1057.

Li, F., C. Li, H. Zhang, Z. Lu, Z. Li, Q. You, N. Lu and Q. Guo (2012). "VI-14, a novel flavonoid derivative, inhibits migration and invasion of human breast cancer cells." Toxicol Appl Pharmacol **261**(2): 217-226.

Li, J., N. White, Z. Zhang, J. Rosenzweig, L. A. Mangold, A. W. Partin and D. W. Chan (2004). "Detection of prostate cancer using serum proteomics pattern in a histologically confirmed population." J Urol **171**(5): 1782-1787.

Li, J., Z. Zhang, J. Rosenzweig, Y. Y. Wang and D. W. Chan (2002). "Proteomics and bioinformatics approaches for identification of serum biomarkers to detect breast cancer." Clin Chem **48**(8): 1296-1304.

Liang, C., G. S. Tan and M. C. Chung (2012). "2D DIGE analysis of serum after fractionation by ProteoMiner beads." Methods Mol Biol **854**: 181-194.

Lima, B. R., L. R. Schoenfield and A. D. Singh (2011). "The impact of intravitreal bevacizumab therapy on choroidal melanoma." Am J Ophthalmol **151**(2): 323-328 e322.

Linge, A., S. Kennedy, D. O'Flynn, S. Beatty, P. Moriarty, M. Henry, M. Clynes, A. Larkin and P. Meleady (2012). "Differential expression of fourteen proteins between uveal melanoma from patients who subsequently developed distant metastases versus those who did Not." Invest Ophthalmol Vis Sci **53**(8): 4634-4643.

Liou, G. I., Y. Fei, N. S. Peachey, S. Matragoon, S. Wei, W. S. Blaner, Y. Wang, C. Liu, M. E. Gottesman and H. Ripps (1998). "Early onset photoreceptor abnormalities induced by targeted disruption of the interphotoreceptor retinoid-binding protein gene." J Neurosci **18**(12): 4511-4520.

Liu, C. (2011). "The application of SELDI-TOF-MS in clinical diagnosis of cancers." J Biomed Biotechnol **2011**: 245821.

Liu, H., Y. Kato, S. A. Erzinger, G. M. Kiriakova, Y. Qian, D. Palmieri, P. S. Steeg and J. E. Price (2012). "The role of MMP-1 in breast cancer growth and metastasis to the brain in a xenograft model." BMC Cancer **12**: 583.

Lobo, A. and S. Lightman (2003). "Vitreous aspiration needle tap in the diagnosis of intraocular inflammation." Ophthalmology **110**(3): 595-599.

Longo, C., G. Gambara, V. Espina, A. Luchini, B. Bishop, A. S. Patanarut, E. F. Petricoin, 3rd, F. Beretti, B. Ferrari, E. Garaci, A. De Pol, G. Pellacani and L. A. Liotta (2011). "A novel biomarker harvesting nanotechnology identifies Bak as a candidate melanoma biomarker in serum." Exp Dermatol **20**(1): 29-34.

Lopez-Arias, E., A. Aguilar-Lemarroy, L. Felipe Jave-Suarez, G. Morgan-Villela, I. Mariscal-Ramirez, M. Martinez-Velazquez, A. H. Alvarez, A. Gutierrez-Ortega and R. Hernandez-Gutierrez (2012). "Alpha 1-antitrypsin: a novel tumor-associated antigen identified in patients with early-stage breast cancer." Electrophoresis **33**(14): 2130-2137.

Lowe, S. W. and A. W. Lin (2000). "Apoptosis in cancer." Carcinogenesis **21**(3): 485-495.

Luchini, A., D. H. Geho, B. Bishop, D. Tran, C. Xia, R. L. Dufour, C. D. Jones, V. Espina, A. Patanarut, W. Zhou, M. M. Ross, A. Tessitore, E. F. Petricoin, 3rd and L. A. Liotta (2008). "Smart hydrogel particles: biomarker harvesting: one-step affinity purification, size exclusion, and protection against degradation." Nano Lett **8**(1): 350-361.

M, D. I. S., M. G. Volpe, G. Colonna, M. Nazzaro, M. Polimeno, S. Scala, G. Castello and S. Costantini (2011). "A possible predictive marker of progression for hepatocellular carcinoma." Oncol Lett **2**(6): 1247-1251.

Maeland Nilsen, M., K. E. Uleberg, E. A. Janssen, J. P. Baak, O. K. Andersen and A. Hjelle (2011). "From SELDI-TOF MS to protein identification by on-chip elution." J Proteomics **74**(12): 2995-2998.

Mahipal, A., L. Tijani, K. Chan, M. Laudadio, M. J. Mastrangelo and T. Sato (2012). "A pilot study of sunitinib malate in patients with metastatic uveal melanoma." Melanoma Res **22**(6): 440-446.

Maldonado, J. L., J. Fridlyand, H. Patel, A. N. Jain, K. Busam, T. Kageshita, T. Ono, D. G. Albertson, D. Pinkel and B. C. Bastian (2003). "Determinants of BRAF mutations in primary melanomas." J Natl Cancer Inst **95**(24): 1878-1890.

Malik, G., M. D. Ward, S. K. Gupta, M. W. Trosset, W. E. Grizzle, B. L. Adam, J. I. Diaz and O. J. Semmes (2005). "Serum levels of an isoform of apolipoprotein A-II as a potential marker for prostate cancer." Clin Cancer Res **11**(3): 1073-1085.

Mallikarjuna, K., V. Pushparaj, J. Biswas and S. Krishnakumar (2007). "Expression of epidermal growth factor receptor, ezrin, hepatocyte growth factor, and c-Met in uveal melanoma: an immunohistochemical study." Curr Eye Res **32**(3): 281-290.

Mao, Y., D. W. Zhang, H. Lin, L. Xiong, Y. Liu, Q. D. Li, J. Ma, Q. Cao, R. J. Chen, J. Zhu and Z. Q. Feng (2012). "Alpha B-crystallin is a new prognostic marker for laryngeal squamous cell carcinoma." J Exp Clin Cancer Res **31**: 101.

Martens-de Kemp, S. R., R. Nagel, M. Stigter-van Walsum, I. H. van der Meulen, V. W. van Beusechem, B. J. Braakhuis and R. H. Brakenhoff (2013). "Functional genetic screens identify genes essential for tumor cell survival in head and neck and lung cancer." Clin Cancer Res **19**(8): 1994-2003.

Martin, M., L. Masshofer, P. Temming, S. Rahmann, C. Metz, N. Bornfeld, J. van de Nes, L. Klein-Hitpass, A. G. Hinnebusch, B. Horsthemke, D. R. Lohmann and M. Zeschnigk (2013). "Exome sequencing identifies recurrent somatic mutations in EIF1AX and SF3B1 in uveal melanoma with disomy 3." Nat Genet **45**(8): 933-936.

Martinez-Outschoorn, U. E., D. Whitaker-Menezes, Z. Lin, N. Flomenberg, A. Howell, R. G. Pestell, M. P. Lisanti and F. Sotgia (2011). "Cytokine production and inflammation drive autophagy in the tumor microenvironment: role of stromal caveolin-1 as a key regulator." Cell Cycle **10**(11): 1784-1793.

Martinez, M., F. Espana, M. Royo, J. M. Alapont, S. Navarro, A. Estelles, J. Aznar, C. D. Vera and J. F. Jimenez-Cruz (2002). "The proportion of prostate-specific antigen (PSA) complexed to alpha(1)-antichymotrypsin improves the discrimination

between prostate cancer and benign prostatic hyperplasia in men with a total PSA of 10 to 30 microg/L." Clin Chem **48**(8): 1251-1256.

Massi, D., A. Franchi, I. Sardi, L. Magnelli, M. Paglierani, L. Borgognoni, U. Maria Reali and M. Santucci (2001). "Inducible nitric oxide synthase expression in benign and malignant cutaneous melanocytic lesions." J Pathol **194**(2): 194-200.

Matassa, D. S., M. R. Amoroso, I. Agliarulo, F. Maddalena, L. Sisinni, S. Paladino, S. Romano, M. F. Romano, V. Sagar, F. Loreni, M. Landriscina and F. Esposito (2013). "Translational control in the stress adaptive response of cancer cells: a novel role for the heat shock protein TRAP1." Cell Death Dis **4**: e851.

Medina, T., M. N. Amaria and A. Jimeno (2013). "Dabrafenib in the treatment of advanced melanoma." Drugs Today (Barc) **49**(6): 377-385.

Mehnert, J. M. and H. M. Kluger (2012). "Driver mutations in melanoma: lessons learned from bench-to-bedside studies." Curr Oncol Rep **14**(5): 449-457.

Melero, I., S. Hervas-Stubbs, M. Glennie, D. M. Pardoll and L. Chen (2007). "Immunostimulatory monoclonal antibodies for cancer therapy." Nat Rev Cancer **7**(2): 95-106.

Metz, C. H., M. Scheulen, N. Bornfeld, D. Lohmann and M. Zeschnigk (2013). "Ultradeep sequencing detects GNAQ and GNA11 mutations in cell-free DNA from plasma of patients with uveal melanoma." Cancer Med **2**(2): 208-215.

Mian, S., S. Ugurel, E. Parkinson, I. Schlenzka, I. Dryden, L. Lancashire, G. Ball, C. Creaser, R. Rees and D. Schadendorf (2005). "Serum proteomic fingerprinting discriminates between clinical stages and predicts disease progression in melanoma patients." J Clin Oncol **23**(22): 5088-5093.

Mimori, K., M. Mori, S. Tanaka, T. Akiyoshi and K. Sugimachi (1995). "The overexpression of elongation factor 1 gamma mRNA in gastric carcinoma." Cancer **75**(6 Suppl): 1446-1449.

Mocellin, S., G. Zavagno and D. Nitti (2008). "The prognostic value of serum S100B in patients with cutaneous melanoma: a meta-analysis." Int J Cancer **123**(10): 2370-2376.

Mouton-Barbosa, E., F. Roux-Dalvai, D. Bouyssie, F. Berger, E. Schmidt, P. G. Righetti, L. Guerrier, E. Boschetti, O. Burlet-Schiltz, B. Monsarrat and A. Gonzalez de Peredo (2010). "In-depth exploration of cerebrospinal fluid by combining peptide ligand library treatment and label-free protein quantification." Mol Cell Proteomics **9**(5): 1006-1021.

Moyano, J. V., J. R. Evans, F. Chen, M. Lu, M. E. Werner, F. Yehiely, L. K. Diaz, D. Turbin, G. Karaca, E. Wiley, T. O. Nielsen, C. M. Perou and V. L. Cryns (2006). "AlphaB-crystallin is a novel oncoprotein that predicts poor clinical outcome in breast cancer." J Clin Invest **116**(1): 261-270.

Munzenrider, J. E. (2001). "Uveal melanomas. Conservation treatment." Hematol Oncol Clin North Am **15**(2): 389-402.

Murali, R., T. Wiesner and R. A. Scolyer (2013). "Tumours associated with BAP1 mutations." Pathology **45**(2): 116-126.

Murrell, J. and R. Board (2013). "The use of systemic therapies for the treatment of brain metastases in metastatic melanoma: Opportunities and unanswered questions." Cancer Treat Rev.

Nagarkatti-Gude, N., I. H. Bronkhorst, S. G. van Duinen, G. P. Luyten and M. J. Jager (2012). "Cytokines and chemokines in the vitreous fluid of eyes with uveal melanoma." Invest Ophthalmol Vis Sci **53**(11): 6748-6755.

Narayana, A., M. Mathew, M. Tam, R. Kannan, K. M. Madden, J. G. Golfinos, E. C. Parker, P. A. Ott and A. C. Pavlick (2013). "Vemurafenib and radiation therapy in melanoma brain metastases." J Neurooncol **113**(3): 411-416.

Negrutskii, B. S. and A. V. El'skaya (1998). "Eukaryotic translation elongation factor 1 alpha: structure, expression, functions, and possible role in aminoacyl-tRNA channeling." Prog Nucleic Acid Res Mol Biol **60**: 47-78.

Neilson, K. A., N. A. Ali, S. Muralidharan, M. Mirzaei, M. Mariani, G. Assadourian, A. Lee, S. C. van Sluyter and P. A. Haynes "Less label, more free: Approaches in label-free quantitative mass spectrometry." Proteomics.

Neri, A., T. Megha, F. Bettarini, D. Tacchini, M. G. Mastrogiulio, D. Marrelli, E. Pinto and P. Tosi (2012). "Is tissue inhibitor of metalloproteinase-1 a new prognosticator for breast cancer? An analysis of 266 cases." Hum Pathol **43**(8): 1184-1191.

Nevins, J. R. (2001). "The Rb/E2F pathway and cancer." Hum Mol Genet **10**(7): 699-703.

Nikkola, J., P. Vihinen, M. S. Vuoristo, P. Kellokumpu-Lehtinen, V. M. Kahari and S. Pyrhonen (2005). "High serum levels of matrix metalloproteinase-9 and matrix metalloproteinase-1 are associated with rapid progression in patients with metastatic melanoma." Clin Cancer Res **11**(14): 5158-5166.

Njauw, C. N., I. Kim, A. Piris, M. Gabree, M. Taylor, A. M. Lane, M. M. DeAngelis, E. Gragoudas, L. M. Duncan and H. Tsao (2012). "Germline BAP1 inactivation is preferentially associated with metastatic ocular melanoma and cutaneous-ocular melanoma families." PLoS One **7**(4): e35295.

Notting, I. C., G. S. Missotten, B. Sijmons, Z. F. Boonman, J. E. Keunen and G. van der Pluijm (2006). "Angiogenic profile of uveal melanoma." Curr Eye Res **31**(9): 775-785.

O'Farrell, P. H. (1975). "High resolution two-dimensional electrophoresis of proteins." J Biol Chem **250**(10): 4007-4021.

Ockner, R. K. and J. A. Manning (1974). "Fatty acid-binding protein in small intestine. Identification, isolation, and evidence for its role in cellular fatty acid transport." J Clin Invest **54**(2): 326-338.

Onken, M. D., L. A. Worley, J. P. Ehlers and J. W. Harbour (2004). "Gene expression profiling in uveal melanoma reveals two molecular classes and predicts metastatic death." Cancer Res **64**(20): 7205-7209.

Onken, M. D., L. A. Worley, M. D. Long, S. Duan, M. L. Council, A. M. Bowcock and J. W. Harbour (2008). "Oncogenic mutations in GNAQ occur early in uveal melanoma." Invest Ophthalmol Vis Sci **49**(12): 5230-5234.

Onken, M. D., L. A. Worley, M. D. Tuscan and J. W. Harbour (2010). "An accurate, clinically feasible multi-gene expression assay for predicting metastasis in uveal melanoma." J Mol Diagn **12**(4): 461-468.

Ouchi, M., K. West, J. W. Crabb, S. Kinoshita and M. Kamei (2005). "Proteomic analysis of vitreous from diabetic macular edema." Exp Eye Res **81**(2): 176-182.

Palmieri, G., M. Capone, M. L. Ascierto, G. Gentilcore, D. F. Stroncek, M. Casula, M. C. Sini, M. Palla, N. Mozzillo and P. A. Ascierto (2009). "Main roads to melanoma." J Transl Med **7**: 86.

Panasiti, V., A. Naspi, V. Devirgiliis, M. Curzio, V. Roberti, G. Curzio, S. Gobbi, S. Calvieri and P. Londei (2011). "Correlation between insulin-like growth factor binding protein-3 serum level and melanoma progression." J Am Acad Dermatol **64**(5): 865-872.

Pande, A., O. Annunziata, N. Asherie, O. Ogun, G. B. Benedek and J. Pande (2005). "Decrease in protein solubility and cataract formation caused by the Pro23 to Thr mutation in human gamma D-crystallin." Biochemistry **44**(7): 2491-2500.

Papaemmanuil, E., M. Cazzola, J. Boultwood, L. Malcovati, P. Vyas, D. Bowen, A. Pellagatti, J. S. Wainscoat, E. Hellstrom-Lindberg, C. Gambacorti-Passerini, A. L. Godfrey, I. Rapado, A. Cvejic, R. Rance, C. McGee, P. Ellis, L. J. Mudie, P. J. Stephens, S. McLaren, C. E. Massie, P. S. Tarpey, I. Varela, S. Nik-Zainal, H. R. Davies, A. Shlien, D. Jones, K. Raine, J. Hinton, A. P. Butler, J. W. Teague, E. J. Baxter, J. Score, A. Galli, M. G. Della Porta, E. Travaglino, M. Groves, S. Tauro, N. C. Munshi, K. C. Anderson, A. El-Naggar, A. Fischer, V. Mustonen, A. J. Warren, N. C. Cross, A. R. Green, P. A. Futreal, M. R. Stratton, P. J. Campbell and C. Chronic Myeloid Disorders Working Group of the International Cancer Genome (2011). "Somatic SF3B1 mutation in myelodysplasia with ring sideroblasts." N Engl J Med **365**(15): 1384-1395.

Pardo, M., R. A. Dwek and N. Zitzmann (2007). "Proteomics in uveal melanoma research: opportunities and challenges in biomarker discovery." Expert Rev Proteomics **4**(2): 273-286.

Pardo, M., A. Garcia, B. Thomas, A. Pineiro, A. Akoulitchev, R. A. Dwek and N. Zitzmann (2005). "Proteome analysis of a human uveal melanoma primary cell culture by 2-DE and MS." Proteomics **5**(18): 4980-4993.

Pardo, M., A. Garcia, B. Thomas, A. Pineiro, A. Akoulitchev, R. A. Dwek and N. Zitzmann (2006). "The characterization of the invasion phenotype of uveal melanoma tumour cells shows the presence of MUC18 and HMG-1 metastasis markers and leads to the identification of DJ-1 as a potential serum biomarker." Int J Cancer **119**(5): 1014-1022.

Partl, R., E. Richtig, A. Avian, A. Berghold and K. S. Kapp (2013). "Karnofsky performance status and lactate dehydrogenase predict the benefit of palliative whole-brain irradiation in patients with advanced intra- and extracranial metastases from malignant melanoma." Int J Radiat Oncol Biol Phys **85**(3): 662-666.

Pass, H. I., Z. Liu, A. Wali, R. Bueno, S. Land, D. Lott, F. Siddiq, F. Lonardo, M. Carbone and S. Draghici (2004). "Gene expression profiles predict survival and progression of pleural mesothelioma." Clin Cancer Res **10**(3): 849-859.

Patel, M., E. Smyth, P. B. Chapman, J. D. Wolchok, G. K. Schwartz, D. H. Abramson and R. D. Carvajal (2011). "Therapeutic implications of the emerging molecular biology of uveal melanoma." Clin Cancer Res **17**(8): 2087-2100.

Paul, D., A. Kumar, A. Gajbhiye, M. K. Santra and R. Srikanth (2013). "Mass spectrometry-based proteomics in molecular diagnostics: discovery of cancer biomarkers using tissue culture." Biomed Res Int **2013**: 783131.

Pelicano, H., D. S. Martin, R. H. Xu and P. Huang (2006). "Glycolysis inhibition for anticancer treatment." Oncogene **25**(34): 4633-4646.

Peng, J., A. J. Stanley, D. Cairns, P. J. Selby and R. E. Banks (2009). "Using the protein chip interface with quadrupole time-of-flight mass spectrometry to directly identify peaks in SELDI profiles--initial evaluation using low molecular weight serum peaks." Proteomics **9**(2): 492-498.

Peric, B., I. Zagar, S. Novakovic, J. Zgajnar and M. Hocevar (2011). "Role of serum S100B and PET-CT in follow-up of patients with cutaneous melanoma." BMC Cancer **11**: 328.

Pietraszek, K., S. Brezillon, C. Perreau, M. Malicka-Blaszkiewicz, F. X. Maquart and Y. Wegrowski (2013). "Lumican - derived peptides inhibit melanoma cell growth and migration." PLoS One **8**(10): e76232.

Pollreisz, A., M. Funk, F. P. Breitwieser, K. Parapatics, S. Sacu, M. Georgopoulos, R. Dunavoelgyi, G. J. Zlabinger, J. Colinge, K. L. Bennett and U. Schmidt-Erfurth (2013). "Quantitative proteomics of aqueous and vitreous fluid from patients with idiopathic epiretinal membranes." Exp Eye Res **108**: 48-58.

Polnaszek, N., B. Kwabi-Addo, L. E. Peterson, M. Ozen, N. M. Greenberg, S. Ortega, C. Basilico and M. Ittmann (2003). "Fibroblast growth factor 2 promotes tumor progression in an autochthonous mouse model of prostate cancer." Cancer Res **63**(18): 5754-5760.

Pons, F., M. Plana, J. M. Caminal, J. Pera, I. Fernandes, J. Perez, X. Garcia-Del-Muro, J. Marcoval, R. Penin, A. Fabra and J. M. Piulats (2011). "Metastatic uveal melanoma: is there a role for conventional chemotherapy? - A single center study based on 58 patients." Melanoma Res **21**(3): 217-222.

Posch, C. and S. Ortiz-Urda (2013). "NRAS mutant melanoma--undrugable?" Oncotarget **4**(4): 494-495.

Prescher, G., N. Bornfeld, H. Hirche, B. Horsthemke, K. H. Jockel and R. Becher (1996). "Prognostic implications of monosomy 3 in uveal melanoma." Lancet **347**(9010): 1222-1225.

Proud, C. G. (1994). "Peptide-chain elongation in eukaryotes." Mol Biol Rep **19**(3): 161-170.

Qi, Y. J., Q. Y. He, Y. F. Ma, Y. W. Du, G. C. Liu, Y. J. Li, G. S. Tsao, S. M. Ngai and J. F. Chiu (2008). "Proteomic identification of malignant transformation-related proteins in esophageal squamous cell carcinoma." J Cell Biochem **104**(5): 1625-1635.

Rabilloud, T. (2002). "Two-dimensional gel electrophoresis in proteomics: old, old fashioned, but it still climbs up the mountains." Proteomics **2**(1): 3-10.

Ramasamy, P., C. C. Murphy, M. Clynes, N. Horgan, P. Moriarty, D. Tiernan, S. Beatty, S. Kennedy and P. Meleady (2013). "Proteomics in uveal melanoma." Exp Eye Res.

Rapanotti, M. C., I. Ricozzi, E. Campione, A. Orlandi and L. Bianchi (2013). "Blood MUC-18/MCAM expression in patients with melanoma: a suitable marker of poor outcome." Br J Dermatol **169**(1): 221-222.

Raskin, L., D. R. Fullen, T. J. Giordano, D. G. Thomas, M. L. Frohm, K. B. Cha, J. Ahn, B. Mukherjee, T. M. Johnson and S. B. Gruber (2013). "Transcriptome Profiling Identifies HMGA2 as a Biomarker of Melanoma Progression and Prognosis." J Invest Dermatol **133**(11): 2585-2592.

Reid, A. L., M. Millward, R. Pearce, M. Lee, M. H. Frank, A. Ireland, L. Monshizadeh, T. Rai, P. Heenan, S. Medic, P. Kumarasinghe and M. Ziman (2013). "Markers of circulating tumour cells in the peripheral blood of patients with melanoma correlate with disease recurrence and progression." Br J Dermatol **168**(1): 85-92.

Ren, D. H., E. Mayhew, C. Hay, H. Li, H. Alizadeh and J. Y. Niederkorn (2004). "Uveal melanoma expression of tumor necrosis factor-related apoptosis-inducing ligand (TRAIL) receptors and susceptibility to TRAIL-induced apoptosis." Invest Ophthalmol Vis Sci **45**(4): 1162-1168.

Rhee, S. G., S. W. Kang, T. S. Chang, W. Jeong and K. Kim (2001). "Peroxiredoxin, a novel family of peroxidases." IUBMB Life **52**(1-2): 35-41.

Richardson, D. R. and E. Baker (1990). "The uptake of iron and transferrin by the human malignant melanoma cell." Biochim Biophys Acta **1053**(1): 1-12.

Riker, A. I., S. A. Enkemann, O. Fodstad, S. Liu, S. Ren, C. Morris, Y. Xi, P. Howell, B. Metge, R. S. Samant, L. A. Shevde, W. Li, S. Eschrich, A. Daud, J. Ju and J. Matta (2008). "The gene expression profiles of primary and metastatic melanoma yields a transition point of tumor progression and metastasis." BMC Med Genomics **1**: 13.

Robert, C., L. Thomas, I. Bondarenko, S. O'Day, D. J. M, C. Garbe, C. Lebbe, J. F. Baurain, A. Testori, J. J. Grob, N. Davidson, J. Richards, M. Maio, A. Hauschild, W. H. Miller, Jr., P. Gascon, M. Lotem, K. Harmankaya, R. Ibrahim, S. Francis, T. T. Chen, R. Humphrey, A. Hoos and J. D. Wolchok (2011). "Ipilimumab plus dacarbazine for previously untreated metastatic melanoma." N Engl J Med **364**(26): 2517-2526.

Roberts, A. S., M. J. Campa, E. B. Gottlin, C. Jiang, K. Owzar, H. L. Kindler, A. P. Venook, R. M. Goldberg, E. M. O'Reilly and E. F. Patz, Jr. (2012). "Identification of potential prognostic biomarkers in patients with untreated, advanced pancreatic cancer from a phase 3 trial (Cancer and Leukemia Group B 80303)." Cancer **118**(2): 571-578.

Roche, S., L. Tiers, M. Provansal, M. Seveno, M. T. Piva, P. Jouin and S. Lehmann (2009). "Depletion of one, six, twelve or twenty major blood proteins before proteomic analysis: the more the better?" J Proteomics **72**(6): 945-951.

Roseanu, A., P. E. Florian, M. Moisei, L. E. Sima, R. W. Evans and M. Trif (2010). "Liposomalization of lactoferrin enhanced its anti-tumoral effects on melanoma cells." Biometals **23**(3): 485-492.

Salama, A. K. (2013). "Evolving pharmacotherapies for the treatment of metastatic melanoma." Clin Med Insights Oncol **7**: 137-149.

Santos, C. R. and A. Schulze (2012). "Lipid metabolism in cancer." FEBS J **279**(15): 2610-2623.

Schilling, B., N. Bielefeld, A. Sucker, U. Hillen, L. Zimmer, D. Schadendorf, M. Zeschnigk and K. G. Griewank (2013). "Lack of SF3B1 R625 mutations in cutaneous melanoma." Diagn Pathol **8**: 87.

Schnaeker, E. M., R. Ossig, T. Ludwig, R. Dreier, H. Oberleithner, M. Wilhelmi and S. W. Schneider (2004). "Microtubule-dependent matrix metalloproteinase-2/matrix metalloproteinase-9 exocytosis: prerequisite in human melanoma cell invasion." Cancer Res **64**(24): 8924-8931.

Scholes, A. G., B. E. Damato, J. Nunn, P. Hiscott, I. Grierson and J. K. Field (2003). "Monosomy 3 in uveal melanoma: correlation with clinical and histologic predictors of survival." Invest Ophthalmol Vis Sci **44**(3): 1008-1011.

Scortegagna, M., R. J. Martin, R. D. Kladney, R. G. Neumann and J. M. Arbeit (2009). "Hypoxia-inducible factor-1alpha suppresses squamous carcinogenic progression and epithelial-mesenchymal transition." Cancer Res **69**(6): 2638-2646.

Sennels, L., M. Salek, L. Lomas, E. Boschetti, P. G. Righetti and J. Rappsilber (2007). "Proteomic analysis of human blood serum using peptide library beads." J Proteome Res **6**(10): 4055-4062.

Seo, M. S., S. W. Kang, K. Kim, I. C. Baines, T. H. Lee and S. G. Rhee (2000). "Identification of a new type of mammalian peroxiredoxin that forms an intramolecular disulfide as a reaction intermediate." J Biol Chem **275**(27): 20346-20354.

Shaheduzzaman, S., A. Vishwanath, B. Furusato, J. Cullen, Y. Chen, L. Banez, M. Nau, L. Ravindranath, K. H. Kim, A. Mohammed, Y. Chen, M. Ehrich, V. Srikantan, I. A. Sesterhenn, D. McLeod, M. Vahey, G. Petrovics, A. Dobi and S. Srivastava (2007). "Silencing of Lactotransferrin expression by methylation in prostate cancer progression." Cancer Biol Ther **6**(7): 1088-1095.

Shitama, T., H. Hayashi, S. Noge, E. Uchio, K. Oshima, H. Haniu, N. Takemori, N. Komori and H. Matsumoto (2008). "Proteome Profiling of Vitreoretinal Diseases by Cluster Analysis." Proteomics Clin Appl **2**(9): 1265-1280.

Shiwa, M., Y. Nishimura, R. Wakatabe, A. Fukawa, H. Arikuni, H. Ota, Y. Kato and T. Yamori (2003). "Rapid discovery and identification of a tissue-specific tumor biomarker from 39 human cancer cell lines using the SELDI ProteinChip platform." Biochem Biophys Res Commun **309**(1): 18-25.

Shors, A. R. and N. S. Weiss (2004). "The co-occurrence of ocular and cutaneous melanomas." Arch Dermatol **140**(7): 884-885; author reply 885.

Siegel, R., D. Naishadham and A. Jemal (2013). "Cancer statistics, 2013." CA Cancer J Clin **63**(1): 11-30.

Simeone, E. and P. A. Ascierto (2012). "Immunomodulating antibodies in the treatment of metastatic melanoma: the experience with anti-CTLA-4, anti-CD137, and anti-PD1." J Immunotoxicol **9**(3): 241-247.

Simo-Servat, O., C. Hernandez and R. Simo (2012). "Usefulness of the vitreous fluid analysis in the translational research of diabetic retinopathy." Mediators Inflamm **2012**: 872978.

Singh, A. D., R. Tubbs, C. Biscotti, L. Schoenfield and P. Trizzoi (2009). "Chromosomal 3 and 8 status within hepatic metastasis of uveal melanoma." Arch Pathol Lab Med **133**(8): 1223-1227.

Sisley, K., M. A. Parsons, J. Garnham, A. M. Potter, D. Curtis, R. C. Rees and I. G. Rennie (2000). "Association of specific chromosome alterations with tumour phenotype in posterior uveal melanoma." Br J Cancer **82**(2): 330-338.

Sisley, K., I. G. Rennie, M. A. Parsons, R. Jacques, D. W. Hammond, S. M. Bell, A. M. Potter and R. C. Rees (1997). "Abnormalities of chromosomes 3 and 8 in posterior uveal melanoma correlate with prognosis." Genes Chromosomes Cancer **19**(1): 22-28.

Smith, M. P., S. L. Wood, A. Zougman, J. T. Ho, J. Peng, D. Jackson, D. A. Cairns, A. J. Lewington, P. J. Selby and R. E. Banks (2011). "A systematic analysis of the effects of increasing degrees of serum immunodepletion in terms of depth of coverage and other key aspects in top-down and bottom-up proteomic analyses." Proteomics **11**(11): 2222-2235.

Snapka, R. M., T. H. Sawyer, R. A. Barton and R. W. Gracy (1974). "Comparison of the electrophoretic properties of triosephosphate isomerases of various tissues and species." Comp Biochem Physiol B **49**(4): 733-741.

Snoek-van Beurden, P. A. and J. W. Von den Hoff (2005). "Zymographic techniques for the analysis of matrix metalloproteinases and their inhibitors." Biotechniques **38**(1): 73-83.

Southan, C. (2013). "BACE2 as a new diabetes target: a patent review (2010 - 2012)." Expert Opin Ther Pat **23**(5): 649-663.

Srinivasan, R., J. Daniels, V. Fusaro, A. Lundqvist, J. K. Killian, D. Geho, M. Quezado, D. Kleiner, S. Rucker, V. Espina, G. Whiteley, L. Liotta, E. Petricoin, S. Pittaluga, B. Hitt, A. J. Barrett, K. Rosenblatt and R. W. Childs (2006). "Accurate diagnosis of acute graft-versus-host disease using serum proteomic pattern analysis." Exp Hematol **34**(6): 796-801.

Stahlecker, J., A. Gauger, A. Bosserhoff, R. Buttner, J. Ring and R. Hein (2000). "MIA as a reliable tumor marker in the serum of patients with malignant melanoma." Anticancer Res **20**(6D): 5041-5044.

Storch, J. and B. Corsico (2008). "The emerging functions and mechanisms of mammalian fatty acid-binding proteins." Annu Rev Nutr **28**: 73-95.

Storch, J. and L. McDermott (2009). "Structural and functional analysis of fatty acid-binding proteins." J Lipid Res **50 Suppl**: S126-131.

Subramanian, P., S. Locatelli-Hoops, J. Kenealey, J. DesJardin, L. Notari and S. P. Becerra (2013). "Pigment epithelium-derived factor (PEDF) prevents retinal cell

death via PEDF Receptor (PEDF-R): identification of a functional ligand binding site." J Biol Chem **288**(33): 23928-23942.

Sun, H., Z. Ma, Y. Li, B. Liu, Z. Li, X. Ding, Y. Gao, W. Ma, X. Tang, X. Li and Y. Shen (2005). "Gamma-S crystallin gene (CRYGS) mutation causes dominant progressive cortical cataract in humans." J Med Genet **42**(9): 706-710.

Sun, Z. L., Y. Zhu, F. Q. Wang, R. Chen, T. Peng, Z. N. Fan, Z. K. Xu and Y. Miao (2007). "Serum proteomic-based analysis of pancreatic carcinoma for the identification of potential cancer biomarkers." Biochim Biophys Acta **1774**(6): 764-771.

Suzuki, K., M. Sakaguchi, S. Tanaka, T. Yoshimoto and M. Takaoka (2013). "Prolyl oligopeptidase inhibition-induced growth arrest of human gastric cancer cells." Biochem Biophys Res Commun.

Szponar-Bojda, A., A. Pietrzak, A. Sobczynska-Tomaszewska, A. Borzecki, A. Kurylcio, W. Polkowski, A. Poluha and G. Chodorowska (2012). "Melanoma and other malignant skin cancers in psoriatic patients treated with phototherapy. Role of the p16 protein in psoriasis." Folia Histochem Cytobiol **50**(4): 491-496.

Takashi, M., S. Katsuno, T. Sakata, S. Ohshima and K. Kato (1998). "Different concentrations of two small stress proteins, alphaB crystallin and HSP27 in human urological tumor tissues." Urol Res **26**(6): 395-399.

Tanaka, T., M. Shnimizu and H. Moriwaki (2012). "Cancer chemoprevention by carotenoids." Molecules **17**(3): 3202-3242.

Terry, K. L., S. S. Tworoger, M. A. Gates, D. W. Cramer and S. E. Hankinson (2009). "Common genetic variation in IGF1, IGFBP1 and IGFBP3 and ovarian cancer risk." Carcinogenesis **30**(12): 2042-2046.

Thierauf, A., F. Musshoff and B. Madea (2009). "Post-mortem biochemical investigations of vitreous humor." Forensic Sci Int **192**(1-3): 78-82.

Thomas, S., C. Putter, S. Weber, N. Bornfeld, D. R. Lohmann and M. Zeschnigk (2012). "Prognostic significance of chromosome 3 alterations determined by microsatellite analysis in uveal melanoma: a long-term follow-up study." Br J Cancer **106**(6): 1171-1176.

Tirumalai, R. S., K. C. Chan, D. A. Prieto, H. J. Issaq, T. P. Conrads and T. D. Veenstra (2003). "Characterization of the low molecular weight human serum proteome." Mol Cell Proteomics **2**(10): 1096-1103.

Tiwari, S., S. Hudson, V. H. Gattone, 2nd, C. Miller, E. A. Chernoff and T. L. Belecky-Adams (2013). "Meckelin 3 is necessary for photoreceptor outer segment development in rat Meckel syndrome." PLoS One **8**(3): e59306.

Toktas, Z. O., A. Bicer, G. Demirci, H. Pazarli, U. Abacioglu, S. Peker and T. Kilic (2010). "Gamma knife stereotactic radiosurgery yields good long-term outcomes for low-volume uveal melanomas without intraocular complications." J Clin Neurosci **17**(4): 441-445.

Topcu-Yilmaz, P., H. Kiratli, A. Saglam, F. Soylemezoglu and G. Hascelik (2010). "Correlation of clinicopathological parameters with HGF, c-Met, EGFR, and IGF-1R expression in uveal melanoma." Melanoma Res **20**(2): 126-132.

Topic, A., M. Ljujic, N. Petrovic-Stanojevic, V. Dopudja-Pantic and D. Radojkovic (2011). "Phenotypes and serum level of alpha-1-antitrypsin in lung cancer." J BUON **16**(4): 672-676.

Torabian, S. and M. Kashani-Sabet (2005). "Biomarkers for melanoma." Curr Opin Oncol **17**(2): 167-171.

Toricelli, M., F. H. Melo, G. B. Peres, D. C. Silva and M. G. Jasiulionis (2013). "Timp1 interacts with beta-1 integrin and CD63 along melanoma genesis and confers anoikis resistance by activating PI3-K signaling pathway independently of Akt phosphorylation." Mol Cancer **12**: 22.

Toyozawa, S., C. Kaminaka, F. Furukawa, Y. Nakamura, H. Matsunaka and Y. Yamamoto (2012). "Chemokine receptor CXCR4 is a novel marker for the progression of cutaneous malignant melanomas." Acta Histochem Cytochem **45**(5): 293-299.

Triozzi, P. L., C. Eng and A. D. Singh (2008). "Targeted therapy for uveal melanoma." Cancer Treat Rev **34**(3): 247-258.

Trout, A. T., R. S. Rabinowitz, J. F. Platt and K. M. Elsayes (2013). "Melanoma metastases in the abdomen and pelvis: Frequency and patterns of spread." World J Radiol **5**(2): 25-32.

Tukey, J. W. (1977). Exploratory Data Analysis, Addison-Wesley.

Turgut, B., F. C. Gul, F. Dagli, N. Ilhan and M. Ozgen (2013). "Impact of ghrelin on vitreous cytokine levels in an experimental uveitis model." Drug Des Devel Ther **7**: 19-24.

Ucar, D. A., E. Kurenova, T. J. Garrett, W. G. Cance, C. Nyberg, A. Cox, N. Massoll, D. A. Ostrov, N. Lawrence, S. M. Sebti, M. Zajac-Kaye and S. N.

Hochwald (2012). "Disruption of the protein interaction between FAK and IGF-1R inhibits melanoma tumor growth." Cell Cycle **11**(17): 3250-3259.

Ugurel, S., J. Utikal and J. C. Becker (2009). "Tumor biomarkers in melanoma." Cancer Control **16**(3): 219-224.

van 't Veer, L. J., B. M. Burgering, R. Versteeg, A. J. Boot, D. J. Ruiter, S. Osanto, P. I. Schrier and J. L. Bos (1989). "N-ras mutations in human cutaneous melanoma from sun-exposed body sites." Mol Cell Biol **9**(7): 3114-3116.

van de Schootbrugge, C., J. Bussink, P. N. Span, F. C. Sweep, R. Grenman, H. Stegeman, G. J. Pruijn, J. H. Kaanders and W. C. Boelens (2013). "alphaB-crystallin stimulates VEGF secretion and tumor cell migration and correlates with enhanced distant metastasis in head and neck squamous cell carcinoma." BMC Cancer **13**: 128.

van den Bosch, T., E. Kilic, D. Paridaens and A. de Klein (2010). "Genetics of uveal melanoma and cutaneous melanoma: two of a kind?" Dermatol Res Pract **2010**: 360136.

van der Watt, P. J., E. Ngarande and V. D. Leaner (2011). "Overexpression of Kpnbeta1 and Kpnalpha2 importin proteins in cancer derives from deregulated E2F activity." PLoS One **6**(11): e27723.

van der Watt, P. J., C. L. Stowell and V. D. Leaner (2013). "The nuclear import receptor Kpnbeta1 and its potential as an anticancer therapeutic target." Crit Rev Eukaryot Gene Expr **23**(1): 1-10.

van Gils, W., E. Kilic, H. T. Bruggenwirth, J. Vaarwater, M. M. Verbiest, B. Beverloo, M. E. van Til-Berg, D. Paridaens, G. P. Luyten and A. de Klein (2008). "Regional deletion and amplification on chromosome 6 in a uveal melanoma case without abnormalities on chromosomes 1p, 3 and 8." Melanoma Res **18**(1): 10-15.

Van Raamsdonk, C. D., K. G. Griewank, M. B. Crosby, M. C. Garrido, S. Vemula, T. Wiesner, A. C. Obenauf, W. Wackernagel, G. Green, N. Bouvier, M. M. Sozen, G. Baimukanova, R. Roy, A. Heguy, I. Dolgalev, R. Khanin, K. Busam, M. R. Speicher, J. O'Brien and B. C. Bastian (2010). "Mutations in GNA11 in uveal melanoma." N Engl J Med **363**(23): 2191-2199.

Velho, T. R., E. Kapiteijn and M. J. Jager (2012). "New therapeutic agents in uveal melanoma." Anticancer Res **32**(7): 2591-2598.

Vereecken, P., F. Cornelis, N. Van Baren, V. Vandersleyen and J. F. Baurain (2012). "A synopsis of serum biomarkers in cutaneous melanoma patients." Dermatol Res Pract **2012**: 260643.

Villanueva, J., A. Vultur, J. T. Lee, R. Somasundaram, M. Fukunaga-Kalabis, A. K. Cipolla, B. Wubbenhorst, X. Xu, P. A. Gimotty, D. Kee, A. E. Santiago-Walker, R. Letrero, K. D'Andrea, A. Pushparajan, J. E. Hayden, K. D. Brown, S. Laquerre, G. A. McArthur, J. A. Sosman, K. L. Nathanson and M. Herlyn (2010). "Acquired resistance to BRAF inhibitors mediated by a RAF kinase switch in melanoma can be overcome by cotargeting MEK and IGF-1R/PI3K." Cancer Cell **18**(6): 683-695.

Wakita, T., T. Hayashi, J. Nishioka, H. Tamaru, N. Akita, K. Asanuma, H. Kamada, E. C. Gabazza, M. Ido, J. Kawamura and K. Suzuki (2004). "Regulation of carcinoma cell invasion by protein C inhibitor whose expression is decreased in renal cell carcinoma." Int J Cancer **108**(4): 516-523.

Wang, F., Z. Bing, Y. Zhang, B. Ao, S. Zhang, C. Ye, J. He, N. Ding, W. Ye, J. Xiong, J. Sun, Y. Furusawa, G. Zhou and L. Yang (2013). "Quantitative proteomic analysis for radiation-induced cell cycle suspension in 92-1 melanoma cell line." J Radiat Res **54**(4): 649-662.

Wang, F., J. Xu, Q. Zhu, X. Qin, Y. Cao, J. Lou, Y. Xu, X. Ke, Q. Li, E. Xie, L. Zhang, R. Sun, L. Chen, B. Fang and S. Pan (2013). "Downregulation of IFNG in CD4(+) T Cells in Lung Cancer through Hypermethylation: A Possible Mechanism of Tumor-Induced Immunosuppression." PLoS One **8**(11): e79064.

Wang, H., L. Feng, J. Hu, C. Xie and F. Wang (2013). "Differentiating vitreous proteomes in proliferative diabetic retinopathy using high-performance liquid chromatography coupled to tandem mass spectrometry." Exp Eye Res **108**: 110-119.

Wang, H., L. Feng, J. W. Hu, C. L. Xie and F. Wang (2012). "Characterisation of the vitreous proteome in proliferative diabetic retinopathy." Proteome Sci **10**(1): 15.

Wang, J., D. Li, L. J. Dangott and G. Wu (2006). "Proteomics and its role in nutrition research." J Nutr **136**(7): 1759-1762.

Wang, J., J. Shafqat, K. Hall, M. Stahlberg, I. L. Wivall-Helleryd, K. Bouzakri, J. R. Zierath, K. Brismar, H. Jornvall and M. S. Lewitt (2006). "Specific cleavage of insulin-like growth factor-binding protein-1 by a novel protease activity." Cell Mol Life Sci **63**(19-20): 2405-2414.

Wang, M., J. You, K. G. Bemis, T. J. Tegeler and D. P. Brown (2008). "Label-free mass spectrometry-based protein quantification technologies in proteomic analysis." Brief Funct Genomic Proteomic **7**(5): 329-339.

Wang, S., Z. F. Boonman, H. C. Li, Y. He, M. J. Jager, R. E. Toes and J. Y. Niederkorn (2003). "Role of TRAIL and IFN-gamma in CD4+ T cell-dependent tumor rejection in the anterior chamber of the eye." J Immunol **171**(6): 2789-2796.

Wang, Y., H. Jiang, D. Dai, M. Su, M. Martinka, P. Brasher, Y. Zhang, D. McLean, J. Zhang, W. Ip, G. Li, X. Zhang and Y. Zhou (2010). "Alpha 1 antichymotrypsin is aberrantly expressed during melanoma progression and predicts poor survival for patients with metastatic melanoma." Pigment Cell Melanoma Res **23**(4): 575-578.

Ward, P. P., E. Paz and O. M. Conneely (2005). "Multifunctional roles of lactoferrin: a critical overview." Cell Mol Life Sci **62**(22): 2540-2548.

Waris, G. and H. Ahsan (2006). "Reactive oxygen species: role in the development of cancer and various chronic conditions." J Carcinog **5**: 14.

Weber, D. C., R. O. Mirimanoff and R. Miralbell (2007). "[Proton beam therapy: clinical indications and summary of the Swiss experience]." Bull Cancer **94**(9): 807-815.

Weber, J., O. Hamid, A. Amin, S. O'Day, E. Masson, S. M. Goldberg, D. Williams, S. M. Parker, S. D. Chasalow, S. Alaparthy and J. D. Wolchok (2013). "Randomized phase I pharmacokinetic study of ipilimumab with or without one of two different chemotherapy regimens in patients with untreated advanced melanoma." Cancer Immun **13**: 7.

Whitaker, H. C., D. Patel, W. J. Howat, A. Y. Warren, J. D. Kay, T. Sangan, J. C. Marioni, J. Mitchell, S. Aldridge, H. J. Luxton, C. Massie, A. G. Lynch and D. E. Neal (2013). "Peroxiredoxin-3 is overexpressed in prostate cancer and promotes cancer cell survival by protecting cells from oxidative stress." Br J Cancer **109**(4): 983-993.

White, V. A., J. D. Chambers, P. D. Courtright, W. Y. Chang and D. E. Horsman (1998). "Correlation of cytogenetic abnormalities with the outcome of patients with uveal melanoma." Cancer **83**(2): 354-359.

Wilson, L. L., L. Tran, D. L. Morton and D. S. Hoon (2004). "Detection of differentially expressed proteins in early-stage melanoma patients using SELDI-TOF mass spectrometry." Ann N Y Acad Sci **1022**: 317-322.

Wistow, G., S. L. Bernstein, M. K. Wyatt, S. Ray, A. Behal, J. W. Touchman, G. Bouffard, D. Smith and K. Peterson (2002). "Expressed sequence tag analysis of human retina for the NEIBank Project: retbindin, an abundant, novel retinal cDNA and alternative splicing of other retina-preferred gene transcripts." Mol Vis **8**: 196-204.

Wolf, M., I. Clark-Lewis, C. Buri, H. Langen, M. Lis and L. Mazzucchelli (2003). "Cathepsin D specifically cleaves the chemokines macrophage inflammatory protein-1 alpha, macrophage inflammatory protein-1 beta, and SLC that are expressed in human breast cancer." Am J Pathol **162**(4): 1183-1190.

Wonsey, D. R., K. I. Zeller and C. V. Dang (2002). "The c-Myc target gene PRDX3 is required for mitochondrial homeostasis and neoplastic transformation." Proc Natl Acad Sci U S A **99**(10): 6649-6654.

Worley, L. A., M. D. Onken, E. Person, D. Robirds, J. Branson, D. H. Char, A. Perry and J. W. Harbour (2007). "Transcriptomic versus chromosomal prognostic markers and clinical outcome in uveal melanoma." Clin Cancer Res **13**(5): 1466-1471.

Wright, P. C., J. Noirel, S. Y. Ow and A. Fazeli (2012). "A review of current proteomics technologies with a survey on their widespread use in reproductive biology investigations." Theriogenology **77**(4): 738-765 e752.

Wu, C. W., J. L. Sauter, P. K. Johnson, C. D. Chen and T. W. Olsen (2004). "Identification and localization of major soluble vitreous proteins in human ocular tissue." Am J Ophthalmol **137**(4): 655-661.

Wu, X., J. Li, M. Zhu, J. A. Fletcher and F. S. Hodi (2012). "Protein kinase C inhibitor AEB071 targets ocular melanoma harboring GNAQ mutations via effects on the PKC/Erk1/2 and PKC/NF-kappaB pathways." Mol Cancer Ther **11**(9): 1905-1914.

Wu, X., M. Zhu, J. A. Fletcher, A. Giobbie-Hurder and F. S. Hodi (2012). "The protein kinase C inhibitor enzastaurin exhibits antitumor activity against uveal melanoma." PLoS One **7**(1): e29622.

www.clinicaltrials.gov. (2013).

Xin, H., J. C. Stephans, X. Duan, G. Harrowe, E. Kim, U. Grieshammer, C. Kingsley and K. Giese (2000). "Identification of a novel aspartic-like protease differentially expressed in human breast cancer cell lines." Biochim Biophys Acta **1501**(2-3): 125-137.

Xu, R. H., H. Pelicano, Y. Zhou, J. S. Carew, L. Feng, K. N. Bhalla, M. J. Keating and P. Huang (2005). "Inhibition of glycolysis in cancer cells: a novel strategy to overcome drug resistance associated with mitochondrial respiratory defect and hypoxia." Cancer Res **65**(2): 613-621.

Xue, A., C. J. Scarlett, L. Chung, G. Butturini, A. Scarpa, R. Gandy, S. R. Wilson, R. C. Baxter and R. C. Smith (2010). "Discovery of serum biomarkers for pancreatic adenocarcinoma using proteomic analysis." Br J Cancer **103**(3): 391-400.

Yan, L. B., K. Shi, Z. T. Bing, Y. L. Sun and Y. Shen (2013). "Proteomic analysis of energy metabolism and signal transduction in irradiated melanoma cells." Int J Ophthalmol **6**(3): 286-294.

Yang, H. and H. E. Grossniklaus (2010). "Constitutive overexpression of pigment epithelium-derived factor inhibition of ocular melanoma growth and metastasis." Invest Ophthalmol Vis Sci **51**(1): 28-34.

Yang, J. C., M. Hughes, U. Kammula, R. Royal, R. M. Sherry, S. L. Topalian, K. B. Suri, C. Levy, T. Allen, S. Mavroukakis, I. Lowy, D. E. White and S. A. Rosenberg (2007). "Ipilimumab (anti-CTLA4 antibody) causes regression of metastatic renal cell cancer associated with enteritis and hypophysitis." J Immunother **30**(8): 825-830.

Yang, Y., E. Spitzer, N. Kenney, W. Zschiesche, M. Li, A. Kromminga, T. Muller, F. Spener, A. Lezius, J. H. Veerkamp and et al. (1994). "Members of the fatty acid binding protein family are differentiation factors for the mammary gland." J Cell Biol **127**(4): 1097-1109.

Yonekawa, Y. and I. K. Kim (2012). "Epidemiology and management of uveal melanoma." Hematol Oncol Clin North Am **26**(6): 1169-1184.

Yoshida, A., N. Okamoto, A. Tozawa-Ono, H. Koizumi, K. Kiguchi, B. Ishizuka, T. Kumai and N. Suzuki (2013). "Proteomic analysis of differential protein expression by brain metastases of gynecological malignancies." Hum Cell **26**(2): 56-66.

Yoshimura, T., K. H. Sonoda, M. Sugahara, Y. Mochizuki, H. Enaida, Y. Oshima, A. Ueno, Y. Hata, H. Yoshida and T. Ishibashi (2009). "Comprehensive analysis of inflammatory immune mediators in vitreoretinal diseases." PLoS One **4**(12): e8158.

Yu, J., R. Peng, H. Chen, C. Cui and J. Ba (2012). "Elucidation of the pathogenic mechanism of rhegmatogenous retinal detachment with proliferative vitreoretinopathy by proteomic analysis." Invest Ophthalmol Vis Sci **53**(13): 8146-8153.

Yu, J. Z., M. A. Warycha, P. J. Christos, F. Darvishian, H. Yee, H. Kaminio, R. S. Berman, R. L. Shapiro, M. T. Buckley, L. F. Liebes, A. C. Pavlick, D. Polsky, P. C. Brooks and I. Osman (2008). "Assessing the clinical utility of measuring Insulin-like Growth Factor Binding Proteins in tissues and sera of melanoma patients." J Transl Med **6**: 70.

Yu, Y., S. Gao, Q. Li, C. Wang, X. Lai, X. Chen, R. Wang, J. Di, T. Li, W. Wang and X. Wu (2012). "The FGF2-binding peptide P7 inhibits melanoma growth in vitro and in vivo." J Cancer Res Clin Oncol **138**(8): 1321-1328.

Zembruski, N. C., V. Stache, W. E. Haefeli and J. Weiss (2012). "7-Aminoactinomycin D for apoptosis staining in flow cytometry." Anal Biochem **429**(1): 79-81.

Zeng, G. Q., H. Yi, P. F. Zhang, X. H. Li, R. Hu, M. Y. Li, C. Li, J. Q. Qu, X. Deng and Z. Q. Xiao (2013). "The function and significance of SELENBP1 downregulation in human bronchial epithelial carcinogenic process." PLoS One **8**(8): e71865.

Zhang, P., D. W. Chan, Y. Zhu, J. J. Li, I. O. Ng, D. Wan and J. Gu (2006). "Identification of carboxypeptidase of glutamate like-B as a candidate suppressor in cell growth and metastasis in human hepatocellular carcinoma." Clin Cancer Res **12**(22): 6617-6625.

Zhou, Y., Z. Zeng, W. Zhang, W. Xiong, M. Wu, Y. Tan, W. Yi, L. Xiao, X. Li, C. Huang, L. Cao, K. Tang, X. Li, S. Shen and G. Li (2008). "Lactotransferrin: a candidate tumor suppressor-Deficient expression in human nasopharyngeal carcinoma and inhibition of NPC cell proliferation by modulating the mitogen-activated protein kinase pathway." Int J Cancer **123**(9): 2065-2072.

Zhou, Y. J., S. P. Zhang, C. W. Liu and Y. Q. Cai (2009). "The protection of selenium on ROS mediated-apoptosis by mitochondria dysfunction in cadmium-induced LLC-PK(1) cells." Toxicol In Vitro **23**(2): 288-294.

Zhu, W., J. W. Smith and C. M. Huang "Mass spectrometry-based label-free quantitative proteomics." J Biomed Biotechnol **2010**: 840518.

Zhu, W., J. W. Smith and C. M. Huang (2010). "Mass spectrometry-based label-free quantitative proteomics." J Biomed Biotechnol **2010**: 840518.

Zinkin, N. T., F. Grall, K. Bhaskar, H. H. Otu, D. Spentzos, B. Kalmowitz, M. Wells, M. Guerrero, J. M. Asara, T. A. Libermann and N. H. Afdhal (2008). "Serum

proteomics and biomarkers in hepatocellular carcinoma and chronic liver disease." Clin Cancer Res **14**(2): 470-477.

Zissimopoulos, A., A. Karpouzis, I. Karaitianos, N. Baziotis, I. Tselios and C. Koutis (2006). "[Serum levels of S-100b protein after four years follow-up of patients with melanoma]." Hell J Nucl Med **9**(3): 204-207.

Zuidervaart, W., P. J. Hensbergen, M. C. Wong, A. M. Deelder, C. P. Tensen, M. J. Jager and N. A. Gruis (2006). "Proteomic analysis of uveal melanoma reveals novel potential markers involved in tumor progression." Invest Ophthalmol Vis Sci **47**(3): 786-793.

SUPPLEMENTARY DATA

AppendixA

Elution 1					Elution 2				Elution 3				Elution 4			
Protein Name	Score	Coverage (%)	MW (Da)	Accession No.	Protein Name	Score	Coverage (%)	MW (Da)	Accession No.	Protein Name	Score	Coverage (%)	MW (Da)	Accession No.	Protein Name	Score	Coverage (%)	MW (Da)	Accession No.
Sulfhydryl oxidase 1	20.23	5.10	82525.7	O00391	Hemoglobin subunit alpha	30.26	30.30	15247.9	P69905	Phosphatidylinositol-glycan-specific phospholip	20.23	3.30	92278.1	P80108	Pregnancy zone protein	20.18	1.30	163759.1	P20742
Coagulation factor X	20.22	5.10	54696.6	P00742	CD5 antigen-like	20.21	9.80	38063.0	O43866	Complement factor H-related protein 5	20.17	3.50	64377.1	Q9BXR6	Phospholipid transfer protein	20.35	8.10	54704.7	P55058
Ig heavy chain V-III region CAM	16.13	18.00	13659.2	P01768	Ig kappa chain V-II region Cum	20.23	13.90	12668.3	P01614	Ig gamma-2 chain C region	40.21	21.80	35877.8	P01859	Apolipoprotein L1	30.21	8.50	43947.0	O14791
Ig heavy chain V-III region GAL	20.18	9.50	12722.2	P01781	Complement component C7	20.21	3.70	93457.3	P10643	Complement component C8 gamma chain	20.21	11.40	22263.6	P07360	Coagulation factor V	20.19	1.30	251543.8	P12259
Platelet factor 4	20.20	11.90	10837.9	P02776	Ig kappa chain V-IV region (Fragment)	20.19	17.40	13371.6	P06312	Ig kappa chain V-III region SIE	30.27	39.40	11767.9	P01620	Apolipoprotein C-IV	20.18	18.90	14543.5	P55056
Lactotransferrin	30.23	4.60	78132.0	P02788	Adiponectin	20.21	14.30	26397.0	Q15848	Alpha-2-macroglobulin	120.25	10.10	163187.4	P01023	Ficolin-2	30.19	6.40	33979.5	Q15485
Salivary acidic proline-rich phosphoprot	20.17	19.30	17006.3	P02810	C4b-binding protein beta chain	20.23	11.50	28338.5	P20851	Complement C5	40.23	3.70	188185.3	P01031	von Willebrand factor	40.23	1.70	309055.6	P04275
Plasma kallikrein	20.19	3.60	71322.8	P03952	Hemopexin	80.33	26.80	51643.3	P02790	Serotransferrin	150.26	26.10	77013.7	P02787	Mannan-binding lectin serine protease	20.17	3.40	75653.7	O00187
Heparin cofactor 2	60.26	13.40	57034.3	P05546	Alpha-1B-glycoprotein	30.33	12.30	54219.7	P04217	Alpha-2-HS-glycoprotein	40.29	18.50	39299.7	P02765	Alpha-2-antiplasmin	30.23	12.80	54531.2	P08697
SPARC	20.27	11.60	34609.7	P09486	Keratin, type I cytoskeletal 14	40.21	11.90	51529.4	P02533	Complement factor B	30.24	3.80	85478.6	P00751	Hyaluronan-binding protein 2	50.16	9.10	62630.5	Q14520
Keratin, type II cytoskeletal 3	30.25	3.50	64377.6	P12035	Keratin, type II cytoskeletal 5	30.20	6.80	62340.0	P13647	Keratin, type II cytoskeletal 4	40.19	9.00	57249.9	P19013	Ig kappa chain V-III region SIE	20.30	31.20	11767.9	P01620
Properdin	20.31	7.90	51242.0	P27918	Azurocidin	20.21	9.60	26868.7	P20160	Haptoglobin	58.24	12.10	45176.6	P00738	Complement component C9	30.34	8.80	63132.8	P02748
Pigment epithelium-derived factor	20.29	11.70	46283.4	P36955	Ceruloplasmin	60.36	8.60	122127.6	P00450	Complement component C9	20.24	6.80	63132.8	P02748	Alpha-2-HS-glycoprotein	30.27	12.00	39299.7	P02765
Complement factor H-related protein 2	20.18	8.50	30630.6	P36980	Alpha-2-macroglobulin	220.29	23.30	163187.4	P01023	Platelet factor 4 variant	20.20	23.10	11545.3	P10720	Complement C1r subcomponent	80.31	19.90	80066.8	P00736
Lysozyme C	20.30	24.30	16526.3	P61626	Vitamin D-binding protein	20.31	9.30	52929.1	P02774	Complement C1r subcomponent	20.23	3.50	80066.8	P00736	Vitamin K-dependent protein S	50.19	9.30	75074.1	P07225
Immunoglobulin lambda-like polypeptic	40.28	27.10	23048.6	B9A064	Complement component C9	20.28	7.00	63132.8	P02748	Keratin, type II cytoskeletal 6A	20.25	4.80	60008.3	P02538	Gelsolin	30.31	6.80	85644.3	P06396
Ceruloplasmin	140.34	22.70	122127.6	P00450	Keratin, type II cytoskeletal 6A	30.28	6.90	60008.3	P02538	Plasma protease C1 inhibitor	30.22	7.80	55119.5	P05155	Lumican	20.26	8.30	38404.8	P51884
Prothrombin	170.30	36.20	69992.2	P00734	Fibulin-1	20.28	3.80	77162.4	P23142	Haptoglobin-related protein	66.23	14.70	39004.7	P00739	Serotransferrin	70.24	14.50	77013.7	P02787
Complement C1r subcomponent	70.22	10.80	80066.8	P00736	Gelsolin	30.29	6.50	85644.3	P06396	Complement component C6	20.20	3.10	104717.9	P13671	Complement component C8 gamma cha	20.20	12.90	22263.6	P07360
Haptoglobin	70.30	22.20	45176.6	P00738	Ig gamma-2 chain C region	50.26	26.40	35877.8	P01859	EGF-containing fibulin-like extracellular matrix	20.17	3.90	54604.3	Q12805	Keratin, type II cytoskeletal 4	60.22	12.90	57249.9	P19013
Haptoglobin-related protein	66.26	15.20	39004.7	P00739	Complement C1q subcomponent subun	20.18	13.10	26000.2	P02745	Alpha-1-acid glycoprotein 1	20.14	11.40	23496.8	P02763	Serum amyloid A-4 protein	30.19	21.50	14737.3	P35542
Plasminogen	30.21	5.30	90510.2	P00747	Alpha-1-antichymotrypsin	58.25	17.50	47620.6	P01011	Kininogen-1	20.17	3.60	71912.1	P01042	Complement component C6	50.20	6.60	104717.9	P13671
Antithrombin-III	28.24	10.10	52569.0	P01008	Complement C1r subcomponent	30.20	4.70	80066.8	P00736	Serum amyloid A-4 protein	30.18	21.50	14737.3	P35542	Keratin, type I cytoskeletal 13	68.22	15.10	49557.4	P13646
Alpha-1-antitrypsin	50.28	16.70	46707.1	P01009	Alpha-1-acid glycoprotein 1	40.24	22.90	23496.8	P02763	Keratin, type I cytoskeletal 13	20.21	4.60	49557.4	P13646	Complement C5	20.23	2.50	188185.3	P01031
Complement C3	1086.39	68.70	187029.3	P01024	Haptoglobin-related protein	48.23	13.20	39004.7	P00739	Apolipoprotein C-I	20.17	24.10	9326.1	P02654	Ig gamma-2 chain C region	20.15	5.20	35877.8	P01859
Complement C5	40.26	5.10	188185.3	P01031	Ig kappa chain V-III region SIE	30.23	39.40	11767.9	P01620	Antithrombin-III	118.30	34.30	52569.0	P01008	Retinol-binding protein 4	40.17	24.90	22995.3	P02753
Kininogen-1	70.22	13.50	71912.1	P01042	Haptoglobin	60.24	16.70	45176.6	P00738	Apolipoprotein A-II	40.22	41.00	11167.9	P02652	Inter-alpha-trypsin inhibitor heavy chai	20.18	2.10	99786.6	Q06033
Ig kappa chain V-III region SIE	30.28	39.40	11767.9	P01620	Complement C5	30.17	2.10	188185.3	P01031	Apolipoprotein E	80.27	28.40	36131.8	P02649	Apolipoprotein E	80.22	25.90	36131.8	P02649
Ig kappa chain C region	40.28	64.20	11601.7	P01834	Hemoglobin subunit beta	20.21	15.60	15988.3	P68871	Ig mu chain C region	50.21	14.80	49275.6	P01871	Fibulin-1	70.29	18.10	77162.4	P23142
Ig gamma-1 chain C region	60.35	29.70	36083.2	P01857	Complement factor B	40.20	7.20	85478.6	P00751	Keratin, type I cytoskeletal 10	60.24	16.40	58791.6	P13645	Ig mu chain C region	60.24	17.30	49275.6	P01871
Ig gamma-2 chain C region	20.18	8.90	35877.8	P01859	Keratin, type II cytoskeletal 4	50.18	10.50	57249.9	P19013	Keratin, type II cytoskeletal 2 epidermal	46.22	5.80	65393.2	P35908	Inter-alpha-trypsin inhibitor heavy chai	70.20	10.40	101325.8	P19827
Ig gamma-3 chain C region	40.22	19.90	41260.4	P01860	Keratin, type I cytoskeletal 13	50.23	11.10	49557.4	P13646	Prothrombin	140.27	32.60	69992.2	P00734	Keratin, type I cytoskeletal 10	70.30	13.00	58791.6	P13645
Ig mu chain C region	110.27	33.80	49275.6	P01871	Retinol-binding protein 4	20.17	10.40	22995.3	P02753	Serum paraoxonase/arylesterase 1	20.23	7.00	39706.3	P27169	Keratin, type I cytoskeletal 9	30.30	8.30	62026.7	P35527
Ig alpha-1 chain C region	50.30	25.50	37630.7	P01876	Antithrombin-III	90.26	29.30	52569.0	P01008	Vitronectin	90.27	29.30	54271.2	P04004	Keratin, type II cytoskeletal 1	90.25	12.90	65998.9	P04264
Apolipoprotein A-I	80.34	22.80	30758.9	P02647	Complement C1q subcomponent subun	20.28	12.20	25757.1	P02747	Alpha-1-antitrypsin	130.30	47.10	46707.1	P01009	Prothrombin	130.28	29.10	69992.2	P00734
C-reactive protein	70.27	31.70	25022.7	P02741	Complement factor H-related protein 1	20.25	11.20	37626.0	Q03591	Apolipoprotein A-IV	220.32	51.00	45371.5	P06727	Alpha-1-antitrypsin	100.32	31.10	46707.1	P01009
Serum amyloid P-component	30.23	14.80	25371.1	P02743	Inter-alpha-trypsin inhibitor heavy chai	60.23	9.40	103293.2	Q14624	C4b-binding protein alpha chain	200.32	44.90	66989.4	P04003	Apolipoprotein B-100	410.32	13.30	515283.6	P04114
Complement C1q subcomponent subun	40.30	24.10	26000.2	P02745	Keratin, type I cytoskeletal 10	70.28	21.10	58791.6	P13645	Complement C3	510.36	39.70	187029.3	P01024	C4b-binding protein alpha chain	90.35	19.60	66989.4	P04003
Complement C1q subcomponent subun	50.24	26.50	26704.5	P02746	Keratin, type II cytoskeletal 1	60.22	12.60	65998.9	P04264	Complement factor H	270.34	30.10	139004.4	P08603	Complement factor H	180.35	20.20	139004.4	P08603
Complement C1q subcomponent subun	60.35	34.70	25757.1	P02747	Keratin, type II cytoskeletal 2 epiderma	26.21	3.30	65393.2	P35908	Fibronectin	508.41	32.90	262457.6	P02751	Fibronectin	410.35	27.90	262457.6	P02751
Complement component C9	90.32	25.90	63132.8	P02748	Prothrombin	100.25	23.30	69992.2	P00734	Plasminogen	210.34	36.50	90510.2	P00747	Ig alpha-1 chain C region	40.23	19.30	37630.7	P01876
Beta-2-glycoprotein 1	30.22	14.20	38272.7	P02749	Serum paraoxonase/arylesterase 1	20.23	7.60	39706.3	P27169	Serum albumin	440.35	71.30	69321.6	P02768	Immunoglobulin lambda-like polypeptic	40.29	32.20	23048.6	B9A064
Fibronectin	278.35	21.80	262457.6	P02751	Vitronectin	30.24	8.80	54271.2	P04004	Apolipoprotein A-I	150.36	58.80	30758.9	P02647	Plasma protease C1 inhibitor	70.22	18.60	55119.5	P05155
Retinol-binding protein 4	70.26	61.70	22995.3	P02753	Alpha-1-antitrypsin	170.30	56.70	46707.1	P01009	Apolipoprotein B-100	310.33	8.70	515283.6	P04114	Plasminogen	150.34	29.50	90510.2	P00747
Protein AMBP	50.33	16.50	38974.0	P02760	Apolipoprotein B-100	170.33	6.10	515283.6	P04114	Apolipoprotein C-III	30.29	34.30	10845.5	P02656	Serum albumin	420.36	70.00	69321.6	P02768
Alpha-1-acid glycoprotein 1	20.19	12.90	23496.8	P02763	Complement C3	608.35	44.90	187029.3	P01024	Apolipoprotein D	60.23	31.20	21261.8	P05090	Antithrombin-III	120.28	36.40	52569.0	P01008
Alpha-2-HS-glycoprotein	30.32	12.00	39299.7	P02765	Complement C4-A	518.32	36.00	192649.5	P0C0L4	Ceruloplasmin	40.28	6.80	122127.6	P00450	Apolipoprotein A-I	188.34	62.20	30758.9	P02647
Transthyretin	90.33	65.30	15877.1	P02766	Complement factor H	370.34	39.20	139004.4	P08603	Clusterin	110.31	25.80	52461.1	P10909	Apolipoprotein A-II	60.26	64.00	11167.9	P02652
Serum albumin	270.33	54.20	69321.6	P02768	Histidine-rich glycoprotein	50.28	13.00	59540.9	P04196	Complement C4-A	418.34	30.80	192649.5	P0C0L4	Apolipoprotein A-IV	210.30	51.00	45371.5	P06727
Vitamin D-binding protein	30.26	10.80	52929.1	P02774	Inter-alpha-trypsin inhibitor heavy chai	170.29	22.90	106396.8	P19823	Complement factor H-related protein 1	30.19	14.20	37626.0	Q03591	Apolipoprotein C-II	20.16	17.80	11276.8	P02655
Serotransferrin	30.22	5.00	77013.7	P02787	Plasminogen	190.31	30.50	90510.2	P00747	Fibulin-1	60.28	12.10	77162.4	P23142	Apolipoprotein D	60.23	25.40	21261.8	P05090
C4b-binding protein alpha chain	40.36	10.20	66989.4	P04003	Serotransferrin	280.32	41.70	77013.7	P02787	Ig alpha-1 chain C region	70.25	26.60	37630.7	P01876	Ceruloplasmin	50.32	8.00	122127.6	P00450
Vitronectin	30.22	7.50	54271.2	P04004	Serum albumin	470.37	70.30	69321.6	P02768	Ig gamma-1 chain C region	70.29	32.70	36083.2	P01857	Clusterin	90.30	25.60	52461.1	P10909
Apolipoprotein B-100	20.16	0.40	515283.6	P04114	Alpha-2-HS-glycoprotein	30.22	17.20	39299.7	P02765	Ig gamma-3 chain C region	30.25	16.40	41260.4	P01860	Complement C3	514.37	42.00	187029.3	P01024
Histidine-rich glycoprotein	20.17	3.60	59540.9	P04196	Apolipoprotein A-I	170.35	53.90	30758.9	P02647	Ig kappa chain C region	40.27	64.20	11601.7	P01834	Complement C4-A	498.33	35.30	192649.5	P0C0L4
Keratin, type II cytoskeletal 1	80.27	14.40	65998.9	P04264	Apolipoprotein A-II	40.24	54.00	11167.9	P02652	Ig lambda-2 chain C regions	20.20	27.40	11286.6	P0CG05	Glutathione peroxidase 3	20.21	14.20	35386.0	P22352
Plasma protease C1 inhibitor	40.17	10.00	55119.5	P05155	Apolipoprotein A-IV	150.23	38.60	45371.5	P06727	Immunoglobulin lambda-like polypeptide 5	30.28	23.40	23048.6	B9A064	Histidine-rich glycoprotein	20.15	3.80	59540.9	P04196
Gelsolin	70.31	13.30	85644.3	P06396	Apolipoprotein C-III	20.19	27.30	10845.5	P02656	Inter-alpha-trypsin inhibitor heavy chain H1	80.31	10.50	101325.8	P19827	Ig gamma-1 chain C region	80.29	40.60	36083.2	P01857
Apolipoprotein A-IV	20.21	6.80	45371.5	P06727	Apolipoprotein D	30.20	18.00	21261.8	P05090	Inter-alpha-trypsin inhibitor heavy chain H2	80.28	8.90	106396.8	P19823	Ig gamma-3 chain C region	30.22	16.40	41260.4	P01860
Complement component C8 beta chain	30.31	9.30	67003.5	P07358	C4b-binding protein alpha chain	200.31	47.10	66989.4	P04003	Inter-alpha-trypsin inhibitor heavy chain H4	70.24	10.10	103293.2	Q14624	Ig kappa chain C region	40.25	65.10	11601.7	P01834
Complement component C8 gamma cha	60.31	48.00	22263.6	P07360	Clusterin	70.24	18.50	52461.1	P10909	Keratin, type I cytoskeletal 9	20.23	6.30	62026.7	P35527	Inter-alpha-trypsin inhibitor heavy chai	100.33	13.50	106396.8	P19823
Thrombospondin-1	80.29	9.10	129299.2	P07996	Complement C1q subcomponent subun	30.25	17.00	26704.5	P02746	Keratin, type II cytoskeletal 1	80.23	16.60	65998.9	P04264	Inter-alpha-trypsin inhibitor heavy chai	160.33	28.60	103293.2	Q14624
Complement factor H	210.34	23.50	139004.4	P08603	Fibronectin	550.40	37.80	262457.6	P02751	Serum amyloid P-component	30.21	15.70	25371.1	P02743	Keratin, type II cytoskeletal 2 epiderma	60.23	8.10	65393.2	P35908
Complement C1s subcomponent	70.25	14.80	76634.9	P09871	Ig alpha-1 chain C region	70.25	28.90	37630.7	P01876	Transthyretin	30.30	39.50	15877.1	P02766	Protein AMBP	20.19	7.40	38974.0	P02760
Complement C4-A	540.36	40.10	192649.5	P0C0L4	Ig gamma-1 chain C region	120.37	54.50	36083.2	P01857	Vitamin D-binding protein	30.23	8.90	52929.1	P02774	Serum paraoxonase/arylesterase 1	38.25	16.60	39706.3	P27169
Ig lambda-2 chain C regions	30.23	52.80	11286.6	P0CG05	Ig gamma-3 chain C region	40.29	22.00	41260.4	P01860	Vitamin K-dependent protein S	20.22	3.80	75074.1	P07225	Transthyretin	50.33	49.00	15877.1	P02766
Platelet factor 4 variant	20.25	23.10	11545.3	P10720	Ig kappa chain C region	50.24	80.20	11601.7	P01834	Serum amyloid A-1 protein	50.28	48.40	13523.5	P0DJI8	Vitronectin	120.26	38.70	54271.2	P04004
Clusterin	30.22	5.30	52461.1	P10909	Ig lambda-2 chain C regions	20.20	27.40	11286.6	P0CG05	Inter-alpha-trypsin inhibitor heavy chain H3	30.20	4.30	99786.6	Q06033	Serum amyloid A-1 protein	50.31	48.40	13523.5	P0DJI8

Keratin, type I cytoskeletal 10	20.20	3.80	58791.6	P13645	Ig mu chain C region	120.27	33.40	49275.6	P01871	Ig lambda chain V-III region LOI	20.14	21.60	11927.8	P80748	Beta-2-glycoprotein 1	20.18	7.00	38272.7	P02749
Lipopolysaccharide-binding protein	20.30	7.70	53350.0	P18428	Immunoglobulin lambda-like polypeptic	50.28	36.00	23048.6	B9A064	Complement C1q subcomponent subunit C	20.19	11.00	25757.1	P02747	Haptoglobin	30.20	9.10	45176.6	P00738
Keratin, type II cytoskeletal 4	40.22	7.50	57249.9	P19013	Inter-alpha-trypsin inhibitor heavy chai	110.35	16.80	101325.8	P19827	C-reactive protein	40.20	19.60	25022.7	P02741	Complement C1q subcomponent subun	20.24	11.50	26704.5	P02746
Inter-alpha-trypsin inhibitor heavy chai	290.38	34.90	106396.8	P19823	Keratin, type I cytoskeletal 9	30.26	10.00	62026.7	P35527	Apolipoprotein C-II	20.24	29.70	11276.8	P02655	Platelet factor 4 variant	20.20	23.10	11545.3	P10720
Inter-alpha-trypsin inhibitor heavy chai	268.37	37.70	101325.8	P19827	Protein AMBP	30.21	10.80	38974.0	P02760	Ficolin-3	30.18	11.00	32882.0	O75636	Alpha-1-antichymotrypsin	30.24	10.40	47620.6	P01011
Keratin, type I cytoskeletal 9	20.26	7.20	62026.7	P35527	Serum amyloid A-4 protein	30.19	21.50	14737.3	P35542	Galectin-3-binding protein	30.21	6.50	65289.4	Q08380	Galectin-3-binding protein	20.22	4.10	65289.4	Q08380
Keratin, type II cytoskeletal 2 epiderma	30.20	4.50	65393.2	P35908	Transthyretin	40.32	55.10	15877.1	P02766	Glutathione peroxidase 3	20.27	14.20	35386.0	P22352	C-reactive protein	40.21	20.10	25022.7	P02741
Lumican	50.29	19.80	38404.8	P51884	Plasma protease C1 inhibitor	30.24	10.00	55119.5	P05155	Hemoglobin subunit beta	50.25	40.80	15988.3	P68871	Kininogen-1	40.17	8.20	71912.1	P01042
Complement factor H-related protein 1	60.27	28.20	37626.0	Q03591	Serum amyloid P-component	30.19	16.10	25371.1	P02743	Protein AMBP	30.18	10.80	38974.0	P02760	Alpha-2-macroglobulin	30.21	2.60	163187.4	P01023
Inter-alpha-trypsin inhibitor heavy chai	130.40	20.30	99786.6	Q06033	Ig lambda chain V-III region L	20.25	21.60	11927.8	P80748	Thrombospondin-1	70.27	7.10	129299.2	P07996	EGF-containing fibulin-like extracellula	20.21	4.50	54604.3	Q12805
Inter-alpha-trypsin inhibitor heavy chai	80.34	13.80	103293.2	Q14624	Apolipoprotein E	70.22	25.90	36131.8	P02649						Complement C1s subcomponent	80.24	15.10	76634.9	P09871
Proteoglycan 4	40.23	4.00	150983.2	Q92954	Apolipoprotein C-I	30.19	28.90	9326.1	P02654						Complement component C8 beta chain	40.29	10.30	67003.5	P07358
					Beta-2-glycoprotein 1	30.26	13.00	38272.7	P02749						Haptoglobin-related protein	48.24	18.70	39004.7	P00739
					Galectin-3-binding protein	30.22	7.20	65289.4	Q08380						Thrombospondin-1	90.28	10.40	129299.2	P07996
					Lipopolysaccharide-binding protein	20.28	6.20	53350.0	P18428						Vitamin D-binding protein	50.25	16.50	52929.1	P02774
					Platelet factor 4 variant	20.20	23.10	11545.3	P10720						Apolipoprotein C-III	30.29	34.30	10845.5	P02656
					Thrombospondin-1	30.25	4.30	129299.2	P07996						Ficolin-3	30.23	13.40	32882.0	O75636
					Vitamin K-dependent protein S	20.24	2.40	75074.1	P07225						Ig lambda-2 chain C regions	20.20	27.40	11286.6	P0CG05
															Lipopolysaccharide-binding protein	20.25	6.20	53350.0	P18428

Table 1 Fractionated cutaneous melanoma sera which were separated by 1-D electrophoresis were sliced up into thin gel sections and digested prior to analysis by LC-MS. The results of this qualitative analysis are shown in the table above. Identifications which were unique to an elution are written in red.

Elution 1					Elution 2				Elution 3					Elution 4				
Protein Name	Score	Coverage (%)	MW (Da)	Accession No.	Protein Name	Score	Coverage (%)	MW (Da)	Accession No.	Protein Name	Score	Coverage (%)	MW (Da)	Accession No.	Protein Name	Score	Coverage (%)	MW (Da)	Accession No.
Alpha-1-acid glycoprotein 1	30.23	15.40	23496.8	P02763	Adiponectin	40.25	31.60	26397.0	Q15848	Keratin, type II cytoskeletal 71	18.24	2.30	57256.1	Q3SY84	Phosphatidylcholine-sterol acyltransferase	20.35	12.00	49546.2	P04180
Complement component C8 beta chain	20.25	7.80	67003.5	P07358	Fibrinogen alpha chain	30.22	5.20	94914.3	P02671	Ig gamma-4 chain C region	20.20	13.50	35917.9	P01861	Complement component C7	30.24	4.60	93457.3	P10643
SPARC	30.22	13.20	34609.7	P09486	Complement factor H-related protein 5	20.23	5.40	64377.1	Q9BXR6	Hemopexin	30.31	10.00	51643.3	P02790	Carboxypeptidase B2	20.18	4.70	48393.5	Q96IY4
Complement C1s subcomponent	38.25	7.40	76634.9	P09871	Apolipoprotein C-IV	20.19	18.90	14543.5	P55056	Glutathione peroxidase 3	20.21	11.90	35386.0	P22352	Keratin-81-like protein KRT121P	68.20	18.80	29098.7	A6NCN2
Coagulation factor V	30.25	2.40	251543.8	P12259	Platelet factor 4	20.23	11.90	10837.9	P02776	Ficolin-3	30.23	12.00	32882.0	O75636	Vitamin K-dependent protein Z	30.24	7.80	44714.7	P22891
Lumican	40.28	13.60	38404.8	P51884	Extracellular matrix protein 1	30.20	9.40	60635.4	Q16610	C4b-binding protein beta chain	30.17	15.90	28338.5	P20851	Neutrophil defensin 1	20.15	19.10	10194.2	P59665
Proteoglycan 4	50.22	5.10	150983.2	Q92954	Properdin	20.16	3.80	51242.0	P27918	Protein crumbs homolog 1	14.14	1.40	154080.4	P82279	Histone H4	20.20	16.50	11360.4	P62805
Immunoglobulin lambda-like polypeptide 5	50.29	36.00	23048.6	B9A064	Ig kappa chain V-III region SIE	20.24	31.20	11767.9	P01620	Antithrombin-III	170.30	45.50	52569.0	P01008	Keratin, type II cytoskeletal 75	18.20	2.20	59524.1	O95678
Mannan-binding lectin serine protease 2	30.29	6.30	75653.7	O00187	Apolipoprotein E	90.26	30.90	36131.8	P02649	Apolipoprotein A-II	60.23	64.00	11167.9	P02652	Vitamin K-dependent protein C	20.19	4.80	52037.5	P04070
Ficolin-3	20.18	6.70	32882.0	O75636	Ficolin-3	40.24	14.00	32882.0	O75636	Apolipoprotein E	130.28	47.60	36131.8	P02649	Keratin, type II cuticular Hb1	30.18	5.70	54892.8	Q14533
Ceruloplasmin	120.34	19.10	122127.6	P00450	Platelet factor 4 variant	20.21	23.10	11545.3	P10720	Ig mu chain C region	90.31	25.20	49275.6	P01871	Alpha-2-antiplasmin	20.18	6.30	54531.2	P08697
Prothrombin	190.30	42.30	69992.2	P00734	Galectin-3-binding protein	20.18	4.40	65289.4	Q08380	Keratin, type I cytoskeletal 10	130.30	31.20	58791.6	P13645	Apolipoprotein C-III	20.24	27.30	10845.5	P02656
Complement C1r subcomponent	60.25	12.80	80066.8	P00736	Apolipoprotein C-I	20.19	26.50	9326.1	P02654	Keratin, type II cytoskeletal 2 epidermal	80.23	11.30	65393.2	P35908	Ficolin-3	60.25	30.10	32882.0	O75636
Haptoglobin	20.18	4.90	45176.6	P00738	Protein crumbs homolog 1	10.15	1.40	154080.4	P82279	Prothrombin	230.35	40.70	69992.2	P00734	Complement C1q subcomponent subunit B	20.28	11.10	26704.5	P02746
Haptoglobin-related protein	30.13	9.80	39004.7	P00739	Antithrombin-III	140.30	41.60	52569.0	P01008	Serum paraoxonase/arylesterase 1	40.28	18.60	39706.3	P27169	Serum amyloid P-component	30.23	14.80	25371.1	P02743
Coagulation factor IX	30.19	7.60	51745.0	P00740	Complement C1q subcomponent subunit C	50.25	29.40	25757.1	P02747	Vitronectin	130.28	33.10	54271.2	P04004	Hyaluronan-binding protein 2	30.17	5.40	62630.5	Q14520
Coagulation factor X	100.32	23.00	54696.6	P00742	Complement factor H-related protein 1	50.29	24.20	37626.0	Q03591	Alpha-1-antitrypsin	20.23	6.50	46707.1	P01009	Kininogen-1	20.13	2.60	71912.1	P01042
Plasminogen	80.22	12.50	90510.2	P00747	Inter-alpha-trypsin inhibitor heavy chain H4	88.32	13.70	103293.2	Q14624	Apolipoprotein A-IV	130.28	37.60	45371.5	P06727	Ig lambda-2 chain C regions	20.20	27.40	11286.6	P0CG05
Antithrombin-III	90.26	21.10	52569.0	P01008	Keratin, type I cytoskeletal 10	140.30	32.20	58791.6	P13645	C4b-binding protein alpha chain	140.34	30.80	66989.4	P04003	Apolipoprotein E	130.30	41.30	36131.8	P02649
Alpha-1-antitrypsin	20.24	4.10	46707.1	P01009	Keratin, type II cytoskeletal 1	140.27	28.10	65998.9	P04264	Complement C3	368.35	32.90	187029.3	P01024	Fibulin-1	100.29	21.50	77162.4	P23142
Complement C3	942.36	64.30	187029.3	P01024	Keratin, type II cytoskeletal 2 epidermal	60.24	8.80	65393.2	P35908	Complement factor H	100.32	11.10	139004.4	P08603	Ig mu chain C region	100.30	27.90	49275.6	P01871
Complement C5	40.29	4.50	188185.3	P01031	Prothrombin	218.33	49.80	69992.2	P00734	Fibronectin	370.34	25.50	262457.6	P02751	Inter-alpha-trypsin inhibitor heavy chain H1	110.31	15.40	101325.8	P19827
Kininogen-1	60.21	13.20	71912.1	P01042	Serum paraoxonase/arylesterase 1	40.27	14.60	39706.3	P27169	Plasminogen	100.36	16.50	90510.2	P00747	Keratin, type I cytoskeletal 10	130.33	30.80	58791.6	P13645
Immunoglobulin J chain	20.16	17.00	18087.0	P01591	Vitronectin	80.25	20.10	54271.2	P04004	Serum albumin	330.33	59.30	69321.6	P02768	Keratin, type I cytoskeletal 9	60.35	16.90	62026.7	P35527
Ig kappa chain V-III region SIE	30.26	39.40	11767.9	P01620	Alpha-1-antitrypsin	40.22	12.40	46707.1	P01009	Apolipoprotein A-I	158.34	52.80	30758.9	P02647	Keratin, type II cytoskeletal 1	140.31	27.80	65998.9	P04264
Ig kappa chain C region	40.33	64.20	11601.7	P01834	Apolipoprotein B-100	100.27	2.80	515283.6	P04114	Apolipoprotein B-100	330.34	9.30	515283.6	P04114	Prothrombin	208.34	40.40	69992.2	P00734
Ig gamma-1 chain C region	100.31	45.50	36083.2	P01857	Complement C3	470.36	36.90	187029.3	P01024	Apolipoprotein C-III	20.28	27.30	10845.5	P02656	Alpha-1-antitrypsin	20.24	6.50	46707.1	P01009
Ig gamma-2 chain C region	20.19	8.00	35877.8	P01859	Complement C4-A	410.32	29.90	192649.5	P0C0L4	Apolipoprotein D	50.21	25.90	21261.8	P05090	Apolipoprotein B-100	270.32	8.70	515283.6	P04114
Ig gamma-3 chain C region	30.29	16.40	41260.4	P01860	Complement factor H	190.30	21.20	139004.4	P08603	Ceruloplasmin	40.24	4.30	122127.6	P00450	C4b-binding protein alpha chain	30.27	8.40	66989.4	P04003
Ig mu chain C region	110.34	30.50	49275.6	P01871	Histidine-rich glycoprotein	30.19	6.90	59540.9	P04196	Clusterin	100.26	25.60	52461.1	P10909	Complement factor H	70.31	8.30	139004.4	P08603
Ig alpha-1 chain C region	60.26	29.70	37630.7	P01876	Inter-alpha-trypsin inhibitor heavy chain H2	120.30	20.00	106396.8	P19823	Complement C4-A	450.33	32.90	192649.5	P0C0L4	Fibronectin	290.31	20.50	262457.6	P02751
Apolipoprotein A-I	120.30	49.10	30758.9	P02647	Plasminogen	120.38	22.30	90510.2	P00747	Complement factor H-related protein 1	30.25	14.80	37626.0	Q03591	Ig alpha-1 chain C region	20.23	9.10	37630.7	P01876
Apolipoprotein E	20.17	6.30	36131.8	P02649	Serotransferrin	20.21	3.90	77013.7	P02787	Fibulin-1	40.21	8.80	77162.4	P23142	Immunoglobulin lambda-like polypeptide 5	20.24	18.20	23048.6	B9A064
Apolipoprotein A-II	20.20	29.00	11167.9	P02652	Serum albumin	300.35	57.60	69321.6	P02768	Ig alpha-1 chain C region	50.25	21.80	37630.7	P01876	Plasma protease C1 inhibitor	30.22	6.20	55119.5	P05155
Apolipoprotein C-I	20.16	24.10	9326.1	P02654	Alpha-2-HS-glycoprotein	30.25	14.40	39299.7	P02765	Ig gamma-1 chain C region	80.28	38.80	36083.2	P01857	Plasminogen	50.17	6.90	90510.2	P00747
Serum amyloid P-component	60.21	24.20	25371.1	P02743	Apolipoprotein A-I	170.34	55.80	30758.9	P02647	Ig gamma-3 chain C region	30.27	16.40	41260.4	P01860	Serum albumin	280.33	57.30	69321.6	P02768
Complement C1q subcomponent subunit A	30.32	22.90	26000.2	P02745	Apolipoprotein A-II	50.26	62.00	11167.9	P02652	Ig kappa chain C region	40.33	67.00	11601.7	P01834	Antithrombin-III	150.32	42.20	52569.0	P01008
Complement C1q subcomponent subunit B	80.27	38.70	26704.5	P02746	Apolipoprotein A-IV	170.28	43.20	45371.5	P06727	Ig lambda-2 chain C regions	20.21	27.40	11286.6	P0CG05	Apolipoprotein A-I	200.39	58.10	30758.9	P02647
Complement C1q subcomponent subunit C	40.30	25.30	25757.1	P02747	Apolipoprotein C-III	20.23	27.30	10845.5	P02656	Immunoglobulin lambda-like polypeptide 5	30.29	25.20	23048.6	B9A064	Apolipoprotein A-II	50.24	64.00	11167.9	P02652
Complement component C9	90.26	23.80	63132.8	P02748	Apolipoprotein D	40.22	25.90	21261.8	P05090	Inter-alpha-trypsin inhibitor heavy chain H1	80.27	10.50	101325.8	P19827	Apolipoprotein A-IV	200.27	50.00	45371.5	P06727
Beta-2-glycoprotein 1	20.21	7.00	38272.7	P02749	C4b-binding protein alpha chain	200.40	43.20	66989.4	P04003	Inter-alpha-trypsin inhibitor heavy chain H2	90.30	15.30	106396.8	P19823	Apolipoprotein C-II	30.19	28.70	11276.8	P02655
Fibronectin	358.33	24.10	262457.6	P02751	C4b-binding protein beta chain	30.22	21.00	28338.5	P20851	Inter-alpha-trypsin inhibitor heavy chain H4	80.26	16.10	103293.2	Q14624	Apolipoprotein D	60.21	30.70	21261.8	P05090
Retinol-binding protein 4	70.25	40.30	22995.3	P02753	Clusterin	90.32	22.30	52461.1	P10909	Keratin, type I cytoskeletal 9	30.25	8.30	62026.7	P35527	Ceruloplasmin	40.25	6.60	122127.6	P00450
Protein AMBP	50.34	16.50	38974.0	P02760	Complement C1q subcomponent subunit B	30.28	15.00	26704.5	P02746	Keratin, type II cytoskeletal 1	100.25	18.60	65998.9	P04264	Clusterin	90.33	25.60	52461.1	P10909
Alpha-2-HS-glycoprotein	30.27	16.10	39299.7	P02765	Fibronectin	560.36	36.40	262457.6	P02751	Serum amyloid P-component	20.19	10.30	25371.1	P02743	Complement C3	456.37	37.60	187029.3	P01024
Transthyretin	50.34	56.50	15877.1	P02766	Ig alpha-1 chain C region	80.27	34.00	37630.7	P01876	Transthyretin	40.32	49.00	15877.1	P02766	Complement C4-A	478.35	35.80	192649.5	P0C0L4
Serum albumin	290.27	57.80	69321.6	P02768	Ig gamma-1 chain C region	90.30	45.50	36083.2	P01857	Vitamin D-binding protein	20.27	7.00	52929.1	P02774	Glutathione peroxidase 3	30.23	19.00	35386.0	P22352
Serotransferrin	50.25	10.50	77013.7	P02787	Ig gamma-3 chain C region	40.28	17.20	41260.4	P01860	Vitamin K-dependent protein S	20.23	3.40	75074.1	P07225	Histidine-rich glycoprotein	20.21	5.70	59540.9	P04196
Angiogenin	40.18	32.70	16539.4	P03950	Ig kappa chain C region	40.32	65.10	11601.7	P01834	Mannan-binding lectin serine protease 2	20.23	4.50	75653.7	O00187	Ig gamma-1 chain C region	88.35	33.90	36083.2	P01857
C4b-binding protein alpha chain	90.43	23.80	66989.4	P04003	Ig lambda-2 chain C regions	20.20	27.40	11286.6	P0CG05	Complement component C6	20.25	3.10	104717.9	P13671	Ig gamma-3 chain C region	20.21	13.30	41260.4	P01860
Vitronectin	60.26	16.10	54271.2	P04004	Ig mu chain C region	100.30	28.50	49275.6	P01871	Histidine-rich glycoprotein	20.23	5.30	59540.9	P04196	Ig kappa chain C region	30.22	50.90	11601.7	P01834
Apolipoprotein B-100	210.33	6.50	515283.6	P04114	Immunoglobulin lambda-like polypeptide 5	40.29	32.20	23048.6	B9A064	Plasma serine protease inhibitor	30.26	11.30	45645.8	P05154	Inter-alpha-trypsin inhibitor heavy chain H2	120.33	19.00	106396.8	P19823
Keratin, type II cytoskeletal 1	110.24	18.50	65998.9	P04264	Inter-alpha-trypsin inhibitor heavy chain H1	120.34	16.20	101325.8	P19827	Beta-2-glycoprotein 1	20.20	9.30	38272.7	P02749	Inter-alpha-trypsin inhibitor heavy chain H4	188.32	30.50	103293.2	Q14624
Plasma protease C1 inhibitor	40.22	13.80	55119.5	P05155	Keratin, type I cytoskeletal 9	50.34	14.60	62026.7	P35527	EGF-containing fibulin-like extracellular matı	60.20	16.00	54604.3	Q12805	Keratin, type II cytoskeletal 2 epidermal	60.24	9.10	65393.2	P35908
Heparin cofactor 2	30.24	9.60	57034.3	P05546	Protein AMBP	30.20	8.80	38974.0	P02760	Complement C1r subcomponent	20.22	4.70	80066.8	P00736	Protein AMBP	20.20	8.80	38974.0	P02760
Ig kappa chain V-IV region (Fragment)	20.16	17.40	13371.6	P06312	Serum amyloid A-4 protein	30.18	13.10	14737.3	P35542	Lipopolysaccharide-binding protein	20.18	4.60	53350.0	P18428	Serum paraoxonase/arylesterase 1	60.26	24.80	39706.3	P27169
Gelsolin	120.33	22.60	85644.3	P06396	Transthyretin	50.30	59.90	15877.1	P02766	Coagulation factor X	20.17	5.50	54696.6	P00742	Transthyretin	60.31	65.30	15877.1	P02766
Apolipoprotein A-IV	70.19	19.20	45371.5	P06727	Immunoglobulin J chain	30.21	23.30	18087.0	P01591	Haptoglobin	20.20	4.90	45176.6	P00738	Vitronectin	110.26	25.70	54271.2	P04004
Vitamin K-dependent protein S	30.17	5.30	75074.1	P07225	Plasma serine protease inhibitor	20.24	7.90	45645.8	P05154	Alpha-2-HS-glycoprotein	40.21	18.50	39299.7	P02765	Gelsolin	70.31	13.60	85644.3	P06396
Complement component C8 gamma chain	50.17	31.20	22263.6	P07360	Procollagen C-endopeptidase enhancer 1	20.21	7.10	47942.0	Q15113	Alpha-2-macroglobulin	90.21	7.60	163187.4	P01023	Complement C1q subcomponent subunit A	20.19	9.40	26000.2	P02745
Thrombospondin-1	50.19	5.40	129299.2	P07996	Complement component C8 gamma chain	20.24	13.90	22263.6	P07360	Apolipoprotein C-II	30.21	40.60	11276.8	P02655	Retinol-binding protein 4	30.22	21.90	22995.3	P02753
Complement factor H	180.32	20.30	139004.4	P08603	Protein Z-dependent protease inhibitor	20.18	5.90	50674.3	Q9UK55	Complement component C9	40.27	12.00	63132.8	P02748	Coagulation factor IX	20.22	5.00	51745.0	P00740
Complement C4-A	670.36	46.20	192649.5	P0C0L4	Secreted phosphoprotein 24	20.20	10.40	24321.8	Q13103	Galectin-3-binding protein	40.20	8.50	65289.4	Q08380	Coagulation factor X	20.17	5.10	54696.6	P00742
Ig lambda-2 chain C regions	20.21	27.40	11286.6	P0CG05	Lysozyme C	20.22	12.80	16526.3	P61626	Haptoglobin-related protein	20.27	8.30	39004.7	P00739	Hemoglobin subunit beta	30.21	21.10	15988.3	P68871
Platelet factor 4 variant	20.21	23.10	11545.3	P10720	EGF-containing fibulin-like extracellular matı	20.22	6.50	54604.3	Q12805	Hemoglobin subunit beta	40.24	36.10	15988.3	P68871	Secreted phosphoprotein 24	20.20	10.40	24321.8	Q13103
Clusterin	50.27	16.50	52461.1	P10909	Kininogen-1	40.16	6.10	71912.1	P01042	Ig gamma-2 chain C region	20.17	8.00	35877.8	P01859	Complement C1q subcomponent subunit C	30.20	15.90	25757.1	P02747
Keratin, type I cytoskeletal 10	70.29	17.60	58791.6	P13645	Alpha-2-macroglobulin	30.19	2.60	163187.4	P01023	Protein AMBP	50.21	17.90	38974.0	P02760	Alpha-2-macroglobulin	70.26	7.90	163187.4	P01023
Lipopolysaccharide-binding protein	30.25	8.70	53350.0	P18428	Ig gamma-2 chain C region	20.23	8.00	35877.8	P01859	Serotransferrin	120.25	21.20	77013.7	P02787	EGF-containing fibulin-like extracellular matı	40.21	11.00	54604.3	Q12805

Inter-alpha-trypsin inhibitor heavy chain H2	300.38	32.50	106396.8	P19823	Beta-2-glycoprotein 1	20.16	7.00	38272.7	P02749	Serum amyloid A-4 protein	40.19	29.20	14737.3	P35542	Mannan-binding lectin serine protease 2	40.21	7.30	75653.7	O00187
Inter-alpha-trypsin inhibitor heavy chain H1	268.37	35.60	101325.8	P19827	Ceruloplasmin	60.33	8.80	122127.6	P00450	Thrombospondin-1	60.28	6.80	129299.2	P07996	Complement C1s subcomponent	30.27	8.40	76634.9	P09871
Glutathione peroxidase 3	20.25	11.50	35386.0	P22352	Complement C1q subcomponent subunit A	20.17	13.10	26000.2	P02745						Complement component C8 beta chain	20.30	7.80	67003.5	P07358
Keratin, type I cytoskeletal 9	40.32	13.00	62026.7	P35527	Complement component C9	50.32	15.90	63132.8	P02748						Haptoglobin-related protein	30.25	10.90	39004.7	P00739
Keratin, type II cytoskeletal 2 epidermal	50.22	9.70	65393.2	P35908	Fibulin-1	30.28	7.10	77162.4	P23142						Thrombospondin-1	40.20	4.90	129299.2	P07996
Pigment epithelium-derived factor	30.21	9.80	46283.4	P36955	Haptoglobin-related protein	20.24	7.50	39004.7	P00739						Vitamin D-binding protein	20.25	4.60	52929.1	P02774
Lysozyme C	30.25	28.40	16526.3	P61626	Hemoglobin subunit beta	40.29	31.30	15988.3	P68871						Vitamin K-dependent protein S	30.25	4.70	75074.1	P07225
Hemoglobin subunit beta	20.26	19.70	15988.3	P68871	Lipopolysaccharide-binding protein	30.28	8.50	53350.0	P18428						Complement component C6	20.22	2.40	104717.9	P13671
Complement factor H-related protein 1	40.28	18.20	37626.0	Q03591	Retinol-binding protein 4	50.27	35.80	22995.3	P02753						Complement component C9	80.29	21.50	63132.8	P02748
Hepatocyte growth factor activator	20.24	4.60	70636.2	Q04756	Thrombospondin-1	20.19	2.60	129299.2	P07996						Ig gamma-2 chain C region	30.19	13.20	35877.8	P01859
Inter-alpha-trypsin inhibitor heavy chain H3	90.27	14.30	99786.6	Q06033	Vitamin D-binding protein	30.16	6.80	52929.1	P02774						Lipopolysaccharide-binding protein	30.29	8.50	53350.0	P18428
Hyaluronan-binding protein 2	20.17	3.60	62630.5	Q14520	Vitamin K-dependent protein S	40.21	7.20	75074.1	P07225						Serum amyloid A-4 protein	30.20	21.50	14737.3	P35542
Inter-alpha-trypsin inhibitor heavy chain H4	90.34	17.10	103293.2	Q14624															
Procollagen C-endopeptidase enhancer 1	20.27	6.70	47942.0	Q15113															
Protein Z-dependent protease inhibitor	20.25	6.10	50674.3	Q9UK55															

Table 2. Fractionated control sera which were separated by 1-D electrophoresis were sliced up into thin gel sections and digested prior to analysis by LC-MS. The results of this qualitative analysis are shown in the table above. Identifications which were unique to an elution are written in red.

Appendix B

017

Elution 1

Description	Score	Coverage (%)	MW (Da)	Accession No.	No. Peptides
Complement C3	1086.39	68.70	187029.3	P01024	110
Complement C4-A	540.36	40.10	192649.5	P0C0L4	54
Inter-alpha-trypsin inhibitor heavy chain H2	290.38	34.90	106396.8	P19823	29
Inter-alpha-trypsin inhibitor heavy chain H3	130.40	20.30	99786.6	Q06033	13
Fibronectin	278.35	21.80	262457.6	P02751	28
Inter-alpha-trypsin inhibitor heavy chain H1	268.37	37.70	101325.8	P19827	27
Haptoglobin	70.30	22.20	45176.6	P00738	7
Complement C1q subcomponent subunit C	60.35	34.70	25757.1	P02747	6
Ig kappa chain C region	40.28	64.20	11601.7	P01834	4
Lumican	50.29	19.80	38404.8	P51884	5
Ceruloplasmin	140.34	22.70	122127.6	P00450	14
Complement factor H-related protein 1	60.27	28.20	37626.0	Q03591	6
Prothrombin	170.30	36.20	69992.2	P00734	17
Ig kappa chain V-III region SIE	30.28	39.40	11767.9	P01620	3
Transthyretin	90.33	65.30	15877.1	P02766	9
Complement factor H	210.34	23.50	139004.4	P08603	21
Complement component C9	90.32	25.90	63132.8	P02748	9
Kininogen-1	70.22	13.50	71912.1	P01042	7
Inter-alpha-trypsin inhibitor heavy chain H4	80.34	13.80	103293.2	Q14624	8
Ig gamma-1 chain C region	60.35	29.70	36083.2	P01857	6
Immunoglobulin lambda-like polypeptide 5	40.28	27.10	23048.6	B9A064	4
Gelsolin	70.31	13.30	85644.3	P06396	7
Ig mu chain C region	110.27	33.80	49275.6	P01871	11
Alpha-2-HS-glycoprotein	30.32	12.00	39299.7	P02765	3
Complement C1q subcomponent subunit A	40.30	24.10	26000.2	P02745	4
Alpha-1-antitrypsin	50.28	16.70	46707.1	P01009	5
Keratin, type II cytoskeletal 1	80.27	14.40	65998.9	P04264	8
Serum albumin	270.33	54.20	69321.6	P02768	27
Complement C1r subcomponent	70.22	10.80	80066.8	P00736	7
Retinol-binding protein 4	70.26	61.70	22995.3	P02753	7
Complement C1q subcomponent subunit B	50.24	26.50	26704.5	P02746	5
Ig gamma-3 chain C region	40.22	19.90	41260.4	P01860	4
Protein AMBP	50.33	16.50	38974.0	P02760	5
Lipopolysaccharide-binding protein	20.30	7.70	53350.0	P18428	2
Complement component C8 gamma chain	60.31	48.00	22263.6	P07360	6
Heparin cofactor 2	60.26	13.40	57034.3	P05546	6
Serotransferrin	30.22	5.00	77013.7	P02787	3
Apolipoprotein A-I	80.34	22.80	30758.9	P02647	8
Apolipoprotein A-IV	20.21	6.80	45371.5	P06727	2
Ig alpha-1 chain C region	50.30	25.50	37630.7	P01876	5
Haptoglobin-related protein	66.26	15.20	39004.7	P00739	7
Vitronectin	30.22	7.50	54271.2	P04004	3
C4b-binding protein alpha chain	40.36	10.20	66989.4	P04003	4
Complement C5	40.26	5.10	188185.3	P01031	4
Ig gamma-2 chain C region	20.18	8.90	35877.8	P01859	2
Antithrombin-III	28.24	10.10	52569.0	P01008	3
Keratin, type II cytoskeletal 2 epidermal	30.20	4.50	65393.2	P35908	3
Complement factor H-related protein 2	20.18	8.50	30630.6	P36980	2
Keratin, type I cytoskeletal 10	20.20	3.80	58791.6	P13645	2
Histidine-rich glycoprotein	20.17	3.60	59540.9	P04196	2
Ig heavy chain V-III region GAL	20.18	9.50	12722.2	P01781	2
Lactotransferrin	30.23	4.60	78132.0	P02788	3
Keratin, type II cytoskeletal 3	30.25	3.50	64377.6	P12035	3
Plasma protease C1 inhibitor	40.17	10.00	55119.5	P05155	4
Ig heavy chain V-III region CAM	16.13	18.00	13659.2	P01768	2
Keratin, type II cytoskeletal 4	40.22	7.50	57249.9	P19013	4
Plasma kallikrein	20.19	3.60	71322.8	P03952	2
Coagulation factor X	20.22	5.10	54696.6	P00742	2
Apolipoprotein B-100	20.16	0.40	515283.6	P04114	2
Serum amyloid P-component	30.23	14.80	25371.1	P02743	3
Salivary acidic proline-rich phosphoprotein 1/2	20.17	19.30	17006.3	P02810	2
Keratin, type I cytoskeletal 9	20.26	7.20	62026.7	P35527	2

Elution 2

Description	Score	Coverage (%)	MW (Da)	Accession No.	No. Peptides
Fibronectin	550.40	37.80	262457.6	P02751	55
Complement C4-A	518.32	36.00	192649.5	P0C0L4	52
Serum albumin	470.37	70.30	69321.6	P02768	47
Ceruloplasmin	60.36	8.60	122127.6	P00450	6
Ig gamma-1 chain C region	120.37	54.50	36083.2	P01857	12
Keratin, type I cytoskeletal 10	70.28	21.10	58791.6	P13645	7
Alpha-2-macroglobulin	220.29	23.30	163187.4	P01023	22
Ig kappa chain C region	50.24	80.20	11601.7	P01834	5
Transthyretin	40.32	55.10	15877.1	P02766	4
Complement factor H	370.34	39.20	139004.4	P08603	37
Vitamin D-binding protein	20.31	9.30	52929.1	P02774	2
Complement component C9	20.28	7.00	63132.8	P02748	2
Plasminogen	190.31	30.50	90510.2	P00747	19
Inter-alpha-trypsin inhibitor heavy chain H1	110.35	16.80	101325.8	P19827	11
Apolipoprotein B-100	170.33	6.10	515283.6	P04114	17
C4b-binding protein alpha chain	200.31	47.10	66989.4	P04003	20
Ig gamma-3 chain C region	40.29	22.00	41260.4	P01860	4
Apolipoprotein A-I	170.35	53.90	30758.9	P02647	17
Complement C3	608.35	44.90	187029.3	P01024	61
Ig mu chain C region	120.27	33.40	49275.6	P01871	12
Alpha-2-HS-glycoprotein	30.22	17.20	39299.7	P02765	3
Keratin, type II cytoskeletal 6A	30.28	6.90	60008.3	P02538	3
Keratin, type II cytoskeletal 1	60.22	12.60	65998.9	P04264	6
Immunoglobulin lambda-like polypeptide 5	50.28	36.00	23048.6	B9A064	5
Alpha-1-antitrypsin	170.30	56.70	46707.1	P01009	17
Ig lambda-2 chain C regions	20.20	27.40	11286.6	P0CG05	2
Complement C1q subcomponent subunit C	20.28	12.20	25757.1	P02747	2
Fibulin-1	20.28	3.80	77162.4	P23142	2
Gelsolin	30.29	6.50	85644.3	P06396	3
Hemoglobin subunit alpha	30.26	30.30	15247.9	P69905	3
Serotransferrin	280.32	41.70	77013.7	P02787	28
Complement factor H-related protein 1	20.25	11.20	37626.0	Q03591	2
Vitronectin	30.24	8.80	54271.2	P04004	3
Antithrombin-III	90.26	29.30	52569.0	P01008	9
Apolipoprotein D	30.20	18.00	21261.8	P05090	3
Prothrombin	100.25	23.30	69992.2	P00734	10
Serum paraoxonase/arylesterase 1	20.23	7.60	39706.3	P27169	2
Ig gamma-2 chain C region	50.26	26.40	35877.8	P01859	5
CD5 antigen-like	20.21	9.80	38063.0	O43866	2
Complement C1q subcomponent subunit A	20.18	13.10	26000.2	P02745	2
Alpha-1-antichymotrypsin	58.25	17.50	47620.6	P01011	6
Apolipoprotein A-IV	150.23	38.60	45371.5	P06727	15
Histidine-rich glycoprotein	50.28	13.00	59540.9	P04196	5
Complement C1r subcomponent	30.20	4.70	80066.8	P00736	3
Inter-alpha-trypsin inhibitor heavy chain H2	170.29	22.90	106396.8	P19823	17
Alpha-1-acid glycoprotein 1	40.24	22.90	23496.8	P02763	4
Apolipoprotein A-II	40.24	54.00	11167.9	P02652	4
Haptoglobin-related protein	48.23	13.20	39004.7	P00739	5
Ig kappa chain V-III region SIE	30.23	39.40	11767.9	P01620	3
Complement C1q subcomponent subunit B	30.25	17.00	26704.5	P02746	3
Ig kappa chain V-II region Cum	20.23	13.90	12668.3	P01614	2
Haptoglobin	60.24	16.70	45176.6	P00738	6
Complement C5	30.17	2.10	188185.3	P01031	3
Complement component C7	20.21	3.70	93457.3	P10643	2
Apolipoprotein C-III	20.19	27.30	10845.5	P02656	2
C4b-binding protein beta chain	20.23	11.50	28338.5	P20851	2
Protein AMBP	30.21	10.80	38974.0	P02760	3
Clusterin	70.24	18.50	52461.1	P10909	7
Ig alpha-1 chain C region	70.25	28.90	37630.7	P01876	7
Hemoglobin subunit beta	20.21	15.60	15988.3	P68871	2
Inter-alpha-trypsin inhibitor heavy chain H4	60.23	9.40	103293.2	Q14624	6
Keratin, type II cytoskeletal 2 epidermal	26.21	3.30	65393.2	P35908	3
Adiponectin	20.21	14.30	26397.0	Q15848	2
Complement factor B	40.20	7.20	85478.6	P00751	4
Keratin, type I cytoskeletal 9	30.26	10.00	62026.7	P35527	3
Ig kappa chain V-IV region (Fragment)	20.19	17.40	13371.6	P06312	2
Keratin, type II cytoskeletal 4	50.18	10.50	57249.9	P19013	5
Keratin, type I cytoskeletal 13	50.23	11.10	49557.4	P13646	5
Serum amyloid A-4 protein	30.19	21.50	14737.3	P35542	3
Retinol-binding protein 4	20.17	10.40	22995.3	P02753	2

Table 1. Complete list of qualitative identifications from elution one and two of cutaneous melanoma sample 017.

036											
Elution 1						Elution 2					
Description	Score	Coverage (%)	MW (Da)	Accession No.	No. Peptides	Description	Score	Coverage (%)	MW (Da)	Accession No.	No. Peptides
Serum albumin	280.38	51.20	69321.6	P02768	28	Keratin, type I cytoskeletal 9	140.53	43.20	62026.7	P35527	14
Complement C1q subcomponent subunit C	50.33	29.40	25757.1	P02747	5	Fibronectin	550.39	35.80	262457.6	P02751	55
Complement C3	1006.35	65.50	187029.3	P01024	101	Keratin, type I cytoskeletal 10	190.33	40.20	58791.6	P13645	19
Complement C4-A	710.36	49.20	192649.5	P0C0L4	71	Ig kappa chain C region	50.31	80.20	11601.7	P01834	5
Fibronectin	370.45	23.40	262457.6	P02751	37	Complement C4-A	520.32	38.80	192649.5	P0C0L4	52
Prothrombin	120.35	25.10	69992.2	P00734	12	C4b-binding protein alpha chain	210.49	48.10	66989.4	P04003	21
Inter-alpha-trypsin inhibitor heavy chain H4	100.30	19.60	103293.2	Q14624	10	Complement C3	470.34	39.00	187029.3	P01024	47
Complement C1q subcomponent subunit A	60.24	26.50	26000.2	P02745	6	Serum albumin	500.38	76.20	69321.6	P02768	50
Complement factor H	320.28	31.90	139004.4	P08603	32	Prothrombin	220.32	43.40	69992.2	P00734	22
Ig gamma-1 chain C region	80.28	39.70	36083.2	P01857	8	Keratin, type II cytoskeletal 1	200.40	41.10	65998.9	P04264	20
Inter-alpha-trypsin inhibitor heavy chain H1	210.34	26.10	101325.8	P19827	21	Plasminogen	120.30	18.80	90510.2	P00747	12
Retinol-binding protein 4	50.24	29.90	22995.3	P02753	5	Ig gamma-1 chain C region	90.35	45.50	36083.2	P01857	9
Inter-alpha-trypsin inhibitor heavy chain H2	260.33	36.70	106396.8	P19823	26	Inter-alpha-trypsin inhibitor heavy chain H4	70.30	13.30	103293.2	Q14624	7
Vitamin D-binding protein	30.26	10.80	52929.1	P02774	3	Antithrombin-III	200.30	43.80	52569.0	P01008	20
Immunoglobulin lambda-like polypeptide 5	40.27	32.20	23048.6	B9A064	4	Hemopexin	80.33	26.80	51643.3	P02790	8
Complement C5	120.29	12.20	188185.3	P01031	12	Apolipoprotein A-I	170.42	58.80	30758.9	P02647	17
Complement component C9	80.24	22.00	63132.8	P02748	8	Ig alpha-1 chain C region	70.27	28.90	37630.7	P01876	7
C-reactive protein	70.27	31.70	25022.7	P02741	7	Alpha-1B-glycoprotein	30.33	12.30	54219.7	P04217	3
Gelsolin	30.29	7.30	85644.3	P06396	3	Alpha-2-HS-glycoprotein	20.20	10.60	39299.7	P02765	2
Heparin cofactor 2	30.20	7.40	57034.3	P05546	3	Complement C5	30.24	3.60	188185.3	P01031	3
Complement C1r subcomponent	130.28	29.50	80066.8	P00736	13	Ig mu chain C region	110.26	33.80	49275.6	P01871	11
Transthyretin	90.30	69.40	15877.1	P02766	9	Immunoglobulin lambda-like polypeptide 5	40.28	32.20	23048.6	B9A064	4
Complement C1s subcomponent	70.25	14.80	76634.9	P09871	7	Fibulin-1	20.26	4.70	77162.4	P23142	2
Serum amyloid P-component	60.23	31.80	25371.1	P02743	6	Serum paraoxonase/arylesterase 1	48.27	20.60	39706.3	P27169	5
Lumican	30.31	12.70	38404.8	P51884	3	Serotransferrin	290.31	48.70	77013.7	P02787	29
Lactotransferrin	140.31	26.90	78132.0	P02788	14	Apolipoprotein A-IV	110.30	30.30	45371.5	P06727	11
Ig kappa chain C region	40.27	61.30	11601.7	P01834	4	Inter-alpha-trypsin inhibitor heavy chain H2	70.35	11.50	106396.8	P19823	7
Ig gamma-3 chain C region	40.28	22.00	41260.4	P01860	4	Vitamin D-binding protein	40.27	13.10	52929.1	P02774	4
Complement C1q subcomponent subunit B	50.26	22.50	26704.5	P02746	5	Keratin, type II cytoskeletal 2 epidermal	178.26	31.10	65393.2	P35908	18
Coagulation factor X	90.28	24.60	54696.6	P00742	9	Complement C1q subcomponent subunit C	30.28	15.10	25757.1	P02747	3
Ig lambda-2 chain C regions	30.23	52.80	11286.6	P0CG05	3	Thrombospondin-1	30.25	4.30	129299.2	P07996	3
Antithrombin-III	64.22	18.80	52569.0	P01008	7	Complement factor H-related protein 1	60.23	28.20	37626.0	Q03591	6
Pigment epithelium-derived factor	20.29	11.70	46283.4	P36955	2	Alpha-1-antitrypsin	100.29	32.80	46707.1	P01009	10
SPARC	20.27	11.60	34609.7	P09486	2	Ceruloplasmin	40.30	6.80	122127.6	P00450	4
Complement factor H-related protein 1	60.32	24.50	37626.0	Q03591	6	Inter-alpha-trypsin inhibitor heavy chain H1	40.23	5.60	101325.8	P19827	4
Protein AMBP	50.30	18.80	38974.0	P02760	5	Ig kappa chain V-III region SIE	30.29	39.40	11767.9	P01620	3
Apolipoprotein A-I	100.37	40.80	30758.9	P02647	10	Alpha-2-macroglobulin	240.27	23.20	163187.4	P01023	24
Plasma protease C1 inhibitor	30.24	8.60	55119.5	P05155	3	Galectin-3-binding protein	30.22	7.20	65289.4	Q08380	3
Ig kappa chain V-III region SIE	20.23	24.80	11767.9	P01620	2	Complement factor H	268.31	27.80	139004.4	P08603	27
Ceruloplasmin	90.30	12.50	122127.6	P00450	9	Apolipoprotein A-II	30.26	54.00	11167.9	P02652	3
Lysozyme C	20.30	24.30	16526.3	P61626	2	Transthyretin	50.22	49.00	15877.1	P02766	5
Lipopolysaccharide-binding protein	80.30	21.20	53350.0	P18428	8	Ig gamma-3 chain C region	40.29	22.00	41260.4	P01860	4
Ig mu chain C region	70.22	19.20	49275.6	P01871	7	Beta-2-glycoprotein 1	30.26	13.00	38272.7	P02749	3
Inter-alpha-trypsin inhibitor heavy chain H3	140.27	23.40	99786.6	Q06033	14	Ig lambda-2 chain C regions	20.22	27.40	11286.6	P0CG05	2
Alpha-1-antitrypsin	20.22	7.20	46707.1	P01009	2	Keratin, type I cytoskeletal 14	40.21	11.90	51529.4	P02533	4
Thrombospondin-1	80.29	9.10	129299.2	P07996	8	Alpha-1-acid glycoprotein 1	40.27	23.40	23496.8	P02763	4
Ig alpha-1 chain C region	50.27	22.70	37630.7	P01876	5	Vitronectin	60.25	16.10	54271.2	P04004	6
C4b-binding protein alpha chain	70.26	16.40	66989.4	P04003	7	Plasma protease C1 inhibitor	30.24	10.00	55119.5	P05155	3
Keratin, type I cytoskeletal 9	30.26	8.30	62026.7	P35527	3	Clusterin	70.28	20.30	52461.1	P10909	7
Platelet factor 4 variant	20.25	23.10	11545.3	P10720	2	Serum amyloid P-component	30.19	16.10	25371.1	P02743	3
Keratin, type II cytoskeletal 1	80.19	14.40	65998.9	P04264	8	Complement component C9	50.23	13.40	63132.8	P02748	5
Proteoglycan 4	40.23	4.00	150983.2	Q92954	4	Apolipoprotein B-100	190.29	6.40	515283.6	P04114	19
Vitronectin	40.21	10.90	54271.2	P04004	4	Alpha-1-antichymotrypsin	48.29	12.50	47620.6	P01011	5
Properdin	20.31	7.90	51242.0	P27918	2	Haptoglobin	78.25	26.60	45176.6	P00738	8
Plasminogen	30.21	5.30	90510.2	P00747	3	Ig gamma-2 chain C region	50.27	25.80	35877.8	P01859	5
Beta-2-glycoprotein 1	30.22	14.20	38272.7	P02749	3	Apolipoprotein E	70.22	25.90	36131.8	P02649	7
Complement component C8 beta chain	30.31	9.30	67003.5	P07358	3	Lipopolysaccharide-binding protein	20.28	6.20	53350.0	P18428	2
Sulfhydryl oxidase 1	20.23	5.10	82525.7	O00391	2	Retinol-binding protein 4	30.21	21.40	22995.3	P02753	3
Kininogen-1	50.20	10.40	71912.1	P01042	5	Apolipoprotein D	50.20	30.70	21261.8	P05090	5
Platelet factor 4	20.20	11.90	10837.9	P02776	2	Ig lambda chain V-III region LOI	20.25	21.60	11927.8	P80748	2
Haptoglobin-related protein	40.21	13.20	39004.7	P00739	4	CD5 antigen-like	20.18	7.20	38063.0	O43866	2
Alpha-1-acid glycoprotein 1	20.19	12.90	23496.8	P02763	2	C4b-binding protein beta chain	30.23	15.10	28338.5	P20851	3
Keratin, type II cytoskeletal 2 epidermal	30.21	5.00	65393.2	P35908	3	Platelet factor 4 variant	20.20	23.10	11545.3	P10720	2
Clusterin	30.22	5.30	52461.1	P10909	3	Haptoglobin-related protein	40.24	7.80	39004.7	P00739	4
Haptoglobin	28.19	5.70	45176.6	P00738	3	Hemoglobin subunit beta	50.20	42.20	15988.3	P68871	5
Ig gamma-2 chain C region	20.22	10.10	35877.8	P01859	2	Keratin, type II cytoskeletal 5	30.20	6.80	62340.0	P13647	3
						Azurocidin	20.21	9.60	26868.7	P20160	2
						Complement C1q subcomponent subunit A	20.16	11.80	26000.2	P02745	2
						Serum amyloid A-4 protein	30.19	21.50	14737.3	P35542	3
						Protein AMBP	30.23	11.90	38974.0	P02760	3
						Apolipoprotein C-I	30.19	28.90	9326.1	P02654	3
						Complement component C7	20.17	2.60	93457.3	P10643	2
						Vitamin K-dependent protein S	20.24	2.40	75074.1	P07225	2

Table 2. Complete list of qualitative identifications from elution one and two of cutaneous melanoma sample 036.

DS114											
Elution 1						Elution 2					
Description	Score	Coverage (%)	MW (Da)	Accession No.	No. Peptides	Description	Score	Coverage (%)	MW (Da)	Accession No.	No. Peptides
Complement C3	942.36	64.30	187029.3	P01024	95	Ig kappa chain C region	40.32	65.10	11601.7	P01834	4
Complement C4-A	670.36	46.20	192649.5	P0C0L4	67	Complement C4-A	410.32	29.90	192649.5	P0C0L4	41
Ceruloplasmin	120.34	19.10	122127.6	P00450	12	Keratin, type I cytoskeletal 10	140.30	32.20	58791.6	P13645	14
Inter-alpha-trypsin inhibitor heavy chain H2	300.38	32.50	106396.8	P19823	30	Serum albumin	300.35	57.60	69321.6	P02768	30
Complement C1q subcomponent subunit C	40.30	25.30	25757.1	P02747	4	Fibronectin	560.36	36.40	262457.6	P02751	56
C4b-binding protein alpha chain	90.43	23.80	66989.4	P04003	9	Complement C3	470.36	36.90	187029.3	P01024	47
Prothrombin	190.30	42.30	69992.2	P00734	19	Apolipoprotein A-I	170.34	55.80	30758.9	P02647	17
Keratin, type I cytoskeletal 10	70.29	17.60	58791.6	P13645	7	Prothrombin	218.33	49.80	69992.2	P00734	22
Inter-alpha-trypsin inhibitor heavy chain H4	90.34	17.10	103293.2	Q14624	9	Ig gamma-1 chain C region	90.30	45.50	36083.2	P01857	9
Keratin, type I cytoskeletal 9	40.32	13.00	62026.7	P35527	4	Plasminogen	120.38	22.30	90510.2	P00747	12
Ig mu chain C region	110.34	30.50	49275.6	P01871	11	Inter-alpha-trypsin inhibitor heavy chain H2	120.30	20.00	106396.8	P19823	12
Gelsolin	120.33	22.60	85644.3	P06396	12	Ig gamma-3 chain C region	40.28	17.20	41260.4	P01860	4
Fibronectin	358.33	24.10	262457.6	P02751	36	Immunoglobulin lambda-like polypeptide 5	40.29	32.20	23048.6	B9A064	4
Transthyretin	50.34	56.50	15877.1	P02766	5	Antithrombin-III	140.30	41.60	52569.0	P01008	14
Complement factor H	180.32	20.30	139004.4	P08603	18	Transthyretin	50.30	59.90	15877.1	P02766	5
Complement C1q subcomponent subunit B	80.27	38.70	26704.5	P02746	8	Inter-alpha-trypsin inhibitor heavy chain H1	120.34	16.20	101325.8	P19827	12
Ig kappa chain C region	40.33	64.20	11601.7	P01834	4	Clusterin	90.32	22.30	52461.1	P10909	9
Ig gamma-3 chain C region	30.29	16.40	41260.4	P01860	3	Keratin, type II cytoskeletal 1	140.27	28.10	65998.9	P04264	14
Complement C1q subcomponent subunit A	30.32	22.90	26000.2	P02745	3	Inter-alpha-trypsin inhibitor heavy chain H4	88.32	13.70	103293.2	Q14624	9
Inter-alpha-trypsin inhibitor heavy chain H3	90.27	14.30	99786.6	Q06033	9	C4b-binding protein alpha chain	200.40	43.20	66989.4	P04003	20
Inter-alpha-trypsin inhibitor heavy chain H1	268.37	35.60	101325.8	P19827	27	Complement factor H-related protein 1	50.29	24.20	37626.0	Q03591	5
Immunoglobulin lambda-like polypeptide 5	50.29	36.00	23048.6	B9A064	5	Complement factor H	190.30	21.20	139004.4	P08603	19
Kininogen-1	60.21	13.20	71912.1	P01042	6	Adiponectin	40.25	31.60	26397.0	Q15848	4
Serum albumin	290.27	57.80	69321.6	P02768	29	Ig lambda-2 chain C regions	20.20	27.40	11286.6	P0CG05	2
Ig gamma-1 chain C region	100.31	45.50	36083.2	P01857	10	Ig alpha-1 chain C region	80.27	34.00	37630.7	P01876	8
Retinol-binding protein 4	70.25	40.30	22995.3	P02753	7	Ig mu chain C region	100.30	28.50	49275.6	P01871	10
Apolipoprotein B-100	210.33	6.50	515283.6	P04114	21	Apolipoprotein A-IV	170.28	43.20	45371.5	P06727	17
Complement factor H-related protein 1	40.28	18.20	37626.0	Q03591	4	Serum paraoxonase/arylesterase 1	40.27	14.60	39706.3	P27169	4
Ig lambda-2 chain C regions	20.21	27.40	11286.6	P0CG05	2	Apolipoprotein C-III	20.23	27.30	10845.5	P02656	2
Ig kappa chain V-III region SIE	30.26	39.40	11767.9	P01620	3	Keratin, type I cytoskeletal 9	50.34	14.60	62026.7	P35527	5
Proteoglycan 4	50.22	5.10	150983.2	Q92954	5	Vitronectin	80.25	20.10	54271.2	P04004	8
Apolipoprotein A-I	120.30	49.10	30758.9	P02647	12	Alpha-2-HS-glycoprotein	30.25	14.40	39299.7	P02765	3
Antithrombin-III	90.26	21.10	52569.0	P01008	9	Apolipoprotein B-100	100.27	2.80	515283.6	P04114	10
Protein AMBP	50.34	16.50	38974.0	P02760	5	Alpha-1-antitrypsin	40.22	12.40	46707.1	P01009	4
Beta-2-glycoprotein 1	20.21	7.00	38272.7	P02749	2	Histidine-rich glycoprotein	30.19	6.90	59540.9	P04196	3
Vitronectin	60.26	16.10	54271.2	P04004	6	Apolipoprotein D	40.22	25.90	21261.8	P05090	4
Ig alpha-1 chain C region	60.26	29.70	37630.7	P01876	6	Apolipoprotein E	90.26	30.90	36131.8	P02649	9
Alpha-2-HS-glycoprotein	30.27	16.10	39299.7	P02765	3	Complement C1q subcomponent subunit B	30.28	15.00	26704.5	P02746	3
Lumican	40.28	13.60	38404.8	P51884	4	Complement C1q subcomponent subunit C	50.25	29.40	25757.1	P02747	5
Coagulation factor X	100.32	23.00	54696.6	P00742	10	Ficolin-3	40.24	14.00	32882.0	O75636	4
Glutathione peroxidase 3	20.25	11.50	35386.0	P22352	2	C4b-binding protein beta chain	30.22	21.00	28338.5	P20851	3
Platelet factor 4 variant	20.21	23.10	11545.3	P10720	2	Apolipoprotein A-II	50.26	62.00	11167.9	P02652	5
Heparin cofactor 2	30.24	9.60	57034.3	P05546	3	Keratin, type II cytoskeletal 2 epidermal	60.24	8.80	65393.2	P35908	6
Complement C1r subcomponent	60.25	12.80	80066.8	P00736	6	Platelet factor 4 variant	20.21	23.10	11545.3	P10720	2
Lysozyme C	30.25	28.40	16526.3	P61626	3	Galectin-3-binding protein	20.18	4.40	65289.4	Q08380	2
Procollagen C-endopeptidase enhancer 1	20.27	6.70	47942.0	Q15113	2	Serotransferrin	20.21	3.90	77013.7	P02787	2
Keratin, type II cytoskeletal 1	110.24	18.50	65998.9	P04264	11	Serum amyloid A-4 protein	30.18	13.10	14737.3	P35542	3
Plasma protease C1 inhibitor	40.22	13.80	55119.5	P05155	4	Apolipoprotein C-I	20.19	26.50	9326.1	P02654	2
Serotransferrin	50.25	10.50	77013.7	P02787	5	Protein AMBP	30.20	8.80	38974.0	P02760	3
Haptoglobin-related protein	30.13	9.80	39004.7	P00739	3	Protein crumbs homolog 1	10.15	1.40	154080.4	P82279	2
Clusterin	50.27	16.50	52461.1	P10909	5						
Hepatocyte growth factor activator	20.24	4.60	70636.2	Q04756	2						
Thrombospondin-1	50.19	5.40	129299.2	P07996	5						
Complement component C8 gamma chain	50.17	31.20	22263.6	P07360	5						
Ig gamma-2 chain C region	20.19	8.00	35877.8	P01859	2						
Apolipoprotein A-II	20.20	29.00	11167.9	P02652	2						
Apolipoprotein A-IV	70.19	19.20	45371.5	P06727	7						
Keratin, type II cytoskeletal 2 epidermal	50.22	9.70	65393.2	P35908	5						
Alpha-1-antitrypsin	20.24	4.10	46707.1	P01009	2						
Haptoglobin	20.18	4.90	45176.6	P00738	2						
Ig kappa chain V-IV region (Fragment)	20.16	17.40	13371.6	P06312	2						

Table 3. Complete list of qualitative identifications from elution one and two of cutaneous melanoma sample DS114.

DS118

Elution 1

Description	Score	Coverage (%)	MW (Da)	Accession No.	No. Peptides
Complement C3	786.37	52.60	187029.3	P01024	79
Ig kappa chain C region	60.30	86.80	11601.7	P01834	6
Fibronectin	398.43	26.10	262457.6	P02751	40
Inter-alpha-trypsin inhibitor heavy chain H2	300.38	36.00	106396.8	P19823	30
Complement factor H	438.38	45.70	139004.4	P08603	44
Complement C4-A	646.36	44.80	192649.5	P0C0L4	65
Ceruloplasmin	148.38	21.50	122127.6	P00450	15
Inter-alpha-trypsin inhibitor heavy chain H4	90.32	15.20	103293.2	Q14624	9
Complement C1q subcomponent subunit C	50.28	25.30	25757.1	P02747	5
Inter-alpha-trypsin inhibitor heavy chain H1	348.37	44.30	101325.8	P19827	35
Keratin, type II cytoskeletal 1	100.27	21.90	65998.9	P04264	10
Serum albumin	330.33	62.10	69321.6	P02768	33
Apolipoprotein B-100	250.31	7.90	515283.6	P04114	25
Ig gamma-1 chain C region	100.38	50.30	36083.2	P01857	10
Ig alpha-1 chain C region	80.25	30.90	37630.7	P01876	8
Gelsolin	110.30	20.80	85644.3	P06396	11
Transthyretin	110.33	69.40	15877.1	P02766	11
Ig gamma-3 chain C region	50.32	25.20	41260.4	P01860	5
Lumican	40.28	18.60	38404.8	P51884	4
Prothrombin	170.32	39.90	69992.2	P00734	17
Immunoglobulin lambda-like polypeptide 5	60.28	40.70	23048.6	B9A064	6
Complement C1q subcomponent subunit A	70.25	27.30	26000.2	P02745	7
Complement C1s subcomponent	38.25	7.40	76634.9	P09871	4
Complement C1r subcomponent	100.24	22.80	80066.8	P00736	10
SPARC	30.22	13.20	34609.7	P09486	3
Complement factor H-related protein 1	40.27	18.20	37626.0	Q03591	4
Retinol-binding protein 4	80.34	60.20	22995.3	P02753	8
Protein AMBP	70.33	31.00	38974.0	P02760	7
Ig lambda-2 chain C regions	20.21	27.40	11286.6	P0CG05	2
Complement C1q subcomponent subunit B	40.26	25.70	26704.5	P02746	4
Plasma protease C1 inhibitor	40.26	12.40	55119.5	P05155	4
Lysozyme C	50.27	45.30	16526.3	P61626	5
Ig mu chain C region	90.25	25.70	49275.6	P01871	9
Procollagen C-endopeptidase enhancer 1	40.22	14.00	47942.0	Q15113	4
Mannan-binding lectin serine protease 2	30.29	6.30	75653.7	O00187	3
Keratin, type I cytoskeletal 10	50.24	11.50	58791.6	P13645	5
Vitronectin	80.24	18.20	54271.2	P04004	8
Serum amyloid P-component	60.21	24.20	25371.1	P02743	6
Beta-2-glycoprotein 1	30.19	11.00	38272.7	P02749	3
Apolipoprotein A-I	100.33	38.60	30758.9	P02647	10
Alpha-1-antitrypsin	20.27	7.90	46707.1	P01009	2
Proteoglycan 4	60.23	5.00	150983.2	Q92954	6
Complement C5	40.29	4.50	188185.3	P01031	4
Coagulation factor X	90.24	23.60	54696.6	P00742	9
Lipopolysaccharide-binding protein	30.25	8.70	53350.0	P18428	3
Inter-alpha-trypsin inhibitor heavy chain H3	140.30	16.00	99786.6	Q06033	14
Protein Z-dependent protease inhibitor	20.25	6.10	50674.3	Q9UK55	2
Hemoglobin subunit beta	20.26	19.70	15988.3	P68871	2
Clusterin	40.18	12.50	52461.1	P10909	4
Plasminogen	80.22	12.50	90510.2	P00747	8
Ig kappa chain V-III region SIE	30.25	39.40	11767.9	P01620	3
Coagulation factor IX	30.19	7.60	51745.0	P00740	3
Complement component C8 gamma chain	30.26	18.80	22263.6	P07360	3
Ig gamma-2 chain C region	40.23	13.20	35877.8	P01859	4
Coagulation factor V	30.25	2.40	251543.8	P12259	3
C4b-binding protein alpha chain	50.27	11.10	66989.4	P04003	5
Apolipoprotein A-IV	80.24	19.70	45371.5	P06727	8
Heparin cofactor 2	20.22	4.80	57034.3	P05546	2
Kininogen-1	50.20	6.40	71912.1	P01042	5
Angiogenin	40.18	32.70	16539.4	P03950	4
Alpha-1-acid glycoprotein 1	30.23	15.40	23496.8	P02763	3
Keratin, type I cytoskeletal 9	50.27	13.30	62026.7	P35527	5
Antithrombin-III	90.25	22.60	52569.0	P01008	9
Pigment epithelium-derived factor	30.21	9.80	46283.4	P36955	3
Complement component C9	90.26	23.80	63132.8	P02748	9
Vitamin K-dependent protein S	30.17	5.30	75074.1	P07225	3
Complement component C8 beta chain	20.25	7.80	67003.5	P07358	2
Platelet factor 4 variant	30.24	37.50	11545.3	P10720	3
Hyaluronan-binding protein 2	20.17	3.60	62630.5	Q14520	2
Apolipoprotein A-II	20.20	43.00	11167.9	P02652	2
Keratin, type II cytoskeletal 2 epidermal	40.23	5.60	65393.2	P35908	4
Immunoglobulin J chain	20.16	17.00	18087.0	P01591	2
Apolipoprotein C-I	20.16	24.10	9326.1	P02654	2
Apolipoprotein E	20.17	6.30	36131.8	P02649	2
Ficolin-3	20.18	6.70	32882.0	O75636	2
Serotransferrin	20.15	2.90	77013.7	P02787	2
Thrombospondin-1	60.22	6.40	129299.2	P07996	6

Elution 2

Description	Score	Coverage (%)	MW (Da)	Accession No.	No. Peptides
Fibronectin	530.41	33.90	262457.6	P02751	53
Complement component C9	50.32	15.90	63132.8	P02748	5
Prothrombin	250.34	43.40	69992.2	P00734	25
Serum albumin	390.36	67.00	69321.6	P02768	39
Keratin, type I cytoskeletal 10	80.28	21.20	58791.6	P13645	8
Plasminogen	140.34	25.80	90510.2	P00747	14
Complement factor H	350.37	37.90	139004.4	P08603	35
Complement C4-A	510.33	36.80	192649.5	P0C0L4	51
C4b-binding protein alpha chain	200.45	47.40	66989.4	P04003	20
Apolipoprotein B-100	310.37	9.80	515283.6	P04114	31
Transthyretin	60.32	68.00	15877.1	P02766	6
Ig kappa chain C region	50.28	80.20	11601.7	P01834	5
Antithrombin-III	220.30	47.20	52569.0	P01008	22
Ceruloplasmin	60.33	8.80	122127.6	P00450	6
Complement C3	390.34	30.90	187029.3	P01024	39
Keratin, type II cytoskeletal 1	140.28	26.20	65998.9	P04264	14
Ig alpha-1 chain C region	80.28	34.80	37630.7	P01876	8
Ig gamma-1 chain C region	90.35	45.50	36083.2	P01857	9
Ig lambda-2 chain C regions	20.19	27.40	11286.6	P0CG05	2
Retinol-binding protein 4	50.27	35.80	22995.3	P02753	5
Ig gamma-3 chain C region	40.30	22.00	41260.4	P01860	4
Clusterin	90.35	22.30	52461.1	P10909	9
Keratin, type I cytoskeletal 9	70.28	26.30	62026.7	P35527	7
Apolipoprotein A-IV	220.32	54.80	45371.5	P06727	22
Inter-alpha-trypsin inhibitor heavy chain H2	110.35	15.00	106396.8	P19823	11
Immunoglobulin lambda-like polypeptide 5	70.25	44.40	23048.6	B9A064	7
Apolipoprotein E	120.25	42.90	36131.8	P02649	12
Apolipoprotein A-I	170.32	61.80	30758.9	P02647	17
Apolipoprotein C-III	20.22	27.30	10845.5	P02656	2
Inter-alpha-trypsin inhibitor heavy chain H1	90.37	13.40	101325.8	P19827	9
Immunoglobulin J chain	30.21	23.30	18087.0	P01591	3
Ficolin-3	50.22	14.70	32882.0	O75636	5
Serum paraoxonase/arylesterase 1	30.22	12.70	39706.3	P27169	3
Alpha-2-HS-glycoprotein	40.33	12.00	39299.7	P02765	4
Complement factor H-related protein 1	40.28	18.20	37626.0	Q03591	4
Apolipoprotein D	40.17	19.60	21261.8	P05090	4
Plasma serine protease inhibitor	20.24	7.90	45645.8	P05154	2
Ig mu chain C region	120.26	36.70	49275.6	P01871	12
Vitronectin	80.28	22.60	54271.2	P04004	8
Protein AMBP	40.23	15.60	38974.0	P02760	4
Haptoglobin-related protein	20.24	7.50	39004.7	P00739	2
Galectin-3-binding protein	40.21	9.10	65289.4	Q08380	4
Alpha-1-antitrypsin	40.23	9.80	46707.1	P01009	4
Fibulin-1	30.28	7.10	77162.4	P23142	3
Inter-alpha-trypsin inhibitor heavy chain H4	70.28	10.10	103293.2	Q14624	7
Histidine-rich glycoprotein	20.22	5.70	59540.9	P04196	2
Ig kappa chain V-III region SIE	20.24	31.20	11767.9	P01620	2
Adiponectin	40.25	29.90	26397.0	Q15848	4
Procollagen C-endopeptidase enhancer 1	20.21	7.10	47942.0	Q15113	2
Complement component C8 gamma chain	20.24	13.90	22263.6	P07360	2
Apolipoprotein A-II	40.23	62.00	11167.9	P02652	4
Lipopolysaccharide-binding protein	30.28	8.50	53350.0	P18428	3
Beta-2-glycoprotein 1	20.16	7.00	38272.7	P02749	2
Protein Z-dependent protease inhibitor	20.18	5.90	50674.3	Q9UK55	2
Complement C1q subcomponent subunit B	30.24	17.00	26704.5	P02746	3
Keratin, type II cytoskeletal 2 epidermal	40.25	4.50	65393.2	P35908	4
Fibrinogen alpha chain	30.22	5.20	94914.3	P02671	3
Complement factor H-related protein 5	20.23	5.40	64377.1	Q98XR6	2
Hemoglobin subunit beta	40.29	31.30	15988.3	P68871	4
Ig gamma-2 chain C region	20.23	8.00	35877.8	P01859	2
Secreted phosphoprotein 24	20.20	10.40	24321.8	Q13103	2
Alpha-2-macroglobulin	30.19	2.60	163187.4	P01023	3
Vitamin K-dependent protein S	40.21	7.20	75074.1	P07225	4
Apolipoprotein C-IV	20.19	18.90	14543.5	P55056	2
Serum amyloid A-4 protein	20.18	13.10	14737.3	P35542	2
Platelet factor 4 variant	20.21	23.10	11545.3	P10720	2
Lysozyme C	20.22	12.80	16526.3	P61626	2
Platelet factor 4	20.23	11.90	10837.9	P02776	2
Vitamin D-binding protein	30.16	6.80	52929.1	P02774	3
EGF-containing fibulin-like extracellular matrix protein 1	20.22	6.50	54604.3	Q12805	2
Thrombospondin-1	20.19	2.60	129299.2	P07996	2
Extracellular matrix protein 1	30.20	9.40	60635.4	Q16610	3
Complement C1q subcomponent subunit A	20.17	13.10	26000.2	P02745	2
Complement C1q subcomponent subunit C	20.21	8.60	25757.1	P02747	2
Kininogen-1	40.16	6.10	71912.1	P01042	4
Apolipoprotein C-I	20.16	26.50	9326.1	P02654	2
Properdin	20.16	3.80	51242.0	P27918	2

Table 4. Complete list of qualitative identifications from elution one and two of cutaneous melanoma sample DS118.

Appendix C

Sample Type	Sex	Age	Stage of Malignancy	Identifier
Control Serum	M	30	-	DS179
Control Serum	F	47	-	DS27
Control Serum	F	55	-	DS38
Control Serum	F	62	-	DS43
Control Serum	F	47	-	DS156
Control Serum	F	33	-	DS22
Control Serum	M	37	-	DS58
Control Serum	M	40	-	DS46
Control Serum	F	52	-	DS34
Control Serum	M	36	-	DS57
Control Serum	M	32	-	DS171
Control Serum	M	48	-	DS56
Control Serum	F	54	-	DS44
Cutaneous Melanoma Serum	F	32	Benign	S1016505
Cutaneous Melanoma Serum	F	24	Benign	S1027507
Cutaneous Melanoma Serum	F	52	Benign	S1000545
Cutaneous Melanoma Serum	M	65	Benign	S1045409
Cutaneous Melanoma Serum	F	39	Benign	S1028513
Cutaneous Melanoma Serum	M	70	Benign	S1012400
Cutaneous Melanoma Serum	F	39	Benign	S1035502
Cutaneous Melanoma Serum	F	23	Benign	S1046506
Cutaneous Melanoma Serum	M	42	Benign	S1054471

Cutaneous Melanoma Serum	F	30	Benign	S1080541
Cutaneous Melanoma Serum	F	23	Benign	S1065568
Cutaneous Melanoma Serum	M	27	Benign	S1019429
Cutaneous Melanoma Serum	F	60	Benign	S1021464
Cutaneous Melanoma Serum	F	44	Benign	S1034536
Cutaneous Melanoma Serum	M	55	Benign	S1017480
Cutaneous Melanoma Serum	F	47	Benign	S1055557
Cutaneous Melanoma Serum	M	81	Benign	S1008454
Cutaneous Melanoma Serum	F	19	Benign	S1058570
Cutaneous Melanoma Serum	M	34	Stage IB	S1096307
Cutaneous Melanoma Serum	F	50	Stage IA	S1009509
Cutaneous Melanoma Serum	M	73	Stage IA	S1089408
Cutaneous Melanoma Serum	M	72	Stage IA	S1087466
Cutaneous Melanoma Serum	M	89	Stage IA	S1059414
Cutaneous Melanoma Serum	F	44	Stage IA	S1022577
Cutaneous Melanoma Serum	M	77	Stage IA	S1093451
Cutaneous Melanoma Serum	M	52	Stage IA	S1026478
Cutaneous Melanoma Serum	M	65	Stage IIB	S1006438

Cutaneous Melanoma Serum	M	44	Stage IB	S1007447
Cutaneous Melanoma Serum	M	46	Stage IB	S1037454
Cutaneous Melanoma Serum	M	39	Stage IB	S1057451
Cutaneous Melanoma Serum	M	36	Stage IIA	S1088486
Cutaneous Melanoma Serum	-	73	Stage IA	S1062509
Cutaneous Melanoma Serum	F	28	Stage IV	023
Cutaneous Melanoma Serum	M	48	Stage IV	BH-M-001
Cutaneous Melanoma Serum	M	45	Stage IV	019
Cutaneous Melanoma Serum	M	84	Stage III	034
Cutaneous Melanoma Serum	F	72	Stage IV	031
Cutaneous Melanoma Serum	F	73	Stage IV	017
Cutaneous Melanoma Serum	F	40	Stage III	039
Cutaneous Melanoma Serum	M	29	Stage III	029
Cutaneous Melanoma Serum	M	67	Stage IV	036
Cutaneous Melanoma Serum	M	36	Stage IV	010
Cutaneous Melanoma Serum	M	82	Stage IV	SVUH-M-006
Cutaneous Melanoma Serum	M	74	Stage III	014
Uveal Melanoma Serum	F	72	Monosomy 3	613325

Uveal Melanoma Serum	M	53	No evidence of Monosomy 3	612963
Uveal Melanoma Serum	M	68	No evidence of Monosomy 3	614618
Uveal Melanoma Serum	M	54	No evidence of Monosomy 3	624972
Uveal Melanoma Serum	M	71	Monosomy 3	608420
Uveal Melanoma Serum	F	72	Monosomy 3	607486
Uveal Melanoma Serum	M	79	No evidence of Monosomy 3	606968
Uveal Melanoma Serum	M	80	Monosomy 3 Loss of Heterozygosity 3	590077
Uveal Melanoma Serum	F	85	Monosomy 3	575817
Uveal Melanoma Serum	-	-	No evidence of Monosomy 3	533028
Uveal Melanoma Serum	-	-	No evidence of Monosomy 3	615989
Uveal Melanoma Serum	M	61	Monosomy 3	619357

Table 1. Comprehensive list of samples used in ELISA analysis in Chapter Five.

Appendix D

Presentations, Posters, and Publications Resulting From This Work:

Presentations:

- ***Proteomic Analysis of Both Uveal and Cutaneous Melanomas for the Identification of Novel Targets***

Irish Mass Spectrometry Society Annual General Meeting. May 2012

- ***Functional Validation of Novel Targets in Uveal Melanoma***

Biotechnology in Action: Stem Cells & Tissue Engineering, Biopharmaceutical Production and Cancer Biomarkers. September 2012

- ***Proteomic Analysis of Cutaneous Melanoma Metastasis using ProteoMiner Fractionation with Reverse Phase Chromatography and LC-MS/MS***

7th Annual Conference on Analytical Sciences Ireland (CASi). July 2013

Posters:

- ***Triosephosphate Isomerase and Fatty Acid Binding Protein, Heart Type as Potential Protein Biomarkers of Metastatic Uveal Melanoma***

2nd Annual Irish Melanoma Forum. November 2012

Publications:

- ***Differential expression of fourteen proteins between uveal melanoma from patients who subsequently developed distant metastases versus those who did not.***

Annett Linge[1], Susan Kennedy[1], Deirdre O'Flynn, Stephen Beatty, Paul Moriarty, Michael Henry, Martin Clynes, Annemarie Larkin[2] and Paula Meleady[2].
Investigative Ophthalmology & Visual Science (IOVS) May 2012